Rear Wheel Steer Bikes

Unconventional stable bicycle

P. H. de Jong

Department of BioMechanical Engineering

TU Delft

Rear Wheel Steer Bikes

Unconventional stable bicycle

by

P. H. de Jong

to obtain the degree of

Master of Science
in Mechanical Engineering

at the Delft University of Technology,
to be defended publicly on Friday February 24, 2017 at 13:00.

Student number:	1538357	
Project duration:	January 1, 2015 – February 24, 2017	
Thesis committee:	Dr. ir. A. L. Schwab,	TU Delft, supervisor
	Dr. ir. R. Happee,	TU Delft
	Prof. dr. ir. M. Wisse,	TU Delft

This thesis is confidential and cannot be made public until February 24, 2022.

TU Delft
Delft University of Technology

Abstract

Keywords bicycle, bike, rear, steer, kinematics, dynamics, lateral, stability, self-stable.

The design of the ordinary bicycle has barely changed since the end of the 19th century. Until then it evolved to a well ridable machine with no need for further drastic modifications. However, around 2011 it was shown that, just like an ordinary bicycle, strange appearing designs could also be stable. One of these designs was a bicycle that steers with the rear wheel instead of the conventional front wheel steering. This was contrary to the popular believe that such a bicycle is inherently unstable. Although it was seen that such a bicycle could be stable, both from a theoretical as well as an experimental point of view, it was not yet revealed why and how this occurs. Now, a thorough study on the stability of rear wheel steered bicycles is conducted to fill up this knowledge gap.

The history of research on rear wheel steered bicycles varying from simple trial-and-error studies, to theoretical researches based on models, is researched and documented. This makes clear where the knowledge on the subject can still be increased and which methods could be used to do that. Subsequently, these deficiencies in the knowledge on rear wheel steering for bicycles are investigated. With the Whipple bicycle model, a quantitative kinematic steer-side definition is found and rear wheel steering is dynamically compared to front wheel steering on bicycles. In this process differences and similarities between the lateral dynamics of different vehicles like bicycles, cars or unicycles are mentioned. Finally, the process of modeling, designing, constructing and validating a self-stable rear wheel steered bicycle is revealed.

Preface

Late 2014 I, Pier, had just finished an internship on the toe pads of treefrogs at the Wageningen University. The only thing left between me and my MSc degree in Mechanical Engineering was a graduation project. Being content about Arend Schwab from whom I took the courses Multibody Dynamics A and B, and Matlab in Engineering, my first choice for supervisor was him. Luckily, Arend recently switched to the BioMechanical Engineering department, which was the department of my master track 'BioMechanical Design' such that there were no bureaucratic obstacles for me to approach him. When sitting down to talk about the graduation opportunities, his enthusiasm soon inspired me to pick up my old BSc graduation subject on rear wheel steered bicycles. Therewith, this conversation marked the start of the creation of this, what I would like to see as the, magnum opus in my academic career so far.

Soon after starting, due to Arend's contagious enthusiasm and the seemingly endless stream of interesting research opportunities, I got entwined in a tangle of theories and analyses on the subject. Luckily, or for some sadly, I appeared not to be in a hurry to leave my student time behind me, and I took the time to investigate all revealed research questions to the best of my capabilities. This included taking some courses on vehicle dynamics and exploring a lot of literature on bicycles. For a large part, this all took place in the bicycle lab (see figure 1) of the TU Delft, where bicycle dynamics are omnipresent.

This bicycle lab harbored some nice people with whom I had fruitful discussions about my project or about nothing at all: Inge Kalsbeek, who helped measuring the prototype parameters and even found RWSB examples like the X-Bike; Patricia Baines, who served nice organic coffee (Simon Lévelt Café Organico Arabica Instant) and flattered me by informally declaring me the lab manager; Tim Huiskens, who passed me his RWSB configurations and helped out when I was not able to read the too tiny letters on a coarse image (stupid 'persevering Peter'); Maryam Sharify, who was busy studying a baseball throw and had nothing to do with bicycles, but to great joy was often around, and I was glad to be her Optitrack vs. IMUs test subject; George Dialynas, the happy Greek bicycle simulator constructing PhD-student with excellent Dutch capabilities, alles goed? prima, geen probleem; Oliver Lee, the PhD-ing cycling open-sourcerer who programmed the bicycle simulator, but was not completely able to circumvent MS Windows; and Niels Lommers, who explained me the use of Shimmer and gave great tips about using TikZ and Inkscape.

Besides the people at the bicycle lab, also the TU Delft people at the 3mE faculty Students' Walk-in Workshop (SWW) and Meetshop (Jos van Driel) were a great help in building the prototype and the

Figure 1: The TU Delft Bicycle Lab.

measurement equipment. Even the people at the Sports Centre, where the experiments were conducted, were so sportive to let me test that heavy steel-pile of a bicycle on their sports hall floor.

To keep my mind running at the absolute smoothest way possible, I shared the occasional distractions, like lunches and coffee breaks with those in the same MSc-graduation boat as me; Those in the bicycle lab as well as Stefan Broxterman, Caspar Banis, and Martijn 'Suud', with whom I even spend an afternoon among the jellyfish at Scheveningen. The coffee consumption, together with my engineering mentality, resulted in a gorgeous triangular coffeecup pyramid. A pyramid that makes the determination of the number of coffeecups, ☕_n, easy by counting the number of stories of the pyramid, n (the n^{th} tetrahedral number) [Tim and Arend]:

$$\text{☕}_n = \frac{n\ (n+1)\ (n+2)}{6} \tag{1}$$

The 10 stories high coffeecup pyramid (see figure 1) can then be seen to consist of 220 cups, which represents only a fraction of the total consumption.

I would like to thank all those people at the university, foremost Arend, for all the help and nice times I received during my graduation. But, although a large part of the graduation happened within the academic walls, I was not always able to leave it there. My thanks go also out to all of those who supported me from the 'normal' world.

First off, my father, mother, and sister for always being me, either mentally, physically, or, how could it be otherwise, financially. My mother, Jelly, never doubted me, my father, Cor, was literally essential for this graduation project by constructing some of the experimental bicycle prototype parts, and Wilke was (almost) always interested in the progression. Furthermore, of course, all my friends and family who showed their support and interest in the process.

Especially 'Ip Man' means a lot to me: Anna Werkman, my family status exceeding friend, who gave me many encouraging words; Remco Langhorst, who was my explosive video-editor; and Arjen Langhorst, with whom I spend time working on our theses and who helped measuring the prototype behavior and getting me some obscure german source material. They were there to share the good and the bad (if I wanted to; sorry for not sharing my awesome literature grade, Anna), or to just relax and forget about bicycles for a moment.

Somewhat a project-within-the-project was the construction of the prototype. Thanks to the bachelor project with Stefan Broxterman, Martijn Korevaar, and Wouter Kuijsters there was already a basis. However, some modifications like different masses and a paint job were required. Rijwielsporthuis Piet Vonk provided excellent service in finding some bicycle parts and Chessa Metaalbewerking delivered great turning work. Spray painting of the bicycle was done in the kitchen and the hallway of my home, so I am grateful for Peter van Dommelen, and Jan van Kampen for living with that crap.

All in all, it turned out to be a bunch of work to finish the project. The literature needed to be found, read and documented, the equations needed to be sorted out and different analyses were carried out, and of course, maybe the nicest part, this report about all this hard work was written. Along with that, also two colloquia (presentations) were given (thanks, Wilma Werkman, for forcing me to do these as quick as possible; it only took a small year to check them off). From time to time all this work made me doubtful and sour, going to a beard and back again, but never did I think of dropping out and here I am writing this preface with joy (although hoping to keep it down-to-earth without much dramatization, i.e. something Erik Werkman would happily read) being all the more convinced I did well; alles komt goed!

P. H. de Jong
Delft, February 2017

Contents

Introduction

A bicycle is a single track vehicle which has two wheels each within a frame and where the frames are connected by a single revolute joint [20]. Not everywhere popular and well established, but in general a bicycle is a well known means of transport taken for granted as an everyday object that works decently (although surprisingly many people are unable to recall the exact bicycle lay-out [21]). That is probably why the bicycle design has barely changed since the end of the 19$^{\text{th}}$ century [13].

Since then, a conventional bicycle has a rider-carrying large 'frame' at the rear and a fork with handlebar at the front. The rotational hinge between the frame and the fork, the headset, is placed in front of the rider and is angled such that the steer axis intersects the ground a little ahead of the front wheel contact point. In this study this bicycle configuration is referred to as the conventional bicycle with the specific numerical benchmark bicycle parameters as working example [22]. A human can comfortably ride such a conventional bicycle by applying propulsion on the pedals that are connected to the driven rear wheel and applying steering via the handlebar.

Although there exist multiple types of bicycles, like the city-bike, a touring bike, a race-bike, a mountain-bike and more, they all share more or less this overall similar conventional design; not many exceptions on this bicycle design can be seen in the 'wild' nowadays. Why is it that there are almost no other bicycle designs? Has the conventional bicycle as we know it the perfect design? Or is it simply because the conventional design works well enough and people stopped applying drastic changes to improve the design? Maybe, the development of the bicycle stopped due to the introduction of the, then novel, motorized transport. It must be admitted that the current conventional bicycle is a pretty good design, but what else is ridable or controllable?

The number of design possibilities for stable bicycles can be increased as some potentially useful design space regions have not yet been explored (sufficiently) during the evolution of the bicycle. Therefore, a broad goal of this study is to confirm that the stable bicycle design space extends beyond the conventional bicycle designs. A bicycle is not exclusively a bicycle when it has its steer axis close to the front wheel intersecting the ground close to the front contact. Many more designs are possible within the technical definition of a bicycle: A single-track machine with two frames connected by a rotational joint with either frame having a turnable wheel. This study focuses on a specific example of bicycle design alteration where the steer-side is changed; rear wheel steering. Specifically, the research aims to investigate the stability of a Rear Wheel Steered Bicycle (RWSB).

RWSBs, as opposed to Front Wheel Steered Bicycles (FWSBs), have the steering wheel at the rear and have been around for years being the interest of bicycle enthusiasts. Many people dream about rear wheel steering as an opportunity of exploring a region in the bicycle innovation domain of which not much is known about, but often RWSBs are simply deemed impossible to ride in any case, and hence, thorough scientific research on RWSBs is scarce. In recent years developments occurred that show that RWSBs can be stable, such that something deemed impossible for a long time, is now possible, creating an urge to investigate all remaining unknowns and theories regarding RWSBs. This discovery marked the start for this research where stable RWSBs are transformed from a myth into science.

Shifting RWSBs from the dream domain towards science is not done by simply looking at the more frequently occurring rear wheel steered multi-track vehicles, like tricycles and cars, which are discussed more often in literature. The stability issues of these vehicles are of a different nature than those of a bicycle, because they are statically stable but can become unstable due to dynamical behavior. These vehicles are only shortly discussed here to relate them to RWSBs, but a full analysis is not conducted. Bicycles also need to stay upright, such that RWSBs impose different challenges on stability analyses.

Illustrative for the challenge in RWSBs is the debate on what actually is a rear wheel steered bicycle, because basically a bicycle is symmetric with two frames connected by a revolute joint. Is the steer-side determined by the location of the rider or the head tube? Does rear wheel steering even exist on a bicycle, or is it the same as front wheel steering? Often people ascribe special cornering properties to RWSBs, but never are they proven. There is much ambiguity in RWSB theories, and indeed, in general, it is hard to say something about a bicycle's stability, because all bicycle parameters interact in a complex manner to create the stability properties [15]. Therefore, there is a need to check all the claims about rear wheel steering and turning it from believe into knowledge, with recent developments giving good hope on a happy conclusion. First, the current knowledge on RWSBs is sought, after which general bicycle theories are presented and linked to RWSBs. Then, a stable RWSB configuration is designed and tested to once and for all show the viability of RWSBs.

Part I Literature

To get a good background on rear wheel steered bicycles (RWSBs), a thorough study is conducted to find the current knowledge about RWSBs and lay a fundament for upcoming research on the subject. This part presents this known information on rear wheel steered bicycles. It has to be admitted that in general, the scientific research on RWSBs is quite scarce and limited, since people might not see added value with respect to conventional bicycles. Moreover, rear wheel steering is often considered inherently unstable on bicycles and although RWSBs were built, they were not easily ridden [23]. Therefore, owning or riding an RWSB is generally considered impractical and a mere gimmick.

The instability presumption makes that primarily the control characteristics of RWSBs are researched and self-stability, where a bicycle stays upright by itself, is only mentioned shortly or not at all. Still some interesting (scientific) literature can be found wherein RWSBs are discussed on different levels. Summaries of these articles are presented in chapter 1, where the only opinions given in the summaries are those of other (third-party) authors.

The articles are discussed in chronological publication order. Some content of the articles here is also used in other parts in the report, hence, some parts are redundant. This is done to make the summaries here as complete as possible, and to keep descriptions in other parts of the report as clear as possible. The summaries are mostly structured to include the following:

Background Why are RWSBs investigated? Are there advantages?

Definition What does the author consider a rear wheel steered bicycle?

(Self-)Stability What is said about (self-)stability and stability theory?

Feasibility What is concluded about the feasibility of RWSBs?

Third parties What do others say about the study?

Quote An appealing quote of the author about the study.

To conclude the RWSB literature, in chapter 2, similar statements from different articles and examples, of both scientific and 'grey' literature, are combined to form general literature statements and interpretations by the author of this study (P. H. de Jong). The transformation from front to rear wheel steering brings several causes for reasoning difficulties and errors with it. These pitfalls as well as other difficulties are presented and discussed here.

Appendix A RWSB literature historical examples

Many bicycle enthusiasts have shown interest in the principle of rear wheel steering [23]. On the internet and in some special interest magazines numerous examples of RWSBs can be found. These examples include hobbyists who try to build something different from conventional bicycles just for the fun of it or students who build an RWSB as school project. In this overview, 101 examples of RWSB designs are presented, making it an overview of 'grey' literature. For example, specific examples of RWSBs built for the researches in the scientific articles, are presented more elaborately in this overview. But also only briefly mentioned RWSB ideas on internet fora are listed to depict the variety.

The list aims to show the interest of people in experimenting with a bicycle by mainly bringing the steer axis more to the rear and/or angle it differently than on the now conventional bicycles. The list consists of an illustrative number of examples, but undoubtedly there are more examples to be found, either on- or offline, in garages or sheds around the world as ongoing projects.

The overview is composed to include all bicycles that pop-up in discussions about rear wheel steering. As such, not all examples are perceived as rear wheel steered by all people, and some are not even true bicycles, since they incorporate multiple steer pivots. To be included in the list, a bicycle is allowed to have an altered or added steer axis, but it can not have more than two wheels.

Part II Bicycle theory

In order to study the stability of bicycles, a sound understanding of bicycle modeling and bicycle dynamics is required. Therefore, the general properties of bicycles and analysis methods need to be known. Then, with that methods the steer-side, i.e. front or rear steered, can be defined and the differences or similarities between the cases can be investigated. This part presents known general bicycle information from literature and expands that at some instances to clarify theories and analyses.

The model chosen to investigate the lateral bicycle dynamics, is the Whipple model [22], because this model is well documented and has already proven that it is able to show self-stable RWSB configurations [16], where other less detailed models used throughout the history did not (see chapter 1 and 2). Chapter 3 describes this Whipple bicycle model and methods to work with it.

From the bicycle model, linearized equations of motion can be used to investigate the stability [22]. In chapter 4 it is explained how the stability qualities of a bicycle follow from these equations as well as how to implement a simple (stabilizing) controller in the model. Moreover, a convenient method to draft parameter requirements for stability is presented, that has proven itself in finding unconventional stable bicycle configurations [15] [16], as is done in this study for rear wheel steering.

Next to a stability analysis, a time response analysis can be used to obtain more insight into bicycle dynamical behavior. Methods to perform this bicycle time response in theory and in real-life are explained in chapter 5. Therefore, an overview of simulation and real-life state measurement methods is presented. When the real time response is obtained, the theory can be compared with measurements, and the time response can even be related to stability theory.

Relating the current state-of-the art bicycle knowledge to rear wheel steered bicycles was not yet clearly done. To investigate the influence of the steer-side on bicycle properties and behavior, one first needs to know what exactly determines the steer-side of a bicycle. Chapter 6 describes how the kinematics are important in bicycle behavior and how the steer-side is defined by those kinematics.

With the steer-side definition in hand a conventional front wheel steered bicycle can easily be converted to a rear wheel steered bicycle. Indeed, there is no reason why the derivations and equations of the bicycle model would not apply to an RWSB, since an RWSB is just a special case of a bicycle (just as an FWSB could be considered a special case). In chapter 7, a conventional bicycle configuration, i.e. the specific numerical benchmark configuration [22], is imagined to be ridden in two different longitudinal directions to compare the behavior of an FWSB with an RWSB. Furthermore, by also comparing the turn behavior for different steer-sides for different vehicles, it is shown that non-leaning vehicles react differently on changing the steer-side than bicycles do.

Part III Self-stable RWSB

By accident Kooijman *et al.* discovered a self-stable, i.e. a system that is stable without external control, RWSB configuration when trying to model a unicycle with the Whipple bicycle model [16]. This discovery serves as basis for the here developed theory on self-stable RWSBs. The study in this part is even set up much alike the study of Kooijman *et al.* where they developed the unconventional self-stable ‘two-mass-skate bicycle’ [15] [16]. Showing how exactly a rear wheel steered bicycle can be self-stable, is never done and might mean a pavement of the way to better ridable RWSBs.

In chapter 8 a reduced set of bicycle parameters is chosen to find clear requirements on their values in order to come up with a theoretical self-stable rear wheel steered bicycle. This bicycle is compared to a unicycle and wheel in chapter 9 to see what the similarities and differences are. Thereafter, in chapter 10 this theoretical bicycle is developed into an experimental RWSB prototype and is compared with the theoretical model by measuring the time response and comparing eigenvalues from a number of experiments at various forward speeds.

Part I

Literature

Chapter 1

RWSB literature summarized

1.1 1869 Rankine [1]

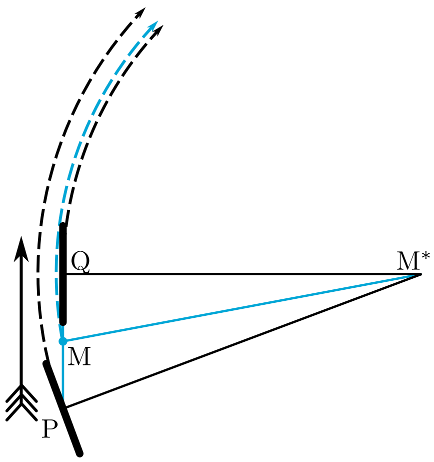

Figure 1.1: Rankine RWSB ground plane depiction in a turn with a single center and riding direction as described by the arrow. It shows projections (traces of the planes) of the wheels, center of mass and their trajectories on the wheelbase $\overline{\mathrm{PQ}}$ on the ground while the bicycle may be leaned. The RWSB has zero rear wheel trail (steer axis passes through rear contact) and vertical steer axis. M depicts the projection of the center of mass on the wheel base, the base-point. Arcs $\widehat{\mathrm{P}}$, $\widehat{\mathrm{Q}}$, and $\widehat{\mathrm{M}}$ are the trajectories of the respective points. (recreated Fig. 7. [1])

William Rankine analyzed the ridability of bicycles with zero trail (steer axis passes either through front or rear wheel contact point), vertical steer axis and front wheel direct drive [24]. Balancing, steering and propulsion of the bicycle with rider are studied with a 'heuristic inverted-pendulum-type model' [25] where the rider is assumed rigidly attached to the frame. The rider can thus not lean with respect to the frame on which he sits. For his analysis of the stability he used the 'base-point'; the perpendicular projection of the center of mass of the total bicycle with rider on the wheel base. The base-point should be coincident with the line of the resultant of the gravity force and the centrifugal force in order to be in balance. Then, normal forces and the centripetal forces at the wheel contacts counteract the gravity and the centrifugal force of the center of mass. Slip is not taken into account in the analysis of Rankine. When the whole system is inclined to one lateral side, the base-point is said to have deviated horizontally to the other side and should be brought underneath the center of mass again to be balanced. In other words, during an imbalance, the center of mass is shifted with respect to the base-point in the direction of the lean. For a conventional front wheel steered bicycle the balance is then kept by actively steering by the rider into the leaned direction (the fall), i.e. contrary to the direction of the base-point deviation, to shift the base-point laterally to the desired position.

Here, steering is the control of the relative angle between the planes of the two wheels in order to indirectly change the position and direction of the forces from the road on the rims and in effect change the track of the bicycle and rider center of mass. The track of all points on the baseline are then assumed concentric and and have a common center which can be found by assuming that the wheel ground projections are tangent to their paths (no slip angle). His front wheel driven model makes that the rider can either control the steered wheel by means of the handlebar or by using his feet which are on the direct-drive of the front wheel, but leaning of the body is said to have no effect on balancing and steering. He seems unaware of the self-stability phenomenon or lean-steer coupling at all and discusses steering only in terms of control by a rider. However, he is probably the first one to notice the existence of counter-steering, which is an initial steer in an undesired direction to initiate the required lean into the desired turn direction [24] [26].

Rankine quantifies the steadiness of a bicycle with the degree of steering into the fall, i.e. the degree of stabilization. This degree at its part is quantified by the speed at which the base-point moves back underneath the center of mass and is called the 'promptitude in recovering the balance'. This promptitude is the lateral velocity of the base-point and is dependent on the forward velocity, v, the radius of curvature of the track of the base-point, $\overline{\mathrm{MM}^*}$, and the location of the base-point with respect to one of the wheels. For an FWSB Rankine defines the 'promptitude of recovery' as $v(\overline{\mathrm{MP}}/\overline{\mathrm{MM}^*})$. Therefore, for an FWSB Rankine's balance promptitude increases with increasing velocity and with a more forwardly placed center of mass position, while it decreases for larger turn radii. Furthermore, a given deviation from the equilibrium position is corrected in less time at higher forward velocities and a higher center of mass is better for steadiness of the bicycle.

In the end Rankine turns to rear wheel steering, because it has the advantage that one does not get the wheel rim against his legs when the wheel is steered (note his assumed direct front wheel drive). Just as his earlier analysis his RWSB example has zero trail, but now for the rear wheel, and the steer axis is vertical. However, he does not state a clear definition of when a bicycle is rear wheel steered other than that the steering wheel is behind.

His reasoning about balancing an RWSB goes as follows: Assume that an RWSB is brought out of balance and is leaned to the left side. Now, to recover the balance, the base-point also needs to be brought to the left side. Referring to figure 1.1 it can be seen that the base-point M moves initially to the left of the initial position when the RWSB is steered to the right (counterclockwise rear wheel steer angle). Then, the RWSB promptitude is $v(\overline{\mathrm{MQ}}/\overline{\mathrm{MM}^*})$ in the beginning and the balance is set to be recovered since M moves in the correct direction. However, after a distance $\overline{\mathrm{MQ}}$, the base-point starts to move in the wrong direction and the bicycle starts to deviate from the balanced position. According to Rankine, if after that small distance in which the base-point moves to the correct side, the balance is not recovered, the bicycle will fall over. And on the other hand, if the balance is recovered sufficiently in that short time, the rider needs to be very alert to neutralize the steering and prevent overturning. This is in contradiction with an FWSB with zero front wheel trail and vertical steer axis which would have the base-point move always in the desired steered direction.

This behavior makes him conclude that for steering or curve following rear wheel steering is just as suitable as front wheel steering, but for balancing it introduces some severe, although not always necessarily insurmountable difficulties.

> "*It is true that for the purpose of steering, or describing curves, as distinguished from balancing, the hind-wheel is quite as suitable as the fore-wheel; but a fatal objection to the proposed alteration arises from the fact that with the steering-wheel behind, it becomes extremely difficult for the rider to keep the balance of the vehicle. . . . A bicycle, then, with the steering wheel behind, may possibly be balanced by a very skillful rider as a feat of dexterity; but it is not suitable for ordinary use in practice.*"

One can wonder if Rankine's analyses of control are not too simple due to the more limited frame of reference of that time. The descriptions and deductions as used by Rankine, although interesting, may need to be interpreted with care as articulated by Limebeer and Sharp [25]:

> "*These papers are interesting from a historical perspective but are of little technical value today.*"

1.2 1896 A. Sharp [2]

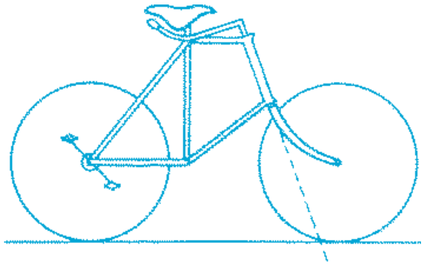

Figure 1.2: Sharp's RWSB example which drives forward to the left in the drawing. [2]

In his 1896 book, Archibald Sharp presented bicycle dynamics theories along with numerous examples of bicycles from that time and before. In that light the possibility of rear wheel steering is then also shortly discussed. An unambiguous example given is the front-driven and rear wheel steered bicycle shown in figure 1.2, but defining RWSBs may not be as easy as appears on first side because several features need to be taken into account:

> "*Proceeding to the further division and classification of bicycles, the first subdivision that suggests itself takes account of the method of steering; a bicycle being said to be a front- or rear-steerer, according as the steering-wheel is in front or behind, while among tricycles there are also side-steerers. A few bicycles have been made with double-steering.*
>
> *The complete frame of the machine is usually divided into two parts, called respectively the front-frame and the rear-frame, united at the steering centre; though sometimes that part to which the saddle is fixed is called the 'frame', to the exclusion of the other portion carrying the steering-wheel. It should be pointed out that the steering portion will sometimes be the larger and heavier of the two, the 'Humber' tricycle affording an example of this. In the 'Chapman Automatic-Steering' Safety the saddle is not fixed direct to the rear-frame, but moves with the steering fork. The complete frame is in this case divided into three parts, which can move relative to each other, on which are fixed the driving-gear, the steering-wheel, and the saddle respectively.*
>
> *Examples of double-steering are afforded by the 'Adjustable' Safety, made by Mr. J. Hawkins in 1884, and by the 'Premier' Tandem Safety, in each of which the forks of both wheels move relative to the backbone.*"

Sharp was probably unaware of the possible existence of self-stability for a bicycle [26]. And regarding stability/ridability of RWSBs it is only claimed that they only have the disadvantage that the rear wheel swings out. Furthermore, the mechanics of steering for RWSBs are not discussed, because rear wheel steering is uncommon:

> "*There have been very few rear-steering bicycles made, though their only evident disadvantage is, that in turning aside to avoid an obstacle, the rear-wheel may foul, though the front-wheel has already cleared. Nearly all successful types of bicycles have been front-steerers. . . . Cycles are front- or rear-steerers, according as the steering-wheel is mounted on the front- or rear-frame. All bicycles that have attained to any degree of public favour are front-steerers.*"

But despite the lack of working examples until then, Sharp was not pessimistic about the possibilities for a successful RWSB:

> "*. . . no successful type of rear-steering bicycle has been evolved. Experimenters might with advantage direct their energies to this comparatively untrodden domain.*"

1.3 1970 Jones [3]

David E. H. Jones did an experimental study to comprehend the stability of bicycles with focus on the ridability under influence of the self-stability. Here, self-stability is the ability of the bicycle to balance itself without rider, and ridability is the ease with which the bicycle could be ridden by a rider. He experimented by changing different parameters and looking what this did for the stability of the bicycle. When the bicycle then turned out to have changed dynamics, the altered parameter was concluded to contribute to the characteristics.

Although he aimed for it, it turned out that it was surprisingly hard to make a bicycle unridable. Some changes like removing front wheel gyroscopy or increasing fork offset (steer axis intersects ground behind front wheel) did remove self-stability, other changes like reversing the fork improved the stability. In his process, Jones also built a fixed (although adjustable) lean bicycle by attaching an outrigger wheel to the rear frame of a conventional bicycle and thereby making it an asymmetric tricycle. Pushing this bicycle backwards and let it run freely without rider essentially makes it rear wheel steered. By performing this unstable backwards run, Jones showed that a reversely moving conventional bicycle is not self-stable. Note that Jones does not mention rear wheel steering at all, but sees this reversing of a bicycle simply as a manner of destabilizing a bicycle. Therefore, he also does not define what makes a bicycle rear wheel steered. He noted that a conventional bicycle ridden backwards has the two wheels moving both an opposite lateral side in contrary with a forward ridden conventional bicycle where both wheel paths tend to align:

> "*I had encountered a very attractive form of self-centering action, not depending directly on variable frictional forces, while trying the naive experiment of pushing a bicycle backwards. Of course it collapsed at once because the two wheels travel in diverging directions. In forward travel the converse applies and the paths of the two wheel converge.*"

1.4 1977 Laiterman [4]

Figure 1.3: Laiterman with his adjustable RWSB. [4]

As an undergraduate project at the Massachusetts Institute of Technology, Lee Howard Laiterman, under supervision of David Gordon Wilson, tried to improve the design of the bicycle for long-distance tour purposes so that the ride is less fatiguing and greater range and speeds are achieved. In his eyes this meant that a small frontal area, protection against the elements, safety and comfort improvement, and high energy efficiency are all necessary. In other words, the physiological requirements of the human were strongly taken into account. This led to the design of a bicycle (see figure 1.3, and section A.26). This bicycle had the requirement that it incorporated a semi-recumbent posture of the rider, i.e. the rider has to sit straight up with the legs pointed frontwards. This position compromises between the efficient leg use of the upright position and the low air resistance of the full recumbent position. Thereby, he states that the bottom bracket should not be higher than the seat for blood circulation considerations. Moreover, the wheel base should not be too long in order to prevent a light loading on the front wheel which could make that wheel to lose contact with the ground. This was quantified as that the front wheel must carry 55% of the rider's weight to optimize the performance. Laiterman also assumes that for stability reasons the rider's center of mass should be as low to the ground as possible. These requirements made that it was hard to make the rider position such that he would not interfere with a steered front wheel and thus Laiterman decided that an RWSB with front wheel drive was the way to go.

In order to come to a good design, the effects of wheel base length, steering-control parameters, and trail (not steer axis angle) on the stability of an RWSB were investigated. Note that a positive trail, for either the front or rear wheel, is when the steer axis intersects the ground ahead of the contact point, and a negative trail is present when the steer axis intersects the ground behind the contact point. A formal definition of an RWSB is not given by Laiterman, but in all his alterations the steer joint stays close to the rear wheel. Moreover, the driving and steering function are separated between the wheels.

No specific bicycle model was used for the stability analysis, but in stead, several theories of bicycle stability were presented, some of which seem to be developed by Laiterman himself. In his discussion of stability, Laiterman makes use of the term '(inherent) stability'. Here, for inherent stability he uses the requirement that a bicycle needs to steer into the leaned direction in order to prevent falling completely. He assumes that this steer into fall behavior is generally caused by the rider leaning in the appropriate direction and thereby influencing the weight carried on the front wheel which on its part steers the front wheel into the fall. Also, the front wheel is assumed to cause a stabilizing gyrostatic effect. These effects make that for all conventional bicycles an increased front wheel trail (more positive, steer axis intersects ground further in front of front contact) is said to result in increased stability.

Laiterman interprets an RWSB physically similar as an FWSB, except for that the steered wheel, i.e. the rear wheel, now has to steer in the opposite direction relative to the main frame to make a turn of equal direction as the front wheel would do in an FWSB case. Since only the direction is different, Laiterman hypothesizes that when slip angles are not taken into account then a rear wheel trail pointing rearwards (negative, steer axis intersects ground behind rear wheel) is required for good stability on an RWSB. However, on an RWSB slip angles supposedly affect bicycle behavior in an opposite manner as for an FWSB since these slip angles are seen by Laiterman as the cause of extra lateral tire contact forces. First, he claims that an RWSB is generally more rotated than an FWSB due to a typical 30% smaller turn radius when all things are equal except for the steered side, presumably resulting in larger slip angles. With this smaller turn radius, he apparently means that an RWSB is much more nosed in a turn as compared to an FWSB. Also, for an RWSB, initially in a corner the rear wheel has a lateral contact force (acceleration) to the outside of the curve and later on it has a (centripetal) force towards the curve inside. In contrary, the front wheel's lateral contact force (acceleration) is always pointed to the inside of the curve. This directional reversal of one of the two wheels lateral forces is not present in an FWSB and makes that whereas an FWSB benefits from trail, an RWSB does not, and thus should have small or no rear wheel trail to minimize slip angles effects, according to Laiterman.

With his theories in hand he built the (very) adjustable prototype and experimented with it. Except for the steer axis angle, the masses of all the parts, and the wheel diameters, everything was more or less adjustable. The much sharper turn for rear wheel steering as compared to front wheel steering makes that small handlebar movements give amplified turn curvature. A reduction ratio from steer input to output may thus make the handling of an RWSB more similar to that of an FWSB. Moreover, to also resemble the movement direction of a conventional bicycle, i.e. a clockwise handlebar turn results in a steer to the right, a cross linkage between the handlebars and rear wheel is required on an RWSB. Therefore, as often in RWSBs, Laiterman included a steering reversal and reduction ratio mechanism from handlebar to headset. He reported that the reduction ratio improved the handling so it was no longer unmanageable, and it opened the way to experimentation with the trail. The cable used to transmit the steer movement to the rear wheel even had a positive effect on ridability, because the rider's job of balancing and steering of the bicycle was easier due to friction and damping in the cables.

A large negative trail (steer axis intersects ground further behind rear contact) caused oversteering. And to his surprise, a positive rear wheel trail (steer axis intersects ground in front of rear contact) showed some beneficial behavior in that it did not worsen handling and it prevented oversteering early in the turn, however, it made it harder to leave the turn and return to a straight ahead trajectory. Experiments showed that the smallest trail (tested minimum was 25 mm), either ahead or behind the rear contact, was favorable for the ridability and that increasing the trail (tested maximum was 203 mm) had a negative effect on the ridability. Cornelius [8] claims that due to an inherent pneumatic caster of tires Laiterman's small negative trail is neutralized and in effect neither stabilizing nor destabilizing dynamics appear. It was also experienced that stability was improved by reducing the length of the wheel base. Probably, because then the angular acceleration around a vertical axis through the center of mass was altered such that it facilitated more accurate leaning and steering corrections, Laiterman reasoned. Moreover, although he had an adjustable seat height, a proper test of the claim that a low rider position, and thus low center of mass of the complete system of bicycle and rider is desirable for stability, was omitted.

As for some general bicycle dynamics he interestingly noticed two phenomena. First, different riders of the bicycle noticed that the long main tube of the bicycle protruding out in front of them first swirls leftward and then rightward when one tries to make a rightward turn. This indicates that the bicycle required counter-steering for the initiation of a curve, just as a conventional bicycle does. Secondly, indirectly a link is created between the extend to which a bicycle can stabilize itself (without controller) and the effort of controlling it. After all, he says his bicycle is not inherently stable since it requires a lot more of man-machine interaction than a conventional bicycle.

Thus, Laiterman constructed an RWSB that was eventually ridable and he thus succeeded in showing the feasibility of such a completely different bicycle. However, riding it required a different technique and more concentration (larger effort) as compared to riding a conventional FWSB; although it can be ridden, it is rather unsteady. Someone who has never ridden a bicycle before may have an easier time learning to ride an RWSB, because then conventional bicycle dynamics are not stored in one's memories. But for everyone these difficulties can be overcome and an RWSB can be just as practical as an FWSB:

> "*I believe that with continued practice, it may be possible for a rider to achieve a level of riding ease comparable to a conventional bicycle.*"

Laiterman's RWSB examples are more extensively described in section A.26. Laiterman also extensively presents the design of a rear wheel steering tricycle. This design is not very relevant in the scope of stabilizing an RWSB and therefore the discussion of this design is omitted here.

1.5 1979 Schwarz [5]

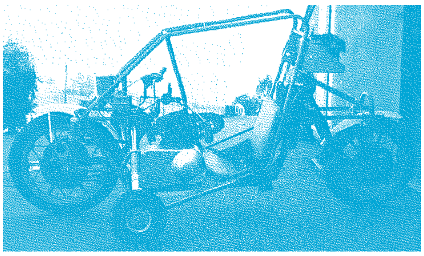

Figure 1.4: NHTSA's and Schwarz' motorcycle. [5]

Robert Schwarz (South Coast Technology, Inc) was contracted by the National Highway Traffic Safety Administration (NHTSA, part of the U.S. government Department of Transportation) to perform an analysis of a rear wheel steered motorcycle concept that would avoid accidents in two ways: it requires less avoidance maneuver time, and it facilitates more efficient and better controlled braking. First, it is argued that by applying rear wheel steering, reverse steer (counter-steer) would be unnecessary to initiate a turn, hence, no lateral movement in the wrong direction would be needed and valuable obstacle avoidance time is gained. Counter-steer is needed for conventional motorcycles in order to initiate a required lean of the vehicle. Secondly, separating the steer and brake behavior by means of rear wheel steering and front wheel braking also increases the stability during braking. This is because front-wheel braking is more effective for a fast deceleration and even a non-experienced rider can keep control of the motorcycle under heavy braking with rear wheel steering. Also, the rear wheel steering facilitates the lower center of mass which should increase stability during braking even further. As basis for the analysis and final design, Schwarz used a reversed conventional elongated wheel base and lower center of mass motorcycle concept of the NHTSA. Peculiarly, Schwarz does not give a clear definition of rear wheel steering.

An analysis of the uncontrolled behavior of the NHTSA concept was performed by an eigenvalue and eigenvector analysis, which gave the dynamical characteristics of the concept. He indirectly indicated that they are aware of self-stability by showing eigenvalue plots of another uncontrolled bicycle that has all negative real eigenvalues for certain velocities. Note that eigenvalues indicate stable behavior when their real part is negative. His analysis is practically showing either whether the motorcycle is self-stable or the degree to which the system could be stabilized by a controller. Schwarz made use of a computer program that incorporated the four degree of freedom motorcycle model of R. S. Sharp [27]. This is a rather complete model with position, mass and inertia parameters for both the main frame, and the front (fork) assembly, and the wheels are defined by position and inertia parameters. Because of assumed non-zero tire slip (with relaxation length) a lateral and yaw degree of freedom are present besides the lean and steer. Although the non-linear model of Sharp is not the most general model, it is mostly in agreement with well-known and checked models [24].

The design space is interpreted by Schwarz as that the motorcycle is made of two parts containing always at least the same components: There is the main frame containing the frame, engine, drivetrain, and rider, and then there is the steering assembly which rotates with respect to the main frame. The only design freedom is thus the choice of which frame to place ahead or behind, and some dimension and mass details. In effect, Schwarz basically made the motorcycle rear wheel steered by simply reversing a conventional motorcycle configuration (maybe just by reversing the forward velocity sign in the equations as suggested by Åström *et al.* [14]). Multiple eigenvalues were calculated for the RWSB, but the most interesting (physically meaningful) eigenvalues of these were found to be a complex pair at high frequencies, an absolute small real eigenvalue or complex pair (depending on speed and geometry) at low frequencies, and a large positive real eigenvalue. Because of the large positive real eigenvalue, a discussion of self-stability is then skipped to go on with a controllability analysis. The modes associated with the first eigenvalues could be stabilized with an appropriate geometry (within Schwarz design space) over an acceptable speed range. However, Schwarz was unable to stabilize the last mentioned largely positive eigenvalue, even when trying different combinations of trail lengths and directions and steer axis angles and directions. The mode associated with this eigenvalue, which he named ‘flop’ mode, is characterized by an increasing steer angle in the opposite direction as the main frame roll and yaw, indicating a steer-out-of-fall dynamic. It typically showed a time constant between 1/4 s and 1/12 s in a 3 m/s to 50 m/s speed range and thus was hard to control (smaller time constant is harder to control) and he declared rear wheel steering inherently unstable and unridable.

Despite those dispromising foresights of the concept’s controllability (and thus ridability), he was obliged contractually to build a prototype and so he did build the ‘best’ configuration he found in his analysis (see figure 1.4, and section A.27). As can be seen, the steer axis is pointing diagonally downwards to the rear and it intersects the ground in front of the rear wheel. As expected the motorcycle turned out to be unridable and this study became infamous in bicycle circles, because of the money waste associated with it [28] [29]; Taxpayers’ money was spent on a motorcycle that was already be hypothyzed to be very difficult or impossible to ride [30]. Jokingly, it can be said that no significant accidents took place with this concept and thus that it was safe [6]:

> “*It turned out to be safe in an unexpected way: No one could ride it.*”

Schwarz’ RWSB example is more extensively described in section A.27. Following his rear steering study, he researched a long wheel base and low center of mass for front wheel steering in the same article, but except for one reference this part is omitted here.

1.6 1982 Whitt and Wilson [6]

Frank Rowland Whitt and David Gordon Wilson discuss RWSBs in their 1982 book ‘Bicycling Science’ (2nd edition) on the dynamics of bicycles. Along with other ‘alternative designs’ they also analyze the balancing and steering of rear-wheel steering bicycles and then especially recumbent bicycles. They lack a definition of an RWSB, but as advantages they bring up the higher efficiency and the (apparently) improved mass distribution over the wheels as noted earlier by Laiterman (section 1.4) and Schwarz (section 1.5):

> “*Many people have seen theoretical advantages in the facts that front-drive, rear-steering recumbent bicycles would have simpler transmissions than rear-drive recumbents and could*

have the center of mass nearer the front wheel than the rear."

However, with reference to the bicycles of Laiterman (section 1.4) and Schwarz (section 1.5), as well as mentioning to a rear wheel steering bicycle with normal 'safety' configuration of the Bendix Company (Elmira, N.Y.), they reason that RWSBs are in general unsteady. The steering behavior is such that initially a fall can be recovered, but then soon thereafter the bicycle will lose its balance:

> "*Even if it were possible to further improve the rear-steering configuration (whether of the recumbent design or not) and to learn how to control such a machine fairly predictably, there would be obvious disadvantages in, for instance, avoiding a suddenly opened car door by first steering into the direction of the car with the rear wheel. The essence of the unsteadiness is related to this aspect of obstacle avoidance: as one begins to fall to one side, one can steer into (or under) the fall with the rear wheel, but then the inertia (the so-called 'centrifugal force') will act to increase the rate of fall.*"

Also a 1974 1st edition [31] is available which only refers to Jones unridable bicycle experiments [3]. The RWSB statements in the 2004 3rd edition [13] of this book will be given later on.

1.7 1989 Price [7]

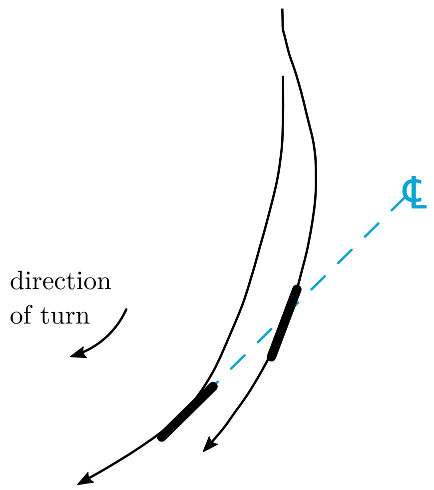

Figure 1.5: Price's representation of rear wheel steering with the wheels represented by two angled bars and a center line connecting them. The front wheel is 'fixed' with respect to the frame and the rear wheel steers, making the wheels follow the tracks as depicted. (recreated Fig. 12. [7])

Price mentions shortly the possibility of rear wheel steering in a discussion of steering and suspension design of two- and fourwheelers. Price states that for well-designed bicycles stability is reached by both wheel aligning due to the caster where the wheel contact patch following the point where the steer axis intersects the ground, and the lowest static position (energy minimum) of the center of mass for a zero steering angle when the bicycle is held upright. Herein, the caster is provided by a trail (distance of contact point to steer axis ground intersection) which can make the bicycle unstable for small values and too stable, i.e. steer insensitive, for large values.

A clear definition of rear wheel steering is not given, but FWSBs have the rear wheel following a track inside the front wheel track and for RWSBs it is then the other way around. Successful RWSBs are the ones that greatly resemble FWSBs, but although being ridable, riding them is not easy:

> "*HPVs* (Human Powered Vehicles) *have been built with front or rear steering. ...for the conventional case, the front wheel is steered in the desired direction and the rear wheel tracks slightly inside the front. Figure* 1.5 *illustrates the rear-steer case where the rear wheel*

is initially steered to aim the front, then partially unsteered to maintain the turn. Successful rear steerers have very conventional fork angle, rake and caster dimensions, but navigating them precisely is an acquired knack."

1.8 1990 Cornelius [8]

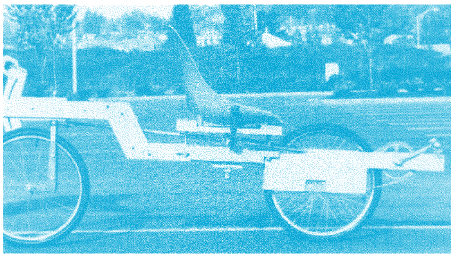

(a)

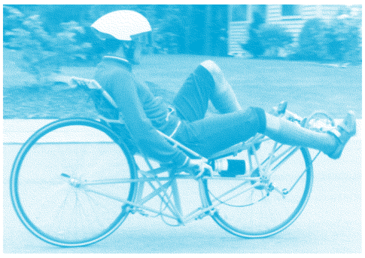

(b)

Figure 1.6: (a) Cornelius 1981 MKI and (b) the 1988 final version, the VelAero. [8]

Craig J. Cornelius built seven rear wheel steered recumbent bicycles in order to experiment with different changes in parameters and come up with the best one (see figure 1.6, and section A.31). The idea was that a rear wheel steered recumbent would make a compacter, lighter, and better packaged bicycle than a front wheel steered recumbent. The driven wheel can be the front wheel, making the drive chain shorter, and the wheel base can be of the same length as a conventional upright ridden bicycle while the center of mass is favorably lowered. This also results in a favorable larger distributed weight on the front wheel and an eased bicycle transportation with respect to front wheel steered recumbents. He states that when stability issues are addressed properly, a rear wheel steered recumbent might even be better than a front steered recumbent due to these advantages.

Cornelius does not explicitly describe how he defines an RWSB, but implicitly he states that it is about mass distribution. He namely discriminates between two frames with different masses where the larger mass contains the main frame, the rider, and the driven wheel, and the smaller mass is made of the steering frame (fork), the steered wheel, and the handlebar. He adds that a bicycle where the seat is attached to the front frame and the front wheel is the driven wheel is technically an RWSB. Dynamically-wise the steered frame can be identified by looking which frame is associated with which disturbance; One can say that a bicycle has a main frame with a rider on it, which is associated with the lean angle, and a steering frame, which is associated with the steering angle. He defines the sign of the trail as dependent on which wheel is steered and on which side of that wheel the steering axis intersects the ground. The front wheel trail is positive when the steer axis intersects the ground in front of the front wheel, and the rear wheel trail is positive when the steer axis intersects in front of the rear wheel. For example, a steer-axis/ground intersection in-between the two wheels gives a negative front wheel trail and a positive rear wheel trail:

> "*Caster, or positive trail, is defined as the distance the steered wheel's ground-contact patch is behind the intersection of the steering axis and the ground, behind being defined as opposite the direction of desired motion.*"

Cornelius uses some theories on bicycle dynamics to develop his designs. Above a certain speed a bicycle is able to remain upright with a hands-off rider or even without rider, he acknowledges. He assumes this 'auto-stability' (self-stability) of a bicycle to be a direct result of both positive (front wheel) trail and a lean-steer mechanism, making these two phenomena the two bicycle stabilizing phenomena. On a conventional bicycle the positive (front) trail corrects a steer angle disturbance by negative feedback where a steer angle decreasing counter torque is produced to align the wheels in a caster fashion. Moreover, the lean-steer mechanism corrects a lean disturbance and brings the bicycle upright again by negative feedback where the bicycle steers into the fall due to its kinematics. Steering into the fall shifts the support line underneath the center of mass and, hence, balances the bicycle. Cornelius states that these two phenomena cannot happen at once for an RWSB: Positive rear wheel trail is necessary to align the wheels after a disturbance (caster), while he claims that, opposed to an FWSB, negative trail of the rear wheel is necessary to steer into the lean. For an RWSB with positive rear wheel trail and negative front wheel trail (steer axis intersects ground in between wheels) the radial (support line) acceleration is assumed directed to the wrong, non-stabilizing, direction. Hence, both stabilizing phenomena never occur simultaneously, because of the different required trail sign. Therefore, Cornelius claims that an RWSB is inherently unstable and one has to compromise between a positive rear trail and the lean-steer behavior, or a neutral configuration (zero trail) where both phenomena are absent. Note that he states that pneumatic caster of tires can make a slightly negative rear trail (as Cornelius saw in Laiterman's study (section 1.4)) neutral, i.e. zero, and thereby removing caster and lean-steer behavior. Hence, no stabilizing effect is present, but neither are destabilizing effects like negative rear trail or steering away from a fall.

Regardless of the supposed impossibility of self-stability Cornelius went on in his quest to build a well-ridable RWSB. With reference to a theory of Laiterman (section 1.4) he assumed that short wheel bases are more stable than long wheel bases. He stays confined to the use of a mass distribution where the centers of mass of both frames are between the rear and front standard bicycle wheels with the steer axis separating the two frames. Moreover, like many RWSB enthusiasts, also Cornelius notes that a steer motion at a handlebar attached to the rear frame of an RWSB results in a turn of the bicycle in the opposite direction, as with the rudder of a boat. Therefore, a linkage system is implemented that inverses the steering motion connection between the handlebar and steered wheel to make the steering more intuitively, i.e. more like a conventional bicycle. Furthermore, a transmission ratio in the steer linkage helps to make the bicycle better ridable.

His experiments gave some interesting insights for which parameter requirements were experienced optimal. A positive rear wheel trail and negative front wheel trail (steer axis intersects ground in-between wheels) resulted in a reversed lean-steer behavior which steers the bicycle away from the leaned direction. However, his bicycle with negative rear wheel trail was harder to control than with a positive rear wheel trail. Furthermore, the bicycle became better controllable when the rear wheel trail was more positive (and the front wheel trail less negative). Although positive rear wheel trail cannot make the radial acceleration point in the correct stabilizing direction, it can reduce the negative effects by being as largely positive as possible. Thus supposedly, with a positive rear (and negative front) wheel trail, the occuring positive feedback effect of steering away from a turn is reduced and it is easier for a rider to withstand the bicycles desire to steer out of a turn. A positive rear wheel trail appeared especially beneficial for the ability to make unassisted starting while accelerating. The main center of mass of the bicycle is of the front frame and rider, and because the driven wheel is placed in front of this, accelerating tends to move the center of mass to the central position. Hence, the destabilizing reversed lean-steer behavior is counteracted during acceleration. Wanting a large positive rear trail means effectively that the bicycle configuration should be shifted more towards a conventional FWSB (but with negative front trail) in order to get dynamics similar to those of an FWSB (this is also noted by Whitehead [9]).

Cornelius based his study mainly on trial-and-error starting from a conventional recumbent bicycle lay-out. Although, quite nice results are shown, a self-stable configuration was not found. He attributes this to the fact that a steering method was not found that combines his necessary assumed positive trail with a steer-into-fall mechanism. However, it seems that Cornelius was aware of the limits of his study, but is positive about the potential possibilities:

> "*The rear-steering-recumbent design revolution is awaiting only the right breakthrough.*"

Cornelius' RWSB examples are more extensively described in sectionA.31. One figure of the article was misprinted and is corrected in a later magazine issue [32]. Cornelius is also known as 'Hephaestus' [33].

1.9 1990 Whitehead [9]

In a summary of known theories, John C. Whitehead discusses rear wheel steering (RWS) for vehicles in general with an emphasize on multi-wheeled (more than two wheels) human powered vehicles. RWS is attractive because of a neater packaging, for example by allowing for easy front wheel drive and thus a more efficient short chain. He states that the unusual behavior of RWS can be attributed to an initial unusual directed lateral movement of the rear wheel to the outside of a wanted curve. However, the problems with RWS arise only during transient behavior, not during a steady movement. Moreover, at higher speeds the effect ceases and there is no fundamental difference in yaw behavior due to steer input in comparison with the front wheel steered (FWS) case.

Whitehead claims that the real issue for RWS multi-wheelers arises for the stability requirement. All vehicles (no matter how many wheels) are desired to have stable behavior from themselves in that they return to a straight ahead path when hands are (momentarily) off steer. This stability also makes that unexpected disturbance torques on the steer can easily be countered by the driver. RWS vehicles, however, have two counteracting phenomena in this regard as transient and steady-state lateral tire forces are opposing in direction. Consider the case for a multi-wheeled vehicle with large main frame in the front and a small rear wheel assembly, where the rear trail is such that the steer axis intersects the ground in front of the rear wheel. Then, transient caster effects make that the rear wheels aligns (zero steer) with the rest of the vehicle and thus stabilizes it. On the other hand, steady state centrifugal accelerations make the center of mass in between the wheels move outwards of a curve, thereby increasing steer angle. The best option for RWS vehicles is then to compromise and take a reversed trail (negative caster, steer axis intersects ground behind rear wheel) and take an unwanted, but best among worst options, oscillation for granted.

Two-wheelers are a special case in that they also need to balance, i.e. they can lean significantly. Whitehead omits to say what makes a two-wheeler exactly RWS and self-stability is not considered at all. However, although very hard to ride, he does not assume it to be impossible since he is aware of the studies of Laiterman (section 1.4 and Cornelius (section 1.8):

> "*RWS bicycles are extremely difficult to ride, because of a problem in addition to the phenomena described above. Two-wheelers must be kept upright during straight riding, which means the center of gravity must be directly above the imaginary balance line connecting the two tire-road contact points. Balancing is nominally controlled by steering to keep the balance line under the center of gravity. With FWS, this results in slight leftward cornering if the bicycle had been leaning too much to the left, which is a stable equilibrium. If a RWS bicycle being ridden straight leans a little to the left, the rear wheel must be steered to the left to move the balance line under the center of gravity. However, this results in a right-turning condition, which tends to make the bicycle lean further to the left, a divergent instability.*
>
> *The above analysis of balancing assumes the rider is rigid relative to the bicycle. However, lateral motion of the rider's torso to shift the center of gravity is an additional control input, which makes it possible to balance an RWS bicycle. The author built a RWS recumbent bicycle in 1983, and could never ride it, but later observed a person riding an upright RWS bicycle. It has been reported that a recumbent RWS bicycle has been ridden at MIT* [6].
>
> *Craig Cornelius has recently published a fascinating article on rear-steered recumbent bicycles (RSRBs) in the spring 1990 issue of Human Power. The effect of his very long trail design may be to make the dynamic behavior similar to that of front-steered bicycles.*"

1.10 1995 Hikichi and Tezuka [10]

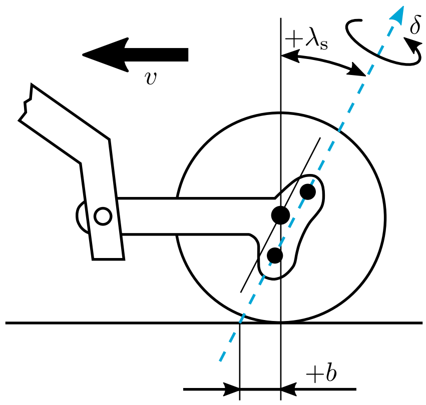

Figure 1.7: Suspended (self-)steered rear wheel of Hikichi *et al.* with dashed blue steer axis. Also depicted are the rear trail, b, steer axis angle, λ_s, forward velocity, v, and steer angle, δ. (recreated from Fig. 2. [10])

As other researchers before them, Toichiro Hikichi and Yoshitaka Tezuka investigated stabilizing a conventional motorcycle at high speed by implementing two steer axes; a supplementary rear wheel steer axis in addition to the still present conventional front steer axis. When riding in a straight line at speeds above 180 km/h, riders of motorcycles may experience an external disturbance induced roll and yaw oscillation (weave mode) of 2 to 5 Hz which can affect the stability [27]. Hikichi *et al.* assume that this motion is caused and sustained by a lateral force at the rear tire which could be decreased by minimizing the slip angle. To this end they implemented, in addition to the conventional steer joint near the front wheel, an extra steer joint near the rear wheel. This allows for a feedback mechanism that decreases the slip angle by aligning the rear wheel when the rear tire lateral force becomes too large. Other researches on this system included an active control of the rear steering angle, but this specific study only uses a passive control (damper) to regulate the rear steering angle and in effect the slip angle, thus making it self-steering.

This is not a case of purely rear wheel steering, but it is rather two wheel steering, although the front wheel is the only actively steered wheel. Either steer axis is close to one wheel and either can thus be associated with one steered wheel. Note that either steer angle (front and rear) is taken positive when rotated counterclockwise with respect to the main (middle) frame. In essence, the rear wheel steer angle follows the motion imposed by the front steer angle and is obstructed in rotational acceleration and speed by a spring and damper. Hikichi and Tezuka performed experiments with the rear wheel as drawn in figure 1.7 with a rear caster angle, $\lambda_s = 15°$, and rear trail, $b = 45$ mm, and various damping coefficients. Whether the motorcycle is self-stable is not discussed by Hikichi *et al.*, but the system indeed seems to make the stability at higher speeds better by improving the damping factor for the weave motion. This is shown in a simulation of a one mass model with two steering axes and allowed slip at both wheels, and subsequently the stability improvement is also confirmed during a real-life test. However, by canceling out some of the front wheel steer angle, the rear wheel steering system may weaken cornering properties. So, although the rear wheel self-steering aids in stability at higher straight line running to a degree determined by the damper characteristics, it changes turning properties at normal speeds. Hence, a trade off needs to be made between low speed handling and high speed stability.

1.11 2002 Suryanarayanan *et al.* [11]

In this article a theoretical study on automatic roll-rate control in the context of high speed bicycles is reported. These highly efficient human powered vehicles gained interest around 2000 and therewith speed contests and world record breaking attempts (record was around 75 mile/h ≈ 120 km/h at time of article) were organized. Matt Weaver (coauthor) is one of the contestants and raced in his low recumbent faired (covered) and front wheel steered bicycle. Notable is the absence of a see through windshield for vision for which in stead a camera and screen is used. It became apparent during the events that at high speeds these low frame bicycles' roll became hard to control by a human rider. Therefore, this study focuses on the dynamics of these race recumbents at high speeds and how the roll can be controlled best, both for front and rear wheel steering.

Rear wheel steering is of special interest because it has potentially a better space utilization inside the fairing, which is important since race recumbents as the one of Matt Weaver have just enough space for legs around the steered front wheel. High speed bicycles such as Matt Weaver's bicycle require special design criteria compared to conventional bicycles, because one wants to get maximum performance from the system. For example, they need to be very low to reduce air resistance. For several reasons, high frequency bandwidth control is required here. First, roll (lean) of the bicycle can be modeled as an inverted pendulum, and just as with an inverted pendulum, the lower center of mass makes stabilization harder and requires higher frequencies to control. Secondly, side wind gusts impose an unwanted moment on the steering axis which can be a challenge for human response time. This could be partly prevented by removing the trail, which serves as a lever arm between the steer axis and the ground contact point, but then still counteracting side winds is not easy for a human. Moreover, removing the trail on its part causes ridability problems which again pleads for automated control. But when these high speed control issues are solved, they expect that the 100 mile/h barrier can be evened.

Aware of rear wheel steer experiments of Klein and control theory by Åström (section 1.14) they performed an analysis on their bicycle. For the analysis a simple one degree of freedom inverted pendulum-like bicycle model is used with a vertical steer axis and zero trail for the steered wheel (naive bicycle). There is one body comprising both the rigid rider and the bicycle's largest frame which is parametrized by the position, the mass, and the mass moment of inertia. The frame center of mass can be positioned anywhere on the vertical plane spanned by the contact point either between the rear and front wheel or even at a theoretical position where the mass is placed behind or in front of either contact point. The lean angle is the degree of freedom, the steer angle is used as control input, and the forward velocity is assumed constant. However, it is not directly clear what the positive steer direction for the rear wheel steered case is. Furthermore, the steer into lean behavior of a bicycle is included by using a control law which feeds back the lean angle to the steer angle with negative gain. By incorporating this feedback mechanism, they make self-stabilizing behavior possible in their model. They simply assume that in a conventional bicycle the front fork design is such that it makes this self-stability possible and that the control behavior that the front fork creates can be modeled by that simple feedback mechanism.

Without presenting a formal definition of what they interpret as an RWSB, they show interesting differences between a naive conventional bicycle and a reversed naive conventional bicycle (their RWSB) with an analysis of the dynamics from the steer angle to the lean angular rate. For the analysis they use the roll rate, because it is the best regulated variable and their aim is to ride in a mere straight line without using large steer angles after lateral disturbances. Moreover, it is the easiest measured variable because one can use a gyro sensor in stead of using inclinometers, which tend to have large settling times to measure the roll angle.

Their model shows that front wheel steering with steer-into-fall behavior gives a stable bicycle while rear wheel steering is inherent unstable due to an always positive real eigenvalue. With increasing speed, the speed dependent eigenvalue becomes more negative for a front wheel steered bicycle while it becomes more positive for a rear wheel steered bicycle. However, both rear and front wheel steered bicycles can be controlled (theoretically) by designing two different controllers. Note that, for some velocities for their rear wheel steering model, the system becomes nearly or completely uncontrollable. Concretely, for Weaver's bicycle parameters example, this means that it is difficult to control between 3 and 40 mile/h. All in all, a suitable controller can in theory stabilize an RWSB by using large control gains [34]. Large steer angles are then required to correct small lean angles and the required roll rate and steer angle are larger for an RWSB compared to an FWSB. This all leads to the conclusion that, although both high speed FWSBs and RWSBs can in theory have an automated roll rate control, the better performance is realized for FWSBs.

Also used largely in a book section by coauthor Tomizuka [34] which does not introduce new theory.

1.12 2004 Karnopp [12]

In his book, Dean Karnopp describes the stability of, mainly four-wheeled, vehicles by using mathematical vehicle models. Here Karnopp defines the stability in vehicle motion as the ability of the vehicle to keep its desired track without spontaneously departing from it. A small section is dedicated to the stability of into-curve-banking two-wheelers and multi-wheelers which are controlled by means of steering. For the tilting vehicles in consideration, the steering does not only maneuver the vehicle, but at high enough speeds it can also be used for stabilizing. For both two- and multi-wheelers rear wheel steering is considered in his discussion where rear wheel steering is thought to be a safety improvement for such tilting vehicles since one might not longer have to counter-steer; one can steer directly away from an obstacle in stead of first steering towards it.

First off, Karnopp analyzes rear wheel steering for vehicles where the tilt is of secondary concern, i.e. four wheel cars. Therefore, he uses the common vehicle bicycle model and it appears that at low enough speeds, stability of these vehicles is rarely a problem, and therefore rear wheel steering can be applied sometimes without too much thought. For example, lawnmowers, forklift trucks, and street sweepers are often equipped with rear wheel steering. At higher speeds however, it becomes more important to look into the stability. He concludes that a rear wheel steered car is a nonminimum phase system which is importantly different from a front steered car. This means that a swift steer input on such a rear wheel steered car will result in a first response that shifts the car center of mass away from the turn to only later on shift it towards the turn. Although the feeling for the driver may be different, this does not say anything about the stability of a vehicle; a vehicle can be stable or unstable with rear wheel steering:

> "*If the rear wheel is steered quickly in one direction, the acceleration will have a 'reverse response'. That is, the acceleration will first be in one direction, and will later be in the opposite direction. A person sitting near the center of gravity of a rear-steering car would feel this back-and-forth acceleration whenever the rear steering angle was suddenly changed. This effect makes rear wheel steering control more difficult than front wheel steering. This is one reason why most people have trouble backing up a car at high speed and why most vehicles capable of high speed are steered from the front.*
>
> *Reverse action acceleration response is an inherent property of rear wheel steering and has nothing to do with stability or instability. Stability has to do with whether the denominator of the transfer functions can be made to vanish for a value of s* (eigenvalue) *lying in the right half of the s-plane. If this were to be the case, there would be an eigenvalue with a positive real part, which would imply that the system is unstable. The reverse action has to do with right half plane zeros of the numerators, rather than the denominator of the transfer functions, and occurs for rear steering cars whether they are stable or unstable.*"

For a vehicle that has major tilting into a curve around an axis close to the ground, Karnopp uses a generalization of the common vehicle bicycle model to come to expressions for the yaw due to the steer angles. His vehicle model steers the front and rear wheel independent of each other with both having a vertical steer axis and zero trail for the wheels respectively. A positive steer angle is when the steered wheel, so either the front or rear wheel, is turned clockwise with respect to the frame. One wheel can be assumed locked to make the other wheel the steered wheel and so a switch is possible between front or rear wheel steering. Moreover, the tires are assumed to be operating in their linear range with slip angles and other effects due to tire characteristics being negligible. Even so, all angles are assumed small and forward speed is taken constant so the entire model is linear, which is especially valid for real-life moderately leaning bicycles. He models the vehicle as one mass with mass moment of inertia around three principal axes plus two massless (and inertialess) wheels which resemble for a multi-wheeled vehicle the two front and/or two rear wheels respectively. The frame is then parametrized by the mass and the mass moment of inertia and its location which can be anywhere in the vertical plane spanned by the wheel contact points; It could also be placed in front of the front wheel or behind the rear wheel. However, his analysis of the dynamics only considers the case when the mass is longitudinally placed in between the wheel contact points. The model for the tilt dynamics can be simply seen as an inverted pendulum with the lean angle as the single geometric degree of freedom and steer angle as input.

The equations of motion are derived via Lagrange's equation and are linearized thereafter. It appears that with steer-locked wheels (zero steer) the model is just that of an inverted pendulum and the vehicle would fall over. For two-wheelers in general one can then already conclude that steering becomes effective for low forward speeds and that both the steer angle and the steer rate do influence lean angle.

Furthermore, from the equation of motion several transfer functions are derived. The most notable two are an equation relating pure front steer input (FWSB) to the lean angle and an equation relating pure rear steer (RWSB) to lean are derived. These equations for either an FWSB and an RWSB indicate unstable behavior when there is no control, i.e. both have a positive real eigenvalue in the open-loop. He simply thinks active control is essential for single-track vehicles to stay upright and in effect self-stability is not considered by Karnopp. Note that ignoring self-stability completely may be appropriate for some simple bicycle models that inherently exclude the self-stable possibility [23]. In trying to stabilize the system, a simple controller with feedback of the lean angle to the steer angle is introduced by Karnopp. Karnopp thus focuses on stabilizing and curve path following of the vehicle through active steering control input where the controller is either the rider or an active automatic computer control system.

It turns out that for FWSBs the simple proportional controller can stabilize the system at sufficiently large forward speeds and even make the lean angle go to a desired lean angle for high speeds. Moreover, he concludes that a conventional FWSB is a nonminimum phase system in closed-loop and has therefore a reverse action between steer angle and lean angle and thus must briefly turn away from a desired turn to initiate a desired lean angle into the desired curve, i.e. counter-steering. On the contrary, Karnopp places RWSBs, whose input-output relation without controller shows a nonminimum phase system and that the action is reversed in the open-loop, which is opposed to a conventional FWSB that had it only in the closed-loop. Presumably this gives the safety advantage that an RWSB no longer requires a counter-steer action to initiate a turn. However, alarming is the fact that the same simple proportional feedback controller can no longer stabilize the system in closed-loop for any gain at all, due to the presence of a real positive eigenvalue, so a more complex controller is required. Moreover, Karnopp claims that by using a more sophisticated model, e.g. with more masses or non vertical steer axis, to analyze an RWSB, even more problems would appear in stabilizing it. (Note that due to his sign convention for the steer angles it appears that for an RWSB in steady state, i.e. in the control law, a positive rear steer angle corresponds to a negative lean angle and vice versa, which is noteworthy, but insignificant for the further analysis since it is just related to the sign convention.)

Karnopp assumes that, in agreement with Schwarz (section 1.5), an RWSB has the advantage that counter-steer is no longer required and one can steer directly into the desired direction and thereby improve obstacle avoidance. Moreover, he concludes that the most important difference between front wheel steering and rear wheel steering is that the latter is harder to control and requires a more complex control scheme. Thus, although it has a supposed safety advantage and it is possible to stabilize it, it requires a lot effort of the controller whether the controller is human or automatic so that any safety advantage is neutralized:

> "*. . . the benefits found so far did not outweigh the disadvantages of the extra complication and expense of introducing a steering mechanism at the rear.*"

Also available in 2$^{\text{nd}}$ edition [35].

1.13 2004 Wilson [13]

Rear wheel steering is shortly brought up in a chapter about steering and balancing a bicycle that is completely written by Jim Papadopoulos. A bicycle can balance itself by self-stability, but the mathematics behind that phenomenon are acknowledged to be difficult. A physical interpretation of balancing a bicycle is done by comparing it to the balancing of a broomstick where the support continually has to be brought under the center of mass to recover a stable upright position. The two contact points that span this support for a bicycle are accelerated differently in order to bring the support under the center of mass, says Papadopoulos. A conventional bicycle, for example, has a front wheel that travels a wavier path with phase lead compared to the rear wheel. For such a bicycle the front wheel has a larger lateral acceleration than the rear and hence, mass at the front is balanced easier:

"*One implication of the delayed and reduced lateral acceleration of a bicycle's rear contact is that mass over the front contact is far more easily balanced than that over the rear. If mass is to be carried over both contacts, keeping that in the rear lower than that in the front will allow the frontsupport acceleration to exert more control over balance. . . . Rear steering would make the rear contact the more controllable one, but a rear-steering bicycle is nearly impossible to ride fast. A major reason for this is that although leftward acceleration of the rear can be achieved rapidly by steering the rear wheel to the left, the resulting steady turn is rightward, that is, with the opposite sense of acceleration. (In the technical discipline of control theory, this is a property that describes a 'non-minimum-phase' system.)*"

This book has contributions by Jim Papadopoulos. 2nd edition of this book [6] is discussed earlier.

1.14 2005 Åström *et al.* [14]

(a)

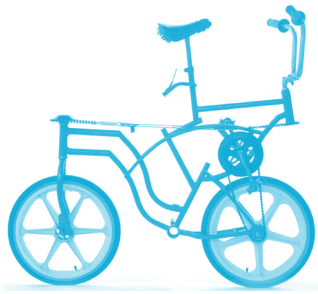

(b)

Figure 1.8: The two Klein RWSBs, (a) unridable RWSB and (b) ridable RWSB. [14] [36]

In this article, bicycle dynamics are described from a control perspective and are related to educational experiments that are attractive for students. A simplified bicycle model is used to describe causes for fundamental control limitations and to give a hands-on experience of the difficulties in controlling this example of a so called 'nonminimum phase' system. Moreover, to show stability issues with conventional rear wheel steered bicycles (RWSBs), two RWSBs were built (figure 1.8) where the second one is designed to improve ridability. Besides the educational purposes, more probable advantages of an RWSB with simple front drive are recognized by referring to Whitt and Wilson (section 1.6). However, aware of the NHTSA (Schwarz) safety motorcycle study (section 1.5) they conclude that systems can be designed that are interesting from a static perspective, while they are useless due to their dynamics. In effect Åström *et al.* go on to explore the stability deficiencies of RWSBs and, although they are aware of the phenomenon for some more conventional bicycles, they do not investigate self-stability of an RWSB. Hence, RWSBs are only described in terms of control.

The bicycle model is developed in stages throughout the paper and eventually several bicycle models of different complexities are presented to analyze balancing and steering. A simple inverted pendulum model, the fourth order linear Whipple model, and nonlinear models are all more or less discussed. These models exclude longitudinal and lateral slippage of the tires from the equations, i.e. they assume idealized contact with non-holonomic constraints.

An example of an expansion of their most simple front steered model is an inclusion of trail and steer axis angle by means of a front fork model. In describing the behavior of a bicycle, especially the self-stability behavior, the front fork is essential. They acknowledge that the steering angle is influenced both by an applied steering torque, and a torque from the design of the bicycle caused by a lean angle (they contribute the coupling of lean and steer to centrifugal force). For a conventional front wheel steered bicycle then the front fork can be modeled by a static torque balance; the front fork steer angle is determined from an external torque applied on the handlebars and a fork feedback torque due to bicycle lean. They say that a front fork design with positive trail (steer axis intersects ground in front of front contact point) causes a feedback that steers the bicycle into a fall and might cause self-stabilizing behavior. Although more trail is better for stability, it makes steering less 'agile', they claim.

A transfer function from steer torque to path deviation of the model with this front fork is used to show existence of the typical 'inverse response behavior' during maneuvering for a 'nonminimum phase' system. This response expresses itself with the 'counter-steering' phenomenon where a bicycle needs a small steer movement in the undesired turn direction to set the bicycle up for the eventual desired lean angle for cornering. However, this physical interpretation is easy to obtain, but precise causal reasoning is hard with a close-loop feedback such as exists between tilt and steer in the system.

Meijaard *et al.* [26] analyzed this article and express their doubts about the usefulness of the simpler models of Åström even when it includes some front fork equation [26]:

> "*In Åström et al. the reductions leading to the simple model come in two stages, mechanical and then mathematical. First Åström et al. assume that the wheels have no spin momentum and are thus essentially skates. They also assume that the front assembly has no mass or inertia. However, both non-zero head angle and non-zero trail are allowed and both point-mass and general inertia rear-frame mass distributions are considered. Åström et al. then add further mathematical simplifications by neglecting non-zero trail contributions except in the static (non-derivative) terms. This eliminates the steer acceleration term in equation (14) therein (lean dynamics), and alters the steer rate term. In equation (9) (steer dynamics), where all torques arise only through trail, this eliminates the terms involving steer rate, steer acceleration, and lean acceleration.*
>
> *Their reduced second order unforced (uncontrolled) steer equation implies that steer angle is proportional to lean angle. . . . The resulting system is thus stabilized in the same way a skateboard is self-stable. In a skateboard mechanical coupling in the front "truck" enforces steer when there is lean, see . . . pages 6 and 17 in Papadopoulos (1987)* [37]. *. . . That bicycle lean and steer coupling might approximately reduce to the much simpler skateboard coupling is certainly an attractive idea.*
>
> *However, the governing stability equation in Åström et al., equation (15) appears to show the emergence of self-stability at high-enough speeds for quite arbitrary bicycle parameters. Examination of the full fourth order equations here (the pair of second order equations) applied to their simplified bicycle (without their additional mathematical simplifications) seems to show that stability is only obtained for special parameters. For example, the point-mass version is never stable. An extended-mass version can be stable, but only with a rather special mass distribution, as discussed in Papadopoulos (1987)* [37], *on page 6 and figure 3 therein. . . . Even for those parameter values in which their mechanical model can have self-stability it is not clear that having steer proportional to lean is an appropriate description of self-steer dynamics. So we have some doubt about the reduction of Åström et al. of even a simple class of bicycle models to second order skateboard-like equations. Limebeer and Sharp* [25] *also question the conclusion of Åström et al. about the central role of trail in stability.*"

Although they are aware of the existence of and even show the more complex models including interesting mechanisms, they use their most simple second-order model for the analysis of an RWSB. Their RWSB model excludes gyroscopic effects of the wheels and models the rider as rigidly attached to the bicycle. Furthermore, the bicycle is considered as consisting of four rigid parts; a frame, a massless fork with handlebars, and two massless wheels. Thus, one mass with mass moment of inertia (lateral direction) is used to describe the whole bicycle and analyze balancing and steering. This mass could be placed anywhere on a plane spanned by the two wheel contact points. For simplicity they assume a zero steer axis angle ($\lambda_s = 0$) and zero trail and thus have a so called naive bicycle. The limits of a naive bicycle model are acknowledged by Åström *et al.* and they are aware that this representation of a bicycle cannot be self-stable (not even for front wheel steering). Since self-stability is not considered at all for RWSBs, such a naive bicycle can still be used for this particular study of RWSB control.

The model has the bicycle lean as its one degree of freedom and assumes the steer angle prescribed on the handlebars as its sole input. The steer angle is implemented as simple proportional feedback on the lean angle in order to model rider behavior as steer-into-fall and make the system closed-loop. Then, the sign of the velocity in the bicycle equation of motion for a conventional bicycle is simply changed from positive to negative to transform an FWSB in an RWSB and a transfer function from steer angle to tilt (lean) angle is derived. (Note that in an eigenvalue plot as function of forward velocity of a conventional front wheel steered bicycle, negative velocities correspond with a rear-steered bicycle.)

Their closed-loop single mass naive model of a bicycle results in a ratio value that needs to be negative for stability:

$$\sqrt{-g/z_\mathrm{T}} \tag{1.1}$$

(pole) Ratio between gravity and total center of mass height, with the gravitational acceleration, g, and the total bicycle mass vertical coordinate, z_T (z-axis positive in downward direction; when mass placed below ground).

However, in their designs with all mass above the ground, this value is always positive such that the system has an eigenvalue with positive real part for all negative velocities. Therefore, this bicycle model can never be asymptotically stable on its own. Due to another ratio value in combination with the previous value, the control effort is determined. This ratio is different between front and rear wheel steered cases, but it should be negative to ease control. For an FWSB this ratio is,

$$-v/(w + d_\mathrm{T}) \tag{1.2}$$

(zero) Ratio between velocity and mass/rear axle distance, with the forward velocity, v, wheel base w, and horizontal distance from front wheel axle to total bicycle mass (including rider mass), d_T (d_T positive in forward bicycle direction; when mass placed ahead of front wheel).

and for an RWSB this ratio is:

$$-v/d_\mathrm{T} \tag{1.3}$$

(zero) Ratio between velocity and mass/front axle distance, with the forward velocity, v, and horizontal distance from front wheel axle to total bicycle mass (including rider mass), d_T (d_T positive in forward bicycle direction; when mass placed ahead of front wheel).

Note that here the forward velocity is for the RWSB positive when its steered wheel is behind in the forward riding direction, thus to have a rear wheel steered bicycle here, $v > 0$. So their bicycle interpretation is not only unstable, but with their assumed negative mass distance, $d_\mathrm{T} < 0$ (center of mass inbetween wheels), the second ratio for an RWSB (1.3) is always positive. In that case, the proportional feedback gain for the lean feedback on the steer angle can never be adjusted such that this bicycle becomes stable and thus a simple proportional control law is not sufficient for stabilizing the bicycle. Even more complex controllers, e.g. a human or even higher bandwidth controllers, have troubles stabilizing such a bicycle due to the fundamental dynamical difficulties accompanying it, simply because robustly controlling of a bicycle with bad system dynamics is difficult [38].

In order to make an RWSB better ridable or more stable certain control strategies can be applied to circumvent the difficulties in dynamics, as Åström *et al.* reason. By sensing the tilt (lean) and yaw (heading) and react on it, the system can be stabilized, but the system becomes dependent on sensing and actuation and control is essential. Maneuvering by means of steer torque, rider lean, and even forward speed are input variables that can eliminate or minimize unstable dynamics of the bicycle.

A more user-friendly way of increasing the ridability, i.e. decrease control effort, (but leaving it unstable) of the bicycle is by altering the construction of the bicycle itself while keeping it rear wheel steered. They reason that for a reduction in control effort the two positive ratios, (1.1) and (1.3), should have very different values; one must be small and the other one large. Because (1.3) increases in value with increasing forward velocity, this ratio is chosen to be as large as possible. Therefore, the distance from the front axle to the center of mass should be as small as possible. The ratio (1.1) is then made as small as possible such that the center of mass height should be as large as possible. This makes placing the center of mass high and longitudinally close to the front wheel results in a less positive eigenvalue thereby reducing control effort such that the bicycle becomes better ridable by humans.

The better ridability of the second Klein RWSB (figure 1.8b) as compared to the first Klein RWSB (figure 1.8a) shows this theory in practice. Note that to improve ridability, these two bicycles both include a steer reversal between the handlebar and the rear wheel to make a clockwise handlebar turn result in a clockwise bicycle turn.

All in all, Åström *et al.* were able to demonstrate in theory and in practice that RWSBs can be made better ridable by changing specific bicycle parameters. However, despite a seemingly thorough analysis, they were not able to find or build a self-stable RWSB, and they remain skeptical about RWSBs:

> "*. . . it is possible to design systems that have many desirable static properties but are practically useless because of their dynamics.*"

Klein's RWSB examples are more extensively described in section A.32. Partly, this article repeats and elaborates on earlier information about conducted RWSB research mentioned [39] and reported about [40] by Klein. Moreover, this article repeats some theory from an earlier article of Åström [38] and it is used in his book [41] and as a basis for a lecture [36].

1.15 2011 Kooijman *et al.* [15] [16]

Figure 1.9: Theoretical self-stable RWSB configuration of Kooijman *et al.* with forward riding direction to the right in the figure. (Recreated with JBike6 from [16])

Kooijman *et al.* proved in their study that gyroscopic effects and a nonzero trail are not necessary for self-stability of bicycles. The overall conclusion is that the degree of stability of a bicycle is dependent on a complex combination of all the bicycle parameters; often a self-stable bicycle can be made unstable by the change of one feature and the other way around. For example, in one particular set of parameters the mass distribution might be as important as the presence of gyroscopic effect, while in other configurations these two parameters are less important. In other words, there is not one factor which determines self-stability; it's a complex interplay between a set of factors and one must really look into the equations to find out the dynamical behavior.

Their research approach was theoretical with a final experimental confirmation of their theory. The Whipple model as described in the benchmark bicycle paper by Meijaard *et al.* [22] is used to analyze the dynamics of the bicycle. The equations of motion from this model and the resulting characteristic equation are used to perform a study on the Routh stability criteria. A difficulty is that the Routh coefficients are all lengthy expressions in the 25 Whipple parameters, such that parameter requirements for stability are hard to obtain. To make the analysis more accessible the full set of 25 Whipple parameters is reduced to a set of only 8 non-zero parameters. The found self-stable bicycle configuration that fulfills the Routh stability criteria is then a theoretical configuration which does not directly represents a physical feasible bicycle design. Therefore, a CAD-aided design process is performed to design a feasible bicycle based on the theoretical configuration that mimics the stability properties. Finally, the bicycle is built and used to test the self-stability hypothesis in real-life, which, in their case, is that a bicycle can be self-stable without gyroscopic and caster effects.

They acknowledge that the lateral acceleration of the support line is important in balancing a bicycle. It determines whether the support line is properly brought back underneath the center of mass. For a moving bicycle, this acceleration has contributions from the steer angle as well as the steer angular rate. This is interesting in the scope of defining the steered wheel of a bicycle which they inexplicitly do. Namely, the definition can be derived from the sign of the contribution of the angular steer rate to the support line lateral acceleration. The steer rate contributes positively to the lateral acceleration of the support line for naive (no trail, vertical steer axis) FWSBs and it contributes negatively to the lateral acceleration for naive RWSBs. The exact in between version where the bicycle steers exactly in the middle has no steer rate contribution. They reason that a negative contribution of the angular steer rate makes a bicycle harder to balance, but by adjusting the mass distribution, an RWSB can be made self-stable and the ridability disadvantage could be circumvented.

In the context of showing that some common bicycle lore is incomplete or incorrect, Kooijman *et al.* experimented with greatly different theoretical bicycle configurations [from personal conversation with A. L. Schwab] and probably were the first ones to notice a self-stable configuration for an RWSB. The configuration came to light when Kooijman *et al.* were trying to (erroneously) model a monocycle with an extra non-rotating mass (as the one of Coleman and Papadopoulos [42]) as a bicycle with a small rear caster wheel. Such a monocycle model requires, besides one wheel contact point, a second frictionless sliding contact point with the ground to prevent the non-rotating mass from rotating. To model this contact in the Whipple model, a small additional trailing massless wheel was used in stead of a sliding stick, because the Whipple model does not support a sliding contact. To their surprise, with this additional wheel the dynamics of the system did not correspond with those of the monocycle with frictionless contact. In hindsight, this was logical because a two wheeled 'monocycle' is essentially different from a monocycle with sliding contact stick since a frictionless contact cannot generate lateral forces whereas a small caster wheel can (therefore a bicycle requires a steer joint to change its heading).

Although the system was different, it turned out after some tweaking that a small rear wheel with trail and vertical steer axis can also make the machine self-stable, and the first self-stable RWSB configuration was found (figure 1.9). Their geometry is a simple one with a point mass representing the front fork and a massless rear frame and a vertical steer axis that intersects the ground just before the rear wheel [16]. With this RWSB configuration they also show that against common lore a bicycle can be self-stable with vertical steer axis (vertical head tube).

Kooijman *et al.* furthermore discuss that due to the symmetric definition of the Whipple bicycle, two frame-wheel assemblies connected by a hinge, a rear wheel steering (or a front wheel steering) definition is problematic. For example, does an objective definition have to do with the location of the hinge and/or with the mass distribution between the two frames? An RWSB as found by Kooijman *et al.* is defined as rear wheel steering because of the 'you know it when you see it' [43] principle. According to Kooijman *et al.* this can be done because the hinge is much closer to the rear wheel and the front assembly has a much larger mass than the rear assembly, but it is not objectively an RWSB:

> "*Our 'rear wheel' steering example is of that nature, not objectively rear-wheel steering, but rear-wheel steering just as much as conventional bicycles have front wheel steering.*"

Kooijman *et al.*'s RWSB example is more extensively described in section A.83. Alongside their main article [15], supplementary online material is provided [16] in which more details and methods are explained. This study is also included in J. D. G. Kooijman's thesis [44].

1.16 2012 Broxterman *et al.* [17]

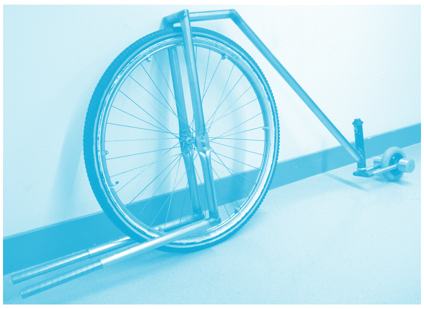

Figure 1.10: Riderless test RWSB of Broxterman *et al.*. [17]

Four students of the Delft University of Technology investigated RWSBs as part of their bachelor degree graduation. Main motivation was to broaden the design space of the bicycle, because the bicycle had essentially not changed much since 1885. The design focused on RWSBs which were not succesfull untill then. Is this because they are per definition unridable or did the bicycle evolution just took one (rather succesful) specific route and never looked at RWSBs again assuming that the current bicycle lay out is near perfect? From a scientific eye-point this is an interesting question. Furthermore, a reason to investigate the stability of RWSBs is because of their presumed reduced frictionlosses due to a shorter drivechain, since the front wheel can easier be used as driven wheel. Also in light of resistance reduction, but now aerodynamic, an advantage might be that it is lowered due to an easier implementable low rider position. The RWSB configuration of Kooijman *et al.* (section 1.15) served as inspiration for this project and the goal was to prove experimentally the theoretical findings of Kooijman *et al.* that an RWSB could be self-stable. Aware of the benchmark bicycle paper of Meijaard *et al.* [22] and the validity of that bicycle model for all bicycles, they used it to design a self-stable and practically realizable RWSB. This bicycle design should be maximal stable to accommodate for possible construction flaws that would lower the stability; a certain margin was desirable. Eventually, they ended up with a riderless bicycle the presence of self-stability above a certain velocity.

The definition of an RWSB (or of an FWSB) is recognized as being a difficult one, because a bicycle is essentially a mechanism made of two wheels, two frames, and three hinges while the location of the steering hinge is not prescribed (section 6.3). When the hinge location would be taken into account, an extreme chopper with the headset closer to the rear wheel than to the front wheel could be wrongly identified as an RWSB. This considering, they come up with the definition of an RWSB based on intuition: An RWSB is a bicycle where the absolute (sign is irrelevant) trail of the rear wheel is smaller than the absolute trail of the front wheel. Here the trail of either wheel is defined as the distance from the wheel contact point to the imaginary point where the steer axis intersects the ground. They claim that with this RWSB definition the wheel that intuitively prescribes the cornering is correctly identified as the steered wheel. Hereby, one wheel steers the bicycle while the other wheel reacts on that steer movement. To bring justice to popular beliefs, they settle with an additional requirement that an RWSB should also have a rear frame which is lighter than the front frame.

Initially, they wanted to find an RWSB that was very self-stable and present a method to do so. To be efficient, they specified 6 independent parameters from which all 25 bicycle parameters could be deducted. This way, the number of design possibilities were reduced which would make the search algorithm faster. For example, they used standard bicycle wheels for which all parameters are determined by only the diameter, and the frames were made of simple straight standard pipes. Unfortunately, this optimization study turned out to be a too drastic simplification and the systematical study where an algorithm tried to find self-stable RWSB configurations failed to come up with good solutions.

The more successful approach was to use the method described by Kooijman *et al.* for finding their ‘two-mass-skate bicycle’. For the RWSB this meant that the RWSB configuration of Kooijman *et al.* was taken as starting point. This configuration with only a small nonzero set of the 25 parameters has no frames and as such is not constructable. In CAD software (SolidWorks) frames were drawn to come to a realistic bicycle with masses and moments of inertia. The stability of that configuration was then checked with JBike6 [45] (section 4.3). Where needed the CAD model was changed and this altered configuration was again checked in JBike6. This process was iterated until the final realizable RWSB design was obtained. The design comprises a large front wheel, a small rear wheel, two frames, and additional masses to obtain stability (figure 1.10).

The design procedure revealed several interesting things. It seems that the center of mass of the bicycle needs to be placed longitudinally close to the front wheel axle as much as possible, while the exact height of the mass seems to be of minor importance. The center of mass was shifted to the front by placing large weights ahead of the front axle. To prevent tipping over frontally, some counterweights were added on the rear axle, i.e. near the rear wheel contact point, following Kooijman *et al.* [16]. This is allowed since masses at or close to the contact points barely influence the lateral stability, i.e. these masses barely move under influence of lean and steer angle. Further worth mentioning is that the relatively high front frame adds inertia about the lean angle and thereby presumably increases the stability of the bicycle. Also, by increasing the front wheel inertia the bicycle becomes self-stable at a lower speed, but at a cost of less negative eigenvalues, i.e. it takes more time to recover from a perturbation. They noted that the importance of self-stability for ridability of a bicycle is not entirely known and thus that the longer perturbation recovery time is of minor importance in this study where only the existence of self-stability, and not the degree of self-stability, has to be shown.

Finally, the design was built (figure 1.10) and the bicycle was tested. Some parameters such as weights and lengths were checked to see how they corresponded with the CAD design. Furthermore, the bicycle was tested in a sports hall where it was pushed to a certain speed after which it was let loose to observe self-stability. A disturbance in the roll rate (lean motion) was applied by hitting the bicycle laterally and a return to the upright equilibrium position could be noted. It turned out that the built bicycle strongly suggests the presence of self-stable behavior. Measuring the lean angular rate along with the forward velocity gave results that showed a harmonic function decreasing in amplitude. However, a quantitative comparison of the measurement results with the theory was not performed.

Broxterman *et al.*'s RWSB examples are more extensively described in section A.84. P.H. de Jong was part of this project.

1.17 2012 Van Dijk *et al.* [18]

Figure 1.11: Ridable RWSB of Van Dijk *et al.* [18]

In an attempt to make a ridable RWSB another group of four bachelor students of the Delft University of Technology, Van Dijk *et al.*, continued the work of Kooijman *et al.* (section 1.15) and Broxterman *et al.* (section 1.16). The RWSBs that were built by enthusiasts until that time are probably not self-stable, but can often be ridden after long practice. By making a ridable RWSB also self-stable, they tried to remove or at least diminish learning time of riding an RWSB.

Besides probable efficiency (short chain and low air drag for recumbent bicycles) and safety (front wheel braking) advantages, RWSBs were mainly in their interest as a way of broadening the design scope of the often presumed fully evolved bicycle. Before Van Dijk *et al.* the presumed advantages of RWSBs were heavily outweighed by the disadvantage that one has to steer earlier into a turn and cannot see the path of the outward moving rear wheel and of course the large disadvantage that RWSBs were not or hardly ridable.

They found the steer-side, i.e. the steering or leading wheel, of a bicycle is difficult to define, because of fore-aft 'symmetry' and riding direction dependency. They make sure that their bicycle is rear wheel steered by giving the rear wheel the smallest of the two wheels' trails and place the center of mass of the total bicycle with rider in front of an imaginary vertical line through the middle of the headset, i.e. to the front wheel side of the head tube. In that way, the steered wheel is the most yawed wheel of the two during a turn and the steered assembly (steered wheel + frame) has the lowest inertia in order to react faster.

For analyzing the stability they used the Whipple bicycle model as described by Meijaard *et al.* [22]. First off, they did some JBike6-aided analyses [45] (section 4.3) of existing RWSBs and found that none of them showed self-stability, although they were ridable as seen in several videos. A difference in the model that they applied with respect to JBike6 is that the rider is included in the front frame parameters in stead of in the rear frame. Therefore, in JBike6 the corresponding code of the program was altered. The exact influence of self-stability on rideability is acknowledged as not being clear at this moment; self-stability most likely reduces control effort on behalf of the rider, but it may also reduce maneuverability since it tends to keep the bicycle in one neutral position. However, they hypothesized that a self-stable bicycle is generally more easily ridable.

Subsequently, they used a self-made Matlab optimalization algorithm (named 'hillclimber') that implemented the differential equations of the Whipple model to find a new self-stable and ridable RWSB configuration. This algorithm takes an existing (theoretic) bicycle configuration from JBike6 and tries one-by-one different variations of different variables to come to new better designs based on that initial configuration. How good a configuration is, is determined by scores that are given to it by comparing it to predefined design specifications. For example, the most important specification here is the weave speed (speed above which the bicycle becomes self-stable) which gives a better score for lower values. After several iterations, where variables are altered multiple times to find better designs, the script saves the best solution. This solution could be only relatively the best, since it is not investigated whether the found configurations are local optima for RWSB configurations or that a global optimum is found. After trying different initial configurations, one final configurations showed up multiple times. Because this configuration had a nice self-stable range and large negative real parts of the eigenvalues in that range, they decided to work out that configuration further into their final RWSB.

Although it has a seat, steering mechanism and paddles, their final solution looked still like the one of Broxterman *et al.* and required the center of mass of the front frame to lie behind the front wheel and the rider's center of mass to lie straight above the front wheel. The rider should sit on the front frame and the rear wheel was small and it was supposedly self-stable with rider mass between 3.2 m/s and 6.1 m/s. Moreover, they decided to incorporate a steer inversion with transmission ratio that makes sure that a clockwise handlebar rotation results in a clockwise bicycle turn and that the steering feels similar to that of a conventional bicycle. Note that their final found configuration was not ideal for frontal tipping over (pitch motion) prevention. Although a self-stable recumbent-like RWSB with lower center of mass was found, they did not use that design because it was less stable and only at higher speeds (7.4 m/s to 8.3 m/s). This recumbent configuration had a rear-upward pointing steer axis and almost equal rear and front wheel trail with an almost horizontal rider with center of mass close to the front wheel center.

After building the final design they were able to ride it and, subjectively experienced, the bicycle was able to bring itself back to the upright equilibrium position with a hands-off rider. Objective measurements of the self-stability were hard to obtain, because the rider was not able to stay completely still (no rigid rider) and thus the possibility of control by the rider could not be ruled out. Some angular rate measurements did however indicate that a disturbance to the bicycle was damped out without direct active steer control (hands-off riding) of the rider. Therefore, it was reasonable to assume that the bicycle with rider was self-stable, but its presence was not indisputable proven. Moreover, the measured rate patterns did not agree with the model predictions which they attributed to a shimmy effect (fast oscillatory steer movements) in the bicycle. At low speeds their specific bicycle showed rather unstable behavior which made it hard to start riding it, but a higher speeds, in the self-stable range, the bicycle was fairly good ridable. Therefore, ridability was assessed, although superficially, by letting people ride on the bicycle with the instruction to get to a high speed as fast as possible and it turned out that within only 2 minutes people were able to ride it. All in all, Van Dijk *et al.* made a ridable and probably self-stable bicycle and herewith they created hope for the future of RWSBs:

> "*This paves the way for other designs to utilize the potential benefits of rear wheel steering.*"

Van Dijk *et al.*'s RWSB examples are more extensively described in section A.85.

1.18 2014 Schwab and Kooijman [19]

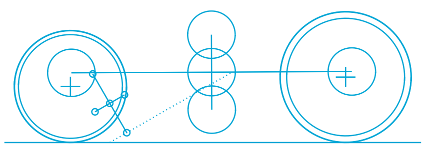

Figure 1.12: RWSVeloX, rightward is forward direction. (Recreated with JBike6 from [19])

This study aimed to improve the performance of the VeloX racing bicycle by implementing rear wheel steering. The VeloX is the race bicycle that the Human Power Team of the TU Delft designed to compete in human powered speed competitions and to break the world speed record for human powered single rider vehicles. Their first bicycle, the VeloX 1, was a fully-faired monocoque front-driven and front-steered recumbent bicycle. Analyses in this study show that the VeloX 1 was self-stable from about 8 m/s to about 17 m/s. It was optimized for having minimal air drag while it remained having enough space for a strong athlete to operate in it. Here, the recumbent position of the rider is preferred over a prone position due to breathing requirements. To minimize the mental workload, the rider should see ahead and is thus positioned such that his feet are in the front of the vehicle. This rider position and posture is a given design limit for further development.

This first configuration of the VeloX turned out to have some disadvantages. The recumbent forward facing rider position is a source for trouble, either when driving the rear or driving the front wheel. Driving the rear wheel would require a long driving chain with subsequent losses. While driving of the steered front wheel causes unwanted steering motions, the correcting of which on its part increases the mental load for the rider. Moreover, and more importantly, the aerodynamics of the bicycle are non optimal when driving the steered front wheel. The wheels require gaps in the fairing where they stick out of the machine to make contact with the ground. The steered wheel needs an extra wide gap to facilitate the turning for the steering. This gap introduces a turbulent air flow which is harmful for the aerodynamics, because the reduction of air drag is benefited by a laminar air flow along the body. At the rear the flow is already turbulent and thus the presence of a gap here is less cumbersome. Moreover, around the driven front wheel the fairing must be extra wide to have enough space for the pedaling feet which also move laterally due to the steering. Additionally this also introduces an extra wide rear in order to keep the air flow laminar. All these issues together plead for the introduction of rear wheel steering or at least the investigation of the possibilities.

Inspired by the finding of Kooijman *et al.* (section 1.15) and the work of Van Dijk *et al.* (section 1.17, referred to as 'Knol *et al.* (2012)') Schwab and Kooijman tried to implement rear wheel steering in the VeloX 1. This made that they were restricted to design within the limited space of the fairing of the VeloX 1. And in effect, they were restricted to change only the steer axis angle, the trail, and the position of the center of mass of the smaller of the two frames (the 'steer assembly'). A strict definition of rear wheel steering is not present, but when the main frame with rider was behind the smaller steer assembly during riding, the bicycle was considered FWS, and vice versa. With trial and error in JBike6 the final theoretical design was found and named 'RWSVeloX'. It turned out that due to their strict design limits, they were not able to come to a self-stable design such as the VeloX 1. In stead they settled with a design that was 'mildly' and slightly increasingly unstable over a velocity range up to 40 m/s which they expected could be balanced by control.

To assess the ridability of the RWSVeloX they put a human rider-like controller, a Least Square Regulator [46], on the bicycle and looked at the control effort of recovering from a lateral perturbation. These perturbations were gusts of side wind modeled as short lean torques of maximal 1 Nm and the control (steer) effort was quantified by the power spectral density of the steer torque. While the steer torques were within physiological human limit (maximum 0.1 Nm) they were about ten times higher than for the VeloX 1. However, the real problem of the RWSVeloX was the mental effort and reaction speed required to ride it at high speeds. The steer effort simply needs too high frequency contents to be comfortably ridable. Therefore, although probably not impossible to ride, the RWSVeloX is considered a bad design. For future work a more flexible design space is needed to improve the ridability of a rear wheel steered VeloX, e.g. the fairing shape might need drastic reshaping.

Schwab and Kooijman's RWSB example is more extensively described in section A.85.

Chapter 2

RWSB literature discussion

2.1 Significance of RWSBs

The exact significance of an RWSB is currently unknown. Although many people saw possible advantages in RWSBs, the stability and therewith the ridability did show to be a problem. Until now, RWSBs were a mere hobbyist subject and they were studied by trial-and-error (see appendix A). Even when modeled and analyzed beyond a trial-and-error approach, a self-stable RWSB was often deemed impossible. That is, until 20112 when Kooijman *et al.* showed an unconventional (front frame mass ahead of front contact) self-stable RWSB configuration [16]. This is where the main significance of a study on RWSBs arises; apparently a solid research considering all design options was never conducted with consequently a lack of knowledge. Making an RWSB self-stable is exciting and would mean a broadening of the bicycle design space which has not changed much since 1885 [18]. Is the conventional bicycle design indeed as ideal as often thought or can it be improved by drastic changes?

But what did many people see in rear wheel steering besides an opportunity of exploring the unknown? Especially recumbent bicycles might benefit from rear wheel steering [8] [18], but also bicycles in general might show interesting rear wheel steered features:

Packaging Some bicycles, e.g. supine recumbent or penny-farthing-like bicycles, have the rider's legs positioned naturally close to the front wheel. With rear wheel steering, the driven wheel can then be the front wheel without a problem. RWS allows for the rider to be placed on the same front frame and the connection between bracket and wheel is not bent during steering. The legs of the rider can even be placed besides the wheel without having the risk of hitting the wheel rim during steering. A chain no longer has to run to the rear wheel and can thus be shorter which reduces friction losses. There could even be a direct front-drive with or without transmission ratio included. Ultimately, due to these measures the bicycle could be more compact with a shorter wheel base and thereby weight distribution over the wheels and aerodynamics might benefit. [1] [4] [6] [8] [9] [17] [18]

Fairing A faired cycling has a cover around the bicycle that, besides protecting the rider against the elements, reduces the air drag of the bicycle. Rear wheel steering is of interest for world speed record breaking faired bicycles, because it could allow for a smaller spaced fairing with better distributed wheel gaps which lowers the air drag further. [11] [19] [appendix A]

Safety Supposedly, RWSBs have generally a lower COM and are therefore less susceptible for pitching over frontally during front wheel braking [5] [18]. Generally, front wheel braking is considered more effective than rear wheel braking due to longitudinal load transfer during braking. Braking the non-steered front wheel is then a good option, because it presumably also does not introduce unwanted unstabilizing steer motions on RWSBs. RWS can also be used in addition to FWS, i.e. having two steer axes, to use it as means of reducing an unwanted and unsafe weave mode at high speeds [10]. A bicycle requires an initial steer motion in the opposite direction to a desired turn in order to set up the bicycle lean in the correct direction, counter-steer. Supposedly, an RWSB might show other dynamical behavior and crucial obstacle avoidance time is gained [5] [12].

Mountability Certain RWSB designs allow for an easy relocation of the handlebar from in front of the rider to alongside the rider. This might benefit or at least change the mountability of the bicycle, because now the rider can mount the bicycle frontally. [appendix A]

Education The changed RWSB dynamics as opposed to FWSB can be illustrative for control theory. It seems ideal as means of relating dynamics and control and to show how control theory can be applied to make RWSBs ridable or unridable. [14]

Handling Like rear wheel steered multi-wheeled vehicles, e.g. forklifts, RWSBs can easier rotate about the front contact (at low forward speed) which may come in handy to aim the front in certain circumstances. [7] [12]

Transportation An RWSB can easy have a shorter wheel base and is generally lighter than ordinary steered bicycles, such that transporting the bicycle is easier [8]. Making an RWSB foldable may be easier due to the separated steer and drive wheel [appendix A].

Of course, RWSBs also have disadvantages. For example, an RWSB has the disadvantage that the rear wheel 'swerves out' during cornering. This makes that one has to steer earlier into a corner to safely negotiate it, which could be a great disadvantage in preventing collisions with suddenly appearing obstacles [18]. Moreover, a rider cannot see the steered (rear) wheel path behind him and could avoid an object with the front wheel while still hitting it with the rear wheel [18]. These examples reduce the ridability of an RWSB, but generally the largest disadvantage of RWSBs is that they cannot be kept upright comfortably, or kept urpight at all.

Therefore, in most studies the advantages do not seem to outweigh the large disadvantage that RWSBs lack ridability whatsoever and RWSBs got a bad name. Added to this, making an RWSB ridable may come at the expense of (some of) these advantages, because some of these supposed advantages are incorrectly assumed to apply. Researchers were simply not able to make the RWSBs ridable and in effect were not able to show that the advantages actually are not present. For example, counter-steer also occurs for stable controlled bicycles (section 7.2).

2.2 Dynamics of RWSBs

Definition

A rear wheel steered bicycle does not exist. Topologically, a bicycle is (longitudinally) symmetrical, having two frames with each one wheel, connected by a hinge. As so, many people are not even aware of a possible distinction between front and rear wheel steered bicycles. But still the term rear wheel steered bicycle pops up from time to time. Sharp showed already in 1896 that an unambiguous definition is not easily formed and did not came further than stating the obvious [2]:

> "*a bicycle being said to be a front- or rear-steerer, according as the steering-wheel is in front or behind*"

Even until now there is no clear definition of the steered side of a bicycle, but some authors try it, either explicitly or implicitly. However, when defined at all, there is no one irrefutable correct definition which can be seen in the different scientific studies and numerous examples of what people interpret as RWSBs (see appendix A). Often the focus is on one or more different aspects of the bicycle:

Rider position RWSB has rider (saddle) on front frame.

Sensors position RWSB has main sensors (yaw, roll, etc.) on front frame.

Handlebar position RWSB has handlebar connected to rear frame.

Driven wheel RWSB has front wheel drive.

Steer hinge position RWSB has steer hinge (headset) behind rider.

Steer hinge angle RWSB has steer hinge (steer axis) diagonally pointing frontally upward.

Mass distribution RWSB has front frame (with or without rider included) heavier than rear frame.

Mass position RWSB has center of mass of total bicycle ahead of steer axis.

Frame size RWSB has largest frame in front.

Wheel paths RWSB has rear wheel path wider than front wheel path.

Wheel yaw RWSB has rear wheel (locally) yawing more than front wheel during steer.

Trail direction RWSB has steer axis intersecting ground behind front wheel contact.

Trail length RWSB has rear wheel trail smaller than front wheel trail.

From this list it becomes clear that a definition can be formed based on kinematics, kinetics, or control. The ideal definition might then distinguish a rear from front wheel steerer in all these three areas.

In general, an RWSB is recognized as one according to 'you know it when you see it' [43]; people identify a bicycle as rear wheel steered, but at second thought do not exactly know why. For reasons of clarity a practical definition that catches the essence of the difference between front and rear wheel steering is required. Preferably this definition should have physical value and most historical examples that people interpret as RWSB should be recognized by the definition as RWSBs.

Before defining the steered side, it makes sense to take a step back and define the front and rear side of a bicycle. The symmetrical nature of a bicycle makes this also a subject for discussion. Here, the front and rear are defined on the basis of the movement direction; the front of the bicycle is the part that has its wheel contact ahead in longitudinal movement. This seems obvious, but this definition has as consequence that an ordinary bicycle that is moving 'backwards' (with the driven wheel ahead in the longitudinal movement) has the main frame as front frame and the fork with handlebar as rear frame. Note that a bicycle has an equal number of steered wheels as there are steer axes. Bicycles with two steered wheels must have two steer axes (and are thus technically not pure bicycles).

As said, most authors omit a clear direct definition of which wheel is steered and just refer to their (example) bicycle as rear wheel steered [1] [4] [5] [6] [7] [8] [9] [10] [11] [12] [13] [14] [19] [appendix A] or they just show rear wheel steering without noting it [3]. Others try, but do not come to an unambiguous clear definition that leaves no room for doubt and is generally accepted by everyone [2] [16]. Still, often a definition can be indirectly distilled from these texts.

There are authors that seem to omit a definition due to their approach of a bicycle as an asymmetrical vehicle, much like a conventional four wheel car [1] [4] [5] [9] [11] [12] [14]. The bicycle is then made of one large frame with mass and a smaller fork with negligible mass as second frame, much alike a conventional car with large main frame and small negligible unsprung mass. For such a simple representation the distinction between front and rear wheel steered is easily made, because the steered wheel is simply the wheel attached to the massless fork and the bicycle is rear wheel steered if this fork is at the rear during forward riding. Sometimes the definition becomes even more easy when the steered wheel is assumed to have always zero trail and there is a vertical steer axis angle (naive bicycle), making the steered wheel simply the one underneath the steer joint [1] [11] [12] [14]. Moreover, rear steering simply arises when a conventional, presumed front wheel steered, bicycle is ridden reversedly [3] [5] [19]. Some bicycles incorporate two steer axis such that the rear steer axis is easily identified [10].

An interesting distinction between the cases of steering from a physics point of view arises by referring to differences in behavior. For example, the relation between paths of the two wheels differ between the cases [1] [7] [13]; rear wheel turn radius is larger than front wheel turn radius for RWSB which is opposite for an FWSB. This is similar to saying that the steered wheel, i.e. leading wheel, is angled (headed) more with respect to the bicycle neutral, such that the steered wheel determines the heading of the total bicycle more [18]. Both turn radius and wheel heading are dependent on the trail of the wheels, i.e. the distance from the wheel contact point to the steer axis ground intersection point.

Another way of defining the side of steering is by looking at the mass of the different parts [8] or by looking at the mass of the total bicycle [18]. One can then look at the mass value and/or at the (center of) mass location or mass distribution among the different bicycle parts where the smaller frame of the bicycle may sometimes be negligible. Often, a mass distribution criterion is included in the definition to ensure that the steering wheel has the lowest inertia and in effect reacts faster and 'leads' the bicycle [18]. The frame assembly with the smallest mass is then taken to have the steered wheel; a bicycle is rear wheel steered when the rear frame has the smaller mass. The rider can be included in the frame mass and then clearly, the frame with the rider is often automatically the heaviest frame. However, inclusion of the rider might make the definition subjective since not all people weigh the same.

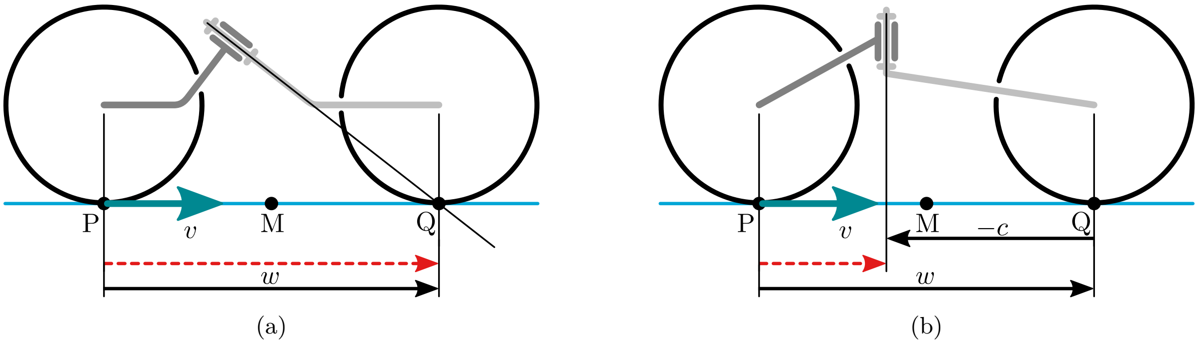

Figure 2.1: Examples of the trails of (a) an FWSB and (b) an RWSB. The movement direction, depicted by forward velocity v, determines which ends of the bicycle are the rear and the front and thus determines which contact is the the rear, P, and front, Q. The rear wheel trail (dashed red arrow) is positive in both cases while the the front wheel trail, c, is respective zero and negative in these two examples. So, although the rear wheel trail is larger in value, in both cases, the absolute length matters and thus the steer-side differs between the cases.

But other than based on intuition, has such a definition any dynamical based substantiation? It may be that the caster mode or transient behavior in cornering would be affected by the mass distribution, but the exact effect of the mass requires a full dynamical analysis. For example, adding much weight at around the wheel contact point makes one assembly probably heavier than the other, but does not necessarily change the dynamics significantly. Certainly, the mass distribution is interesting for stability analysis and makes bicycles behave different, but it might not give a direct simple distinguishing between rear and front wheel steering.

Maybe the definition should be based simultaneously on different elements like mass, steer axis angle, and trail altogether. For example, besides a trail requirement, one can complementarily add a mass location requirement [17] [18]. This thought is illustrated by the following statement where no clear one turning point between front and rear wheel steering is presented, but the shift from front wheel pivoting to rear wheel pivoting in order to steer occurs gradually [47]:

> "*There is not a hard line defined between front steering and rear steering. Instead there is just a continuous spectrum from most of the mass in the rear to most of the mass in the front, head angle positive to head angle negative, and trail positive to trail negative.*"

Those who give a clear definition do seem to come with similar multifeature (simultaneously trail and mass requirements) definitions, but base them on different reasoning [16] [17] [18]. Based on intuition, an RWSB is a bicycle where the absolute rear wheel trail is larger than the absolute front wheel trail [17] [18] (see figure 2.1b) and where the front frame has the largest mass [17] or the center of mass of the total bicycle lies ahead of the (possibly diagonal) steer axis [18].

Finally, the most intuitive as well as somewhat vague definition would be that the steering wheel is the wheel that leads the bicycle into a direction making the rest of the bicycle follow that steering wheel [13]:

> "*Rear steering would make the rear contact the more controllable one*"

Luckily, the message of this definition might be practically captured by looking at the contribution of the steer rate on the lateral acceleration of the midpoint of the support line spanned by the wheel contact points [16] (see chapter 6). The support line movement is important, because this line is the base that can counteract unbalancing forces. Its midpoint is of interest since it is often close to a vertical projection of the center of mass of the bicycle and allows for an analysis taking the longitudinal 'symmetry' of a bicycle into account. A bicycle is then rear wheel steered when the steer angular rate contributes negatively to the lateral acceleration of this support line midpoint, in stead of the positive contribution for a front wheel steered bicycle [16] (see section 6.3). This steer rate support acceleration contribution sign is determined completely by the bicycle kinematics and is the only practical difference between the steer-side cases. Concretely, it means that the support line can initially shift away from the direction of an initiated curve (see section 6.4).

With this steer rate contribution steer-side definition, the turning point can be shown to lie at the point when both trails are precisely the half of the wheel base length (section 6.3). Thus, this definition from lateral support line acceleration is a mathematical way of describing the definition by trail lengths, where the steered wheel has the smallest absolute trail of the two wheels (see figure 2.1b), in a purely kinematic and mass independent manner. The definition can almost always (not for two equal trail lengths) objectively distinguish bicycles from each other based on their steered side, whether they are (self-)stable or not. A definition by wheel turn radii or by local wheel heading is also dependent on the trail lengths and comes down to the same definition. Finally, the most practical applicable version of the definition is looking at the steer-axis and midpoint M: The side of M, i.e. at the rear or in front of M, where the steer-axis intersects the ground, is the same as the steer-side (section 6.3).

Research methods, models, self-stability, and ridability

An important feature for a bicycle's usefulness are its dynamics, which can be expressed in its ridability; the ease by which it can be ridden by a human. Often, this ridability is assessed indirectly by looking at the self-stability; the ability by which it can stay upright by itself without control. The two features can be analyzed by using different methods and models.

In that light, most interesting about the literature is what the authors state about the (self-)stability of RWSBs (or RWS motorcycles) and how they came to their statements. In the RWSB literature, just as in many other topics, there is a variety of detail in the analysis of the dynamics. Some authors analyze it by looking simply at the motion of points on the ground with respect to the center of mass [1] [7] [9] [13] or experimenting by trial and error based on theorizing [3] [4] [8]. Others use Newtonian dynamical models of varying order and detail [11] [12] [16] [19] after which some even built and test the design [5] [10] [14] [17] [18]. The last category is authors referring to the other experiments or studies to come to conclusions about RWSBs [2] [6].

The exact relation between self-stability and ridability is not known, but it is assumed that a self-stable bicycle is better ridable [46] and unexpected disturbance torques can easier be counteracted by a controller or control can be even temporarily interrupted [9], but self-stability might come at the expense of maneuverability. Although self-stability of a bicycle might make the ridability better, it is not essential for riding a bicycle upright rather stable. Both Self-stability and ridability are discussed in literature although the distinction is often blurry. Often for an RWSB, more so than with conventional bicycles, only the control part is discussed and self-stability is only mentioned shortly or not at all.

This under-exposure of self-stability occurs for instance because self-stability is simply assumed impossible [8], or the model used is so simple that self-stability is never an option [12]. Until 2011, when Kooijman *et al.* [16] presented their theoretical RWSB, all authors concluded that RWSBs are never self-stable. Some of the authors are even unaware of the existence of self-stability for bicycles at all [1] [12]. However, they also all claim that, although thorough practice may be required and RWSBs exist that are impossible to ride [14], RWSBs can be made such that they are ridable.

The simple analysis of the motion of points on the ground with respect to the center of mass without using a complete dynamical model is presented by several authors [1] [7] [9] [13]. This can be seen a 'heuristic inverted-pendulum-type model' [25]. However, often dynamical means of recovering balance are neglected and it turns into a mere kinematic analysis of the movement of the bicycles contact points, and self-stability is not mentioned at all. This analysis, if done correctly by understanding the true dynamics, might be helpful in a qualitative analysis, but exact trajectories cannot be calculated.

A somewhat more useful analysis is a trial-and-error approach. Of the authors that built RWSBs, two adjusted and optimized their bicycle and reported extensively about the process: Laiterman [4] and Cornelius [8]. Note that this trial-and-error approach is more often done in the past, but other reports are less explicit (see appendix A, where Laiterman's and Cornelius' bicycles are also described in more detail). Both aim for a wheel base as short as possible, because it makes the bicycle swifter in moving the center of mass laterally, after all the whole dynamics time scale with wheel base over velocity. However, peculiarly enough, they come to different conclusions about the trail. The steer axis cannot intersect the ground behind the rear wheel, because then the wheel will flip around instantly as a caster wheel. However, when the steer axis intersects the ground ahead of the rear wheel, the center of mass in-between the wheels will presumably steer the bicycle always out of a fall. Therefore, such a trail is tricky and while Laiterman thus prefers a zero rear wheel trail, Cornelius, aware of Laiterman's results, wants the rear wheel trail as largely positive as possible (while keeping the bicycle

RWS, so steer axis still intersects ground around the support line middle point), thus shifting it more and more towards front wheel steering. Laiterman notices that a larger positive rear trail is better for holding balance, but he does not find it to weigh up against a worsened maneuvering. These different conclusions seem illustrative for the complex interaction between parameters on a bicycle, and proper modeling and analyzing of the bicycle dynamics is required to understand the influence of parameter changing better. Note that these specific trial-and-error studies rely heavily on slip angles in their explanation of the dynamics [4] [8]. However, many of the behaviors also occur in models when tire dynamics are neglected and are assumed infinity stiff.

Most authors see the bicycle as an inverted pendulum where the balance can be recovered by accelerating the support (base) towards underneath the center of mass (COM). Therefore, a popular and simple model for the analysis of an RWSB is a one point mass inverted pendulum model [11] [12] [14] (figure 2.2). In this model the wheels are taken massless and without mass moment of inertia. It is naive, meaning that the bicycle has a vertical steer axis running through the steered wheel contact point without a trail. An FWSB has then zero front wheel trail, $c = 0$, and an RWSB has zero rear wheel trail, $w = -c$ (wheel base equal to front wheel trail). Furthermore, the mass of the steer assembly is neglected leaving only the mass and mass moment of inertia of the larger frame attached to the non-steered wheel with the other wheel pivoting around a vertical axis. This longitudinally asymmetric model can either be used for a rear wheel steer analysis by transforming from front to rear wheel steering by changing the sign of the forward velocity [14], or by defining a rear wheel steer angle with respect to the main frame [12]. There is no lean-to-steer coupling because of the one mass and the lack of trail and precession, making it a one degree of freedom model with one equation of motion. The lean angle is the one degree of freedom while the steer angle is the control variable (input).

A steer into the fall feedback control law of the lean angle to the steer is used to stabilize the model where this control can be considered exerted on the bicycle by an external controller [12] [14] or as a bicycle's own inherently self control quality (self-stability) [11] [14]. A simple feedback model where steer is directly proportional to lean only ($\delta = -K_{\mathrm{f}}\phi$), alike a skateboard, can never show a self-stable bicycle with the single mass naive bicycle model [14] [26]. Even for an FWSB this simple bicycle model does have positive eigenvalues for all feasible bicycle configurations (mass above ground) [14]. But where such an FWSB can be stabilized by the simple controller, an RWSB described by this single mass naive bicycle model is cannot even be stabilized by this control law due to the 'bad' system dynamics [14].

However, with a more complicated steer into fall feedback control, e.g. besides the proportional feedback of the lean angle also the lean rate ($\delta = -K_{\mathrm{f}}\phi - C_{\mathrm{f}}\dot{\phi}$), even the single mass naive RWSB model can be stabilized. Some argue that precise steer angle control may not be a realistic representation of what humans actually do for the controlling of vehicles and it is rather torque input control [9], or that a human uses a combination of both steer angle and torque input, i.e. stiffness control. These ideas can be included by changing the control law and the model can even be extended to some height by altering control; trail, steer-axis angle, or gyroscopy of a wheel or both wheels can all be included to influence control [14]. To aid these more complicated controllers, e.g. a human, in stabilizing the RWSB, the dynamics of the simple model can be improved by changing some parameters to make ridability better, but self-stability remains impossible with this simple model [14].

All in all, for control purposes, a one mass bicycle model might actually be a good approximation of a bicycle, e.g. to make a robust controller that can handle variations in rider properties without problem. However, for finding a self-stable RWSB configuration, a single mass naive bicycle model is too simplified and too limited.

A more detailed two frame masses (main frame and fork) model is used by Schwarz [5] who, apparently, makes a front wheel steered motorcycle model (from Sharp [27]) rear wheel steered by simply reversing the forward velocity [14]. The only substantial difference with a conventional motorcycle is the elongated wheel base and a reversed trail (steer axis intersects ground ahead of steered rear wheel). His model does incorporate gyroscopic effects of the wheels and is rather similar to the Whipple model as described by Meijaard *et al.* [22] and later used by Kooijman *et al.* [16] to show a self-stable RWSB. However, Schwarz stays close to a conventional motorcycle design geometry, i.e. basically rides a conventional motorcycle backwards, and concludes that rear wheel steering is inherently unstable in theory due to always present real positive eigenvalues as confirmed in practice by his unridable motorcycle.

The 25 parameter and two degree of freedom (fourth order) linear Whipple bicycle model is used for the studies at Delft [16] [17] [18] [19] [appendix A], with the aid of Matlab software JBike6 [45] (section 4.3) in order to rapidly see the effect of parameter changes on the eigenvalues. Lean and steer are here

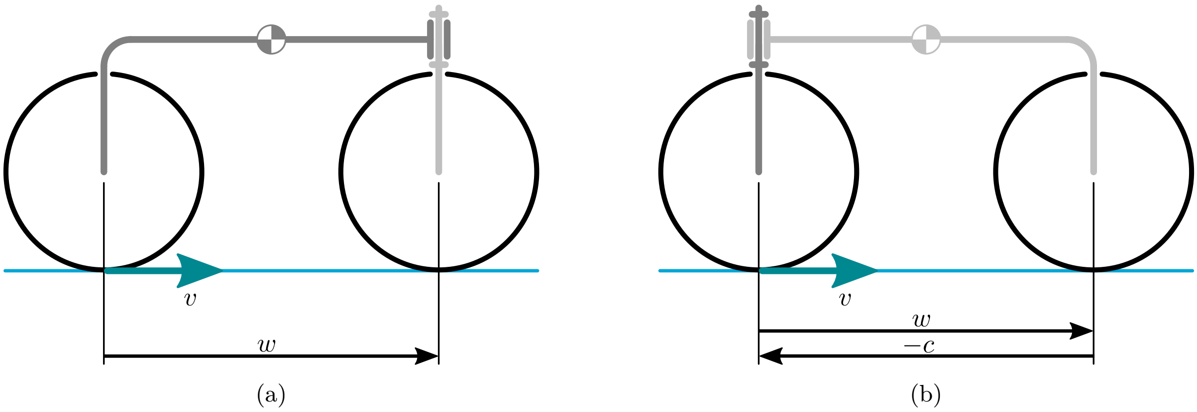

Figure 2.2: Single mass naive bicycle model as (a) FWSB and (b) RWSB as used by many authors to illustrate several bicycle features [1] [4] [5] [9] [11] [12] [14]. It is a so called naive bicycle since it has a vertical steer axis and one zero trail; steer axis angle, $\lambda_s = 0$, and the front wheel trail, c, is either zero or equal in length to the wheel base, w. This model has the lean dynamics as its single degree of freedom with the steer angle as kinematic variable, and is too simplified to model self-stable RWSBs.

the degrees of freedom and one can prescribe the torques on them as inputs. By including gyroscopic effects in the front wheel and placing the front frame mass ahead of the front wheel, a self-stable RWSB configuration is found, even with some parameters being zero, e.g. a zero steer axis angle [16] [appendix A]. Following this analysis, Broxterman *et al.* show that such a theoretical configuration can be self-stable in practice by building and testing it [17]. Next, Van Dijk *et al.* went a step further by making it ridable in a practical manner by starting from a self-stable design which includes passive rider [18]. However, due to restrictions in the parameter design space dictated for a low frag faired recumbent bicycle design, an attempt to incorporate self-stable rear wheel steering in a streamlined bicycle did not succeed [19].

Interesting is that directly or indirectly several authors conclude that a bicycle needs two features in order to be stable [4] [5] [8]. First, a caster effect is needed where the two wheels are aligned such that during a forward motion no flip (or ‘flop’ [5]) occurs where one wheel immediately tends to rotate a half cycle about the steer axis, e.g. like a swivel wheel on a shopping cart would do when the cart is suddenly pushed backwards after a forward motion. This unstable flipping needs to be prevented by designing the bicycle such that the castering wheel is already in the stable aligned position. Secondly, a steer into-fall-mechanism is required that tends to shift the support underneath the center of mass to recover balance. Both features are simultaneously present on conventional self-stable bicycles, but in the past it was often experienced to be impossible to implement both simultaneously on RWSBs. That is, until the self-stable theoretical and real RWSBs were created in Delft [16] [17] [18].

In the light of these findings, self-stability for rear wheel steered bicycles stays undiscovered mainly because of two reasons: Either the model is too simplified and/or the design space is too limited. The one mass inverted pendulum model is basically a very simplified Whipple model with many zero parameters due to which even a degree of freedom is lost. Compared to the simple one mass inverted pendulum model, the most simple theoretical bicycle of Kooijman *et al.* [16] has added trail and wheel gyroscopy with the front wheel inertia being two orders larger than the rear. This indicates that a nonzero front and rear trail and a front wheel gyroscopic effect, along with their ‘strange’ location of the front frame mass ahead of the front contact, might be essential in making an RWSB self-stable. So, although the one mass model is useful in some cases, it has an incomplete selection of nonzero parameters for the self-stable RWSB analysis, and thus shows that the selection of nonzero parameters has to be made cleverly to not overlook self-stability.

But even when the models include this gyroscopy and they allow for masses in unconventional places, e.g. in front of the front wheel, authors fail to find a self-stable configuration due to the limited design space they acknowledge [5]. They stay within a rather conventional design frame which is heavily influenced by conventional bicycle and motorcycle designs and thus the design options are probably not investigated to the full potential. In practice this means simply reversing conventional designs and not deviate far from such a reversing design. For example, the center of mass is placed often in the middle (which seems logical from pitch stability considerations) between the wheels and geometry angles are modified only slightly. However, using some more unconventional designs can results in self-stable bicycles. Even the simple models of rear wheel steered bicycles, that can never be self-stable, could be improved in ridability terms by placing the mass ahead of the front wheel, causing a negative so-called zero which benefits controllability [14]. It is not easy to think besides the paved paths and indeed, it was only by accident, when trying to model M. Coleman's monocycle [42] in JBike6, that Kooijman *et al.* found their self-stable theoretical RWSB which forms the basis for the later presented theoretical RWSB with minimal number of nonzero parameters (chapter 8).

Steer angle definition

A common reason for confusion and wrong conclusions is an unclear or inconsistent positive sign convention for the steer angle [1] [4] [10] [11] [12] [14]. The steering angle is sometimes defined with respect to the frame on which the rider sits [4] [10] [12]; for example, positive when seen from above the steer frame rotates clockwise with respect to the main frame whether the steer frame is in front are at the rear. The issue arises from the simple model that assumes one frame with respect to which the two wheels steer. It is then straightforward to say that for either the front or rear wheel a positive steer angle is when it is turned clockwise with respect to the frame when seen from above. Because a positive front wheel steer and a positive rear wheel steer then result in opposite turning and thus opposite leaning directions, confusion looms.

A similar issue arises when one reverses the velocity sign [14]. Reversing the sign in the equations is a simple way of making a conventional bicycle rear wheel steered in the model. The rear (main frame) of a conventional bicycle then becomes the front frame which is handy because it occurs naturally. However, the positive direction of the steer angle results now in an opposite turning direction as for the reversely ridden case and, hence, is again cause for confusion. So, although not wrong when well defined and understood, it is advisable to take a precaution into account and keep the steer angle consistent as described next.

To circumvent the issues one must stay true to the definition of steering and see it as the changing of the relative angle between the two frames. It is just a matter of perspective, i.e. which frame is chosen to be the reference. The most convenient way of thinking about rear wheel steering is to look at it as just a gradual backwards shift of the head tube (steer axis) without marking one the two frames as being the main frame. When shifting the headset backward there is never a moment when the positive steer angle is defined in a counter rotated fashion; when a front wheel steered bicycle seen from above has a positive steer angle defined as a clockwise rotating front frame with respect to the rear frame, then this is still applicable to a rear wheel steered bicycle (see the grey wheel steer visualization in figure 2.3 while neglecting the lateral accelerations for now).

Balancing the relevant center of mass

In order to stabilize an inverted pendulum, such as the bicycle, the support needs to intercept the resultant force on the center of mass (see section 4.1). Therefore, the (lateral) movement of the support is important, and for a bicycle this support is spanned by the wheel contact points. Then, for a balance analysis, the most interesting point on this support line, is the point that has to 'catch' the resultant force on the center of mass: the base-point, i.e. the vertical projection of the center of mass on the support line [1]. For conventional bicycles this base-point is close to the support line middle point, such that often this middle point can be selected for lateral support line motion analyses [16].

However, it might not always be the desired geometrical point to discuss the balance recovery. Apparently, for an RWSB with the front frame center of mass at a location similar to a conventional FWSB, the lateral acceleration of the support line middle point cannot be directed correctly by the bicycle system itself and thus self-stability is impossible in that case. Luckily, the center of mass of the front frame can be brought more to the front in order to make the RWSB self-stable (chapter 8). In that case it would make sense to use another point on the support line that is more directly underneath that COM. Ahead of an RWSB front wheel the lateral dynamics of ground points may be as desired for stability so that there the main center of mass needs to be placed. Then, it might make more sense to place the base-point also there. For a complete picture the support line as a whole support line is probably more suitable for an analysis of the recovery of the stability as compared to a single base-point.

In line with this it is questionable if the center of mass of the complete bicycle or only one of the individual frames or that both frames masses need to be included separately for a balancing analysis. For example, Kooijman *et al.* showed that solely the front frame mass, when positioned correctly, is enough to make an RWSB steer into the fall by itself and thus create self-stability [16] (chapter 8). Moreover, a large mass may be added at the wheel contact point without severely affecting the dynamics, although the center of mass position of the total bicycle system may be shifted a lot. It is quite possible that the choice of important mass(es) is different from case to case.

Note that at least for a tipping fore-aft analysis a total COM analysis is useful, since a high total bicycle center of mass close to the rear or front wheel can cause pitching over during acceleration or braking. A center of mass placed behind or ahead of the rear and front contact respectively will pitch over the bicycle even in a static case, such that this total bicycle COM location should be avoided on real-life bicycles. Therefore, in the further discussion here, the COM of the total bicycle system is assumed to be placed in between the wheel contacts.

Stable turning and balancing

It is proven that to hold all (self-)stable bicycles in a steady turn a handlebar torque is required that is opposing to the turn direction; a clockwise turn requires a counterclockwise handlebar torque [15]. When in a steady turn the torque is released, then all stable bicycles will turn further into the turn in order to recover from it (section 7.2 and 7.3). Even when only leaned, all bicycles are assumed to require a steer into fall in order to recover from the undesired lean. By such a steer motion, the support line is accelerated towards underneath the leaned over COM of the bicycle and, hence the bicycle uprightens, like is done by balancing an inverted pendulum. A bicycle is then stable when its own dynamics or an applied control mechanism is able to produce correctly aimed and fast enough support line movement to counteract every unbalancing motion. Similarly, when initiating a turn from a straight up and ahead position on a stable bicycle, one first needs to steer away from the desired turn in order to set up the correct lean, i.e. counter-steering (see section 7.2 and 7.3 for an elaborate explanation and mathematical expressions).

A difference in the support line midpoint lateral motion between FWSBs and RWSBs gives rise to theories about dynamical differences between the steer-side cases. Some authors notice that, when initiating a turn to one side, the support lateral motion is in opposed directions for the two steer-side cases [1] [4] [9] [12] [13]. For example, when applying a rightward steer motion on an RWSB, a rider above the support midpoint initially experiences a leftward lateral acceleration, and the rear is felt to break out away from the turn [12]. This happens because just after initiating a turn, the lateral acceleration of the support line midpoint is pointed in the opposite direction as the steer is pointed in (acceleration outwards of curve) under influence of the initial rear contact lateral acceleration; a clockwise steer (of front frame with respect to rear frame) is reasoned to result in an initial movement of the support midpoint to the left (figure 2.3b). Hence, from an upright straight position, a clockwise steer of the front frame with respect to the rear frame on an RWSB shifts the support line to the left and thus makes the bicycle fall to the right when the center of mass is placed at a conventional location in between the wheel contact points.

The authors then reason that if one can manage to reach a steady state corner, which requires high skill, the centripetal acceleration is again pointed to the inside of the corner and a steady rightward corner is negotiated. Throughout the literature this notion that the initial turn direction might be the same as in the steady state makes some think that counter-steer at initiating a corner is no longer required and an RWSB can directly steer in a desired direction [5] [7] [12]. Counter-steering can be defined as a difference in steering direction between initial and steady state corner negotiation. This absence of counter-steer theory is persistent and recurring.

Indeed, as opposed to an FWSB, a steer rate in the same direction as the steer angle can cause an RWSB to have a lateral acceleration of support line in-between the wheels that is pointed to the opposite side of the initiated turn; the support line middle point is accelerated to the outside of the curve. This occurs due to the angular steer rate whose lateral acceleration contribution has a different sign for an FWS as for an RWS case. This situation is illustrated in figure 2.3 for the initiation of steering the bicycle into a clockwise corner. As steer rate damps out only a steer angle remains in steady state and during such a steady corner the support line middle point is accelerated neatly to the inside of the curve and balance is kept for both an FWSB and RWSB (see section 7.2 and 7.3). When

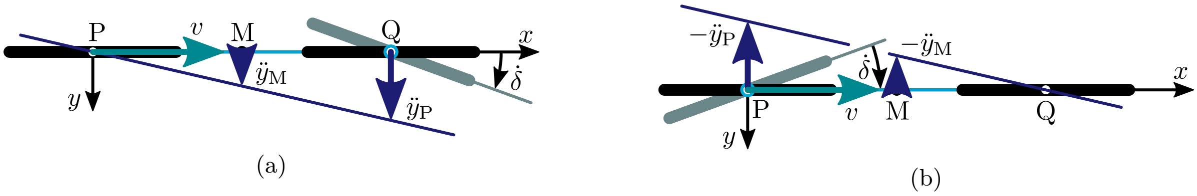

Figure 2.3: Depiction of the lateral acceleration, $\ddot{y}$, of the support line of a naive bicycle ($\lambda_s = 0$ and either one wheel's trail is zero) riding with a forward velocity, v, with wheelbase $w = 1$ m and front wheel trails (a) $c = 0$ and (b) $c = -w$. The lateral acceleration of the midpoint, M, on the support line is oppositely directed among the steer-side cases for equally directed angular steer rate (see chapter 7). The steer angle is defined as the angle that the front frame makes with the rear frame, so this positive steer rate depicts that the front frame is going to rotate clockwise with respect to the rear frame; the rear wheel will thus rotate counterclockwise about it's contact point, P, with respect to the front wheel, which rotates about it's contact, Q. The drawing is based and scaled according to a bicycle with forward velocity $v = 4.5$ m/s, steer angle $\delta = 0$ and steer angular rate $\dot{\delta} = \pi/6$ rad/s.

the center of mass of the bicycle is placed between the wheel contact points, the initial middle point acceleration of an RWSB will shift the support line away from underneath the COM and the bicycle will fall directly into the steered direction. So as far as that goes, the authors have a sane point, but this does not state anything about counter-steering since there is no requirement that the bicycle is stable (balanced). It just tells whether the support line midpoint lateral acceleration is pointed in- or outwards a curve at a certain time. A proper analysis would take both a self-stability case and a control-stable case in consideration (section 7.2 and 7.3).

It appears that for all bicycles that are self-stable, counter-steer occurs, and even for bicycle that are controlled to be stable (stabilized), counter-steer occurs (section 7.2 and 7.3). Surely, for stabilized bicycles all real part of the eigenvalues of the complete linear system (with potentially necessary controller included) are negative. As Kooijman *et al.* [16] showed from these negative real parts by using Routh criteria (see section 7.2), the initial response and steady state response to a constant steer torque reference for such a self-stable upright and straight bicycle are directed oppositely; to initiate a rightward turn, first a small leftward turn has to be performed, and vice versa. For all stabilized bicycles this should hold, so also, for example, for not self-stable but control-stable RWSBs, although for controlled bicycles the input steer torque obviously cannot be constant.

It is thought that counter-steering is associated with initiating a desired lean angle for turning [1] [5] [12] [14] [26]. This physical interpretation is easy to obtain, but causal reasoning is difficult due to the closed-loop feedback coupling between tilt and steer in the system [14]. Even more, because stable RWSBs also can show counter-steer (section 7.2), which is unexpected for many. Sometimes motions are experienced on RWSBs that indicate that counter-steering is still required. For example, first the front would dip to the left before pointing to the right when a rightward curve is initiated [4].

Related to the supposed absence of counter-steering, is the believe that an RWSB does not require steer into the fall in order to recover balance, but rather steer out of the fall [1] [6]. Surely, on an RWSB, a steer rate results in a support midpoint lateral acceleration away from the steer rate direction. Thus, when one wants to always shift the support towards underneath a leaned COM in between the wheel contacts, one should initially not steer into the fall, but first away from the fall and then gradually into the fall [1]. That all stable bicycles need to steer into a general fall (so also when there is no steer) to recover balance, is unproven but likely. However, equivalently to the counter-steer phenomenon, it is proven that all stable bicycles in a steady turn (fall with steer), first steer further into the turn in order to come straight upright again [15] [16], no matter which side of the bicycle is steered (section 7.2, 7.3, and 7.4).

It is not certain that the acceleration always has to be pointed in the correct direction. Why could it not be possible that first the acceleration destabilizes the bicycle somewhat more after which it will make up for it and stabilize the bicycle? And thus, that recovering from an unbalance by steering the rear wheel of a stable bicycle, just as is assumed for steering with the front wheel, is done by steering into the fall. This would first shift the support line a little away from underneath a conventional placed COM due to a nonzero steer rate, but later the acceleration of the complete support line is towards the inside of the turn. Of course, for stability, the controlling mechanism (either self or external) should always be fast enough to neutralize destabilizing motions, even those initial destabilizing motions caused by the controlling mechanism itself.

In stead of the lateral support line acceleration one might also want to look at the lateral velocity of support line in the direction of a leaned center of mass [1]. However, velocity does not seem to be the balance recovering phenomenon; if the acceleration is still pointed in a balance recovering direction then the velocity will be led correctly by the acceleration eventually if the bicycle does not fall over too fast. Moreover, in a no tire slip model, a bicycle in a turn has the support line resultant velocity always pointing tangential to the path, while the support resultant acceleration is pointed perpendicular to the path to the center of the curve which explains the rotating velocity vector aligned with the rotating bicycle support. Only in a special theoretical case when the COM has zero lateral velocity, which is not the general case, then a pure velocity of the base indeed shifts the base-point relatively to the COM.

The lateral support line midpoint motion is different for an RWSB, because the angular steer rate contributes negatively to it as opposed to an FWSB where a positive steer rate increases the support line midpoint positive lateral acceleration. With a constant steer angle, the support line makes a constant circular motion around a turn center and has thus a constant lateral acceleration to the inside of a curve for both stable FWSBs and RWSBs. However, many authors do not take steer rate into account for the lateral motion and attribute the different support line motion to other things, e.g. slip angles. Some have the steer rate appear in the equations of motion [5] [11] [12] [14], but only one mentions steer rate influence on support line motion (by means of the trail) [16].

Ridability improvements

When the rider sits on the front frame and the handlebar is attached to the rear frame, a difference in steering experience between front and rear wheel steering occurs. A clockwise steer movement of the handlebar then results in a bicycle turn in counterclockwise direction; steer reversal. Most RWSB experimenters decouple the handlebar from the rear frame to get rid of this steer reversal [4] [8] [14] [18]. The necessity of this correction is not undisputed, because steering of a bicycle seems largely a matter of learning and familiarization of the dynamics of the bicycle [48] [49] [50]. After all, it is just a relative motion between two in essence equivalent frames and when and if reversal is necessary for a comfortable ride reamins an unanswered question. The human is a very adaptive controller as illustrated by Jones [3] and even conventional bicycles equipped with such a steer-reversal are ridable after practice [48].

Although the human is a versatile adaptable controller, balancing might require such high bandwidth controlling or such large forces that it exceeds human capabilities [19]. A human can only act in a limited reaction time and speed. Therefore, on top of or besides the steer reversal, a steering ratio can be implemented, as many have done [4] [8] [14] (appendix A); a steer angle of the handlebar then does result in a smaller or larger steer angle of the wheel. It was shown in practice that ridability can indeed benefit from a steer ratio by experimenting with different ratios [4] [8]. Even on a conventional bicycle altering the steer ratio by grabbing the handlebar at different locations changes a rider's riding experience. Another aid in affecting the required bandwidth is the implementation of a damper in the steering mechanism. For different bicycle designs, different effectiveness of steer ratios is to be expected, because trail and steer axis angle also affect the steering.

Most RWSB builders want to sit as low as possible for aerodynamic resistance reasons [4] [8] [11] [19] (appendix A) or braking stability [5]. However, this is disadvantageous for the stability, because the moment of inertia around the lean/roll axis is smaller as opposed to high bicycles, just as a longer inverted pendulum is easier to stabilize. A low center of mass may be good for maneuverability (swift obstacle avoidance) and braking, but it certainly is not beneficial for the stability. Higher center of mass has a higher inertia against rolling over laterally during forward motion and makes the lateral dynamics slower so that it is easier for a human to control. Therefore, so far the designs proved to be not comfortably controllable by humans [11] [19], and possibly one could better focus on higher COMs.

Some think that an RWSB can make sharper turns than an FWSB [4] (appendix A), but this is incorrect. Under the no slip assumption, the center of rotation is always the intersection of perpendicular lines through the wheels. For example, with zero trail and zero steer axis angle for one of the wheels, a 90° steer angle will result in a turn radius of zero with the turn center at the non-steered wheel contact point. Note that in practice such an implementation would require the driving of the steered wheel in order to pull the vehicle around the turn center. What actually might be different for certain RWSBs is that the the rider moves more sideways through the corner with his frontal area pointing inward of the curve due to the rear wheel making the larger radius. This can be a cause for a sensation of making a sharper turn as compared with front wheel steering.

A different approach of rear wheel steering is sometimes also under consideration as Hikichi *et al.* show [10]. In order to decrease a cumbersome motorcycle weave motion at high speed they use a model similar to the one point mass inverted pendulum model, but with two steer axes and allowing for slip. Passive rear wheel steering is implemented in addition to the regular front wheel steering and is shown to reduce rear slip angles and therewith the weave upto a certain degree [10].

Single- and Multi-wheeled vehicles

Often, rear wheel steering is discussed in relation to vehicles with more than two wheels, where leaning is of secondary importance [51] [52] [7] [9] [12] (see section 7.1). Also, 'steering' a one-wheeled vehicle might be considered rear wheel steering, as well as simultaneously being front wheel steering (see chapter 9). Moreover, rear steering can be implemented on all vehicles, but there are differences, as well as similarities, for applying rear steering on different vehicles.

The self-stable theoretical RWSB of Kooijman *et al.* was discovered by accident, when they tried to model a (one-wheeled) monocycle/unicycle with the Whipple bicycle model. However, when a monocycle is modeled with one non-rotating mass and a frictionless sliding stick contact, such as the one of Coleman and Papadopoulos [42] [53], then it cannot be straightforwardly described by the Whipple bicycle model (see section 9.2). A vehicle with two or more wheels in line requires a steer joint to allow for a change in heading, because both contacts can create lateral forces. With only one wheel (plus a frictionless contact) the heading can be changed, without steering, i.e. without changing the relative angle between two parts. In effect, without a steer joint, lean and wheel yaw are decoupled in a static case and thus a monocycle cannot be modeled as a bicycle, which couples static lean and yaw by the non-rotating mass. Note that a single wheel without non-rotating mass can be modeled correctly by the Whipple bicycle model, because a single wheel in the bicycle model has also no static coupling between lean and wheel yaw (see section 9.3).

Also being a riding transportation, the comparison between a bicycle and a conventional car, or another multi-track and multi-wheeled road vehicle, is easily made. In general, a car is different in that it has a well-defined main frame. The steered wheels are then easily recognized as being in the front or in the rear of that main frame and the wheel axles steer with respect to that frame. But essentially, a car's lay-out is the same as that of a bicycle, especially when modeled with the bicycle model where the two front wheels are combined in one front wheel and the two rear wheels are combined in one rear wheel. When viewed as a conventional bicycle, the car's chassis is the rear frame and the nonrotating unsprung mass of the front wheels is the front frame (fork). Note that some multi-wheeled vehicles, e.g. some shovels, have a more distinct rear and front frame than conventional multi-wheeled vehicles. The steering then occurs by changing the angle between those frames much alike the steering (without lean) of a bicycle.

The difference between multi-track vehicles and a bicycle is that they do not lean and cannot fall over laterally, such that stability is somewhat different. Non-leaning vehicles are laterally roll stable, but they still need directional-(self-)stability to prevent severe yaw motions [9]. The slip angle of compliant tyres is a major reason for why rear wheel steering is often deemed impossible to be stable [51] [52]. However, even when slip is disregarded (which is often not realistic) in the analysis, there is still a cause for instability: the trail or caster [52]. Although, just as for bicycles, initiating a steer on a rear wheel steered car results in an initial lateral motion of the rear outwards of the desired turn direction, the directional stability for a non-leaning vehicle requires a different mass distribution than the lateral/directional stability of a bicycle (see section 7.1).

With rear wheel steering, a non-leaning vehicle is always directionally unstable when the center of mass is located longitudinally inbetween the front and rear wheels. Then, a fully developed rear wheel skid can never be recovered [52] (see section 7.1). In figure 2.4a it can be seen that the accelerations (and the not drawn forces) are perpendicular to the non-slipping tires. The trail provides lever arms with respect to the steer axis for all lateral contact forces, and the centrifugal force on the vehicle COM tends to push the vehicle out of a turn. For conventional cars with rear wheel steering and positive rear trail (steer axis intersects ground ahead of rear wheels) as in figure 2.4a with their COM in between the wheels, the steer angle will increase due to this forces and the vehicle might even turn around in an unstable fashion which is known as the tea-trolley effect [52] or ground looping [54].

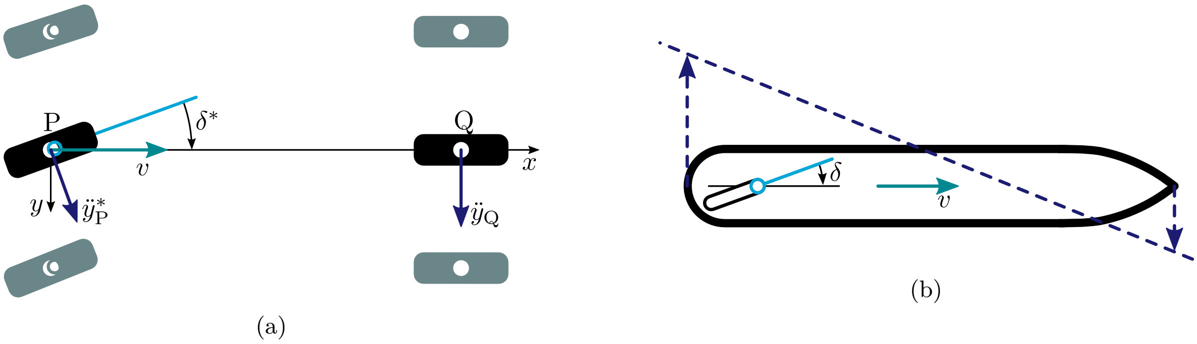

Figure 2.4: Lateral support accelerations for a constant forward velocity and steer angle of (a) non-leaning, e.g. multi-track and multi-wheeled, no-slip vehicles and (b) vehicles in fluids. The essential difference between a car and a bicycle is that lean is assumed to have another (minor) influence. A car can therefore be modeled by a bicycle without lean, depicted here by thick wheels. This car has a wheelbase, $w = 2.6$ m, wheel radius $r = 0.3$ m, and a small caster angle ($\lambda_s = 5°$) and a small rear trail (front trail, $c = -2.57$ m), causing a projected steer angle, δ^*, to occur on the ground. The trail causes a steering moment due to the arms of the forces at both wheels and the centrifugal tendency of the vehicle to fly outward of a turn. A vehicle in a fluid, e.g. a boat or airplane, is not kinematically constraint with a limited number of contact points (like a no-slip rolling vehicle) and thus for a certain steer angle with zero steer rate, the lateral accelerations are undetermined. The situation depicted here shows a constant steer angle and a possible lateral acceleration situation that results in a rotation about a vertical axis of the vehicle. However, the same constant steer angle at the same forward speed can also have other lateral accelerations.

In general, for all vehicles with multiple axles with two or more wheels, the wheel with the smallest trail makes the largest turn radius of the two wheels, regardless the steer axis angle (section 6.2). Thus, for a rear wheel steered vehicle the front wheels have the smallest turn radius (compared to the rear wheels) which is different from front wheel steering. This might be beneficial for certain maneuverability such as for aiming of the front and is why vehicles as forklifts or drivable lawnmowers with their equipment at the front often have rear wheel steering. Likewise, parallel parking with rear wheel steering requires a forwardly insert motion as opposed to conventional front wheel steered parking.

Also vehicles in fluids like boats and planes have different influence of rear steering. A vehicle in a fluid has another relation with the environment than a vehicle with a finite number of (point)contacts (see figure 2.4b). Boats and airplanes generally have one main frame to which the steering services are attached in order to change the yaw of the vehicle. Such fluid vehicles are not kinematically constraint and their lateral accelerations are not solely determined by the steer motion. During a steady turn with constant steer the accelerations are pointed to the turn center just as for a no-slip rolling vehicle, but during the transient, even with a constant steer angle, the lateral accelerations can fluctuate. As opposed to bicycles, and to somewhat lesser extent cars, boats and even more, airplanes, are heavily influenced by the vertical and pitch motion degrees of freedom. For all airplanes and many (smaller) boats, there is a coupling between the yaw and roll (just as for a bicycle) and even pitch motion that cannot be neglected.

A boat generally steers by adjusting the angle of a vertically positioned rudder during a longitudinal motion. On a boat, a bow rudder (front steering) may affect the streamline of a boat negatively and the chance of damaging the rudder by hitting an object is larger than for a stern rudder [personal communication J. P. Meijaard]. Moreover, for maneouvrability the placement of the rudder at either the bow or at the stern is a consideration between obstacle avoidance (bow rudder preferred) and steering effectiveness (stern rudder preferred), but from a stability point of view it does not matter [55]. Moreover, a boat has no kinematic constraint as opposed to a no-slip rolling vehicle; it can move sidewards regardless the position of the rudder.

A conventional airplane mainly steers by adjusting its roll (lean) with the flaps on the main wings, while the rear tail flap is often only included for stability reasons. Canard design airplanes like the Wright Flyer [56] contain a foreplane that can be used to modify the airflow and change pitch or roll and in effect yaw motion. Stability of all degrees of freedom of an airplane are certainly affected by the placement of the wings, all the more because often the center of mass is ahead of the main wings. Just as a bicycle, an airplane also requires leaning (rolling or banking) during cornering to remain stable. And just as a boat, in principle, an airplane also has no kinematic constraints and can move sidewards regardless the position of the rudder, but to keep flying it always needs a longitudinal movement such that pure lateral skidding is impossible.

2.3 Literature knowledge gaps on RWSBs

Up till recently, RWSBs were thought to be always unstable and they were considered more of a hobby object (see appendix A) than scientific material. Since it is not yet performed or documented, there was room for an elaborate analysis of RWSBs with the 25 parameter Whipple model that already had proven to be able to capture self-stable behavior of an RWSB [16]. As shown above, there were even still gaps or misunderstandings in the general thought about RWSBs which can be refuted with general bicycle theory. The following subjects are investigated with the Whipple model and are discussed in this study:

Steer-side definition How to define which side is the steered-side of a bicycle.

Dynamical behavior How compares RWSB turn behavior to the turn behavior of FWSBs. Do both show the counter-steer phenomenon?

Routh analysis A stability analysis in the style of Kooijman *et al.* [16] gives insight in the requirements for certain parameters to come up with a self-stable RWSB. For example, nonzero trail is not necessary and front wheel trail can be negative [15] [16] [17] [18]. However, can both front wheel trail and rear wheel trail be negative? (steer axis intersects ground behind rear wheel contact point) Probably no unambiguous answer; all factors like steer axis angle, mass distribution etc. come into play again.

Quantitative measurements The results of the modeled RWSB should be quantitatively in accordance with the measured results of a to-be built RWSB.

Eigenmode analysis An eigenmode analysis can reveal how an RWSB behaves. Is Kooijman *et al.* configuration [16] stable because the main center of mass (COM of front frame) is in front of the front wheel, such that the 'base-point' accelerates towards a position beneath the COM of the front frame when steered into a fall? And when the main COM would be between the two wheels a steer toward the fall will not (necessarily) result in a base-point acceleration towards the inside of the turning radius?

Comparison other vehicles What are the differences between an RWSB and other (non-leaning) rear steered vehicles such as cars. And why is the RWSB alike Kooijman not the same as a monocycle or simply a disk?

All in all, rear wheel steering is just another case of steering on a bicycle. An RWSB is not very different from an FWSB and the shift between the cases does not alter the model. It is important to realize this and to not make unnecessary alterations in definitions and thinking patterns that are a cause for confusion. Although, an RWSB is just another bicycle, it does require unconventional geometry and mass properties as shown by the most promising existing RWSBs (section A.32, A.53, A.55, A.65, A.75, A.83, A.85).

Part II

Bicycle theory

Chapter 3

Linear bicycle model

3.1 Whipple model

To gain inside in the bicycle dynamics, a model of a bicycle is used that describes the dynamics of a bicycle by applying several assumptions. By using linear kinematic relations, the model is rather useful for describing many bicycle motions. Even a controller can be applied to investigate a bicycle's reaction on control. All these dynamics are based on the most essential parameters that describe and can be extracted from real-life bicycles.

Description and assumptions

The used bicycle model is the (Carvallo-)Whipple model as described by Meijaard *et al.* in their benchmark bicycle paper [22]. This rigid-body model describes the most essential parts that make a bicycle: Two wheels connected by two two revolution joints to two frames interconnected by a hinge. Other (rotating) parts that are present on actual bicycles like chains, pedals, brake mechanisms or saddles are not separately included in this model. The laterally symmetric bicycle (left-right symmetry) has both perfectly circular wheels constantly contacting a flat surface and controlling the hinge angle between the two frames is the steering [16]. Furthermore, the model is somewhat simplified in that structural compliances, dampers, joint friction, and tire models with compliance and slip are all not included in the model [22]:

> "*The model here includes all the sharply-defined rigid-body effects, while leaving out a plethora of terms that would require more subtle and less well-defined modelling.*"

Thus, it is a conservative system (only workless kinematic constraints), and the axisymmetric wheels make a no-slip ideal knife-edge rolling contact point with the ground.

To describe this bicycle quantitatively there are 25 parameters defined for a straight up and zero steer positioned bicycle in the vehicle standard coordinate system of SAE J670 [57] as displayed in figure 3.1. These parameters include masses, m, and mass moments of inertia of all the bodies, I, the positions of the center of mass of the two frames, (x, y), the radii of the wheels, r the wheel base w, the front wheel trail c (distance from front contact point Q to the steer axis ground intersection point, positive in direction depicted in figure 3.1a), and the steer axis angle λ_s (positive as depicted in figure 3.1a). In the neutral straight up and ahead position the coordinates of parts are given with respect to the nominal local origin rear contact P. The local frame has its x-axis always through the rear contact P and front contact Q, with a perpendicular y-axis in the ground plane. The assumption is made that masses cannot be negative and cannot be placed below the surface on which the bicycle rides; the z-position value of a part can only be negative. For clarity, the steer axis angle is assumed $-\pi/2 < \lambda_\mathrm{s} \leq \pi/2$. Note that the particular set of parameters of Meijaard *et al.*, as presented later, can be referred to as the (numerical) 'benchmark bicycle' and has a common bicycle configuration as depicted in figure 3.1.

Moreover, mass moments of inertia are around the centers of mass along the coordinate system axes and no one moment of inertia can be larger than the other two combined. The frames are generally only laterally symmetric, and therefore there are four distinct globally referenced moments and products of

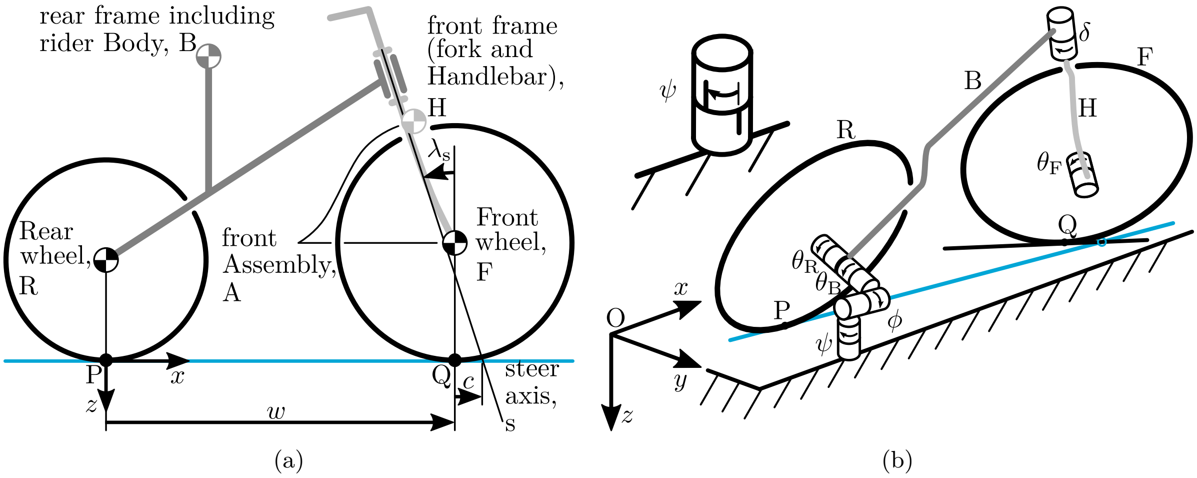

Figure 3.1: (a) The bicycle model parameters and configuration and (b) dynamic variables as defined by Meijaard *et al.* in their benchmark bicycle paper [22]. Three bicycle parameters depicted here are the wheel base, w, front wheel trail, c and steer axis angle, λ_s. The rear and front contact points are given by a point P and Q respectively, and the rear wheel heading is depicted by a cyan line. The steer axis intersects the ground where the cyan rear wheel heading line crosses the black front wheel line heading. The accessible configuration space is parametrized by the xy-position of rear contact point P relative to a global fixed coordinate system with origin O and 5 angles (θ_B not included since this angle follows from the other DOFs when the front wheel is assumed always in contact with the ground) drawn as 'cans in series' [58]. The velocity degrees of freedom are only the rear frame lean angular rate, $\dot{\phi}$, steer angular rate, $\dot{\delta}$, and rear wheel pitch rate, $\dot{\theta}_R$. [22]

inertia, I_{xx}, I_{yy}, I_{zz}, and $I_{xz} = I_{zx}$. The wheel inertias can have any value as long as $I_{yy} \leq 2I_{xx}$ to ensure planar mass distribution. The wheels are assumed symmetric about three orthogonal planes and so products of inertia are zero. Since they are also assumed symmetric about any radial axis, i.e. axisymmetric, only two mass moments of inertia are required to define them; a radial mass moment of inertia, $I_{xx} = I_{zz}$, and a mass moment of inertia about the axle, I_{yy}.

The bicycle has a 7-dimensional accessible configuration space (7 degrees of freedom) as shown in 3.1b). These include the coordinates of point P, x_P and y_P, the yaw angle of the rear frame ψ, the lean (or roll in vehicle terms) angle of the rear frame ϕ, the steer angle δ, and the two rotational angles of the rear and front wheel respectively θ_R and θ_F. The pitch angle of the rear frame θ_B is not a degree of freedom, because it is determined by a trigonometric relation when the front (and rear) wheel is required to be always in contact with the ground, which is assured by holonomic vertical constraints. Due to 4 non-holonomic constraints (no-slip in longitudinal and lateral direction at both wheels) the velocity degrees of freedom are reduced to 3: The lean rate of the rear frame, $\dot{\phi}$, the steer rate, $\dot{\delta}$, and the rear wheel rotation rate relative to B, $\dot{\theta}_R$ (which is directly related to the forward velocity v for no-slip assumption).

From symmetry principles of the bicycle it can be seen that several ignorable (or cyclic) coordinates can be recognized that do not show up in any lateral forces, moments, or potential/kinetic energies expressions for any part [22]: bicycle (rear contact) position, (x_P, y_P), heading (global rear assembly yaw angle), ψ, and wheel to frame rotations, θ_R and θ_F. This allows for a reduction in the set of dynamic equations to only have equations in the non-ignorable coordinates: lean, ϕ, and steer, δ. Which can come in handy, since often the main interest in bicycle dynamical analyses is the lateral (balancing) stability which is dominantly determined by those non-ignorable lean and steer motions. The ignorable coordinates can then have any arbitrary value for the reduced set of dynamic equations in non-ignorable coordinates to have the same solution. Hence, the ignorable variables can never be asymptotically stable, because their equilibrium can be any value. In the end, to fully define the bicycle in the global frame, their values can be obtained from the lean and steer angles and rates and wheel rotation rate by kinematic relations after those angles and rates are known from some time response analysis (see section 5.1).

The model is assumed to be operated with no-hands, but a rigid rider can be included. This is done in the benchmark bicycle parameters by taking a no-hands rider into account making it rigidly attached to a frame by including its parameters in the frame on which the rider is positioned (in the Benchmark paper this is the rear frame, but this can just as easy be the front frame). Rider control of the system can be modeled only by translating the forces he creates to the generalized forces (lean torque and steer torque and propulsion torque) of the model. Despite the simplifications it turns out that the model is detailed enough for some correct and interesting stability analyses. Self-stability, for example, can be explained with this model, but why it stays up on itself is only explained by showing that it follows from the equations; lean and steer are coupled in such a way that one simple physical explanation is difficult. This model is pretty accurate for riderless bicycles with speeds up to about 5 m/s, but for higher speeds some more details may need to be included to make the model representative [46] [59]. Tyre behavior and the high frequency shimmy (wobble) phenomenon require attention at those higher velocity levels. Peculiarly, for understanding active control of a bicycle for example, the model might even be unnecessarily complex.

Linearized Equations of Motion

In order to properly understand the dynamics, the linear equations of motion (EOM) are derived. By putting them in a mechanical equations representation, it becomes clear where separate terms originate from and what their respective influences are (the matrix terms are color coded to make tracking them easier). Eventually, this is helpful in understanding the dynamical differences between different kinds of bicycles or between bicycles and other vehicles. Here the derivation as in the (appendix of the) benchmark paper [22] is repeated, but is presented as a more step-by-step derivation as in a draft on bicycle dynamics [37].

Coefficient definitions

Several coefficients made up of the 25 parameters are defined to make the upcoming equations of motion clearer. As in figure 3.1 subscript R is used for the rear wheel, B is for the rear frame, H is used for the front frame, and F is used to describe the front wheel properties. Furthermore, T is for the total assembly and A depicts the front assembly (front frame plus front wheel). The total mass with its position with respect to rear contact point P is then:

$$m_{\mathrm{T}} = m_{\mathrm{R}} + m_{\mathrm{B}} + m_{\mathrm{H}} + m_{\mathrm{F}} \tag{3.1}$$
$$x_{\mathrm{T}} = \left(x_{\mathrm{B}} m_{\mathrm{B}} + x_{\mathrm{H}} m_{\mathrm{H}} + w m_{\mathrm{F}}\right) / m_{\mathrm{T}} \tag{3.2}$$
$$z_{\mathrm{T}} = \left(-r_{\mathrm{R}} m_{\mathrm{R}} + z_{\mathrm{B}} m_{\mathrm{B}} + z_{\mathrm{H}} m_{\mathrm{H}} - r_{\mathrm{F}} m_{\mathrm{F}}\right) / m_{\mathrm{T}} \tag{3.3}$$

While the mass moment of inertia and products of inertia along the global axes with respect to point P are

$$I_{\mathrm{T}xx} = I_{\mathrm{R}xx} + I_{\mathrm{B}xx} + I_{\mathrm{H}xx} + I_{\mathrm{F}xx} + m_{\mathrm{R}} r_{\mathrm{R}}^2 + m_{\mathrm{B}} z_{\mathrm{B}}^2 + m_{\mathrm{H}} z_{\mathrm{H}}^2 + m_{\mathrm{F}} r_{\mathrm{F}}^2 \tag{3.4}$$
$$I_{\mathrm{T}xz} = I_{\mathrm{B}xz} + I_{\mathrm{H}xz} - m_{\mathrm{B}} x_{\mathrm{B}} z_{\mathrm{B}} - m_{\mathrm{H}} x_{\mathrm{H}} z_{\mathrm{H}} + m_{\mathrm{F}} w r_{\mathrm{F}} \tag{3.5}$$

For the axisymmetric front and rear wheel the moment of inertia along the x- and z-axis are dependent:

$$I_{\mathrm{R}zz} = I_{\mathrm{R}xx}, \qquad I_{\mathrm{F}zz} = I_{\mathrm{F}xx} \tag{3.6}$$

The moment of inertia of the whole assembly about the z-axis is then

$$I_{\mathrm{T}zz} = I_{\mathrm{R}zz} + I_{\mathrm{B}zz} + I_{\mathrm{H}zz} + I_{\mathrm{F}zz} + m_{\mathrm{B}} x_{\mathrm{B}}^2 + m_{\mathrm{H}} x_{\mathrm{H}}^2 + m_{\mathrm{F}} w^2 \tag{3.7}$$

Now, these same properties are defined for the front assembly A only,

$$m_{\mathrm{A}} = m_{\mathrm{H}} + m_{\mathrm{F}} \tag{3.8}$$
$$x_{\mathrm{A}} = \left(x_{\mathrm{H}} m_{\mathrm{H}} + w m_{\mathrm{F}}\right) / m_{\mathrm{A}} \tag{3.9}$$
$$z_{\mathrm{A}} = \left(z_{\mathrm{H}} m_{\mathrm{H}} - r_{\mathrm{F}} m_{\mathrm{F}}\right) / m_{\mathrm{A}} \tag{3.10}$$

and the moments of inertia along the global axes are taken with respect to the center of mass of the front assembly,

$$I_{\mathrm{A}xx} = I_{\mathrm{H}xx} + I_{\mathrm{F}xx} + m_{\mathrm{H}}\left(z_{\mathrm{H}} - z_{\mathrm{A}}\right)^2 + m_{\mathrm{F}}\left(r_{\mathrm{F}} + z_{\mathrm{A}}\right)^2 \tag{3.11}$$
$$I_{\mathrm{A}xz} = I_{\mathrm{H}xz} - m_{\mathrm{H}}\left(x_{\mathrm{H}} - x_{\mathrm{A}}\right)\left(z_{\mathrm{H}} - z_{\mathrm{A}}\right) + m_{\mathrm{F}}\left(w - x_{\mathrm{A}}\right)\left(r_{\mathrm{F}} + z_{\mathrm{A}}\right) \tag{3.12}$$
$$I_{\mathrm{A}zz} = I_{\mathrm{H}zz} + I_{\mathrm{F}zz} + m_{\mathrm{H}}\left(x_{\mathrm{H}} - x_{\mathrm{A}}\right)^2 + m_{\mathrm{F}}\left(w - x_{\mathrm{A}}\right)^2 \tag{3.13}$$

A perpendicular distance to the steer axis, s, through the headset with angle λ_{s} to the vertical (see figure 3.1a), is defined

$$u_{\mathrm{A}} = \left(x_{\mathrm{A}} - w - c\right)\cos\lambda_{\mathrm{s}} - z_{\mathrm{A}}\sin\lambda_{\mathrm{s}} \tag{3.14}$$

Three special inertia quantities are required which are the moment of inertia around the steer axis and the products of inertia relative to crossed, skew axes, taken about the points where they intersect. The last two give the torque about one axis due to an angular acceleration about the other:

$$I_{\mathrm{Ass}} = m_{\mathrm{A}}u_{\mathrm{A}}^2 + I_{\mathrm{A}xx}\sin^2\lambda_{\mathrm{s}} + 2I_{\mathrm{A}xz}\sin\lambda_{\mathrm{s}}\cos\lambda_{\mathrm{s}} + I_{\mathrm{A}zz}\cos^2\lambda_{\mathrm{s}} \tag{3.15}$$
$$I_{\mathrm{As}x} = -m_{\mathrm{A}}u_{\mathrm{A}}z_{\mathrm{A}} + I_{\mathrm{A}xx}\sin\lambda_{\mathrm{s}} + I_{\mathrm{A}xz}\cos\lambda_{\mathrm{s}} \tag{3.16}$$
$$I_{\mathrm{As}z} = m_{\mathrm{A}}u_{\mathrm{A}}x_{\mathrm{A}} + I_{\mathrm{A}xz}\sin\lambda_{\mathrm{s}} + I_{\mathrm{A}zz}\cos\lambda_{\mathrm{s}} \tag{3.17}$$

A ratio of mechanical trail (i.e. the distance of the front wheel contact point Q perpendicular to the steer axis) to wheel base is

$$\mu = (c/w)\cos\lambda_{\mathrm{s}} \tag{3.18}$$

The wheels are sources of gyroscopic effect and their angular momenta along the y-axis, divided by the forward speed is the gyrostatic coefficient:

$$S_{\mathrm{R}} = I_{\mathrm{R}yy}/r_{\mathrm{R}}\left(= I_{\mathrm{R}yy}\dot{\theta}_{\mathrm{R}}/v\right), \qquad S_{\mathrm{F}} = I_{\mathrm{F}yy}/r_{\mathrm{F}}\left(= I_{\mathrm{F}yy}\dot{\theta}_{\mathrm{F}}/v\right), \qquad S_{\mathrm{T}} = S_{\mathrm{R}} + S_{\mathrm{F}} \tag{3.19}$$

and a frequently appearing static moment term is

$$S_{\mathrm{A}} = m_{\mathrm{A}}u_{\mathrm{A}} + \mu m_{\mathrm{T}}x_{\mathrm{T}} \tag{3.20}$$

Finally, note that also the non-design parameters gravitational acceleration, g, and forward velocity, v, are used in the upcoming equations of motion. Where the gravitational acceleration is defined as positive in the positive z-direction.

Dynamic equations

Now, the dynamic governing equations can be drafted with help of the several defined coefficients [22] [37]. Lateral symmetry of the equations and the bicycle make that straight up and straight ahead bicycle rolling is a solution for any longitudinal velocity, v [22]. Furthermore, with respect to this symmetric solutions, a lateral perturbation to one side must result in the same forward velocity change as a perturbation to the opposite side. However, linearity dictates that the effects need to be the negative of each other and thus there can be no first-order (linear) coupling between lean/steer and forward velocity. Hence, linearized fore-aft EOM are completely decoupled from lateral EOM. The concern for a lateral stability analysis makes that the bicycle lateral motion and thus the lateral equations of motion are of main interest, which due to the linear decoupling has no influence on the forward velocity.

For the derivation, the two lateral ground contact forces, F_y, are first assumed unknown and alongside of the vertical contact forces, the gravity force, and the lean and steer torque, they influence the EOM [37]. Then, the contacts can slip longitudinally and sideways and their position is not directly related to the lean and steer. The non-holonomic constraints later make that the two contact points are only able to move in the direction of the respective wheel headings.

With unknown contact forces, the four lateral global degrees of freedom, rear frame rightward lean ϕ, rightward handlebar steer, δ, the rear frame yaw, ψ, and the y-position of the rear contact point P, y_{P}, are used to find the EOM for the lateral dynamics [22]. Since a linear model is sufficient for stability analyses, the EOM are set up here by an *ad hoc* linearization, around a vertically upright, $\phi = 0$, and straight-ahead, $\delta = 0$, position approximately parallel to the x-axis, $\psi \approx 0$ (y_P = any value). Thus, to only keep first order configuration variables consequences, ϕ, δ, as well as $\dot{y}_\mathrm{P}/v \approx \psi$ are assumed small. Small is here assumed to be $< \pi/9$ for angles such that sines and cosines can be approximated, and products of small quantities are neglected. In effect, the equations as given here only apply for small propulsive and small additional (besides gravity) forces.

The EOM can be derived from force and angular momentum balances. Here, the left side includes conjugate force or moment required to accelerate mass on the bike in whatever motion [22] [37]. The right side includes the applied forces and moments. For the angular momentum, concretely, this means that the left side of the angular momentum balance is the rate of change of angular momentum about the fixed axis and consists of three different kind of terms: the angular momentum due to translational acceleration, the angular momentum due to angular acceleration, and the angular momentum due to gyroscopic effects. Here, the perpendicular distances (arms) of each body center of mass with respect to the fixed axis is needed. The righthand side of the angular momentum balance contains the torques created by external forces. To understand the single terms in the EOM better, one can imagine that only the DOFs concerned with the term under consideration are free and that the rest are held fixed.

The power, P, of all arbitrary forces applied at various bicycle points (sum of products of all those forces with their respective velocity), is a linear combination of the three generalized forces (torques) associated with three velocities that are allowed by the hinge and ground contact constraints [22]:

$$P = T_\phi \dot{\phi} + T_\delta \dot{\delta} + T_{\theta_\mathrm{R}} \dot{\theta}_\mathrm{R} \tag{3.21}$$

General dynamics dictate that virtual power can define the forcing terms [22]. When the velocities in (3.21) are replaced with virtual perturbations of those velocities, the expression for the virtual power is obtained and it can be seen that the torques in (3.21) can be used in the equations of motion as the external applied torques around the different axis. The propulsion torque is often assumed zero to have constant forward velocity such that it also not contributes to the virtual power.

$\boldsymbol{\theta}_\mathrm{R}$ angular momentum balance whole bicycle The linearized EOM for forward motion is derived with simple planar mechanics [22] and although in the linearized case it is decoupled from the lateral motion, it is presented here for some more completeness in the dynamical descriptions. The propulsion torque can be on either wheel, but in this specific case it is on the rear wheel. The linearized equation of the radial rotation angle of the wheel is then simply obtained from two-dimensional mechanics and deals with only one degree of freedom.

$$M_{\theta\mathrm{R}} \ddot{\theta}_\mathrm{R} = T_{\theta_\mathrm{R}} \tag{3.22}$$

with,

$$M_{\theta\mathrm{R}} = r_\mathrm{R}^2 m_\mathrm{T} + I_{\mathrm{R}yy} + (r_\mathrm{R}/r_\mathrm{F})^2 I_{\mathrm{F}yy} \tag{3.23}$$

$\boldsymbol{r_\mathrm{R}^2 m_\mathrm{T} \ddot{\theta}_\mathrm{R}}$ Rear axle moment required to accelerate the total bicycle center of mass longitudinally.

$\boldsymbol{\left(I_{\mathrm{R}yy} + (r_\mathrm{R}/r_\mathrm{F})^2 I_{\mathrm{F}yy}\right) \ddot{\theta}_\mathrm{R}}$ The rear wheel axle moment required to rotationally accelerate the wheels. A difference in radii between the two wheels results in a transmission ratio that makes the rotational speed of the wheels different. This causes that the effective mass moment of inertia of the front wheel is differently 'felt' at the rear wheel axle.

$\boldsymbol{T_{\theta_\mathrm{R}}}$ Propulsive external moment at the rear wheel axle. For most bicycles in normal operation, the main contributor to this moment is the torque on the pedals. But also a forward push or an engine torque (like on a moped or an electrical bicycle) can contribute.

$\boldsymbol{y}$ force balance whole bicycle This EOM can be used with upcoming equations to solve for the lateral rear contact force. The equation describes a simple force balance for a lateral translational motion [37].

$$m_\mathrm{T} \ddot{y}_\mathrm{P} - m_\mathrm{T} \ddot{\phi} z_\mathrm{T} + m_\mathrm{T} \ddot{\psi} x_\mathrm{T} + m_\mathrm{A} \ddot{\delta} u_\mathrm{A} = F_{\mathrm{R}y} + F_{\mathrm{F}y} \tag{3.24}$$

$\boldsymbol{m_\mathrm{T} \ddot{y}_\mathrm{P}}$ Lateral acceleration force total assembly due to lateral acceleration of rear contact only.

$\boldsymbol{-m_\mathrm{T} \ddot{\phi} z_\mathrm{T} + m_\mathrm{T} \ddot{\psi} x_\mathrm{T}}$ The whole bicycle y-acceleration force due to lean and yaw respectively.

$\boldsymbol{m_{\mathrm{A}}\ddot{\delta}u_{\mathrm{A}}}$ The y-acceleration force of the whole bicycle due to steering only.

$\boldsymbol{F_{\mathrm{R}y}+F_{\mathrm{F}y}}$ Lateral contact forces at rear and front contact point respectively.

ϕ angular momentum balance whole bicycle Lean angular momentum balance about the axis in the ground plane that is instantaneously aligned with the rear wheel at its contact point P (axis is aligned with the rear wheel and due to a possible trail and steer motion does not generally passes through front contact Q):

$$-m_{\mathrm{T}}\ddot{y}_{\mathrm{P}}z_{\mathrm{T}}+I_{\mathrm{T}xx}\ddot{\phi}+I_{\mathrm{T}xz}\ddot{\psi}+I_{\mathrm{A}sx}\ddot{\delta}+\dot{\psi}vS_{\mathrm{T}}+\dot{\delta}vS_{\mathrm{F}}\cos\lambda_{\mathrm{s}}=T_{\phi}-gm_{\mathrm{T}}z_{\mathrm{T}}\phi+gS_{\mathrm{A}}\delta \tag{3.25}$$

$\boldsymbol{-m_{\mathrm{T}}\ddot{y}_{\mathrm{P}}z_{\mathrm{T}}}$ ($C_{1\phi\delta}$, $K_{2\phi\delta}$) The ϕ moment required for accelerating the center of mass of the whole total assembly laterally.

$\boldsymbol{I_{\mathrm{T}xx}\ddot{\phi}}$ ($M_{\phi\phi}$) The ϕ moment required for angular accelerating ($\ddot{\phi}$) the total assembly about point P about the lean axis.

$\boldsymbol{I_{\mathrm{T}xz}\ddot{\psi}}$ ($M_{\phi\delta}$, $C_{1\phi\delta}$) The ϕ moment required for angular accelerating ($\ddot{\psi}$) the total assembly about point P about the yaw axis.

$\boldsymbol{I_{\mathrm{A}sx}\ddot{\delta}}$ ($M_{\phi\delta}$) The ϕ moment required for angular accelerating of the front assembly about the steer axis.

$\boldsymbol{\dot{\psi}vS_{\mathrm{T}}}$ ($C_{1\phi\delta}$, $K_{2\phi\delta}$) The gyroscopic ϕ moment required for yawing of the whole bike about a vertical axis.

$\boldsymbol{\dot{\delta}vS_{\mathrm{F}}\cos\lambda_{\mathrm{s}}}$ ($C_{1\phi\delta}$) The gyroscopic ϕ moment required for the precession of the front wheel about the vertical axis of the front wheel.

$\boldsymbol{T_{\phi}}$ Externally applied generalized lean moment on the rear frame abound the ground contact line, or the work-conjugate of bicycle lean [16]. With a rigid rider this cannot be caused by rider upper body lean. A sideways wind gust or someone helping another one on a bicycle to hold it upright or pushing it over sideways are the main causes for such a moment. In control terms, this moment is not practically implemented as a control measure, because it has to be applied from outside the bicycle/rider system.

$\boldsymbol{-gm_{\mathrm{T}}z_{\mathrm{T}}\phi}$ ($K_{0\phi\phi}$) The moment of the gravity force acting at the center of mass of the total bicycle when it only leans.

$\boldsymbol{gS_{\mathrm{A}}\delta}$ ($K_{0\phi\delta}$) The moment of gravity force acting at the center of mass of the front assembly when the bicycle only steers. Plus the moment of the vertical front contact force which is offset from the horizontal ground axis aligned with the rear wheel due to steer (by means of the trail) only.

ψ angular momentum balance whole bicycle Yaw angular momentum balance for the whole bicycle about the z-axis, which is vertical for small angles, that instantaneously passes through point P.

$$m_{\mathrm{T}}\ddot{y}_{\mathrm{P}}x_{\mathrm{T}}+I_{\mathrm{T}xz}\ddot{\phi}+I_{\mathrm{T}zz}\ddot{\psi}+I_{\mathrm{A}sz}\ddot{\delta}-\dot{\phi}vS_{\mathrm{T}}-\dot{\delta}vS_{\mathrm{F}}\sin\lambda_{\mathrm{s}}=wF_{\mathrm{F}y} \tag{3.26}$$

$\boldsymbol{m_{\mathrm{T}}\ddot{y}_{\mathrm{P}}x_{\mathrm{T}}}$ ($C_{1\delta\delta}$, $K_{2\delta\delta}$) The ψ moment required for accelerating the center of mass of the whole total assembly laterally.

$\boldsymbol{I_{\mathrm{T}xz}\ddot{\phi}}$ ($M_{\delta\phi}$) The ψ moment required for angular accelerating ($\ddot{\phi}$) the total assembly about a horizontal axis through point P.

$\boldsymbol{I_{\mathrm{T}zz}\ddot{\psi}}$ ($M_{\delta\delta}$, $C_{1\delta\delta}$) The ψ moment required for angular accelerating ($\ddot{\psi}$) the total assembly about a vertical axis through point P.

$\boldsymbol{I_{\mathrm{A}sz}\ddot{\delta}}$ ($M_{\delta\delta}$) The ψ moment required for angular accelerating of the front assembly about the steer axis.

$\boldsymbol{-\dot{\phi}vS_{\mathrm{T}}}$ ($C_{1\delta\phi}$) The gyroscopic ψ moment required for rolling of the whole bicycle about the rear assembly heading line.

$\boldsymbol{-\dot{\delta}vS_{\mathrm{F}}\sin\lambda_{\mathrm{s}}}$ ($C_{1\delta\delta}$) The precession of the front wheel about the horizontal axis of the steered front wheel.

$\boldsymbol{wF_{\mathrm{F}_y}}$ External yaw torque due to the lateral ground force at front wheel contact point.

δ angular momentum balance front assembly Steer angular momentum balance for the whole bicycle about a fixed axis that instantaneously aligned with the steer axis.

$$m_{\mathrm{A}}\ddot{y}_{\mathrm{P}}u_{\mathrm{A}} + I_{\mathrm{A}sx}\ddot{\phi} + I_{\mathrm{A}sz}\ddot{\psi} + I_{\mathrm{Ass}}\ddot{\delta} + vS_{\mathrm{F}}\left(-\dot{\phi}\cos\lambda_{\mathrm{s}} + \dot{\psi}\sin\lambda_{\mathrm{s}}\right) \\ = T_{\delta} - cF_{\mathrm{F}y}\cos\lambda_{\mathrm{s}} + g\left(\phi + \delta\sin\lambda_{\mathrm{s}}\right)S_{\mathrm{A}} \quad (3.27)$$

$\boldsymbol{m_{\mathrm{A}}\ddot{y}_{\mathrm{P}}u_{\mathrm{A}}}$ ($C_{1\delta\delta}$, $K_{2\delta\delta}$) The δ moment required for accelerating the center of mass of the front assembly laterally.

$\boldsymbol{I_{\mathrm{A}sx}\ddot{\phi}}$ ($M_{\delta\phi}$) The δ moments required for angular accelerating ($\ddot{\phi}$) the total front assembly about the x-axis. Required moment about one axis for angular acceleration about another axis is the same is the same as the required moment for the reversed case.

$\boldsymbol{I_{\mathrm{A}sz}\ddot{\psi}}$ ($M_{\delta\delta}$, $C_{1\delta\delta}$) The δ moments required for angular accelerating ($\ddot{\psi}$) the total front assembly about the z-axis.

$\boldsymbol{I_{\mathrm{Ass}}\ddot{\delta}}$ ($M_{\delta\delta}$) The δ moment required for angular accelerating of the front assembly about the steer axis.

$\boldsymbol{vS_{\mathrm{F}}\left(-\dot{\phi}\cos\lambda_{\mathrm{s}} + \dot{\psi}\sin\lambda_{\mathrm{s}}\right)}$ ($C_{1\delta\phi}$, $C_{1\delta\delta}$, $K_{2\delta\delta}$) The gyroscopic δ moment required for precession about an axis in the bicycle plane perpendicular to the steer axis.

$\boldsymbol{T_{\delta}}$ Internally applied generalized steering torque. This work-conjugate of steer acts positively on the front assembly and negatively on the rear assembly [16]. The rider applies this torque on the handlebars. Alternatively, another controlling mechanism can be implemented that applies this torque to the handlebars.

$\boldsymbol{-cF_{\mathrm{F}_y}\cos\lambda_{\mathrm{s}}}$ Torque from the unknown lateral contact force on the front assembly.

$\boldsymbol{g\left(\phi + \delta\sin\lambda_{\mathrm{s}}\right)S_{\mathrm{A}}}$ ($K_{0\delta\phi}$, $K_{0\delta\delta}$) Torque from the gravity force on the the front assembly leaned by angle $(\phi + \delta\sin\lambda)$.

Kinematic equations

For a no slip (infinite friction force availability) assumption, the geometry of a bicycle determines how different rotations and translations are related in a kinematic sense. This relations are described by non-holonomic (rolling) constraints. As was done for the dynamical equations, also here the angles are assumed small to obtain simple linear expressions. Moreover, the constraints are not presented here in the order of derivation by Meijaard *et al.*, but are grouped together for clarity. Furthermore, some angles that appear throughout the EOM and that are also useful in upcoming analyses are presented.

Generally, the angles of the rear assembly are presented, but also the front assembly angles are of interest. These global lean and yaw angles and angular rates of the assemblies are equal to those of separate bicycle parts. Rear wheel and rear frame lean and yaw angle (and rate) are equal to the rear assembly lean and yaw angle (and rate),

$$\begin{cases} \phi = \phi_{\mathrm{R}} = \phi_{\mathrm{B}} \\ \psi = \psi_{\mathrm{R}} = \psi_{\mathrm{B}} \end{cases} \quad (3.28)$$

And the front frame and front wheel lean and yaw angle (and rate) are equal to those angles (and rates) of front assembly, A,

$$\begin{cases} \phi_{\mathrm{A}} = \phi_{\mathrm{H}} = \phi_{\mathrm{F}} \\ \psi_{\mathrm{A}} = \psi_{\mathrm{H}} = \psi_{\mathrm{F}} \end{cases} \quad (3.29)$$

Forward velocity With the no-slipping assumed, the forward speed and wheel angular velocity are directly. Note that with no propulsive force, which is not generally the case, the forward velocity is constant.

$$v = -\dot{\theta}_{\mathrm{R}}\, r_{\mathrm{R}} = -\dot{\theta}_{\mathrm{F}}\, r_{\mathrm{F}} \quad (3.30)$$

Projected steer The projected true (ground) steer angle appears in many terms of the EOM. Due to the steer axis angle, the steer angle around the steer axis is projected generally smaller on the ground (see figure 3.2):

$$\delta^* = \delta \cos \lambda_s \tag{3.31}$$

Rear assembly yaw/heading In the end the global rear yaw (or heading) angle (see figure 3.2) is an ignorable coordinate (can have any value), but for now it is assumed small to make the derivation easier, so $\psi \approx 0$. The rates and accelerations of the yaw angle do appear in the EOM and with the no-slip can be expressed as function of the steer angle.

$$\dot{\psi} = ((v\delta + c\dot{\delta})/w) \cos \lambda_s \tag{3.32}$$

$$\ddot{\psi} = ((v\dot{\delta} + c\ddot{\delta})/w) \cos \lambda_s \tag{3.33}$$

Rear contact The coordinates are ignorable and can have any value without influencing the local lateral motion, so (x_P, y_P) can have any value. In the linear domain and for the small assumed yaw angle, the velocities and accelerations in the x-direction are constant, and in first order those in the y-direction are linearly dependent on the bicycle rear yaw angle (see figure 3.2):

$$\dot{x}_P = v \quad , \quad \dot{y}_P = v\psi \tag{3.34}$$

$$\ddot{x}_P = 0 \quad , \quad \ddot{y}_P = v\dot{\psi} = ((v^2\delta + vc\dot{\delta})/w) \cos \lambda_s \tag{3.35}$$

Front assembly lean The front assembly, A, or equivalently the front frame or front wheel, have their own global lean and yaw angle, because both, front frame and front wheel, yaw about a vertical axis through the front wheel contact point. The lean angle of the front assembly is almost the same as the rear frame and wheel, because the roll axes are coincident. Only a projection of the steer angle on the rear frame lean angle has to be added. The equations for the front frame lean in the global frame are then [22],

$$\phi_A = \phi + \delta \sin \lambda_s \tag{3.36}$$

$$\dot{\phi}_A = \dot{\phi} + \dot{\delta} \sin \lambda_s \tag{3.37}$$

Front assembly yaw/heading Likewise, the small assumed front yaw angle is a linear combination of the small rear yaw angle and the true steer angle. For both global coordinates rear (ψ) and front (ψ_A) assembly yaw, the velocity dependent component of the yaw rate is the same, because at one specific steer angle the bicycle yaws as one whole body. However, the steer rate dependent part is different for the front yaw rate, because its yawing axis is not coincident with the rear frame yaw angle axis. In figures 3.1b and 3.2 it can be seen that a positive steer angular rate has a positive effect on the rear yaw rate when the trail is positive (clockwise steer rotates rear frame also clockwise with positive front trail). The effect on the front yaw rate is equal and thus the steer rate also adds positively to the front yaw rate with positive front trail. However, the scaling is different which makes that the length from the steer axis ground intersection point to the rear wheel, $w + c$, must be used in stead of length from that point to the front wheel, c.

$$\psi_A = \psi + \delta \cos \lambda_s \tag{3.38}$$

$$\dot{\psi}_A = \dot{\psi} + \dot{\delta} \cos \lambda_s = ((v\delta + (w + c)\dot{\delta})/w) \cos \lambda_s \tag{3.39}$$

Front contact The global front contact coordinates, velocities and accelerations for small yaw angles are those of the rear frame augmented with terms dependent on the front frame yaw:

$$x_Q = x_P + w \quad , \quad y_Q = y_P + w\psi - c\delta\cos\lambda_s \tag{3.40}$$

$$\dot{x}_Q = v \quad , \quad \dot{y}_Q = \dot{y}_P + w\dot{\psi} - c\dot{\delta}\cos\lambda_s = v(\psi + \delta\cos\lambda_s) \tag{3.41}$$

$$\ddot{x}_Q = 0 \quad , \quad \ddot{y}_Q = \ddot{y}_P + w\ddot{\psi} - c\ddot{\delta}\cos\lambda_s = ((v^2\delta + v(c+w)\dot{\delta})/w)\cos\lambda_s \tag{3.42}$$

Mechanical 'Lean and Steer' equations

By substituting the necessary non-holonomic rolling constraints into the equations, the heading, ψ, and lateral position, y_P are eliminated and equations are obtained that are only expressed in lean and steer and their respective derivatives [22]. Then, equation (3.25) turns into the so called lean equation. If then also equations (3.26) and (3.27) are combined to eliminate the front wheel lateral force, the steer equation is obtained. Finally, the terms of the two equations are rearranged to put them in the neat mechanical equations form to give the fourth-order (highest derivative in equations times the number of degrees of freedom) bicycle model for the two degree of freedom lateral motion:

$$\mathbf{M}\ddot{\mathbf{q}} + v\mathbf{C}_1\dot{\mathbf{q}} + \left[g\mathbf{K}_0 + v^2\mathbf{K}_2\right]\mathbf{q} = \mathbf{f} \tag{3.43}$$

with time-varying quantities,

$$\mathbf{q} = \begin{bmatrix} \phi \\ \delta \end{bmatrix} \quad , \quad \mathbf{f} = \begin{bmatrix} T_\phi \\ T_\delta \end{bmatrix} \tag{3.44}$$

Here, the torques are the generalized forces on the system and all other external forces can be translated to these two forces. Note further that the linearity requires that the equations only hold for turns with a large radius of curvature where the bicycle stays in the linear regime. The angles in the equations of motion may not be too large. The matrices are constructed in terms of the 25 parameters and the subscripts are such that they match the multipliers of the corresponding v. The trail, the steer axis angle, the gyroscopic terms from rotation of the wheels, and the mass distribution of front and rear assembly are all responsible for the coupling of the roll angle to the steer equation [46]. For the coupling of the steer angle to the roll equation, the same parameters are important, although the degree to which they contribute may be different. Furthermore, the qualitative and quantitative contribution of all of the parameters may differ among different bicycle designs and can even change with varying forward velocity as can be clearly seen next for the separate explanations of the matrices.

Mass matrix A symmetric positive-definite matrix giving the kinetic energy at zero forward speed by $\dot{\mathbf{q}}^\intercal\mathbf{M}\dot{\mathbf{q}}/2$.

$$\begin{gathered} M_{\phi\phi} = I_{\mathrm{T}xx} \quad , \quad M_{\phi\delta} = I_{\mathrm{A}sx} + \mu I_{\mathrm{T}xz} \\ M_{\delta\phi} = M_{\phi\delta} \quad , \quad M_{\delta\delta} = I_{\mathrm{Ass}} + 2\mu I_{\mathrm{A}sz} + \mu^2 I_{\mathrm{T}zz} \\ \mathbf{M} = \begin{bmatrix} M_{\phi\phi} & M_{\phi\delta} \\ M_{\delta\phi} & M_{\delta\delta} \end{bmatrix} \end{gathered} \tag{3.45}$$

The first entry is simply the total mass moment of inertia of the whole assembly. It is used to calculate the lean moment required for angular lean accelerating about the rear contact point P. The second entry is the mass moment of inertia of the front assembly coupling the steer angular acceleration to the lean angular acceleration. Added is the moment of inertia of the total assembly coupling the steer angular acceleration to the lean angular acceleration by multiplicating the mechanical trail to wheelbase ratio, μ, in order to obtain the yaw acceleration around point P from the steer acceleration. The third entry is identical to the second one since the coupling in accelerations is the same the other way around. Specifically, the μ comes now from the ratio of arms between the front lateral force to the steer axis and to the vertical axis through P. Finally, the fourth entry is a translation of all angular accelerations to the steer axis. It is made up of a front assembly mass moment of inertia about the steering axis. A mass moment of inertia corresponding to the required total assembly yaw moment to steer the front assembly and the steer moment required to yaw the front assembly. And a total assembly mass moment of inertia multiplicated by μ^2 in order to translate the total assembly yaw angular acceleration to the steer angular acceleration.

Velocity-dependent 'damping' matrix Damping-like matrix which is linear with the forward speed in the equations of motion: $v\mathbf{C}_1$. The matrix deals with gyroscopic torques from steer and lean rate, inertial reactions of the rear frame yaw rate due to trail effects, and inertial reactions from yaw acceleration which is proportional to steer rate.

$$
\begin{aligned}
&C_{1\phi\phi} = 0 \quad , \quad C_{1\phi\delta} = \mu S_\mathrm{T} + S_\mathrm{F}\cos\lambda_\mathrm{s} + (I_{\mathrm{T}xz}/w)\cos\lambda_\mathrm{s} - \mu m_\mathrm{T} z_\mathrm{T} \\
&C_{1\delta\phi} = -\left(\mu S_\mathrm{T} + S_\mathrm{F}\cos\lambda_\mathrm{s}\right) \quad , \quad C_{1\delta\delta} = (I_{\mathrm{A}sz}/w)\cos\lambda_\mathrm{s} + \mu\left(S_\mathrm{A} + (I_{\mathrm{T}zz}/w)\cos\lambda_\mathrm{s}\right) \\
&\mathbf{C}_1 = \begin{bmatrix} C_{1\phi\phi} & C_{1\phi\delta} \\ C_{1\delta\phi} & C_{1\delta\delta} \end{bmatrix}
\end{aligned}
\tag{3.46}
$$

The first entry of the damping matrix is always zero. The lean rate does not contribute to the lean torque since gyroscopy only effects in perpendicular direction. The second entry of the matrix contains the steer rate contributions to the lean torque. Two terms are associated with the gyrostatic coefficients of the bicycle and come into the equations from the steer rate induced yaw rate gyroscopic lean torque. The remaining terms come from an inertial reaction of the whole bicycle due to a steer rate induced translational acceleration and a steer rate induced yawing acceleration of the bicycle. The third entry contains solely the gyroscopic effect of the lean rate on the yaw angular momentum translated to a steering torque. Finally, the fourth entry contains a steer rate induced yawing acceleration of the total assembly that contains the wheel inertia (yaw is translated into steer). Furthermore, the S_A coefficient shows up in this entry and deals with the steer rate induced lateral acceleration which results in a whole bicycle yaw torque (which is translated to a steer torque) and a steer torque. Note, that here the front wheel gyrostatic coefficient does not show up because it affects the yaw angular momentum negatively and the steer angular momentum positively such that these effects cancel out.

Gravity-dependent stiffness matrix A velocity-independent symmetric matrix proportional to the gravitational acceleration; $g\mathbf{K_0}$. The entries of this matrix can be used to analyse a static (unstable) equilibrium of the bicycle, because it can be used for calculating changes in potential energy with $\mathbf{q}^\intercal\left[g\mathbf{K}_0\right]\mathbf{q}/2$.

$$
\begin{aligned}
&K_{0\phi\phi} = m_\mathrm{T} z_\mathrm{T} \quad , \quad K_{0\phi\delta} = -S_\mathrm{A} \\
&K_{0\delta\phi} = K_{0\phi\delta} \quad , \quad K_{0\delta\delta} = -S_\mathrm{A}\sin\lambda_\mathrm{s} \\
&\mathbf{K}_0 = \begin{bmatrix} K_{0\phi\phi} & K_{0\phi\delta} \\ K_{0\delta\phi} & K_{0\delta\delta} \end{bmatrix}
\end{aligned}
\tag{3.47}
$$

The first entry is used to calculate the lean torque when the bicycle is solely leaned, i.e. no steering. This is just the separate mass times the corresponding arm multiplied by the lean angle. The second entry is the lean torque due to steering only. By steering the front assembly, this front assembly mass and in effect the total mass are offset from the horizontal line parallel to the rear wheel and through the rear contact point. The third entry is equal to the second, because a lean only motion requires a steer torque that counteracts the tendency to steer due to the front fork mass. the fourth entry captures that a steering movement only does result in a torque about the steering axis. A nonzero steer axis angle makes that there is a certain point when the bicycle is at a potential energy minimum such that the mass can be lifted by solely steering which introduces a recovering steer torque.

Velocity-dependent stiffness matrix A non-symmetric stiffness matrix due to gyroscopic and centrifugal effects (centripetal force induced) due to cornering motion which is proportional to the quadratic forward speed; $v^2\mathbf{K}_2$.

$$
\begin{aligned}
&K_{2\phi\phi} = 0 \quad , \quad K_{2\phi\delta} = \left(\left(S_\mathrm{T} - m_\mathrm{T} z_\mathrm{T}\right)/w\right)\cos\lambda_\mathrm{s} \\
&K_{2\delta\phi} = 0 \quad , \quad K_{2\delta\delta} = \left(\left(S_\mathrm{A} + S_\mathrm{F}\sin\lambda\right)/w\right)\cos\lambda_\mathrm{s} \\
&\mathbf{K}_2 = \begin{bmatrix} K_{2\phi\phi} & K_{2\phi\delta} \\ K_{2\delta\phi} & K_{2\delta\delta} \end{bmatrix}
\end{aligned}
\tag{3.48}
$$

The first entry is always zero, because only leaning does not introduce a centrifugal effect (no cornering) and the gyroscopy of the wheel works only on perpendicular axes. The second entry captures the lean torque corresponding with a steer angle in combination with a forward speed. With a forward speed, the wheels are spinning around their central y-axles and together with the z-axis yaw motion due to the steer angle, a gyroscopic precession moment around the remaining lean axis is created. Furthermore, a lean torque is required to counteract centrifugal forces pushing the bicycle out of the corner about the lean axis when only steering is prescribed. The third entry is always zero, because lean angle only has no velocity dependent effect on the steer torque. Finally, The fourth term includes the steering torque required to counteract the centrifugal force created by the front fork and total bicycle mass in a corner as well as the front wheel precession about the steer axis. Here, the total bicycle mass contributes by the trail to wheelbase ratio.

3.2 Transformation of generalized coordinates

A transformation to other generalized coordinates can be done by plugging a transformation multiplication in the mechanical equations (3.43). For new coordinates, for example coordinates of the several parts depicted by a pre-subscript $p(=\mathrm{R, B, H, F, A}$, see figure 3.1), the transformation is

$$\mathbf{q} = {}_p\mathbf{T}\ {}_p\mathbf{q} \tag{3.49}$$

However, preservation of the power balance (3.21) [22] prescribes that the generalized forces in the new coordinates of the several parts are related to the old coordinates with the transpose of the transformation matrix in order to summate the power of all separate degrees of freedom:

$${}_p\mathbf{f} = {}_p\mathbf{T}^\intercal\ \mathbf{f} \tag{3.50}$$

Therefore, both the generalized coordinates and the forces need to be multiplied by the transformation matrix for a coordinates translation. Bringing all transformations to one side of the lean and steer equations (3.43) then gives the equations in the new set of coordinates and forces with transformed mass, damper and stiffness matrices:

$${}_p\mathbf{M}\ {}_p\ddot{\mathbf{q}} + v\ {}_p\mathbf{C}_1\ {}_p\dot{\mathbf{q}} + \left[g\ {}_p\mathbf{K}_0\ + v^2\ {}_p\mathbf{K}_2\right]\ {}_p\mathbf{q} = {}_p\mathbf{f} \tag{3.51}$$

where,

$$\begin{aligned}
{}_p\mathbf{M} &= {}_p\mathbf{T}^\intercal\ \mathbf{M}\ {}_p\mathbf{T} \\
{}_p\mathbf{C}_1 &= {}_p\mathbf{T}^\intercal\ \mathbf{C}_1\ {}_p\mathbf{T} \\
{}_p\mathbf{K}_0 &= {}_p\mathbf{T}^\intercal\ \mathbf{K}_0\ {}_p\mathbf{T} \\
{}_p\mathbf{K}_2 &= {}_p\mathbf{T}^\intercal\ \mathbf{K}_2\ {}_p\mathbf{T}
\end{aligned} \tag{3.52}$$

Bicycle local coordinates

Sometimes it might be interesting to look at the coordinate angles of a bicycle part in the bicycle local frame with x-axis through the two contact points (so x-axis not necessarily aligned with rear wheel). The yaw angles in the global coordinate system are ignorable coordinates since they do not show up in the final lateral mechanical equations; they can have any value and the EOM will still be satisfied. However, in the local frame, the both lean and yaw are completely defined by the global lean and steer angle: The lean angles in the local frame for both wheels are only different from the lean angle in the global frame for the front assembly, but the yaw angles in the local frame are for both assemblies determined from the steer angle by some transmission ratio due to the trail and wheel base (see figure 3.2).

The coordinates in the local frame are depicted by a pre-subscript symbol where the exact symbol is dependent on the specific part under consideration. For the rear wheel (or equivalently rear frame or rear assembly) the lean and yaw angle in the local frame can then be written as,

$${}_\mathrm{R}\phi = \phi \tag{3.53}$$

$${}_\mathrm{R}\psi = (c/w)\delta\cos\lambda_\mathrm{s} \tag{3.54}$$

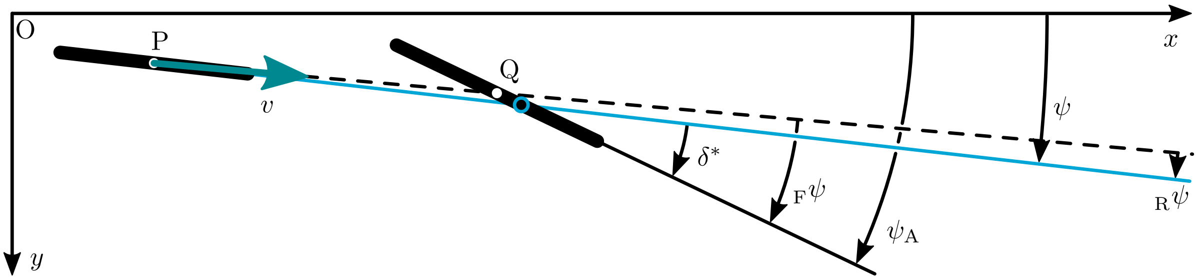

Figure 3.2: The heading (yaw) angles for the benchmark bicycle. The support line through contacts P and Q is depicted by a dashed line, while the rear and front wheel heading are respectively depicted by a solid cyan and black line. The ground projected steer angle, δ^*, creates the local rear heading angle, ${}_{\mathrm{R}}\psi$, and the local front heading angle, ${}_{\mathrm{F}}\psi$. The global rear heading, ψ, and front assembly heading, ψ_{A}, are not directly affected by the steer angle and can generally have any value.

This results can be put in a transformation matrix form to obtain a transformation from the standard benchmark coordinates to bicycle local frame rear wheel angles:

$$\begin{bmatrix} {}_{\mathrm{R}}\phi \\ {}_{\mathrm{R}}\psi \end{bmatrix} = \begin{bmatrix} 1 & 0 \\ 0 & \frac{c}{w}\cos\lambda_{\mathrm{s}} \end{bmatrix} \begin{bmatrix} \phi \\ \delta \end{bmatrix}, \quad {}_{\mathrm{R}}\mathbf{q} = {}_{\mathrm{R}}\mathbf{T}^{-1}\mathbf{q} \quad \rightarrow \quad \mathbf{q} = {}_{\mathrm{R}}\mathbf{T}\,{}_{\mathrm{R}}\mathbf{q} \tag{3.55}$$

The global yaw rate of the rear and front assembly can be calculated from the local yaw in a similar way as it is related to the steer angle in (3.32) and (3.39):

$$\dot{\psi} = {}_{\mathrm{R}}\dot{\psi} + \frac{v}{c}\,{}_{\mathrm{R}}\psi \tag{3.56}$$

$$\dot{\psi}_{\mathrm{A}} = \left(1 + \frac{w}{c}\right){}_{\mathrm{R}}\dot{\psi} + \frac{v}{c}\,{}_{\mathrm{R}}\psi \tag{3.57}$$

Similarly, the local front wheel (or equivalently front frame or front assembly) lean and yaw angle can be obtained with reference to global frame angles (3.36) and (3.38):

$${}_{\mathrm{F}}\phi = \phi + \delta\sin\lambda_{\mathrm{s}} \tag{3.58}$$

$${}_{\mathrm{F}}\psi = {}_{\mathrm{R}}\psi + \delta\cos\lambda_{\mathrm{s}} = (1 + (c/w))\,\delta\cos\lambda_{\mathrm{s}} \tag{3.59}$$

And also these can be put in a transformation form:

$$\begin{bmatrix} {}_{\mathrm{F}}\phi \\ {}_{\mathrm{F}}\psi \end{bmatrix} = \begin{bmatrix} 1 & \sin\lambda_{\mathrm{s}} \\ 0 & (1 + \frac{c}{w})\cos\lambda_{\mathrm{s}} \end{bmatrix} \begin{bmatrix} \phi \\ \delta \end{bmatrix}, \quad {}_{\mathrm{F}}\mathbf{q} = {}_{\mathrm{F}}\mathbf{T}^{-1}\mathbf{q} \quad \rightarrow \quad \mathbf{q} = {}_{\mathrm{F}}\mathbf{T}\,{}_{\mathrm{F}}\mathbf{q} \tag{3.60}$$

The global yaws are then,

$$\dot{\psi} = \frac{c}{c+w}\,{}_{\mathrm{F}}\dot{\psi} + \frac{v}{c+w}\,{}_{\mathrm{F}}\psi \tag{3.61}$$

$$\dot{\psi}_{\mathrm{A}} = {}_{\mathrm{F}}\dot{\psi} + \frac{v}{c+w}\,{}_{\mathrm{F}}\psi \tag{3.62}$$

3.3 Linear controller

A controller can be added to the mechanical equations (3.43) in order to investigate the behavior of all facets of a system under influence of certain inputs. Here, a rather general controller is added to the system; a linear time-invariant Proportional-Derivative-controller (PD-controller) that allows for a full state (both the degrees of freedom and their derivatives) feedback law on all inputs. Note that, since there is no input of the global coordinates of the bicycle, this controller is not suitable for path following. However, a reference torque can be followed such that the control law with a reference, $\mathbf{f}_{\mathrm{r}}$, input to the system is,

$$\mathbf{f} = \begin{bmatrix} T_\phi \\ T_\delta \end{bmatrix} = \mathbf{N}\mathbf{f}_{\mathrm{r}} - \mathbf{K}\begin{bmatrix} \dot{\mathbf{q}} \\ \mathbf{q} \end{bmatrix} = \mathbf{N}\begin{bmatrix} T_{\phi\mathrm{r}} \\ T_{\delta\mathrm{r}} \end{bmatrix} - \mathbf{K}\begin{bmatrix} \dot{\mathbf{q}} \\ \mathbf{q} \end{bmatrix} \tag{3.63}$$

with feedback gain matrix,

$$\mathbf{K} = [\mathbf{C}_\mathrm{f}\,\mathbf{K}_\mathrm{f}] = \begin{bmatrix} C_{\mathrm{f}\phi\phi} & C_{\mathrm{f}\phi\delta} & K_{\mathrm{f}\phi\phi} & K_{\mathrm{f}\phi\delta} \\ C_{\mathrm{f}\delta\phi} & C_{\mathrm{f}\delta\delta} & K_{\mathrm{f}\delta\phi} & K_{\mathrm{f}\delta\delta} \end{bmatrix}, \tag{3.64}$$

and a reference gain matrix to correct for a steady-state error in the final output value compared with the reference torques [41],

$$\mathbf{N} = \begin{bmatrix} N_{\phi\phi} & N_{\phi\delta} \\ N_{\delta\phi} & N_{\delta\delta} \end{bmatrix}, \tag{3.65}$$

In order to obtain information about the system's own dynamics with the control included, the control law can be plugged into the bicycle model equations (3.43). The control then alters the dynamics of the total system and its reaction on an applied input external force reference. However, because the matrices have constant entries without adaptive control, the system remains a linear time-invariant system with equations of motion,

$$\mathbf{M}\ddot{\mathbf{q}} + [\mathbf{C}_\mathrm{f} + v\mathbf{C}_1]\,\dot{\mathbf{q}} + \left[g\mathbf{K}_0 + \mathbf{K}_\mathrm{f} + v^2\mathbf{K}_2\right]\mathbf{q} = \mathbf{N}\mathbf{f}_\mathrm{r}, \tag{3.66}$$

The feedback gains can be chosen such that certain dynamical behavior is present. For example, it is often important that the system is stabilized. When stabilization has to be done one way or another, the exact control manner is not important and so this simple controller with appropriate gains is convenient to use. Moreover, in general, with simply just a reference, the system will not end up at the desired (torque) reference value, because the obtained output is never compared to the exact reference [41]. The reference gains can then be used to correct for the error between output torques and its desired reference values. Methods to determine desired values of the gains are discussed later on in section 4.4 and 4.5.

3.4 State-space representation

The linear time-invariant system can be put in the state-space representation [41] by rewriting the equations of motion into a set of first order differential equations. This representation provides tools for both (control) stability (section 4.4) and time response (section 5.1 and 5.3) analyses. Stability with or without control can be investigated and this along with integration to time is done easily in software such as Matlab. Here, a time-invariant version can be used since the matrices are independent of time. The state-space form of a system with state, $\mathbf{x}$, and input, $\mathbf{u}$, looks as,

$$\begin{aligned} \dot{\mathbf{x}}(t) &= \mathbf{A}\mathbf{x}(t) + \mathbf{B}\mathbf{u}(t) \\ \mathbf{y}(t) &= \mathbf{C}\mathbf{x}(t) + \mathbf{D}\mathbf{u}(t) \end{aligned} \tag{3.67}$$

A state-feedback can be included as input to change system dynamical characteristics by means of control with reference, $\mathbf{r}$, reference gains, (3.65), and feedback gains, (3.64):

$$\mathbf{u}(t) = \mathbf{N}\mathbf{r}(t) - \mathbf{K}\mathbf{x}(t) \tag{3.68}$$

In Matlab the state space system can be created with the function `ss`, and tools are available for a simple check of, for example, stability or controllability (or observability). For a time response analysis, the input needs to be the system initial state conditions, the reference actuation and a specification for the time. The output and state as function of time are then the obtained results. Moreover, the system can be represented in a block diagram as shown in figure 3.3 where the in- and outputs can be identified.

In the case of the bicycle equations (3.43) the state, input and reference are,

$$\mathbf{x} = \begin{bmatrix} \dot{\mathbf{q}} \\ \mathbf{q} \end{bmatrix}, \quad \mathbf{u} = \mathbf{f} = \begin{bmatrix} T_\phi \\ T_\delta \end{bmatrix}, \quad \mathbf{r} = \mathbf{f}_\mathrm{r} = \begin{bmatrix} T_{\phi r} \\ T_{\delta r} \end{bmatrix} \tag{3.69}$$

And the state-space matrices for the system can be constructed from (3.43) with the output chosen to be the two external input torques:

$$\begin{aligned} \mathbf{A} &= \begin{bmatrix} -\mathbf{M}^{-1}v\mathbf{C}_1 & -\mathbf{M}^{-1}\left[g\mathbf{K}_0 + v^2\mathbf{K}_2\right] \\ \mathbf{I} & \mathbf{0} \end{bmatrix}, & \mathbf{B} &= \begin{bmatrix} \mathbf{M}^{-1} \\ \mathbf{0} \end{bmatrix} \\ \mathbf{C} &= \mathbf{0}, & \mathbf{D} &= \mathbf{I} \end{aligned} \tag{3.70}$$

Here, $\mathbf{0}$ and $\mathbf{I}$ are a zero and an identity matrix respectively of size 2×2.

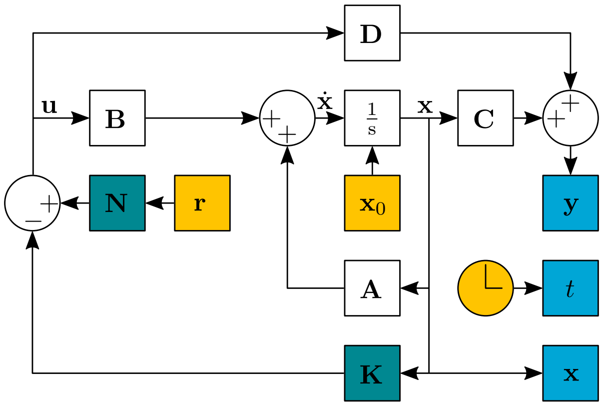

Figure 3.3: Block diagram for the state space representation of a linear time-invariant system with state feedback implementable in, for example, the Simulink software. The state-space matrices **A** and **B** are dependent on the system dynamics with respect to state x and input **u**, whereas the matrices **C** and **D** are determined by the desired output **y**. A possible state-feedback control can be implemented with feedback gains matrix **K** and reference gains matrix **N**. Stability characteristics are determined completely by the four state-space and two control matrices, but for a time response analysis one has to specify reference values, **r**, initial conditions (integration constants), $\mathbf{x}_0$, and time requirements. The system then gives the output as well as the state, both as function of time t.

3.5 Obtaining bicycle parameters

To determine the dynamical qualities of bicycle designs, one requires the 25 benchmark parameters of such a bicycle. Parameters can be obtained by measuring real-life bicycles or by calculating them from a design by using geometry and material density, whether or not aided by (CAD-)software. When a (rigid) rider needs to be included, he/she needs can be everywhere on the bicycle (no hands on handlebar and feet off the ground) wherever possible, and the parameters need to be included into the frame parameters on which he/she is seated.

Experimental measuring

The parameters can be collected by using several methods that are different per kind of parameter [60] (also shortly described in [61] including determination of rider parameters). The here presented methods and calculations are as complete and general for all kinds of bicycles as possible. During the measurements correct tire pressure is important, as well as the presence or absence of a rider.

Wheel radii

The effective wheel radii can be determined by measuring the traversed distance for a certain natural number of wheel rotations. This can be done by placing a long ruler on a flat ground and marking one point on the wheel. Then, by counting the number of rotations, $\mathcal{N}_\theta$, and measuring the traveled distance (displacement), $\mathcal{S}$, the wheel radii can be obtained for either wheel, $p(=\mathrm{R},\mathrm{F})$ by

$$r_p = \frac{\mathcal{S}}{2\pi\mathcal{N}_{\theta,p}} \tag{3.71}$$

Steer axis angle

Measuring the headtube angle, λ_h, between the ground and the headtube is the easiest way of measuring the steer axis angle. This can be done by several kinds of angle finders. The steer axis angle is the complement and can be described (with an optional conversion from ° to rad) by,

$$\lambda_\mathrm{s} = (90° - \lambda_\mathrm{h})\,\frac{\pi}{180°} \tag{3.72}$$

Trail

Trail can be indirectly determined from the fork offset (sometimes called rake), $\mathcal{O}$, which is the perpendicular distance from the wheel axle to the steer axis. To measure this distance, the head tube part of a frame can be aligned with a flat table while the fork blades are aligned such that the axle axis is parallel to the table. Then the difference in height between the head tube and axle can be measured with a ruler and one directly has the fork offset. The front wheel trail, c, follows then from the front frame fork offset by,

$$c = \frac{r_{\mathrm{F}} \sin \lambda_{\mathrm{s}} - \mathcal{O}}{\cos \lambda_{\mathrm{s}}} \tag{3.73}$$

Wheel base

The wheel base, w, can simply be measured by using a ruler to measure the distance between the wheel contact points. Alternatively, one can measure the distance between the wheels axles and parallel to the ground (which might be difficult for different sized wheels).

Mass

The masses, m, of all parts, $p(=\mathrm{R, B, H, F})$, can be simply obtained by putting all four bodies separately on a scale.

Center of Mass

Wheels In order to be in accordance with the Whipple model, the locations of the centers of mass of the two wheels, $(x_{\mathrm{R}}, z_{\mathrm{R}})$, and $(x_{\mathrm{F}}, z_{\mathrm{F}})$, are assumed to be at the centers of the wheels.

Frames To determine the location of the center of mass of the two frames, each frame should be hung separately on a thin shaft as a torsional pendulum (see figure 3.5a). Therefore, a clamp is used which attaches the frame to the torsional spring shaft with one looking at the, in forward riding direction, right side of the frame. This clamp is attached such that the bicycle can freely rotate about the origin in the pendulum coordinate system $\mathcal{XZ}$-plane (see figure 3.4). Then, due to gravity, the center of mass aligns itself underneath the pendulum coordinates origin where the bicycle is clamped. The pendulum coordinates $\mathcal{X}$-axis passes through the center of mass of the frame, and by placing the clamp at different locations on the frame at different locations the bicycle is orientated differently and several of those pendulum axes can be obtained. The intersection of the axes is the location of the center of mass. Figure 3.4 shows the interesting distances and angles in one specific bicycle rotation orientation.

Per rotational orientation of either frame an angle and a distance need to be measured. The headtube angle relative to the ground (or relative to the pendulum $\mathcal{Z}$-axis), γ, can be measured with an angle finder (possibly with level). The distance from the wheel axle to the pendulum axis (wheel axle $\mathcal{Z}$-coordinate) for either frame, $\mathcal{Z}_p$, can be determined by aligning a string with the pendulum $\mathcal{X}$-axis and measure the perpendicular distance to the axle with a ruler (see figure 3.5b). This distance is positive when the string hangs to the right of the axle (axle has a positive $\mathcal{Z}$ value in pendulum coordinates). And the distance is negative when the string falls to the left of the axle (axle has a negative $\mathcal{Z}$ value in pendulum coordinates).

The coordinate system rotation angles from the bicycle nominal configuration to the pendulum hanging orientation for different frames, $p(=\mathrm{B, H})$, and different hanging orientations, j, follow as,

$$\beta_{p,j} = \lambda_{\mathrm{s}} - \gamma_{p,j} \tag{3.74}$$

This angle is important in determining the equation for the pendulum axes, $\mathcal{X}$, of every specific pendulum orientation in the nominal bicycle coordinates. The axis is a simple line in that coordinates,

$$z = \mathcal{V}_{p,j} x + \mathcal{W}_{p,j} \tag{3.75}$$

with a slope, $\mathcal{V}$, and a z-intercept, $\mathcal{W}$. With reference to figure 3.4 (note the positive direction of the z-axis), it can be shown that the slope is

$$\mathcal{V}_{p,j} = -\tan \beta_{p,j} \tag{3.76}$$

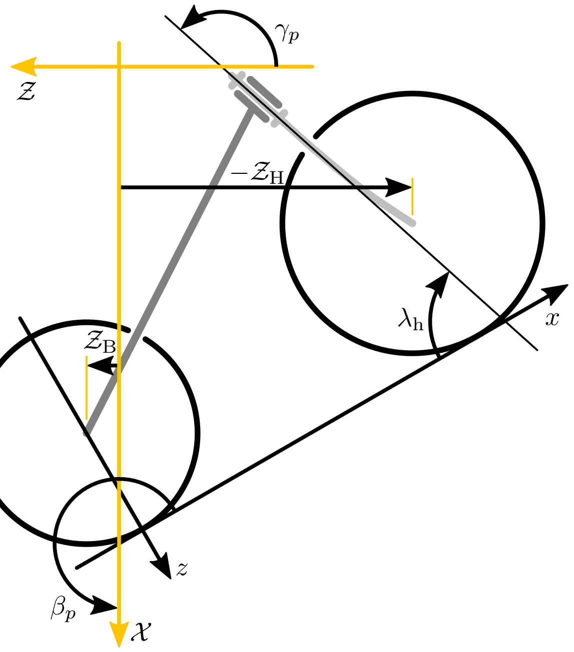

Figure 3.4: Angles and dimensions of a bicycle hung as a torsional pendulum with pendulum reference frame $\mathcal{XZ}$. The part counter does only represent the two frames here, $p(=\mathrm{B},\mathrm{H})$. The headtube orientation angle, γ_p, and the frame rotation angle, β, are used equally for rear and front frame in the bicycle frame xz. However, the horizontal distances between the axles and the vertical pendulum axis, $\mathcal{Z}_{\mathrm{B}}$ and $\mathcal{Z}_{\mathrm{H}}$, have a different translation to the bicycle frame. Note that in measuring the parameters of the wheels and frames, the bicycle is disassembled in the four parts and they are all measured separately, and not as depicted here, as the total bicycle. Moreover, the headtube angle, λ_{h}, must not be mixed up with the steer axis angle, λ_{s}.

The z-intercept is different for the the rear and front frame, since the origin of the nominal bicycle coordinates lies underneath the rear axle. It can be shown that for the rear frame,

$$\mathcal{W}_{\mathrm{B},j} = -\left(\frac{\mathcal{Z}_{\mathrm{B},j}}{\cos\beta_{\mathrm{B},j}} + r_{\mathrm{R}}\right) \tag{3.77}$$

and for the front frame,

$$\mathcal{W}_{\mathrm{H},j} = w\tan\beta_{\mathrm{H},j} - \left(\frac{\mathcal{Z}_{\mathrm{H},j}}{\cos\beta_{\mathrm{H},j}} + r_{\mathrm{F}}\right) \tag{3.78}$$

Due to experimental errors, more than two determined pendulum axes do not intersect at the same location in the nominal bicycle coordinates. Therefore, the center of mass location needs to be determined from the measured intersections of the lines close to the actual common intersection. This estimation becomes more accurate when the number of determined axes is increased.

First, one might look at the centroid between the intersections of the multiple pendulum axes and take that centroid as center of mass. For a number of n different measured frame rotation orientations, the centroid can be found by calculating the intersections between all line pairs and then averaging those intersection locations by the total number of intersections. Alternatively, the n lines can be considered an over-determined linear system and the least squares method can be used to find a unique solution for either bicycle frame p:

$$\begin{bmatrix} -\mathcal{V}_{p,1} & 1 \\ -\mathcal{V}_{p,2} & 1 \\ \vdots & \vdots \\ -\mathcal{V}_{p,n} & 1 \end{bmatrix} \begin{bmatrix} x_p \\ z_p \end{bmatrix} = \begin{bmatrix} \mathcal{W}_{p,1} \\ \mathcal{W}_{p,2} \\ \vdots \\ \mathcal{W}_{p,n} \end{bmatrix} \tag{3.79}$$

Those two methods give generally a different outcome and therefore the method with the higher accuracy is preferred, which, for example, can be determined by plotting the lines.

Mass Moment of Inertia

Since the parts are assumed symmetrical in the xz-plane, the mass moments of inertia can be determined by hanging them separately as both compound and torsional pendulums. By then measuring the period of free oscillation after a small angle perturbation, the mass moment of inertia, which determines this period, can be deducted. The period of oscillation on its part can be determined by measuring the angular rate of the body with a rate gyro during the oscillation. A harmonic function is then fitted to the signal with a nonlinear least squares routine to obtain the natural oscillation frequency, ω, and the damping ratio, ζ, as well as the quantities, $\mathcal{A}$, $\mathcal{B}$, and $\mathcal{C}$. Including the damping ratio is useful when there is significant friction in the pendulum joint, e.g. a frame oscillating as compound pendulum about the wheel axle of an e-bike with motor at the axle. For different bodies, $p(=\text{R, B, H, F})$, along the different pendulum axes, j, the following fit function can be used:

$$\mathcal{A}_{p,j} + e^{-\zeta_{p,j}\,\omega_{p,j}\,t}\left(\mathcal{B}_{p,j}\cos\left(\sqrt{1-\zeta_{p,j}^2}\,\omega_{p,j}\,t\right) + \mathcal{C}_{p,j}\sin\left(\sqrt{1-\zeta_{p,j}^2}\,\omega_{p,j}\,t\right)\right) \tag{3.80}$$

The damped oscillation period, $\mathcal{T}$, can be calculated from the natural oscillation frequency and damping ratio,

$$\mathcal{T}_{p,j} = \frac{2\pi}{\sqrt{1-\zeta_{p,j}^2}\,\omega_{p,j}} \tag{3.81}$$

To correct for experimental errors an average oscillation period, $\overline{\mathcal{T}}$, can be determined by repeating an identical measurement several times.

Hanging the parts as a torsional pendulum requires a torsional spring with clamp. As spring, a simple thin long torsion rod, e.g. a 2.5 mm radius, 1 m long mild steel rod, can be used. The clamp should be such that it is lightweight in order to not influence the measurement too much, but it should be able to clamp the frame as well as the wheels with tires while not allowing the wheel to move with respect to the torsion rod (only possible motion should be due to the rod compliance). The parts are then hung just as with the center of mass location determination with different clamp locations on the bicycle frame giving the different orientation angles, $\beta_{p,j}$. Again, one looks at the frame from the right side in forward riding direction. First, the part should be hung freely and let the gravity align the center of mass with the pendulum $\mathcal{X}$-axis, i.e. the torsion rod longitudinal axis, and then the clamp must be secured. After a small perturbation about the $\mathcal{X}$-axis, the parts oscillate about that axis, and the mass moments of inertia about the x- and z-axis can be determined.

The torsional pendulum is calibrated by using an object with known mass moment of inertia, $\mathcal{I}^*$, to determine the spring stiffness of the pendulum. For example, a relatively heavy (with respect to the torsion rod and clamp), calibration rod with mass, $\mathcal{M}^*$, radius, $\mathcal{R}^*$, and length, $\mathcal{L}^*$, would suffice, since its mass moment of inertia can easily be calculated: $\mathcal{I}^* = \frac{\mathcal{M}^*}{12}(3(\mathcal{R}^*)^2 + (\mathcal{L}^*)^2)$. The stiffness of the torsional pendulum can be estimated by fitting and calculating the period for the oscillating calibration rod:

$$\mathcal{E} = \frac{4\,\mathcal{I}^*\,\pi^2}{\overline{\mathcal{T}^*}^2} \tag{3.82}$$

For lightweight bodies, even though kept small, the clamps weight might still affect the measurement significantly. Therefore, an estimation of the unloaded pendulum and clamp construction mass moment of inertia, $\mathcal{I}^{**}$, is made by letting it oscillate without a load:

$$\mathcal{I}^{**} = \frac{\mathcal{E}\,\overline{\mathcal{T}^{**}}^2}{4\,\pi^2} \tag{3.83}$$

This mass moment of inertia of rod and clamp needs to be subtracted from every mass moment of inertia about a certain pendulum axis determined with the torsional pendulum in order to correct for the nonzero clamp mass moment of inertia.

Wheels The radial mass moment of inertia is determined from hanging the wheel as torsional pendulum and determining the average oscillation period, for either wheel, $p(=\text{R, F})$:

$$I_{pxx} = \frac{\mathcal{E}\overline{\mathcal{T}}_{pxx}^2}{4\pi^2} - \mathcal{I}^{**} \tag{3.84}$$

(a)

(b)

(c)

(d)

Figure 3.5: Several bicycle parts hung as pendulum to determine the COM location and mass moments of inertia. (a) The frame hung as torsional pendulum with a digital angle meter to determine the headtube angle, γ_p, in the pendulum frame, and (b) a ruler to determine the distance from the wheel axle to the pendulum $\mathcal{X}$-axis (determined with a not shown vertical plumb bob hanging from the clamp), $\mathcal{Z}_p$, which is negatve in this case ($\mathcal{X}$-axis/string is to the left of the wheel axle). The frame is clamped such that its COM hangs right underneath the torsional spring shaft with clamp, and it can oscillate about the (vertical) axis running through this spring shaft. It hangs such that one looks at the frame from the right side in forward riding direction, and by changing the clamp location, the frame rotates about its y-axis and the pendulum axes can be positioned differently with respect to the bicycle axes. The other frame (fork) and a wheel can be clamped in a similar fashion as torsional pendulum. (c) The frame hung as compound pendulum with the wheel axle as pivot point (other frame (fork) can be hung in a similar manner), and (d) a wheel hung as compound pendulum with its rim on a steel staff. (Photos from [60])

Furthermore, the mass moment of inertia about the axle can be determined by hanging the wheels as compound pendulums (see figure 3.5d). This can be done by simply hanging the wheel on its rim on a horizontal rod. A wheel pendulum length, $\mathcal{L}$, is the length from the axle to the inside of the rim where the wheel hangs on, and can be determined by measuring the inside diameter of the rim and divide it by two. Then, the moment of inertia about the wheel axle follows from the average oscillation period when the wheel oscillates in its xz-plane:

$$I_{pyy} = \left(\frac{\overline{\mathcal{T}}_{pyy}}{2\pi}\right)^2 m_p g \mathcal{L}_p - m_p \mathcal{L}_p^2 \tag{3.85}$$

Note that due to measurement errors, $I_{yy} \leq 2I_{xx}$, might not hold. This has to be corrected to be in accordance with the Whipple model.

Frames By hanging the frame as both torsional and compound pendulum, all four distinct global moments and products of inertia can be determined. To determine all moments and products of inertia with respect to the x- and z-axis of the two frames, they are hung as torsional pendulum in the same different orientations as used for the center of mass location determination (see figure 3.5a). In order to increase the accuracy, the angles should be as far apart from each other as possible, e.g. for three orientation angles a separation of 120° is ideal, and increasing the number of used angles increases the accuracy even further. From the different orientations, j, the same amount of mass moments of inertia about the pendulum axes, $\mathcal{I}$, can be calculated after letting the frames, $p(=\mathrm{B}, \mathrm{H})$, oscillate between the xy- and yz-plane:

$$\mathcal{I}_{p,j} = \frac{\mathcal{E}\overline{\mathcal{T}}_{p,j}^2}{4\pi^2} - \mathcal{I}^{**} \tag{3.86}$$

Translating these mass moments and product of inertia in the pendulum coordinates to the nominal bicycle coordinate system can be done by using a standard 2D-rotation matrix [60]. It then follows that the mass moments of inertia in the nominal bicycle configuration for n different orientations can be found by solving,

$$\begin{bmatrix} \mathcal{I}_{p,1} \\ \mathcal{I}_{p,2} \\ \vdots \\ \mathcal{I}_{p,n} \end{bmatrix} = \begin{bmatrix} \cos^2\beta_{p,1} & -2\sin\beta_{p,1}\cos\beta_{p,1} & \sin^2\beta_{p,1} \\ \cos^2\beta_{p,2} & -2\sin\beta_{p,2}\cos\beta_{p,2} & \sin^2\beta_{p,2} \\ \vdots & \vdots & \vdots \\ \cos^2\beta_{p,n} & -2\sin\beta_{p,n}\cos\beta_{p,n} & \sin^2\beta_{p,n} \end{bmatrix} \begin{bmatrix} I_{pxx} \\ I_{pxz} \\ I_{pzz} \end{bmatrix} \tag{3.87}$$

The remaining mass moment of inertia, I_{yy}, can be determined by hanging both frames separately as compound pendulum (see figure 3.5c). Thereto, the wheel can be fixed somewhere uphigh such that the frame can oscillate around the wheel axle with low friction thanks to the bearings. Then the pendulum lengths, $\mathcal{L}_p$, for the rear and front frame are respectively,

$$\mathcal{L}_\mathrm{B} = \sqrt{x_\mathrm{B}^2 + (z_\mathrm{B} + r_\mathrm{R})^2} \tag{3.88}$$

and

$$\mathcal{L}_\mathrm{H} = \sqrt{(x_\mathrm{H} - w)^2 + (z_\mathrm{H} + r_\mathrm{F})^2} \tag{3.89}$$

With these lengths the mass moment of inertia about the y-axis can be calculated similarly to those of the wheels:

$$I_{pyy} = \left(\frac{\overline{\mathcal{T}}_{pyy}}{2\pi}\right)^2 m_p g \mathcal{L}_p - m_p \mathcal{L}_p^2 \tag{3.90}$$

Note that I_{zz} is corrected with respect to the other moments of inertia to make sure that no one moment of inertia is larger than the other two combined, which might occur due to measurement errors. Here the mass moment about the z-axis is taken because this is the least important moment of inertia due to the minor pitch dynamics.

Theoretical measuring

Bicycle parameters can also be calculated from theoretical exact bicycle geometry design and material densities. This can be done by hand or with the use of computer software. Besides being able to extract length parameters some Computer-Aided Design (CAD) software, e.g. Solidworks, can also perform mass property calculations. The Whipple parameters as lengths and mass properties can then be directly taken from the software.

To obtain correct values, one has to be careful that mass properties of the correct separate parts are extracted in software. For example, mass properties of either of the several four parts might be obtained by suppressing the other three parts or by using different configurations. Moreover, attention ha to be paid on taking coordinates with respect to the correct nominal bicycle coordinates origin and make sure that the mass moments of inertia or taken at the centers of mass and aligned with the nominal bicycle coordinate system. Note that sometimes the inertia tensor matrix is presented by software or other sources with negative cross terms [62]:

$$\begin{bmatrix} I_{\mathrm{xx}} & -I_{\mathrm{xy}} & -I_{\mathrm{xz}} \\ -I_{\mathrm{xy}} & I_{\mathrm{yy}} & -I_{\mathrm{yz}} \\ -I_{\mathrm{xz}} & -I_{\mathrm{yz}} & I_{\mathrm{zz}} \end{bmatrix} \tag{3.91}$$

Chapter 4

Bicycle stability

4.1 Bicycle balancing and eigenmodes

To use a bicycle practically, one has to be able to balance and maneuver it. Of those, the balancing can be regarded the most important act, since there is no way of maneuvering without balancing. Due to the longitudinally placed two wheels, balancing a bicycle longitudinally is generally no problem such that when one talks about bicycle balancing it comprehends the preventio of falling over laterally. Due to the only two contact points with the ground a bicycle is inherently laterally unstable giving it a tendency to fall to either side [46]. Therefore, investigating the lateral stability is of importance in bicycle research and there are several methods to investigate it.

Balancing

When the lateral bicycle motion is stable, the bicycle stays close to an equilibrium position. A bicycle is in balance when the resultant forces on the bicycle pass exactly through the straight infinitely long support line spanned by the two wheel contacts. Two cases of equilibrium can be distinguished where on a stable bicycle disturbances will be corrected to return to one of those positions: A straight upward and ahead riding position, and a steady turn. The straight riding position has solely gravitational forces that pass through the support line right underneath the center of mass. For a steady turn, the centripetal force created at the contact points cancels out the centrifugal force in a corner and all destabilizing torques around the support line are counteracted by stabilizing torques.

When a bicycle is undesirably leaned to a side, the support line needs to move laterally to the leaned direction of the bicycle to move the support underneath the forces on the center of mass of the total bicycle-rider system [16], similar to balancing of an inverted pendulum. Actually just as an inverted pendulum, a bicycle is never exactly in balance and needs a constant lateral shift of the support line. On a forwardly moving bicycle this lateral movement can be done by steering. It is generally assumed that this steering for balance recovery occurs as steering into the fall where the support line is directed towards an undesired lean to recover from it. However, although steering into the fall is often assumed to occur for all canceling of undesired leans for all bicycles, it is only proven to occur for stable bicycles to come straight up again from a steady (leaned) turn [15] (see section 7.2).

At zero velocity, balancing can only be done after severe training and even then large disturbances cannot be counteracted. Moreover, it can be reasoned that a larger forward velocity makes balancing easier, because a correction of the centrifugal force can then be reached with a smaller steering angle. But even at very high speeds, the steering cannot be locked. Thus for effective balancing, a longitudinal motion as well as a free steer are required [3]; to facilitate support line shifting control, a hinge between the two frames, as well as a means of longitudinal propulsion required.

Two systems contribute to bicycle balancing: The bicycle itself, and a (potential) added controller. Hence, the bicycle stability features can be described also in two ways [22]. First, by means of the bicycle uncontrolled dynamics, and secondly, by looking at the total system of bicycle and controller combined. These features can be captured in two separate bicycle qualities: self-stability, and control-stability.

Eigenmodes

The eigenmodes of a system describe the dynamics of a system and consist of the eigenvalues with corresponding eigenvectors. For example, for a linear time-invariant model, i.e. a linearized model of a nonlinear system close to equilibrium, the stability can be assessed by looking at the eigenvalues. The eigenvalues are independent of the choice of coordinate system or form of the equation, and are therefore convenient instruments for comparing behavior of different configurations or models of the same system. A dynamical analysis can be conducted on the system with or without linear time invariant control and the eigenvalues and eigenvectors can be obtained by solving the characteristic equation of a system.

The oscillation frequencies of the motion of the eigenmodes are called the eigenfrequencies and it appears that these follow from the eigenvalues. The shape of a motion corresponding with an eigenfrequency is described by the mode shape and follows from the eigenvectors of the system. With system eigenvalues, λ_j, and system eigenvectors, $\widehat{\mathbf{q}}_j$, the dynamic system (3.43) can be assumed to have a solution, $\mathbf{q}$, for the movement of the system that is of an exponential form: $\mathbf{q} = \widehat{\mathbf{q}}_j \, e^{\lambda_j t}$.

Eigenvalues

Eigenvalues show how the solution varies in time. In general these eigenvalues are complex numbers of the form $\lambda_j = \Re(\lambda_j) + \Im(\lambda_j)i$ with $i = \sqrt{-1}$. With some rewriting and Euler's formula it can be seen that the real part of the eigenvalue is a measure for the exponential decrease or increase of the solution, and the imaginary part is a measure for the oscillation frequency:

$$\begin{aligned} \mathbf{q} &= \widehat{\mathbf{q}}_j e^{\lambda_j t} \\ &= \widehat{\mathbf{q}}_j e^{(\Re(\lambda_j)+\Im(\lambda_j)i)\,t} \\ &= \widehat{\mathbf{q}}_j e^{\Re(\lambda_j)\,t} e^{\Im(\lambda_j)\,i\,t} \\ &= \widehat{\mathbf{q}}_j e^{\Re(\lambda_j)\,t} \left(\cos\left(\Im(\lambda_j)\,t\right) + i \sin\left(\Im(\lambda_j)\,t\right)\right) \end{aligned} \tag{4.1}$$

The real part of an eigenvalue should then be negative in order for the exponential solution of the system to converge to zero. And thus, the system is asymptotically stable when all real parts of the eigenvalues are negative (and marginally or neutral stable for a zero real part). Moreover, the magnitude value of the eigenvalue is a measure of how stable a system is, i.e. for the degree of stability. A larger negative eigenvalue lets the solution converge faster to the steady state value, whereas a large positive value lets the solution diverge faster. Equivalently to the eigenvalue, one can give the eigenvalue inverse; the time constant. A small time constant means that a smaller time is required for the solution to reach its end state. For stable systems this end state is the steady state value while for unstable systems it is an infinite value. Furthermore, it is generally known that eigenvalues are composed of the eigenfrequency and damping of a system.

Recap single DOF system eigenvalue composition For a single degree of freedom second order system of the form $\mathcal{A}\ddot{q} + \mathcal{B}\dot{q} + \mathcal{C}q = 0$ with $\mathcal{A} > 0$, the eigenvalues are negative, and the system thus stable, when $\mathcal{B} > 0$ and $\mathcal{C} > 0$. A second order system with one degree of freedom can be put in a second-order normal (canonical) form that fits this three scalar coefficients mechanical equation: $\ddot{q} + 2\zeta\omega\dot{q} + \omega^2 q = f$. Then, the eigenvalues can be obtained straightforwardly from the eigenfrequency and damping ratio and vice versa.

Recap multiple DOF system eigenvalue composition A system with more than one coupled degree of freedom cannot straightforwardly be represented in this normal form, because the damping in the system often couples the normal equations for the different degrees of freedom. The damping ratio and eigenfrequency can then not be determined directly from the eigenvalue. However, the other way around, the eigenvalues can still be expressed in terms of the natural (eigen-) frequencies, ω_j, and the respective damping ratios, ζ_j. Eigenvalues thus contain damping and oscillation information of the two degrees of freedom and can be written in the form [41],

$$\lambda_{j,(j+1)} = -\zeta_j\omega_j \pm \sqrt{\omega_j^2\left(\zeta_j^2 - 1\right)} \tag{4.2}$$

It can be seen that indeed the eigenvalue can be complex. When rewritten in the complex polar form it turns out that the natural frequency is the modulus of the eigenvalue:

$$\omega_j = |\lambda_j| = \sqrt{\left(\Re\left(\lambda_j\right)\right)^2 + \left(\Im\left(\lambda_j\right)\right)^2} \tag{4.3}$$

and the damping ratio can be defined as [41],

$$\zeta_j = \frac{-\Re\left(\lambda_j\right)}{|\lambda_j|} = \frac{-\Re\left(\lambda_j\right)}{\sqrt{\left(\Re\left(\lambda_j\right)\right)^2 + \left(\Im\left(\lambda_j\right)\right)^2}}. \tag{4.4}$$

For $\zeta_j < 0$, the system is unstable. The solution can then oscillate with an increasing amplitude, or there may not be an oscillation at all and it just increases. On the other hand, the system might be so stable that no oscillation occurs (highly damped), $\zeta_j > 1$, and there is no natural frequency to be found. For an underdamped system (lightly damped), $0 < \zeta_j < 1$, the system oscillates stably and the solution is damped out. In that stable case the actual oscillation frequency is lowered by the damping so that one can speak of the damped frequency,

$$\omega_{\zeta,j} = \Im\left(\lambda_j\right) = \omega_j \sqrt{1 - \zeta_j^2} \tag{4.5}$$

The oscillatory solution to an oscillating system, either stable, $0 < \zeta_j < 1$, or unstable, $-1 < \zeta_j < 0$, can be written with damping ratio, damped frequency, offset, and amplitudes [41]:

$$\mathcal{A} + e^{-\zeta_j\, \omega_j\, t}\left(\mathcal{B}\cos\left(\omega_{\zeta,j}\, t\right) + \mathcal{C}\sin\left(\omega_{\zeta,j}\, t\right)\right) \tag{4.6}$$

Eigenvectors

The eigenvectors, $\widehat{\mathbf{q}}_j$, contain quantitative information of the relative motion between the generalized coordinates. It presents the solution 'shape' and is thus also called the mode shape. For each eigenvalue there is an eigenvector that describes the motion corresponding with the specific eigenvalue, by containing multiple possibly complex entries each corresponding with one of the generalized coordinates.

For a given mode the ratios between the individual components of the eigenvector are constant [41]. Therefore, an eigenmode can easily be normalized which is done by dividing all eigenvector entries by one of the entries values (one entry, generally the largest, is set to one and the others are scaled accordingly). This can be done since only the magnitude (modulus) ratio between the eigenvector components is important in the analysis of relative motion between the degrees of freedom.

Purely real eigenvalues indicate only magnitudes of the degrees of freedom and mean that they move either precisely in phase or precisely in anti-phase (when the signs are opposite), while a complex eigenvector also contains the exact phase difference between the components. This phase difference is simply the difference between the phases (arguments) of the entries. Which one of the degrees of freedom leads the others is just a matter of interpretation, because one can round the origin of the complex plane as many times as wanted. The rule is that the phase is positive in the counterclockwise direction starting on the positive (horizontal) real axis with zero imaginary value such that. For example, a vector aligned with the positive (vertical) imagininary axis can be said to lead a pure real positive vector by $\pi/2$ rad (90°) or lag it by $3\pi/2$ rad (270°). Note that the argument can often be calculated in software with the `atan2` function (implemented as `atan2(imag(..),real(..))`).

The magnitude ratio and phase can be used to plot an eigenvector or multiple eigenvectors in a phasor diagram (in Matlab one can use `compass` or `polarplot`). Alternatively, a phase portrait in 2D or 3D for two or three degrees of freedom respectively can be plotted. Calculating eigenvalues and eigenvectors of linear polynomials is easily done in Matlab by using `polyeig`, where even a mass, damper, spring system can directly be put in.

The two degrees of freedom bicycle model, used here, has eigenvectors with the lean and steer angle as entries. As said, they can be possibly complex numbers, and thus the eigenvector looks as follows:

$$\widehat{\mathbf{q}}_j = \begin{bmatrix} \widehat{\phi}_j \\ \widehat{\delta}_j \end{bmatrix} = \begin{bmatrix} \Re(\widehat{\phi}_j) + \Im(\widehat{\phi}_j)\, i \\ \Re(\widehat{\delta}_j) + \Im(\widehat{\delta}_j)\, i \end{bmatrix} \tag{4.7}$$

The possible phase difference between those entries is then,

$$\varphi_{\phi\delta} = \arg(\widehat{\phi}_j) - \arg(\widehat{\delta}_j) \tag{4.8}$$

4.2 Self-stability

The extent to which a bicycle with or without no-hands rigid rider can stay upright (stabilize) by itself is described by the self-stability. The bicycle, just like any other dynamical system, has dynamics of its own. When self-stable, the bicycle has dynamics due to geometric, inertial, and gyroscopic features which make that stabilizing steering torques are produced by the system itself. It is generally assumed that these steering torques make sure that the ground-contact points, which span the support line, are brought at the correct location underneath the COM by steering into the fall (an undesired lean). This means that a bicycle requires an inherently coupling between the leaning and steering for self-stability.

A self-stable bicycle without control will always return to a straight up position riding in a straight ahead line after a limited disturbance. With one constant applied steer torque, the self-stable bicycle can stay in a constant turn [16]. Thus, a bicycle is self-stable when it automatically, without control, comes back to an upright position both after a disturbance, or when a steer torque is released in a steady turn [37]. Note that this self-stable behavior is often only present, if present at all, in a specific forward speed range (see figure 4.1) that differs from bicycle to bicycle.

Different mechanisms that might stabilize a bicycle can be identified. One can think of when the bicycle leans, the front wheel precesses about the steer axis due to the front wheel gyroscopy and thereby stabilizes by steering into the fall, or, this steering into-the-fall can be cause by a nonzero trail that makes that the potential energy minimum occurs when the bicycle is leaned and the front fork is steered into the lean [3]. Moreover, in most instances the trail allows for a self-aligning effect of the wheels like that of a swivel wheel. However, the lean angle of a conventional bicycle is dominantly affected by a gravity torque that destabilizes the bicycle and the movement of the support line due to steering that can stabilize the bicycle. Other effects, like wheel gyroscopy, ground contact displacement due to not knife-edged wheels, rider bending, center of mass displacement due to trail, etc., generally have negligible effects on lean angle and thus the stability [16].

Although these mechanisms can often be recognized on conventional bicycles, what exactly determines if a bicycle has the correct coupling between leaning and steering is a question which cannot be answered straightforwardly [15]. Bicycle dynamics simply depend on too many factors and the parameters interact in a complex manner to create those dynamics. It appears that no specific geometric or mass properties are necessary nor sufficient individually for self-stability, and no easy physical explanation is found (yet) that describes why a bicycle is self-stable and at what speeds. For example, neither gyroscopic effects of the wheels nor castering effects due to trail are necessary or sufficient for self-stability [15] (gyroscopy is even the reason why all known bicycles lose self-stability at higher speeds). Other parameters like the front assembly mass distribution can be at least as important due to the complex way of interaction between them all. This complexity can be summarized in the notion that a bicycle can be made self-stable or unstable by changing just one thing; there is a thin, and often unknown, line between self-stability and -instability for bicycles [15].

However, although general steering into a fall alone is insufficient to assure self-stability [15], conversely, the only physically interpretable condition for self-stability seems to be that a self-stable bicycle must steer into a fall [44]. In fact, at least one factor coupling the lean and steer inherently needs to be present for self-stability: a 'cross term' in the upper right of the matrices of (3.43) is required that makes a lean result in a steer [15]. Even then it is not to say if a bicycle is self-stable by just looking at geometrical features; a mathematical analysis is necessary to draw conclusions about the self-stability.

Bicycle characteristic equation

A mathematical self-stability analysis of the system can be performed by looking at the homogeneous solution, $\mathbf{f} = \mathbf{0}$, of the linear lean and steer equations (3.43). This way the eigenvalues and eigenvectors of the system can be found and thus information about the system's own dynamics are obtained. The exponential solution, $\mathbf{q} = \widehat{\mathbf{q}}_j e^{\lambda_j t}$ (4.1), with eigenvalues, λ_j, and corresponding eigenvectors (the mode shapes), $\widehat{\mathbf{q}}_j$, is assumed for the homogeneous equations. Plugging this solution in equation (3.43), with the zero external forces and some rewriting, gives the following expression:

$$e^{\lambda_j t}\left[\mathbf{M}\lambda_j^2 + v\mathbf{C}_1\lambda_j + g\mathbf{K}_0 + v^2\mathbf{K}_2\right]\widehat{\mathbf{q}}_j = \mathbf{0} \tag{4.9}$$

To have a non-trivial solution, the exponential cannot be zero, $e^{\lambda_j t} \neq 0$, and thus:

$$\left[\mathbf{M}\lambda_j^2 + v\mathbf{C}_1\lambda_j + g\mathbf{K}_0 + v^2\mathbf{K}_2\right]\widehat{\mathbf{q}}_j = \mathbf{0} \tag{4.10}$$

A non-trivial solution also requires a non-zero eigenvector, $\widehat{\mathbf{q}}_j \neq \mathbf{0}$, which means that the matrix in equation (4.10) is singular (or non-invertible), requiring that its determinant is zero. This gives the

Table 4.1: Numerical benchmark bicycle of Meijaard *et al.* high precision parameter values [22].

Parameter	**Symbol**	**Value**
Wheel base	w	1.02 m
Front wheel trail	c	0.08 m
Steer axis tilt	λ_s	$\pi/10$ rad
Gravity	g	9.81 N/kg
Rear wheel R radius	r_R	0.3 m
Rear wheel R mass	m_R	2 kg
Rear wheel R MMOI	(I_{Rxx}, I_{Ryy})	(0.0603, 0.12) kgm^2
Rear frame B COM	(x_B, z_B)	(0.3, −0.9) m
Rear frame B mass	m_B	85 kg
Rear frame B MMOI	$\begin{bmatrix} I_{Bxx} & 0 & I_{Bxz} \\ 0 & I_{Byy} & 0 \\ I_{Bxz} & 0 & I_{Bzz} \end{bmatrix}$	$\begin{bmatrix} 9.2 & 0 & 2.4 \\ 0 & 11 & 0 \\ 2.4 & 0 & 2.8 \end{bmatrix}$ kgm^2
Front frame H COM	(x_H, z_H)	(0.9, −0.7) m
Front frame H mass	m_H	4 kg
Front frame H MMOI	$\begin{bmatrix} I_{Hxx} & 0 & I_{Hxz} \\ 0 & I_{Hyy} & 0 \\ I_{Hxz} & 0 & I_{Hzz} \end{bmatrix}$	$\begin{bmatrix} 0.05892 & 0 & -0.00756 \\ 0 & 0.06 & 0 \\ -0.00756 & 0 & 0.00708 \end{bmatrix}$ kgm^2
Front wheel F radius	r_F	0.35 m
Front wheel F mass	m_F	3 kg
Front wheel F MMOI	(I_{Fxx}, I_{Fyy})	(0.1405, 0.28) kgm^2

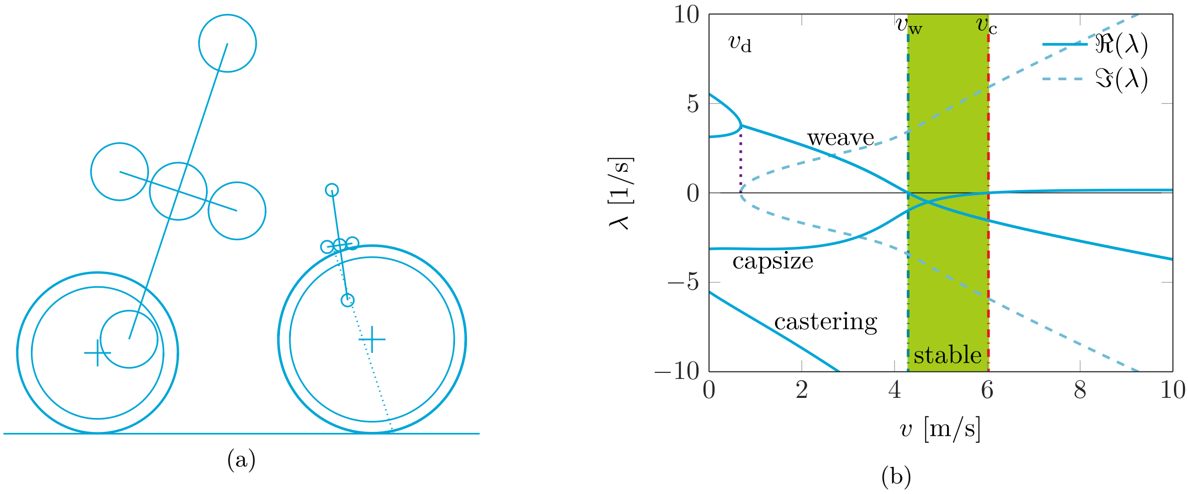

Figure 4.1: Numerical benchmark bicycle of Meijaard *et al.* [22] (a) visual parameter representation in the style of JBike6 (see section 4.3) where the bicycle is seen from the right and (b) the eigenvalues from linearized stability analysis as function of the forward bicycle velocity. Solid lines show the real parts of eigenvalues and the dashed line corresponds with the imaginary part of the eigenvalue. Three modes corresponding with the eigenvalues can be recognized: The complex weave mode (complex eigenvalue pair), the real capsize mode, and the real castering mode. Oscillations from the weave mode start to appear at the real double root at $v_d \approx 0.7\,\mathrm{m/s}$. This specific bicycle shows self-stable behavior in the speed range $v_w(\approx 4.3\,\mathrm{m/s}) < v < v_c(\approx 6.0\,\mathrm{m/s})$, where all real parts of the eigenvalues are negative.

characteristic equation for the lateral bicycle motion model:

$$\det\left(\mathbf{M}\lambda_j^2 + v\mathbf{C}_1\lambda_j + g\mathbf{K}_0 + v^2\mathbf{K}_2\right) = 0 \tag{4.11}$$

This determinant of the two by two second order system is a quartic polynomial in system eigenvalues, λ_j, which are the roots, of this characteristic polynomial. Thus, the characteristic equation can be solved to find the eigenvalues and thereby determine the stability of the uncontrolled bicycle. The eigenvectors, on their part, can then be found by solving (4.10) with the found eigenvalues.

Bicycle eigenmodes

This fourth order uncontrolled bicycle system has generally also four distinct eigenmodes [22]. Only for some special parameter values there exist multiple roots such that less than four distinct eigenmodes are present. Generally, for one specific forward velocity, there are either four real eigenvalues, two real and one complex pair, or two complex pairs. With varying velocity, two real eigenvalues can coalesce and split in a complex pair, or a complex pair coalesces at the real axis into two real eigenvalues. Not only a change in velocity alters the eigenvalues, but a change in whichever one of the 25 parameters alters the eigenvalues. For asymptotic self-stability all real parts of the eigenvalues of a bicycle (without controller, but with possible no-hands and no-control rigid rider) need to be negative. Both lean and steer angle are then converging to zero whether or not by oscillation. The eigenvectors corresponding with the eigenvalues describe how this lean and steer angle are present in the mode.

For conventional common bicycles, e.g. the well-defined numerical benchmark configuration [22] shown in table 4.1 and figure 4.1, several modes corresponding with different eigenvectors can be identified. This bicycle represents a rather conventional bicycle configuration with a rigid no-hands rider on it. There are four real roots that turn into two real roots and a complex pair at higher speeds (figure 4.1b). Note that the bicycle modes are named from a conventional bicycle perspective and correspond with the motion shapes shown in figure 4.2 for a specific forward velocity. More alternative bicycle designs may have eigenmodes that are different combinations of the two degrees of freedom.

The two most important modes for self-stability of a conventional bicycle at higher speeds are the so-called capsize mode and the weave mode (see figure 4.1b). The oscillatory weave mode shows a sinusoidal steer and lean motion about the heading angle, where the steering follows the leaning with a small phase lag (figure 4.2a). The complex eigenvalue of this mode contains the frequency of this weave motion and tells whether the motion is decaying or increasing. As seen in figure 4.2a the weave mode contains both a significant lean and significant steer motion and shows a steer-into-fall principle that uprights the bicycle in periods. The lean dominated capsize mode is associated with a smaller real eigenvalue that has a lean dominated eigenvector (barely steering) (see figure 4.2b). This means that the lean angle, ϕ, and a steer angle, δ, of an unstable capsizing bicycle are progressively increasing such that the bicycle falls over in a tightening spiral. During this unstable capsizing, the bicycle lean and steer are to the same side, but the steer is not sufficient to correct the lean and balance the bicycle.

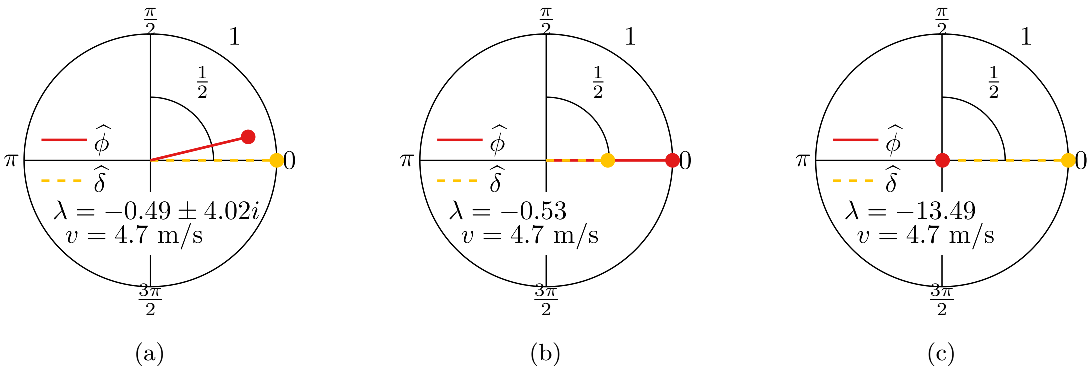

Figure 4.2: Phasor diagrams of the eigenvectors (mode shapes) of the benchmark bicycle at $v = 4.7$ m/s corresponding with (a) the weave mode, (b) the capsize mode, and (c) the castering mode. The (peripheral) angular value shows the phase of the eigenvector while the radial value shows the normalized magnitude.

The third mode is the castering mode, which is associated with a large negative real eigenvalue for a conventional bicycle. It tells something about the aligning of the wheels where one wheel follows the other by a tractrix-like pursuit trajectory, and it covers an effect like the straightening of a shopping cart front swivel wheel. It is highly steer dominated, as can be seen in figure 4.2c. In the numerical benchmark model, this castering mode is mainly caused by the front contact point aligning with the rear wheel and frame under influence of the trail. The castering mode is present for all bicycle configurations being either positive or negative. This mode must not be confused with the fast oscillating steer motion

Table 4.2: Reversed numerical benchmark high precision parameter values.

Parameter	**Symbol**	**Value**
Wheel base	w	1.02 m
Front wheel trail	c	−1.10 m
Steer axis tilt	λ_s	$-\pi/10$ rad
Gravity	g	9.81 N/kg
Rear wheel R radius	r_R	0.35 m
Rear wheel R mass	m_R	3 kg
Rear wheel R MMOI	(I_{Rxx}, I_{Ryy})	(0.1405, 0.28) kgm^2
Rear frame B center of mass	(x_B, z_B)	(0.12, −0.7) m
Rear frame B mass	m_B	4 kg
Rear frame B MMOI	$\begin{bmatrix} I_{Bxx} & 0 & I_{Bxz} \\ 0 & I_{Byy} & 0 \\ I_{Bxz} & 0 & I_{Bzz} \end{bmatrix}$	$\begin{bmatrix} 0.05892 & 0 & 0.00756 \\ 0 & 0.06 & 0 \\ 0.00756 & 0 & 0.00708 \end{bmatrix}$ kgm^2
Front frame H center of mass	(x_H, z_H)	(0.72, −0.9) m
Front frame H mass	m_H	85 kg
Front frame H MMOI	$\begin{bmatrix} I_{Hxx} & 0 & I_{Hxz} \\ 0 & I_{Hyy} & 0 \\ I_{Hxz} & 0 & I_{Hzz} \end{bmatrix}$	$\begin{bmatrix} 9.2 & 0 & -2.4 \\ 0 & 11 & 0 \\ -2.4 & 0 & 2.8 \end{bmatrix}$ kgm^2
Front wheel F radius	r_F	0.3 m
Front wheel F mass	m_F	2 kg
Front wheel F MMOI	(I_{Fxx}, I_{Fyy})	(0.0603, 0.12) kgm^2

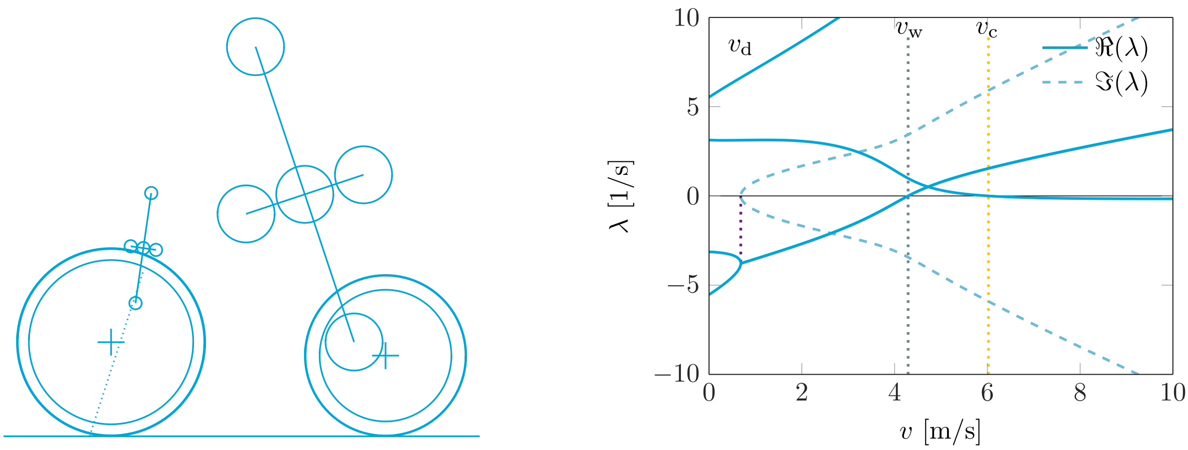

(a) (b)

Figure 4.3: Reversed numerical benchmark bicycle (a) visual parameter representation in the style of JBike6 (see section 4.3) where the bicycle is seen from the right (the rider posture may require some minor adaptations to make it practically implementable), and (b) the eigenvalues for a backwards ridden benchmark bicycle. It is never stable which is not surprising, because a bicycle that is (self-)stable ridden in one direction is per definition (self-)unstable when ridden in the other direction.

of mainly the front wheel in conventional two-wheelers, the wobble motion or shimmy, which is caused by features not included in the Whipple-model such as frame flexibility and tire dynamics.

As said, these eigenmode descriptions hold for common bicycles, for other arbitrary bicycles at different speeds the roots are harder to categorize so straightforwardly. A new analysis of the eigenvectors corresponding with the eigenvalues is then required.

Several interesting speeds that correspond with eigenvalues can be identified for most conventional bicycles. The weave speed, v_{w}, is the speed where the real part of the eigenvalue of the weave mode becomes zero. And for most conventional bicycles, the capsize speed, v_{c}, is the speed where the capsize eigenvalue reaches zero. Conventional bicycles like the numerical benchmark bicycle, can then be seen to be self-stable in a velocity region bounded by the weave speed and the capsize speed. Note that the weave and capsize speed are in general defined somewhat more complex, as will be shown later in section 4.5). Furthermore, speeds at which double roots appear, v_{d}, can be identified. The speed where the stability is 'maximal', i.e. where the real part of the eigenvalues are at a combined minimum, for the benchmark bicycle lies around 4.7 m/s. This speed can be used in simulations to find a reasonable fast converging solution.

Due to the workless kinematic constraints and state dependent forces a bicycle shows exactly the opposite dynamical behavior when ridden in a reversed direction as opposed to the other direction [22]. This means that when a bicycle shows an exponentially decaying disturbance when ridden in one direction, it will show an exponentially increasing disturbance when ridden in the opposite direction. Therefore, a bicycle that is exponentially stable in forward direction, must be exponentially unstable in the reverse direction and vice versa [22]. The eigenvalue plot as function of the forward velocity, is thus point symmetric about the vertical axis at zero speed (see figure 4.5).

This also makes that a fore-aft symmetric bicycle (two equal frames with two equal wheels connected by a vertical or horizontal steer axis exactly in the middle between the wheels) can never be self-stable. Because of symmetry it needs both exponentially growing and decaying solutions at the same time in either riding direction. And thus never are solely decaying solutions present in one riding direction, and hence, such a bicycle is never asymptotically stable. However, it can be neutrally stable, showing a constant oscillating motion.

Investigating a reversely ridden bicycle can simply be done by setting the forward velocity to an opposite, negative, value in the equations. The eigenmodes then obtained are for that reversed bicycle. However, this might be a cause for misconceptions of what frame is the front or the rear, and which direction of the angles is the positive direction. Therefore, one could more conveniently reverse a bicycle by mirroring the parameters about the bicycle vertical axis.

A conventional bicycle ridden normally is self-stable, so when reversely ridden it is not. This can be seen when the numerical benchmark bicycle is reversed such that a positive forward velocity corresponds with a situation when the smaller wheel is ahead in the riding direction. The parameters and corresponding eigenvalues of such a mirroring of the numerical benchmark bicycle are displayed in table 4.2 and figure 4.3. Indeed, as compared to figure 4.1b, the eigenvalue plot figure 4.2b is 'mirrored' about the zero speed vertical axis. It can then be directly seen that the castering mode which was increasingly negative for increasing velocity of the numerical benchmark bicycle, becomes increasingly

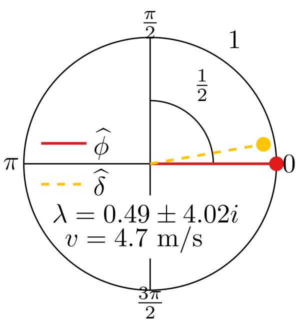

(a)

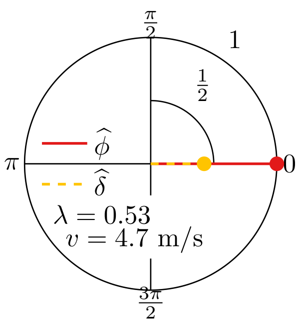

(b)

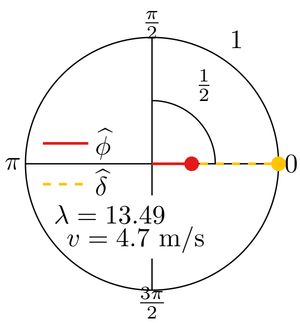

(c)

Figure 4.4: Phasor diagrams of the eigenvectors (mode shapes) of the reversed benchmark bicycle at $v = 4.7$ m/s corresponding with (a) the weave mode, (b) the capsize mode, and (c) the castering mode.

positive for the reversed numerical benchmark bicycle and thus the bicycle never is self-stable. The eigenvectors (mode shapes) are qualitatively very similar to the normal benchmark bicycle, but there are some phase shifts (see figure 4.4).

4.3 Self-stability analysis: JBike6 software

A tool for researching the self-stability of bicycles is the Matlab program JBike6 (version February 2015) [45] [47] [15]. This program solves the eigenvalue problem and the stability of a 25 parameter bicycle configuration is expressed with the use of these eigenvalues. In figure 4.5 the interface of JBike6 is shown with the in- and outputs for the high-precision parameter values of the benchmark bicycle. The usage of JBike6 with this interface will be described next [16].

The 25 parameters are specified in the different input boxes. The wheel base and trail are defined the same as in the benchmark bicycle; wheel base is positive in positive x direction from the origin at the rear wheel ground contact point, and the trail is positive in positive x direction from the front wheel ground contact point. Just as in the benchmark bicycle, the round axisymmetric wheels require only two mass moments of inertia to be defined. However, the rear frame, rider and rear rack can be specified separately, but are combined in terms of mass and inertia (this can be a cause for errors when one means to put the rider on the front frame). The same holds for the front frame (fork) and front basket. All bodies are assumed symmetric about the vertical plane and three principal values are used to describe their mass moment of inertia about their three principal axes. The principal 1-axis can be rotated in the vertical plane by specifying the angle, α, with the x-axis in the xy-plane.

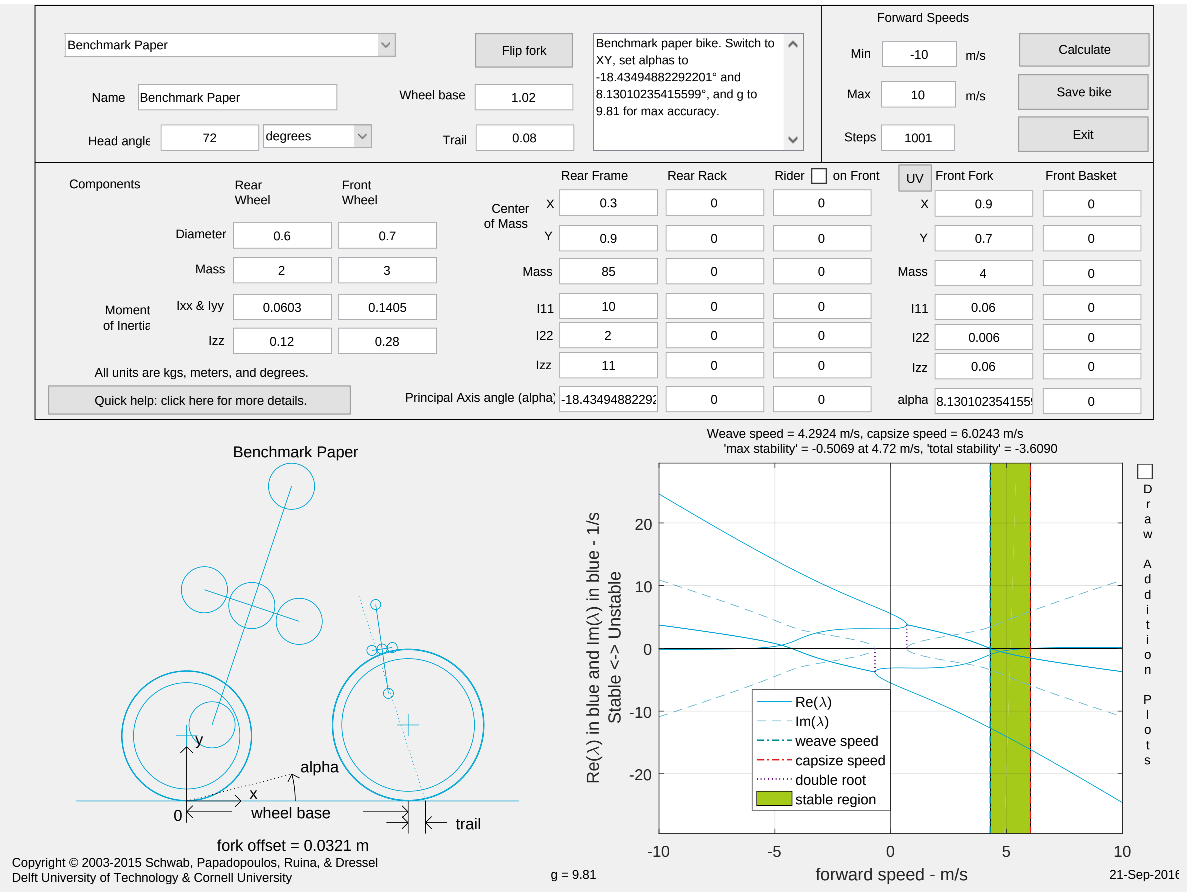

Figure 4.5: Screenshot of the JBike6 Graphical User Interface (GUI) with the parameters of the benchmark model of Meijaard *et al.* [22]. This is a modified version of JBike6 February 8, 2015 that incorporates a function for including the rider in the front assembly when a separate (no-hands) rider is defined.

The program puts out two figures; a graphical sketch of the bicycle to scale, and an eigenvalue plot. The bicycle sketch shows a graphical representation of the input parameters with a bicycle-like silhouette with forward riding direction (positive x and v) to the right. It shows the length based parameters as well as a graphical representation of the mass moments of inertia of all separate bodies. For the wheels mass moment of inertia a radius of gyration circle is used which is concentric with the wheel perimeter circle, where a larger circle represents a larger mass moment of inertia. The moments of inertia of other bodies are shown by means of 6 mass balls which are lined up in pairs along the three principal directions. The middle circle then represents a left and a right ball that lie directly behind each other in the direction perpendicular to the drawing plane. Every ball represents 1/6 of the total body mass and the volumes of them (cubed diameter of circles) are a measure for the masses of the balls. Furthermore, the farther away the balls lie from the center of mass, the higher their inertia is about the center.

The main purpose of JBike6 is the eigenvalue plot in the lower right of the screen. For specified forward velocities, the corresponding real parts and imaginary parts are depicted by different lines. Two complex conjugate eigenvalues are both drawn by the software and thus appear symmetrically about the speed axis at a speed where two real parts merge. For a stable configuration all real parts are negative, and the speed area where this occurs is marked by a shaded region which is bounded by JBike6 by the weave and capsize speed as lower and upper bound respectively (Note that JBike6 does not use the formal definition of the weave and capsize speed, but simply takes them as stable boundaries). The values of these velocities are printed above the graph and when they are present in the research forward velocity region these velocities as well as double root velocities are drawn by vertical lines. Furthermore, the ‘max stability’ where the value of the real parts at the speed where the real parts have the lowest (most negative) value when a stable region is presented, as well as the ‘total stability’ which is the area between the real parts and the horizontal axis in the stable region and is a measure for how stable a bicycle is over the speed range.

JBike6 uses some other definitions than the benchmark bicycle. The head angle in JBike6 is defined zero when the steering axis is horizontal and positive in a clockwise direction. Furthermore, both use the rear wheel contact point as origin for the mass positions, but the axis are defined differently. JBike6 has a forward pointing x-axis, an upward pointing y-axis and a rightward pointing z-axis (from the view of a potential rider, outwards of the drawing plane). The benchmark paper uses the SAE J670e standard [57] coordinate system where the x-axis points forward, the y-axis points rightward (from the view of a potential rider) and the z-axis points downward which makes the coordinates related as ${}_{\text{Benchmark}}[x,\, y,\, z] = {}_{\text{JBike6}}[x,\, z,\, -y]$. In matrix form the transformation from the JBike6 coordinates, with pre-subscript J, to benchmark bicycle coordinates is,

$$\begin{bmatrix} x \\ y \\ z \end{bmatrix} = \begin{bmatrix} 1 & 0 & 0 \\ 0 & 0 & 1 \\ 0 & -1 & 0 \end{bmatrix} \begin{bmatrix} {}_{\text{J}}x \\ {}_{\text{J}}y \\ {}_{\text{J}}z \end{bmatrix}, \quad \mathbf{p} = {}_{\text{J}}\mathbf{T}\;{}_{\text{J}}\mathbf{p} \quad \rightarrow \quad {}_{\text{J}}\mathbf{p} = {}_{\text{J}}\mathbf{T}^{\intercal}\,\mathbf{p} \tag{4.12}$$

A second order tensor transforms the mass moments of inertia to JBike6 coordinates by premultiplying the inertia tensor in benchmark coordinates with the transpose of the transformation matrix, ${}_{\text{J}}\mathbf{T}^{\intercal}$, and postmultiply the benchmark coordinates tensor with simply the transformation matrix, ${}_{\text{J}}\mathbf{T}$. In stead of the moments of inertia around the global coordinate axes, JBike6 uses the moments of inertia around the principal axes. The inertia values correspond with the eigenvalues of the moments of inertia tensor while the angles of the alignment of the principal axes with respect to the global frame are captured by the eigenvectors of the moments of inertia tensor. JBike6 specifies the mass moments of inertia of the bicycle bodies by the three principal values ${}_{\text{J}}I_{11}$, ${}_{\text{J}}I_{22}$, ${}_{\text{J}}I_{zz}$ and the counterclockwise angle α that the 1-axis of the specific body makes with the x-axis in the xy-plane:

$${}_{\text{J}}I_{11,22} = \frac{{}_{\text{J}}I_{xx} + {}_{\text{J}}I_{yy}}{2} \pm \sqrt{{}_{\text{J}}I_{xy}^2 + \left(\frac{{}_{\text{J}}I_{xx} - {}_{\text{J}}I_{yy}}{2}\right)^2}, \qquad \alpha = \frac{1}{2}\arctan\left(\frac{2\,{}_{\text{J}}I_{xy}}{{}_{\text{J}}I_{xx} - {}_{\text{J}}I_{yy}}\right) \tag{4.13}$$

The JBike6 as depicted in figure 4.5 is a modified JBike6 February 8, 2015 and has an extra checkbox to include the rider in the front assembly. This is done in the JBike6 code by changing `fa=[1 2 3]` to `fa=[1 2 3 7]` in the `JBmck.m` file for a checked box. The front assembly then also includes the rider parameters that have index `7`. This is done to allow for a better way of modeling a bicycle with the rider on the front assembly, such as most rear wheel steered bicycle have. Furthermore, implementing rear wheel steering in JBike6 can be done in several ways [47]. First, the speed can be made negative, which shows that the eigenvalues are 'wonderfully' mirrored or inverse symmetric about the $\Re(\lambda)$-axis. Secondly, one can specify a backwards bike with negative wheel base, trail, a head angle greater than 90°, etc. [47]. This second method is similar to flipping the bicycle parameters about the central vertical axis of the bicycle as is done for the benchmark bicycle in table 4.2.

4.4 Control-stability

Next to self-stability, there is control-stability. The bicycle is then not stabilized by its own dynamics, but rather by means of a control input on the degrees of freedom (see section 3.3). The controller makes the dynamics of the bicycle such that it is able to stay upright, and move the support line in the correct manner to the correct location under the COM. A bicycle that would be unstable on its own with no control can often still be made stable by a controller; it might even improve or worsen the dynamics of an already self-stable bicycle. These self-stability characteristics on their part, can determine the required control effort.

A controller can actually have two tasks: balancing the bicycle by counteracting undesired leans, and tracking a desired trajectory. Therefore, control-stability comprises some ambiguously and sometimes redundantly defined properties such as maneuverability, accident avoidance, riding stability, directional stability and tracking qualities of the bicycle. In this study, the balancing of not self-stable bicycles is of main interest.

In this model there are two degrees of freedom with torques, and thus a controller can ultimately control two torques: lean torque at the rear contact and steer torque. All forces on the bicycle can be translated to these two generalized forces. For a real-life bicycle the steer torque can easily be controlled, for example by a motor acting on the steer hing or by a human rider acting on the handlebar. A lean torque can in real-life be achieved by the rider leaning with respect to the bicycle, but this model assumes a rigid rider and modeling a leaning rider would require an extra degree of freedom [63]. With a rigid rider, still a bicycle lean torque input can be implemented, for example, by pushing against the bicycle by an external system [22] or by using jets or rotors on the bicycle. All these methods would not be very practical, but in a theoretical (mathematical) model this real-life limitations would not cause a problem (other than that it is unrealistic) and one can always apply an input lean torque.

When a controller stabilizes an unstable bicycle, the whole system of bicycle and controller has negative eigenvalues and thus might have qualitatively the same features as a self-stable bicycle. The weave, capsize, and castering mode are identified for a conventional (self-stable) bicycle, but may appear also on a controlled bicycle. However, a linear time invariant controller alters the eigenvalues and eigenshapes of the system and therefore the mentioned modes might no longer be recognizable. Still, the (now altered) eigenmodes of the system with control are a measure of the stability. Note that more difficult (adaptive) controllers may have no (one set of) eigenvalues and such an analysis would no longer hold.

Bicycle control characteristic equation

To obtain the eigenvalues of the bicycle system with linear time invariant control, the characteristic equation of the bicycle with control can be derived from (3.66) in a similar fashion as was done for the bicycle without control (4.11). First an intermediate equation is obtained with now the feedback control stiffness gains matrix, $\mathbf{K}_\mathrm{f}$, and 'damping' gains matrix, $\mathbf{C}_\mathrm{f}$, included:

$$\left[\mathbf{M}\lambda_j^2 + \left[\mathbf{C}_\mathrm{f} + v\mathbf{C}_1\right]\lambda_j + g\mathbf{K}_0 + \mathbf{K}_\mathrm{f} + v^2\mathbf{K}_2\right]\widehat{\mathbf{q}}_j = \mathbf{0} \tag{4.14}$$

And the determinant in the characteristic equation is once again a quartic polynomial in the system eigenvalues, λ_j, but now for the controlled system such that investigation of both self-stable and control-stable bicycle cases is possible:

$$\det\left(\mathbf{M}\lambda_j^2 + \left[\mathbf{C}_\mathrm{f} + v\mathbf{C}_1\right]\lambda_j + g\mathbf{K}_0 + \mathbf{K}_\mathrm{f} + v^2\mathbf{K}_2\right) = 0. \tag{4.15}$$

Again, the eigenvectors can be found by solving (4.14) for the found eigenvalues. And as said, calculating eigenvalues and eigenvectors of linear polynomials is done in Matlab by using `polyeig`.

Note that the characteristic equation, (4.15), can equivalently be found in state-space form. In that form it becomes directly clear, as expected, that the output of the state-space system has no influence on the stability, but only the first order differential equations with the feedback matrices are influential. To check for this stability, one can calculate the eigenvalues from the state space representation with or without state feedback ($\mathbf{K} \neq \mathbf{0}$ or $\mathbf{K} = \mathbf{0}$) by solving for λ_j (eigenvalues of matrices are in Matlab found with `eig`),

$$\det\left(\lambda_j \mathbf{I} - [\mathbf{A} - \mathbf{B}\mathbf{K}]\right) = 0 \tag{4.16}$$

Bicycle controller design

To stabilize a bicycle, a controller in the form of (3.63) can be designed that makes the eigenvalues of the total system negative. Some things can be said about how the controller should look like globally, but exact gain values are best calculated with the use of the state-space representation (see section 3.4).

Full state feedback (see section 3.3), where the steer angle and the lean angle and their derivatives are fed back to control the input torques, can be used to stabilize unstable bicycles. With correctly chosen feedback gains, such a controller can stabilize any bicycle. Even a fore-aft symmetric bicycle which can never be asymptotically self-stable or a bicycle at zero forward velocity can be stabilized with control. State feedback in this cases is only useful in balancing the bicycle; For controlling the following of a path, i.e. tracking, an additional controller is required. Such a controller could, for example, couple the xy-path of a trajectory and the current xy-position and their derivatives of the bicycle to a steer input torque.

As said, however, the rigid rider model does not allow a practical way of applying an external lean torque. To incorporate this 'limitation' in the control model, the lean torque and the associated feedback gains can be set to zero. The reference gain associated with the lean reference becomes one, because there is no feedback on that specific input

$$\mathbf{f}_\mathrm{r}^* = \begin{bmatrix} 0 \\ T_{\delta\mathrm{r}} \end{bmatrix} \quad , \quad \mathbf{K}^* = \begin{bmatrix} 0 & 0 & 0 & 0 \\ C_{\mathrm{f}\delta\phi} & C_{\mathrm{f}\delta\delta} & K_{\mathrm{f}\delta\phi} & K_{\mathrm{f}\delta\delta} \end{bmatrix} \quad , \quad \mathbf{N}^* = \begin{bmatrix} 1 & 0 \\ N_{\delta\phi} & N_{\delta\delta} \end{bmatrix} \tag{4.17}$$

Note that control can be removed completely from the equations by making the feedback gains all zero and the relevant reference gains equal to one. When there is no control included in the system, the feedback and reference gains matrices are a zero, $\mathbf{0}$, and an identity matrix, $\mathbf{I}$, respectively of size 2×4 and 2×2. However, the external torque reference can still be nonzero so that an uncontrolled-stable (self-stable) bicycle can still have a torque input:

$$\mathbf{f}_\mathrm{r}^{**} = \begin{bmatrix} 0 \\ T_{\delta\mathrm{r}} \end{bmatrix} \quad , \quad \mathbf{K}^{**} = \mathbf{0} \quad , \quad \mathbf{N}^{**} = \mathbf{I} \tag{4.18}$$

Feedback gains

To stabilize the bicycle one can intuitively chose the feedback gains in the feedback gain matrix, $\mathbf{K}$, in (4.15) such that it incorporates the steer-into(-undesired)-fall mechanism to stabilize the bicycle [46]. Then, a positive lean angle or rate results into a positive controlled steer angle, and the other way around. The gains can then often be found such that only the states associated with the lean are used as stabilizing feedback input to the steer torque. Moreover, when the gain values turn out to be within human capacity, this method gives a controller that is somewhat similar to a human controller [63]. However, this simple controller has limits and might not stabilize all bicycles.

A general method for designing the feedback controller is the Linear Quadratic Regulator (LQR) method. This method often results in large gains that are not realistic for human capacity, but it can theoretically stabilize bicycles that are unridable by most humans. With this method the full state-feedback gains are found by minimizing $J = \int_0^\infty (\mathbf{x}^\intercal\mathbf{Q}\mathbf{x} + \mathbf{u}^\intercal\mathbf{R}\mathbf{u})\,\mathrm{d}t$, with weighted state and control costs. Balancing means that the lean angle needs to be minimized, i.e. go to zero, which can be done by using a unity state weight on the lean angle, $\mathbf{Q} = \mathrm{diag}([0, 0, 1, 0])$. Moreover, the control effort can be simply taken to be $\mathbf{R} = \mathbf{I}$ [63]. Again, for practical reasons, the state feedback might only be applied on the steer torque as in (4.17) [63]. In that case, only the second column (corresponding with the steer torque input) of $\mathbf{B}$ is used to optimize while the other column is neglected. Matlab has the function `lqr` to calculate the feedback gains from the system and weight matrices with the LQR method.

Reference gains

A ‘problem’ of the input not ending up at the reference value in steady-state arises, because the input is not compared with the reference in the current control mechanism. In stead the states multiplied by the feedback gains are compared with the reference by subtracting them from that reference (see figure 3.3), which is generally expected to give a different steady-state value than the wanted input that should be equal to the reference [41]. Besides having an incorrect magnitude, the steady-state value might even have the wrong sign. Luckily, the steady-state error in the final input can be corrected rather simply by scaling the reference input to make it equal to the steady-state states multiplied by the feedback gains. Thus, the reference gains matrix, $\mathbf{N}$, can be determined by looking at the error between the steady-state input value and the desired reference value that one wants it to be. Due to the steady-state dependency, the sign of the reference gains is related to the bicycle stiffness that only acts on angles and not their derivatives (see section 4.5).

Before going further, note that in the state-space representation as used here, (3.67) with (3.70), the input is equal to the output which are the generalized forces; $\mathbf{y} = \mathbf{u} = \mathbf{f}$. The reference, $\mathbf{r}$, is used to determine the input.

As said, the reference gains matrix is chosen such that the input/output torque is equal to the reference torque in steady-state. Therefore, to correct for the steady control effects, the reference gain cannot only alter the magnitude of the reference to input relation, but also the sign. However, since the reference is always multiplied by the reference gains, the input torques are constantly affected. Before steady-state, generally the input torque is not equal to the reference and, for example, the short time response of the system is majorly determined by the accelerations, $\ddot{\mathbf{q}}$, which do not show up in the control law (3.63). So at short time the feedback control implemented here has initially no influence on the input and the input is completely determined by the reference; $\mathbf{f}_{(t=0)} = \mathbf{N}\mathbf{f}_{\mathrm{r}}$. In steady-state, only the angles, $\mathbf{q}$ (no derivatives), are nonzero and thus the input torque is also partly determined by the controller and should end up at the reference values when the reference gains are chosen correctly; $\mathbf{f}_{(t\to\infty)} = \mathbf{N}\mathbf{f}_{\mathrm{r}} - \mathbf{K}\mathbf{q} = \mathbf{f}_{\mathrm{r}}$.

The reference gains are used to correct for the steady-state error between the desired reference and the input torque value. Therefore, they need to be calculated as the inverse of the ratio between the reference and the steady-state output of the system. With the state-space model (3.67) the input torques are retrieved as the system outputs. The expression for the reference gains follows from the relation in (3.67) between the reference and the output in steady-state when input, state and reference, 3.68 and 3.69, are put in (3.67) in the frequency domain with a frequency of zero:

$$\mathbf{N} = \left(\mathbf{D} - \frac{\mathbf{C} - \mathbf{D}\mathbf{K}}{\mathbf{A} - \mathbf{B}\mathbf{K}}\mathbf{B}\right)^{-1} \tag{4.19}$$

Matlab has the function, `dcgain`, that performs the calculation of the ratio from reference to steady-state output value, i.e. the DC-gain, of a state-space model. The reference gains are then simply the inverse of those DC-gain values.

Ridability

The most obvious controller is the human rider, and therefore a special case of control-stability is introduced: ridability [3]. This is the most common control-stability for a bicycle, since it takes a human into account as controller. Because ridability is a form of control-stability it is not synonymous; ridability is limited by human capacity, while general control-stability is limited by the capacity of any type of control. The ridability is thus a broad aspect that describes the ability of a bicycle to be ridden by a human. This term describes the ease by which a bicycle can be balanced and maneuvered around and is a mere control qualification of the stability [3]. It deals with the handling of a bicycle in both balancing and maneuvering sense.

Using a human controller might introduce the difficulty that not all humans are equal and that thus the experience of control-stability might differ from human to human, making it a more subjective stability quality. A human is a powerful and versatile controller and can (with practice) stabilize many bicycle designs. Many bicycles are therefore ridable, but the degree to which differs from person-to-person. To make the analysis more objective, the human rider could be considered in control terms after which an assessment in objective aspects is possible. Lower or upper limits of average human capacities can be expressed in time-constants or bandwidths for example, after which one can compare these with a bicycle control requirements. Ridability can then be judged by looking at either physical and mental workload and when a bicycle is said to be ridable, its dynamics are within human limits and a human is able to stabilize the system.

Controllers can be designed based on requirements for the extent of stability that lie within human capacity. For example, to be ridden comfortably by a human (neural delay for bicycle steering is approximately 0.2 s [14]), a bicycle can have an unstable real eigenvalue of maximal 1 rad/s [14] [38]. By implementing a controller that meets this requirement, human behavior can be mimicked. Moreover, looking at the exact eigenmodes of a bicycle can give inside into the extend to which a human may ride a bicycle. For instance, in practical ridability terms the capsize mode of conventional bicycles is of little importance, because its absolute real value is smaller than 0.2 1/s upto $v = 10$ m/s and can be corrected easily by human manual feedback [14]. However, a more unconventional bicycle that is almost symmetrical bicycle with $c = -w/2$ is reportedly difficult to ride [64] [16].

Although full state feedback with an LQR designed controller stabilizes bicycles, it demands unrealistically large steering torques for human controllers and is thus not quite representive for human behavior [63]. Better might be to use intuitive control where only the strictly necessary states are fed back, which can result in lower feedback gains and, in effect, in lower required torques. For example, steer-into-undesired-lean behavior can be implemented. For the benchmark bicycle this can be done by using the lean angular rate below the weave speed, while above the capsize speed, the lean angle suffices, because there the drift from the vertical position is slow.

In real-life, practical control of a human rider on the bicycle can be done by steering and leaning the bicycle; applying torques around the corresponding axes. Steering is done by turning the handlebar and leaning by moving the upper body with respect to the bicycle. These two motions are coupled such that a steer results in a lean and on many bicycles a hands-off rider can create an appropriate steer motion by leaning the bicycle. With hands-on riding, maneuvering by steer input is much more effective than lean input, and probably lean is not used at all when one is able to generate a direct steer input [63] [46]. In modeling terms then, control of solely the steer torque based on information of the roll angle is a reasonable stabilizing mechanism [46]. Therefore, it is justifiable to implement the rider as rigidly attached to the frame and thereby losing the practical means of applying a lean input. Note that it is assumed that a human uses stiffness control to balance a bicycle, in stead of solely the steer torque or steer angle.

Often self-stability is used to say something about the ridability of a bicycle, because self-stability is easier to determine as it excludes influence of a subjective human rider. One known relation between self-stability and ridability is that self-stability has the effect on a controlled bicycle that a constant turn can be initiated and maintained with one constant torque input (see section 7.2) [15] [16] [44]. However, the further effects of self-stability on ridability are not clear as of yet. A ridable bicycle can be made stable by a human controller, but is not necessarily self-stable. On the other hand, a self-stable bicycle is stable from itself, but its ridability might be experienced differently by different riders. It is, however, suspected that the ridability does correlate with self-stability and that ridability can benfeit from self-stability [46] [44].

Self-unstable bicycles are usually hard to ride [15], while self-stable bicycles are often pretty ridable. Illustrative for this is that some unconventional bicycle designs that are hard to ride by a human with hands on or off are often not self-stable [3] [14]. Moreover, since an unstable bicycle requires active control, it is often hypothesized that for comfort and safety reasons probably a self-stable bicycle is preferred [46] [23]. A self-stable bicycle stays upright when control is briefly interrupted which indicates the lower control effort required and external control effort might be completely put in maneuvring. Indeed, control effort (or steer effort) can be reduced by changing certain characteristics such as handling quality and (self-)stability [46].

Although many bicycles show self-stability, none of them are self-stable at all forward velocities. There is a speed above which the bicycle becomes self-stable and often there is also a speed above which the bicycle becomes unstable again. In the unstable forward velocity regions a controller (in general the rider) has to apply input on the system to balance it. In this light it could be possible that a bicycle is self-stable at high speeds, but very unstable at low speeds. It might not be practical to ride such a bicycle, because starting it is very hard.

A very self-stable bicycle may be hard to be deviated from the stable neutral equilibrium position and in effect may be hard to maneuver. In other vehicles such as jet-fighters or rally cars this sometimes leads to intentionally bringing them (momentarily) out of their stable motions in order to increase the maneuverability. Likewise, one could imagine that a little unstable behavior is beneficial for agility of the bicycle. A very stable system is sluggish while a nearly or slightly unstable system is more responsive [3]. When a bicycle is required to be swifter and maneuverability needs to be increased, one might consider to make the bicycle 'less' or not self-stable. Balancing and maneuvering are separate things, but one cannot maneuver without balancing and one cannot easily maneuver on a very stable bicycle. Therefore, bicycle manufacturers or purchasers can chose whether they want an emphasis on stability or on maneuverability. Which one of these features does represent a 'better' ridability is source for discussion and depends on what is desired of the bicycle.

Recap bicycle control lore

The 'technical discipline of control theory' [13] has some lore that can often be related to classical mechanics. Since bicycles are often researched from a control perspective with the accompanying control terms, here a short enumeration of these terms is presented.

Control can be applied in two ways: open-loop and closed-loop [41]. In open-loop, the outputs of a system are not used as input to a controller, such that a system's outputs have no influence on its inputs and the loop is 'open'. A system is said to be open-loop when a controller does not use feedback of the outputs to the inputs in order to close the loop. On the contrary, with closed-loop the controller uses the system outputs as its own inputs to determine and 'feed' that system certain inputs, i.e. it uses feedback of the outputs on the inputs. For robust control, i.e. control that maintains stability under different circumstances, closed-loop control is important in order to deal with uncertainties. When the system is unstable, one might check whether the system is controllable and thus if simple control is effective. For an $\mathbf{A}$-matrix size of $n \times n$, the system is controllable when the rank, i.e. the number of linearly independent rows, of the controllability matrix is equal to the size of $\mathbf{A}$,

$$\mathrm{rank}\left(\begin{bmatrix} \mathbf{B} & \mathbf{AB} & \mathbf{A}^2\mathbf{B} & \dots & \mathbf{A}^{n-1}\mathbf{B} \end{bmatrix}\right) = n \tag{4.20}$$

In control theory, often transfer functions representing the system differential equations are formed with zeros in the numerator and poles in the denominator. For example, the transfer function from steer torque to lean angle for the numerical benchmark bicycle with Laplace (complex) frequency parameter, s, is,

$$\phi = -\frac{s^2 + 14.60vs + 33.02v^2 - 10.99}{8.059s^4 + 25.71v^2s^3 + (28.31v^2 - 325.6)s^2 + (28.08v^3 - 214.0v)s - 66.62v^2 + 2418} T_\delta \tag{4.21}$$

An output is calculated by multiplying an input with the transfer function in the frequency domain. Putting in a frequency value corresponding with a zero makes the numerator zero such that there is no transfer from input to output, while putting in a frequency value corresponding with a pole value makes the denominator zero, such that the transfer becomes infinite. These poles and zeros define the system response, just as roots of the characteristic equation, i.e. eigenvalues, do, which can be seen when transfer functions would be composed from (3.66).

The specific bicycle EOM give specific transfer functions. First, from input torque to output angle, a transfer function would have a single one in the numerator and a mass-damper-spring (mechanical) equation corresponding with the angle in the denominator. The poles of the denominator are therefore equal to the eigenvalues of the mass-damper-spring polynomial. Secondly, a transfer function from one angle to the other angle would have both in the numerator and in the denominator a mass-damper-spring mechanical equation either corresponding with one of the angles. Eigenvalues of the numerator and denominator mechanical equation would respectively correspond with the zeros and poles.

This last form of transfer functions is often presented in bicycle literature from a single degree of freedom (lean) model with the steer angle as input and the lean angle as output. For a multiple degree of freedom model, also multiple transfer functions from one of several DOFs to another DOF can be extracted, and so the eigenvalues of the complete model will not necessarily correspond with one set of poles or zeros. Furthermore, poles and zeros are dependent on bicycle geometry and may or may not vary with varying forward velocity.

For stability all poles of a system should be in the left complex half-plane (all negative real parts), while zeros can be in the complete complex plane. However, attention has to be paid to the type of transfer function that is used. A linear time-invariant open-loop system is stable when all the poles of the open-loop transfer function are in the left complex half-plane. Furthermore, a linear time-invariant closed-loop system is stable when all the poles of the closed-loop transfer function are in the left complex half-plane. However, a linear time-invariant closed-loop system is stable when all the zeros of its open-loop transfer function are in the left complex half-plane, because the zeros in the open-loop transfer function become poles when trasnformed to the closed-loop transfer function. Generally, poles and zeros in the right-half of the complex plane are a cause for fundamental control limitations [14].

To get rid of unstable zeros for control purposes, all state variables must me measured [14]. For an unstable bicycle, a feedback control with tilt and yaw sensors eliminate the problems from a right-half plane zero. An alternative way of eliminating the problems caused by the right-half plane zeros is by maneuvering. Steer torque, rider lean, and even forward speed are input variables that can be used to eliminate or minimize the effect of unstable zeros [14]. For example, increasing the velocity shifts the pole and zero away from each other. Moreover, altering geometry influences the required control effort. For example, for a reversed ridden conventional bicycle, placing the center of mass high and longitudinally close to the front wheel does shift the pole and zero away from each other and thus makes the closed-loop controlled system more robust [14].

Systems with all poles and zeros in the complex left half-plane (negative eigenvalue real part and thus stable from themselves) show a smaller phase lag than systems with poles and zeros in the right half-plane [41]. Therefore, inherently stable systems are called minimum phase systems and systems with zeros and poles in the right half-plane are called nonminimum phase systems. The poles and zeros in minimum phase systems are in the left half-plane and can thus be canceled freely to create any desired loop function and performance is limited only by the controller limitations [38]. A nonminimum phase system with zeros in the complex right-half plane can still be stable, but some 'strange' dynamics occur.

Practically, a nonminimum phase system might be hard to control, because it has as effect that a response to a step input has an undershoot; the output to a certain input is initially in the wrong direction before changing direction and becomes directed as desired. A bicycle is a nonminimum phase system [14] and this undershoot behavior can be seen on bicycles. For example, when one wants to make a certain radius turn, a certain corresponding steer torque can be applied. However, for all stable bicycle, a constant steer torque input initially results in a steer angle in the direction of the steer torque, and eventually in the steady state, due to bicycle dynamics, the steer angle is directed opposed to the applied input torque. This is known as the counter-steer phenomenon. For a controller this might cause trouble, because first it might notice a wrongly directed steer angle and react to that angle by a counter measure, but ends up at an even more undesired steer angle eventually. Counter-steering will be discussed in more detail in section 7.2 and 7.3.

Besides the place of the poles and zeros, i.e. either in the left half or right half in the complex plane, another measure for the ease of control of a system is available. This is the zero/pole ratio which is the distance of the zero to the origin divided by the distance of the pole to the origin in the complex plane. This ratio requirement originates from some robust control of the system requirements. If the unstable pole and zero move too close to each other a system is highly uncontrollable up to the point where they coincide and no control is possible. For high robustness of the complete system with controller a phase margin of 60° ($= \pi/3$) and a slope of the transfer function at the gain crossover frequency of -1 can be chosen reasonably. While for lower robustness a phase margin of 45° ($= \pi/4$) and a slope of -1/2 are admissible [41]. These phase margin and slope choices dictate requirements for the zero/pole ratio of the system to still be well controllable [38]. When high robustness control is desired a zero/pole ratio smaller than about 1/60 or larger than about 60 are allowed. However, when the robustness can be lesser, the zero/pole ratio requirement is also less strict and can be below about 1/6 or above about 6.

A system is proper when its transfer function has the same or lower degree in the numerator as/than in the denominator (equal or lower number of zeros as/than number of poles). Such a proper system cannot be stabilized by a stable controller if the unstable zero is smaller than the unstable pole. For example, a linear time-invariant system with an odd number of real unstable poles between two real unstable zeros [11]. Thus in that case the controller needs to be unstable [38], e.g. controller has negative zero and positive pole.

As said before, in stead of the eigenvalue, sometimes the time constant is presented which is the inverse of the eigenvalue. In terms of control a small time constant of an unstable system means that the instability of the system is harder to control because the system diverges faster from the desired state. The bandwidth of a control scheme describes the width of the range of the required frequencies, such that a higher bandwidth requires more frequencies and is a measure for the control effort.

A nice instrument for stability analysis is the root locus diagram [41]. The roots are then plotted in the complex plane and the effect of changing a variable (often the gain) can be seen. For a bicycle an analysis of the influence of the forward velocity on the root locus is interesting. One can then see for what velocity (if any) all roots lie in the left (stable) half-plane.

4.5 Self- and control-stability analysis: Routh-Hurwitz criterion

To analyse the stability of both self- and control-stable system, the Routh-Hurwitz criterion is presented here. The stability of a system is depicted by its eigenvalues which show if a system shows converging or diverging behavior. To see whether a system has negative real eigenvalues and is stable, the Routh(-Hurwitz) stability criterion can be used. In first instance this method tells if the real parts of the eigenvalues are negative, not what their values are. An analysis of the Routh coefficients can even lead to some interesting conclusions about bicycle behavior, such as the required turn torque for self-stable bicycles and the notion of the counter-steering phenomenon [16].

For this bicycle model the characteristic equation (4.15), which reduces to (4.11) for no control, is a fourth order polynomial in λ with eigenvalues λ_j as roots [16],

$$A\lambda^4 + B\lambda^3 + C\lambda^2 + D\lambda + E = 0 \tag{4.22}$$

For the 25 parameter bicycle model, these polynomial roots are polynomials in the forward speed, v:

$$\begin{aligned} A &= A_0 \\ B &= B_1 v \\ C &= C_0 + C_2 v^2 \\ D &= D_1 v + D_3 v^3 \\ E &= E_0 + E_2 v^2 \end{aligned} \tag{4.23}$$

For the stability analysis also the Routh determinant X is required [65]. This determinant is a combination of the previous polynomial coefficients and can be written as a sixth order polynomial in v:

$$X = BCD - ADD - EBB = X_2 v^2 + X_4 v^4 + X_6 v^6 \tag{4.24}$$

All separate Routh coefficients within the characteristic polynomial coefficients 4.23 (A_0 in A, B_1 in B, etc.) are large expressions including the 25 bicycle parameters of the Whipple model. Only the A and E coefficient have a physical interpretation; they are namely the determinant of the mass and stiffness matrix respectively:

$$A = \det(\mathbf{M}), \quad E = \det\left(\left[g\mathbf{K}_0 + \mathbf{K}_\mathrm{f} + v^2\mathbf{K}_2\right]\right) \tag{4.25}$$

For example, without control, the coefficients in E are $E_0 = -g^2 S_\mathrm{A}(m_\mathrm{T} z_\mathrm{T} \sin\lambda_\mathrm{s} + S_\mathrm{A})$ and $E_2 = g\cos\lambda_\mathrm{s}(S_\mathrm{F} m_\mathrm{T} z_\mathrm{T} \sin\lambda_\mathrm{s} + (S_\mathrm{F} + S_\mathrm{R})S_\mathrm{A})/w$.

If all eigenvalues must have a negative real part, the Routh stability criterion [65] states that all coefficients A, B, C, D, E as well as the determinant X need to have the same sign. The mass matrix is positive semi-definite for positive masses, meaning that its determinant is equal or larger than zero. Only for some singularities due to strange mass distributions is the determinant of the mass matrix zero. The first Routh coefficient is this determinant of the mass matrix, so for stability the first coefficient is larger than zero; $A > 0$. Hence, for stability all other coefficients (4.23) and (4.24) need to have the same sign and thus need to be positive.

Requirements for the parameters can be extracted from the Routh coefficients to give those coefficients a certain sign (often thus positive) and design a stable system. However, the complexity of all separate Routh coefficients makes it apparent that it is very hard to say which bicycles are self-stable and at what speed [15]; with the full 25 parameter Whipple model, general statements about when a bicycle is self-stable are hard to make. The Routh coefficients become complicated and all bicycle parameters contribute in another way to the values.

A reduction of the set of parameters (eliminating some of the 25 parameters by setting them to zero) can be helpful to make the coefficients more insightful and to better understand what is needed for stability [15]. From such a set, some general requirements of the demands regarding the parameter values for self-stability might be created. Relations between and limits of the parameters can be found by using that the coefficients should be larger than zero. The parameters in the coefficient expressions should be such that this stability requirement is met. Then, if chosen wisely, a reduced set of parameters can ease the finding of this parameter limits and relations and can help to build a physical feasible full parametrized self-stable bicycle eventually.

In some theoretical studies it is sufficient to just demonstrate that stability is possible at all, no matter at what speed. The easiest approach is then to seek a stable configuration that is stable from a random forward speed to infinite speed, so without upper stable speed limit. Then the analysis can be focused on the leading terms which are the terms in the polynomial coefficients corresponding with the highest velocities orders in the specific coefficients: A_0, B_1, C_2, D_3, E_2, and X_6. These are the most important terms, because eventually the higher order terms always become the largest parts of the expressions when the velocity is increased. A negative lower order coefficient can thus be compensated by a positive higher order coefficient. This makes the number of individual coefficients that should be positive a little smaller and thus the analysis a little easier.

Transitional speeds

Although all coefficients, A to E and X, need to be positive for stability in bicycles in general, the E and X coefficients need can be used to tell at what speeds some transitional speeds are located [16]. From a stable situation with all positive coefficients, stability is lost when either E or X pass through zero (it is possible in singular cases that they both turn zero simultaneously) [16], because they vanish before B, C, or D do.

When $E = 0$ there is an eigenvalue that passes through zero and the corresponding single eigenmode (not necessarily the complete bicycle) changes from stable to unstable or from unstable to stable for changing forward speed. This transition occurs when E changes sign which can be seen from (4.23) to happen at the speed, $v_c = \sqrt{-E_0/E_2}$. This speed is sometimes referred to as the capsize speed [16] and marks a speed above or below which self-stability is impossible.

For example, for a conventional bicycle like the benchmark bicycle, $E_0 > 0$ and $E_2 < 0$ and self-stability is only possible at speeds below the capsize speed. In general, a bicycle can also be only stable above the capsize speed ($E_0 < 0$, $E_2 > 0$), or the transitional speed might be completely absent ($E_2 = 0$, or $\mathrm{sgn}(E_0) = \mathrm{sgn}(E_2)$) for certain parameter combinations when E has no real root v. With the definition of the capsize speed, the following can be said of the speed bounds where self-stability is potentially possible:

$\boldsymbol{E_0 > 0,\ E_2 < 0}$ self-stability only possible below capsize speed. (conventional bicycle)

$\boldsymbol{E_0 < 0,\ E_2 < 0}$ self-stability impossible.

$\boldsymbol{E_0 > 0,\ E_2 > 0}$ self-stability possible for all speeds.

$\boldsymbol{E_0 < 0,\ E_2 > 0}$ self-stability only possible above capsize speed.

However, for self-stability, also other Routh criteria need to be taken into account. For example, E might change from negative to positive at a point for increasing velocity while not all other Routh coefficients are positive (yet). It can even be that E stays either positive or negative for the complete forward speed range. The self-stability bounds from E are simply minima or maxima above or below which self-stability is possible, and thus they are not necessarily bounds of the self-stable speed region.

For a conventional bicycle the capsize speed and the upper bound of the self-stable speed region are coinciding. The speed where $E = 0$ is then associated with the speed where the capsize mode becomes unstable, hence the name. In that case the capsize speed might be simply taken as that upper bound (as done in JBike6 February 8, 2015 [45], section 4.3), but this would not work in general. The eigenmode that flips sign at $E = 0$ might even not be associated with a lean dominated capsize mode shape in

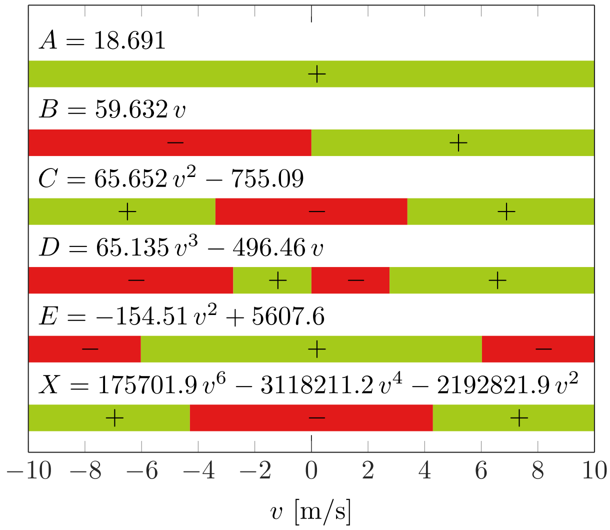

Figure 4.6: Routh Hurwitz coefficients for the benchmark bicycle parameters as function of the forward velocity. The reversed benchmark bicycle is represented by the negative forward velocities. It can be seen for $v > 0$ that the bicycle becomes stable, i.e. all positive Routh coefficients, when $X = 0$ and it becomes unstable again at $E = 0$.

more unconventional bicycles. A more accurate name, applicable to all bicycles, for the speed at $E = 0$ could be chosen, for example one that uses that the steer stiffness is zero at E_0.

Moreover, another transitional speed, the weave speed, v_w, occurs at $X = 0$. Just as $E = 0$ it is possible that $X = 0$ corresponds with different modes (not weave mode) crossing the zero axis such that the name may also not that appropriate. Also, it is not necessary that stability is lost or gained when the coefficient turns zero. The transitional speed corresponding with $E = 0$ is not necessarily a higher velocity than the one corresponding with $X = 0$. Furthermore, also the weave speed might not be at a point where a harmonic weave mode crosses the horizontal zero axis, but it does so for a conventional bicycle and in effect is called 'weave' speed. There might even be multiple speeds where $X = 0$, and hence, there might also be multiple 'weave' speeds.

For the conventional-like benchmark parameters, the coefficients are as displayed in figure 4.6. It can be seen in combination with figures 4.1b and 4.2b (or more precisely figure 4.5) that for this bicycle indeed the weave and capsize speed correspond with the velocities where $X = 0$ and $E = 0$ respectively. For the forwardly ridden benchmark bicycle the velocity region between the weave and capsize speed is the stable region, but for the reversed benchmark bicycle (negative forward velocity) this region is not stable. So indeed, not for all bicycles the weave and capsize speed are a stability boundary, because all other coefficients, besides E and X, also need to be positive in that speed region.

Reference gains signs

The sign of the reference gains is dependent on how the bicycle acts in steady-state. In steady-state, only the angles of the degrees of freedom are nonzero while their derivatives are zero. Then only the stiffness matrix, and thus the E coefficient, has influence on the sign of the reference gains. Because the forward velocity has influence on the stiffness the sign of the control reference gain is ultimately dependent on the forward velocity and its relation to the capsize speed determined by E.

During a constant turn (the bicycle is thus either self- or control-stable) the bicycle stays upright by a constant steer torque on the steer joint. At the capsize speed a 'control reversal' occurs that makes that the lean direction corresponding with a certain torque direction flips around at the capsize speed [16]. Where first a certain directed steer torque was needed to keep the bicycle in a constant turn, when the capsize speed is reached this direction changes sign. This is why a conventional bicycle loses its self-stability above the capsize speed; below the capsize speed it steers sufficiently much into the fall (which is needed for balancing), while above the capsize speed it steers not enough into a fall to return to an upright position. Exactly at the capsize speed where $E = 0$ there is no steer stiffness; changing the steer angle does not take any effort.

The reference following gain $N_{\delta\delta}$ is calculated such that the potential 'control reversal' at v_c is taken into account. This v_c is the capsize speed of the uncontrolled bicycle: $E = E_0 + E_2 v^2 = \det\left(\left[g\mathbf{K}_0 + v^2\mathbf{K}_2\right]\right) = 0$. Here the uncontrolled bicycle dynamics hold since a control-stable bicycle has changed dynamics of the whole system and may have a different capsize speed or no capsize speed at all. It appears that then for a conventional bicycle:

$$E_0 > 0,\ E_2 < 0 \Rightarrow \begin{cases} N_{\delta\delta} < 0, & \text{if } v > v_c \\ N_{\delta\delta} = 0, & \text{if } v = v_c \\ N_{\delta\delta} > 0, & \text{if } v < v_c \end{cases} \tag{4.26}$$

and for example a more unconventional bicycles may show different behavior:

$$E_0 < 0,\ E_2 > 0 \Rightarrow \begin{cases} N_{\delta\delta} < 0, & \text{if } v < v_c \\ N_{\delta\delta} = 0, & \text{if } v = v_c \\ N_{\delta\delta} > 0, & \text{if } v > v_c \end{cases} \tag{4.27}$$

Chapter 5

Bicycle time response

5.1 Simulating global coordinates

The behavior of the bicycle in time can be investigated by performing a linear time response simulation which gives the development of the states. Thus, the generalized coordinates are obtained as function of time. All simulations are done by numerical integration of the model (3.66) and require a specified time step and end as well as initial condition for the degrees of freedom (often zero), $\mathbf{x}_0$, and reference torques, $\mathbf{f}_\mathrm{r}$.

The bicycle model (3.66) can be rewritten to represent an Ordinary Differential Equation (ODE) such as the equation with $\mathbf{A}$ and $\mathbf{B}$ matrix in the state-space form, (3.67). This ODE can be integrated for example with the help of Matlab. Then, a Matlab `ode`-solver might be used or the system can be modeled in Simulink (see figure 3.3). Similarly, the model can be put in the complete state-space form (3.67) in order to simulate it (see section 3.4). In Matlab, a state-space model created with `ss` can be simulated with the `lsim` function. In all cases a timestep, time length, reference torque, and initial conditions have to be specified. After the simulation, the complete state of the bicycle in the global coordinate system can be calculated from the obtained generalized coordinates values.

Large global coordinates

For a time response analysis it is interesting to have the bicycle coordinates in the global frame to see what path the bicycle follows. However, in section 3.1 where the dynamical equations were derived, the bicycle was assumed to move only closely aligned with the global x-axis, such that the global coordinates remained small. To have a good image of how the bicycle can actually moves in the global frame, large coordinate values are desired.

The complete bicycle state is described by the generalized coordinates, lean angle ϕ and steer angle δ, as well as the ignorable coordinates, rear contact location (x_P, y_P), heading (global rear assembly yaw angle), ψ, and wheel to frame rotations, θ_R and θ_F. These last five coordinates are ignorable, because non-holonomic constraints make that they do not show up in the final lateral EOM (see section 3.1). Therefore, the bicycle does not need to be aligned with the global coordinate system and these coordinates can be arbitrary large such that the bicycle can be located everywhere on the ground plane with any heading angle [22].

Although they do not appear in the final equations, the ignorable coordinates are still needed to fully define the bicycle orientation in the global frame in order to get a complete image of the bicycle motion in time, e.g. for visualization [22]. When the states of the degrees of freedom of the bicycle in time are known from some time simulation, the kinematic constraint equations can be integrated and the full bicycle configuration as a function of time is obtained [22]. Although the lean and steer are assumed linear, the overall motion of the bicycle in the global frame can be described in a nonlinear manner: [22]:

> "*This situation is somewhat analogous to, say, the classical elastica where the displacements and angles used in the strain calculation are small yet the displacements and angles of the elastica overall can be arbitrarily large.*"

Thus several equations are obtained that describe the relation between the bicycle generalized coordinates and the remaining bicycle coordinates. Note that integration of a vector can be done in Matlab by applying `cumsum` and multiplying with the time step.

Global large assembly yaws The global yaw angles of the rear assembly, ψ, and front assembly, ψ_A, determine the heading of the wheels in the global frame (see figure 3.2). Only for the derivation of the equations of motion did the yaw angle need to be assumed small. Since it is an ignorable coordinate it can be a large angle and can be calculated by integrating (with certain initial condition) the rear yaw angular rate from kinematics with the steer angle, from constraint equation (3.32):

$$\psi = \int \dot{\psi}\,\mathrm{d}t \tag{5.1}$$

The large front assembly yaw can then be calculated from (3.38) with (5.1) plugged in.

Global large contacts positions For large yaw angles the rear wheel contact point velocities are dependent on forward velocity and yaw angle by simple trigonometry:

$$\dot{x}_P = v\cos\psi \quad , \quad \dot{y}_P = v\sin\psi \tag{5.2}$$

The positions follow by simple integration (with certain initial conditions),

$$x_P = \int \dot{x}_P\,\mathrm{d}t \quad , \quad y_P = \int \dot{y}_P\,\mathrm{d}t \tag{5.3}$$

The front wheel contact point in the global frame is determined by the rear wheel contact point, the yaw angle and bicycle parameters as in (3.40). From simple 2D rotation matrix theory where the small angle yaw coordinates of Q are taken in a local coordinates frame aligned with the rear assembly (not aligned with the support line), the large yaw angle position then follows:

$$\begin{bmatrix} x_Q \\ y_Q \end{bmatrix} = \begin{bmatrix} x_P \\ y_P \end{bmatrix} + \begin{bmatrix} \cos\psi & -\sin\psi \\ \sin\psi & \cos\psi \end{bmatrix} \begin{bmatrix} x_Q \\ y_Q \end{bmatrix}_{(x_P, y_P, \psi=0)} \tag{5.4}$$

with, from (3.40),

$$\begin{bmatrix} x_Q \\ y_Q \end{bmatrix}_{(x_P, y_P, \psi=0)} = \begin{bmatrix} w \\ -c\,\delta\cos\lambda_s \end{bmatrix} \tag{5.5}$$

Which can be shown to be the same as,

$$\begin{aligned} x_Q &= x_P + (w+c)\cos\psi - c\cos\psi_A \\ y_Q &= y_P + (w+c)\sin\psi - c\sin\psi_A \end{aligned} \tag{5.6}$$

Wheel rotation angles For completeness also a linear time response of the rotation angle of the rear wheel can be conducted. The wheel rotation angles can be calculated from the rotational velocity:

$$\theta_R = \int \dot{\theta}_R\,\mathrm{d}t \quad , \quad \theta_F = \int \dot{\theta}_F\,\mathrm{d}t \tag{5.7}$$

The angular rate is directly related to the forward velocity, v, by (3.30). With no propulsion the torque vanishes from (3.22), and $\dot{\theta}$ (and v) is constant. With certain initial conditions than the wheel rotation angles can easily be obtained.

5.2 Measuring global coordinates

To see how the dynamics of a bicycle are in real-life, one can measure experimentally, the time response of a bicycle. The real-life bicycle can then be ran with or without a known linear controller and the movements can be measured. Optionally, these measurements can be compared with simulations (see section 5.3).

The two generalized coordinates, the global lean and especially the relative steer angle between the frames, can be measured directly. Absolute angles in the global frame can be obtained from the rates by integration, but this is prone to errors, so preferably they are accurately measured directly. However, global frame, angular rates around the several axes are obtained easier and more accurate than absolute angles. For these rates, often one gyroscope per angular rate is enough to measure the movements. The full bicycle configuration in time can be possibly derived from the wheel angular rate and lean and yaw rate of one of either assembly (see section 5.3).

All sensors have some collective requirements. Most importantly, the measuring system should minimally influence the bicycle system in order to measure the pure bicycle dynamics. Therefore, a low mass and mass moment of inertia is required for the sensors, and they should introduce minimal friction in the bicycle system. For some experiments the sensors are required to work in the open-air and -road, but sometimes it is enough that they work inside in an enclosed limited environment.

Note that care has to be taken in whether the angles are presented in degrees or the desired radians. When needed, degrees can be translated to radians per second by multiplying the degrees with $\pi/180$ or, alternatively, the Matlab function `deg2rad` and its counter part `rad2deg` are available.

Wheel rotation/forward velocity

An important degree of freedom, which is ignorable for the lateral EOM, is the wheel rotation angle of the bicycle. The wheel rotation could be measured with some rotary encoder. Its derivative, the angular rotation rate is directly coupled to the forward velocity for a no-slip assumption. So basically, all methods of determining the forward velocity can also be used to measure the angular rate. Here, the calculations are described to obtain the forward velocity, but the wheel angular rate can easily be obtained from (3.30) when the wheel radius is known.

All methods can either measure the front or rear wheel rotation rate and, thus both wheels can be either used to determine the forward velocity (see (3.30)). However, not all methods can determine the riding direction.

Gyroscope

A gyroscope, i.e. angular rate sensor, can be directly put in a wheel to measure the wheel's angular rate. For example, an IMU with gyroscope can be used to measure the angular rate around a certain axis by placing it at the wheel hub or in the spokes. Minimal effect on the wheel inertia is caused when it is placed at the hub. For example, a Shimmer can be used for which a holder can be made that fits around the hub or in the spokes (see figure 5.2). A device like a Shimmer has as extra benefit that several of them can be synchronized, such that their timestamp and sample rate coincide.

By measuring the velocity with this method, the direction of riding can also be determined. If calibrated and placed correctly, the forward riding direction corresponds with negative angular rate and a reversed direction corresponds with a positive rate. The forward velocity follows directly from the wheel angular rate (see (3.30)):

$$v = -\dot{\theta}\, r \tag{5.8}$$

Voltage generator

To measure the forward speed of a bicycle, a tachometer can be used that generates a certain voltage corresponding with a certain speed. A continuous, although possibly alternating, voltage signal with an amplitude that depends on forward bicycle speed is then required. For example, a classic wheel or modern hub dynamo or a Direct Current (DC) motor are able to do this.

A classic dynamo generates an Alternating Current (AC). To rectify the current, i.e. make it DC, a (diode) bridge rectifier circuit should be added to the dynamo output terminals and create a good (linear) relation between rotational speed and output voltage. However, the wheel turning direction, or equivalently the bicycle riding direction, cannot be determined with a dynamo, because its output signal is the same in both turning direction.

A DC-motor has two terminals, but which one of the two terminals is the positive one and which one is the ground depends on the turning direction of the motor. Therefore, it is important to let the motor rotate (or likewise connect the terminals correctly) in the direction that gives the desired voltage output at normal operating. For clarity, the tachometer should be placed such that forwards movement gives a positive voltage and a negative voltage is created when the bicycle is ridden backwards. This method is potentially able to determine the riding direction, because the voltage sign depends on the DC-motor rotational direction. However, the processor that takes the voltage should be able to handle negative input voltages.

Some processor units, e.g. Shimmer (see table 5.2 and figure 5.2), can only process voltages within a certain voltage range. If that is the case a circuit as shown in figure 5.1c can be applied. When the voltage is outside the allowed voltage range the Zenerdiode closes the circuit over the motor so that the output to the processor does not get a negative voltage. The one zenerdiode does provide an over-voltage protection and in theory also deals with negative voltage by letting voltage true when negative. However, to really make sure that negative voltage is stopped in time a second diode (Schottky) is added. To not short the circuit over the motor when the circuit through the diodes is open, the resistor, is added. The current over the motor stays limited, because the resistor takes some away.

Furthermore, a motor will generally not generate a constant valued voltage due to it's architecture. It will give a voltage of peaks and valleys and therefore a capacitor, is placed to attenuate this phenomenon and other noise. If the finally obtained signal still contains electrical or mechanical noise, the signal can be post-facto filtered, for example, with Matlab function `filtfilt` that filters without phase shift.

Note, that the circuit could be made more complex to make the reach in the Shimmer range more precise. It could be even made such that the circuit does not short-circuit outside of the range or that a backwards bicycle ride results also in a positive voltage. Furthermore, if the tachometer puts out a to high voltage at a to-be-reached forward velocity, a voltage divider can be designed to keep the full resolution of the tachometer.

At low enough speeds, the bicycle forward speed, v, is linearly related to the output voltage of the tachometer, $\mathcal{U}$, by the bicycle wheel radius, r, and a tachometer specific velocity constant, $\mathcal{K}_v$, as,

$$v = \mathcal{K}_v \, r \, \mathcal{U} \tag{5.9}$$

This tachometer velocity constant can be determined by calibration; $\mathcal{K}_v^*$. Thereto, the tachometer output voltage is measured for specific accurately known forward velocities of a running band, drum, or other machine. These measurement points are fitted with a linear function which is allowed when the complete tachometer, just as its voltage generator, has a linear voltage/velocity ratio. Alternatively, the tachometer velocity constant can be calculated when the generator rotational speed constant, $\mathcal{K}_\omega$, and transmission ratio, μ_ω, are known, which gives generally a slightly different result than the calibration,

$$\mathcal{K}_v = \mathcal{K}_\omega \, \mu_\omega \tag{5.10}$$

If the rotational speed constant of the motor is not known from the specifications, but the nominal voltage, $\mathcal{U}_\mathrm{n}$, and motor nominal/no load rotational speed, ω_n, are, it can be calculated from those values:

$$\mathcal{K}_\omega = \frac{\omega_\mathrm{n}}{\mathcal{U}_\mathrm{n}} \tag{5.11}$$

These calculations hold for the tachometer when it is placed on the wheel tire like an old dynamo or when it is attached to the the wheel hub/axle with some transmission.

Tire measurement A way of applying a forward velocity dependent voltage generator is the well-known classic dynamo design that uses a runner wheel on the tire [66]. When a generator is used with a runner wheel on the bicycle wheel tire to measure the velocity, the input output ratio, μ_ω becomes dependent on the bicycle wheel radius. In that case for a bicycle wheel/tire of radius, r, and a runner wheel of radius, $\mathcal{R}$, which runs on the bicycle tire at a distance from the bicycle wheel axle, $\mathcal{L}$:

$$\mu_\omega = \frac{\mathcal{R}\, r}{\mathcal{L}^2} \tag{5.12}$$

This transmission ratio can be used in (5.10) in order to calculate the tachometer velocity constant. However, note that the ratio is dependent on several factors that are different for different bicycles such that the ratio must be calculated every time this method is used in other situations.

Axle measurement The generator can be attached at the wheel axle with some transmission mechanism to rotate with the wheel hub. This way the friction caused by the tachometer is probably

Table 5.1: Tachometer important specifications.

Parameter	Symbol	Value
Mass	–	0.2031 kg
Dimensions	–	137×Ø33 mm
Calibrated velocity constant	$\mathcal{K}_v^*$	43.63 1/(Vs)
Maxon DC motor 2028.948-12.161-025		
Rotational speed constant	$\mathcal{K}_\omega$	30.3π 1/(Vs)
Worm drive		
I/O ratio	μ_ω	9/20

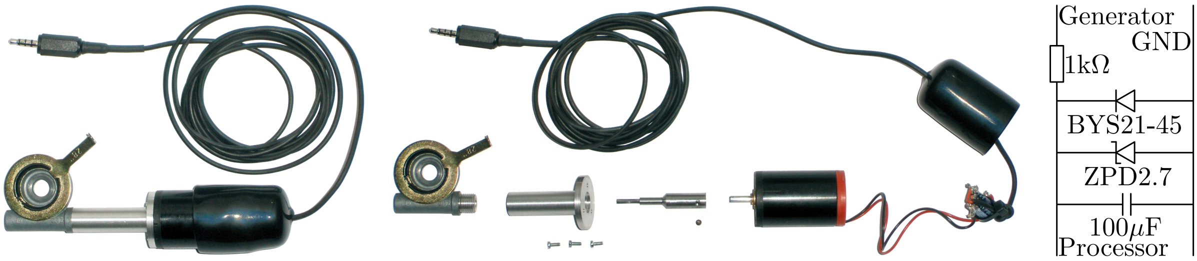

(a) (b) (c)

Figure 5.1: The wheel hub tachometer (a) assembled and (b) exploded, and (c) the connected electronic circuit between the generator (DC-motor) and the processor (Shimmer allowing voltage of 0-3V). The yellow pin grabs on in the wheel and rotates along with it. Via a transmission in the worm drive between the yellow ring and the grey tube, the wheel drives the DC-motor which, on its part, generates a voltage corresponding with its rotational speed. The circuit provides a negative- and over-voltage protection by reverse-biased diodes, signal flattening by capacitor, and short-circuit current limiting by resistor, and connects to a 3.5 mm jack plug.

less than when placed at the wheel. However, with such a design the bicycle needs to be inconveniently dissembled to install sensor. A system with a chain or belt can be applied, as well as a system with a worm drive. An example of such a worm drive design tachometer is depicted in table 5.1 and figure 5.1.

The bicycle is assumed to run at a low enough speed such that the rotational speed and output voltage have a linear relation such that a velocity constant is available that relates the values. As seen, this tachometer has a measured calibrated velocity constant, $\mathcal{K}_v^*$, to be used with (5.9). The tachometer velocity constant calculated with (5.10) from the motor rotational speed constant and the worm drive transmission ratio is only slightly different from the calibrated value.

This specific tachometer uses a Maxon DC-motor 2028.948-12.161-025 with a 'Messgeräter, Montage GmbH Beierfeld (MMB)' perpendicular rotation converter to generate a continuous voltage from the wheel rotation. The motor is supposed to function in its linear domain at normal bicycle speed and the faster the motor runs, the higher its output voltage.

The small perpendicular rotation converter is a worm drive that creates a rotation perpendicular to the wheel hub and originates from classic analogues bicycle and moped tachometers. It is placed at the wheel hub where the worm wheel rotates with the wheel, while the worm screw is stationary around the non-rotating wheel hub axle. The pin from the worm wheel grabs in between the spokes and can be secured to them with a tie-wrap. Thus, input of the worm drive is the part attached to the wheel and the output is attached to the generator, making an input/output ratio from wheel rotation to output rotation as listed in table 5.1.

The specific tachometer circuit components (figure 5.1c) are designed for use with a Shimmer. The added terminal connection together with the electronic circuit makes that the tachometer can only be placed at the right side of a wheel to give a correct voltage output. By switching the motor terminals on the circuit, the tachometer can be used on the other (left) side of a wheel.

This design has as disadvantage that it adds mass to the bicycle (see table 5.1). Furthermore, it also appeared to cause periodical mechanical noise due to imperfections in the worm drive.

Rotary encoder

A pulse sensor can be used that measures pulses of a rotating wheel. There exist rotary encoders that can determine the absolute angle, the angular rate, and the turning direction. However, here a simple and common example for bicycles is worked out: Magnetic pulse counter tachometer.

In the wheel a magnet can be used to create voltage pulses upon passage of a magnetic switch such that a wheel rotation is registered. From the pulses due to the wheel rotation the pulse periods can be determined. However, these pulses are direction independent and can thus not discriminate between riding directions. This sensor requires a voltage which is passed back to the processor whenever the circuit is closed by the pulse creator. This voltage can be supplied by a battery or by the processor itself, e.g. a Shimmer (see figure 5.2).

To increase the accuracy of the measurement, the number of pulses per wheel rotation, $\mathcal{N}_\mathrm{p}$, should be increased. However, the pulse creators, i.e. magnets, must be uniformly distributed around the wheel. The number of spokes are then convenient to use to determine this number, and place the pulse creators evenly distributed over the wheel. Wide magnets would create longer pulses which are easier to register and prevent misses of pulses with a processor with limited sample rate. A possible issue in pulse counting is namely that pulses can be missed due when there are no measuring samples taken during a pulse.

It is a semi-post-facto measurement, because the velocity can only be determined over a pulse period after that pulse period occurred. This can be done by hand or, for example, in Matlab with `pulseperiod`, which gives the generally alternating periods between the pulses. For a fluctuating forward velocity, also the pulse period fluctuates such that there is no one pulse period. For example, with decreasing v, the pulse period increases. Finally, the forward velocity follows from the pulse period between two specific consecutive pulses, $\mathcal{T}_\mathrm{p}$, as,

$$v = \frac{2\,\pi\,r}{\mathcal{N}_\mathrm{p}\,\mathcal{T}_\mathrm{p}} \tag{5.13}$$

Videocamera

A videocamera with known image frame rate, ω_i, can also be used to determine the forward velocity [15] [16] [44]. One can then determine the number of wheel rotations, $\mathcal{N}_\theta$, per number of frames required for those rotations, $\mathcal{N}_\mathrm{i}$. To make noticing a complete rotation in the video image frames easier, a wheel could have a mark on it, e.g. the valve, or a sticker/tape. A larger number of wheel rotations and number of frames can increase the precision of the measurement, but when the velocity changes fast these values cannot be too large or else the accuracy of the measured velocity value decreases. Of course, the riding direction can easily be seen from the video and from a number of wheel rotations per second and the wheel radius, r, the forward velocity can be determined post-facto, i.e. after the measurement, as follows:

$$v = \frac{2\,\pi\,r\,\omega_\mathrm{i}\,\mathcal{N}_\theta}{\mathcal{N}_\mathrm{i}} \tag{5.14}$$

Step pacer

Counting the steps of a human running next to a bicycle is another way of measuring the forward velocity. The step gait of walking can be seen as a sequence of pulses, where every pulse corresponds with a certain displacement distance. Although it is not a very accurate method, it is handy as pacer in bringing a coasting bicycle to an approximate speed. The desired speed is then known beforehand, and a matching gait step length and gait frequency should be applied to come to that forward velocity.

The step length can be reached, for example, by placing markers on the floor separated by a distance equal to the step length. At low forward velocities, the gait step length and forward velocity are approximated by a linear relation. Therefore, gait step length and forward velocity data [67] is taken and a linear fit is performed on a mean of all the data for a separate male and female category, resulting in two equations linking forward velocity, v, to a comfortable human gait/step length, $\mathcal{L}_\mathrm{g}$:

Male

$$v = 4.32\,\mathcal{L}_\mathrm{g} - 1.48 \tag{5.15}$$

Female

$$v = 5.14\,\mathcal{L}_\mathrm{g} - 1.73 \tag{5.16}$$

The step length alone is not sufficient to reach a certain velocity, it is just an indication of what step length is comfortable to walk by at a certain forward velocity. Therefore, the step length should also be matched with a certain gait frequency, $\omega_\}$. This gait frequency can be reached by using a constant step ticker, e.g. a metronome, and trying to match one's gait frequency with the ticker frequency. Note that a metronome often gives its ticks in Beats Per Minute (BPM), i.e. 1 [BPM] $= 60\,\omega_\mathrm{g}$ [1/s]. With a certain step length, the forward velocity follows then from the step frequency as,

$$v = \omega_\mathrm{g}\,\mathcal{L}_\mathrm{g} \tag{5.17}$$

Steer angle

The steer angle is a relative angle between two frames and requires a special manner of measuring. Two IMU's, one on either assembly, could be used to measure the yaws of either assembly. Then, the steer angle is the difference (augmented by the steer-axis angle, λ_s) between the rear and front assembly yaw angle/rate, (3.38) and (3.39). Furthermore, a manner of determining the steer angle is by direct measurement with a sensor that measures angles between two bodies. For example, a rotary encoder or a potential meter with one end attached to the rear assembly and the other end to the front assembly, e.g. by means of a pulley and rope, would suffice.

Global angles

The global angles around the different axes are another important state representation of the bicycle. The drift free orientation yaw/heading angle can be measured with 3D accelerometers and magnetometers. Less prone to measurement errors is the measuring of the angular rates around all axes which can be done with 3D gyroscopes. Just as in many cases, separate sensors and processors can be used or integrated sensor and processing devices are available.

Separate sensor

Separate sensors can be used to determine the angle or the angular rate [17] [18]. For an analog sensor an Analog to Digital (A/D) converter might be required to convert an analog voltage signal to a digital one, and some storage or sending device might be needed to bring the data to a PC. For example, an Arduino unit would do as a processor of data.

Integrated sensor

To measure the angular rate (and absolute heading) one can use one single device that measures and logs the data. For example an Inertial Measurement Unit (IMU) like a Philips Pi-Node [15] [16] [44] or a Shimmer [71] would suffice. These units have integrated 3D accelerometers, magnetometers, and gyroscopes, as well as a processor to log the data and to store or stream the data and bring it to a PC. Here, the usage of a Shimmer3 is used as example of measuring angular rates and possibly processing forward velocity measurements [71].

A Shimmer (see table 5.2 and figure 5.2) can be placed on a bicycle by using a holder, e.g. the custom designed 3D-printable holder for round tubes as displayed in figure 5.2d. The Shimmer can be manually calibrated such that, when placed on the bicycle, its axes align with the bicycle benchmark coordinate system [22] of SAE J670 [57]. Furthermore, the round orange button on the Shimmer can be set to start and stop the measurement and its recording upon pressing. These recorded results can be saved internally on its (SD-card) memory and/or stream the results via Bluetooth to another device, e.g. PC. Moreover, with the Consensys software several Shimmers can be connected via Bluetooth to operate in synchronization and thus to measure simultaneously with a synchronized time stamp.

Measurement configurations such as sample frequency and sensor range with according sensitivities (higher sensitivity is more accurate) can all be set. Also, the exact output of the Shimmer is manually

Table 5.2: Inertial measurement unit, Shimmer, important specifications. (LSB: Least Significant Bit)

Parameter	Symbol	Value
Shimmer3 (Shimmer PROTO3)		
Mass (PROTO3)	–	0.0236 (0.028) kg
Dimensions (PROTO3)	–	50.5 (65.0) × 34.0 × 14.0 mm
Clock rate [68]	ω_t	32768 ticks/s
Maximum sample rate [68]	–	1024 Hz
Accelerometer wide range [69]	–	$\pm 2.0g \ldots \pm 16.0g$ m/s^2
Accelerometer sensitivity (per range) [69]	–	1000 . . . 83.3 LSB/g
Gyroscope range [69]	–	±250 . . . ±2000 °/s
Gyroscope sensitivity (per range) [69]	–	131 . . . 16.4 LSB/(°/s)
Magnetometer range [69]	–	±0.00013 . . . ±0.00081 T
Magnetometer sensitivity (per range per axis) [69]	–	1100/980 . . . 230/205 ·10^4LSB/T
Input voltage range [70]	–	0 - 3000 mV
Output voltage [70]	–	3 V

(a) (b) (c) (d)

Figure 5.2: An inertial measurement unit (IMU) and processor; (a) Shimmer3 [71] and (b) the Shimmer PROTO3 Deluxe [71] with (c) 3.5mm jack plug connections: Two Analog to Digital converter (A/D) positions, one 3V output, and one Ground (GND) [70]. (d) A 3D-printable Shimmer holder (compatible with the Shimmer3 and Shimmer PROTO3 Deluxe) attachable to a round tube with, for example, tie wraps.

selectable, but the most important ones in this case are the angular rates and the time stamp. The Shimmer presents the angular rates per axis as ‘Gyroscope’ output in degrees per second, such that it first needs to be translated into radians per second. The most ‘pure’ time signal of the Shimmer is the raw time stamp, $\mathcal{N}_t$, that is presented as a tick, t, count in the output ‘Timestamp’ column. With the clock rate, ω_t, this tick time stamp can be translated to the time in seconds. Generally, the time stamp does not start at zero. To correct for this, the first time stamp value, $\mathcal{N}_{t0}$, must be subtracted from all time values:

$$t = \frac{\mathcal{N}_t - \mathcal{N}_{t0}}{\omega_t} \tag{5.18}$$

Besides the Shimmer3 internal sensors, by implementing expansion boards, external sensors can be connected in order to let the Shimmer3 process their measurements. A Shimmer PROTO3 expansion board can be used to ‘interface the Shimmer3 with an analogue output sensor, a digital output sensor, a serial UART or a parallel bus interface’ [70]. One of these expansion boards is the Shimmer PROTO3 Deluxe which has two 3.5 mm 4-position jack connectors (see figure 5.2b). The jack plug connectors (see figure 5.2c) provide means of supplying a to-be-recorded voltage signal to the Shimmer (two A/D channels), as well as means of supplying a voltage (a 3V channel) to an external sensor. For example, a voltage from a tachometer can be put on an ‘Int A’ port of the Shimmer and is then presented in the output file in mV.

5.3 Comparing simulation and measurement

Experimentally measured bicycle coordinates can be compared with the bicycle model. Thereto a measured signal can be fitted with the bicycle model in the specific bicycle parameters. Generally, next to the forward velocity (or wheel rotation rate), the global lean rate and global heading rate of either frame/assembly are measured and compared, but also the rates of the two generalized coordinates, lean rate and steer rate, could be the comparable signal.

To compare motions between a real bicycle and its model a certain motion can be applied on the real bicycle in an experiment. For example, when stable the bicycle can be brought out of its equilibrium position by a sidewards push against the frame while moving it forward. Its behavior after the push is dependent on its dynamics and can be compared with the simulated behavior from the model. When unstable, a motion is already started when the bicycle is let loose without applying a push.

Wheel rotation rate/forward velocity

In the linear domain, the longitudinal EOM are decoupled from the lateral EOM (see section 3.1), but to perform a simulation, first the bicycle wheel angular rate is required. The angular rate of the wheels relative to the frames is directly related to the bicycle forward velocity with a no-slip assumption.

For an experiment with $\mathbf{f} = 0$ and $T_\theta = 0$, measurements show a decreasing velocity due to friction in the system. However, here the data needs to be fitted on a linear model with constant v. The 'fit' of the forward velocity then consists of taking the initial value of the measured (and filtered) velocity signal. This launch speed at the beginning of the experiment is the most important velocity during the experiment [16] [44].

Angular rates

Fit specific bicycle configuration

A method of comparing the measured angular rate values with simulated ones is fitting a simulation with the state-space representation (see section 3.4) of the specific real-life measured bicycle by using Matlab function `ssest`. Thereto, the measured data, the state-space model, and the to-be estimated initial conditions must all be converted to identifiable parameters with Matlab functions, `iddata`, `idss`, and `idpar` respectively. Then, with `ssestOptions` the options can be set such as the fitting method and which state-space parameters may be varied, i.e. the free variables, and within what boundaries they can be changed. With measured bicycle parameters (including the already fitted forward velocity), the state-space matrices are not free to chose and, in effect, the fit algorithm must be set to only vary the initial state for the simulation. Finally, a good time sample should be chosen from the complete measured signal where the bicycle is supposed to move in accordance with its model, e.g. when no external torques are assumed in the model then the data should correspond with a free running bicycle.

What initial conditions can be chosen to be free or not, is open for discussion and should be determined with trial-and-error. The initial lean and steer angular rate can always be set free, because those or the states of interest here. However, the angles themselves may not be measured, but should be given an initial value for the simulation fit. It turns out that the fit algorithm, when allowed to change them, tends to chose them inaccurately large and not corresponding with what is seen in real-life experiments. Therefore, a safe bet is to give the initial angles a set value of 0.

The fit quality of the model output in time, $\mathbf{y}_j$, and the measured output, $\mathbf{y}_j^*$, for either output channel, j, can be visually checked by plotting it. However, there are some more objective measures, for example, presented by Matlab in a report with the estimation, `Report.Fit`. One measure between the difference of the measured signal and the model is the Mean Squared Error (MSE), $\mathcal{D}$, between the signals, where its value should be lower to have a better fit. It is simply the mean of the squared differences between measurement and model (also in the Matlab report; `MSE`):

$$\mathcal{D} = \overline{[\mathbf{y}_j^* - \mathbf{y}_j]^\intercal [\mathbf{y}_j^* - \mathbf{y}_j]} \tag{5.19}$$

Another, derived, measure for the quality of the fit is the Normalized Root Mean Square Error (NRMSE), $\mathcal{D}^*$. This value can be calculated to compare between data or models with different scales. Matlab expresses this value as a percentage of one and presents it in a report as `FitPercent`, such that the higher this value, the better the fit. It can be calculated by taking the Euclidean norm (2-norm) of the errors, i.e. the difference between measurements and model, and normalizing it and converting it to a percentage:

$$\mathcal{D}^* = 100\left(1 - \frac{||\mathbf{y}_j^* - \mathbf{y}_j||}{||\mathbf{y}_j^* - \overline{\mathbf{y}_j^*}||}\right) = 100\left(1 - \left(\mathcal{D}/\sqrt{[\mathbf{y}_j^* - \overline{\mathbf{y}_j^*}]^\intercal\,[\mathbf{y}_j^* - \overline{\mathbf{y}_j^*}]}\right)\right) \tag{5.20}$$

Unfortunately, this estimation/fit function can only fit stable (converging) signals, or when stable, the fit may not be visually satisfactory. When that is the case, one might chose to fit the model in another way on the measured values. For example, a fit of a linear first order polynomial can be performed on a certain number of values that are close to $t = 0$, and hence, the estimation of the initial condition is then the value of the polynomial for $t = 0$. This is simply the polynomial coefficient of order zero, and these polynomial coefficients can easily be calculated in Matlab with `polyfit`. The number of values used for the fit can be chosen by trial-and-error to get the best estimation. Alternatively, the initial conditions can be chosen or tweaked by hand, or the time sample from the measured data can be chosen differently, to make the fit better.

State-space fitting requires that the state-space model (3.67) outputs the same variables as the measured ones. Therefore, depending on what is measured, the state-space output requires different $\mathbf{C}$ and $\mathbf{D}$ matrices.

Generalized coordinates To just fit the generalized coordinates rates when these are directly measured, the `ssest` function requires simple output matrices:

$$\mathbf{C}^* = \begin{bmatrix} 1 & 0 & 0 & 0 \\ 0 & 1 & 0 & 0 \end{bmatrix} \quad , \quad \mathbf{D}^* = \mathbf{0} \tag{5.21}$$

Global (ignorable) coordinates When the lean and yaw rate of the rear assembly are measured, i.e. sensor on rear assembly, the state-space model must output the lean generalized coordinate and the rear frame yaw rate from (3.32) for the fit:

$$\mathbf{C}^{**} = \begin{bmatrix} 1 & 0 & 0 & 0 \\ 0 & \frac{c}{w}\cos\lambda_\mathrm{s} & 0 & \frac{v}{w}\cos\lambda_\mathrm{s} \end{bmatrix} \quad , \quad \mathbf{D}^{**} = \mathbf{0} \tag{5.22}$$

Likewise, the two output matrices of the state-space model for an output of the front frame lean and yaw rate can be composed with (3.37) and (3.39),

$$\mathbf{C}^{**}_\mathrm{A} = \begin{bmatrix} 1 & \sin\lambda_\mathrm{s} & 0 & 0 \\ 0 & \left(1 + \frac{c}{w}\right)\cos\lambda_\mathrm{s} & 0 & \frac{v}{w}\cos\lambda_\mathrm{s} \end{bmatrix} \quad , \quad \mathbf{D}^{**}_\mathrm{A} = \mathbf{0} \tag{5.23}$$

(Note that, alternatively, to get the front frame angles and rates the bicycle parameters can be reversed and the velocity can be made the opposite sign to make the reversed bicycle appear to ride forwards. This makes the DOF lean and yaw angles and rate the angles and rates of the front wheel and frame. This method is not ideal, because it can cause confusion. When the lean angle has the same sign as for the forward case, the corresponding yaw angle is of an opposite angle. And the other way around, when the yaw angle is of the same sign as for the forward case, then the lean angle has an opposite sign. This is because the bicycle rides now in another quadrant of the reference frame.)

With the model, a prediction can be made of the ratio between the initial input angular rates, as consequence of a sideward impulse applied on the bicycle at point I. Not only can the ratio between steer and lean angular rate be calculated, but with an initial zero assumed steer angle, also the ratio from yaw angular rate to lean angular rate can be calculated, becuase then the initial global angular rates are equal to the initial local angular rates. The ratios are dependent on the location of the impulse, $(x_\mathrm{I},\, z_\mathrm{I})$, and on which of the two assemblies of the bicycle it is applied.

Rear assembly impulse The lateral velocity at the location of the impulse on the rear frame right after the impulse is applied can be described by a kinematic relation with the initial angular rates. By using 3.53 and 3.54, this velocity can be expressed both in lean/yaw and lean/steer:

$$\begin{aligned} \dot{y}_{\mathrm{I}0} &= -z_\mathrm{I}\ {}_\mathrm{R}\dot{\phi}_0 + x_\mathrm{I}\ {}_\mathrm{R}\dot{\psi}_0 \\ &= -z_\mathrm{I}\,\dot{\phi}_0 + x_\mathrm{I}\,(c/w)\,\dot{\delta}_0\cos\lambda_\mathrm{s} \end{aligned} \tag{5.24}$$

These expressions for the lateral velocity can be used to derive two expressions for the initial motion as consequence of an applied impulse, $\int F_{\mathrm{I}y}\,\mathrm{d}t$. Thereto, a transformation with (3.55) might be needed to obtain the correct mass matrix (3.52):

$$
{}_{\mathrm{R}}\mathbf{M}\begin{bmatrix} {}_{\mathrm{R}}\dot{\phi}_0 \\ {}_{\mathrm{R}}\dot{\psi}_0 \end{bmatrix} = \begin{bmatrix} -z_{\mathrm{I}} \\ x_{\mathrm{I}} \end{bmatrix} \int F_{\mathrm{I}y}\,\mathrm{d}t \tag{5.25}
$$

$$
\mathbf{M}\begin{bmatrix} \dot{\phi}_0 \\ \dot{\delta}_0 \end{bmatrix} = \begin{bmatrix} -z_{\mathrm{I}} \\ x_{\mathrm{I}}\,(c/w)\,\cos\lambda_{\mathrm{s}} \end{bmatrix} \int F_{\mathrm{I}y}\,\mathrm{d}t \tag{5.26}
$$

The equations can be solved for the unknown initial conditions for any arbitrary nonzero impulse to find the ratios between the initial values, $\frac{{}_{\mathrm{R}}\dot{\psi}_0}{{}_{\mathrm{R}}\dot{\phi}_0}$ and $\frac{\dot{\delta}_0}{\dot{\phi}_0}$, from the model.

Front assembly impulse With the use of (3.58) and (3.59), the lateral velocity at the impulse location on the front frame can be expressed as,

$$
\begin{aligned}
\dot{y}_{\mathrm{I}0} &= -z_{\mathrm{I}}\ {}_{\mathrm{F}}\dot{\phi}_0 + (x_{\mathrm{I}} - w)\ {}_{\mathrm{F}}\dot{\psi}_0 \\
&= -z_{\mathrm{I}}\,\dot{\phi}_0 + ((x_{\mathrm{I}} - w - c + x_{\mathrm{I}}\,(c/w))\cos\lambda_{\mathrm{s}} - z_{\mathrm{I}}\,\sin\lambda_{\mathrm{s}})\,\dot{\delta}_0
\end{aligned} \tag{5.27}
$$

And the initial motions expressions follow, where for the local lean and yaw, (3.60) is used to obtain the mass matrix (3.52):

$$
{}_{\mathrm{F}}\mathbf{M}\begin{bmatrix} {}_{\mathrm{F}}\dot{\phi}_0 \\ {}_{\mathrm{F}}\dot{\psi}_0 \end{bmatrix} = \begin{bmatrix} -z_{\mathrm{I}} \\ x_{\mathrm{I}} - w \end{bmatrix} \int F_{\mathrm{I}y}\,\mathrm{d}t \tag{5.28}
$$

$$
\mathbf{M}\begin{bmatrix} \dot{\phi}_0 \\ \dot{\delta}_0 \end{bmatrix} = \begin{bmatrix} -z_{\mathrm{I}} \\ (x_{\mathrm{I}} - w - c + x_{\mathrm{I}}\,(c/w))\cos\lambda_{\mathrm{s}} - z_{\mathrm{I}}\,\sin\lambda_{\mathrm{s}} \end{bmatrix} \int F_{\mathrm{I}y}\,\mathrm{d}t \tag{5.29}
$$

Solving these for an arbitrary nonzero impulse gives the ratios between the initial values, $\frac{{}_{\mathrm{F}}\dot{\psi}_0}{{}_{\mathrm{F}}\dot{\phi}_0}$ and $\frac{\dot{\delta}_0}{\dot{\phi}_0}$, from the model for an impulse on the front frame.

Fit exponential function

In order to compare the measured values with the model further, the eigenvalues of the measured signals can be extracted by fitting a function on them. When the bicycle shows an oscillating motion during the experiment, the oscillating exponential function (4.6) can be fitted on the signal in order to find the frequency and damping ratio (and remaining coefficients). Then, the eigenvalues of the signal follow from (4.2).

As known, the Whipple model gives four eigenvalues (see section 4.2), but with this fitting method generally only a single complex eigenvalue pair is obtained. This is because such a complex eigenvalue corresponds with the dominating oscillatory motion. Both a lean and a yaw/steer angular rate signal are dominantly determined by this same eigenvalue, and thus both angular rate signals can be used for the fit. Since both should be equivalent in this situation, the mean of the eigenvalues from both signals can be taken as the eigenvalue of the measured signals.

A convenient way of performing the fitting is with the Matlab `fit` function. With `fitType` and `fitOptions` the exact fitting preferences can be set, such as the fitting method, and lower/upper bounds and starting points of the several to-be fitted coeffients and parameters. These starting points can be chosen such that they correspond with the values that are expected by the model.

Chapter 6

Kinematics: Support motion and steer-side definition

6.1 Support line lateral acceleration

The kinematics of the Whipple bicycle model determine how the support line accelerates laterally for given forward velocity and steer angle. For balancing and maneuvering it is important that the support of the bicycle can be moved laterally such that it can be brought underneath resultant forces on the center of mass (COM). The support of a bicycle is spanned by its contact points and is thus the infinitely long support line PQ (see figure 3.2). As will be shown later on, not only is the kinematic motion of the support line important in balancing, but the kinematics are also important in distinguishing the steer-side of a bicycle (see section 6.3).

During balancing the support line is constantly moved to intercept the resultant force on the center of mass on the bicycle; during straight movement the support is supposed to be brought vertically underneath the center of mass to counteract gravity and during a corner it should generally be positioned somewhere diagonally below the COM to also counteract a centripetal acceleration. The support line should be moved back to a stable position to recover balance when the line is shifted away, or equivalently, when the bicycle is leaned over to one side. Here, the movement of the support line in the ground plane under influence of steering is discussed in a kinematic sense with only superficial discussing dynamics of balancing. If the bicycle is actually balanced and whether this fall-avoidance is due to self-stability or an external controller is determined by the dynamics and is not considered here.

The lateral ground motion of the support line is described both by its lateral velocity and the lateral acceleration. The lateral velocity (in fall direction) of the support line should be larger than the lateral velocity (in fall direction) of the COM in order to recover from falling laterally. It is essential that the support moves faster relative to the COM in order to 'catch up' with it. The lateral acceleration of the support line already captures this recovering force and it ultimately determines if the support line moves in the correct balancing direction, i.e. that it shifts in a desired position underneath the COM eventually. The lateral velocity direction is of less importance, because the velocity is affected by the acceleration eventually. Therefore, the lateral acceleration of the support line is the best measure for the force that brings the support back under the COM and thus for the lateral motion. In other words, the support line generally needs to be accelerated into the lean direction to recover balance. The only way this can be done on a bicycle is indirectly by changing the trajectories of the wheel contact points; steering. This is where the assumption of steering into a fall to recover balance comes from physically. Both steer angle and steer angular rate have effect on the support line lateral acceleration.

With a no-slip condition assumed for the contact points, the directions of the absolute velocities and accelerations of the contact points and different points on the support line are completely defined by the wheel yaws (inclination about vertical axis). The resultant forward velocity of the points on the support line are always tangent to the trajectory of those points in the ground plane. This means that the velocity direction is aligned with the rear and front wheel at the contact points and that it changes direction in the bicycle frame linearly in between. On the contrary, the acceleration is always perpendicular to the trajectories of the points on the support line, such that they are aligned with a line through the instantaneous curvature center and a point on the support line (see figure 2.4). At the contact points the acceleration is perpendicular to the wheels and just as the velocity it changes direction linearly in the bicycle local frame along the support line. The lateral acceleration acts through forces at the contact points that change the bicycle velocity direction in the global frame. So in this frictionless model, the forward velocity does not change in magnitude and the acceleration only changes the direction of the velocity in the global frame.

The lines of action are thus definite, but the direction and magnitude are not. The lateral acceleration of the support line between the front and rear contact point is a function of both steering angle and steering angular rate [15]. The contribution of the steer angle on the support line lateral acceleration is equal along the support line. However, the steer rate contribution is generally different at the rear contact point as compared with the front contact point, because under influence of the bicycle parameters, the kinematics can alter such that the sign of the contribution of the steer rate might change along the length of the support line. This makes the prediction of the lateral acceleration of the support-line less straightforward; One portion of the rear and front resultant acceleration is equal, while another part is different following a certain ratio dependent on the trail and wheel base length. Moreover, the steer angle has relatively more influence at high forward velocities compared to the steer rate, because it scales with the squared velocity.

The influence of the steer rate makes that the support line can move different initially than it does in steady state. For a conventional bicycle ridden with small steer rates, i.e. barely fluctuating steer angles, the lateral acceleration of the support line in between the wheels is always pointed to the inward of the curve. However, quick steer movements might alter the magnitude and direction. A steer rate can even make that the lateral acceleration of the rear wheel is initially pointed outwards of the curve during transient behavior, while in steady state when the curve motion is more settled and the steer rate is zero the lateral acceleration is a centripetal force pointing inwards of the curve. Note that, with appropriate control (section 7.2 and 7.3) or appropriate mass distribution (chapter 8), positive angular steer rate contributing negatively to the lateral acceleration of the support line in between the wheels is not necessarily problematical for dynamical stability purposes.

On top of the no-slip assumption, the linearity assumption, makes the analysis even simpler by assuming small angles. The small steer angle approximately always aligns the wheels with the x-axis. Then the complete support line can be assumed to have constant forward velocity v and lateral accelerations of the support line that are actually on lines intersecting at the turn center can be approximated by the accelerations in the y-direction of the coordinates frame, $\ddot{y}_x$ (see figure 6.1).

The overall lateral motion of PQ is a kinematic linear combination of the lateral contact points motions which are described by the rolling constraints. For the rear wheel contact point the lateral acceleration is described by (3.35) and the front wheel contact point lateral acceleration is described by (3.42). Since it is a linear gradient, specific points on the support line with longitudinal coordinate, x, have a lateral acceleration that is a weighted average of those of the contact points as given by (3.35) and (3.42):

$$\begin{aligned} \ddot{y}_x &= \left(1 - \frac{x}{w}\right) \ddot{y}_{\mathrm{P}} + \frac{x}{w} \ddot{y}_{\mathrm{Q}} \\ &= \left(v\delta + (c + x)\,\dot{\delta}\right) \frac{v}{w} \cos\lambda_{\mathrm{s}} \end{aligned} \tag{6.1}$$

This relation is illustrated for the numerical benchmark bicycle [22] (section 4.2 and 4.4) in figure 6.1 and figure 6.2. Since the support line lateral acceleration varies linearly along its length, the weights of the contact point accelerations on a specific support line point can easily be obtained. At the contact points the weights are simply 1 and 0 for either contact point acceleration. A nonzero steer angle laterally accelerates the support line as a whole with an acceleration that is equal along the whole support line. However, (6.1) shows that a steer rate accelerates the support line according to a gradient along the support line depending on the bicycle geometry. This gradient along the support line under influence of a nonzero steer rate makes that the lateral acceleration line crosses the x-axis (where $\ddot{y}_x = 0$) somewhere; from (6.1) this is seen to be at

$$x_{(\ddot{y}_x = 0)} = -v\frac{\delta}{\dot{\delta}} - c \tag{6.2}$$

To illustrate some different interesting cases for the behavior of the support line under influence of (opposing) geometry, the numerical benchmark bicycle is considered ridden in two different directions;

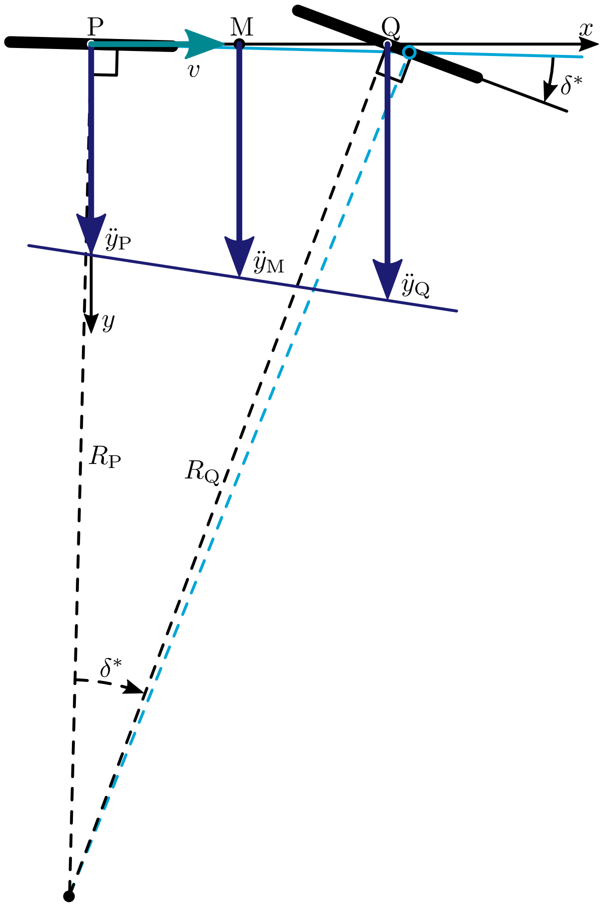

Figure 6.1: The ground plane projection of the Benchmark bicycle during an unsteady turn with forward velocity, $v = 4.7$ m/s, and lateral accelerations, $\ddot{y}$. No actual physical bicycle parts are shown in this drawing; $\overline{\mathrm{PQ}}$ is the support line with midpoint M, and the two black bars are projections of the wheels on the ground plane with the contact points P and Q. The steer axis intersects the ground at the small blue circle where also an imaginary line through the rear wheel crosses a similar line through the front wheel. $\overline{\mathrm{PQ}} = w$ and in the linear domain the distance from P and Q to the steer axis ground intersection are approximately $w + c$ and c respectively. There is a positive steer axis angle and trail which yaw both rear and front wheel in the local frame under influence of the positive instantaneous steer angle, $\delta \approx \pi/9$ rad ($\delta^* = \delta \cos \lambda_\mathrm{s}$), and positive steer rate, $\dot{\delta} \approx \pi/9$ rad/s ($\dot{\delta}^* = \dot{\delta} \cos \lambda_\mathrm{s}$) with a small assumed lean angle. For a positive steer rate on the benchmark configuration, the front lateral acceleration is larger than the rear. Another steer rate would show different acceleration magnitudes or possibly even accelerations pointing outward of the curve. The not drawn trajectories are also only instantaneous since the nonzero steer rate changes the steer angle and therewith the trajectories. Note that the accelerations with no slip are actually aligned with the turn radii, R, pointing to the center of the curve, but due to linearization they are approximated by the y-accelerations.

the conventional manner with the larger wheel ahead and a reversed manner with the larger wheel behind. Even with a (instantaneously) zero steer angle, the lateral accelerations can be nonzero under influence of a nonzero steer rate as displayed in figure 6.2. The two bicycles give different lateral accelerations between the wheel contacts ($0 < x < w$) for the same angular steer rates, because the steer rate contribution sign is trail dependent as can be seen in (6.1). The gradient line describing this acceleration is shifted along the support line between the two cases. The point where the support line crosses the x-axis (where $\ddot{y}_x = 0$) for a zero steer angle can be seen from (6.2) to lie at $x = -c$. Thus, under influence of only steer rate, the conventional benchmark bicycle has a negative lateral acceleration behind a point behind the rear contact, and the reversed benchmark bicycle has this negative acceleration behind a point in front of the front contact.

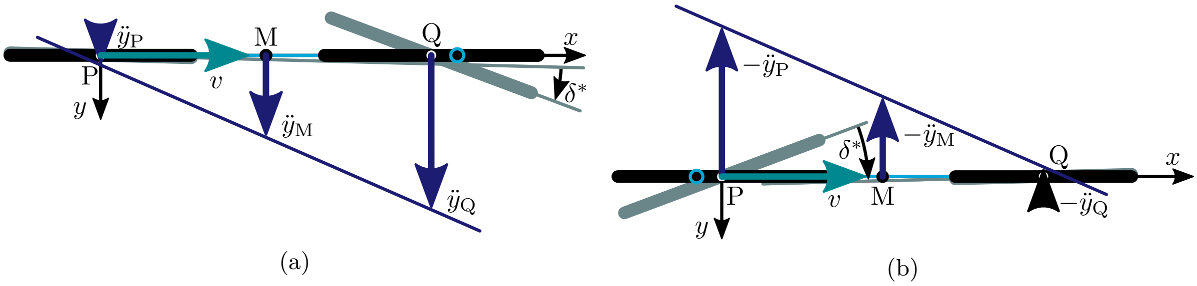

Figure 6.2: Depiction of the support line lateral accelerations for $\delta = 0$ and $\dot{\delta} = 1$ rad/s ($\dot{\delta}^* = 1 \cos \lambda_s$) and $v = 4.7$ m/s for (a) the benchmark bicycle and (b) a reversed benchmark bicycle. Note that the steer angle δ (and accordingly also steer rate $\dot{\delta}$ is defined such that a positive angle depicts a clockwise rotation of the front frame with respect to the rear frame; in both figures a rightward (clockwise) steer motion is depicted.

For the conventional benchmark bicycle the steer rate has a larger effect on the front than on the rear contact lateral acceleration. For the reversed benchmark this behavior is opposing and the rate has a small contribution to the front wheel and a larger contribution to the rear wheel acceleration, such that the rear can now be experienced to 'swerve out'. This swerving out happens behind (often out of vision) of the rider and may pose a problem since one might hit curbs with the rear wheel. Besides these two specific benchmark examples, an infinite amount of different bicycle geometries is possible which have different contributions of the steer rate. In extremis, for a bicycle with $c = 0$, the rear wheel will have no contribution of the steer rate on its lateral acceleration, and for $c = -w$ the front wheel lateral acceleration is unaffected by the steer rate.

To have one measure for the support line motion, one can simply look at its midpoint M between the wheels contacts where $x = w/2$. M is chosen since a bicycle is in essence fore-aft 'symmetrical' (two wheel, two frames, three hinges) and a midpoint makes the analysis as general as possible. Moreover, this choice makes sense because this is the location above which often the center of mass of the bicycle is placed for longitudinally fore-aft (pitch) stability considerations. Note that it is not a physical material point of the bicycle, it is just an imaginary point on the ground close to a perpendicular projection of the COM on the support line. For the support line midpoint a simple kinematic expression from (6.1) can be derived with equal weights of the rear and front lateral acceleration:

$$\begin{aligned} \ddot{y}_M &= \frac{\ddot{y}_P + \ddot{y}_Q}{2} \\ &= \left(v\delta + \left(c + \frac{w}{2} \right) \dot{\delta} \right) \frac{v}{w} \cos \lambda_s \end{aligned} \tag{6.3}$$

Indeed, as for all support line points, the magnitude of the lateral acceleration is dependent on bicycle parameters and steer motions. As can be seen from (6.3), the lateral acceleration from the steer angle is always pointed towards the steered side; clockwise steer angle gives rightward acceleration. However, the contribution of the steer rate depends on the ratio between the difference between trail and wheel base, i.e. it depends where and under which angle the headset is placed. In theory, the steer rate contribution can thus be changed continuously to whichever value is desired if the headset is moved and rotated longitudinally or vertically. Some extraordinary bicycle designs (for example Suijker's 'The Wave', see section A.46) can change the trail and steer axis angle, and in effect kinematics as well as COMs and inertias, by adjusting angles between tubes. In practice, generally the headset is fixed and the kinematics of a specific bicycle cannot be changed. As can be expected, the different lateral acceleration of the support line in between the wheel contact points has direct consequences for the acceleration of the important midpoint of the support line in between the wheels.

First, consider the conventional benchmark bicycle, i.e. $c > 0$ (figure 6.2a). In that case a positive steer angle and angular rate (as in figure 6.2a) both add to the midpoint lateral acceleration, while both negative steer angle and rate contribute negatively. Initially, from a straight ahead position, when such a bicycle is steered to a side, point M laterally accelerates in the steer direction. In steady-state a clockwise steer results in a constant lateral acceleration in the same stabilizing positive direction. When leaned to a side, a steer into that lean always shifts M underneath the fall.

Secondly, a reversely ridden benchmark bicycle is considered, i.e. $c < -w$ (figure 6.2b). Note that the steer angle is still positive when the front assembly rotates clockwise with respect to the rear assembly. The steer angle contribution to the lateral acceleration is still positive, but now a positive steer angular rate contributes negatively to the M acceleration. Moreover, it means that a sufficiently large positive steer rate can cause a lateral acceleration of the support line in the opposite direction of that steer rate, and from a straightforward zero steer angle position an initial steer motion accelerates M outwards of the curve under influence of purely steer rate. When steered into a fall, the initial M motion is away from the leaned side. However, in steady state, with a steer angle in the fall direction without a steer rate, M is accelerated towards the leaned side.

A turning point in the steer rate contribution to the middle point lateral acceleration, i.e. its contribution flips sign, occurs when $c = -w/2$ (see (6.3)). Then, only the steer angle contributes to the lateral support line midpoint M with a certain constant, because the negative steer rate contribution at the rear contact and the positive steer rate contribution at the front contact cancel each other in the middle. Note, that this would be equivalent to a 'bicycle' with two vertical steer axes through both wheels centers (This is not a bicycle in the pure sense, because it has three frames; two forks and one connecting main frame, e.g. Maebe 'Bicycle with steerable wheels', see section A.29) where both wheels steer exactly equally, but also exactly oppositely with respect to the main frame. A kinematic coupling between the two wheel assemblies, such as on a skateboard, could make sure that the wheels are exactly oppositely steered.

6.2 Support points turn radii

Kinematics also determine that a certain steer angle defines certain turn radii for the support line. Generally, there is a difference between the rear and front wheel path radius. This difference can be derived by looking at figure 6.1 where the situation is drawn for instantaneous rear turn radius R_{P}, and instantaneous front turn radius R_{Q}. Also drawn is that the steer axis intersects the ground at the point where the line parallel through the rear wheel projection intersects the front wheel projection. The distance from Q to this intersection point is the trail, c, and the distance between P and Q is the wheel base, w. An average of the turn radii can be described by a simple trigonometrical linear ($\delta \ll 1 \Rightarrow \tan\delta^* \approx \delta^*$) relation with the assumption that the radii are always positive,

$$\frac{R_{\mathrm{P}} + R_{\mathrm{Q}}}{2} = \frac{w}{|\delta^*|} \tag{6.4}$$

Furthermore, R_{P} and R_{Q} can be related by noticing that there are two triangles sharing one side. This side is the line from the instantaneous turn center (where the turn radii intersect) to the steer axis ground intersection point. Expressing this side length with Pythagorean theorem from the two separate triangles gives the equality,

$$R_{\mathrm{P}}^2 + (w + c)^2 = R_{\mathrm{Q}}^2 + c^2 \tag{6.5}$$

which can be rearranged and rewritten:

$$(R_{\mathrm{P}} + R_{\mathrm{Q}})\,(R_{\mathrm{P}} - R_{\mathrm{Q}}) = -w\,(w + 2c) \tag{6.6}$$

Combining (6.4) and (6.6) gives the difference between R_{P} and R_{Q} as function of three bicycle parameters and the steer angle,

$$2\frac{w}{|\delta^*|}\,(R_{\mathrm{P}} - R_{\mathrm{Q}}) = -w\,(w + 2c) \tag{6.7}$$

and with some rewriting and the steer angle ground projection expression, (3.27),

$$R_{\mathrm{P}} - R_{\mathrm{Q}} = -\left(c + \frac{w}{2}\right)|\delta|\cos\lambda_{\mathrm{s}} \tag{6.8}$$

To calculate the turn radius of either contact point, equation (6.4) and (6.8) can be substituted in each other. Furthermore, the points of the complete support line, i.e. points in between or behind/ahead of P and Q at any x-position, have turn radii that are linear combinations of the two contact point turn radii:

$$R_x = \frac{w}{|\delta|\cos\lambda_{\mathrm{s}}} + \left(\frac{x}{w} - \tfrac{1}{2}\right)\left(c + \frac{w}{2}\right)|\delta|\cos\lambda_{\mathrm{s}} \tag{6.9}$$

The turn radii of the points on the support line are related to the lateral acceleration. When at a zero steer angle a rate steer rate is applied, then soon the paths of the wheels will be curved. Here, a larger lateral acceleration of a point on the support line corresponds with a larger upcoming radius and a smaller upcoming curvature (inverse of radius). Moreover, a point with smaller lateral acceleration gets a larger turn radius change than a point with a larger lateral acceleration. Similarly it can be said that for the conventional benchmark bicycle the radius of the rear wheel path is determined largely by the steer angle and only a small part by the angular rate, while the steer angular rate adds more to the radius of the front wheel path. For the reversed benchmark bicycle this is exactly the opposite. The 'swerving out' of the rear wheel for the reversed benchmark bicycle corresponds with the larger radius of the rear wheel path as compared to the front wheel path.

6.3 Steer-side definition

Because a bicycle is essentially a symmetric machine, one specific steer-side does not exist for a bicycle. Therefore, a front wheel steered bicycle, nor a rear wheel steered bicycle does not exist. Steering happens around a headset that can be placed anywhere in the plane of the bicycle and is always a relative motion between two frames. Which one of those frames is chosen as reference to which the other frame rotates might determine the front or rear wheel steering. However, this choice of reference frame is arbitrary, and one should rather think of a bicycle as really two equally valued frames. For a clockwise turn seen from above, the front frame rotates clockwise with respect to the rear frame while the rear frame rotates counterclockwise with respect to the front frame.

Generally, people do not think of which side of a bicycle is steered. People, perhaps correctly, just do not realize that an RWSB is that different from a conventional bicycle. Someone might notice that a bicycle looks or feels strange, but still acknowledges that it is a bicycle and does not attribute the strangeness to an altered steer-side. However, when specifically asked, it can be expected that they discriminate different steer cases, i.e. front or rear steered, by argumenting that they 'know it when they see it' [43]. Often, conventional bicycles are considered front wheel steered and strange bicycles that are basically reversed conventional bicycles are considered rear wheel steered.

Although the steering occurs symmetrically and people perhaps do not care which side is steered, still differences are experienced between presumed different cases of steering, e.g. the ridability of most presumed RWSBs is dramatic. To gain clarity, a steer-side definition is required here that captures differences in behavior. Unfortunately, an unambiguous definition is not yet clearly formulated.

Literature shows that different authors attribute their definition of the steer-side to different bicycle features (see section 2.2). For example, the location of the largest frame or the frame that carries the rider or the location of the head tube. Or one can compare a bicycle with a car and note that a car has often a well-defined main frame which make the steered wheels easily identifiable, so that this could also apply to a bicycle. The most elegant definition seems to arise from the previous support line motion discussion [16]. The lateral acceleration of the midpoint namely shows a turning point that marks an essential difference in kinematics between front and rear wheel steering.

Because many people label a steer-side of a bicycle, a practical steer-side definition might be useful. Therefore, it is first convenient to define the front and rear side of a bicycle, which is harder than it sounds like due to the fore-aft symmetry. It is chosen here to label the front and rear part based on the longitudinal movement direction; the front of the bicycle is the assembly that contains the wheel contact that is ahead in the riding direction (and the rear is then behind). This definition has as consequence that a 'backwards' moving conventional bicycle, such as the reversed benchmark, has the main frame as front frame and the fork with handlebar as rear frame. Likewise the contact points are also flipped.

Steer-side coefficient

To find the steered-side, either front or rear, of a bicycle, the wheel (and frame) that dominantly 'leads' the bicycle needs to be found. Of the two wheels, this leading wheel primarily determines the riding direction. It appears that the steer-side is completely determined by the bicycle kinematics, such that the kinematics can be used to distinguish which side, front or rear, is the steer-side of the bicycle.

The wheel contact point with the largest lateral acceleration has the largest effect on the support line lateral motion. The wheel that thus dominantly 'steers' the support line is this wheel with the largest lateral acceleration. Since the difference between the front and rear wheel acceleration lies with the steer rate (section 6.1), the wheel contact point with the largest absolute lateral acceleration under steer rate influence is the leading wheel.

Due to the linear acceleration gradient along the support line, the wheel that contributes most to the support line midpoint acceleration reveals itself in the sign of the steer rate contribution to that acceleration. For a positive steer rate contribution sign, the absolute lateral acceleration under influence of the steer rate is larger at the front wheel than at the rear wheel and vice versa. Thus, the 'leading' wheel in the lateral acceleration of the support line changes when the steer rate contribution to the midpoint lateral acceleration changes from positive to negative or vice versa [16]. As seen in (6.3), the sign of the contribution of the steer rate is solely dependent on the bicycle geometry and changes when $c = -w/2$.

Based on this turning point, here a coefficient is introduced that determines whether and the degree to which a bicycle is front or rear wheel steered, the steer-side coefficient:

$$\Delta_\mathrm{s} = 2\frac{c}{w} + 1 \tag{6.10}$$

With the assumptions $w > 0$ and $-\pi/2 < \lambda_\mathrm{s} \leq \pi/2$, the following rewritten (6.3) has the turning point when the coefficient changes sign:

$$\ddot{y}_\mathrm{M} = \left(v\delta + \tfrac{1}{2}w\Delta_\mathrm{s}\dot{\delta}\right)\frac{v}{w}\cos\lambda_\mathrm{s}, \tag{6.11}$$

Since the turn radii of the support line points are closely related to the lateral accelerations, the steer-side coefficient can also be recognized in the instantaneous turn radii difference between the contacts, 6.8, and the equation can be rewritten:

$$R_\mathrm{Q} - R_\mathrm{P} = \tfrac{1}{2}w\Delta_\mathrm{s}|\delta|\cos\lambda_\mathrm{s} \tag{6.12}$$

The equations (6.11) and (6.12) are intentionally rewritten in such a way that the steer-side coefficient can be written in its particular way. Now, not only the sign, but also the exact value of the steer-side coefficient tells something about the support line motion. It is composed such that when it is zero, the bicycle is front nor rear wheel steered. When the coefficient is positive, the steer rate contributes positively to a positive middle point M lateral acceleration, making the bicycle front wheel steered, and when the coefficient is negative, the steer rate contributes negatively to a positive middle point M lateral acceleration, making the bicycle rear wheel steered. With negative steer gradient it is thus possible that the lateral acceleration sign is opposite to the steer angle sign while the steer rate has equal sign as the steer angle. The steered, i.e. 'leading', wheel thus indeed changes depending on the sign of the steer coefficient. Moreover, the coefficient gives an indication of how much a bicycle is front or rear wheel steered. When the coefficient is 1 or -1 the trail of respectively the front wheel or the rear wheel is exactly zero, making the bicycle semi-naive (steer axis angle can still be non-zero), such that at either wheel the lateral acceleration under influence of steer rate is zero and a turning point in the direction of either wheel's contact lateral acceleration under influence of steer rate occurs:

$$\begin{cases} \text{front wheel steered,} & \text{if } \Delta_\mathrm{s} > 0 \quad \text{(semi-naive if } \Delta_\mathrm{s} = 1) \\ \text{middle steered,} & \text{if } \Delta_\mathrm{s} = 0 \\ \text{rear wheel steered,} & \text{if } \Delta_\mathrm{s} < 0 \quad \text{(semi-naive if } \Delta_\mathrm{s} = -1) \end{cases} \tag{6.13}$$

A difference between rear and front wheel steering is the ratio between the rear and front wheel turn radii. The 'leading' or steered wheel dominantly determines the bicycle kinematics by having the largest radius. The steered wheel can be imagined to require the largest turn radius in order to 'push' the other wheel in a yaw motion into the corner. By combining 6.13 and 6.12 it is clear that FWSBs have a larger front turn radius while RWSBs have a larger rear wheel turn radius:

$$\begin{cases} R_\mathrm{Q} > R_\mathrm{P}, & \text{if } \Delta_\mathrm{s} > 0 \\ R_\mathrm{Q} = R_\mathrm{P}, & \text{if } \Delta_\mathrm{s} = 0 \\ R_\mathrm{Q} < R_\mathrm{P}, & \text{if } \Delta_\mathrm{s} < 0 \end{cases} \tag{6.14}$$

Besides having the largest lateral acceleration or turn radius, the leading wheel has another similar property. Namely, the steered wheel is the wheel that changes the direction of the bicycle the most and is thus the wheel that is angled the most with respect to the bicycle local frame with x-axis through the two wheel contacts. From the local wheel heading (yaw) expressions of rear wheel R, (3.54), and front wheel F, (3.59), it can be seen that the steer-side coefficient can also plugged into those expression,

$$ {}_{\mathrm{R}}\psi = \tfrac{1}{2}\left(\Delta_{\mathrm{s}} - 1\right)\delta\cos\lambda_{\mathrm{s}} \tag{6.15}$$
$$ {}_{\mathrm{F}}\psi = \tfrac{1}{2}\left(\Delta_{\mathrm{s}} + 1\right)\delta\cos\lambda_{\mathrm{s}} \tag{6.16}$$

And indeed the wheel with the largest absolute heading angle, is the steered-wheel according to the steer-side coefficient:

$$\begin{cases} |{}_{\mathrm{F}}\psi| > |{}_{\mathrm{R}}\psi|, & \text{if } \Delta_{\mathrm{s}} > 0 \\ |{}_{\mathrm{F}}\psi| = |{}_{\mathrm{R}}\psi|, & \text{if } \Delta_{\mathrm{s}} = 0 \\ |{}_{\mathrm{F}}\psi| < |{}_{\mathrm{R}}\psi|, & \text{if } \Delta_{\mathrm{s}} < 0 \end{cases} \tag{6.17}$$

Note that besides the front trail and wheel base length bicycle parameters, the motion of M is also dependent on the steer axis angle. The lateral direction of the support line middle-point, however, is only different between cases of different trails, and therefore the steer axis angle does not show up in the steer-side coefficient or in the steer-side definition whatsoever.

Recapitulating, the sign of the steer coefficient is both the sign of the angular steer rate contribution on the positive lateral acceleration of the midpoint of the support line, and it is the sign of the relative length of the front contact turn radius to the rear contact turn radius. Although, the kinematics change with changing steer-side coefficient, it does not necessarily says anything about the stability. However, the definition does capture the difference in the riding experience between cases. For example, an RWSB seems to be more angled in a turn, i.e. it seems to drift (without slipping) through a corner, and similarly, the rear wheel 'swerves out'.

Qualitative definition

To illustrate the consequences of the steer-side coefficient a verbal description is given here. In order to come to that, first the trail of either wheel is defined. The trail is the horizontal distance from a wheel's contact point to the point where the steer axis intersects with the ground plane. A bicycle can then be seen to have two trails; one for either wheel: The front wheel trail is the distance of the front wheel contact point to the steer axis ground intersection denoted by c. Similarly, the rear wheel trail is the distance of the rear wheel to the steer axis ground intersection. Then, when one wheel's trail is zero the other wheel's trail is of the length of the wheel base. By definition, the wheel trail is positive when the steer axis ground intersection is ahead of the wheel contact point in the positive forward riding direction. So, three combinations can be identified:

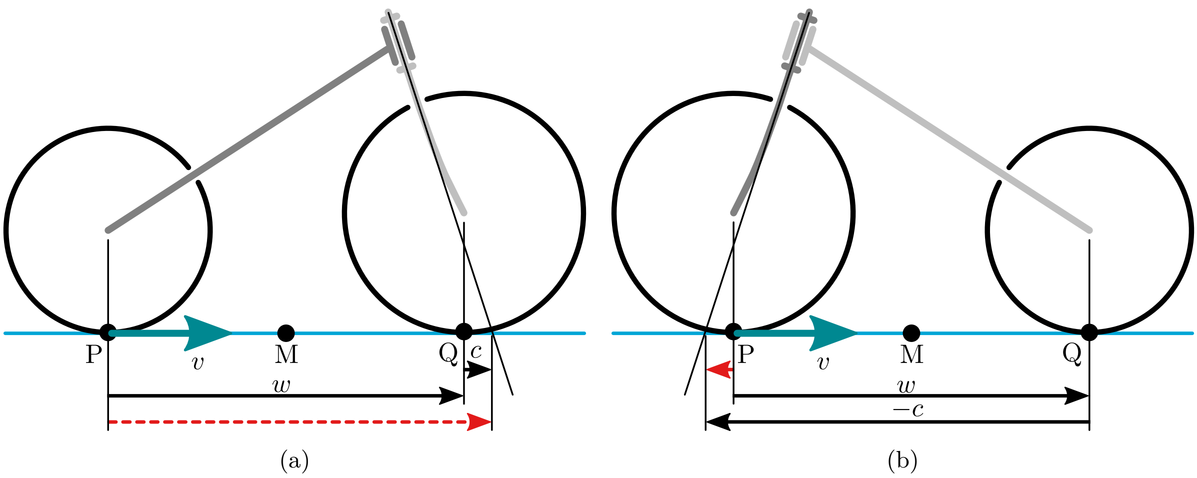

Figure 6.3: The rear wheel trail (dashed red arrow) and front wheel trail, c, of (a) the front wheel steered benchmark bicycle and (b) a rear wheel steered reversely ridden benchmark bicycle for a forward riding direction at speed v.

(+) rear and (+) front wheel trail The steer axis ground intersection is ahead of the front wheel contact point, e.g. conventional bicycles like the benchmark bicycle (figure 6.3a).

(+) rear and (−) front wheel trail The steer axis ground intersection is between the rear and front wheel contact points, e.g. bicycles in figure 6.4.

(−) rear and (−) front wheel trail The steer axis ground intersection is behind the rear wheel contact point, e.g. a reversed Benchmark bicycle (figure 6.3b).

As said, it follows from the definition of the steer side by the steer gradient that the turning point between steer-side cases lies at $c = -w/2$ and with the trails definition one can draft the following description:

Absolute trail lengths A bicycle is front wheel steered when the absolute front wheel trail is smaller than the absolute rear wheel trail. And vice versa, a bicycle is rear wheel steered when the absolute rear wheel trail is smaller than the absolute front wheel trail. Two equal trails make the bicycle middle steered.

Equivantly, one can simply look to the location of the steer axis ground intersection with respect to the support line midpoint M in a neutral straight up and straight ahead position:

Steer axis ground intersection to M A bicycle is front wheel steered when the steer axis intersects ground ahead of M, and it is rear wheel steered when the steer axis intersects ground behind M. A bicycle with steer axis intersecting the ground exactly at M is middle steered.

Several cases of steered sides on bicycles are displayed in figures 6.3 and 6.4. At first glance some of these bicycles' steered side may subjectively be qualified incorrectly, due to the position and angle of the steer hinge. However, the definition by trail makes the steer-side indisputable. Think about an exaggerated chopper where the headset is closer to the rear wheel, but the steer axis would still point in the direction of the front wheel. Such a chopper would still be front steered.

Note that all bicycles, except for middle steered ones, can be made from FWSB to RWSB and vice versa by flipping the forward velocity direction (changing sign). This is due to the front and rear definition which is dependent on the longitudinal movement direction. This can best be seen in figure 6.3 where the benchmark bicycle is ridden in either direction and can both be an FWSB and RWSB.

6.4 Bicycle kinematics and steer-side discussion

The distinction in steer-side is purely based on kinematics (support midpoint motion for different trail lengths) and captures essential behavioral differences in the support line movement between different cases. This is an objective way of defining the steer-side, because it is solely dependent on specific clear length bicycle parameters and changing the steer-side is the only possible way of changing the kinematic support lateral motion. Moreover, the kinematics are fundamental in that they are a base for the dynamics, and whereas kinematics have influence on dynamics, dynamics do not influence kinematics. Dynamics determine the progress of the degrees of freedom, but they do not change the kinematic relations that determine the support acceleration from those DOFs. This one-way relation between kinematics and dynamics and the fact that kinematics are not influenced by mass parameters while dynamics are certainly dependent on those (rider) mass (distribution) and inertias, as well as on control, makes the kinematics a more unique feature for steer-side distinction.

For example, instinctively, the mass (distribution) might also be important for the definition. However, changing a mass does only change dynamics and not change the kinematics and is therefore not so fundamental as changing the kinematic influencing parameters. Moreover, point M is similar, but in general not equal, to a base-point [1] which is a perpendicular projection of the center of mass on the support line; For conventional bicycles the support line midpoint and base-point coincide approximately. When the COM does not lie approximately directly above the midpoint M the important point to consider on the support line may be a specific base-point and not M. For example, a simple steer-side coefficient (without semi-naive calculation) that takes mass distribution into account can be derived from (6.1) with the x-coordinate of the total mass, T: $\Delta_{\mathrm{s}}^{*} = c + x_{\mathrm{T}}$.

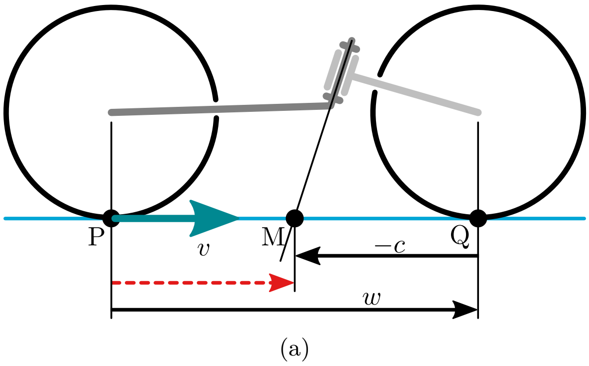

Figure 6.4: Two unconventional bicycle configurations which represent either (a) neutral steered ($c = -w/2$) and (b) front wheel steered ($c > -w/2$) bicycles.

However, it is questionable what then the important mass is, e.g. masses added to the bicycle close to the contact points to prevent pitching over do not alter the dynamics very much, but can shift the center of mass of the total bicycle assembly significantly. Is then the front assembly or frame, the rear assembly or frame, or the total assembly COM important in dynamics and determining the steer-side? When dynamics are changed significantly by using a different mass distribution, then the kinematics are still unaffected, and the fundamental support line motion for specific steer angles and angular rates is still the same. For example, take a conventional FWSB bicycle, e.g. benchmark bicycle, and place a lot of mass or a rider on the front frame, is it now an RWSB? Furthermore, including the rider mass or position in a steer-side definition is subjective since humans differ in mass and size. All in all, the mass (distribution) seems an inappropriate feature to define the steer-side by.

Also, one can look at the rear contact point and lay the turning point from rear to front steering when that contact point accelerates in the opposite direction under influence of the steer rate. This would lay the emphasis on the swinging out of the rear wheel only. In that case the turning-point from FWSB to RWSB occurs when $\Delta_s = -1$. Likewise, one might also look at the front contact point or any other point on the support line. However, changing the support point under consideration for the steer-side definition would do no justice to the fore-aft symmetry of a bicycle, and the emphasis would be on one of the steer cases (FWSB or RWSB) which would decrease the generality of the definition.

That kinematics have effect on the dynamics (and ridability) can be seen from a conventional (benchmark) bicycle perspective, where making the front wheel trail more positive improves stability, but lessens the 'agility' of steering [14]. Presumably, 'strange' RWS kinematics make a bicycle generally harder to balance, because it is counter intuitive that the support line midpoint initially accelerates away from a turn (see figure 6.2b). This happens since the rear 'swerves out' which is, to say the least, not the familiar kinematic for most riders accustomed to riding conventional bicycles. This swerving out of the rear wheel is fundamental to RWSBs and can decrease ridability, because the rider can hit curbs with the rear wheel that is out of the rider's vision. Furthermore, kinematics may create such fast unstable dynamics when other parameters like masses and inertias are not altered properly, that riding such a 'weird' bicycle has decreased ridability and riding it is beyond human capacity.

So, the steer-side definition does influence the dynamics in that different kinematics give different dynamics. However, the steer-side alone does not determine whether a bicycle is or can be dynamically self- or control-stable (section 7.2 and 7.3 and chapter 8). Just as with changing whatever parameter, also with a changed steer-side, other parameters, e.g. mass distribution, may need to be altered to obtain better stability (chapter 8). For all bicycles, either front, rear, or middle steered, the dynamics can be altered in many ways, for the good or the worse, while keeping its kinematics (and thus steer-side) equal. Changing the steer-side does in the first place change the kinematics without changing masses, in the second place it also changes the dynamics via altered kinematics.

Chapter 7

Dynamics: Stable turning behavior

7.1 Turn without leaning

Interesting dynamics occur for a vehicle with the initiation or maintaining of a turn. For both leaning vehicles, such as bicycles, and vehicles where leaning is of minor importance, such as cars, the stability in a turn can be investigated. However, the behavior of both sorts of vehicles is crucially different for different cases of steer-sides, i.e. front or rear steered vehicles.

For a vehicle with minor lean there is no need to balance laterally, but still the stability during a turn, which is determined by the system dynamics, is important [52]. During riding it is important that the dynamics of non-leaning vehicles tend to return the vehicle to a straight course, to prevent it from uncontrollable spinning. This directional stability is different than lateral stability, but they are associated with each other; a (laterally) self-stable bicycle follows a straight course when there is no control and is thus directionally stable. It happens to be that without leaning the mechanical trails as well as the location of the COM have influence on the stability.

Here a case is considered where both wheels have a nonzero mechanical trail. Then, the reaction forces at the wheel contacts during a turn cause a torque about the steer axis. To maintain the turn, this torque needs to be counteracted by an applied input steer torque. Thus, when the input torque is released, the reaction forces will change the steer angle. Therefore, to investigate stability of an non-leaned vehicle, these contact forces during a constant turn need to be analyzed.

To model the behavior of a non-leaning vehicle, the leaning Whipple bicycle model is transformed to a version of the car 'bicycle' model where the front and rear wheels of a car are combined in one front and one rear wheel (see figure 2.4a). Since the bicycle can no longer lean, ϕ, $\dot{\phi}$, $\ddot{\phi} = 0$, and all lean associated terms in the equations of motion become zero. Furthermore, because a constant turn is assumed, $\dot{\delta}$, $\ddot{\delta} = 0$, it follows from (3.35) and (3.42)that, $\ddot{\psi} = 0$ and $\ddot{y}_\mathrm{P} = (v^2/w)\delta\cos\lambda_\mathrm{s}$. Then, 3.24 and 3.26 reduce to,

$$m_\mathrm{T}(v^2/w)\delta\cos\lambda_\mathrm{s} = F_{\mathrm{R}y} + F_{\mathrm{F}y} \tag{7.1}$$

$$m_\mathrm{T}(v^2/w)x_\mathrm{T}\delta\cos\lambda_\mathrm{s} = wF_{\mathrm{F}y} \tag{7.2}$$

Substituting the second equation into the first and some rearranging results in the expressions for the rear and front lateral contact force during a constant turn without lean:

$$F_{\mathrm{R}y} = m_\mathrm{T}(v^2/w)\left(1 - \frac{x_\mathrm{T}}{w}\right)\delta\cos\lambda_\mathrm{s} \tag{7.3}$$

$$F_{\mathrm{F}y} = m_\mathrm{T}(v^2/w)\frac{x_\mathrm{T}}{w}\delta\cos\lambda_\mathrm{s} \tag{7.4}$$

It can be seen that the two reaction forces during a constant turn have equal sign, i.e. both pointed in same direction, when the total center of mass, T, is located somewhere between the contact points, $0 < x_\mathrm{T} < w$. When it lies behind the rear or ahead of the front contact point (only theoretically possible due to tipping over longitudinally), the reaction forces are directed oppositely. During a constant turn, the centripetal acceleration of the COM, $\ddot{y}_\mathrm{T}$, is pointed to the center of the turn under influence of the friction forces at the wheel contacts. The centrifugal acceleration of the COM is exactly equal in value

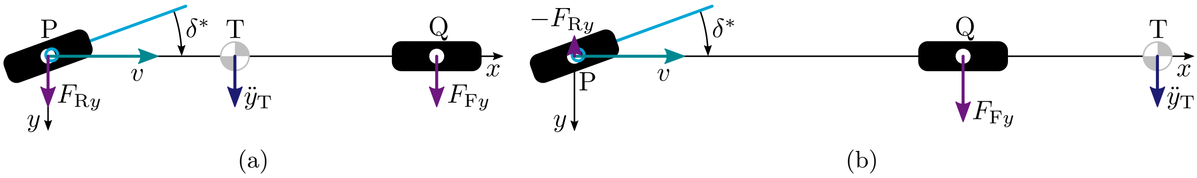

Figure 7.1: Ground projection of a rear wheel steered no-leaning vehicle during a constant turn with the total center of mass (COM), T, placed (a) inbetween the wheels, and (b) ahead of the front wheel. The vehicle rides with constant velocity, v, and projected steer angle, δ^*, and has the steer axis ground intersection (depicted by the blue circle) slightly ahead of the rear contact, i.e. a small nonzero rear mechanical trail and a larger front mechanical trail. Shifting the COM, with centripetal acceleration, $\ddot{y}_{\mathrm{T}}$, ahead of the front wheel makes that the lateral contact forces, $F_{\mathrm{R}y}$ and $F_{\mathrm{F}y}$, get opposed signs, resulting in a differently directed torque about the steer axis due to both trails (rear and front) being nonzero. When the steer torque is released, a COM placed inbetween the wheels results in an unstable increase of steer angle, while a COM placed ahead of the front wheel results in stable aligning of the two wheels.

but directed oppositely, causing a centrifugal force: $-m_{\mathrm{T}}\,\ddot{y}_{\mathrm{T}}$. The centrifugal 'force' is always pointed to the outside of the curve. In combination with the location of the steer axis ground intersection all these forces determine whether the vehicle is directionally stable.

Two examples of directional stability analyses for a clockwise turn are shown in figure 7.1 for a rear wheel steered, small mechanical rear wheel trail, non-leaning vehicle, either with the COM inbetween the wheels, or with the COM ahead of the front wheel. Such a rear wheel steered case, i.e. rear wheel steered with positive rear wheel trail, $-w < c < -w/2$, is interesting when one considers that a positive rear wheel trail (steer axis intersects ground ahead of rear wheel contact) is desirable for caster effect considerations. By then looking at the torque the three forces, i.e. two lateral contact forces and one centrifugal 'force', create about the steer axis, one can deduct whether this torque tends to make the steer smaller (stable) or larger (unstable). Note that for this clockwise turn analysis, the centrifugal force is always in the negative y-direction, opposed to the centripetal force.

As seen in figure 7.1a for a rear wheel steering vehicle with positive rear wheel (mechanical) trail and a COM in between the wheels, a torque is created by the forces that tends to increase the steer angle. This phenomenon where a rear wheel steered vehicle has increasing steer angle and tends to turn around such that the rear wheel comes in front, is known as ground-loop in the aircraft field [54].

However, a similar analysis with the COM ahead of the front wheel contact as shown in figure 7.1b shows that the reaction forces tend to decrease the steer angle. With the COM placed ahead of the front wheel, the lateral contact forces are aimed oppositely and due to leverage, a torque is created that tends to align the wheels. So, in order to be directionally stable, a non-leaning vehicle with rear wheel steering and steer-axis intersecting the ground in between the wheels, requires a COM placed ahead of the front wheel.

Such force analyses are done for all 9 distinct cases of mass location and steer-axis ground intersection in order to create table 7.1. Note that, because of swivel wheel effects, when $c < -w$, the vehicle might be unstable no matter what center of mass location is used. This is opposed to what table 7.1 states, since this table does not include these swivel effects. Moreover, the turning point between the cases does not lie at the turning point from front to rear wheel steering, $c = -w/2$ (see section 6.3). A front wheel steered vehicle with a mass in between the wheels can be stable when its front trail is positive, or unstable when its front trail is negative ($-w/2 < c < 0$). A similar, but opposite, case arises for a rear wheel steered vehicle.

Table 7.1: Directional stability for a non-leaning vehicle dependent on trails signs and total COM longitudinal location.

T location \ front trail	$c > 0$	$-w < c < 0$	$c < -w$
$x_{\mathrm{T}} < 0$	unstable	stable	stable
$0 < x_{\mathrm{T}} < w$	stable	unstable	stable
$x_{\mathrm{T}} > w$	stable	stable	unstable

7.2 Bicycle turn responses

For a vehicle that needs to balance laterally, the dynamics of balancing are interesting. The support needs to be brought underneath the COM in an appropriate manner such that the forces on the COM are directed through the support line (see section 4.1). The dynamics determine whether the movement of the support line happens in a sufficiently directed and timed manner to guarantee stability. Interesting dynamical behavior is shown when a bicycle initiates and maintains a turn [16]. Both the initial response and the steady-state response to a steer input corresponding with a turn radius are considered here to see the difference between those cases.

The maneuver is made such that a reference steer torque, $T_{\delta\mathrm{r}}$, is followed, which for a certain bicycle at a certain stable speed is equivalent to negotiating a turn with certain steer angle. This constant reference torque is applied on a straight-up, straight-forward riding bicycle at $t = 0$ and is maintained to $t \to \infty$. To make the analysis as general as possible within the scope of this study, the controlled bicycle system with EOM (3.66) is used. However, a control law is introduced, during this study, that gives only feedback on the steer torque input, (4.17), to resemble a realistic case (see section 4.4). This still allows for analyzing both self-stable and control-stable bicycles. Note that although this analysis requires a torque on the handlebars, the upcoming analysis of the steer torque in a steady turn can also be applied on self-stable bicycles [16]. It is the reaction of a bicycle on an applied external torque, and for a self-stable bicycle the controller gains are then simply zero.

Remember that a positive steer angle, $\delta > 0$, is an angle where the front assembly is rotated clockwise with respect to the rear assembly when looking from above (see figure 3.1b). Seen from a conventional bicycle perspective, this is a rightward handlebar turn when looking ahead on a bicycle with of a positive forward velocity. Likewise, a positive lean angle, $\phi > 0$, is a rightward lean when looking ahead on a bicycle with a positive forward velocity.

Initial turn response

All bicycles riding forwardly straight up happen to make qualitatively the same movement when a sudden torque input is placed on the steer joint. From such a neutral position, a suddenly applied torque has the largest effect on the angular accelerations, i.e. $\dot{\mathbf{q}} = \mathbf{q} = \mathbf{0}$ and $\mathbf{N}\mathbf{f}_\mathrm{r} = \mathbf{f}$ (see section 4.4), and the initial short time response can be extracted from (3.66),

$$\mathbf{M}\begin{bmatrix}\ddot{\phi}\\ \ddot{\delta}\end{bmatrix} = \mathbf{N}\begin{bmatrix}T_{\phi\mathrm{r}}\\ T_{\delta\mathrm{r}}\end{bmatrix} \quad = \begin{bmatrix}T_{\phi}\\ T_{\delta}\end{bmatrix} \tag{7.5}$$

The first row of (7.5) gives an expression for the lean angular acceleration at the onset of a turn:

$$\ddot{\phi} = -\frac{M_{\phi\delta}}{M_{\phi\phi}}\ddot{\delta} + \frac{N_{\phi\phi}T_{\phi\mathrm{r}} + N_{\phi\delta}T_{\delta\mathrm{r}}}{M_{\phi\phi}} \tag{7.6}$$

Furthermore, substituting the first row of (7.5) in the second and solving this for the steer angle acceleration, gives the initial reaction to an applied torque

$$T_{\delta\mathrm{r}} = \frac{\det(\mathbf{M})}{N_{\delta\delta}M_{\phi\phi} - N_{\phi\delta}M_{\delta\phi}}\ddot{\delta} + \frac{N_{\phi\phi}M_{\delta\phi} - N_{\delta\phi}M_{\phi\phi}}{N_{\delta\delta}M_{\phi\phi} - N_{\phi\delta}M_{\delta\phi}}T_{\phi\mathrm{r}} \tag{7.7}$$

Since there is a rigid rider there are no practical means of giving a lean torque and therefore the lean torque reference can be set zero, $T_{\phi\mathrm{r}} = T_\phi = 0$ (see section 4.4). Without the ability of giving a lean torque input, the feedback to the lean can also be zero, $K_{\mathrm{f}\phi\phi} = 0$, $K_{\mathrm{f}\phi\delta} = 0$, and in effect the reference following gain from the lean to the steer is also zero $N_{\phi\delta} = 0$ (but $N_{\phi\phi} = 1$). With these assumptions and noting from (3.45) that, $M_{\phi\phi} = I_{\mathrm{T}xx}$, equation (7.6) becomes,

$$\ddot{\phi} = -\frac{M_{\phi\delta}}{I_{\mathrm{T}xx}}\ddot{\delta} \tag{7.8}$$

and (7.7) becomes

$$T_{\delta\mathrm{r}} = \frac{\det(\mathbf{M})}{N_{\delta\delta}I_{\mathrm{T}xx}}\ddot{\delta} \quad = \frac{T_\delta}{N_{\delta\delta}} \tag{7.9}$$

So the initial responses of the system become rather simple. However, one general statement about the directions of the two angles with respect to each other can not be formulated from (7.8); Although, the denominator is always positive since $I_{\mathrm{T}xx} > 0$, the sign of the numerator is dependent on the geometry and mass distribution of the bicycle and thus differs from case to case. But two cases can be identified for the initial response of the bicycle:

$$t \approx 0: \quad \begin{cases} \mathrm{sgn}(\ddot{\phi}) = \mathrm{sgn}(\ddot{\delta}), & \text{if } M_{\phi\delta} < 0 \\ \mathrm{sgn}(\ddot{\phi}) = -\mathrm{sgn}(\ddot{\delta}), & \text{if } M_{\phi\delta} > 0 \end{cases} \tag{7.10}$$

From (3.45) it can be seen that the mass cross term is a combination of a product of inertia of the front assembly about the steer axis and a trail/wheel base scaled product of inertia of the total bicycle: $M_{\phi\delta} = I_{\mathrm{A}\mathrm{s}x} + \mu I_{\mathrm{T}xz}$. When both these products of inertia are positive, as is often the case, then via μ (3.18), a negative front wheel trail can still make the total mass cross term negative.

Conventional bicycles have $M_{\phi\delta} > 0$, and the bicycle falls away from an initial steer angular acceleration. When $M_{\phi\delta} < 0$, the support line right underneath the COM of the total bicycle shifts away to the outside of a steered direction, and the bicycle thus starts to lean in the steer direction directly. It can be shown that with initial zero steer, $\delta = 0$, this happens when $x_{\mathrm{T}} < -c$ (see section 6.1 with (6.2)). For example, this happens for a naive rear wheel steered bicycle ($c = -w$, $\lambda_{\mathrm{s}} = 0$) with the total bicycle COM behind the front wheel contact, $x_{\mathrm{T}} < w$. But it also happens for example, for a naive front wheel steered bicycle ($c = 0$, $\lambda_{\mathrm{s}} = 0$) with the total bicycle COM behind the rear wheel contact, $x_{\mathrm{T}} < 0$ (this might be impossible in practice considering pitch stability).

For the reaction of the steer angle to an input torque a more general statement can be made. Since the mass matrix is positive definite, the numerator $\det(\mathbf{M})$ is always positive, and one part of the denominator is also always positive, $I_{\mathrm{T}xx} > 0$. The reference gain $N_{\delta\delta}$ can have either sign depending on the feedback gains and bicycle geometry, but for the input torque, T_δ, the reference gain disappears and the initial steer reaction is always in the same direction as the input torque. This is true for stable and unstable as well as controlled and uncontrolled bicycles. Due to the reference gain, the initial input torque can have another sign and magnitude than the reference torque. However, for all systems in Newtonian mechanics, and thus also for a bicycle, it can be seen that the initial reaction to a sudden applied force results in a movement in the same direction as that applied force [16]:

$$t \approx 0: \quad \mathrm{sgn}(T_\delta) = \mathrm{sgn}(\ddot{\delta}) \tag{7.11}$$

Steady turn response

For a stabilized bicycle, either self-stable or control-stable, there is another equilibrium position besides the upright one (see section 4.1): A position with constant lean and constant steer angle under the control of a constant handlebar torque; a steady turn. The support-line spanned by the two contact points then intersects with the resultant of the gravity and a centrifugal force on the total system center of mass. When that is the case, those forces are exactly counteracted by normal and centripetal forces at the wheel contacts (with enough lateral friction). In a steady turn, all terms involving velocities and accelerations of the degrees of freedom are zero, i.e. $\ddot{\mathbf{q}} = \dot{\mathbf{q}} = \mathbf{0}$ and $\mathbf{f}_{\mathrm{r}} = \mathbf{f}$ (see section 4.4) and vanish from equations (3.66):

$$\left[g\mathbf{K}_0 + \mathbf{K}_{\mathrm{f}} + v^2\mathbf{K}_2\right] \begin{bmatrix} \phi \\ \delta \end{bmatrix} = \mathbf{N} \begin{bmatrix} T_{\phi\mathrm{r}} \\ T_{\delta\mathrm{r}} \end{bmatrix} \quad = \mathbf{N} \begin{bmatrix} T_\phi \\ T_\delta \end{bmatrix} \tag{7.12}$$

The first row gives the steady-state lean as function of steer and applied torques (note $K_{2\phi\phi} = K_{2\delta\phi} = 0$),

$$\phi = -\frac{gK_{0\phi\delta} + K_{\mathrm{f}\phi\delta} + v^2 K_{2\phi\delta}}{gK_{0\phi\phi} + K_{\mathrm{f}\phi\phi}}\delta + \frac{N_{\phi\phi}T_{\phi\mathrm{r}} + N_{\phi\delta}T_{\delta\mathrm{r}}}{gK_{0\phi\phi} + K_{\mathrm{f}\phi\phi}} \tag{7.13}$$

Using the first line to eliminate the lean from the second gives the expression for steady steer torque,

$$\begin{aligned} T_{\delta\mathrm{r}} = & \frac{\det\left(g\mathbf{K}_0 + \mathbf{K}_{\mathrm{f}} + v^2\mathbf{K}_2\right)}{N_{\delta\delta}\left(gK_{0\phi\phi} + K_{\mathrm{f}\phi\phi}\right) - N_{\phi\delta}\left(gK_{0\delta\phi} + K_{\mathrm{f}\delta\phi}\right)}\delta \\ & + \frac{N_{\phi\phi}\left(gK_{0\delta\phi} + K_{\mathrm{f}\delta\phi}\right) - N_{\delta\phi}\left(gK_{0\phi\phi} + K_{\mathrm{f}\phi\phi}\right)}{N_{\delta\delta}\left(gK_{0\phi\phi} + K_{\mathrm{f}\phi\phi}\right) - N_{\phi\delta}\left(gK_{0\delta\phi} + K_{\mathrm{f}\delta\phi}\right)}T_{\phi\mathrm{r}} \end{aligned} \tag{7.14}$$

As with the initial torque response, again, the lean torque reference can be set to zero, $T_{\phi\text{r}} = 0$, as well as the feedback to the lean, $K_{\text{f}\phi\phi} = 0$, $K_{\text{f}\phi\delta} = 0$, and the reference following gain from the lean to the steer, $N_{\phi\delta} = 0$ (but $N_{\phi\phi} = 1$). Now, with the notion from (3.47) that, $K_{0\phi\phi} = m_{\text{T}} z_{\text{T}}$, (7.13) becomes easier to interpret:

$$\phi = -\frac{gK_{0\phi\delta} + v^2 K_{2\phi\delta}}{gm_{\text{T}} z_{\text{T}}}\delta \tag{7.15}$$

and likewise, (7.14) becomes,

$$T_{\delta\text{r}} = \frac{\det\left(g\mathbf{K}_0 + \mathbf{K}_\text{f} + v^2\mathbf{K}_2\right)}{N_{\delta\delta} g m_{\text{T}} z_{\text{T}}}\delta \quad = T_\delta \tag{7.16}$$

The sign of the relation between the steady-state lean angle and steer angle, (7.15, is dependent on bicycle geometry and thus the sign can be different for different bicycles. The denominator in (7.15) is always negative since, $g > 0$, $m_{\text{T}} > 0$, and $z_{\text{T}} < 0$, while the second part of the numerator, $K_{2\phi\delta} = \left(\left(S_{\text{T}} - m_{\text{T}} z_{\text{T}}\right)/w\right)\cos\lambda_{\text{s}}$ (3.48), is always positive. However, the first part of the numerator, $K_{0\phi\delta} = -S_{\text{A}}$ (3.47), can have either sign dependent on bicycle geometry, and thus the total ratio can have either sign. The two angles in steady-state are then related as follows:

$$t \to \infty : \quad \begin{cases} \operatorname{sgn}(\phi) = \operatorname{sgn}(\delta), & \text{if } \left(K_{0\phi\delta} < 0 \text{ and } v > \sqrt{-gK_{0\phi\delta}/K_{2\phi\delta}}\right) \text{ or } K_{0\phi\delta} > 0 \\ \operatorname{sgn}(\phi) = -\operatorname{sgn}(\delta), & \text{if } \left(K_{0\phi\delta} < 0 \text{ and } v < \sqrt{-gK_{0\phi\delta}/K_{2\phi\delta}}\right) \end{cases} \tag{7.17}$$

For increasing speed the speed dependent positive part of the numerator gets the upper hand and the relation will always be positively signed. However, at low speeds, the relation might be somewhat counter-intuitive, because the steady lean angle can be opposite to the steer angle and the bicycle thus seems to lean stably to the outside of a curve. This happens when in a static case a steer angle causes a lateral shift of the COM to the inside of a curve under influence of the bicycle geometry and mass distribution. At low speeds, the bicycle is almost straight up and the COM is placed almost vertically above the support line. However, it can be shown that the COM is still somewhat to the inside of the curve with respect to the support line, as would be expected. This is because the lean angle of interest for this 'inverted-pendulum-balancing' is the angle at the support line between a vertical line and a line to the COM of the total bicycle. This angle is dependent on the rear assembly lean, ϕ, and front assembly lean, ϕ_{A} (which on its part is determined by ϕ and δ, see (3.36)). In a steady turn this 'pure' lean angle is still in the direction of the inside of the curve, while either the rear or front assembly lean angle might be directed outwards of the curve. Note that depending on the bicycle lay-out, i.e. which frame contains the major COM, either rear or front frame lean is the angle of greater interest.

For the torque input to steer angle relation, (7.16), first off, the sign of the numerator depends on whether the bicycle is stable. The determinant of the stiffness matrix is the constant term E of the characteristic equation (4.22), $E = \det\left(g\mathbf{K}_0 + \mathbf{K}_\text{f} + v^2\mathbf{K}_2\right)$ (see section 4.5). With this torque to angle relation, the stability condition $E > 0$ is thus expressed as the control torque in a steady turn. When this stability condition is met, which is the case for self-stable and control-stable bicycles, the numerator of (7.16) is positive. For a bicycle to be self-stable it is necessary that E is positive and the numerator is thus always positive for self-stable bicycles. Bicycles that ride at a speed outside the self-stable speed region should be controlled in order to be stable, but when stabilized, also $E > 0$ and the numerator is again positive. One part of the denominator, $gm_{\text{T}} z_{\text{T}}$, is always negative, and hence for a stable bicycle the sign of the total ratio is determined by the sign of the reference gain, $N_{\delta\delta}$:

$$\text{stability} \Rightarrow E > 0 \Rightarrow \quad t \to \infty : \quad \begin{cases} \operatorname{sgn}(T_\delta) = \operatorname{sgn}(\delta), & \text{if } N_{\delta\delta} < 0 \\ \operatorname{sgn}(T_\delta) = -\operatorname{sgn}(\delta), & \text{if } N_{\delta\delta} > 0 \end{cases} \tag{7.18}$$

Note that the sign of the reference gain, on its part, is determined by the bicycle geometry, or equivalently by the signs of the individual coefficients of E, and whether it rides below or above the capsize speed (see section 4.4 and 4.5). Thus, the sign of the ratio for a control-stable bicycle riding at a forward speed where the bicycle is not self-stable, depends on the sign of $N_{\delta\delta}$. The turning point where $N_{\delta\delta}$ turns from positive to negative is at the capsize speed of the uncontrolled bicycle such that the steady-state steer torque to steer angle ratio changes sign at the capsize speed and reverses the reaction on an input torque; a 'control reversal' [16] (see section 4.5). For most conventional self-stable bicycles, the self-stable forward speed region is finite with the capsize speed as upper limit. So, conventional control-stable bicycles with $v < v_c$ have a positive denominator and conventional control-stable bicycles with $v > v_c$ have a negative denominator.

For an uncontrolled bicycle, all control gains are zero and in effect, $N_{\delta\delta} = 1$ (see section 4.4), and the denominator in (7.16) is always negative. Among others, this can be the case for a self-stable bicycle, because such a bicycle would not require control to be stabilized. Therefore, for a (uncontrolled) self-stable bicycle, the steady-state steer torque direction is always opposed to the steer angle direction; to maintain a constant turn on a self-stable bicycle, a constant counter (to the steer angle) torque is required on the handlebar [16]. This is a necessary condition for a bicycle to be self-stable. It means that the self-stable bicycle itself produces a torque in the direction of the steady steer angle and thus when the bicycle is self-stable and one releases hands from the handlebars (no control) during a steady turn, the initial immediate motion is a turn towards the turn direction. This is in approval with the more general theory that a bicycle must turn towards a fall in order to come upright again.

Counter-steering

Comparing the initial response and the steady-state response to an input torque shows some interesting behavior of a stable bicycle [16]; counter-steering. Suppose that one wants to follow a certain reference torque, $T_{\delta r}$, starting from an upright straight ahead (neutral) riding position ($\ddot{\mathbf{q}} = \dot{\mathbf{q}} = \mathbf{q} = 0$). This is equivalent to following a certain steer angle, since steer torque and angle are related by a constant ratio (see (7.16)). The reference torque is constant over the full time period and the initial response, (7.9), can be compared with the steady-state response, (7.16). Since both responses have the same constant reference gain, $N_{\delta\delta}$, in the denominator, both responses are affected equally by this gain. Then, it can be seen that when a bicycle is stable, in either case, both for negative or positive $N_{\delta\delta}$, the responses to one reference input torque are oppositely:

$$\text{stability} \Rightarrow E > 0 \Rightarrow \begin{cases} N_{\delta\delta} < 0: & \begin{cases} \operatorname{sgn}(T_{\delta r}) = -\operatorname{sgn}(\ddot{\delta}), & \text{if } t \approx 0 \\ \operatorname{sgn}(T_{\delta r}) = \operatorname{sgn}(\delta), & \text{if } t \to \infty \end{cases} \\ N_{\delta\delta} > 0: & \begin{cases} \operatorname{sgn}(T_{\delta r}) = \operatorname{sgn}(\ddot{\delta}), & \text{if } t \approx 0 \\ \operatorname{sgn}(T_{\delta r}) = -\operatorname{sgn}(\delta), & \text{if } t \to \infty \end{cases} \end{cases} \tag{7.19}$$

This phenomenon where a stable bicycle has to have an initial steer motion into the other direction than the eventual desired steady steer direction is called counter-steering. It can be seen from (eqn:countersteer) that the only requirement for this phenomenon to occur is that the bicycle is stable. In that stabilized case the eigenvalues of the total system (whether or not with controller included) are all negative and thus $E > 0$. So for all bicycles, either front wheel steered, rear wheel steered, or middle steered, counter-steer occurs for making a turn as long as the bicycle is self- or control-stable with linear PD-control.

The counter-steer phenomenon has proven to be a fascinating as well as long known aspect of riding a bicycle [1] [56] [14] [26]. At first glance it seems counter-intuitive, that to initiate a turn with a bicycle, first a small steer motion to the opposite direction of the wanted turn direction has to be made before bringing the handlebar in the turn direction. One can philosophize about its role in safety. Due to the nature of the dynamics, i.e. first a steer towards an undesired direction is required, several motorcycle accidents have happened when a (novice) rider fails to counter-steer in a reflex and ends up turning towards the obstacle [14]. On real-life bicycles, steering can also be initiated by only applying a lean angle, but counter-steer is necessary for fast obstacle avoidance, since the steer dynamics for solely leaning have a long response time. Furthermore, also from a control perspective it is interesting, because this counter-steer behavior typically corresponds with a system that has control issues [14].

The occuring of counter-steering is physically explained as a way of setting up a certain lean angle that corresponds with a certain desired corner radius [1] [5] [12] [14]. This is directly seen for conventional bicycles ridden at high enough speed. Then, to initiate a corner, first the bicycle needs the required lean angle which could be set up by the counter-steer. For example, to steer right from a straight ahead riding position, initially a leftward counter-steer is applied which, due to momentum of the bicycle center of mass creates, a rightward fall of he total bicycle, then a rightward steer is applied to follow the fall direction and prevent falling over.

However, comparing (7.10) and (7.17) shows that different combinations are possible between the initial and steady-state lean to steer angle relation under influence of mass and stiffness properties. Thus, for more unconventional bicycle designs, during the motion from initial to steady turn, the rear frame lean angle can change direction, which is unexpected when a counter-steer is assumed to set up the correct directed lean. Apparently, to set up a correct lean angle for a turn, a stable bicycle with certain geometries might require a small lean in the wrong direction, i.e. 'counter-lean', to make the support line move in such a direction that ultimately the lean is correct. In other words, for a stable bicycle, counter-steer is even present when initially that counter-steer results in a lean directed to an opposite side as the steady turn lean. For negotiating a stable turn it is thus more important that the initial steer is in the opposite direction of the steady steer angle, even if this means that the initial lean is directed to a not ideal opposite side of the steady state lean.

The theory that the counter-steer sets up the correct directed lean angle for a steady turn, assumes that the lean angle is the angle at the support line between the vertical and a line from the support line to the total bicycle COM, which is not the same as the rear frame lean angle. This 'pure' lean angle is indeed pointed to the inside of a steady curve for a stable bicycle. Between the initial state and steady state, however, even this latter lean angle can change sign, because both rear and front frame initial lean angular acceleration can have the same sign as the initial steer angular acceleration.

For a self-stable bicycle, a constant turn can be set up by applying and sustaining one constant torque [16]. Such a self-stable bicycle does not require feedback control and thus, $\mathbf{K} = \mathbf{0}$, $N_{\delta\delta} = 1$, and for the whole time span the input steer torque is equal to the reference torque, $T_\delta = T_{\delta r}$. From the positive reference gain it can be seen in (7.19) that a steer torque must be opposed to the steer angle to maintain a steady curve. Furthermore, (7.19) shows that by applying a sudden constant torque to one side, first the bicycle will steer shortly to that side and then steer to the opposite side of the applied torque. All bicycles have an initial steer motion in the same direction as the applied torque, (7.11), but a self-stable bicycle also has a long time response where that same torque results in a steer to the reversed direction. As shown a state feedback PD-controlled bicycle also shows counter-steer, but the movement is generally not done by one torque in one direction. The controller alters the system and thereby the steady state relation. For control-stable bicycles with, $N_{\delta\delta} = 1$, the input torque is initially and in steady-state equal to the reference torque, but in-between they will be different most of the time. Note that in practice, when one wants to maneuver on a self-stable bicycle, also control is applied to get faster to the steady state turn. First a large torque is applied to make the bicycle roll faster, and then the torque is reduced to maintain the turn [16].

The occurring of counter-steer is similar to the behavior that, for a stable bicycle in a steady turn, when the handlebar torque is released, the first steer motion will be to steer more into the the fall direction. Conversely, to leave a constant turn, one has to shortly steer further into the leaned direction (counter-steer) in order to bring the support line straight underneath the COM again. In general it is assumed, but unproven, that all stable bicycles need to steer into a fall to come straight up again, so also when they are not in a steady curve and are trying to recover from an undesired lean only [15].

7.3 Bicycle turn simulations

To illustrate the results obtained in section 7.2, some time response simulations are performed. Several simulations are performed to show the effects of the forward speed on two different bicycles; the high precision benchmark bicycle configuration [22] and the reversed version of that same bicycle (see section 4.2). In this way the behavior of a rather conventional bicycle and its opposite can be compared.

The simulations are performed as a linear time response (see section 5.1) of the initiating and maintaining of a constant clockwise turn (seen from above) corresponding with a certain steer torque reference from initial straight up and ahead riding:

$$\begin{bmatrix} \dot{\mathbf{q}}_0 \\ \mathbf{q}_0 \end{bmatrix} = \mathbf{0}, \quad T_{\delta\mathrm{r}} \neq 0 \tag{7.20}$$

In all cases the only input is this steer torque which, at $t = 0$, is given a certain nonzero constant reference value which differs from case to case. This constant reference value corresponds with a certain turn radius and is chosen for the different cases such that all angles are kept within the linear region ($< \pi/9$ or $< 20°$). For a case where no control is applied, the actual applied steer torque, T_δ, is always equal to the reference torque. However, for a controlled case, the actual steer torque is controlled to end up at the reference value in steady state, but generally differs from the difference in the transient period.

Then, the bicycle model is either stable by itself and no control is required such that the input torque is simply the reference torque, or the bicycle requires control and the input torque is not constant and only equal to the reference in steady-state. The controller is designed separately for all specific bicycle configurations with the LQR-method to minimize the lean angle (see section 4.4). Note, that the controlled bicycle is 'magically' controlled to be balanced; it may not be a realistic representation of human capabilities and thus the bicycle without non-human control may not be ridable. Moreover, the motion is generally not an accurate representation of what a human rider would do to negotiate a turn, e.g. on a self-stable bicycle a human would apply first a large torque and then a smaller torque to faster obtain the required turn radius [16].

Benchmark bicycle

The first simulation is one in the self-stable forward velocity region of the benchmark bicycle, at the velocity where all eigenvalues together have the largest negative value, i.e. 'maximum stability'. For the benchmark bicycle this is at $v = 4.7$ m/s and in figure 7.2 the wheel paths as well as the lean and steer angles are displayed for a steer torque of -0.4 Nm. Because the bicycle is self-stable, no additional control is required in the control law (3.63):

$$\mathbf{N} = \mathbf{I} \quad , \quad \mathbf{K} = \mathbf{0} \tag{7.21}$$

It can be seen that one constant applied torque makes this bicycle negotiate a constant turn due to the self-stability. Initially the bicycle moves to the left with a negative steer angle (this translational motion

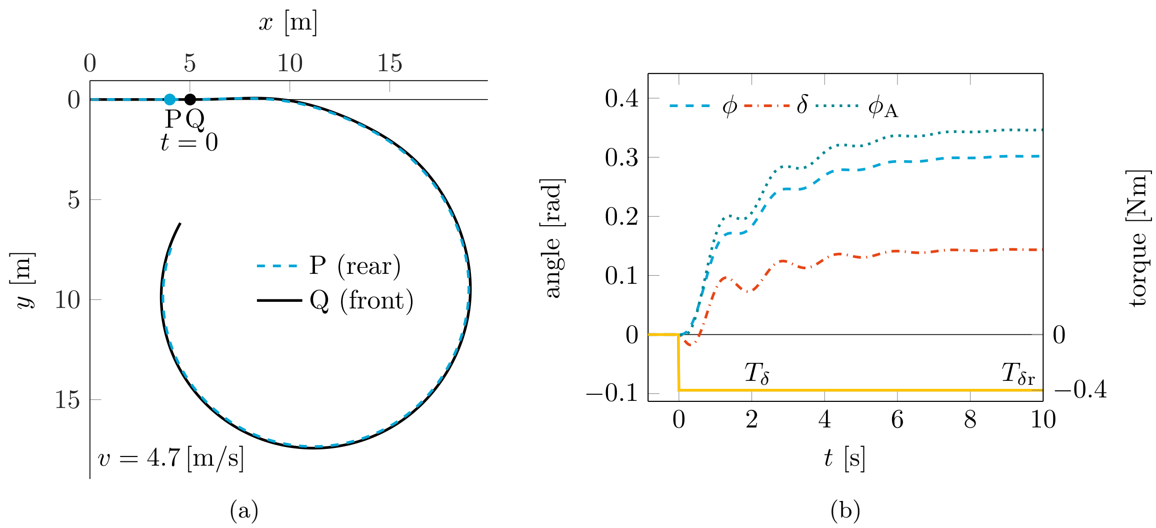

Figure 7.2: Dynamical simulation of the benchmark bicycle at $v = 4.7$ m/s showing (a) the wheel paths and (b) the corresponding angles and torque. The two global generalized coordinates, lean angle, ϕ, and steer angle, δ, as well as the global front assembly lean angle, ϕ_A are presented. The constant forward speed is chosen to be at the 'max stability' value, $v = 4.7$ m/s. The bicycle starts of in a straight-ahead stable riding position and the desired input steady reference steer torque, $T_{\delta r}$, corresponding with the steady turn is put on the steer axis at $t = 0$ and is exactly followed by the actual steer torque, T_δ, for this self-stable bicycle. A small, barely noticeable, counter-steer ($\delta < 0$ is a counterclockwise handlebar turn) is performed afterwhich the bicycle turns the other way and ends up in a steady turn. The exact values of these figures are dependent of the bicycle parameters; the positions, the paths positions with respect to each other, the transitional behavior and steady-state values of the angles can all differ for other bicycle configurations. Note that, although the larger front wheel path circle is only barely visible, due to this benchmark bicycle's (a conventional bicycle design) kinematics the front wheel makes a larger turn radius than the rear wheel. (figures inspired by [16])

is small, so barely visible in the paths figure), but due to that motion the bicycle starts leaning (with both the rear and front assembly) to the right and in effect a rightward/clockwise turn is negotiated. This is in accordance with the theory as presented earlier in section 7.2 and shows that there is a counter-steer motion. Moreover, kinematics determine that this front wheel steered bicycle has the front wheel making a larger turn path than the rear wheel; the front wheel is more on the outside of the corner than the rear wheel which is as expected (see section 6.3).

Now, the behavior of the benchmark bicycle outside of the self-stable speed region is investigated. Therefore, the controller needs to keep the bicycle upright and the input steer torque will thus not be constant. Both a very low speed of $v = 0.1$ m/s and a speed above the stable speed region of $v = 6.5$ m/s are used and the results are shown in figure 7.3. The gains on the steer torque are determined by (4.19) for the reference, and by the LQR-method for the feedback. For this bicycle they are in all cases such that a positive lean angle or angular rate, results in a positive steer torque from the control law (3.63), i.e. steer into fall. This can be seen from the feedback matrix for the $v = 0.1$ m/s case (note that the control law has already a minus sign for the feedback matrix),

$$\mathbf{N} = \begin{bmatrix} 1 & 0 \\ 3.9976 & 1.0000 \end{bmatrix} \quad , \quad \mathbf{K} = \begin{bmatrix} 0 & 0 & 0 & 0 \\ -1013.5 & -25.154 & -3174.6 & -98.881 \end{bmatrix} \tag{7.22}$$

and also from the $v = 6.5$ m/s case where the bicycle is less unstable, and the gains can be smaller,

$$\mathbf{N} = \begin{bmatrix} 1 & 0 \\ 0.15064 & -3.6280 \end{bmatrix} \quad , \quad \mathbf{K} = \begin{bmatrix} 0 & 0 & 0 & 0 \\ -0.093570 & 0.064949 & -1.6019 & 1.1114 \end{bmatrix} \tag{7.23}$$

At the low speed of 0.1 m/s it can be seen that the turn is negotiated eventually with the controller controlling the steer torque. The bicycle is stable and so a counter-steer is still present. However, a difference with the self-stable case is that the torque fluctuates and the front assembly lean angle initially follows the steer direction. More peculiar is that the lean angle of the rear is negative in steady-state. This happens because of the low speed which makes the relation between the steer and rear lean angle negative as can be seen in (7.17). Due to the large positive front assembly lean angle it can be seen that the total bicycle COM lies still inside of the curve, and the total bicycle thus leans towards the inside of the curve. This is as expected for all leaning single-track vehicles in a stable steady turn.

The higher speed of 6.5 m/s is above the capsize speed of the bicycle. This means that there is a ‘control reversal’ and that the torque to maintain a positive steer angle is also positive now (see section

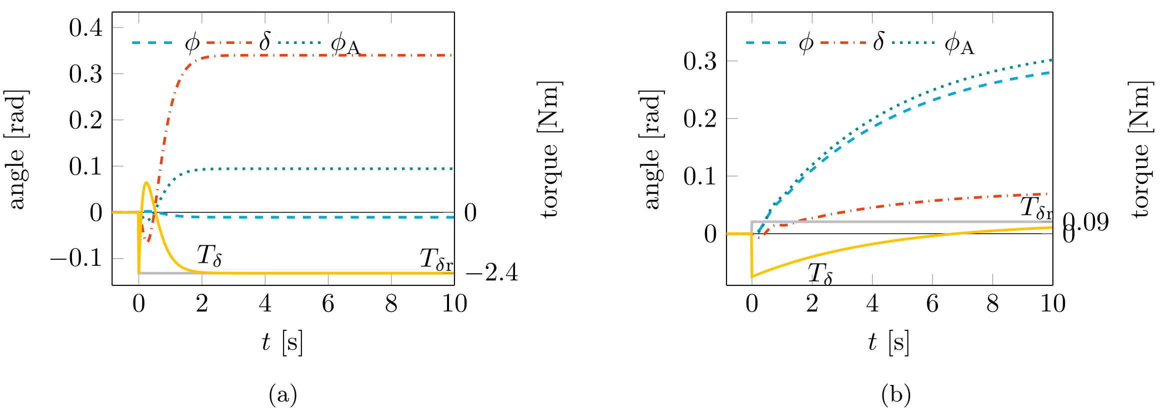

Figure 7.3: Angles and input steer torque during the initiation and maintaining of a steady turn for a control-stable benchmark bicycle riding at (a) $v = 0.1$ m/s and (b) $v = 6.5$ m/s. For this steady turn a constant steer torque reference, $T_{\delta\mathrm{r}}$, is trying to be followed by the actual steer torque, T_δ. The two global generalized coordinates, lean angle, ϕ, and steer angle, δ, as well as the global front assembly lean angle, ϕ_A are presented. The bicycle at 0.1 m/s can be seen to show counter-steer since the steer angle is initially opposed to the steady steer angle. The global rear and front assembly lean angles are also initially opposed to their steady values, but they end up either leaning to another side. At 6.5 m/s, only the steer angle shows initially an opposed direction to the steady value (counter-steering), but now the steer torque is directed in the same direction as the steady steer angle.

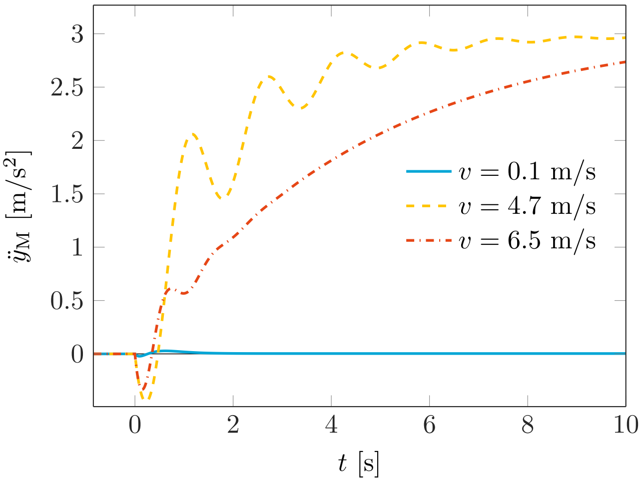

Figure 7.4: Benchmark bicycle support line midpoint M lateral acceleration. For different riding velocities, the exact magnitude and propagation of the lateral acceleration is different, but the overal pattern is for all forward velocities the same. Initially, the lateral acceleration is negative, meaning that the support line midpoint shifts to the left of the bicycle (seen from above) which makes this bicycle lean to the right. Eventually, when the transient response dampes out it is positive and thus points to the right of the bicycle which corresponds with a constant stable clockwise turn.

4.5). Indeed, for this bicycle conventional bicycle at this higher speed, $N_{\delta\delta} < 0$ (see (4.26)), and from (7.18) it can be seen that then the signs of torque and steer angle are equal. Since this bicycle is stabilized, there is still a counter-steer, but the controlled input torque has initially a different sign as in steady state. Because of the relative high velocity, a much smaller torque is required to make the same lean and steer angles as before.

The lateral accelerations of the midpoint on the support line for the three forward velocity cases are plotted in figure 7.4. The exact values and progression differ for the different velocities, but for all cases the pattern is the same. The lateral acceleration is initially in the negative direction, meaning that it accelerates first to the left, giving a rightward lean to this bicycle. After some transient behavior, in steady state all lateral accelerations are to the right pointing to the inside of the constant turn and maintaining the rightward lean.

Reversed benchmark bicycle

The same simulations at 4.7, 0.1 and 6.5 m/s are performed for a benchmark bicycle that is ridden in a reversed direction. Note that the rear frame is now the smaller frame (fork), while the front frame is the larger frame with the rider attached to it. According to the definition such a bicycle is rear wheel steered. However, as said before, a bicycle that is self-stable in one direction can never be self-stable when ridden in the opposite direction. So this reversed benchmark bicycle always requires control in order to balance. This is illustrated by the three feedback matrices determined with the LQR-method. The matrices are now also nonzero for the $v = 4.7$ m/s case,

$$\mathbf{N} = \begin{bmatrix} 1 & 0 \\ 0.10266 & 1.3263 \end{bmatrix} \quad , \quad \mathbf{K} = \begin{bmatrix} 0 & 0 & 0 & 0 \\ -9.5611 & 9.6847 & -9.7650 & 22.609 \end{bmatrix} \tag{7.24}$$

just as for the $v = 0.1$ m/s case (where the steer torque feedback on the lean has an opposite sign),

$$\mathbf{N} = \begin{bmatrix} 1 & 0 \\ -2.7665 & 1.0008 \end{bmatrix} \quad , \quad \mathbf{K} = \begin{bmatrix} 0 & 0 & 0 & 0 \\ 699.96 & -192.13 & 2197.1 & -610.52 \end{bmatrix} \tag{7.25}$$

and for the $v = 6.5$ m/s case,

$$\mathbf{N} = \begin{bmatrix} 1 & 0 \\ -1.3401 & -3.8850 \end{bmatrix} \quad , \quad \mathbf{K} = \begin{bmatrix} 0 & 0 & 0 & 0 \\ -12.321 & 13.119 & -10.005 & 37.881 \end{bmatrix} \tag{7.26}$$

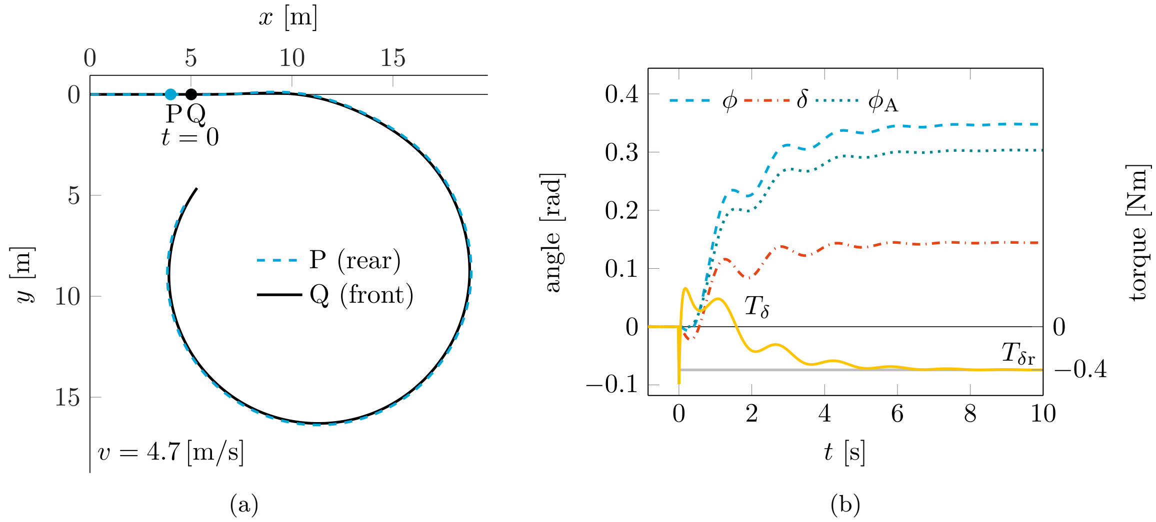

Figure 7.5: Dynamical simulation of the reversed benchmark bicycle at v = 4.7 m/s showing (a) the wheel paths and (b) the corresponding angles and torque. The two global generalized coordinates, lean angle, ϕ, and steer angle, δ, as well as the global front assembly lean angle, ϕ_A are presented. The constant forward speed is chosen to be at the 'max stability' value, $v = 4.7\,\mathrm{m/s}$. The bicycle starts of in a straight-ahead stable riding position and the desired input steady reference steer torque, $T_{\delta\mathrm{r}}$, corresponding with the steady turn is put on the steer axis at $t = 0$ and the actual steer torque, T_δ, is controlled to eventually and up at the reference torque. A small barely noticeable counter-steer ($\delta < 0$ is a counterclockwise handlebar turn) is performed afterwhich the bicycle turns the other way and ends up in a steady turn. The two lean angles also show a 'counter' movement where they initially move in the opposite direction to the steady direction. Note that, although the larger rear wheel path circle is only barely visible, due to this reversed benchmark bicycle's kinematics the front wheel makes a smaller turn radius than the rear wheel. (figures inspired by [16])

For a forward velocity of 4.7 m/s the results of the simulation are displayed in figure 7.5. It is directly clear that now the input torque is controlled, in stead of being held constant. However, the counter-steer phenomenon is still present at the initialization of the turn as witnessed by an initial steer angle with different sign as in the steady turn (the translational motion is small, so barely visible in the paths figure). This is as is expected for all stabilized bicycles, so also for rear wheel steered bicycles (see section 7.2). Different with the normal benchmark riding case is that now initially the lean angles are in the same direction as the counter-steer steer angle, i.e. all angles are initially briefly negative (although only slightly). The counter-steer is thus not used to initiate the correct lean angle directly, but apparently this small 'counter-leaning' movement is required by the dynamics to make the correct leaning possible eventually (see section 7.2). Furthermore, kinematics determine that the wheel paths are now such that the rear wheel makes a larger radius path than the front wheel.

The lower speed of 0.1 m/s simulation for the reversed benchmark depicted in figure 7.6a shows similar results as the conventional benchmark case. Again, the counter-steer phenomenon is present, but different is that here the front assembly is the assembly that leans to the outside of the turn, while the rear assembly is still relatively largely angled to the same side as the steer angle (see also (7.17)). The COM of the total bicycle is thus still dislocated to the inside of the curve. Note that, as said, in this case the front assembly is the larger assembly of the bicycle that incorporates the rider.

In figure 7.6b the results for the simulation of a stable turn at 6.5 m/s can be seen. The input torque develops more turbulent as compared to the normal ridden benchmark case, but eventually the torque still settles on a value that corresponds with control reversal above the capsize speed. Besides the counter-steer, just as at the other two forward velocities for the reversed benchmark, also here a 'counter-lean' occurs where the initial lean angles are opposed to the steady angles.

The main difference between the normal ridden benchmark and the reversely ridden benchmark is the lateral acceleration of the support line midpoint. It can be seen in figure 7.7 that initially this acceleration is directed to the inside of the desired turn direction, after which it becomes directed to the other side, to eventually end up pointing again to the inside of the turn. The initial movement towards the desired curve is apparently needed for a stable bicycle with this geometry to prepare the movement of the support line to move away from a desired curve to set up a correct lean for a constant turn.

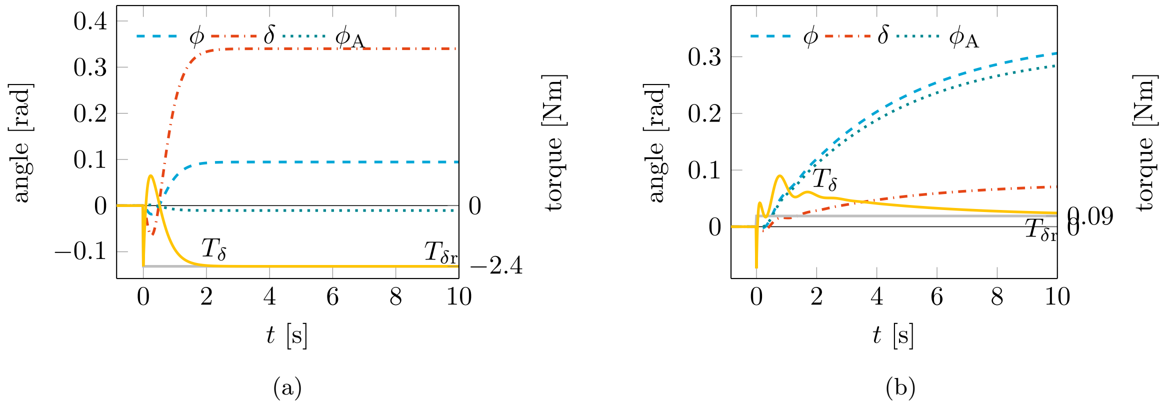

Figure 7.6: Angles and input steer torque during a turn for a control-stable reversed benchmark bicycle at (a) $v = 0.1$ m/s and (b) $v = 6.5$ m/s. For this steady turn a constant steer torque reference, $T_{\delta\mathrm{r}}$, is trying to be followed by the actual steer torque, T_δ. The two global generalized coordinates, lean angle, ϕ, and steer angle, δ, as well as the global front assembly lean angle, ϕ_A are presented. The bicycle at 0.1 m/s can be seen to show counter-steer since the steer angle is initially opposed to the steady steer angle. The global rear and front assembly lean angles are also initially opposed to their steady values, but they end up either leaning to another side. At 6.5 m/s, all angles show initially an opposed direction to the steady value, i.e. 'counter-steering' and 'counter-leaning', with the steer torque ending up directed in the same direction as the steady steer angle.

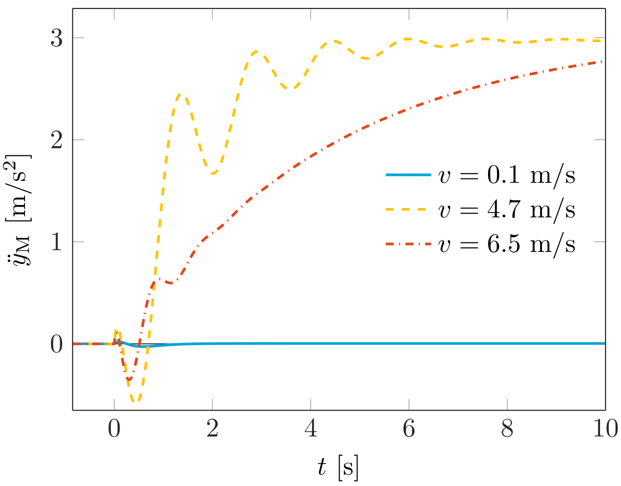

Figure 7.7: Reversed benchmark bicycle support line midpoint M lateral acceleration. For different riding velocities, the exact magnitude and propagation of the lateral acceleration is different, but the overal pattern is for all forward velocities the same. Initially the support line midpoint shifts to the right of the bicycle, although only for a small amount as can be seen in the figure by the small positive acceleration just after $t = 0$, which makes this bicycle lean to the left. Soon thereafter the lateral acceleration becomes negative, shifting the support midpoint to the left making the bicycle lean to the right. Apparently, to move to the left side to set up the correct lean angle, first the dynamics determine that a rightward motion is required. Eventually, when the transient response dampes out the lateral acceleration becomes again positive and thus points to the right to the constant turn center.

7.4 Bicycle dynamics and steer-side discussion

All stable bicycles show qualitatively the same dynamical behavior. Of course, bicycle parameters can be changed such that they become unstable or stable, but this holds for all bicycle designs. Although quantitative characteristics may change, every machine with two wheels possible within the Whipple model is still a bicycle, and for all bicycles, its characteristics are dependent on all parameters in a complex way and stability is determined by a combination of parameters. Changing a feature like the steer-side, changes kinematics (see section 6.3), and in effect the dynamics, but it does not change the fact that the machine is a bicycle and still has bicycle dynamics such as counter-steering and control reversal at a certain velocity.

The ability to lean of a bicycle is of essential influence on the stability [72]. Leaning provides a manner of intercepting the gravitational and centrifugal forces on the bicycle COM with the support. Peculiar is that for a non-leaning vehicle the stable configuration with mass ahead of the front wheel tends to straighten out the vehicle as described in section 7.1. This makes sure that the vehicle straightens out when there is no torque on the steer axis. For a leaning vehicle, one wants it to steer into a fall in order to recover balance. The straightening out of a non-leaning vehicle is then precisely the opposite of that steering into fall, because this straightening out would mean that the vehicle would steer away from the fall, and thus fall over.

An example of typical bicycle dynamics due to the lean ability is counter-steering to initiate a turn, which occurs for bicycles when they are either self- or control-stable with constant input torque reference, no matter what steer-side they have. So, opposed to what is often thought, a control-stable rear wheel steered bicycle has the counter-steer phenomenon. Counter-steer is already sometimes experienced on RWSBs in real-life when stabilized and initiating a turn to one side, first the bicycle points to the other side before aiming to the correct desired side [4]. Equivalently, for all stable bicycles, one has to steer further into a constant turn to come straight up again. A steer towards the other side will then result in falling over. If one definitely wants to get rid of the counter-steer phenomenon, the instability (and unridability) of the bicycle must be taken for granted which seems a very undesirable side effect to put it lightly.

The occurring of counter-steer can be somewhat counter-intuitive on a stable rear wheel steered bicycle with conventional-like design with COM in between the wheels, e.g. the reversed benchmark, because then initially the lean is directed outward of the desired turn. As said before, the lateral acceleration of the support line is key in balancing; it should be brought underneath the resultant forces on the COM. When initially the support line motion is balance disturbing, i.e. when initially the bicycle falls out of a desired turn, control dynamics need to be fast enough, to redirect the support line motion to a balancing motion. It may be needed to take a 'wrongly' directed transient lean angle for granted and rely on control to stabilize the bicycle and end up at a correct directed lean angle (see section 7.3). This 'wrongly' directed lean, i.e. a support line midpoint that first makes the bicycle lean out of a desired turn, is apparently required by the dynamics to make the ultimate correct lean to the inwards of a turn possible.

On such an RWSB, i.e. a simply reversed conventional bicycle, this counter-intuitive initial lean comes due to the total bicycle COM position in combination with changed kinematics that 'swerves out' the rear under influence of a steer motion (see section 6.3). The 'swerving out' makes the feeling of the bicycle different, i.e. strange for humans accustomed to conventional bicycles, as noted in practice by many (see appendix A), but does not essentially make controlling the bicycle impossible. When the dynamics are control-stable, they are qualitatively the same between steer-side cases. However, the kinematics are still different between steer-side cases.

Simply reversing a good design as the benchmark bicycle can cause troubles, because the control effort might be changed heavily by reversing a bicycle. This can be seen from the heavily fluctuating input torque pattern for the reversed benchmark which indicates that it is hard to control, which is why a human can hardly achieve this. Whether the balance can be recovered eventually is a question of how fast the dynamics occur and if the control system, e.g. the human rider, has enough time or has learned to deal with this 'strange' dynamics and the system time constant is now of importance. But if correct controlled, simply reversely riding a benchmark-like bicycle does not even have a severely changed angle propagation with respect to the normal riding case (see section 7.3).

By not solely reversing a design, but also changing other parameters, like mass-distribution, dynamics can be altered such that better stability characteristics are possible [16] (see chapter 8). However, when a parameter is changed, often other parameters should be changed in an accordingly and appropriate way to make the new design stable again. The undesired dynamics of a bicycle with other steer-side are thus not primarily determined by its steer-side, but rather by the lack of changing other parameters like the mass distribution accordingly. When the two trails (rear and front) of a bicycle are changed, then kinematically the lateral acceleration of the support line under influence of steer motion does also change (section 6.1). However, changing the steer-side, i.e. making a front wheel steered bicycle rear wheel steered, is not that different from changing any other parameters of a bicycle. In stead of 'rear wheel steering' one could make a bicycle for example 'rear wheel heavy' with a larger rear wheel mass. Just as changing trails to make a bicycle rear wheel steered makes the bicycle dynamics different, making the rear wheel heavier does also change the dynamics. However, changing a mass does not change the kinematics, whereas changing the trails does.

Changing the steer-side basically means practically nothing more than changing some kinematics such that the turn radii of the wheels are different. For a rear wheel steering vehicle, the rear wheels describe a wider path than the front wheels. A rider has to be aware of this, because the rear wheels swing out behind the riders vision; Even when the front wheels pass an obstacle, the rear wheels can still hit it. For example, the very common ordinary curbs might become an obstacle for a rear wheel steered bicycle. The steer side is just a fascinating and appealing bicycle alternation that looks significant such that many have tried it. But because they were not able to find values for the other parameters to make such bicycles ridable, changing the steer-side got a bad name it does not necessarily deserve.

The steer-side of a bicycles does not drastically change this dynamical behavior as long as the bicycle is stabilized. On a kinematics level, changing of the steer-side is the only way of changing the support line lateral motion. However, on dynamics level, changing the steer-side is just another way of changing the dynamics, just as, for example, changing a mass. All parameters affect the bicycle dynamics, while only lengths and angles of axes influence the kinematics. Changing the steer-side can be considered a change of trail parameters that influence dynamics, just as changing a mass changes dynamics. Changing the steer-side is then one of many ways to change the dynamics and other parameters might need to be changed in accordance to make the bicycle self-stable or ridable again. In that light it should not come as a surprise that all bicycles can be made better ridable and even self-stable and all steer-side cases can be either stable or unstable.

The kinematics determine the support acceleration from the steer motion and they influence the dynamics. On its part, the exact steer motions are determined by the dynamics. It might look like that the dynamics influence the kinematics, but although the dynamics determine the steer motion, they do not influence how the acceleration of the support follows from this steer motion. The relation between the kinematics and dynamics is thus one-directional and dynamics determine the stability under influence of kinematics, all bicycle parameters, and applied torques. In other words, support acceleration happens on all stable or unstable bicycles under influence of the kinematics and the dynamics determine if this support acceleration occurs in a stabilizing or unstabilizing way. Whether a bicycle with a certain steer-side is stable, is thus independent on its steer-side, but rather on the dynamics caused by all parameters.

It is then the question whether the kinematics or the dynamics are more important. Concretely this comes down to a choice between comfort/safety or usefulness: Kinematics play a role in ridability by moving the support-line differently, e.g. the rear wheel can 'swerve out' invisible for the rider and hit a curb, while dynamics determine if a bicycle is ridable at all. Generally, dynamics are considered more important and the steer-side is not important, because, as said, changing the steer-side is just one of many ways to alter the dynamics. Then, the desire to label the steer-side can be considered essentially unnecessary and is an exponent or expression of the psychological/philosophical human desire to label, even when there are no noteworthy differences; a rear wheel steered bicycle is just another bicycle.

Part III

Self-stable RWSB

Chapter 8

Minimal theoretical self-stable RWSB

8.1 Minimal parameters set and equations of motion

An RWSB is just a bicycle with an unconventional positioned steer axis, but an RWSB can, just as other bicycles can, be self-stable. However, since bicycle parameters all interact in a complex manner with each other to create the bicycle dynamics, changing the steer axis position does also change the requirements for the other parameters on order to create stable dynamics. Therefore, here a study is conducted to find parameters requirements for making an RWSB self-stable.

The full 25-parameter Whipple bicycle model (see section 3.1) is too complex to 'probe for theoretical insights' [16]. In effect, a minimal set of parameters is chosen in order to draw conclusions about parameter requirements for a self-stable RWSB. With the theoretical RWSB of Kooijman *et al.* (see section A.83) as basis, a trial-and-error study is performed with the Whipple model tool Matlab software JBike6 [45] (Remember slightly different parameter definitions, see section 4.3) to select a set of nonzero parameters that is sufficiently small to find clear parameter requirements, while simultaneously still being extensive enough to find a self-stable RWSB, i.e. to obtain theoretical insights in the bicycle configuration requirements.

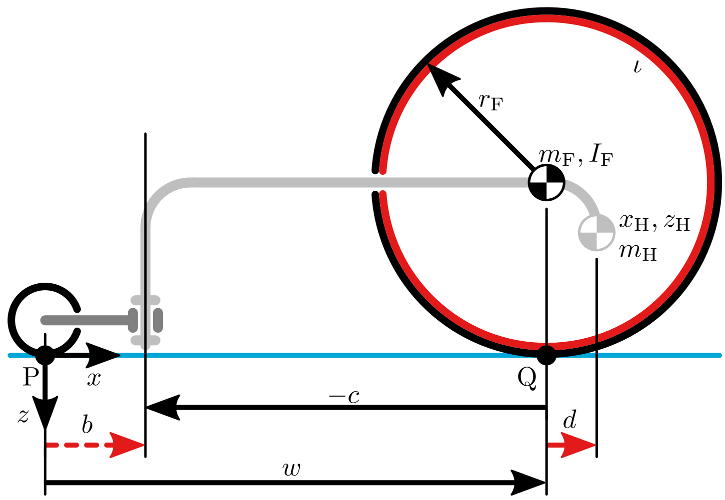

Figure 8.1: The eight nonzero parameters of the minimal RWSB: wheel base, w, front wheel trail, c, front frame mass, m_H, and coordinates, (x_H, z_H, front wheel mass, m_F, mass moment of inertia, I_F, and wheel radius, r_F. Depicted in red are the three redundant variables that are introduced to make the equations better readable: rear wheel trail, b, front mass to axle distance, d, and inertia factor, ι. Moreover, the rear and front wheel contact points, respectively P and Q, are indicated.

Figure 8.1 displays the minimal set of eight nonzero parameters that was found for which an RWSB can be self-stable and is comprehensive enough to describe a bicycle (a self-stable example of eight specific values is shown in table 8.1). The remaining 17 parameters of the Whipple model, i.e. those for the rear frame, the rear wheel, inertia of the front frame, and the steer axis angle, are all set to zero. Note that it is assumed that the front wheel is flat in the xz-plane, i.e. its thickness is much smaller than the radius, as well as symmetrical, which makes that the mass moments of inertia about the axle and the other two axes are dependent as $I_{\mathrm{F}_{yy}} = 2I_{\mathrm{F}_{xx}} (= 2I_{\mathrm{F}_{zz}})$. Furthermore, note that the additional front point-mass, H, can be imagined to be a frame only or a rigid rider and frame and all other added parts together.

All remaining nonzero parameters can easily be put together in the mass, damping, and stiffness matrix form as presented in section 3.1 to obtain the linear equations of motion for this minimal bicycle, i.e. the lean and steer equation. Due to the reduced set of parameters, this minimal RWSB set results in simpler and clearer matrices:

$$\mathbf{M} = \begin{bmatrix} m_\mathrm{H}\, z_\mathrm{H}{}^2 + (1+\iota)\, m_\mathrm{F}\, r_\mathrm{F}{}^2 & -\left(m_\mathrm{H}\, b\, d\, z_\mathrm{H}\right)/w \\ -\left(m_\mathrm{H}\, b\, d\, z_\mathrm{H}\right)/w & \left(m_\mathrm{H}\, d^2 + \iota\, m_\mathrm{F}\, r_\mathrm{F}{}^2\right) b^2/w^2 \end{bmatrix} \tag{8.1}$$

$$\mathbf{C}_1 = \begin{bmatrix} 0 & \left(-m_\mathrm{H}\,(b+d)\, z_\mathrm{H} + (1+2\,\iota)\, m_\mathrm{F}\, b\, r_\mathrm{F}\right)/w \\ -\left(2\,\iota\, m_\mathrm{F}\, b\, r_\mathrm{F}\right)/w & \left(m_\mathrm{H}\,(b+d)\, d + \iota\, m_\mathrm{F}\, r_\mathrm{F}{}^2\right) b/w^2 \end{bmatrix} \tag{8.2}$$

$$\mathbf{K}_0 = \begin{bmatrix} m_\mathrm{H}\, z_\mathrm{H} - m_\mathrm{F}\, r_\mathrm{F} & -\left(m_\mathrm{H}\, b\, d\right)/w \\ -\left(m_\mathrm{H}\, b\, d\right)/w & 0 \end{bmatrix} \tag{8.3}$$

$$\mathbf{K}_2 = \begin{bmatrix} 0 & \left(-m_\mathrm{H}\, z_\mathrm{H} + (1+2\,\iota)\, m_\mathrm{F}\, r_\mathrm{F}\right)/w \\ 0 & \left(m_\mathrm{H}\, b\, d\right)/w^2 \end{bmatrix} \tag{8.4}$$

Here, three redundant variables are introduced that proved to simplificate the long expressions in the matrices. In stead of the front wheel trail, c, the rear wheel trail, b is used, and in stead of the front mass horizontal coordinate, x_H, its distance from the wheel axle, d, is used. Moreover, a factor, ι, is introduced that is a measure for how the mass is distributed over the wheel. It can vary continuously from representing a hoop wheel with all the mass on the perimeter, $\iota = \frac{1}{2}$, to a solid disk with equal radially distributed mass, $\iota = \frac{1}{4}$, or even to a theoretical wheel where all mass is located at the axle, $\iota = 0$, or outside the perimeter, $\iota > \frac{1}{2}$. These three redundant parameters are shown in figure 8.1 and are related to the standard benchmark paper [22] parameters as:

b Rear wheel trail: $c = b - w$

d Horizontal front mass/axle distance: $x_\mathrm{H} = d + w$

ι Front wheel inertia: $I_{\mathrm{F}yy} = 2\,\iota\, m_\mathrm{F}\, r_\mathrm{F}{}^2 \quad (= 2\, I_{\mathrm{F}xx} = 2\, I_{\mathrm{F}zz})$

8.2 Stability conditions

For the Routh stability analysis described in section 4.5, now the polynomial coefficients of the characteristic equation (4.11) are required as well the Routh determinant. The polynomial coefficients (4.23) are,

$$\begin{aligned}
A_0 &= m_\mathrm{F}\, b^2\, r_\mathrm{F}{}^2 \left(\iota\, m_\mathrm{H}\, d^2 + m_\mathrm{H}\, d^2 + \iota\, m_\mathrm{H}\, z_\mathrm{H}{}^2 + \iota^2\, m_\mathrm{F}\, r_\mathrm{F}{}^2 + \iota\, m_\mathrm{F}\, r_\mathrm{F}{}^2\right)/w^2 \\
B_1 &= m_\mathrm{F}\, b\, r_\mathrm{F} \left(m_\mathrm{H}\, b\, d\, z_\mathrm{H} + \iota\, m_\mathrm{H}\, z_\mathrm{H}{}^2\, r_\mathrm{F} + \iota\, m_\mathrm{H}\, d^2\, r_\mathrm{F} + m_\mathrm{H}\, d^2\, r_\mathrm{F} + \iota\, m_\mathrm{H}\, b\, d\, r_\mathrm{F} + m_\mathrm{H}\, b\, d\, r_\mathrm{F}\right. \\
&\quad \left. +\iota^2\, m_\mathrm{F}\, r_\mathrm{F}{}^3 + \iota\, m_\mathrm{F}\, r_\mathrm{F}{}^3\right)/w^2 \\
C_0 &= -\,g\, b^2 \left(m_\mathrm{H}\, m_\mathrm{F}\, d^2\, r_\mathrm{F} + m_\mathrm{H}{}^2\, d^2\, z_\mathrm{H} - \iota\, m_\mathrm{H}\, m_\mathrm{F}\, r_\mathrm{F}{}^2\, z_\mathrm{H} + \iota\, m_\mathrm{F}{}^2\, r_\mathrm{F}{}^3\right)/w^2 \\
C_2 &= m_\mathrm{F}\, b\, r_\mathrm{F} \left(m_\mathrm{H}\, d\, z_\mathrm{H} - 2\,\iota\, m_\mathrm{H}\, b\, z_\mathrm{H} + m_\mathrm{H}\, d\, r_\mathrm{F} + \iota\, m_\mathrm{H}\, d\, r_\mathrm{F} + 2\,\iota\, m_\mathrm{F}\, b\, r_\mathrm{F} + 4\, b\, \iota^2\, m_\mathrm{F}\, r_\mathrm{F}\right)/w^2 \\
D_1 &= -\,g\, m_\mathrm{F}\, b\, r_\mathrm{F} \left(m_\mathrm{H}\, d^2 - \iota\, m_\mathrm{H}\, z_\mathrm{H}\, r_\mathrm{F} + \iota\, m_\mathrm{F}\, r_\mathrm{F}{}^2\right)/w^2 \\
D_3 &= 2\,\iota\, m_\mathrm{F}\, b\, r_\mathrm{F} \left(-m_\mathrm{H}\, z_\mathrm{H} + m_\mathrm{F}\, r_\mathrm{F} + 2\,\iota\, m_\mathrm{F}\, r_\mathrm{F}\right)/w^2 \\
E_0 &= -\,g^2\, m_\mathrm{H}{}^2\, b^2\, d^2/w^2 \\
E_2 &= 2\,\iota\, g\, m_\mathrm{H}\, m_\mathrm{F}\, b\, d\, r_\mathrm{F}/w^2
\end{aligned} \tag{8.5}$$

and the Routh determinant coefficients (4.24) have the long expressions,

$$
\begin{aligned}
X_2 =\; & g^2\, m_{\mathrm{H}}\, m_{\mathrm{F}}^2\, b^4\, d\, r_{\mathrm{F}}^2\, \left(z_{\mathrm{H}} + r_{\mathrm{F}} + \iota\, r_{\mathrm{F}}\right) \big(\iota\, m_{\mathrm{H}}^3\, b^2\, d^3\, r_{\mathrm{F}} + m_{\mathrm{H}}^3\, b^2\, d^3\, r_{\mathrm{F}} + m_{\mathrm{H}}^3\, b^2\, d^3\, z_{\mathrm{H}} \\
& + 2\,\iota\, m_{\mathrm{H}}^3\, b\, d^4\, r_{\mathrm{F}} + m_{\mathrm{H}}^2\, m_{\mathrm{F}}\, b\, d^4\, r_{\mathrm{F}} + 2\, m_{\mathrm{H}}^3\, b\, d^4\, r_{\mathrm{F}} + m_{\mathrm{H}}^3\, b\, d^4\, z_{\mathrm{H}} + 2\,\iota^2\, m_{\mathrm{H}}^2\, m_{\mathrm{F}}\, b\, d^2\, r_{\mathrm{F}}^3 \\
& + 2\,\iota\, m_{\mathrm{H}}\, m_{\mathrm{F}}^2\, b\, d^2\, r_{\mathrm{F}}^3 + 2\,\iota\, m_{\mathrm{H}}^2\, m_{\mathrm{F}}\, b\, d^2\, r_{\mathrm{F}}^3 - \iota\, m_{\mathrm{H}}^2\, m_{\mathrm{F}}\, b\, d^2\, z_{\mathrm{H}}\, r_{\mathrm{F}}^2 + \iota\, m_{\mathrm{H}}^3\, b\, d^2\, z_{\mathrm{H}}^2\, r_{\mathrm{F}} \\
& + \iota^2\, m_{\mathrm{F}}^3\, b\, r_{\mathrm{F}}^5 - 2\,\iota^2\, m_{\mathrm{H}}\, m_{\mathrm{F}}^2\, b\, z_{\mathrm{H}}\, r_{\mathrm{F}}^4 + \iota^2\, m_{\mathrm{H}}^2\, m_{\mathrm{F}}\, b\, z_{\mathrm{H}}^2\, r_{\mathrm{F}}^3 + \iota\, m_{\mathrm{H}}^3\, d^5\, r_{\mathrm{F}} + m_{\mathrm{H}}^3\, d^5\, r_{\mathrm{F}} \\
& + 2\,\iota^2\, m_{\mathrm{H}}^2\, m_{\mathrm{F}}\, d^3\, r_{\mathrm{F}}^3 + 2\,\iota\, m_{\mathrm{H}}^2\, m_{\mathrm{F}}\, d^3\, r_{\mathrm{F}}^3 + \iota\, m_{\mathrm{H}}^3\, d^3\, z_{\mathrm{H}}^2\, r_{\mathrm{F}} + \iota^3\, m_{\mathrm{H}}\, m_{\mathrm{F}}^2\, d\, r_{\mathrm{F}}^5 \\
& + \iota^2\, m_{\mathrm{H}}\, m_{\mathrm{F}}^2\, d\, r_{\mathrm{F}}^5 + \iota^2\, m_{\mathrm{H}}^2\, m_{\mathrm{F}}\, d\, z_{\mathrm{H}}^2\, r_{\mathrm{F}}^3\big) / w^6 \\
X_4 =\; & -g\, m_{\mathrm{H}}\, m_{\mathrm{F}}^2\, b^3\, d\, r_{\mathrm{F}}^2\, \big(8\,\iota^3\, m_{\mathrm{H}}\, m_{\mathrm{F}}^2\, b^2\, d^2\, r_{\mathrm{F}}^3 + 2\,\iota^3\, m_{\mathrm{H}}^2\, m_{\mathrm{F}}\, b^2\, d^2\, r_{\mathrm{F}}^3 \\
& + 4\,\iota^3\, m_{\mathrm{H}}^2\, m_{\mathrm{F}}\, b^2\, d^2\, r_{\mathrm{F}}^2\, z_{\mathrm{H}} + 12\,\iota^2\, m_{\mathrm{H}}\, m_{\mathrm{F}}^2\, b^2\, d^2\, r_{\mathrm{F}}^3 + 8\,\iota^2\, m_{\mathrm{H}}\, m_{\mathrm{F}}^2\, b^2\, d^2\, z_{\mathrm{H}}\, r_{\mathrm{F}}^2 \\
& + 4\,\iota^2\, m_{\mathrm{H}}^2\, m_{\mathrm{F}}\, b^2\, d^2\, r_{\mathrm{F}}^3 + 6\,\iota^2\, m_{\mathrm{H}}^2\, m_{\mathrm{F}}\, b^2\, d^2\, z_{\mathrm{H}}\, r_{\mathrm{F}}^2 + 4\,\iota^2\, m_{\mathrm{H}}^2\, m_{\mathrm{F}}\, b^2\, d^2\, z_{\mathrm{H}}^2\, r_{\mathrm{F}} \\
& - 2\,\iota^2\, m_{\mathrm{H}}^3\, b^2\, d^2\, z_{\mathrm{H}}^2\, r_{\mathrm{F}} + 4\,\iota\, m_{\mathrm{H}}\, m_{\mathrm{F}}^2\, b^2\, d^2\, r_{\mathrm{F}}^3 + 4\,\iota\, m_{\mathrm{H}}\, m_{\mathrm{F}}^2\, b^2\, d^2\, z_{\mathrm{H}}\, r_{\mathrm{F}}^2 \\
& + 2\,\iota\, m_{\mathrm{H}}^2\, m_{\mathrm{F}}\, b^2\, d^2\, r_{\mathrm{F}}^3 + 2\,\iota\, m_{\mathrm{H}}^2\, m_{\mathrm{F}}\, b^2\, d^2\, z_{\mathrm{H}}\, r_{\mathrm{F}}^2 - 2\,\iota\, m_{\mathrm{H}}^3\, b^2\, d^2\, z_{\mathrm{H}}^2\, r_{\mathrm{F}} \\
& - 2\,\iota\, m_{\mathrm{H}}^3\, b^2\, d^2\, z_{\mathrm{H}}^3 + 8\,\iota^4\, m_{\mathrm{F}}^3\, b^2\, r_{\mathrm{F}}^5 - 8\,\iota^4\, m_{\mathrm{H}}\, m_{\mathrm{F}}^2\, b^2\, z_{\mathrm{H}}\, r_{\mathrm{F}}^4 + 12\,\iota^3\, m_{\mathrm{F}}^3\, b^2\, r_{\mathrm{F}}^5 \\
& + 8\,\iota^3\, m_{\mathrm{F}}^3\, b^2\, z_{\mathrm{H}}\, r_{\mathrm{F}}^4 - 16\,\iota^3\, m_{\mathrm{H}}\, m_{\mathrm{F}}^2\, b^2\, z_{\mathrm{H}}\, r_{\mathrm{F}}^4 - 8\,\iota^3\, m_{\mathrm{H}}\, m_{\mathrm{F}}^2\, b^2\, z_{\mathrm{H}}^2\, r_{\mathrm{F}}^3 \\
& + 4\,\iota^3\, m_{\mathrm{H}}^2\, m_{\mathrm{F}}\, b^2\, z_{\mathrm{H}}^2\, r_{\mathrm{F}}^3 + 4\,\iota^2\, m_{\mathrm{F}}^3\, b^2\, r_{\mathrm{F}}^5 + 4\,\iota^2\, m_{\mathrm{F}}^3\, b^2\, z_{\mathrm{H}}\, r_{\mathrm{F}}^4 - 8\,\iota^2\, m_{\mathrm{H}}\, m_{\mathrm{F}}^2\, b^2\, z_{\mathrm{H}}\, r_{\mathrm{F}}^4 \\
& - 8\,\iota^2\, m_{\mathrm{H}}\, m_{\mathrm{F}}^2\, b^2\, z_{\mathrm{H}}^2\, r_{\mathrm{F}}^3 + 4\,\iota^2\, m_{\mathrm{H}}^2\, m_{\mathrm{F}}\, b^2\, z_{\mathrm{H}}^2\, r_{\mathrm{F}}^3 + 4\,\iota^2\, m_{\mathrm{H}}^2\, m_{\mathrm{F}}\, b^2\, z_{\mathrm{H}}^3\, r_{\mathrm{F}}^2 \\
& + 4\,\iota^3\, m_{\mathrm{H}}^2\, m_{\mathrm{F}}\, b\, d^3\, r_{\mathrm{F}}^3 + 4\,\iota^3\, m_{\mathrm{H}}^2\, m_{\mathrm{F}}\, b\, d^3\, z_{\mathrm{H}}\, r_{\mathrm{F}}^2 + 9\,\iota^2\, m_{\mathrm{H}}^2\, m_{\mathrm{F}}\, b\, d^3\, r_{\mathrm{F}}^3 \\
& + 10\,\iota^2\, m_{\mathrm{H}}^2\, m_{\mathrm{F}}\, b\, d^3\, z_{\mathrm{H}}\, r_{\mathrm{F}}^2 - 2\,\iota^2\, m_{\mathrm{H}}^3\, b\, d^3\, z_{\mathrm{H}}^2\, r_{\mathrm{F}} + 6\,\iota\, m_{\mathrm{H}}^2\, m_{\mathrm{F}}\, b\, d^3\, r_{\mathrm{F}}^3 \\
& + 8\,\iota\, m_{\mathrm{H}}^2\, m_{\mathrm{F}}\, b\, d^3\, z_{\mathrm{H}}\, r_{\mathrm{F}}^2 - 2\,\iota\, m_{\mathrm{H}}^3\, b\, d^3\, z_{\mathrm{H}}^2\, r_{\mathrm{F}} + m_{\mathrm{H}}^2\, m_{\mathrm{F}}\, b\, d^3\, r_{\mathrm{F}}^3 + 2\, m_{\mathrm{H}}^2\, m_{\mathrm{F}}\, b\, d^3\, z_{\mathrm{H}}\, r_{\mathrm{F}}^2 \\
& + m_{\mathrm{H}}^2\, m_{\mathrm{F}}\, b\, d^3\, z_{\mathrm{H}}^2\, r_{\mathrm{F}} + 4\,\iota^4\, m_{\mathrm{H}}\, m_{\mathrm{F}}^2\, b\, d\, r_{\mathrm{F}}^5 + 4\,\iota^4\, m_{\mathrm{H}}\, m_{\mathrm{F}}^2\, b\, d\, z_{\mathrm{H}}\, r_{\mathrm{F}}^4 \\
& + 9\,\iota^3\, m_{\mathrm{H}}\, m_{\mathrm{F}}^2\, b\, d\, r_{\mathrm{F}}^5 + 10\,\iota^3\, m_{\mathrm{H}}\, m_{\mathrm{F}}^2\, b\, d\, z_{\mathrm{H}}\, r_{\mathrm{F}}^4 - \iota^3\, m_{\mathrm{H}}^2\, m_{\mathrm{F}}\, b\, d\, z_{\mathrm{H}}\, r_{\mathrm{F}}^4 \\
& + 2\,\iota^3\, m_{\mathrm{H}}^2\, m_{\mathrm{F}}\, b\, d\, z_{\mathrm{H}}^2\, r_{\mathrm{F}}^3 + 4\,\iota^3\, m_{\mathrm{H}}^2\, m_{\mathrm{F}}\, b\, d\, z_{\mathrm{H}}^3\, r_{\mathrm{F}}^2 + 6\,\iota^2\, m_{\mathrm{H}}\, m_{\mathrm{F}}^2\, b\, d\, r_{\mathrm{F}}^5 \\
& + 8\,\iota^2\, m_{\mathrm{H}}\, m_{\mathrm{F}}^2\, b\, d\, z_{\mathrm{H}}\, r_{\mathrm{F}}^4 - 2\,\iota^2\, m_{\mathrm{H}}^2\, m_{\mathrm{F}}\, b\, d\, z_{\mathrm{H}}\, r_{\mathrm{F}}^4 + 6\,\iota^2\, m_{\mathrm{H}}^2\, m_{\mathrm{F}}\, b\, d\, z_{\mathrm{H}}^3\, r_{\mathrm{F}}^2 \\
& - 2\,\iota^2\, m_{\mathrm{H}}^3\, b\, d\, z_{\mathrm{H}}^4\, r_{\mathrm{F}} + \iota\, m_{\mathrm{H}}\, m_{\mathrm{F}}^2\, b\, d\, r_{\mathrm{F}}^5 + 2\,\iota\, m_{\mathrm{H}}\, m_{\mathrm{F}}^2\, b\, d\, z_{\mathrm{H}}\, r_{\mathrm{F}}^4 + \iota\, m_{\mathrm{H}}\, m_{\mathrm{F}}^2\, b\, d\, z_{\mathrm{H}}^2\, r_{\mathrm{F}}^3 \\
& - \iota\, m_{\mathrm{H}}^2\, m_{\mathrm{F}}\, b\, d\, z_{\mathrm{H}}\, r_{\mathrm{F}}^4 - 2\,\iota\, m_{\mathrm{H}}^2\, m_{\mathrm{F}}\, b\, d\, z_{\mathrm{H}}^2\, r_{\mathrm{F}}^3 - \iota\, m_{\mathrm{H}}^2\, m_{\mathrm{F}}\, b\, d\, z_{\mathrm{H}}^3\, r_{\mathrm{F}}^2 \\
& + 2\,\iota^3\, m_{\mathrm{H}}^2\, m_{\mathrm{F}}\, d^4\, r_{\mathrm{F}}^3 + 5\,\iota^2\, m_{\mathrm{H}}^2\, m_{\mathrm{F}}\, d^4\, r_{\mathrm{F}}^3 + 4\,\iota\, m_{\mathrm{H}}^2\, m_{\mathrm{F}}\, d^4\, r_{\mathrm{F}}^3 + \iota\, m_{\mathrm{H}}^2\, m_{\mathrm{F}}\, d^4\, z_{\mathrm{H}}\, r_{\mathrm{F}}^2 \\
& + m_{\mathrm{H}}^2\, m_{\mathrm{F}}\, d^4\, r_{\mathrm{F}}^3 + m_{\mathrm{H}}^2\, m_{\mathrm{F}}\, d^4\, z_{\mathrm{H}}\, r_{\mathrm{F}}^2 + 4\,\iota^4\, m_{\mathrm{H}}\, m_{\mathrm{F}}^2\, d^2\, r_{\mathrm{F}}^5 + 10\,\iota^3\, m_{\mathrm{H}}\, m_{\mathrm{F}}^2\, d^2\, r_{\mathrm{F}}^5 \\
& - \iota^3\, m_{\mathrm{H}}^2\, m_{\mathrm{F}}\, d^2\, z_{\mathrm{H}}\, r_{\mathrm{F}}^4 + 4\,\iota^3\, m_{\mathrm{H}}^2\, m_{\mathrm{F}}\, d^2\, z_{\mathrm{H}}^2\, r_{\mathrm{F}}^3 + 8\,\iota^2\, m_{\mathrm{H}}\, m_{\mathrm{F}}^2\, d^2\, r_{\mathrm{F}}^5 \\
& + 2\,\iota^2\, m_{\mathrm{H}}\, m_{\mathrm{F}}^2\, d^2\, z_{\mathrm{H}}\, r_{\mathrm{F}}^4 - 2\,\iota^2\, m_{\mathrm{H}}^2\, m_{\mathrm{F}}\, d^2\, z_{\mathrm{H}}\, r_{\mathrm{F}}^4 + 4\,\iota^2\, m_{\mathrm{H}}^2\, m_{\mathrm{F}}\, d^2\, z_{\mathrm{H}}^2\, r_{\mathrm{F}}^3 \\
& + 2\,\iota\, m_{\mathrm{H}}\, m_{\mathrm{F}}^2\, d^2\, r_{\mathrm{F}}^5 + 2\,\iota\, m_{\mathrm{H}}\, m_{\mathrm{F}}^2\, d^2\, z_{\mathrm{H}}\, r_{\mathrm{F}}^4 - \iota\, m_{\mathrm{H}}^2\, m_{\mathrm{F}}\, d^2\, z_{\mathrm{H}}\, r_{\mathrm{F}}^4 + \iota\, m_{\mathrm{H}}^2\, m_{\mathrm{F}}\, d^2\, z_{\mathrm{H}}^3\, r_{\mathrm{F}}^2 \\
& + 2\,\iota^5\, m_{\mathrm{F}}^3\, r_{\mathrm{F}}^7 + 5\,\iota^4\, m_{\mathrm{F}}^3\, r_{\mathrm{F}}^7 - \iota^4\, m_{\mathrm{H}}\, m_{\mathrm{F}}^2\, z_{\mathrm{H}}\, r_{\mathrm{F}}^6 + 4\,\iota^4\, m_{\mathrm{H}}\, m_{\mathrm{F}}^2\, z_{\mathrm{H}}^2\, r_{\mathrm{F}}^5 + 4\,\iota^3\, m_{\mathrm{F}}^3\, r_{\mathrm{F}}^7 \\
& + \iota^3\, m_{\mathrm{F}}^3\, z_{\mathrm{H}}\, r_{\mathrm{F}}^6 - 2\,\iota^3\, m_{\mathrm{H}}\, m_{\mathrm{F}}^2\, z_{\mathrm{H}}\, r_{\mathrm{F}}^6 + 4\,\iota^3\, m_{\mathrm{H}}\, m_{\mathrm{F}}^2\, z_{\mathrm{H}}^2\, r_{\mathrm{F}}^5 - \iota^3\, m_{\mathrm{F}}\, m_{\mathrm{H}}^2\, r_{\mathrm{F}}^4\, z_{\mathrm{H}}^3 \\
& + 2\,\iota^3\, m_{\mathrm{F}}\, m_{\mathrm{H}}^2\, r_{\mathrm{F}}^3\, z_{\mathrm{H}}^4 + \iota^2\, m_{\mathrm{F}}^3\, r_{\mathrm{F}}^7 + \iota^2\, m_{\mathrm{F}}^3\, z_{\mathrm{H}}\, r_{\mathrm{F}}^6 - \iota^2\, m_{\mathrm{H}}\, m_{\mathrm{F}}^2\, z_{\mathrm{H}}\, r_{\mathrm{F}}^6 \\
& + \iota^2\, m_{\mathrm{H}}\, m_{\mathrm{F}}^2\, z_{\mathrm{H}}^3\, r_{\mathrm{F}}^4 - \iota^2\, m_{\mathrm{H}}^2\, m_{\mathrm{F}}\, z_{\mathrm{H}}^3\, r_{\mathrm{F}}^4 - \iota^2\, m_{\mathrm{H}}^2\, m_{\mathrm{F}}\, z_{\mathrm{H}}^4\, r_{\mathrm{F}}^3\big) / w^6 \\
X_6 =\; & 2\,\iota\, m_{\mathrm{H}}\, m_{\mathrm{F}}^3\, b^3\, d\, r_{\mathrm{F}}^3\, \left(z_{\mathrm{H}} + r_{\mathrm{F}} + \iota\, r_{\mathrm{F}}\right) \left(-m_{\mathrm{H}}\, z_{\mathrm{H}} + m_{\mathrm{F}}\, r_{\mathrm{F}} + 2\,\iota\, m_{\mathrm{F}}\, r_{\mathrm{F}}\right) \big(4\,\iota^2\, m_{\mathrm{F}}\, b^2\, r_{\mathrm{F}} \\
& + 2\,\iota\, m_{\mathrm{F}}\, b^2\, r_{\mathrm{F}} - 2\,\iota\, m_{\mathrm{H}}\, b^2\, z_{\mathrm{H}} + \iota\, m_{\mathrm{H}}\, b\, d\, r_{\mathrm{F}} + m_{\mathrm{H}}\, b\, d\, r_{\mathrm{F}} + m_{\mathrm{H}}\, b\, d\, z_{\mathrm{H}} + \iota\, m_{\mathrm{H}}\, d^2\, r_{\mathrm{F}} \\
& + m_{\mathrm{H}}\, d^2\, r_{\mathrm{F}} + \iota^2\, m_{\mathrm{F}}\, r_{\mathrm{F}}^3 + \iota\, m_{\mathrm{F}}\, r_{\mathrm{F}}^3 + \iota\, m_{\mathrm{H}}\, z_{\mathrm{H}}^2\, r_{\mathrm{F}}\big) / w^6
\end{aligned}
\tag{8.6}
$$

These expressions seem very complicated, but due to terms outside the brackets they appear to be neat enough to extract requirements for the parameters in a stability study with the Routh stability criterion (see section 4.5). To make the analysis even simpler, first off a stable configuration is sought that is stable from a certain forward speed to infinite speed; no upper speed bound is present. In such a case it is only important that eventually the system becomes stable, and thus only the leading terms of the coefficients corresponding with the highest powers of the velocity are important. A negative lower order coefficient can thus be compensated by a positive higher order coefficient.

As explained in section 4.5, all following Routh conditions are necessary for self-stability. If one condition is not met, the bicycle is not self-stable. Note that it is directly assumed that masses, inertia's, and the radius cannot be negative, $m_{\mathrm{H}} \geq 0$, $m_{\mathrm{F}} \geq 0$, $I_{\mathrm{F}}(,\iota) \geq 0$, $r_{\mathrm{F}} \geq 0$, and masses cannot be located underneath the ground (positive z-axis points down), $z_{\mathrm{H}} \leq 0$. The gravitational acceleration, g, is defined as always positive. For further parameter requirements, the Routh conditions must be used:

$\boldsymbol{A = A_0 > 0}$ The coefficient A_0 is positive as long as the mass-matrix is non-singular, since it is the determinant of that positive semi-definite matrix. The term outside the brackets shows that the mass matrix can be singular in two ways: First, it is singular when the front wheel has zero mass and radius, and secondly, when there exists a combination of lean and steer that does not move any mass. From the term outside brackets it can be concluded that $A_0 > 0$ is met when $m_{\mathrm{F}} > 0$, $r_{\mathrm{F}} > 0$ (they are already assumed non-negative), and $b \neq 0$, $w \neq 0$ ($w = 0$ gives division by zero).

$\boldsymbol{B = B_1 v > 0}$ When the bicycle moves forward ($v > 0$), B_1 must be positive for self-stability. Even by applying the parameter requirements from A_0, the sign of the terms outside and inside brackets is uncertain. The term inside brackets contains a term with the always negative mass height that might make or might not make the term inside brackets negative. In effect, from B_1, no extra conclusions can be drawn about parameter requirements at all.

$\boldsymbol{C = C_0 + C_2 v^2 > 0}$ The first coefficient is always negative, but with increasing velocity the second coefficient will weigh more on the sign of the total coefficient and C will eventually be positive when C_2 is positive. However, just as for B_1, the term inside the brackets can be either positive or negative depending on different parameter combinations, thus from C_2 no extra parameter requirements arise.

$\boldsymbol{D = D_1 v + D_3 v^3 > 0}$ At higher positive velocities, the leading coefficient, D_3, becomes the most important. It can directly be seen from the term outside the brackets that the mass moment of inertia cannot be zero, and it was already assumed that it can also not be negative. Then, when remembering $m_{\mathrm{F}} > 0$, $r_{\mathrm{F}} > 0$, and $z_{\mathrm{H}} \leq 0$, it can be concluded that the leading coefficient D_3, is only positive for $\iota > 0$, $b > 0$.

$\boldsymbol{E = E_0 + E_2 v^2 > 0}$ The leading coefficient E_2 determines that at higher velocities the total coefficient is positive when E_2 is positive. It can directly be seen that the front frame mass and its distance to the wheel axle cannot be zero. Then, remembering the sign of the other coefficients, $m_{\mathrm{F}} > 0$, $\iota > 0$, $r_{\mathrm{F}} > 0$, $b > 0$, and taking the assumption into account that masses cannot be negative, it is concluded for E_2 to be positive that $m_{\mathrm{H}} > 0$, $d > 0$.

$\boldsymbol{X = X_2 v^2 + X_4 v^4 + X_6 v^6 > 0}$ At higher velocities the leading coefficient X_6 needs to be positive to assure self-stability. The term outside brackets and the second term inside brackets are positive when all previously deducted parameter requirements are applied. The first term inside brackets reads $z_{\mathrm{H}} + r_{\mathrm{F}} + \iota\, r_{\mathrm{F}}$ and the third term inside brackets contains the same pattern so that the sign of the total coefficient is dependent on the signs of these two bracket terms. The complete coefficient X_6 is positive when the first and third term in brackets are either both positive or both negative. The individual terms inside the third term inside brackets can also be found distributed over B_1 and C_2 such that this bracket term can be rewritten,

$$\begin{aligned} X_6 = 2\,\iota\, m_{\mathrm{H}}\, {m_{\mathrm{F}}}^3\, b^3\, d\, {r_{\mathrm{F}}}^3\, \left(z_{\mathrm{H}} + r_{\mathrm{F}} + \iota\, r_{\mathrm{F}}\right) \left(-m_{\mathrm{H}}\, z_{\mathrm{H}} + m_{\mathrm{F}}\, r_{\mathrm{F}} + 2\,\iota\, m_{\mathrm{F}}\, r_{\mathrm{F}}\right) \\ \left(w^2\, \left(B_1/b + C_2\right) / \left(m_{\mathrm{F}}\, r_{\mathrm{F}}\right) - m_{\mathrm{H}}\, b\, d\, \left(z_{\mathrm{H}} + r_{\mathrm{F}} + \iota\, r_{\mathrm{F}}\right)\right) / w^6 \end{aligned} \tag{8.7}$$

So when $\iota > 0$, $m_{\mathrm{F}} > 0$, $r_{\mathrm{F}} > 0$, $b > 0$, $d > 0$, $z_{\mathrm{H}} \leq 0$ and $B_1 > 0$, $C_2 > 0$, as is required for stability, then the first and third bracket terms can never be simultaneously negative due to the minus sign inside the third term. Hence, the two bracket terms should be simultaneously positive to make all coefficients, B_1, C_2, and X_6, positive; and thus, $(z_{\mathrm{H}} + r_{\mathrm{F}} + \iota\, r_{\mathrm{F}}) > 0$, making the front frame mass height limit front wheel inertia dependent, being at least the wheel radius ($\iota > 0$): $z_{\mathrm{H}} > -(1+\iota)\, r_{\mathrm{F}}$.

To summarize the findings from the Routh conditions, the requirements on the parameters for a self-stable minimal bicycle with these specific eight parameters are shown in figure 8.2. It can be seen

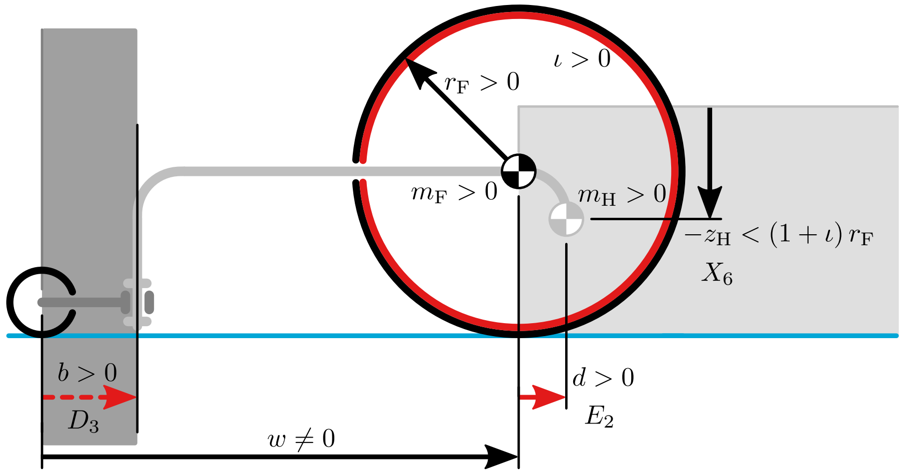

Figure 8.2: Illustration of the stability conditions. The highlighted area shows the region where the front assembly mass can be placed

that $w \neq 0$, $m_F > 0$, and $r_F > 0$ from A_0, $\iota > 0$ and $b > 0$ from D_3, $d > 0$ and $m_H > 0$ from E_2, and finally $0 \leq -z_H < (1 + \iota)\, r_F$ from X_6. The three introduced redundant parameters can then be translated to requirements for their relevant benchmark parameters: $x_H > w$, $c > -w$, and $I_F > 0$.

In theory there is now upper bound for the value of the rear wheel trail (or no lower bound on the front wheel trail) for this minimal bicycle parameter set to be self-stable. However, the kinematic definition of the steer-side of a bicycle does set an upper bound to the rear trail value in order make the bicycle rear wheel steered; $b < w/2$ (see section 6.3). When this upper bound is ignored one can get a self-stable FWSB with infinite long positive front wheel trail; (vertical) steer axis intersects the ground way ahead of the front wheel. So to make sure to end up with an RWSB, this rear wheel trail limit should be taken into account. Peculiarly, the found configuration with a larger and heavier front assembly and steer axis located close to the rear also meets the subjective 'you know it when you see it' definition of a rear wheel steered bicycle (see section 6.3).

Although causal reasoning is hard due to the complex interaction nature of all bicycle parameters, some physical explanations can be given for the requirements. The rear wheel needs a positive trail, which seems logical since it is a caster wheel that always tends to follow the front wheel. With negative rear wheel trail it would soon align to a positive trail, destabilizing the bicycle in the process.

Furthermore, the front frame mass ahead of the front wheel levers about the front wheel contact point and tends to steer the front wheel into a fall when the bicycle is leaned, thereby recovering balance. When the bicycle gets out of its upright stable position it leans to one side. When leaned, the mass ahead of the front wheel pulls the front down about an axis through the front contact point and the steer angle gets directed into the fall. Note that even simpler models of rear wheel steered bicycles could benefit lateral stability-wise by placing the mass ahead of the front wheel. For example, the simple single-mass inverted pendulum model gets a negative control parameter (a zero) which benefits controllability [14] (section 1.14). Furthermore, note that in real-life a center of mass ahead of the front wheel would flip the bicycle over forwardly which might be why this configuration is minimally investigated in literature. Luckily, just as for the two-mass-skate bicycle of Kooijman *et al.*, extra (point-)masses can be added exactly at either contact point without affecting lateral dynamics [16].

In a similar fashion one can look at the turn response as described in section 7.2. A self-stable bicycle namely can negotiate a turn with a single constant torque on the steer joint. During a forward motion, when such a torque is applied, the frame mass ahead of the front wheel of this RWSB lies above a point on the support line where the support line is accelerated into the curve during an initiation of a curve. This is similar to a conventional self-stable bicycle where the mass lies above such a point on the support line in between the wheels (see section 6.1, figure 6.2). This means that during the initiation the support line is shifted away underneath the mass to initiate a lean to the outside of the curve, i.e. a counter-steer. While leaning to one side, the mass ahead of the front wheel then acts in combination with other parameters to angle the steer into the lean, i.e. steer-into-fall, and recovers balance.

A front wheel mass moment of inertia is required for self-stability and the height of the front frame mass is bounded by this inertia and the front wheel radius. The wheel inertia makes that the wheel precesses (steers) into the fall under influence of a lean angle of the wheel; the larger the wheel inertia, the larger this precession. On the other hand, a high front frame increases the inertia about the lean axis and thereby increases the resistance against leaning of the bicycle, and thus a higher front frame mass makes the tendency to lean smaller. These two phenomena go hand-in-hand since lean causes steer and vice versa, but they also counteract each other since lateral stability requires that the lean is reduced. Therefore, the timing between the phenomena is important and thus stability requires an appropriate phase between lean and steer, setting a front wheel inertia dependent limit on the front frame mass height. Note that a bicycle with mass below (and ahead of) the front axle is stable regardless the front wheel inertia. As seen in section 8.4, the bicycle can be stable for a finite forward velocity region with a high mass with appropriate horizontal distance to the wheel axle.

Summarizing, this RWSB thus incorporates a positive rear wheel trail which is important for caster purposes, with a steer-into-fall behavior by means of a special mass-distribution, as is sought by some authors in literature [5] [4] [8] (see appendix A). Note that the mass only is not enough to assure self-stability, it remains an interplay of different features, e.g. the front wheel inertia is also important.

8.3 Numerical example

To get more insight in the dynamics of a self-stable RWSB, a numerical example is generated which allows for some numerical analyses. For this theoretical RWSB a numerical example is generated whose

Table 8.1: The 8 parameters of a self-stable RWSB configuration with minimal set of parameters. The remaining parameters are zero.

Parameter	**Symbol**	**Value**
Wheel base	w	1 m
Front wheel trail	c	-0.8 m
Gravity	g	9.81 N/kg
Front frame H mass	m_{H}	8.5 kg
Front frame H center of mass	$(x_{\mathrm{H}}, z_{\mathrm{H}})$	$(1.1, -0.25)$ m
Front wheel radius	r_{F}	0.35 m
Front wheel mass	m_{F}	5 kg
Front wheel inertia	$I_{\mathrm{F}yy}$ $(= 2I_{\mathrm{F}xx})$	0.45 kgm^2

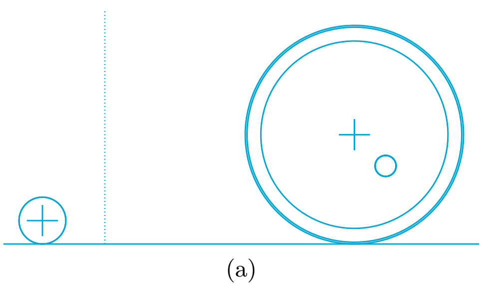

(a)

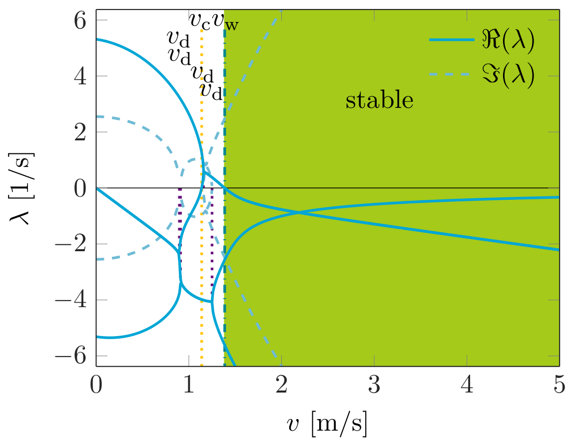

(b)

Figure 8.3: Numerical theoretical RWSB (a) visual parameter representation in the style of JBike6 (see section 4.3) where the bicycle is seen from the right, and (b) the corresponding eigenvalues. It has double root velocities $v_{\mathrm{d}} \approx 0.898, 0.910, 1.157, 1.251$ m/s, a capsize speed of $v_{\mathrm{c}} \approx 1.139$ m/s, and a weave speed of $v_{\mathrm{w}} \approx 1.387$ m/s.

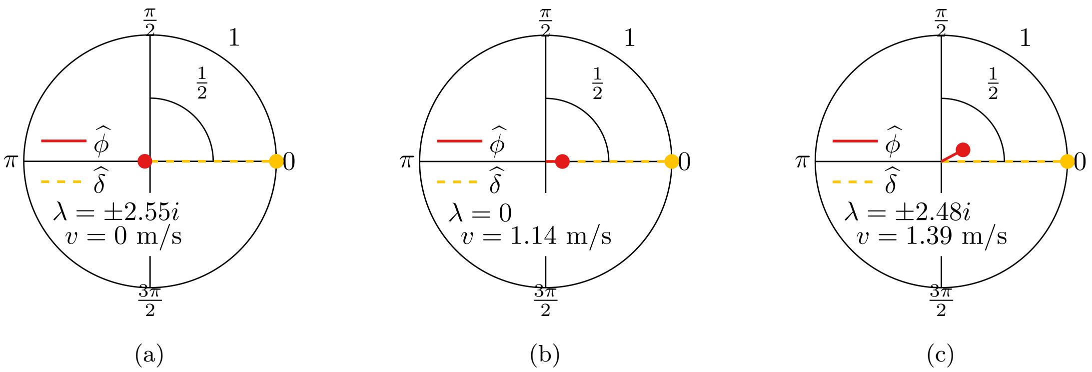

Figure 8.4: Phasor diagrams of some eigenvectors (mode shapes) of the numerical theoretical RWSB. (a) A purely imaginary mode shape at $v = 0$, (b) the mode shape associated with the eigenvalue that turns 0 at the 'capsize' speed ($E = 0$), and (c) one of the two mode shapes corresponding with the weave speed ($X = 0$) where the bicycle becomes stable.

parameters are shown in table 8.1 and a graphical representation along with its eigenvalues are presented in figure 8.3. Moreover, the coefficients of the characteristic polynomial are shown in figure 8.5 and some interesting mode shapes are depicted in figure 8.4. These figures give rise for notions about peculiar things about this unconventional bicycle configuration, e.g. this specific theoretical RWSB is self-stable for $1.39 < v < \infty$.

Eigenmodes

With reference to the eigenvalue plot, figure 8.1b, there is an eigenmode at $v = 0$ m/s that is purely imaginary with a mode shape that has a large steer angle motion with an exactly opposing (in anti phase) small lean angle, as shown in figure 8.4a. This mode is such that it oscillates without damping with the energy minimum in the upright ahead position; when leaned rightwards the steer is to the left and vice versa, such that the lowering of the mass due to the lean is counteracted by the steer.

At some higher velocities the eigenvalue plot, figure 8.1b, shows multiple velocities where a double root occurs. These make the eigenvalue plot somewhat cluttered, but are not of special interest for the eigenmode analysis other than that they are boundaries for oscillating motions.

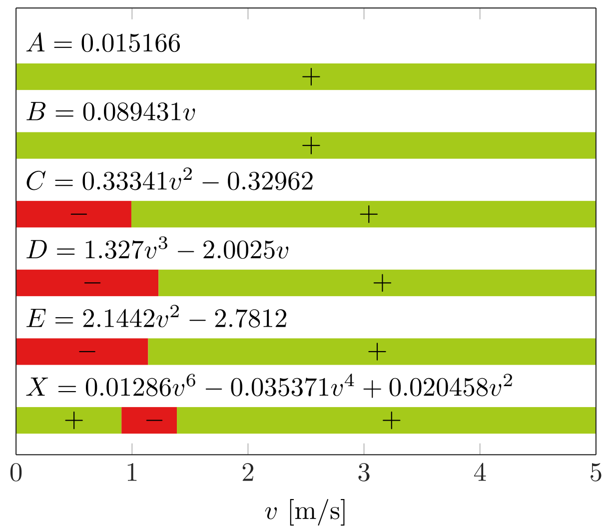

Figure 8.5: Routh Hurwitz coefficients for the numerical theoretical RWSB as function of the forward velocity. It can be seen that there are actually two weave speeds (also one at 0.909 m/s), because $X = 0$ at two velocities.

The eigenmode associated with $E = 0$ crosses zero at around 1.14 m/s such that there the capsize speed lies according to its definition (see section 4.5). The capsize speed is located at a lower speed than the weave speed, but although it is a lower limit of where the bicycle can be self-stable, it is not a boundary of the stable speed region. This is in accordance with the theory that for a bicycle with $E_0 < 0$, $E_2 > 0$, as this bicycle has (see figure 8.5), stability is only possible somewhere above the capsize speed (see section 4.5). The bicycle becomes only stable at a higher speed (for this biycle the weave speed) than the capsize speed, because first, besides E, also the other coefficients (here D and X) need to become positive.

However, the mode shape associated with the eigenmode crossing the zero line at the capsize speed does not correspond with a 'capsize' shape; it is steer dominated in stead of lean dominated (see figure 8.4b). This is oppositely to a conventional bicycle that has a capsize shape which is lean dominated (see section 4.2). The name 'capsize' may thus not be in place for this eigenmode with the critical speed where $E = 0$ for this specific bicycle.

In stead of that the self-stable speed region begins at the weave speed and ends at the capsize speed, as is often the case for a conventional bicycle (see section 4.2), it starts at the weave speed and reaches to infinity. As stated by the definition (see section 4.5), the weave speed is calculated as the speed where $X = 0$, which is here at $v_{\mathrm{w}} \approx 1.39$ m/s. Figure 8.4c shows that the mode shape associated with the weave speed where the bicycle becomes stable is associated with a 'traditional' weave shape with a lot of steer and a significant lean contribution, just as seen on a conventional bicycle (see section 4.2). Note that figure 8.5 shows that there are actually two weave speeds, since there are two velocities where $X = 0$. So actually, starting from zero forward speed with increasing speed, the weave is stable, becomes unstable, and later becomes stable again. However, in the eigenvalue plot, the lower weave speed is not depicted, because it almost coincides with a double root and does not show special behavior.

Above the weave speed, the RWSB is thus self-stable with two all real negative eigenvalues and a complex eigenvalue with negative real part. At 2.18 m/s the eigenvalues are combined at their most negative value, such that one can speak of the 'maximal' stability. This speed can be used to find reasonable fast converging solutions in time analyses.

Time response

A linear time response simulation (see section 5.1) is carried out for different values of d and z_{H}, in order to show that the RWSB indeed shows stable converging behavior for a certain set of parameters. Focus is here on the location of the front frame mass, which is varied while all other parameters are kept constant. Four simulations are performed as shown in figure 8.6 with small initial perturbations in the lean angular rate, while no additional torques are applied:

$$\mathbf{x}_0 = \begin{bmatrix} \dot{\phi}_0 \\ \dot{\delta}_0 \\ \phi_0 \\ \delta_0 \end{bmatrix} = \begin{bmatrix} \pi/9 \\ 0 \\ 0 \\ 0 \end{bmatrix}, \qquad \mathbf{f} = \begin{bmatrix} T_\phi \\ T_\delta \end{bmatrix} = \mathbf{0} \tag{8.8}$$

The mass is positioned in different quadrants around the intersection between the lines $d = 0$ and $z_{\mathrm{H}} = -(1+\iota)\,r$ to show stable and unstable behavior. Indeed, for a figure where the RWSB rides forward to the right, it can be seen that the RWSB is only stable for a frame mass located in the lower right area as depicted in figure 8.6e for the numerical parameter values of table 8.1. The mass is then ahead the front wheel axle and below the wheel inertia dependent height limit. For this front frame mass position, the oscillating weave motion after the perturbation damps out to a straight up and ahead forward motion.

With the mass placed in the upper left or lower left quadrant, the bicycle soon starts to deviate from the zero stable position in a capsize fashion; the lean and steer increase making the bicycle fall over in an ever-tightening spiral. When the front frame mass is placed in the upper right quadrant, a harmonic weave motion can be seen that is somewhat similar to the stable RWSB with mass in the lower right quadrant. However, here the harmonic motion is almost stable, but not quite as it is still diverging. Note that when the mass is placed correctly in this upper right quadrant, the minimal RWSB can be still self-stable, but then for a finite forward speed region as shown in section 8.4.

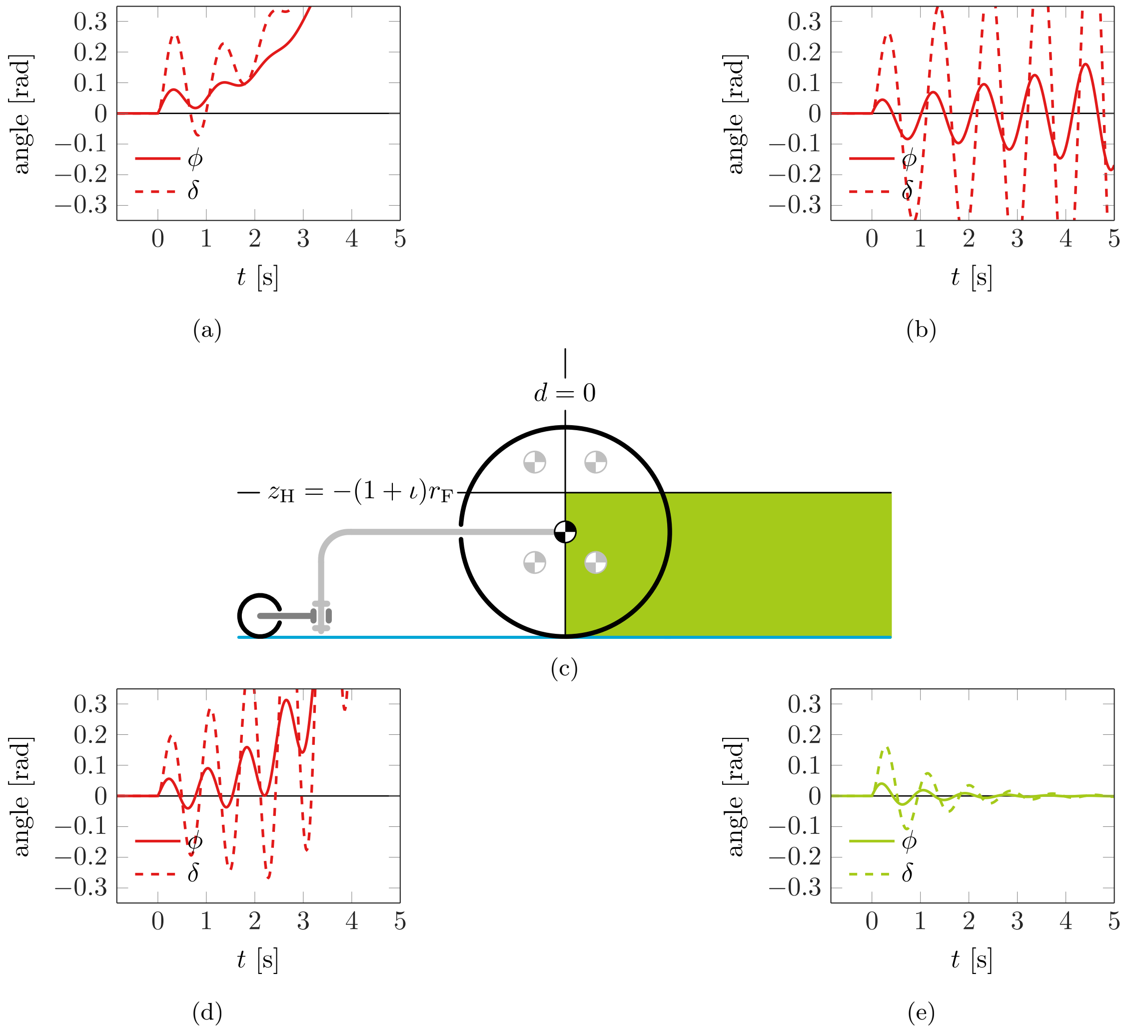

Figure 8.6: Linear time response of the minimal theoretical RWSB for different values of d and z_{H} (other parameters kept equal) at $v = 2.18$ m/s with initial disturbances, $\dot{\mathbf{q}}_0 = [\pi/9,\, 0]^{\mathsf{T}}$. (a) $d = -0.1$, $z_{\mathrm{H}} = -(1+\iota)r_{\mathrm{F}} - 0.1$; Unstable, (b) $d = 0.1$, $z_{\mathrm{H}} = -(1+\iota)r_{\mathrm{F}} - 0.1$; Unstable, (e) $d = -0.1$, $z_{\mathrm{H}} = -0.25 (> (1+\iota)r_{\mathrm{F}})$; Unstable, (e) $d = 0.1$, $z_{\mathrm{H}} = -0.25 (> (1+\iota)r_{\mathrm{F}})$, the specific numerical RWSB parameters; Stable. Summarizing, (c) shows whether the bicycle is stable when the front frame mass is placed in a certain quadrant; red is unstable, green is stable.

8.4 Finite speed region stability

In stead of the theoretical minimal RWSB parameter conditions that result in self-stability from a certain forward velocity onward without upper speed bound, also parameter values of the minimal parameter set can be found that result in a finite self-stability speed region. Then, a minimal and maximal forward speed are present between which the bicycle is stable. This means that the RH-coefficients are not all positive for infinite increasing forward speeds, but only at some forward speeds they are all positive. This is in contrast with the previous where stability for a region from a minimal speed up to infinite speed was sought.

By trial-and-error an example of such a finite self-stable speed region bicycle was found which has $d > 0$ and $-z_{\mathrm{H}} > (1+\iota)\, r_{\mathrm{F}}$. As seen in section 8.2, such parameter values cannot result in a self-stable minimal theoretical RWSB that is self-stable to infinite speed due to the height of the mass. Here, a the numerical example is generated that has the same parameter values as the numerical RWSB except for the front mass location which is now located at $d = 0.4$ m ($x_{\mathrm{H}} = 1.4$ m) and $z_{\mathrm{H}} = -0.55$ m. This configuration is given in table tab:RWSBMinB and it can be seen from figure 8.7 that indeed there is

Table 8.2: The 8 parameter values of a finite self-stable speed region RWSB configuration.

Parameter	**Symbol**	**Value**
Wheel base	w	1 m
Front wheel trail	c	-0.8 m
Gravity	g	9.81 N/kg
Front frame H mass	m_{H}	8.5 kg
Front frame H center of mass	$(x_{\mathrm{H}}, z_{\mathrm{H}})$	$(1.4, -0.55)$ m
Front wheel radius	r_{F}	0.35 m
Front wheel mass	m_{F}	5 kg
Front wheel inertia	$I_{\mathrm{F}yy}$ $(= 2I_{\mathrm{F}xx})$	0.45 kgm^2

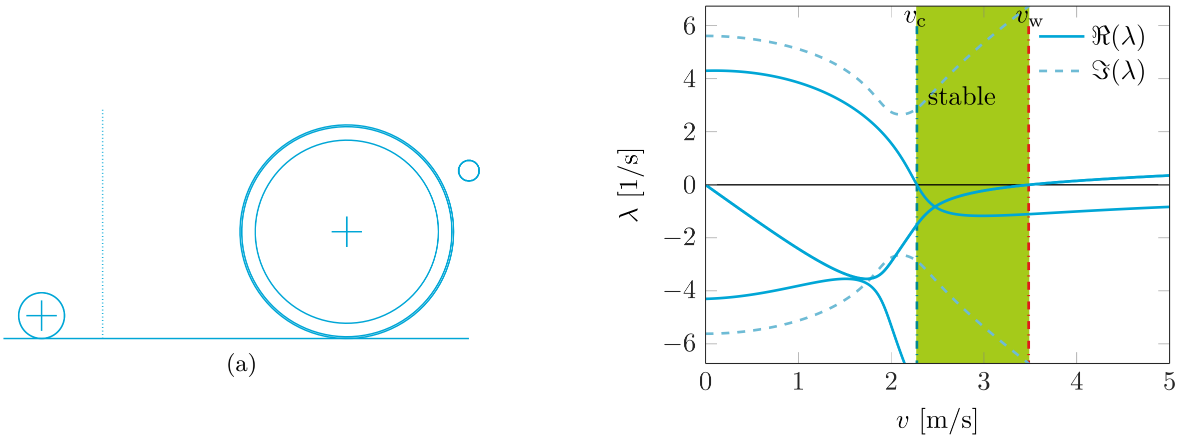

(a) (b)

Figure 8.7: Finite self-stable speed region numerical theoretical RWSB (a) visual parameter representation in the style of JBike6 (see section 4.3) where the bicycle is seen from the right, and (b) the corresponding eigenvalues. It has a capsize speed of $v_{\mathrm{c}} \approx 2.278$ m/s, and a weave speed of $v_{\mathrm{w}} \approx 3.482$ m/s.

a stable speed region.

Such a configuration can show stability, because the Routh determinant (8.6) is positive at certain speeds under influence of the positive X_4 coefficient (see figure 8.8). At lower speeds, when the X_2 coefficient still plays a significant role, and at higher speeds, when X_6 dominates the total coefficient, their negativity makes the total coefficient also negative. Unfortunately, as (8.6) shows, the expression for X_4 is very long and contains an interaction of all eight parameters. Therefore, straightforward parameter conditions for when X_4 is positive and outweighs a negative X_2 and X_6 cannot easily be extracted.

The configuration as given here is apparently such that physically the high front mass position is nullified by a large forward horizontal distance of the same mass. As said, a higher position of the front mass makes the inertia about the lean axis larger which results in slow lean dynamics and in effect in slow wheel precession. The further horizontal distance makes the lever arm of the front mass about the front wheel yaw axis larger and makes a stabilizing steer-into-fall dynamic at certain speeds possible. However, as said, it is not easy to obtain exact stability conditions for d and z_{H} when a finite self-stable speed region is desired.

In this specific case the stable speed region starts at the capsize speed and ends at a weave speed, which is opposite to ordinary bicycles where the stable speed region starts at the weave speed and ends at the capsize speed. Furthermore, both the mode shape associated with the capsize speed and the mode shape associated with the weave speed are steer dominated, in stead of lean dominated as for a conventional bicycle.

Besides the existence of a finite self-stable speed region RWSB with this specific minimal set of parameters, another set of minimal parameters might also turn out to give a self-stable RWSB. For

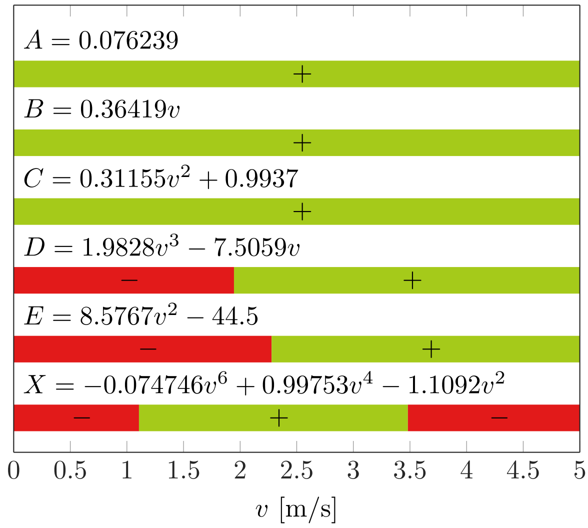

Figure 8.8: Routh Hurwitz coefficients for the finite self-stable speed region numerical theoretical RWSB as function of the forward velocity.

example, this set arose from an attempt to model a simple unicycle, but another starting point is also possible. Removing parameters from this set is impossible, because it was seen that none of them can be zero for self-stability. However, adding nonzero parameters is no problem, but can change specific parameter requirements and thus change the self-stable configuration. Introducing extra nonzero parameters from the total of 25, e.g. make the front mass moment of inertia nonzero, does change the dynamical characteristics of the RWSB. The stability limit requirements may then be changed somewhat, but broadly speaking the stable mass distribution stays the same. An example of a fully parametrized RWSB with infinite stable forward velocity range is presented in section 10.1, but other examples with infinite or finite stable forward velocity range are also possible (see section A.85).

Chapter 9

Single wheel vehicle comparison

9.1 RWSB EOM in local Front coordinates

One might think that the self-stable RWSB configuration as described in section 8.3 is simply a rolling wheel with some mass attached to its axle. Especially since, due to the large mass in front of the axle and the massles rear wheel and frame, the ground contact pressure at the rear wheel can be small in a real-life realization of this bicycle. However, although the configuration of the RWSB presented here looks like a uni- or mono-cycle (vehicles are generally the same, but are sometimes distinguished by the place of the extra mass; above or inside the wheel respectively [42]), or just a single large wheel, its behavior is essentially different. This is shown by comparing the RWSB equations of motion with those of a unicycle model and with those of a single wheel.

The benchmark model uses a different set of generalized degrees of freedom, i.e. rear wheel roll angle, ϕ, and steer angle δ, as is used for a one wheel model lacking a steer pivot like the unicycle or single wheel. To make comparing of the RWSB with these one wheel models possible, a translation for the RWSB is performed to describe the local lean and yaw angle of the parametrized front wheel, ${}_{\mathrm{F}}\phi$, and ${}_{\mathrm{F}}\psi$. The unicycle and wheel model have no difference between local and global coordinates, so that it is allowed to translate the bicycle model to the local coordinates. These are the angles as they could be used in the benchmark model if one chooses to make the local front wheel angles the degrees of freedom by performing a transformation with (3.60) on the matrices (see section 3.2). Here, $\lambda_{\mathrm{s}} = 0$ and $c = b - w$, such that the transformation matrix becomes,

$$
{}_{\mathrm{F}}\mathbf{T} = \begin{bmatrix} 1 & 0 \\ 0 & w/b \end{bmatrix} \tag{9.1}
$$

By transforming the minimal RWSB matrices, (8.1), (8.2), (8.3), and (8.4), the following matrices for the minimal RWSB in front wheel local coordinates are obtained:

$$
{}_{\mathrm{F}}\mathbf{M} = \begin{bmatrix} m_{\mathrm{H}}\, {z_{\mathrm{H}}}^2 + (1+\iota)\; m_{\mathrm{F}}\, {r_{\mathrm{F}}}^2 & -m_{\mathrm{H}}\, d\, z_{\mathrm{H}} \\ -m_{\mathrm{H}}\, d\, z_{\mathrm{H}} & m_{\mathrm{H}}\, d^2 + \iota\, m_{\mathrm{F}}\, {r_{\mathrm{F}}}^2 \end{bmatrix} \tag{9.2}
$$

$$
{}_{\mathrm{F}}\mathbf{C}_1 = \begin{bmatrix} 0 & \left(-m_{\mathrm{H}}\;(b+d)\;z_{\mathrm{H}} + (1+2\,\iota)\, m_{\mathrm{F}}\, b\, r_{\mathrm{F}}\right)/b \\ -2\,\iota\, m_{\mathrm{F}}\, r_{\mathrm{F}} & \left(m_{\mathrm{H}}\,(b+d)\;d + \iota m_{\mathrm{F}} {r_{\mathrm{F}}}^2\right)/b \end{bmatrix} \tag{9.3}
$$

$$
{}_{\mathrm{F}}\mathbf{K}_0 = \begin{bmatrix} m_{\mathrm{H}}\, z_{\mathrm{H}} - m_{\mathrm{F}}\, r_{\mathrm{F}} & -m_{\mathrm{H}}\, d \\ -m_{\mathrm{H}}\, d & 0 \end{bmatrix} \tag{9.4}
$$

$$
{}_{\mathrm{F}}\mathbf{K}_2 = \begin{bmatrix} 0 & \left(-m_{\mathrm{H}}\, z_{\mathrm{H}} + (1+2\iota)\; m_{\mathrm{F}}\, r_{\mathrm{F}}\right)/b \\ 0 & m_{\mathrm{H}}\, d/b \end{bmatrix} \tag{9.5}
$$

By examining the matrices for both generalized coordinates it can be seen that the transformation comes down to putting $w = b$ in the matrices of the minimal RWSB. This occurs because the transformation acts by letting the steer axis and the front wheel vertical yaw axis coincide, $c = 0$, making the steer angle equal to the front wheel yaw.

9.2 Unicycle

To compare the minimal RWSB with a unicycle, the unicycle model as presented by Coleman and Papadopoulos [42] [53] is used, but somewhat altered to make the parameters resemble those of the minimal RWSB. This 'generalized' unicycle has two bodies: A wheel with mass and mass moment of inertia, and an added point mass representing rider and frame that follows the wheel lean and yaw, but has no pitching motion (see figure 9.1). The wheel is modeled in the same way as the wheels in the bicycle Whipple model (section 3.1) and thus has a planar mass distribution and is knife edged, with a no-slip, non-penetrating, non-dissipative, rolling point contact. In order to hold the added second mass into place with respect to the wheel in a fore-aft asymmetric fashion, a second frictionless contact is added. In figure 9.1) this is depicted by the curve from the fork center of mass to the ground at contact point, P*, which represents a massless bar that is required to hold the added point mass at a constant position in the vehicle's local coordinate frame. At the contact point, P*, there is no friction in any direction, but contact with the ground is always kept, e.g. this could be realized in real-life by using a roller ball. Then, the vehicle 'steers' by somehow yawing its single wheel about its own vertical axis.

Now, the minimal RWSB model is transformed to the unicycle model, in order to see what the differences are. Since the minimal RWSB has only one wheel with nonzero parameters, it is chosen to use that front wheel as the single wheel of the unicycle. All geometrical and mass properties are now taken from a neutral upright position with the coordinate system origin at the front wheel contact point. A unicycle is then sort of a naive 'bicycle' with zero front wheel trail, $c = 0$, and due to its single wheel has an infinite wheel base, $w \to \infty$, and an equal rear wheel trail, $b = w \to \infty$. Note that this is different from taking a zero rear wheel trail, $b = 0$, which at first sight might seem a way of transforming a bicycle into a unicycle, but does not result in a workable model. Therefore, a first step in conversing the RWSB model into the unicycle is to take $\lim_{b\to\infty}$ of the matrices (9.2), (9.3), (9.4), and (9.5). The vanishing matrix terms then show that the finite bicycle wheel base and trail make that the front frame mass on the RWSB contributes different to the motion than it does on the unicycle.

However, with the trail terms removed, the Coleman unicycle model [42] [53] is not yet acquired. A second difference is namely the static lean-yaw coupling. The unicycle is modeled as a one wheel vehicle with an extra frictionless ground point contact to ensure the location of the front frame mass.

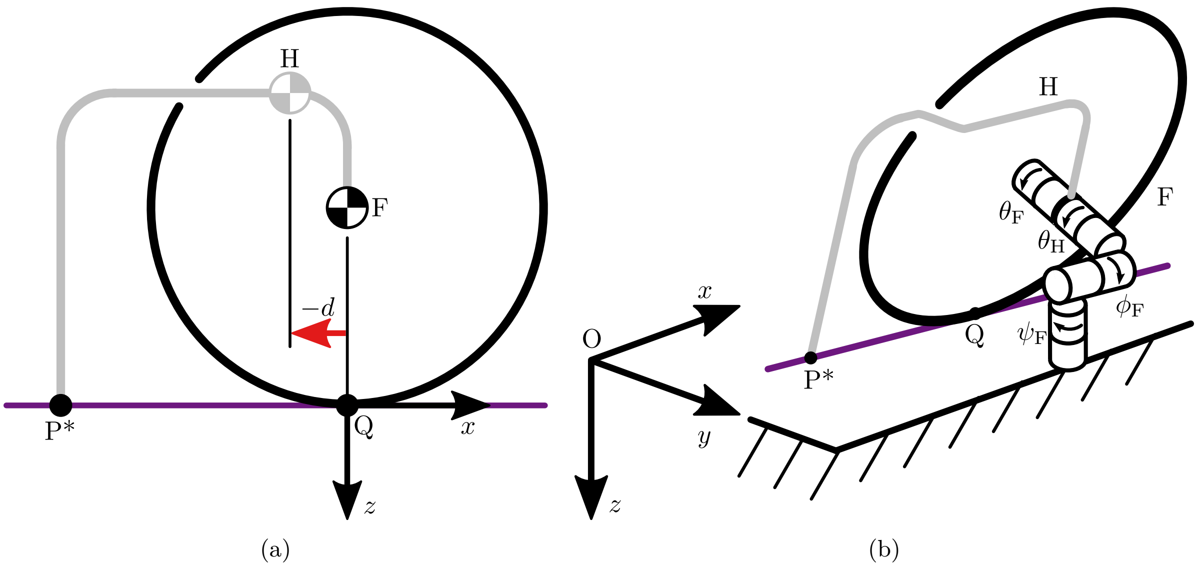

Figure 9.1: Unicycle model depiction as presented by Coleman and Papadopoulos [42] [53] with the purple line displaying the heading of the wheel. (a) The single wheel, F, has a point mass, H, attached to it which is held at a certain position, (d, z_H), with respect to the wheel axle by a massless bar. This bar is imagined to slide on the ground at the frictionless contact, P^*, while the wheel has a no-slip contact, Q. (b) The unicycle has several degrees of freedom, of which only the wheel lean angle, ϕ_F, yaw angle, ψ_F, and pitch angle, θ_F parametrize the accessible configuration space. Here, $\dot{\theta}_F$, is used as representation for the forward velocity, v.

This extra contact point location is directly related to the wheel yaw in contrary to a bicycle where either contact point does not move laterally under the influence of wheel yawing of either wheel due to the steer pivot between the two frames. A yaw on the unicycle rotates the support line spanned by the contact points and always keeps the frame mass above this support line. This is in contrast to what happens for a bicycle for a local wheel yaw, where the frame mass is moved to one side of the support line which creates a lean moment. This modeling makes that the cross terms in the unicycle $\mathbf{K}_0$ matrix are lost such that a static lean only does not yaw the unicycle and vice versa. Therefore, along with taking $\lim_{b\to\infty}$, these static cross terms need to be removed from the velocity-independent stiffness matrix to convert the RWSB model into the Coleman unicycle model with six nonzero parameters [42]:

$$
{}^{\mathrm{U}}\mathbf{M} = \begin{bmatrix} m_\mathrm{H}\, z_\mathrm{H}{}^2 + (1+\iota)\, m_\mathrm{F}\, r_\mathrm{F}{}^2 & -m_\mathrm{H}\, d\, z_\mathrm{H} \\ -m_\mathrm{H}\, d\, z_\mathrm{H} & m_\mathrm{H}\, d^2 + \iota\, m_\mathrm{F}\, r_\mathrm{F}{}^2 \end{bmatrix} \tag{9.6}
$$

$$
{}^{\mathrm{U}}\mathbf{C}_1 = \begin{bmatrix} 0 & -m_\mathrm{H}\, z_\mathrm{H} + (1+2\,\iota)\, m_\mathrm{F}\, r_\mathrm{F} \\ -2\,\iota\, m_\mathrm{F}\, r_\mathrm{F} & m_\mathrm{H}\, d \end{bmatrix} \tag{9.7}
$$

$$
{}^{\mathrm{U}}\mathbf{K}_0 = \begin{bmatrix} m_\mathrm{H}\, z_\mathrm{H} - m_\mathrm{F}\, r_\mathrm{F} & 0 \\ 0 & 0 \end{bmatrix} \tag{9.8}
$$

$$
{}^{\mathrm{U}}\mathbf{K}_2 = \begin{bmatrix} 0 & 0 \\ 0 & 0 \end{bmatrix} \tag{9.9}
$$

In practice, e.g. in incorporated models as in JBike6, removing wheel base/trail terms is easier than removing the static cross terms. By numerically setting $b = w \to \infty$ all undesired terms relating to the wheel base/trail in all matrices vanish. However, the cross terms should only disappear from the static $\mathbf{K}_0$-matrix, and not from other matrices. So by simply taking $m_\mathrm{H} = 0$ or $d = 0$ not only the static cross terms are removed, but also other terms in other matrices that are desirable to keep are removed, and the RWSB model is not transformed into a unicycle, but into a single wheel (see section 9.3). Were it not for these static cross-terms, then the unicycle could be modeled correctly by the bicycle model as a special naive bicycle case with infinite long wheel base. However, the absence of a static lean and yaw coupling due to different support line behavior makes a unicycle crucially different from a bicycle.

The difference between the unicycle and the bicycle can also be seen as that the unicycle has two contacts of which one contact cannot generate lateral (or longitudinal) contact forces, whereas a bicycle has two lateral force generating contacts. This is also why a bicycle needs a steer joint to change the heading of its wheels, and a unicycle does not.

All in all, a bicycle cannot be modeled by the unicycle model, but maybe more peculiarly, a unicycle can also not be modeled with the bicycle model due to the presence of static cross terms that originate from a support line reacting different on wheel yaw. For a unicycle the support line yaws along with the wheel, while on a bicycle the support line does not move for local wheel. Then, an additional mass yawing along with the wheel does only create a lean moment for a bicycle.

Stable unicycle conditions

As for the minimal RWSB, also for the unicycle the Routh coefficients can be determined in order to find the unicycle stability conditions (here the analysis of Coleman and Papadopoulos [42] is repeated in the style of Kooijman *et al.* [16], see section 4.5). Since several terms have disappeared from the equations of motions, the unicycle model has also fewer and simpler nonzero Routh coefficients:

$$
\begin{aligned}
A_0 &= m_\mathrm{F}\, r_\mathrm{F}{}^2 \left(\iota\, m_\mathrm{H}\, d^2 + m_\mathrm{H}\, d^2 + \iota\, m_\mathrm{H}\, z_\mathrm{H}{}^2 + \iota^2\, m_\mathrm{F}\, r_\mathrm{F}{}^2 + \iota\, m_\mathrm{F}\, r_\mathrm{F}{}^2\right) \\
B_1 &= m_\mathrm{H}\, m_\mathrm{F}\, d\, r_\mathrm{F}\, (z_\mathrm{H} + r_\mathrm{F} + \iota\, r_\mathrm{F}) \\
C_0 &= -\,g\, (-m_\mathrm{H}\, z_\mathrm{H} + m_\mathrm{F}\, r_\mathrm{F}) \left(m_\mathrm{H}\, d^2 + \iota\, m_\mathrm{F}\, r_\mathrm{F}{}^2\right) \\
C_2 &= 2\,\iota\, m_\mathrm{F}\, r_\mathrm{F}\, (-m_\mathrm{H}\, z_\mathrm{H} + m_\mathrm{F}\, r_\mathrm{F} + 2\,\iota\, m_\mathrm{F}\, r_\mathrm{F}) \\
D_1 &= -\,g\, m_\mathrm{H}\, d\, (-m_\mathrm{H}\, z_\mathrm{H} + m_\mathrm{F}\, r_\mathrm{F}) \\
X_2 &= g^2\, m_\mathrm{H}{}^2\, m_\mathrm{F}\, d^2\, z_\mathrm{H}\, r_\mathrm{F}\, (-m_\mathrm{H}\, z_\mathrm{H} + m_\mathrm{F}\, r_\mathrm{F})^2 \left(m_\mathrm{H}\, d^2 - \iota\, m_\mathrm{H}\, z_\mathrm{H}\, r_\mathrm{F} + \iota\, m_\mathrm{F}\, r_\mathrm{F}{}^2\right) \\
X_4 &= -\,2\, g\, \iota\, m_\mathrm{H}{}^2\, m_\mathrm{F}{}^2\, d^2\, r_\mathrm{F}{}^2\, (-m_\mathrm{H}\, z_\mathrm{H} + m_\mathrm{F}\, r_\mathrm{F})\, (z_\mathrm{H} + r_\mathrm{F} + \iota\, r_\mathrm{F})\, (-m_\mathrm{H}\, z_\mathrm{H} + m_\mathrm{F}\, r_\mathrm{F} \\
&\quad +2\,\iota\, m_\mathrm{F}\, r_\mathrm{F})
\end{aligned} \tag{9.10}
$$

When masses and radii are assumed to be non-negative, it can easily be seen that just as for the minimal RWSB the masses, radius and inertia should be larger than zero for stability (for stability all Routh coefficients need to have the same sign, section 4.5): $m_\mathrm{F} > 0$, and $r_\mathrm{F} > 0$ from A_0, $m_\mathrm{H} > 0$ from B_1, and $\iota > 0$ from C_2. However, due to the unicycle system being crucially different, two differences with the bicycle requirements for self-stability can be noted. For the unicycle, the added mass, m_H, has to be placed behind the front wheel axle and above a certain inertia dependent height [42]: $d < 0$ from D_1, and $z_\mathrm{H} < -(1+\iota)\, r_\mathrm{F}$ from X_4. This requirement is opposite to the self-stable RWSB requirement, where the additional mass should be in front of the axle, $d > 0$, and below a certain height, $z_\mathrm{H} > -(1+\iota)\, r_\mathrm{F}$. Once again, redundant parameters, d and ι, can be translated to requirements for their relevant benchmark parameters: $x_\mathrm{H} < 0$, and $I_\mathrm{F} > 0$.

Numerical unicycle example

Based on the minimal self-stable RWSB parameter values (table 8.1), a numerical unicycle example is created that satisfies the unicycle stability requirements (table 9.1 and figure 9.2). An eigenvalue analysis reveals some of the dynamical behavior of the unicycle (see figure 9.2). The unicycle as modeled here has only three nonzero eigenvalues, with two of three real eigenvalues joining at a certain forward velocity to form a complex eigenvalue pair. This is one less nonzero eigenvalue in comparison with the bicycle model: the unicycle has no caster mode, because it has only one wheel and, therefore, the wheels cannot align. However, just as for all systems, when all real parts of the eigenvalues are negative, as occurs for this specific configuration, the unicycle becomes asymptotically stable.

A linear time response simulation (section 5.1) with no external forces of the Coleman unicycle model shows how the unicycle two generalized coordinates freely develop in time after a perturbation (figure

Table 9.1: The 6 parameters of a self-stable unicycle configuration.

Parameter	**Symbol**	**Value**
Gravity	g	9.81 N/kg
Front frame H mass	m_H	8.5 kg
Front frame H center of mass	$(x_\mathrm{H}, z_\mathrm{H})$	(−0.1, −0.55) m
Front wheel radius	r_F	0.35 m
Front wheel mass	m_F	5 kg
Front wheel inertia	$I_{\mathrm{F}yy}$ $(= 2I_{\mathrm{F}xx})$	0.45 kgm^2

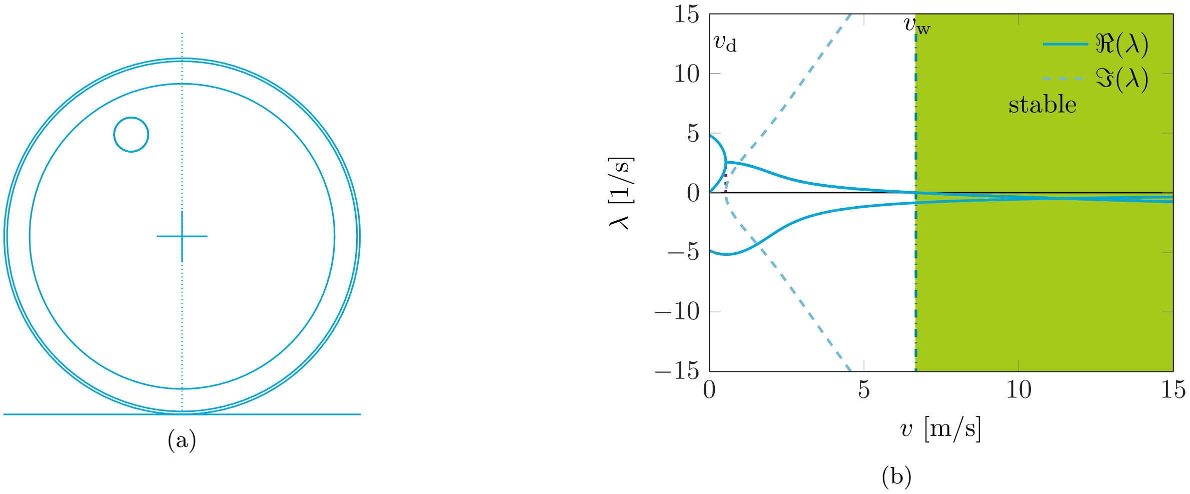

Figure 9.2: Unicycle (a) visual parameter representation in the style of JBike6 and (b) the eigenvalues of the unicycle model of Coleman and Papadopoulos [42] with specific parameter values chosen to resemble the minimal RWSB. $v_\mathrm{d} \approx 0.531$, and $v_\mathrm{w} \approx 6.678$ m/s. (not created with JBike6; that software uses the non-applicable bicycle model)

9.3). With the mass at the right position in the unicycle local frame, behind the wheel axle and above a wheel inertia dependent threshold height, the two DOF converge to a constant stable value. Thus, a wheel with non-holonomic rolling contact in combination with a correctly located front frame mass and a high enough forward velocity, makes the system such that a harmonic weave mode is damped out [42]; a self-stable unicycle. Then, a disturbance in lean and heading is corrected to come to a straight up and ahead motion, although the absolute heading is arbitrary (see figure 9.3a) [53]. Note, that when the frame mass has a mass moment of inertia, stability is possible for a lower mass height [42].

However, the mass can also be placed ahead or below the height threshold, such that the DOFs values do not converge to a stable constant value. Interestingly, it can be seen that the unicycle and RWSB are indeed crucially different due to the lack of static lean to wheel heading coupling for this unicycle model: Where the RWSB was self-stable with the mass in the bottom-right quadrant when riding forward is to the right in the figure, the unicycle is self-stable with the mass in the top-left quadrant (see figure 8.6 and 9.3). When the mass is placed exactly at the vertical wheel axis, $d = 0$, then the system becomes fore-aft symmetric and some terms with the additional mass disappear from (9.6), (9.7), (9.8), and

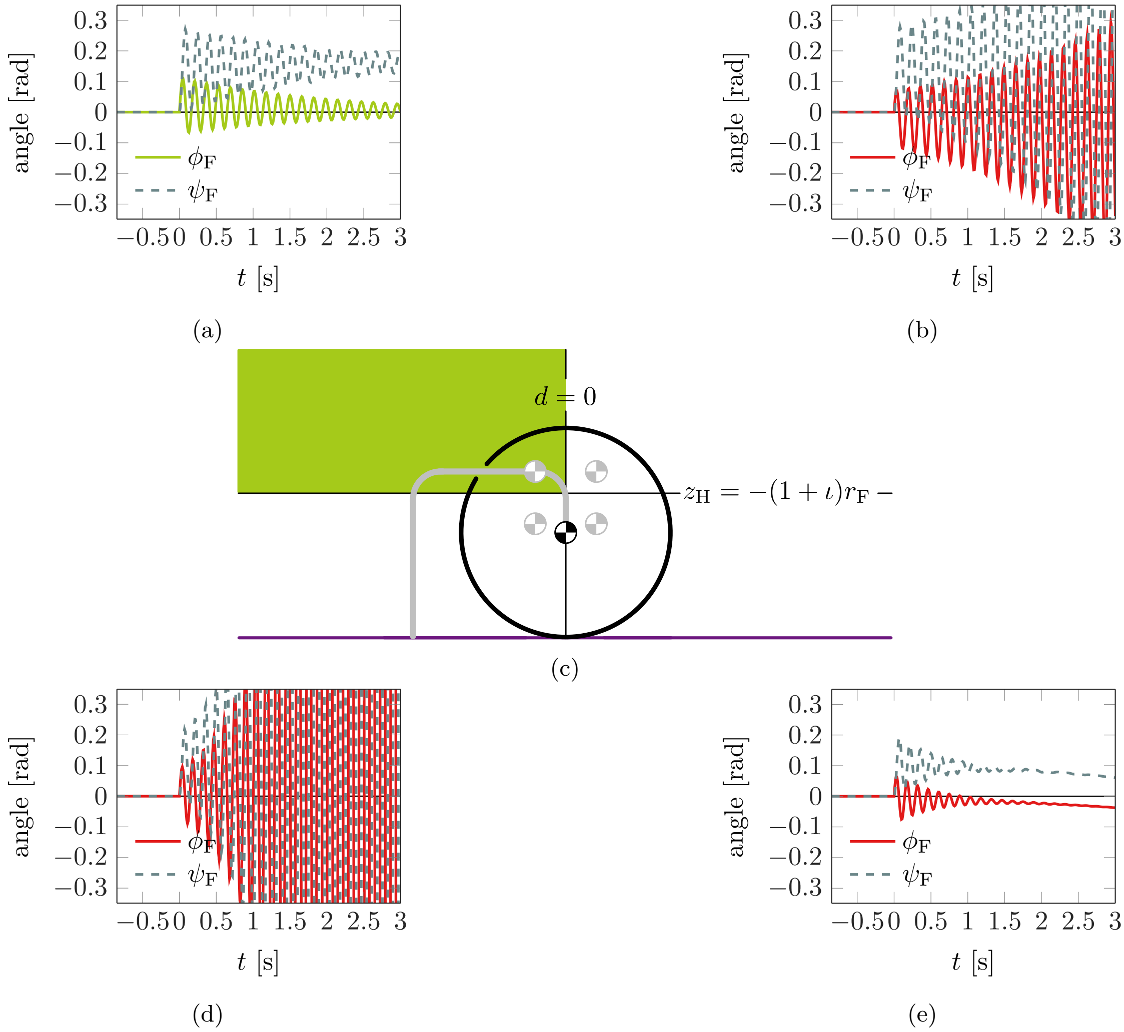

Figure 9.3: Linear time response of the unicycle for different values of d and z_H (other parameters kept equal) at $v = 11.4$ m/s with initial disturbances, $\dot{\mathbf{q}}_0 = [10\pi/9, 0]^\intercal$. (a) $d = -0.1$, $z_H = -0.55$, the specific numerical unicycle parameters; Stable, (b) $d = 0.1$, $z_H = -0.55$; Unstable, (d) $d = -0.1$, $z_H = -(1+\iota)\, r_F + 0.1$; Unstable, (e) $d = 0.1$, $z_H = -(1+\iota)\, r_F + 0.1$; Unstable. Summarizing, (c) shows whether the unicycle is stable when the front frame mass is placed in a certain quadrant; red is unstable, green is stable. Since the yaw angle is an absolute angle in the global frame, it can have any value, but during a straight ahead stable motion it should settle at a constant, generally nonzero, value.

(9.9). This makes the eigenvalues qualitatively the same as those of a single wheel, which prohibits the system from being asymptotically stable (although neutral stability is possible, see section 9.3) [42].

9.3 Wheel

The most simple rolling vehicle is a single wheel without any added mass. Such a wheel can be modeled just as the idealized wheels of a bicycle or unicycle with planar mass distribution and being knife-edged with a no-slip and no-dissipation rolling contact with the ground (see figure 9.4) [53] [42] [73].

To transform the minimal RWSB or unicycle model into a wheel, one can simply take $\lim_{b\to\infty}$ (or $\lim_{w\to\infty}$) and put in $m_\mathrm{H} = 0$ to make the trail (or wheel base) terms and the superfluous front frame mass terms disappear from the equations of motion. Both, the bicycle model and unicycle model, then result in the same wheel model, which can be a hoop, $\iota = \frac{1}{2}$, a solid disk, $\iota = \frac{1}{4}$, or theoretically anything else. Again, just as for the unicycle, here the front wheel is the single wheel. Many terms drop from the equations of motion matrices and the only coupling between lean and heading is under influence of angular rates by cross-terms in the 'damping' matrix for the wheel in the front wheel coordinates:

$$ {}^{\mathrm{W}}\mathbf{M} = \begin{bmatrix} (1+\iota)\, m_\mathrm{F}\, {r_\mathrm{F}}^2 & 0 \\ 0 & \iota\, m_\mathrm{F}\, {r_\mathrm{F}}^2 \end{bmatrix} \tag{9.11} $$

$$ {}^{\mathrm{W}}\mathbf{C}_1 = \begin{bmatrix} 0 & (1+2\,\iota)\, m_\mathrm{F}\, r_\mathrm{F} \\ -2\,\iota\, m_\mathrm{F}\, r_\mathrm{F} & 0 \end{bmatrix} \tag{9.12} $$

$$ {}^{\mathrm{W}}\mathbf{K}_0 = \begin{bmatrix} -m_\mathrm{F}\, r_\mathrm{F} & 0 \\ 0 & 0 \end{bmatrix} \tag{9.13} $$

$$ {}^{\mathrm{W}}\mathbf{K}_2 = \begin{bmatrix} 0 & 0 \\ 0 & 0 \end{bmatrix} \tag{9.14} $$

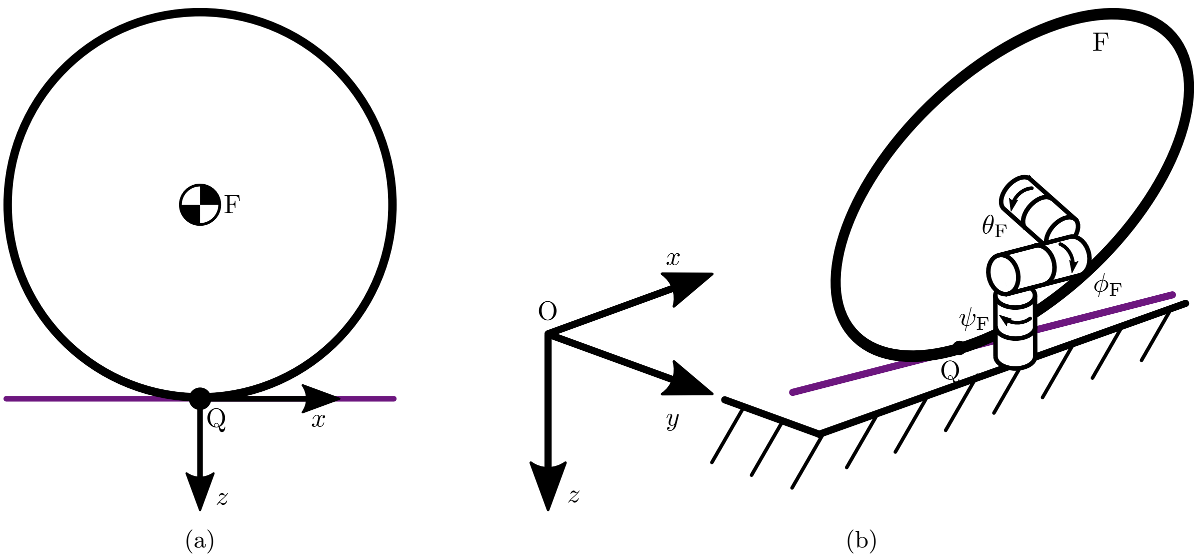

Figure 9.4: Wheel model depiction with the purple line displaying the heading of the wheel. (a) The single wheel, F, has no additional masses and only one contact point. (b) The three degrees of freedom, wheel lean angle, $\dot{\phi}_\mathrm{F}$, yaw angle, ψ_F, and pitch angle, θ_F parametrize the accessible configuration space.

Stable wheel conditions

To investigate the stability of the wheel, the Routh coefficients are drafted from the EOM (section 4.5):

$$\begin{aligned} A_0 &= (1+\iota)\, \iota\, {m_\mathrm{F}}^2\, {r_\mathrm{F}}^4 \\ C_0 &= -\,\iota\, g\, {m_\mathrm{F}}^2\, {r_\mathrm{F}}^3 \\ C_2 &= 2\,(1+2\,\iota)\, \iota\, {m_\mathrm{F}}^2\, {r_\mathrm{F}}^2 \end{aligned} \tag{9.15}$$

Because these are the only nonzero coefficients, the Routh determinant, (4.24), is always zero, $X = 0$, and all coefficients plus the determinant can never all have the same sign being nonzero. However, they can all be zero at the same time, resulting in neutral stability. An idealized non-dissipative wheel as modeled here is fore-aft symmetrical and just as all fore-aft symmetrical mechanisms cannot be asymptotically stable due to a required time reversibility which would require (the impossible) simultaneous existence of decaying and growing motions (section 4.2) [22] [42], but neutral stability, i.e. constant oscillating motion, is possible [42]. It turns out that there is a speed above which this neutral stability is possible and the wheel weaves constantly without falling completely [73]. This critical speed, corresponding with a double root, can be derived from the Routh coefficients, or more precisely, since $A = A_0 > 0$, it can be derived from $C = C_0 + C_2 v^2 = 0$ [74] [75] [76]:

$$v_\mathrm{d} = \sqrt{-\frac{C_0}{C_2}} = \sqrt{\frac{g\, r_\mathrm{F}}{(2+4\,\iota)}} \tag{9.16}$$

Numerical wheel example

A numerical example is created to see how the eigenvalues develop in a specific wheel case (table 9.2 and figure 9.5). There are only two nonzero real eigenvalues with one eigenmode representing arbitrary

Table 9.2: The 3 nonzero parameters of a wheel configuration.

Parameter	Symbol	Value
Gravity	g	9.81 N/kg
Front wheel radius	r_F	0.35 m
Front wheel mass	m_F	5 kg
Front wheel inertia	$I_{\mathrm{F}yy}$ $(= 2I_{\mathrm{F}xx})$	0.45 kgm^2

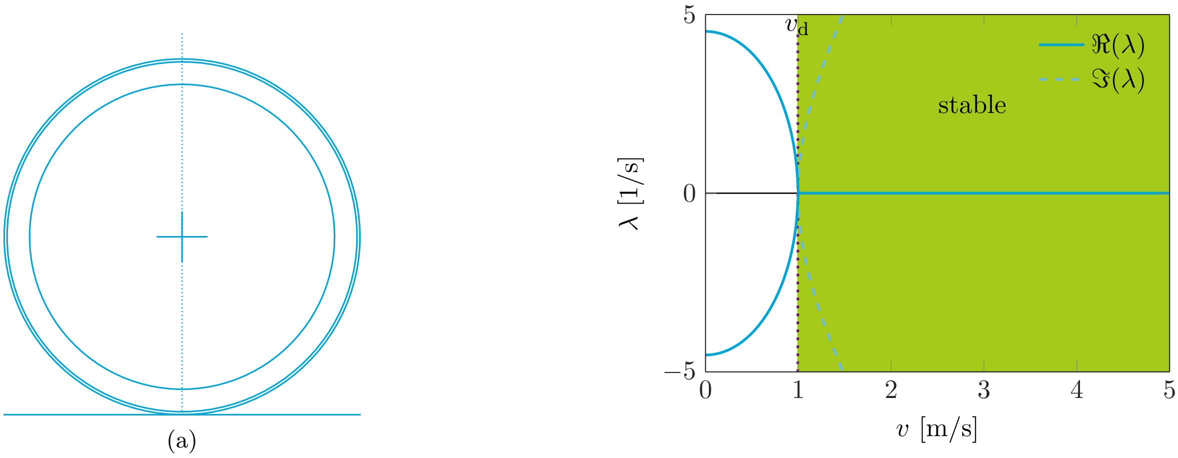

(a)

(b)

Figure 9.5: Wheel (a) visual parameter representation in the style of JBike6, and (b) the eigenvalues of the wheel model with specific parameter values chosen to resemble the minimal RWSB. The wheel is only marginally stable, because real parts of the eigenvalues are never all negative but only all zero; $v_\mathrm{d} \approx 0.995$ m/s. (not created with JBike6, because that software uses the non-applicable bicycle model)

heading, and the other representing arbitrary lean coupled to a heading rate [42]. These eigenvalues coalesce into a purely imaginary eigenvalue pair, i.e. zero real part, at the critical speed, describing an undamped weave motion superimposed on a constant lean circular trajectory above this critical speed [73] [42]. With the two real eigenvalues coalescing into a complex pair, the wheel eigenvalues look qualitatively somewhat like the numerical minimal RWSB eigenvalue plot (figure 8.3). Indeed, the numerical minimal self-stable RWSB has a very present front wheel, but the single wheel is essentially different from the minimal RWSB (and unicycle), because it can never return to a straight up and ahead motion after a perturbation.

However, in real-life, a fast enough rolling disk or hoop can return to straight up and ahead motion after a perturbation [42]. The linearized equations lacking the real-life dissipation are not able to capture this asymptotic stability, and some form of dissipation, like tire spin friction, should be included to simulate stable decaying motions [42].

Chapter 10

Experimental validation

10.1 Experimental RWSB prototype

The minimal theoretical RWSB from the previous chapters shows that an RWSB can be self-stable. However, this minimal configuration assumes point masses and has more nonzero parameters that cannot be physically nonzero for a real-life bicycle. This theoretical configuration needs to be converted into a real-life experimental RWSB prototype, in order to check if self-stable rear wheel steering is also practically implementable. Therefore, first a practically realizable self-stable RWSB design is required which is converted into a construction, in order to further test the stability features. The parameters of the parts of a constructed bicycle can be measured, such that it can be confirmed that a constructed RWSB based on the design is indeed self-stable according to the bicycle model.

Design

To increases the chance of finding a self-stable realizable design it is important for the design of the experimental bicycle that it comes close to the minimal theoretical bicycle design, both in configuration and in the assumptions of the Whipple model. This means that the rear assembly, i.e. rear wheel and rear frame, should be small and light, while the front frame mass can be large, but should be located ahead of the front wheel axle. Furthermore, this means that parts should be sufficiently rigid, friction in joints should be near zero, and the wheels must be as planar and axisymmetric as possible with close to knife-edged contacts. Furthermore, the experimental bicycle has some design requirements that should be met:

Reasonable self-stability characteristics The bicycle should be such that it can be brought upto a certain self-stable speed by a human while running next to it in a sports hall with flat floor. Concretely, this means that the bicycle should be self-stable in average human walking speed limits, $v < 5$ m/s, and it should be self-stable to a sufficient degree, i.e. eigenvalues should be sufficiently negative at a certain velocity, to compensate for unexpected discrepancies between model, design, and construction.

Experimental comfort The bicycle should be such that an average human can comfortably hold it and push it laterally when running next to it. Therefore, the bicycle must be high enough, and it may not be too heavy, e.g. a 200 kg motorcycle-like bicycle is hard to bring upto a certain speed in a limited distance.

Practically representative scale It should be on a length and weight scale, i.e. normal bicycle scale, to convince that self-stable rear wheel steering can be applied in practice. This includes the usage of standard parts.

Adjust- and disassemblable There should be some room for making corrections of miss-alignments or other discrepancies with the design when it turns out that the observed stability features or not satisfactory. In the same light the bicycle should give the opportunity to disassemble it.

From these requirements and for reasons of simplicity, three components of the bicycle are already taken as definite before the design process starts. As rear wheel a standard air pressurized wheel chair wheel is used with its standard bearings. The front wheel is a standard bicycle wheel which can be given an increased mass moment of inertia by placing two bent shaft rings in them. And a complete conventional head-tube with head-set is used to create the steer joint in order to make the steer axis easily recognizable and ease construction.

The RWSB of Broxterman *et al.* [17] (this study was a BSc graduation project of a student group containing the current author, P. H. de Jong, see section A.84) is used as base for the iterative prototype design process [16]. This iterative process includes drawing the bicycle design in Computer Aided Design (CAD) software (SolidWorks) and extracting masses, center of mass locations, and mass moments of inertia properties of the four rigid bodies (see section 3.5). These properties are put in the dynamical model and the eigenvalues are evaluated to see whether the design is sufficiently stable at a low enough speed. As long as the design stability properties are unsatisfying, the CAD design is modified, and the new mass properties are extracted and dynamically evaluated.

This resulted in the design as displayed in figure 10.1, with the 25 bicycle parameters and their visualization in table 10.1 and figure 10.1a, and the eigenvalues as shown in figure 10.1b. The model includes almost all important components, except the front wheel ball bearings and front wheel inertia rings holders. To distinguish the several parts easily, several colors are used: A grey rear frame, a yellow front frame, and red added weights. Note that, to-be used sensors (Shimmer and tachometer) are not included in the design and its parameters.

As known from the theoretical point mass configuration, the front frame mass needs to be located ahead of the front axle. This is done by placing a large weight with small mass moment of inertia, i.e. high density in a sphere-like shape, on the front frame ahead of the front axle. In real-life such a forwardly placed front frame mass needs to be balanced by a rear frame mass behind the front axle to prevent statically forward tipping which would make the rear wheel lose contact with the ground. However, in the self-stable theoretical model the rear frame was assumed to have no mass and inertia at all (see section 8.1) which is preferably mimicked in the real-life model. Luckily, mass can be added close to the wheel contact points with only small influence on the lateral dynamics, because such masses barely move under influence of lean and steer angle. By also making this mass small in dimension, i.e. sphere-like with high density material, the mass moment of inertia is kept acceptable. Thus, the required extra rear frame counterweight mass is placed close to the rear contact point at the rear axle with spere-like cylinders with a mass value that brings the center of mass of the total bicycle only slightly longitudinally behind the front axle to minimally influence the lateral stability [16] [17].

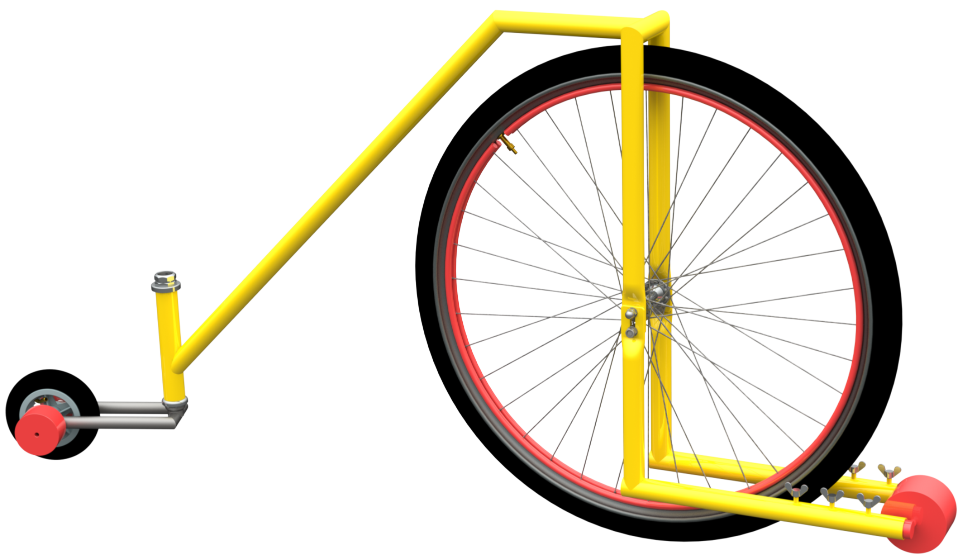

Figure 10.1: 3D CAD drawing of the RWSB prototype design. This design has a larger front wheel and a smaller rear wheel with grey rear frame and yellow front frame. Added weights at the rear and front frame and in the front wheel are coloured red.

To balance the bicycle statically, the frame masses are only limited in size relative to each other, with their absolute size limited by usefulness for experiments. The masses are a combination of the part structure and sizes and are dependent on the specified material density of the specific part.

The design procedure revealed several interesting things, which are applicable to this specific bicycle

Table 10.1: RWSB prototype design parameter values from the CAD software. Note that the weights on the rear and front frame and the front wheel are included in those respective parts.

Parameter	**Symbol**	**Value**
Wheel base	w	1.00 m
Front wheel trail	c	-0.80 m
Steer axis tilt	λ_s	0 rad
Gravity	g	9.81 N/kg
Rear wheel R radius	r_R	0.076 m
Rear wheel R mass	m_R	0.263 kg
Rear wheel R MMOI	(I_{Rxx}, I_{Ryy})	(0.0003966, 0.0007330) kgm^2
Rear frame B COM	(x_B, z_B)	(0.0345, -0.0894) m
Rear frame B mass	m_B	3.251 kg
Rear frame B MMOI	$\begin{bmatrix} I_{Bxx} & 0 & I_{Bxz} \\ 0 & I_{Byy} & 0 \\ I_{Bxz} & 0 & I_{Bzz} \end{bmatrix}$	$\begin{bmatrix} 0.0196 & 0 & 0.0072 \\ 0 & 0.0251 & 0 \\ 0.0072 & 0 & 0.0285 \end{bmatrix}$ kgm^2
Front frame H COM	(x_H, z_H)	(1.075, -0.252) m
Front frame H mass	m_H	8.601 kg
Front frame H MMOI	$\begin{bmatrix} I_{Hxx} & 0 & I_{Hxz} \\ 0 & I_{Hyy} & 0 \\ I_{Hxz} & 0 & I_{Hzz} \end{bmatrix}$	$\begin{bmatrix} 0.412 & 0 & -0.318 \\ 0 & 1.506 & 0 \\ -0.318 & 0 & 1.117 \end{bmatrix}$ kgm^2
Front wheel F radius	r_F	0.359 m
Front wheel F mass	m_F	4.889 kg
Front wheel F MMOI	(I_{Fxx}, I_{Fyy})	(0.226, 0.451) kgm^2

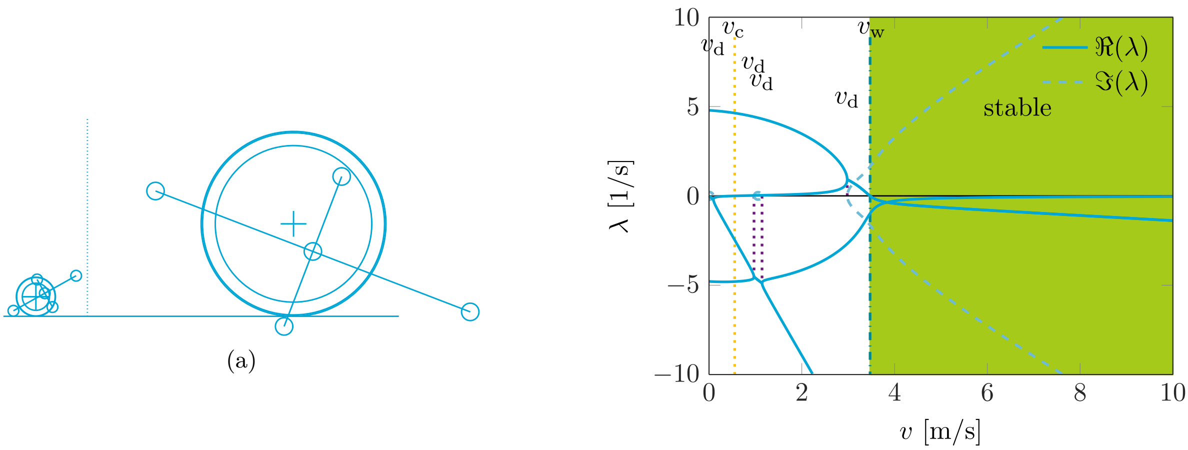

(a) (b)

Figure 10.2: RWSB prototype design (a) visual parameter representation in the style of JBike6 (see section 4.3) where the bicycle is seen from the right and (b) the eigenvalues from linearized stability analysis as function of the forward bicycle velocity. Solid lines show the real parts of eigenvalues and the dashed line corresponds with the imaginary part of the eigenvalue. Capsize speed at $v_c \approx 0.55$ m/s and double roots at $v_d \approx 0.096, 0.97, 1.14, 2.98$ m/s. This specific bicycle shows self-stable behavior for $v > v_w (\approx 3.47)$ m/s, where all real parts of the eigenvalues are negative. Its 'maximal' stability is reached at $v \approx 3.84$ m/s.

design. Because all parameters interact with each other to determine the dynamics/stability (see section 4.2), these findings apply only for limited changes of one parameter at a time. For small parts with small moments of inertia, small changes in geometry or material (density) can affect their moment of inertia drastically percentage-wise. However, these parts then often remain small, and do not alter the dynamics much. Changing the parameters of the more present parts significantly, can drastically alter the dynamics. For example, increasing the bicycle front wheel inertia makes the bicycle become self-stable at a lower speed at the cost of less negative eigenvalues. Furthermore, in accordance with the minimal theoretical RWSB, the height of the front frame is limited by the mass moment of inertia of the front wheel, i.e. a higher front wheel inertia allows a higher placed front frame mass. However, a higher placed mass makes tipping over for- or backwardly in real-life more likely to occur.

Construction

The RWSB prototype is constructed from the CAD drawing and only at some points does the construction deviate from the design (see figure 10.3). The inertia weight rings in the front wheel, one on either side of the spokes, are attached by using tie wraps. Moreover, some components are added to make the bicycle safer for its environment and change the appearance. This includes bump rubbers at the front weight, covering caps on the ends of the wheel weight rings and in the head tube, stickers with the Delft University of Technology (DUT) logo, and a paint job in the DUT corporate colors. Moreover, a removable stand is added to hold the bicycle upright statically for display.

The four bodies of the bicycle model (see section 3.1) are in this case all composed of separate mostly stiff parts themselves as listed in table 10.2 and can be seen in figure 10.4. Besides trying to make the construction rigid by using stiff components, other measures are also taken to approach the Whipple model assumptions. To make the friction in the joints almost absent, as is assumed in the model, ball bearings are used in all joints. To keep them as frictionless, wear is reduced by means of grease in the ball bearings of the front wheel and head-set. In order to approximate the model's infinitesimally small no-slip contact points, the tires are maximally inflated.

The two frames cannot be taken fully apart since they are mainly constructed by sawing and welding together several tubes in almost all mitered joints. Herein, the head tube and set are taken as a whole from a conventional donor bicycle with some parts being welded to the rear and others to the front frame. The small rear frame is made as one piece with a wheel fork, a custom-made axle, and the inner

Figure 10.3: The RWSB experimental prototype construction in overview. The smaller rear wheel and larger front wheel (including inertia-increasing weight rings) are black, the rear frame white, the front frame cyan, and the added weights are black. Note that a detachable stand is added to keep the prototype statically upright for display.

tube of the head-set. The non-rotating rear axle passes through two Ø8 mm holes, and on its ends two separate cylindrical (counter-)weights are screwed on to the rear frame axle. The larger front frame consists of three parts; a large part with diagonal tube, head-set outer tube and wheel fork, and two

Table 10.2: Parts of constructed experimental prototype RWSB.

Part	**Material**	**Mass** [kg]	**Notes**
Rear wheel			
Rim	Plastic	0.0967	Black wheelchair rim. Includes ball bearings
Tire	Rubber	0.176	Black pneumatic wheelchair tire. C-179-1 (6” $\times$ $1\frac{1}{4}$) 2.5 bar. Includes outer tire and inner tire with valve
Rear frame			
Frame	Steel EN-S235JR(G2)	0.776	White (RAL 9016) welded tubes (EN-1.0305-3-S2) Ø20×2 mm. Includes Ø8 mm rear axle, nuts and rings, nylon spacers, headset bearing cone, and headset cone nut
Weight	Stainless steel EN-1.4307	2.415	$2\times$ Black (RAL 9005) round staff Ø70×40 mm with M8 hole
Front frame			
Frame	Steel EN-S235JR(G2)	4.660	Cyan (RAL 5015) welded tubes (EN-1.0305-3-S2) Ø30×2 mm. Includes (wing) bolts, nuts and rings, headset bearing cups, and headset bearing balls
Weight	Stainless steel EN-1.4307	3.595	Black (RAL 9005) round staff Ø90×60 mm, $2\times$ round staff Ø10×12 mm, and $2\times$ tubes $200 \times 25 \times 2$ mm
Front wheel			
Rim	Steel	1.854	Black (RAL 9005) ‘omafiets’ wheel rim. Includes hoop, spokes, hub, axle, and ball bearings
Tire	Rubber	0.798	Black pneumatic bicycle tire. 40-635 (28” $\times\, 1\frac{1}{2}$) 5 bar. Includes outer tire and inner tire with valve
Weight	Steel EN-S235JR(G2)	2.329	$2\times$ Black (RAL 9005) bent round staff Ø10 mm, tie-wraps

(a) (b) (c)

Figure 10.4: The RWSB experimental prototype construction (a) rear view, (b) right side view, and (c) front view. The several black weights can be seen to be part of the white rear frame, the cyan front frame, and the black front wheel. Note that a detachable stand is added.

L-shaped weight holders that are bolted to the larger part at the front axle in such a way that they cannot rotate with respect to the larger part; The milled slots in the L-shaped holders are secured at the wheel axle with cap nuts, and extra bolts and nuts are added to prevent the rotation. At the front axle, the tubes are pressed flat and 8 mm width sleeves are milled in them to attach the front wheel.

Table 10.3: RWSB prototype construction parameter from measurements. Note that the weights on the rear and front frame and the front wheel are included in those respective parts, while the detachable stand is not included at all since it is removed during experimenting.

Parameter	**Symbol**	**Value**
Wheel base	w	0.991 m
Front wheel trail	c	-0.796 m
Steer axis tilt	λ_s	-0.0244 rad
Gravity	g	9.81 N/kg
Rear wheel R radius	r_R	0.0752 m
Rear wheel R mass	m_R	0.273 kg
Rear wheel R MMOI	(I_{Rxx}, I_{Ryy})	(0.000380, 0.000639) kgm^2
Rear frame B COM	(x_B, z_B)	(0.0379, -0.0947) m
Rear frame B mass	m_B	3.191 kg
Rear frame B MMOI	$\begin{bmatrix} I_{Bxx} & 0 & I_{Bxz} \\ 0 & I_{Byy} & 0 \\ I_{Bxz} & 0 & I_{Bzz} \end{bmatrix}$	$\begin{bmatrix} 0.0179 & 0 & 0.0061 \\ 0 & 0.0269 & 0 \\ 0.0061 & 0 & 0.0287 \end{bmatrix}$ kgm^2
Front frame H COM	(x_H, z_H)	(1.0798, -0.233) m
Front frame H mass	m_H	8.255 kg
Front frame H MMOI	$\begin{bmatrix} I_{Hxx} & 0 & I_{Hxz} \\ 0 & I_{Hyy} & 0 \\ I_{Hxz} & 0 & I_{Hzz} \end{bmatrix}$	$\begin{bmatrix} 0.460 & 0 & -0.375 \\ 0 & 1.404 & 0 \\ -0.375 & 0 & 1.0419 \end{bmatrix}$ kgm^2
Front wheel F radius	r_F	0.356 m
Front wheel F mass	m_F	4.980 kg
Front wheel F MMOI	(I_{Fxx}, I_{Fyy})	(0.230, 0.448) kgm^2

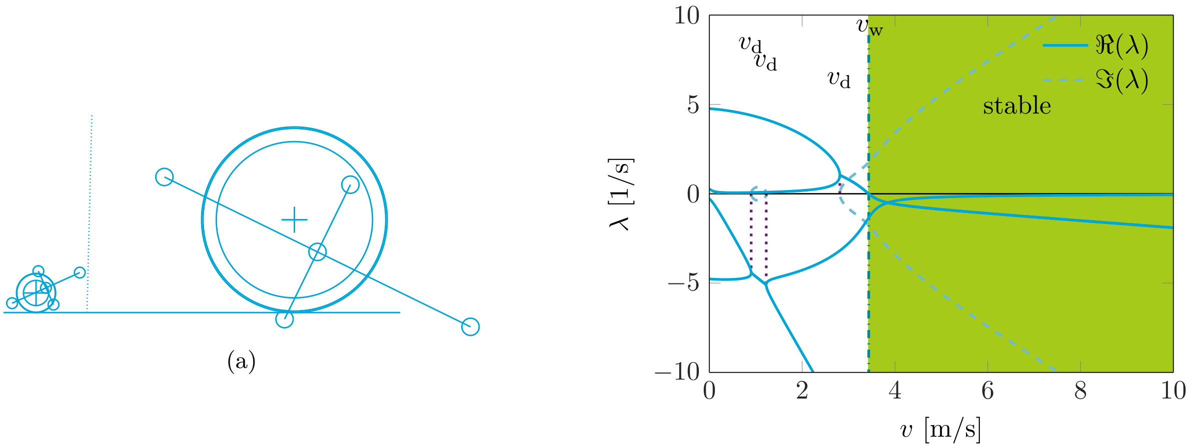

(a) (b)

Figure 10.5: RWSB prototype construction (a) visual parameter representation in the style of JBike6 (see section 4.3) where the bicycle is seen from the right and (b) the eigenvalues from linearized stability analysis as function of the forward bicycle velocity. Solid lines show the real parts of eigenvalues and the dashed line corresponds with the imaginary part of the eigenvalue. Double roots at $v_d \approx 0.90, 1.23, 2.81$ m/s. This specific bicycle shows self-stable behavior for $v > v_w (\approx 3.44)$ m/s, where all real parts of the eigenvalues are negative. Its 'maximal' stability is reached at $v \approx 3.85$ m/s.

The L-shaped holders are not welded with a mitered joint, but instead, the lower horizontal tube has two open ends to allow the usage of other-shaped and other-placed front weights. The front weight is made of a heavy cylinder with two tubes welded on it that can be shoved into the two L-shaped weight holders. The weight's longitudinal location is slightly adjustable and is set by tightening wing bolts in the holders. Of course, these weights at the rear and front frame can be replaced by different custom-made weights if desired.

The bicycle is measured to obtain the 25 parameters used to describe a bicycle model in the Whipple model (see section 3.5). Therefore, the four bodies that the Whipple model assumes (bold parts in table 10.2, and not all separate components of those parts) are measured separately to obtain their mass properties. The results of these measurements along with a visualization and the resulting eigenvalues are given in table 10.3 and figure 10.5. Note that also for the final construction, no to-be-attached sensors are included in the parameters.

The bicycle parameters from the CAD-design and the actual built prototype are very similar. Although the standard wheels and headset have unknown exact material and (internal) dimension, the constructed (welded) parts are somewhat different, and the measurements are not perfectly accurate, the construction shows a satisfactory resemblance of the design. This gives the important result that the eigenvalues are also very similar with both the design and realization having a self-stable speed region starting around $v = 3.45$ m/s and ending, if at all, far above 10 m/s.

10.2 Experimental set up and method

To check whether the built RWSB prototype is indeed self-stable and shows behavior in accordance with the Whipple model, the time response transient motions during coasting (free-running) are measured (see section 5.2). Therefore, three time-dependent variables are measured: The angular front frame lean rate, the angular front frame yaw rate, and the forward velocity. Here, the lean rate is a lateral motion about the longitudinal horizontal axis, the yaw rate is a rotational motion about the vertical axis through the front wheel contact point, and the forward velocity describes simply the longitudinal motion of the complete bicycle.

Two devices are placed on the front frame for the measurements (see figure 10.6b): an IMU with processor and 3D gyroscope, the Shimmer PROTO3 (see section 5.2), and an in-house fabricated calibrated tachometer at the wheel axle which works as a velocity dependent voltage generator (see section 5.2). The sensor placement on the front frame around the axle is better than placing on the rear frame, because this influences the lateral dynamics minimally. The Shimmer is placed behind and on the front

(a) (b) (c)

Figure 10.6: (b) The sensors attached to the RWSB prototype construction behind the front fork, with (a) left the Shimmer (used solely as gyroscope and processing unit), and (c) right the tachometer (DC-motor picking up the front wheel rotation).

fork with an in-house designed and 3D-printed holder leftwards of the front wheel (see figure 10.6a). The tachometer, on the other hand, is mounted together with the front wheel at its axle at the right side of the front wheel connected via a jack plug to the Shimmer (see figures 10.6c and 10.6b). The Shimmer is set to use a sample rate of about 100 Hz and the (high) maximum gyroscope sensitivity of 2000°/s, and the button on the Shimmer is configured to start measurement recording upon pressing. A camera is used by a second experimenter to film the experimental runs and have a visual check.

To make the experimental conditions closely match the assumptions of the Whipple model, the experiment is conducted in a sports hall with minimal disturbing external factors and a hard rubber level floor. Measurements at several different forward velocities in a wide-spectrum as possible are required to get a complete as possible image of the bicycle behavior in comparison with the model. However, the forward velocity by the tachometer is not available in real-time to the experimenter, such that a second forward velocity measurement is introduced to give an indication of the forward velocity. Therefore, a pacer is created by placing markers on the floor corresponding with a specific step length (one is visible in 10.7) to use in combination with a metronome with different gait frequency beats corresponding with different forward velocities (see section 5.2).

The actual experimental method comes down to measuring the bicycle motions while letting the bicycle coast at certain velocities. Therefore, the bicycle is brought upto a certain speed corresponding with a gait step length and step frequency and as soon the speed is reached, the bicycle is released (see figure 10.7 and videos [77]). From here, two experimental methods are distinguished:

Self-stable experiment Because the bicycle is here self-stable, it is given some time to go to a neutral straight up and straight ahead riding position. Then, in order to obtain nice harmonic decaying angular rate data, it is perturbed laterally by applying an impulse by hand at the horizontal longitudinal bar above the front wheel at around $(x_\mathrm{I}, z_\mathrm{I}) = (0.835, -0.75)$ m. The bicycle is caught and brought to a stop when the end of the sports hall is near.

Not self-stable experiment Now, the bicycle tends to diverge from a stable straight up and ahead riding position, so the measurement starts as soon as the bicycle is released; there is no time for the application of an impulse. The bicycle is caught and brought to a stop when its lean and steer angle become too large, which might happen rather quickly.

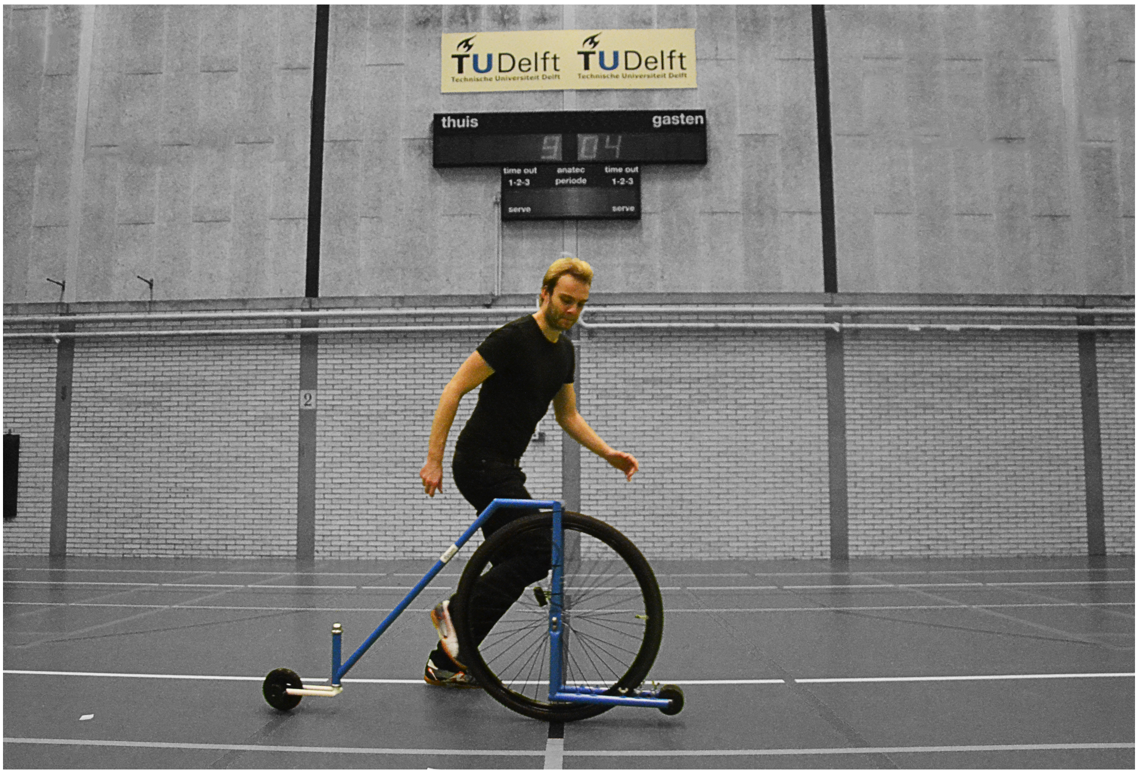

Figure 10.7: Run with the RWSB experimental prototype in the sports hall.

These cases can be predicted beforehand, because of the intended forward velocity one wants to reach in combination with the eigenvalue plot of the bicycle to see whether the bicycle is self-stable or not. However, because the intended forward velocity is not reached perfectly accurate, it might be needed, when the intended velocity is close to the stability limit, to determine the case mid-experiment by noticing if the bicycle falls over or not.

10.3 Comparing measurement and simulation

That the bicycle is self-stable can easily be seen subjectively by noticing that the bicycle stays upright by itself, even after a lateral perturbation after it is brought up to a certain speed and let free to run (see videos [77]). However, to demonstrate self-stability objectively, and also to show that the unstable behavior is as expected, measured behavior (see raw data [77]) is compared with simulated behavior (see section 5.3).

Specific bicycle configuration fit

The measured time response of the bicycle can be compared with the expected time response from the measured bicycle parameters of table 10.3. Therefore, the linearized equations of motion (3.43) of this specific bicycle are obtained by determining the matrix coefficients from the parameters,

$$\begin{aligned}\mathbf{M} &= \begin{bmatrix} 1.817638 & -0.097708 \\ -0.097708 & 0.076646 \end{bmatrix}, \quad \mathbf{C}_1 = \begin{bmatrix} 0 & 0.521760 \\ -0.2409832 & 0.331945 \end{bmatrix} \\ \mathbf{K}_0 &= \begin{bmatrix} -4.018884 & 0.043268 \\ 0.043268 & -0.001057 \end{bmatrix}, \quad \mathbf{K}_2 = \begin{bmatrix} 0 & 5.329365 \\ 0 & -0.074611 \end{bmatrix}\end{aligned} \tag{10.1}$$

These equations are then transformed to the state space representation (3.70) in order to perform the simulation (see section 3.4 and 5.1). Since the measured coordinates or the front assembly lean rate, $\dot{\phi}_\mathrm{A}$, and yaw rate, $\dot{\phi}_\mathrm{A}$, the simulated generalized coordinates need to be converted to these ignorable coordinates (see section 5.3). The front assembly lean angular rate can be calculated from (3.37) and the yaw angular rate of that assembly can be calculated with (3.39). This is implemented in a state-space model by letting it put out these coordinates by letting the output matrices be as (5.23). Putting in the RWSB prototype parameters gives the output:

$$\begin{bmatrix} \dot{\phi}_\mathrm{A} \\ \dot{\psi}_\mathrm{A} \end{bmatrix} = \begin{bmatrix} 1 & -0.024432 & 0 & 0 \\ 0 & 0.197115 & 0 & 1.008475\, v \end{bmatrix} \begin{bmatrix} \dot{\phi} \\ \dot{\delta} \\ \phi \\ \delta \end{bmatrix} \tag{10.2}$$

From the raw data, first the most interesting time span has to be selected where the movement of the bicycle is clearly free and develops smoothly as can be seen from videos and the data itself. For an unstable experimental run, $t = 0$ when the bicycle is released, and for a self-stable run, $t = 0$ when the impulse is applied. The end time of the 'clean' data is selected such that the forward velocity has approximately a linear decreasing development over the entire time span.

The actual comparison between simulation and measurements is done by fitting the simulation on the measured values (see section 5.3). First, a single constant forward velocity is 'fitted' on the filtered measured velocity signal by simply taking the velocity value at $t = 0$. This fitted forward velocity is then used in the state-space model to create the specific matrices for all forward velocity cases. Then only the initial state values have yet to be chosen to match the model with the measurements. However, the fit algorithm tends to make the chosen initial angles unrealistically large, such that the absolute steer angle is often way larger than the absolute lean angle and also larger than the linear limit of $\pi/9$. This can be seen from the videos to be not the case during the experiments, and therefore, for this fitting only the angular rate initial conditions for the simulation are set free to chose:

$$\mathbf{x}_0 = \begin{bmatrix} \dot{\phi}_0 \\ \dot{\delta}_0 \\ 0 \\ 0 \end{bmatrix} \tag{10.3}$$

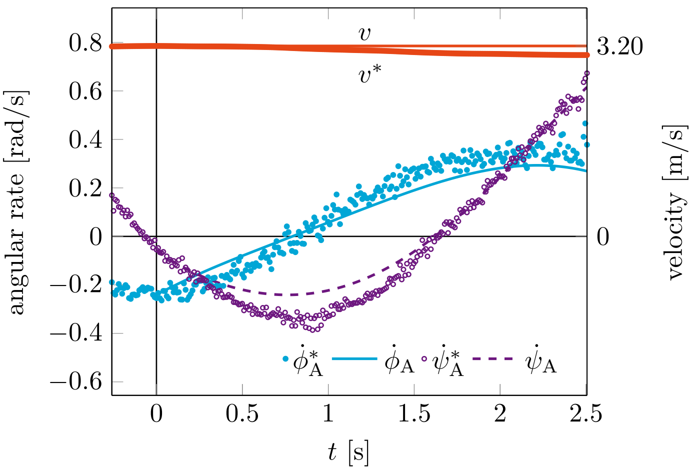

Figure 10.8: RWSB prototype construction measured and modeled unstable time response. The measured values are, filtered v^*, ϕ^*_A, and ψ^*_A, and the simulated values are, v, ϕ_A, and ψ_A which are fitted for the initial conditions.

These initial generalized coordinates can be translated to the front assembly coordinates, as is done automatically during the fitting process, with (10.2).

From all experimental runs, several are selected by video analysis that satisfy the model assumptions of constant wheels floor contact and small angles. Furthermore, they correspond with sufficiently different forward velocities to compare model and measurements over a large velocity range. The comparisons of the measured values, filtered v^*, ϕ^*_A, and ψ^*_A, with the best fit simulated values, v, ϕ_A, and ψ_A are displayed in figures 10.8 and 10.9 for respectively unstable and stable experiments.

At the low forward velocity of $v = 3.20$ m/s, the bicycle is unstable. Figure 10.8 shows that the angular angular rates could not make a full period before the experiment was stopped, and especially the yaw rate is seen to diverge from an equilibrium. However, the simulated and measured response correspond rather well with each other. Furthermore, the unstable experiment has no applied impulse, and in stead the initial angular rates are determined by the angular rates upon release.

The higher forward velocities are all in the self-stable velocity area of the bicycle and show a converging response (see figure 10.9). For these velocities, the measurements and simulations do correspond well. As can be seen, the initial condition are completely determined by the impulse that is applied at $t = 0$, because the angular rates are approximately zero beforehand.

As explained in section 5.3 the initial input ratio between the angular rates of the two measured rates as consequence of an applied impulse is predictable. This ratio is solely dependent on the bicycle parameters and the place where the impulse is applied, and not on the magnitude of the impulse. During this experiment, a rightward impulse was applied on the front frame around $(x_\mathrm{I}, z_\mathrm{I}) = (0.835, -0.75)$ m. Table 10.4 shows that the measured ratios which come from the fit algorithm are close to the calculated predicted ratios. Of course, for the unstable experiment where no impulse is applied, the ratio between the inputs cannot be predicted. Note that, in order to show that the ratio is indeed independent of the

Table 10.4: Fitted and predicted ratios between initial angular rates after application of a lateral impulse. The ratios are forward velocity independent, but the velocites are used here to refer to the different experimental runs. The impulse is applied at the front frame around $(x_\mathrm{I}, z_\mathrm{I}) = (0.835, -0.75)$ m which results in predicted ratios by the calculation as presented in section 5.3. Variations from the predicted value arise from the variation in actual impulse application location, and not from variations in forward velocity. The unstable bicycle has no applied impulse and so also no predictable input ratio.

Ratio	**3.20**	**3.93**	**4.22**	**4.44**	**5.10**	**5.80**	**6.09**	**Predicted**
$\dot{\delta}_0/\dot{\phi}_0$	–	−0.119	−0.429	−0.185	−0.313	−0.506	−0.180	−0.304
$\dot{\psi}_{\mathrm{A}0}/\dot{\phi}_{\mathrm{A}0}$	–	−0.0233	−0.0836	−0.0364	−0.0612	−0.0984	−0.0352	−0.0595

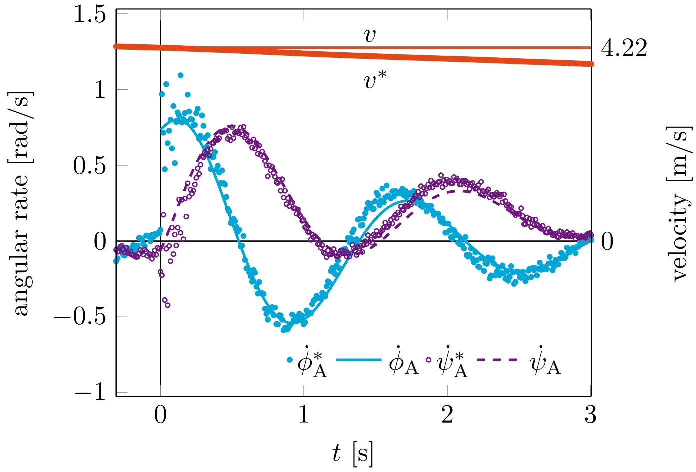

(a)

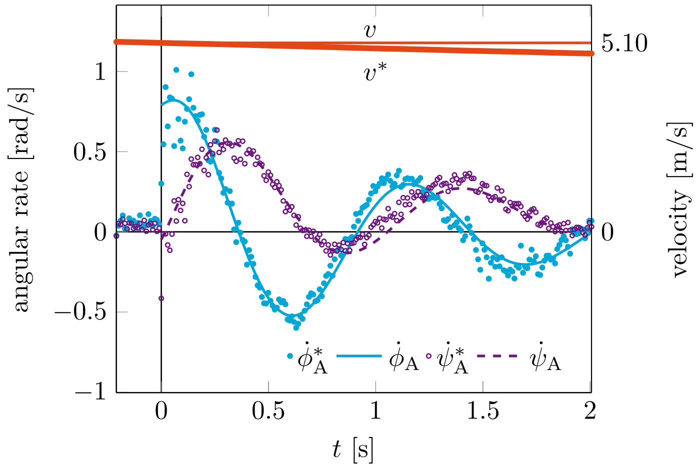

(b)

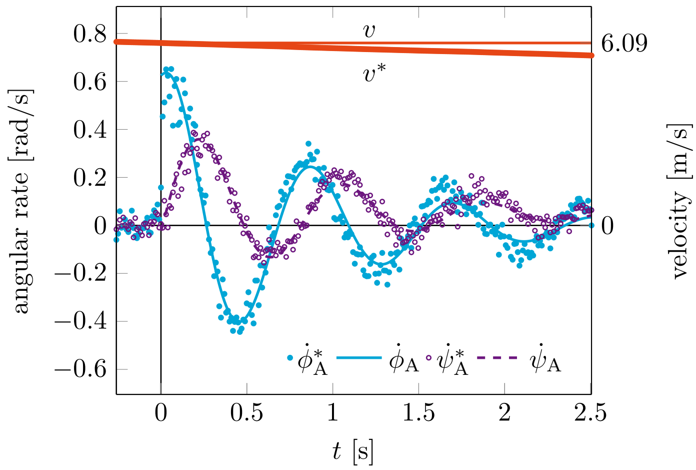

(c)

Figure 10.9: RWSB prototype construction measured and modeled stable time responses for (a) $v = 4.22$, (b) $v = 5.10$, and (c) $v = 6.09$ m/s. The measured values are, filtered v^*, $\dot\phi^*_\mathrm{A}$, and $\dot\psi^*_\mathrm{A}$, and the simulated values are, v, $\dot\phi_\mathrm{A}$, and $\dot\psi_\mathrm{A}$ which are fitted for the initial conditions.

forward velocity, some ratios for other model assumptions satisfying experimental runs are also shown.

It can be seen that the initial yaw rate is slightly negative, giving the front assembly a counterclockwise rotation. This happens because the sideward impulse to the right is applied at the front frame behind a vertical line through the front contact point, and because the COM of the front assembly that resists against the lateral displacement is ahead of the front wheel. The value of the yaw angular rate is much smaller than the lean angular rate because the impulse has a larger arm about the lean axis.

Exponential function fit

Another way of comparing the results of the measurements with the simulations is by fitting an exponential function on the measured data. The eigenvalues corresponding with the two measured signals, i.e. front lean and yaw angular rate, are then determined by fitting an harmonic exponential function

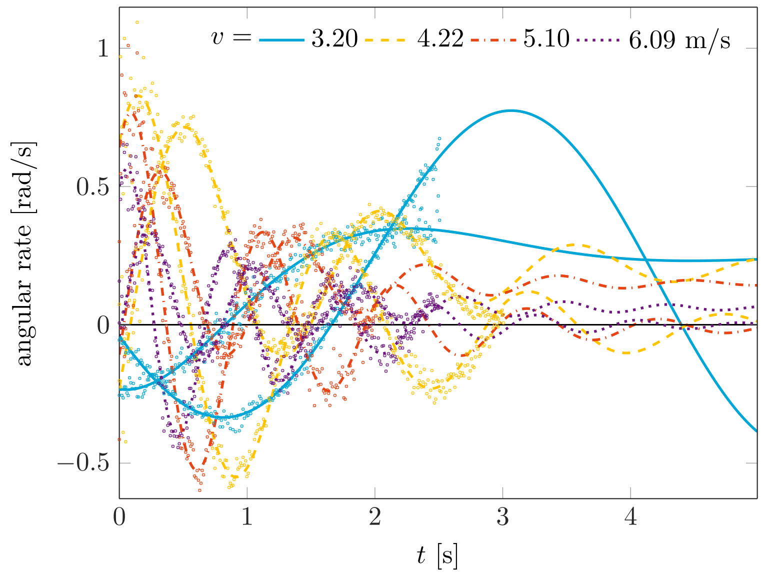

(a)

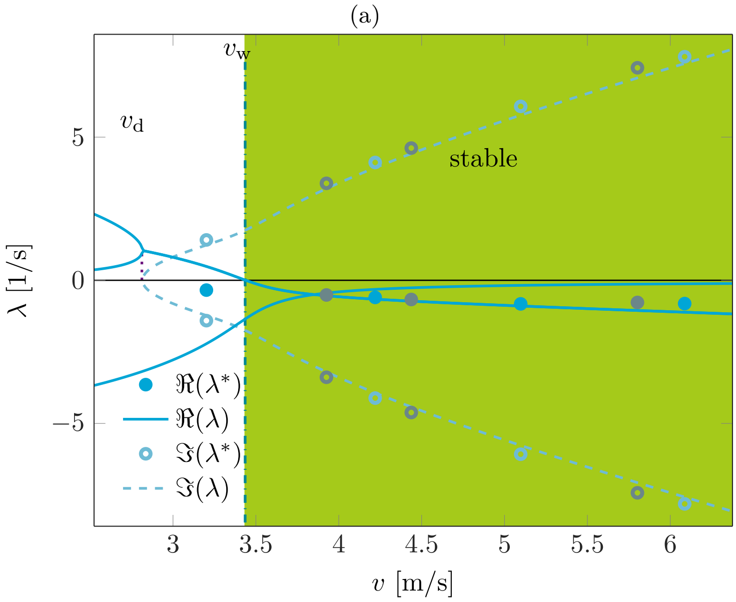

(b)

Figure 10.10: RWSB experimental prototype (a) time response fit of exponential functions on the measured front assembly lean and yaw angular rate for different forward velocities, v, and (b) the resulting fitted measured eigenvalues, λ^*, compared with the simulated eigenvalues, λ.

with a non-linear least squares algorithm (see section 5.3). This is done on the same time region as was selected for the time response model fit.

The fitting of the exponential function (with steady-state offset) on the measured front assembly lean and yaw angular rate data signals is shown in figure 10.10a. From these fits the eigenfrequencies and damping coefficients can be determined for all forward velocities. Generally, both fit signals, i.e. lean and yaw angular rate, result in a slightly different eigenfrequency and damping coefficient due to fitting artifacts, so the mean of the two frequencies and damping coefficients from the two measured signals per forward velocity is taken as the one measured fitted eigenfrequency and damping ratio for this specific forward velocity. With this eigenfrequency and damping ratio, the eigenvalue can be composed (see section 5.3). These measured fitted eigenvalue, λ^*, are displayed on the modeled eigenvalue plot in figure 10.10b.

Since the dominantly measured eigenmode is the oscillating weave mode, the eigenvalues correspond with the complex eigenvalue pair. The real part of the eigenvalues is a measure for the damping in the signal, while the imaginary part represents the damped frequency. It can then be seen from the figure that the frequency fit is pretty accurate over the complete measure velocity range, but the damping is only accurate in the mid-range velocities.

10.4 RWSB self-stability analysis discussion

Some remarks can be made about the testing of the constructed prototype RWSB. The tachometer showed some problems like mechanical noise and it did malfunction in the end due to a broken worm-drive. Moreover, it is hard to install on the bicycle; the wheel needs to be taken of to place sensor on the hub. Better would be to use a gyroscope to measure wheel rate or use magnets to measure pulses. With the extra gyroscope in stead of the separate tachometer, the two gyroscopic devices can be both placed in the longitudinal vertical 'median' midplane of the bicycle (instead of at one pin of the front fork); one device is placed at the horizontal transverse tube above the front wheel of the bicycle to measure the lean and yaw angle about two axes, and the other device is placed at the front wheel axle to register the wheel angular rate (and forward velocity). In that way, although the sensor's mass properties are assumed negligible with respect to the bicycle mass properties, the bicycle is more laterally symmetrical than with the separate tachometer.

Furthermore, the Shimmer angular rate range was now set to the highest value (2000°/s). This reduces the sensitivity. It appeared that this highest value was not reached by the angular rates by far, so that it could have been lowered to increase sensitivity. In the same regard, the sample rate could have also be different.

Comparing the measurements with the simulations did also show some interesting phenomena. The Whipple model is most accurate in the stable speed region upto a forward velocity of about $v = 6$ m/s [59] [46]. Fitting is hard in the unstable speed region, because the signal is then far from a complete oscillation cycle in a relative long time span (see figure 10.8) which makes it hard to 'predict' the harmonic wave of which the signal is part of; the time that the bicycle stays upright is simply too short compared to the time period of the weave mode. For the exponential function fit, the frequency is still quite accurate, but the 'damping' is off and corresponds with stable behavior, while the bicycle was clearly not stable during the experiment (see video).

Moreover, at higher velocities, the Whipple model starts to deviate from actual bicycle motion, due to real-life non-linear behavior like tire compliance, tire slip, and structural compliances, and as a consequence the eigenvalue from the model differs also from the measured eigenvalue [59] [46]. This becomes clear in figure 10.10b for the $v = 6.09$ m/s measurement, where the real part of the eigenvalue, i.e. the damping part, is somewhat different than the simulated value.

The inaccuracy in the forward velocity fit itself is also a cause for errors. At lower forward velocities, just below the stability speed, a small fluctuation in forward velocity results in significant changes in the dynamics, i.e. significantly changed eigenvalues (see figure 10.3b). So when the forward velocity decreases only a little during the experiment, or when the forward velocity measurement is a little inaccurate, then already the slightly inaccurately fitted velocity used in the model can result in an inaccurate simulation. For the higher velocities, a small perturbation in forward velocity does not result in severely changed dynamics, and hence fitting with an inaccurate velocity can still result in reasonable fits. Nevertheless, on confined time scales, the low forward speed experiments can also have reasonable fits. Moreover, at low speeds, the large yaw and lean angles are out of the linear domain. This makes that the nonlinear coupling between angles and forward velocity becomes noticeable, such that the forward velocity does not decrease linearly, but faster when the angles become large.

But all in all, the stability analysis for RWSBs turned out to be a success. For the first time it is shown how an RWSB can be made self-stable in theory. A Routh-Hurwitz stability analysis showed that a rear wheel steered bicycle can theoretically be made self-stable by using a specific set of parameters requirements. Interestingly, the mode shapes that such a self-stable RWSB shows do not all correspond with those of a conventional bicycle, making clear that the conventional FWSB does not have all generally present bicycle behavior. Thus, an FWSB is just as a special case of a bicycle, as an RWSB is.

The parameter requirements for stability make the bicycle look like a unicycle or single wheel, but the theoretical bicycle configuration is crucially different from those vehicles by having two non-sliding contacts and a steer pivot. For example, a unicycle needs an additional mass placed behind the wheel axle and above a certain threshold to be self-stable, while the RWSB needs the mass ahead the front wheel axle and below a certain threshold.

Self-stability on RWSBs could even be proven in practice by translating the theoretical self-stable RWSB configuration into a real constructed self-stable RWSB and testing it on stability. Interestingly, the self-stable RWSB design has a lot in common with some of the seemingly best ridable RWSB examples (see section A.32, A.53, A.55, A.65, A.75, A.83, A.85). Maybe more peculiarly is that the final design has quite a lot in common with the classic penny farthing, e.g. a large front wheel and the center of mass close to the front axle, although the penny farthing main center of mass is that of the rear frame plus rider.

Modeling made clear that the theoretical minimal RWSB could be made stable for a finite forward velocity range by placing the front frame mass ahead of the axle but above the height threshold. However, by placing the same mass below the height threshold, the bicycle becomes stable to infinite forward velocity. Even fully defining the 25 parameters of the RWSB, but keeping the front frame mass below the height threshold, keeps the RWSB stable upto infinite velocity according to the Whipple bicycle model. Thus, adding nonzero parameters does not necessarily change the stability limits drastically, as confirmed by measurements on a constructed version of the design. Herewith, the modeling, design, construction, and validation of a self-stable rear wheel steered bicycle is brought to a successful conclusion.

Conclusion

Up to now, the rear wheel steered bicycle (RWSB) was a mere hobbyist fascination. Science lacked thorough research on RWSBs, because RWSBs were simply deemed impractical due to a believed inherent instability. And even when an attempt was made to approach RWSB scientifically with models, then soon the conclusion was drawn that RWSBs are unstable, due to over-simplificated models or a too narrow design space. However, recent developments showed that stable RWSBs are possible and thus, a knowledge gap existing since the 19^{th} century was uncovered that was waiting to be filled [2]:

> "*... no successful type of rear-steering bicycle has been evolved. Experimenters might with advantage direct their energies to this comparatively untrodden domain.*"

Luckily, a rear wheel steered bicycle is just another example of a bicycle, which is essentially a symmetric vehicle with its two wheel/frame assemblies connected by a revolute joint. All bicycles, either front or rear wheel steered, can be investigated with the same well-known and documented analysis methods. However, the symmetry of a bicycle makes it hard to get a grasp on what exactly makes a bicycle front or rear wheel steered, and the definition was a mere subjective one until now.

The Whipple bicycle model allows for drafting a handy practical objective steer-side definition which assumes that a difference in steer-side, either front or rear wheel steered, is only a difference in kinematics that are determined by the location where the steer axis intersects the ground: When the steer axis intersects the ground closer to the front wheel, a bicycle is front wheel steered, and when it intersects the ground closer to the rear wheel, the bicycle is rear wheel steered. The location of masses, the headset, the driven wheel and so on, do not change the kinematics and thus also not the steer-side according to this practical definition.

Changing the steer-side changes the bicycle kinematics, but dynamically a steer-side change is not essentially different from a parameter change like, for instance, an altered mass location. Such a change alters the dynamics and may destabilize the bicycle, but can be corrected by changing another parameter. Thus, by changing the steer-side the dynamics are altered, but not drastically and the vehicle remains a bicycle with its characteristic dynamics, e.g. a counter-steer is still required to initiate a stable turn and one has to steer into a fall to recover from it.

That an RWSB is still just a bicycle makes that, just as a conventional FWSB with its specific parameter configuration can stay upright by itself, i.e. be self-stable at certain forward velocities, also an RWSB can be self-stable with an appropriate parameter configuration. An RWSB described by a reduced set of bicycle parameters turns out to be self-stable up to infinite forward velocity for specific parameter requirements: The vertical steer axis must intersect the ground ahead of the rear wheel, and the front frame center of mass must be located ahead of the front wheel axle below a front wheel inertia dependent height.

Interestingly, the eigenmodes of the self-stable RWSB are different from those of a conventional FWSB, but they are still those of a bicycle. The required front wheel inertia makes the bicycle front wheel larger than the rear wheel, but, although the final self-stable RWSB configuration and its eigenmodes look like a single wheel vehicle, its dynamics are crucially different from those of a unicycle or a separate wheel. A single wheel can never be asymptotically stable, and a unicycle cannot be modeled with the bicycle model and vice versa, due to the different support line orientation with respect to the wheels under influence of wheel yaw. This is also illustrated by the fact that a minimal RWSB configuration is self-stable for a front frame mass location with respect to the front wheel axle exactly opposite to the required front frame mass location for a self-stable unicycle.

A conversion of the theoretical reduced parameter set configuration to a fully parametrized model and even a full size constructed experimental bicycle, shows that an RWSB can indeed be self-stable, as simulated with the Whipple model and confirmed with the experimental bicycle. For the experimental RWSB, the Whipple model simulations even compare accurately with the measured behavior. And moreover, although the conversion requires some alterations in the design, like placing weights close to the rear contact point to prevent tipping over forwardly, the main self-stable minimal theoretical configuration remains recognizable. This results in a structure of the eigenvalues and eigenmodes over the complete forward speed range for the experimental RWSB which is comparable to the theoretical minimal eight parameter bicycle model.

So all in all, known bicycle theories have been applied on rear wheel steered bicycles to get a grip on their dynamics. These dynamics turned out to be 'just' bicycle dynamics, proving that an RWSB is nothing more or less than a bicycle. This encouraged the finding of the 'right breakthrough' [8] that the rear wheel steering bicycle design has waited for, for so long: A practically implementable self-stable RWSB configuration. The key to this success was a sufficiently elaborate bicycle model with appropriately chosen set of parameters representing an unconventional bicycle design. Until recently this was never done in literature, although in retrospective there were hints to how self-stable RWSB would look like, since some of the seemingly most ridable known RWSBs have the mass on the front frame shifted to the front. Nevertheless, as of yet, it is known for sure that RWSBs can be stable and obstacles for a further development towards a comfortably ridable RWSB are removed.

Recommendations

The self-stable configuration as found here is not commercially interesting, since it is not ridable. Besides the obvious issues of lacking a saddle, driving mechanism, brakes, and handlebar, it is also rather heavy and sensitive for tipping frontally. Therefore, when trying to be commercialized, it needs to be altered such that it becomes more practically usable. This is not expected to be a problem, because it was already seen that other finite forward velocity region stable configurations are possible (see section 8.4 and A.85). Adding, for example, a non-vertical steer axis as done by Van Dijk *et al.* [18] (see section A.85) opens up a new territory of the design space.

It would make sense to place the rider on the front frame and drive the front wheel, but due to the kinematic steer-side definition, this is not essential for a bicycle to be marked as rear wheel steered. What is the most comfortable remains a question. Moreover, often a steer-reversal is used on RWSBs to make sure that a clockwise handlebar turn results in a clockwise bicycle turn, but as witnessed by some ridden RWSBs lacking such a mechanism, this is not essential.

Besides these research opportunities on practical feasibility of RWSBs, this study also leaves some theoretical questions about bicycle dynamics in general. The eigenmodes of the self-stable RWSB contain motions that do not all correspond with the motions on conventional bicycles. So, some motions of the conventional FWSB are not generally present for all bicycles and an FWSB and RWSB are to a certain extent both separate cases within the bicycle design domain, just as there might be more of those cases. Thus, within the bicycle domain, stable behavior is possible in ways that were not yet discovered, leaving the question if there is not even more unknown about bicycles. In short, just as all bicycles, the RWSB remains an interesting machine full of features to be studied.

Appendix

Appendix A

RWSB literature historical examples

To delineate this list of RWSB-like examples some limits are taken into account. Main requirement for a bicycle to be included into this list is that it is interpreted by (some) people as rear wheel steered. This means that the practical technical definition as drafted in section 6.3 to distinguish the steer-side of a bicycle does not always mark the bicycles in this overview as rear wheel steered. This makes that in some cases sitting on the front frame is enough to make a bicycle rear wheel steered, even though the trail and steer axis angle might be similar to those of an FWSB. Similarly, placing the drive train on the front wheel and shifting the headset can also be considered as a shift towards rear wheel steering. However, the listed structures here are limited to fulfill the requirement for a bicycle that it has two wheels. Generally also the two frames requirement is met, except for some bicycles (having three frames and four hinges) that deserve some attention.

Several languages are used to search for the RWSB examples. To help in this search a table is drafted (table A.1) that includes free translations of bicycle jargon. The table content can be used as search words to find bicycle articles or pictures on internet, or it can help in understanding bicycle discussions in different languages.

The found examples are often presented along with the riding characteristics. These, mainly qualitative, characteristics are either taken from the builder's comments or are estimated from videos of the bicycles in action. For some bicycles exact parameters with a graphical representation and stability plot are presented. These are extensively explained in chapter 4, but can be interpreted shortly as follows.

The parameters are the 25 Whipple parameters in the symbols as defined and used in the benchmark bicycle paper by Meijaard *et al.* [22]. The steer axis tilt is thus positive counterclockwise from vertical and the trail is positive with respect to the front wheel pointing forward. Where the original reported models had sometimes separate front and rear baskets as well as a separate rider, here they are all combined in one rear and one front assembly. The graphical representation of the parameters and the stability plot are made with help of the Matlab software JBike6 [45]. In the graphical representation the forward direction (positive v) is always to the right. Moreover, the steer axis is a dotted line and the wheels are simply made of two circles where one circle depicts the circumference and the other the radius of gyration. The masses and moments of inertia are depicted by balls and circles where the middle ball is located at the center of mass of the particular part of the assembly. Larger balls and longer lines depict larger masses and larger moment of inertia respectively. For the stability plot, the eigenvalues of the specific bicycle parameter system are plotted against the bicycle forward speed. The system shows (self-)stability at the forward velocity region where the real part of all eigenvalues ($\Re(\lambda)$) are all negative. The velocities where an eigenvalue crosses the zero line are depicted by the weave and capsize speed (v_w and v_c). Moreover, speeds where double roots occur (v_d) are also depicted.

Table A.1: Bicycle jargon in different languages. Some words and terms are not literal translations, but they show how they are used (sometimes ambiguously) in discussions about bicycles. Often the english word is used in other languages as well. As such, this list should be regarded a loose guideline to aid in comprehending bicycle discussions and finding those discussions in different languages; it does not represent a dictionary.

English	**Dutch**	**French**	**German**	**Italian**	**Spanish**
bicycle, bike, velocipede	fiets, tweewieler	vélo, bicyclette, vélocipede	Fahrrad, Zweirad	bicicletta, bici	bicicleta
rear	achter	arrière	hinter	posteriore	trasera, posterior
front	voor	avant	vorder	anteriore	delantera
wheel	wiel	roue	Rad	ruota	rueda
trail, caster	naloop, naspoor	chasse	Nachlauf	avancorsa, radrizzante	avance
wheelbase	wielbasis	empattement	Radstand	passo, interasse	batalla, distancia entre ejes
rake, offset	sprong, vlucht	cintre, déport	(Vor)Biegung, Rücksprung	avanzamento	desplazamiento
fork	vork	fourche	Gabel (scheide)	forcella	horquilla, horca, tijera
handlebar(s)	stuur	guidon	Lenker(bügel, Hebel)	manubrio	manillar
headset (head tube)	balhoofd	tube (douille) de direction	Steuersatz, -kopf, -rohr	tubo (serie) sterzo	telescopio, tubo de dirección
(steer(ing)) axis, axle	(stuur)as	axe (de direction)	(Lenk)achse	asse, albero (dello sterzo)	eje (de dirección)
tilt, inclination, angle	hoek, helling	tilt, incline, angle	Winkel	angolo	ángulo
caster(castor) / rake angle	balhoofdhoek, askanteling	angle avant	Lenkwinkel	angolo d'incidenza, angolo dello sterzo	Lanzamiento, cáster, ángulo de viraje
steering	stuurinrichting, besturing, stuur	(système de) direction	Lenkung, Lenkeinrichtung	sterzo, sterzando	dirección
steered	bestuurd, gestuurd	conduiré, guidé, dirigé	gesteuerd, gelenkt	guidato	dirigido
frame	frame	cadre, frame	Rahmen	telaio	cuadro
saddle, seat	zadel, zitting	selle	Sattel, Sitz	sella	sillín, asiento
(semi-)recumbent (bicycle)	ligfiets	vélo couché	(Sessel-)LiegeFahrrad	reclinate	Bicicleta reclinada
drive(n), traction	aandrijving	drive, traction	Antrieb	motrici	drive, propulsión, tracción

A.1 186- W. F. Reynolds and Mays 'Phantom'

Another mid-steered bicycle is the Phantom of W. F. Reynolds and J. A. Mays, 10 King Street, Tower Hill, London [79] (figure A.1). Tie-rods connect the handlebar to the rear frame at the pivot in the middle, thereby creating two equal steered wheels [80]. They seem to be mounted in a crossed fashion in order to make a clockwise handlebar rotation result in a clockwise turn. The steer axis is vertical and the front and rear wheel trail are equal. Examples of a bicycle alike this one are said to date from 1865 [80] and Velorama in Nijmegen also has one in its collection dated 1871 (figure A.2), but officially the bicycle is described in English Patent No. 1216, 1869 [81] [82]:

> "–*'The wheels of the machine are constructed on the suspension principle.' This is one of the earliest instances of suspension wheels. It will be noted that the spokes are in pairs, one wire making two spokes: the ends of the wire are held between the two halves of the hub-flange, and the wire is threaded through an 'eye' screwed into the wooden rim or felloe. The hub is built up of three parts; centre barrel carrying the inner half of each flange, and the two outer halves of the two flanges: the whole is fastened together with screws, gripping the spoke ends as previously mentioned. The main subject of the invention was the principle of hinging the frame between the two wheels, which enabled the machine to be turned in a small circle; but it was extremely 'tricky' to steer. This was one of the first machines to be fitted with rubber tyres: the rubber was vulcanised to a strip of canvas, and nailed to the wooden felloe with ordinary nails about 1.5 inches apart. Note the foot-rests for use when running down hill.*
>
> *The 'Phantom' made its first appearance in a race on the top terrace at the Crystal Palace, Sydenham, London, on 27th May, 1869, its rider winning the event. Wheels 36 inch front, 32 inch back. Weight 63 lbs. Purchased in Brighton, Sussex. The earliest instance of the use of rubber tyres on a bicycle locates the date as November, 1868, and the rider one J. Hastings, who is stated to have tested the innovation over thirty miles of snow-covered roads. His tyres were flat or convex shaped strips of canvas-backed rubber, nailed on top of the usual iron rim or felloe. I have a 'boneshaker' fitted with such tyres*"

Figure A.1: Phantom Velocipede 1869. The first English velocipede with a suspension wheel and solid rubber tires. [78]

Hadland also noticed this bicycle and describes some more objective features of the bicycle [83]:

> "*A Successful patent application was filed by Reynolds & Mays of London for improvements of velocipedes and other wheeled vehicles (British patent 1,216 of april 21, 1869); French patent 85,885 of 1869). Their Phantom, a wire-wheeled cranked velocipede with a jointed frame, was produced until October of 1872. Their wheels still had a bent wooden rim with a metal tire shrunk on. These used doubled spokes, fed through staples at the rim with the ends clamped at the hub. The hub flanges were then forced apart, tensioning the spokes. For a year the Phantom was a favorite on the track. Its unthreaded spokes didn't break, but neither could they be tensioned individually to true the wheel. This, and the fact that the hinged frame of the Phantom made steering an art, gave it a unique but eventually terminal disadvantage [The Field, October 5, 1872].*"

Figure A.2: Phantom Velocipede of Velorama in Nijmegen, The Netherlands. [Photo by A.L. Schwab]

A.2 1869 McDonald 'Improved style of velocipedes'

C.E. McDonald (Amsterdam, New York) pended a patent for an RWSB in 1869 through the Scientific American Patent Agency [84]. It is an RWSB where the rear wheel rotates about it's vertical mid axle in a ring-shaped frame resulting in zero rear wheel trail and a vertical steer axis. From inspection of the picture shown in figure A.3, the bicycle was self-stable nor ridable [85]. The bicycle lay-out and the supposedly easy construction and operation are described [84]:

> "*The frame is of hollow pipe, the rear being a complete circle in which the steering wheel rotates on its axis, the driving wheel running between the parallel bars of the front portion. The axle of this wheel passes through boxes secured to the parallel bars by set screws, so it may be adjusted forward or back to suit the physique of the rider. The axle of the steering wheel runs in boxes secured to sliding bars curved to fit the inner diameter of the circular portion of the frame, thus allowing this wheel with its axle to perform an entire revolution within the frame on a horizontal plane. Its movements are controlled by means of rods attached at one end to the ends of the axle, and at the other brought together to the lower end of a lever directly under the rider's seat, the handle of which comes up in front of the rider, the fulcrum being on a cross piece between the rear portion of the parallel bars, serving not only that purpose but that of a brace. It will be seen from the figure that the guiding of the vehicle may be effected by one hand. The seat need not be so high as represented in the engraving; it may be lowered until nearly to the level of the reach, which is the horizontal line of the axles.*
>
> *The reach, which in the ordinary bicycle extends in an upward curve from the level of the rear axle to the top of the driving wheel, is easily made, while in others its forging adds greatly to the cost of the vehicle. In mounting the ordinary two-wheeled velocipede the rider must spring from the ground to a hight not easily reached by persons of obesity or of sluggish habits, and the danger of damage to both rider and vehicle is greatly enhanced by hight from the ground. If overturned, this machine cannot fall upon the rider, as the circular formation of the rear portion forbids a complete inversion. The danger of overturning this machine is still further diminished by the weight of the rider being brought nearer the center of suspension, as his seat may be brought very near the horizontal line of the axles without preventing or interfering with the action of his legs. The ease of guiding is sufficiently clear by an examination of the engraving* (figure A.3)*, where the rider is shown as using only one hand for this purpose.*"

Figure A.3: McDonald's adjustable bicycle. [84] [86]

A.3 1869 Combs 'Improved Velocipede'

In 1869 A. Combs patented the design of his 'improved velocipede' (figure A.4) [87]. The drive train is made such that the pedals only grab in the pinion during the downward motion of the pedal. In the upward motion, the pedals run free from the pinion. The force for this upward motion is provided by leaf springs. The pedals make a more linear motion as opposed to the circular motion on ordinary bicycles. Moreover, the pedals are not rigidly connected to each other. It is possible to let the left and right pedals be out of phase where one goes up and the other one goes down, or you can both press and release them at the same time. This last option would resemble more the wobbling rider motion on a horse.

To accommodate his new propulsion mechanism, Combs shifted the steering from the front wheel to the rear wheel. Connected by crossed linkages a clockwise motion of the handlebars result in a rightward turn of the bicycle. Combs does not claim to have invented this rear wheel steering, but he himself is more interested in the spring suspension of the rear wheel. To complete the picture, it should be said that braking is done by pressing the handlebars downward against the front wheel. Combs did not build this bicycle and therefore does not report on the rideablity:

> "*I do hereby declare that the following is a full, clear, and exact description thereof, which will enable others skilled in the art to make and use the same, reference being had to the accompanying drawing, forming part of this specification. This invention relates to a new manner of propelling velocipedes, and of steering the same, and of arranging elastic support. The object of the invention is to simplify the construction of the apparatus, to facilitate its operation, and to improve its appearance.*"

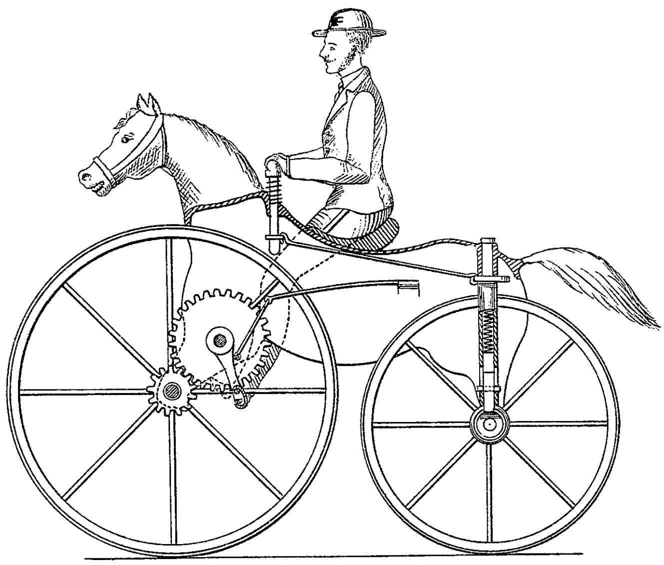

(a)

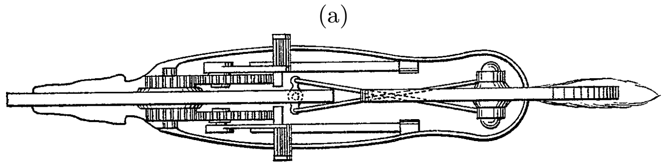

(b)

Figure A.4: Combs' Improved Velocipede resembling a horse. The driving train (a) is such that the rider can make a wobbling motion with the feet. (b) The steering mechanism has a crossed linkage. [87]

A.4 1869 Stassen 'Eagle'

In 1869 John Isack Stassen issued a patent request for a rear wheel steered bicycle [88] in order to make front wheel drive more comfortable. As can be seen in figure A.5 the connecting rods from the handlebar to the rear wheel are crossed, so when the handlebars are turned to the right, the bicycle steers to the right. Whether this bicycle was really built and how the ridability was is not known. The reason for building this RWSB and some construction and operation details are described in the patent [88]:

> "*My invention particularly refers to the construction of velocipedes known as the bicycle or two-wheeled velocipedes, but it is also applicable to velocipedes with more than two wheels. Heretofore the velocipede has been steered or guided by the fore or leading wheel being supported in a frame which is free to turn upon a pivot; by this means the fore or guiding wheel when in certain positions becomes placed or pressed against the legs of the driver, and in many cases where the curve is sharp compels him to raise his feet off the cranks.*
>
> *Now according to my Invention I steer the velocipede by the hind or rear wheel or wheels and avoid the aforesaid objection. I carry my Invention into effect in the following manner: -The front or driving wheel, the shaft of which carries the ordinary cranks, is supported and free to revolve in bearings formed in the apex of a frame, by preference somewhat of a bell-crank shape; the upright rods of this frame embrace the wheel, and are united at top by a pin and bolts. Through the pin uniting the frame a vertical rod passes carrying the steering handle; the lower end of this rod is joined to a yoke, to which rods extending to the forked frame carrying the rear wheel are attached. The forked frame is supported at top and free to move in the tail end of the bell-cranked shaped lever. By moving the steering handle motion is thus given to the hind wheel, and according to the direction in which the handle is turned so the velocipede is guided. Sometimes instead of the rods I place pulleys on the vertical steering rod and the top of the forked rod supporting the hind wheel, and pass a stiff cord or wire rope round and so steer with it instead of with the rigid rods.*"

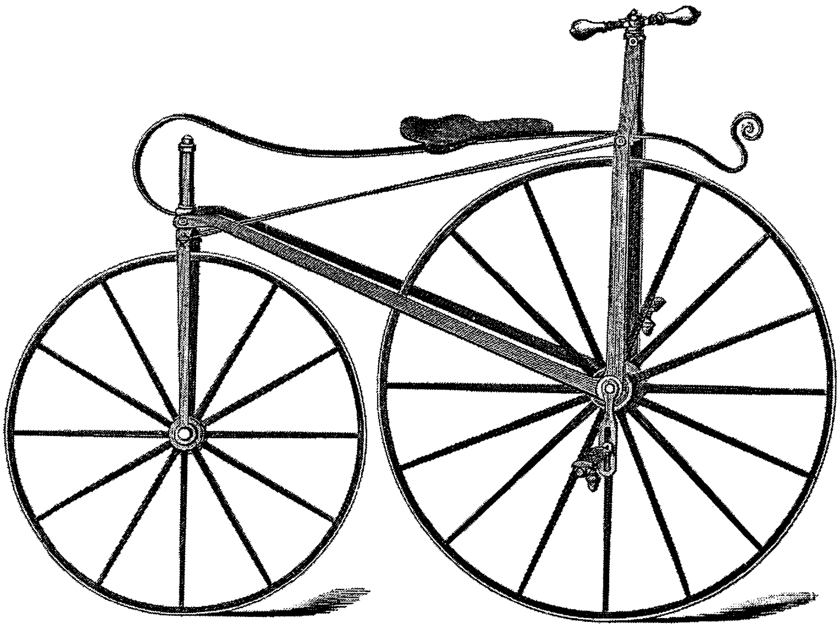

Figure A.5: Drawing of the Stassen 'Eagle' from a flyer. [89]

A.5 1869 Laubach 'Improvement in velocipedes'

The 1869 Laubach Velocipede, although technically considered mid-steered, is a shift towards rear wheel steering and therefore included here. In figure A.6 the bicycle is shown and it can be seen that the bicycle has a direct front wheel drive and the driver seat is attached to the front frame. Thus, the handlebars move with respect to the front frame with an opposite turning direction as the rear frame. A fore-aft bicycle can never be stable due to the point-symmetric about zero speed axis eigenvalue plot, but the original Laubach design is not exactly symmetrical, because the rider adds a lot of wight to one of the two frames. The design in figure A.8 is more symmetric and may be harder to stabilize.

The National Museum of American History has one in its collection that is built in 1869 in New York, Pennsylvania (figure A.7). Their description explains some of the background of the bicycle and how their specimen is constructed [90] (Edited version of section in [91]):

> "*This velocipede was donated to the Museum in 1971. It is one of the few departures from conventional velocipede construction that achieved any appreciable popularity. The design was invented by Dr. William H. Laubach, of Philadelphia and assigned U.S. Patent 86,235 on 26 January 1869* [64]. *Laubach's velocipede also came to be known as the Pearsall velocipede after Laubach sold his patent to the Pearsall brothers, who operated New York City's first and most successful velocipede school. The New York Coach-Maker's Magazine, the Coach-Makers' International Journal, and the Eclectic Medical Journal all were profuse in their praise of this "most scientific velocipede." Among the claims made for it were the statements that both wheels were always in the same arc when turning and that, due to its peculiar construction, the rider's weight kept it running in a naturally straight line. The many favorable comments made of it seem unwarranted, however, for it proved to be far less manageable than velocipedes of the usual design.*
>
> *Dr. Laubach is said to have traveled one hundred miles in five hours on one of these velocipedes, seemingly a rather unlikely feat. The Pearsalls were so impressed with the design that they reportedly formed a stock company with a capital of $300,000.00 to manufacture Laubach patent velocipedes, but it is not known to what extent they produced them, or used them in their riding school. Laubach velocipedes cost $125.00.*
>
> *The construction of this velocipede differs from the more common variety in that this one is articulated, being constructed of two separate frames, one for each wheel, pivoted together in the center. Each frame consists of four iron rods, secured together by cast bronze fittings. The fittings securing the axles are split, and are held together by two bolts. The central fittings of the two frames pivot on a vertical iron pin. A gear segment, integral with the upper pivot joint of the rear section, engages a gear segment on the steering column, the latter being mounted in the forward frame section. Turning the wood-grip handlebars causes both wheels to swing, so that both assist in steering, yet the rear wheel appears to be doing the greater portion of the work because the seat remains in the same plane with the front wheel. The 12-spoke wheels are both 36 1/2 inches in diameter, and carry a 3/4-inch iron tire. The pedal cranks are in the conventional position on the front wheel, and carry 3-sided bronze pedals that can be fitted in either of two holes in the cranks, giving a throw*

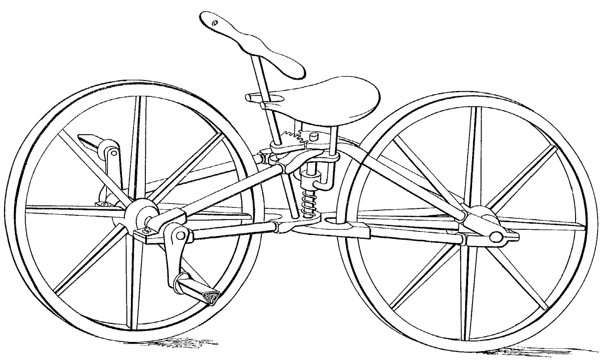

Figure A.6: The Laubach Velocicpede from 1869 in a patent drawing. [64]

Figure A.7: Laubach Velocipede picture from a museum archive [90]. It has 927 mm wheels, a trail of about 508 mm and the seat attached to the front frame.

> *of either 5 1/2 or 6 1/2 inches. The wooden seat is old, but may not be original, for it does not agree with three contemporary illustrations of the cycle. Tack holes on the underside indicate that the seat was once covered. The seat support rests on a coil spring around the central pivot pin, allowing the seat to move freely up and down. Two of the three existing drawings of this velocipede show some type of footrest beneath the rider, just in front of the pivot joint, but there is no evidence that this machine was ever fitted with such rests. Neither is there evidence of any finish on this velocipede, yet in view of the existing finishes on other velocipedes, it does not seem unlikely that this one, too, was once brightly painted and striped.*"

A variation of the Laubach Velocipede is displayed in figure A.8. It seems that the seat is attached in such a manner that it serves as a spring (and damper) that affects the movement of the joint between the frames. Static steering can only be done by bending the bicycle with your whole body. It is not clear directly if dynamically a lean-steer coupling is present.

Figure A.8: 1869 Boneshaker Velocipede from Canada Science & Technology Museum collection. [92]

A.6 1882 Crane 'Bicycle'

Moses G. Crane patented this 'Improvement in Bicycles' in 1882 [93]. The bicycle positions the rider on the front frame and has a vertical steer axis running through the rear wheel. The rear wheel fork is connected with a crossed linkage to the handlebar in front of the rider. A clockwise handlebar turn thus results in a clockwise corner. Moreover, the front wheel is driven by a mechanism where the pedals are moved up and down without a rotary movement. The chain on the crank arm is only there to be able to shift the location of engagement of the drive strap, such that the leverage arm can be varied by rotating the foot platforms about their axle. Crane describes his bicycle as follows [93]:

> "*In this my improved bicycle the rider's seat is supported at the rear of the largest or front wheel and between it and the smaller or rear wheel, which has its axle in a fork pivoted in a bearing at the rear end of the backbone, the said rear wheel being made available as the steering-wheel, and being connected by a suitable chain or cord, or link, with the steering-handle located in front of the rider's seat. The main or front wheel, having the bearings for its axle fixed to the backbone near its front end, is driven by pawl-and-ratchet or friction-clutch mechanism each side of it, the pawl-carriers being operated by levers having foot-pieces, the point of connection of the straps for moving the pawl-carriers with the said levers being quickly adjustable by means of the rider's feet on the said levers, whereby the leverage to be gained by the use of the levers may be increased or decreased at will, according to the condition of the road being traveled.*"

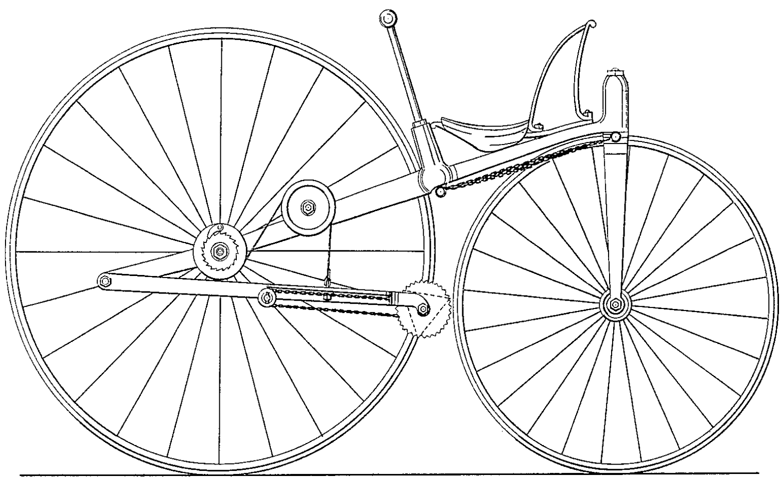

(a)

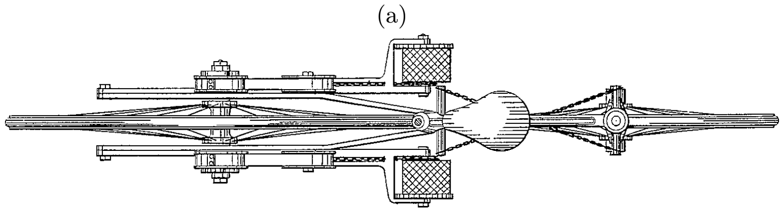

(b)

Figure A.9: Crane's Improved in Bicycles seen (a) from the left and (b)from above. Note that the steering mechanism has a crossed linkage. [93]

A.7 1883 McCall 'Bicycle'

Robert S. McCall and Joseph W. McCall invented a 'new and improved Bicycle' and patented it in 1883 [94]. The bicycle has wires running from the handlebar, through the front frame, to the rear fork at the headset, in order to provide steering of the rear wheel. It is not clear whethet a clockwise steer results in clockwise or in counterclockwise bicycle cornering, but this could be easily implemented. Apparently, it is supposed to be a very manageable bicycle [94]:

> "*The object of our invention is to provide a new and improved bicycle, which is so constructed that the center of gravity is very low, and the vehicle will not be apt to tilt. It can be mounted easily, and the rider is not liable to be thrown over the front wheel when the same strikes against obstructions.*
>
> *The invention consists in a bicycle constructed with a reach having a depression for the seat between the front and rear wheels, and with springs secured to the pivot of the fork in which the rear wheel is journaled, for the purpose of holding the rear or steering wheel in line with the front or driving wheel. The fork is turned by means of wires or cords secured to the pivot of the same, and to a vertical steering-shaft in front of the seat, which wires or cords pass through a longitudinal recess in the bottom of the reach.*"

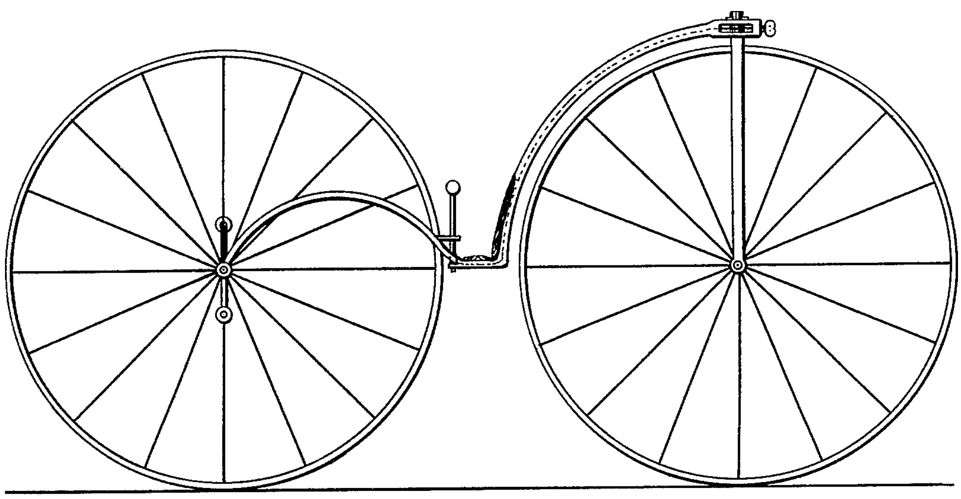

Figure A.10: The bicycle of Robert and Joseph McCall from 1883. [94]

A.8 1883 De Lancy Kennedy 'Bicycle'

De Lancy Kennedy invented a bicycle in 1883 [95]. His design shows that a bicycle does not necessarily uses the feet to propel and hands to steer, while it incorporates steering of the rear wheel. The steer axis of the bicycle is nearly vertical and goes through the rear axle. He uses rear wheel steering to allow for interchanging the roles of the hands and feet; The hands do now deliver the propelling force, while the feet steer the bicycle. Supposedly, then a greater speed with the same or less effort can be achieved than on a more conventional design [95]:

> "*In the use of the ordinary foot-propelled bicycle it is obvious that only about one-third of the stroke of the crank is effective, the remaining portion of the stroke being an inoperative return movement. This difficulty cannot be avoided in those machines which are propelled by foot. It is also apparent that in order that the rider may conveniently work the cranks the seat must be placed nearly over the center of the main wheel, which throws the center of gravity so far forward as to render the machine dangerous on downgrades or rough roads, or if any obstruction is met with by the wheel. My invention obviates these defects of the ordinary bicycle by dispensing with foot-propelling mechanism and substituting hand-propelling devices therefor, whereby the entire revolution of the crank is made effective, the feet of the rider being only used in steering the machine, and resting upon supports which have substantially the same function as the common stirrup attached to a riding-saddle. The seat may therefore be placed sufficiently far in the rear of the center of the machine to afford a secure seat for the rider, who can maintain his equilibrium on downgrades or rough roads, and cannot be thrown forward from the machine should the main wheel strike an obstructing object. It will be understood that the fork of the main wheel is not vertically pivoted, this wheel not being used for steering, but that the steering is done by means of the rear or small wheel, whose fork is pivoted, and to which proper connection is made from the foot steering devices.*"

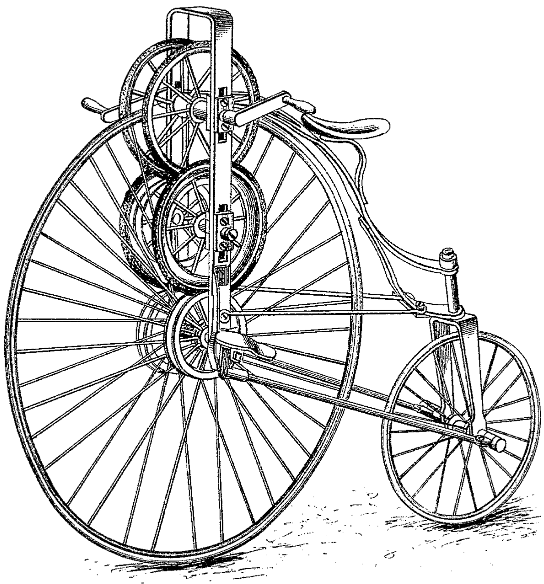

(a)

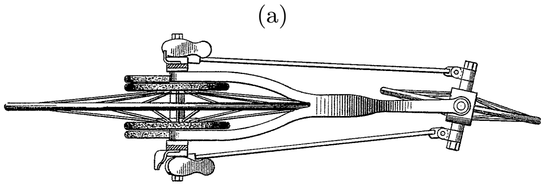

(b)

Figure A.11: The bicycle of De Lancy Kennedy seen (a) from a left perspective, and (b) from a top section (plan) view. [95]

A.9 1884 Hawkins ‘Adjustable Safety’

The ‘Adjustable Safety’ made by mr. J. Hawkins in 1884 is a ‘double-steering’ bicycle [2]. Figure A.12 shows that the bicycle is made of three ’frames’; two forks and one saddle frame. The forks are connected by a rod and thereby both wheels can rotate with respect to the saddle frame by rotating the front fork handlebar. The steering mechanism is implemented such that a clockwise handlebar turn results in a counterclockwise rear wheel turn with respect to the saddle frame in order to make corners. Note furthermore that the front wheel is the driven wheel by implementation of a chain drive.

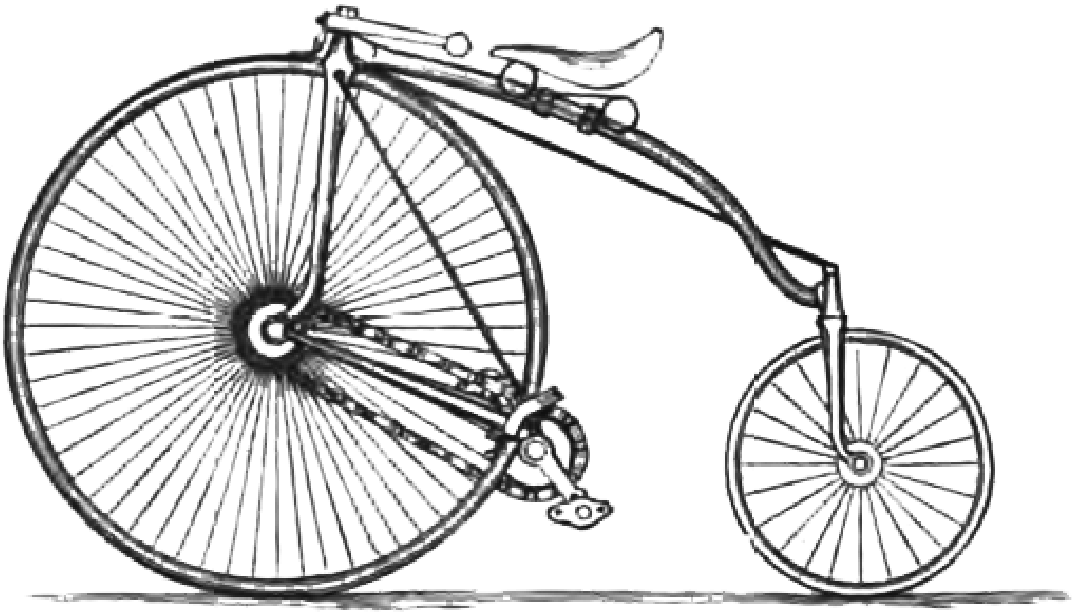

Figure A.12: The 1884 ‘Adjustable Safety’ of Hawkins is a two wheel steered bicycle. [2]

A.10 188- Leddell 'Bicycle'

Charles S. Leddell presented two versions of a 'useful improvement' in bicycles in 1884 [96] and 1885 [97]. Opposed to what is often done on classic penny farthing bicycles, Leddell makes the smaller wheel the steered wheel. The steer axis runs through or close to the axle of the small wheel. However, he has not necessarily designed the bicycle with rear wheel steering, because he suggests that the bicycle can be ridden in either direction without mentioning stability [96]:

> "*If it be desired to operate the machine with the steering-wheel behind, a saddle might be mounted as shown by dotted lines in Fig. 1* (figure A.13a)."

Also on the 1885 version he included this feature of a reversible saddle, but now also with a shiftable dust shield [97]:

> "*To shift the dust shield or guard, it is only necessary to raise the forward end to disengage the links from the heads, and then move the shield ahead and hook the links upon the studs, which are on the clamps. The saddle may then be reversed in position, as shown by dotted lines in Fig. 1* (figure A.13b)."

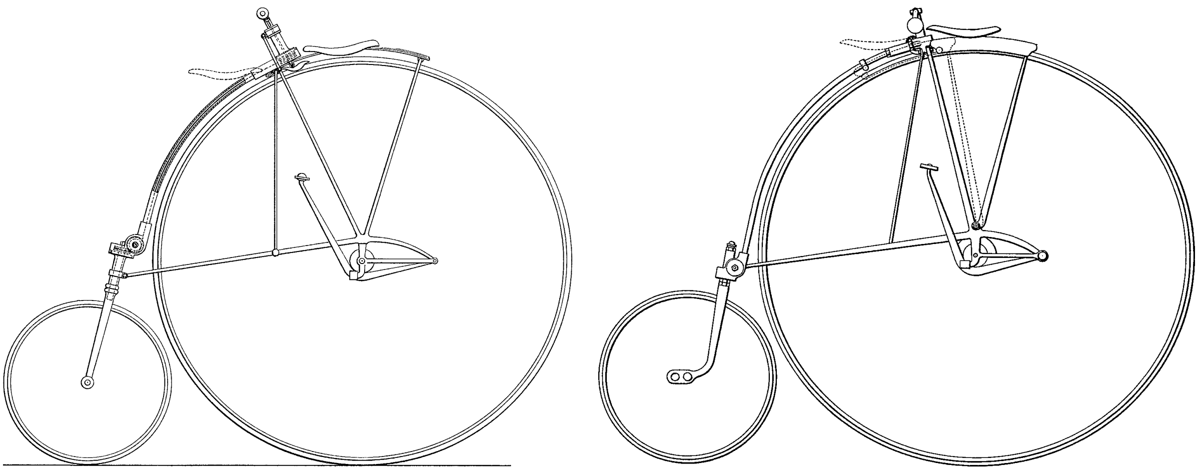

(a) (b)

Figure A.13: Two patented bicycle designs of Leddell from (a) 1884 [96] and (b) 1885 [97].

A.11 1887 Hillman *et al.* 'Premier Tandem Safety'

This Safety Tandem made by Hillman, Herbert, and Cooper in 1887 is a 'double-steering' tandem bicycle [2]. The bicycle is made of three parts with one rider placed on the front fork and one rider on the middle frame while the rear fork is simple. Without the front rider, the bicycle looks very symmetric in the longitudinal direction. It resembled a rather conventional bicycle design with this difference that it incorporated front wheel drive and a steering rear wheel. Both riders drive the front wheel by means of a chain drive. Furthermore, by use of a connecting rod, both wheels turn with respect to the middle frame during steering although in an opposite direction to make cornering possible. It seems that the rear rider on the middle frame was the one steering the bicycle by the handlebar and the front rider turned along with the front wheel. There is even a small wheel placed in front to prevent tipping over frontally under the front rider's weight.

Figure A.14: The 1887 'Premier Tandem Safety' of Hillman *et al.*[2]

A.12 1889 S. D. Reynolds ‘Bicycle’

Stephen D. Reynolds designed his ‘Bicycle’ in 1889 in order to improve bicycles [98]. The bicycle has a ‘front drive-wheel’ and a ‘rear guide wheel’ connected by a large hollow tube front frame and a smaller rear fork.

Gears provide two different transmission ratios between the pedals and the driven wheel which can be set by moving the upper gears up and down manually. Next to the transmission, a free-run mechanism is included that connects the pedals and the driving wheel only in one turning direction due to a system of pawls and ratchet teeth between horizontally adjacent gears. Lifting of the upper gears can be used to make the free-running even better, which may come in handy for example during hill descending. Furthermore, a braking machanism is placed at the front wheel with a shaft that runs through the vertical part of the handlebar. The steer joint is placed vertically above the ‘rear-steering wheel’ and this bicycle is thus naive and can be considered a rear wheel steered bicycle:

> “*. . . the guide-wheel is arranged in rear of the machine, and may be manipulated by the hands of the operator while grasping the handle portions of the cross-bar.*”

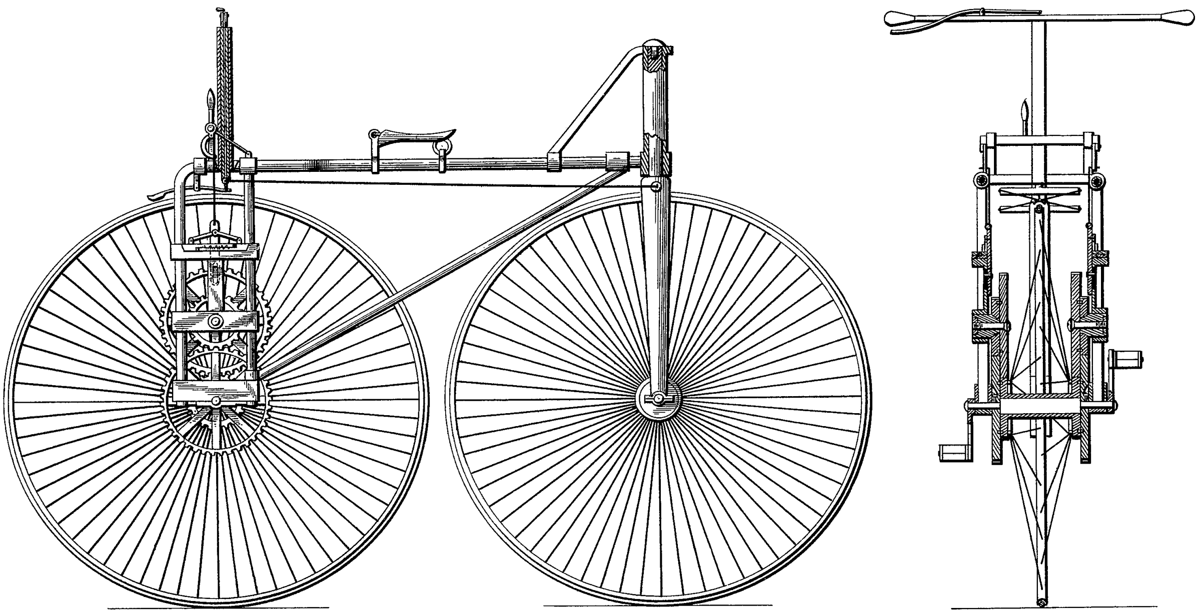

(a) (b)

Figure A.15: The 1889 bicycle of S. D. Reynolds from (a) a side view with part in section and part broken away, and (b) a section view through the front wheel. [98]

A.13 1891 Stroud 'Velocipede'

In 1891 Edward Mansfield Stroud patented his 'improvements in frame, steering device, and device for taking up the slack in the driving-chain of safety bicycles', 'Velocipede' [99]. His objective was to make the bicycle as simple and light as possible, which he tries to accomplish by using the main frame both as 'backbone' and as steering-head as can be seen in figure A.16. With the steering wheel at the rear, Stroud hopes to have some advantages with respect to the ordinary (Safety) bicycle design:

> "*The object of this invention is ... to overcome sensitiveness in steering by having the steering centers so arranged in their relation to the steering-wheel that the combined weight of the rider and the machine upon the lower bearing of the steering-shaft tends to keep both wheels pointed upon the same line, so that the forward course of the bicycle cannot be altered except by a voluntary movement of the handles; to cause the back wheel, which is the steering-wheel, to caster in such a manner as to maintain a straightforward course except when either handle is pressed downward on the side to which the rider desires to go; ... to lessen side sliding or skidding while rapidly turning a corner by having the rear wheel course in the direction which, in a machine having it fixed, it would otherwise skid; ... to have the driving-gear attached to the front wheel, making it pull the rest of the machine after it instead of pushing it, as in the ordinary Safety bicycle.*"

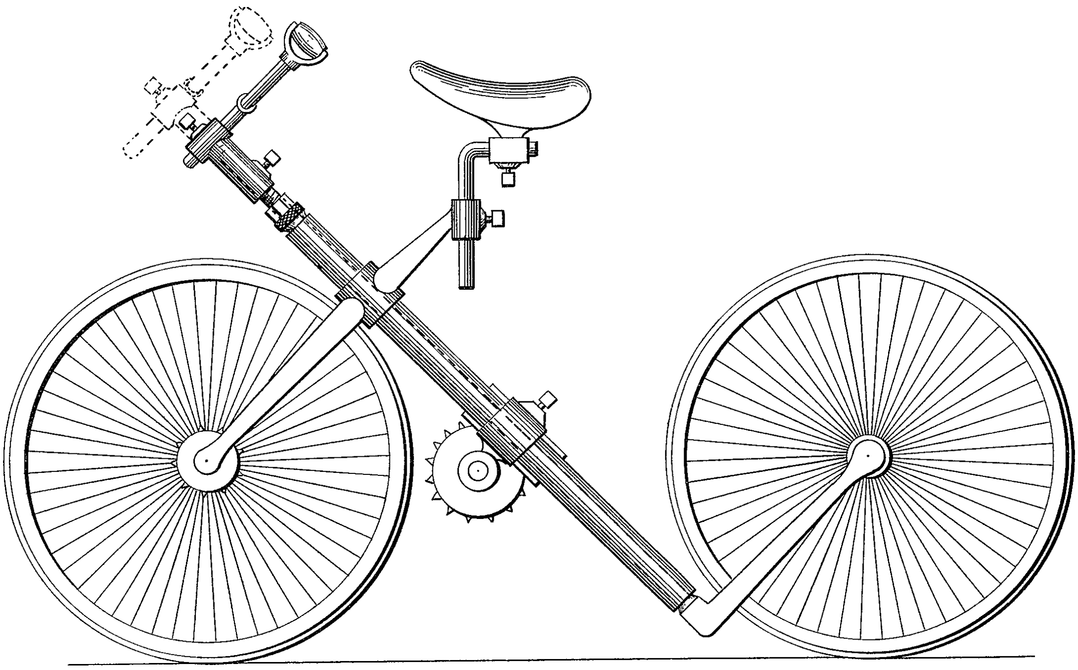

Figure A.16: The 1891 velocipede of Stroud with steering head as main frame, seen from the left. [99]

A.14 189- Valère et Cie 'Unidentified Bicycle'

In the National Technical Museum in Prague an example of an unortodox bicycle from 1893/94 (figure A.17) can be found. It is driven by pedaling with your feet as well as pushing and pulling levers with your hands. Steering is done by rotating the lever mechanism as a whole. This frontally placed mechanism is connected to the headset at the rear with a crossed linkage. Rotating the two levers to the right results in a corner to the right and the other way around. A small chain transmission is included between the crank and front wheel to provide a comfortable pedal height and transmission ratio. Furthermore, the steer axis intersects the ground behind the rear wheel. From the description of the bicycle it turns out that actually little is known about the bicycle [100]:

> "*Unidentified bicycle, mid-1890s (?)*
> *In 1893 and 1894, Valère et Cie in Paris designed two types of bicycles with a conventional frame, whose rear wheel was driven by the rider with his feet and also with his hands through levers. The design, where the rider operates the front wheel with all his limbs and steers the back wheel, is so complicated that it is unique. There has been no success to date in finding a similar machine anywhere else, nor has any mention of it been discovered in the literature.*
> *producer unknown, France (?)*"

(a) (b)

Figure A.17: French bicycle seen from the right side in the National Technical Museum in Prague, Czech Republic. (a) Overview from the rear right side and (b) some more detail from the front right side. [Photos by A.L. Schwab]

A.15 1893 Libbey 'Bicycle'

Hosea W. Libbey patented his 'new and useful Improvements in Biycles' in 1893 [101]. His main objective was to implement steam power on a bicycle, and apparently he found steering of the rear wheel to be the best way of implementing this (see figure A.18). The steer axis runs vertical through the center of the rear wheel and the steering is controlled by means of a two armed lever attached to the top of the rear fork. In much the same way as steering with a rudder on a small boat, this bicycle is steered. Moreover, Libbey was probably aware of some stability difficulties since he prefers two tires at the rear 'so that the vehicle will have three resting points'. However, as said, his main focus lies on the steam engine implementation:

> "*The invention consists of a front wheel and a rear steering wheel, preferably having a double tread, connected together by suitable frame work to which frame is secured a casing divided so as to form a water reservoir and a boiler, to the sides of which are secured steam cylinders the piston rods of which are connected by pitmen to the cranks on the axle of the front wheel ...*"

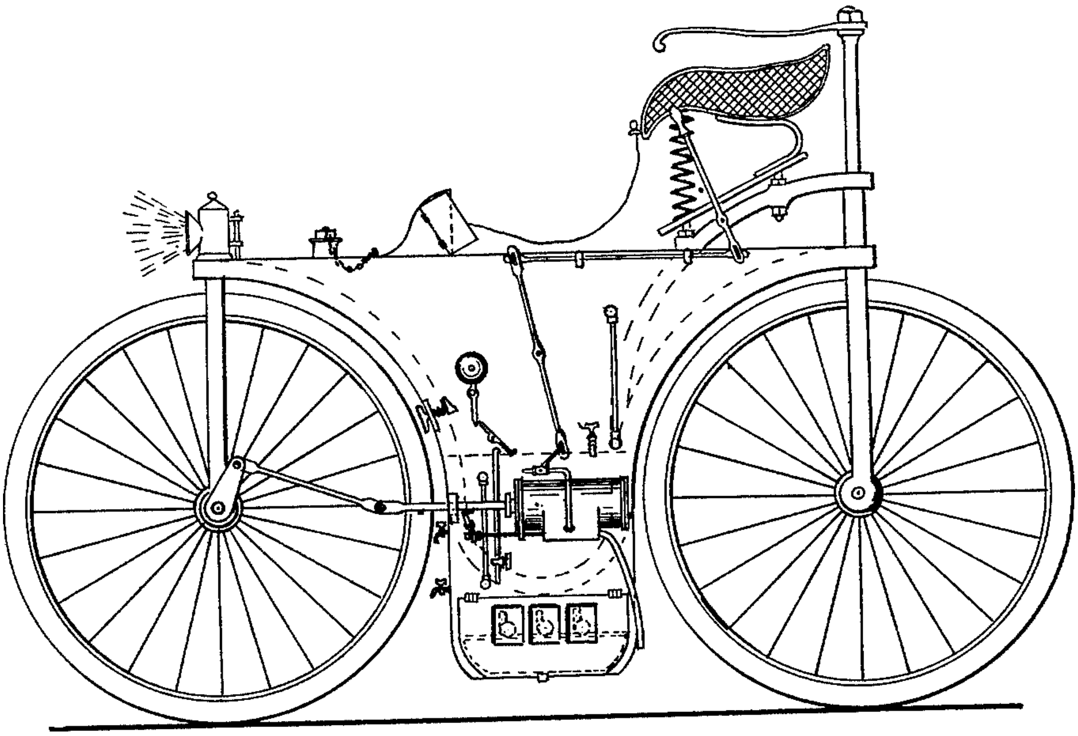

Figure A.18: Left side view of the 1893 bicycle of Libbey. [101]

A.16 1894 Fenner 'Rear Steerer Front Driver'

Mr. Fenner of the Rear Steer (R. S.) Company designed this bicycle in 1894 [102]. Presumably a direct drive of the front wheel with a geared hub is the most advantageous way of powering a bicycle. However, with the rider on the rear frame and the feet on the front frame, pedaling becomes inefficient due to the steering between the frames. Therefore, Fenner designed this bicycle where the rider sits on the same front frame onto which also the driven wheel is attached. The steer hinge is located vertically in the middle of the bicycle and the handlebar is connected by a 'tubular steering rod' to the rear frame (figure A.19).

The 0.76 m diameter front driving wheel is geared by a 'narrow-tread Hall central bevel gear' to feel like a 1.5 m diameter wheel. The rear wheel is 0.6 m in diameter and both wheels have pneumatic tyres. Moreover, all hinges have ball bearings while the saddle is from Brooks and the pedals from Bown and all costed only £25.-.

Reportedly, the bicycle is well ridable, as witnessed by some customer reviews. The catalogue of the company itself does even claim that everyone can cycle on this bicycle:

> "*...the steering of the Rear-steerer feels more like the R.D.* (Rear Drive) *safety than the F.D.* (Front Drive)*, but is dissimilar to either. The machine, nevertheless, is ridden by everbody at the first attempt.*"

Figure A.19: Right side view of the 1894 Fenner Rear Steerer Front Driver. [103]

A.17 1895 Krieger 'Bicyclette'

The Bicyclette Krieger (figure A.20) from 1895 is an example of an unconventional bicycle design. It's near vertical steer axis intersects the ground slightly in front of the rear wheel contact point. A German text describes the bicycle and why rear wheel steering can be an advantage [104] [translation by P.H. de Jong]:

> "*Wie Fig. 4 ersehen lässt, zeichnet sich diese Maschine durch Einfachheit aus. Das vordere Rad dient als Triebrad, das Hinterrad zur Lenkung. Eine Kette besitzt das Bicyclette nicht; sie ist durch eine wechselbare Uebersetzungsvorrichtung ersetzt. Das Gewicht des Fahrers wirkt gleichmässig auf die ganze Maschine im Gegensatz zu dem gewöhnlichen Niederrade, dessen Hinterrad alles Gewicht zu tragen hat. Der Sattel ruht auf einer kräftigen, elastischen Feder, wodurch das Stossen auf schlechten Wegen verschwindet. (Radfahr-Chronik, 1895 S. 497.)*
>
> *Der Grund, warum sich die Vordertreiber nicht einführten, war der, dass man jeden Tritt auf das Pedal mit den Armen pariren musste, was sich besonders beim Bergauffahren unangenehm fühlbar machte. Diesem Uebelstande abzuhelfen, baut die Firma B. S. Roberts und Co. in Birmingham einen Front Driver, der mit dem Hinterrade gesteuert wird. Um dies zu ermöglichen; laufen von der Lenkung zur Gabel des Hinterrades zwei dünne Stangen, ähnlich wie bei den neueren Tandems solche nach vorne gehen. (Radfahr-Chronik, 1895 S. 1153.)*"

> "*As can be seen in Fig. 4* (figure A.20)*, this machine is characterized by simplicity. The front wheel is used as a driving wheel, the rear wheel for steering. The Bicyclette has no chain; it is replaced by an exchangeable transmission mechanism. The driver's weight is equally distributed over the whole machine, as opposed to the common safety bicycle whose rear wheel has to bear all the weight. The saddle rests on a hefty, elastic spring, through which the shocking on bad roads disappear. [Radfahr-Chronik, 1895 S. 497.]*
>
> *The reason why front-drive was not introduced, was that you had to parry every step on the pedal with the arms, which is particularly unpleasant to the feeling when driving uphill. To fix this inconvenience, the company B.S. Roberts and Co. in Birmingham build a Front Driver, which is steered with the rear wheel. To make this possible; two thin rods run from the steer to the fork of the rear wheel, similar to the newer tandems where such rods run forwards. [Radfahr-Chronik, 1895 S. 1153.]*"

Figure A.20: 1895 Bicyclette Krieger seen from the left. [104]

A.18 1896 Sharp 'Front-Driving Rear-Steering Geared Bicycle'

Sharp presents a simple rear steering design in his 1896 book [2]. It is brought up as possible implementation of a gear in the front hub in order to make the driving easier (Sharp specifically opts to incorporate a 'Crypto' or 'equivalent' gear). The bicycle as shown in figure A.21 is ridden forwards to the left in the figure. The rider sits on the saddle on the front frame and he can move the rear fork handlebar whose bars are placed beside the rider.

It is pretty much a standard bicycle ridden backwards with the difference that the steer axis intersects the ground in front of the rear wheel contact point. On a conventional bicycle the steer axis intersects the ground in front of the front wheel (positive trail) and thus if such a bicycle is reversed the steer axis would intersect the ground behind the rear wheel. Note that the wheel base looks also shorter than on a conventional bicycle, but this may be deception. The headset is brought closer to the saddle and the fork offset is larger (fork more curved) in order to facilitate that the steer axis intersects the ground in front of the rear wheel. Although this makes the main frame shorter, it does not necessarily shorten the wheelbase.

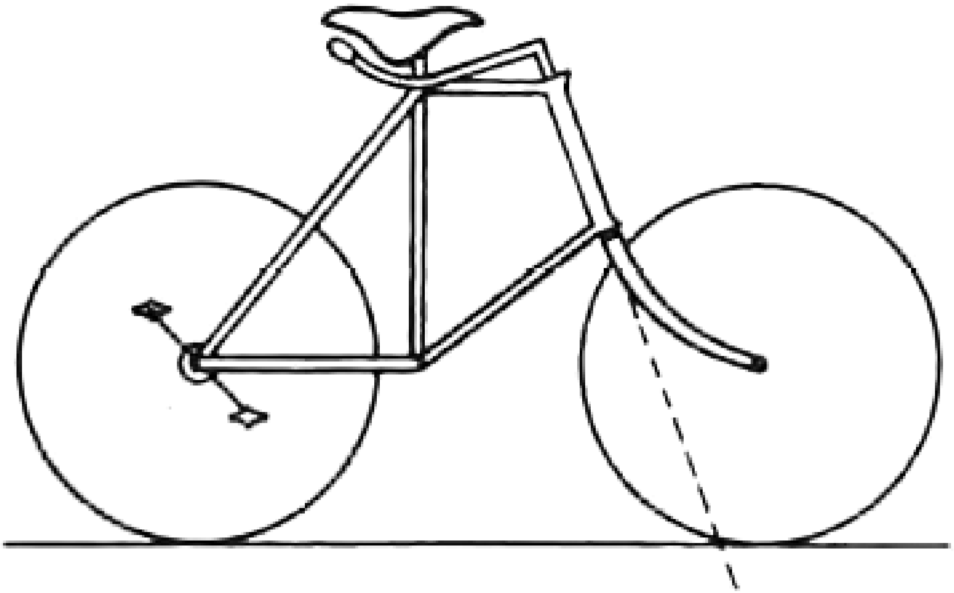

Figure A.21: Sharp's 1896 possible front-driving rear-steering geared bicycle with forwards riding direction to the left in the drawing. [2]

A.19 1899 Stephens 'Steering Mechanism for Cycles'

Anson P. Stephens designed a bicycle steering mechanism in 1897 and patented it in 1899 [105]. His bicycle (figure A.22) makes use of sprockets and chains to transmit the steering motion of the handlebars to the rear wheel. Hereby, the mechanism is such that a clockwise handlebar motion results in a rightward turn. He implements two equal sprockets which means that there is no transmission ratio between the handlebars angle and the rear wheel angle. The linkage bars are flattened in the middle so that they do not rub on each other and the saddle can be placed around and over them.

He is unaware or neglects any lean and steer coupling mechanisms and assumes that a bicycle with rear wheel steering is easy to ride due to a self-aligning effect on the rear wheel similar to that of a caster wheel [105]:

> "*I find it advantageous to mount the rear wheel so that it may trail and follow behind the front and driving wheel with little or no attention from the rider, and by connecting the rear steering-wheel to the handle-bar in front the rider is enabled to steer with great ease and reliability, especially as the movement given to the rear wheel in steering acts in a manner similar to the rudder of a vessel and tends to carry the rear of the cycle to the outer side of the curve that is described, and in so doing the weight of the rider is thrown inward and less effort is required to maintain the proper balance while the cycle is passing around a curve.*
>
> *In this improvement the weight of the rider is nearly uniformly taken by the front and rear wheels, because the saddle can be moved along upon the perch T to the desired position, and in consequence of the driving mechanism being applied to the axle of the front wheel the movements of the feet in giving motion to such front wheel are entirely in front of the rear wheel, so that the latter can be turned in steering without the feet coming into contact therewith even when the rear steering-wheel is closely adjacent to the front driving-wheel, and for this reason the cycle can be made very compact and lighter and stronger than cycles of this general class as heretofore constructed.*"

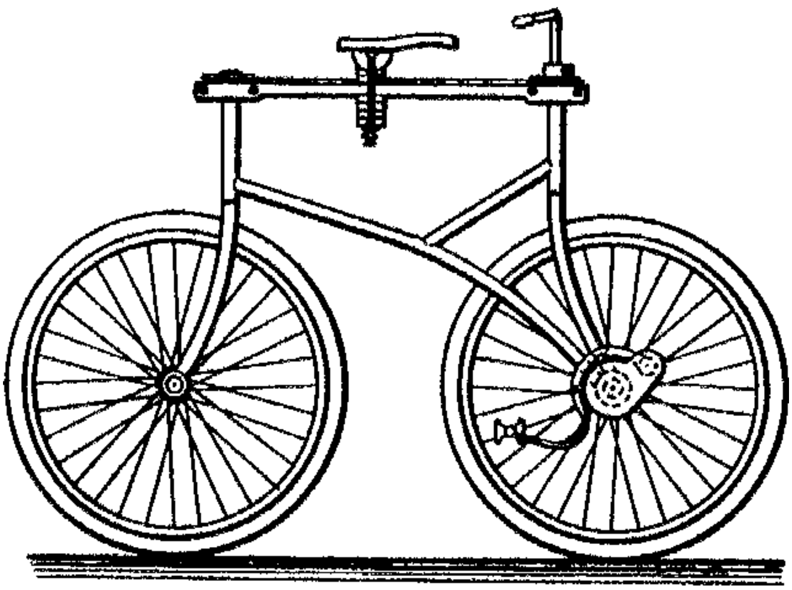

(a)

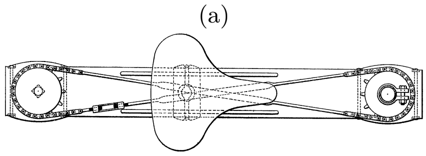

(b)

Figure A.22: The 1899 bicycle steering mechanism of Stephens as (a) implemented on a bicycle seen from the right side, and (b) a detail of the steering mechanism seen from above. [105]

A.20 1899 Anderson 'Military Bicycle'

James C. Anderson patented his 'Military Bicycle' in 1899 [106] (not to confuse with his other patents [107] [108] which are variations on this RWSB, but then reversely ridden). Since the handlebars are attached to the front frame, steering is done by rotating the saddle which is attached to the rear frame carrying the smaller rear wheel (see figure A.23). The steer axis is angled diagonally upwards to the front and intersects the ground slightly ahead of the rear wheel. Note that the handlebar also includes tube that can hold a knapsack, haversack, blanket, etc., and more obscure is that the bicycle supports the attachment of a rifle. Anderson sees some interesting benefits in his unorthodox bicycle design:

> "*My present invention has for its object to provide a bicycle suitable for use in the military service and with the small steering-wheel arranged at the rear of the machine and the larger driving-wheel in front, whereby I am enabled to very considerably shorten up the frame and make the machine compact. The result of this shortening of the frame not only makes the machine more compact, as stated, but it also overcomes the inherent defect in long-coupled machines having a rear steer ing-wheel, because in the latter class of machines it is obvious that the long distance between the wheels renders the front or driving wheel slow or sluggish in responding to the influence of the rear steering-wheel. In other words, the longer the distance between the axes of the front and rear wheels the slower will be the change made in the course or direction of the front wheel, and the converse is also true. Another disadvantage in a long coupled machine lies in the fact that the farther away from the front wheel the steering wheel is located the greater will be the disturbance in the equilibrium of the rider and the more difficult it is for him to retain his seat.*
>
> *In a machine for personal locomotion, propelled wholly by the human body, whether used for transportation of the rider only or for the additional service of a carrier, especially for carrying the necessary equipments of a soldier, it is not only desirable that the machine should be compact and small as possible, but it should, as it were, fit the rider mounted thereon in an upright soldierly position, which position is manifestly best suited to the human anatomy and best conserves the human force of the body in propelling the machine, as well as in maintaining the proper equilibrium. . . . the articulation of the body of the rider and of the machine should compensate each other, and in such a wheel it is also desirable that the rider should be able to mount in front, and when occasion requires to dismount forwardly or in the direction of the motion of the wheel, and hence it is important that his movements should not be obstructed by the usual arrangement of handle-bars in front of him.*"

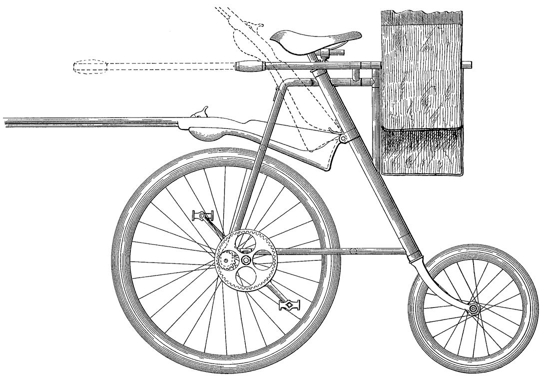

(a)

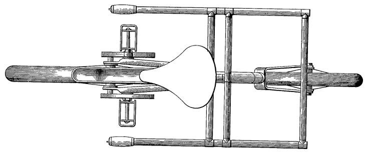

(b)

Figure A.23: Anderson's 1899 Military Bicycle seen (a) from the left and (b) from above. [106]

A.21 1914 Smith 'Push-Bike'

In 1914 a single image cartoon of Alfred Talbot Smith was published that stars an unconventional bicycle design [109]. It appears to be a mere reversed ridden conventional bicycle that is adjusted to give the rider a recumbent position. The steer axis is angled and intersects the ground close to the rear wheel contact point. Moreover, the handlebar is placed over the rider's shoulders. The accompanying text (see figure A.24) suggests that the bicycle is well ridable, but due to the commercial nature of the drawing this is probably not an accurate description.

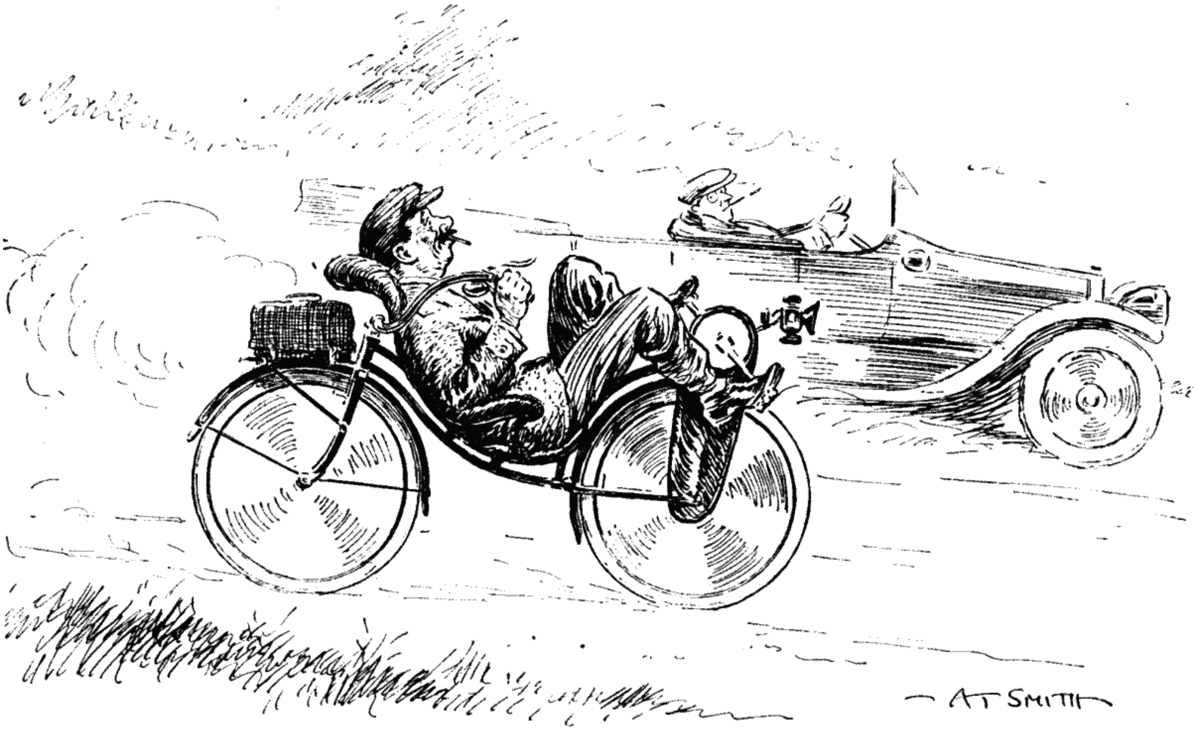

Figure A.24: "*Why should not persevering Peter of the push-bike adopt, when travelling, the same supercilious attitude as languid Lionel of the touring-car de luxe.*" [109]

A.22 1935 Kirby 'Front-Wheel-Drive Recumbent'

Len Kirby designed a 'front-wheel-drive recumbent' bicycle that incorporates rear wheel steering around 1935 [110]. The headset is placed close above and ahead to the small rear wheel while the bracket and pedals are placed above the larger front wheel (see figure A.25). Moreover, the steer axis runs through the rear wheel intersecting the fround just behind the rear wheel contact. A small text accompanying the photo provides some background information [111]:

> "*Sid Rose and an experimental front-wheel-drive recumbent designed by Len Kirby, circa 1935, which he found to be unridable. However, an acrobat from the Boswell circus, while recovering from an injury in Cape Town, not only rode the experimental recumbent, but was able to do figures of eight in Rouwkoop Road.*"

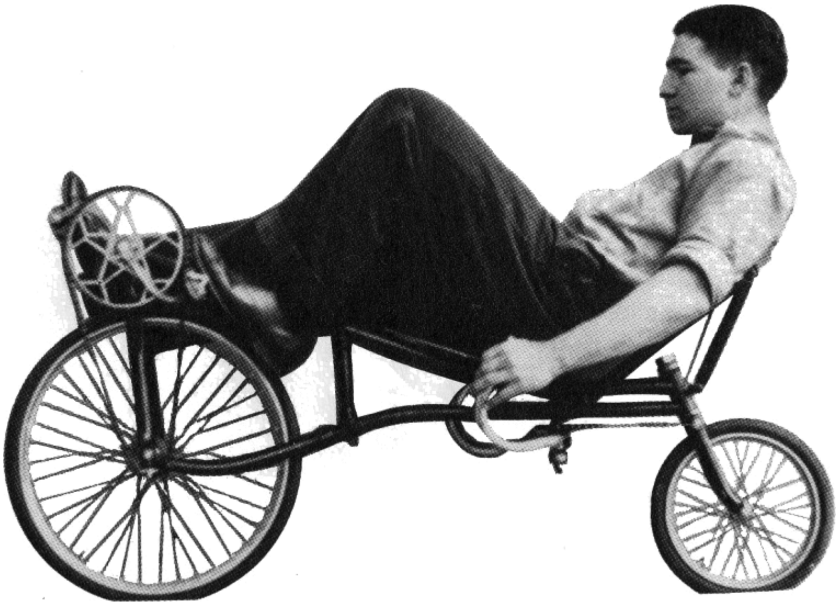

Figure A.25: Kirby's 1935 bicycle ridden by Sid Rose [111] (Scan by Stephen Nurse via [110])

A.23 1939 Mieher 'Bicycle'

Gustav H. Mieher patented a bicycle in 1939 that should distribute the weight of extra load better over the base of support [112]. He achieves this by including a potential comfortable front seat for a passenger or load on the front of the bicycle in such a way that the steered wheel and the handlebar as well as the rider's vision are not bothered with the extra weight or volume (see figure A.26). Therefore, rear wheel steering is incorporated:

> "*Referring to the preferred construction of my bicycle, it will be noted that an outstanding feature of this invention is the provision whereby the frame therefor is constructed and arranged to permit the drive wheel to operate in front and the steering wheel controlled by the handle bars pivotally mounted adjacent the top central portion of the frame and controllably connected with the rearwardly disposed steering wheel by a steering link.*"

To make this rear wheel steering comfortable, the handlebar is connected to the rear fork with the mentioned link in a crossed manner such that a clockwise steer results in a clockwise turn, and both the rider and extra passenger are placed on the front frame. The extra traction required to accelerate a higher load is supposedly created by placing that same load above the driven wheel, while the extra weight does not make the steering of the steered wheel much harder. A gearshift must then make sure that driving does not become too heavy.

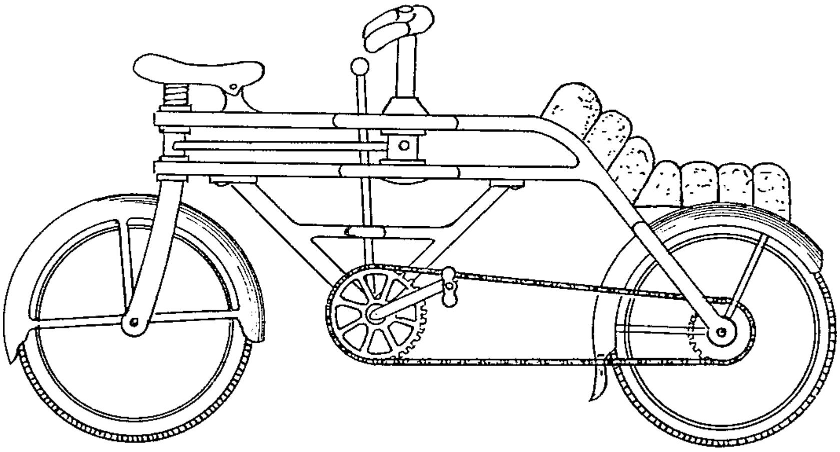

(a)

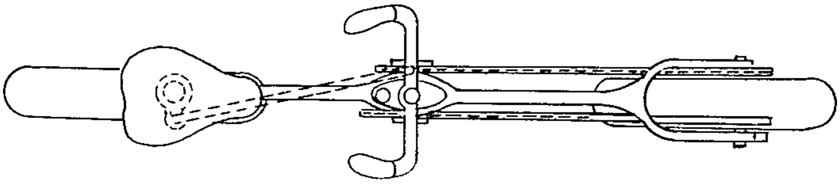

(b)

Figure A.26: Mieher's 1939 bicycle seen from (a) the right side and (b) from above. [112]

A.24 1974 Belden 'Pivotable rear wheel' or 'Swing Bike'

In 1974 Ralph A. Belden patented his 'bicycle with pivotable rear wheel' which has two steered wheels [113]. Different from some other earlier two wheel steered designs is that here the two wheels can be steered separately (figure A.27a). The original design has a rather conventional front part with accompanying headset between the main frame and the front wheel assembly providing a steer axis angle and trail. Furthermore, the rear wheel assembly includes a conventional drive train and ordinary coaster brake. However, the rear part also includes an extra angled joint to allow the rear wheel assembly to steer with respect to the main frame. It seems from the drawing that the rear wheel has barely a trail with respect to the rear steer axis. Note that the seat is vertically adjustable, but attached to the main frame.

The front wheel can be steered by turning the handlebar and the rear wheel is steered by rotating the pedals about the rear steer joint by 'pediatric' input. It is acknowledged that this kind of bicycle has different dynamics and riding it may be erratic. Therefore, to aid the rider Belden added two measures. First, in order to tend to improve the 'linear stability of motion' an extension spring is included between the rear assembly and the main frame such that these two frames are naturally aligned. Secondly, he incorporated a pin lock in the rear joint to, if desired, fix the rear steering entirely and make it an ordinary bicycle.

A commercialization of Belden's design is the Swing bike. As can be seen in figure A.27b it is a little different from Belden's patent, because the saddle is attached to the rear wheel assembly. On the Swing Bike the rider thus turns along with the rear wheel and can thus also steer by rotating his complete lower-body with respect to the main frame. The Swing Bike is considered more of a gimmick than a serious transport measure, probably because of an inherent unstable behavior as can also be deducted from a quote by Museum The Strong [114]:

> "*In 1974 Ralph Belden received a patent for the mechanism on his Swing Bike which allowed independent steering for both the front and back wheel. The bike appeared on the market in 1975 and sold for just three years. Ad copy for the bike boasted: 'With Swing Bike, you can invent wacky maneuvers which leave everyone else bug-eyed in amazement!' Unfortunately, the wacky maneuvers often led to spills, crashes, and injuries, which perhaps explains the company's closing in 1978.*"

(a) (b)

Figure A.27: (a) Drawing from Belden's patent [113] and (b) a Swing Bike from 1975 [114].

A.25 1976 Häggkvist ‘Bicycle of Low Wind Resistance’

Björn Häggkvist patented in 1976 his ‘bicycle (and tricycle) of low wind resistanc and of low center of gravity’ [115]. In order to increase comfort and obtainable riding speed of bicycles, he tries to reduce air resistance and optimally utilize the power of the rider. Therefore, a simple and efficient power transmission and steering mechanism are included that keep the weight of the vehicle low. Moreover, the rider is given a supposed low and comfortable sitting position on the front frame while the front wheel has exactly no trail (see figure A.28).

Häggkvist mentions a steer reversal mechanism, but uses a direct linkage from handlebar to steered wheel in the design of figure A.28. However, for a rear wheel steered bicycle he assumes that a steer reversal is necessary:

> “*... the steering handle can also act directly upon the steering link without any transmissions of steering movements from the steering handle to the rear wheel, which are necessary features in connection with rear wheel steered bicycles.*”

Supposedly, the stability of the bicycle is not a problem due to the nonzero steer axis angle:

> “*By the inclination of the link the rear portion of the forward frame together with part of the rider is lifted during the pivoting movement in connection with a steering deflection. The lifted up mass, which under certain geometrical conditions can be great, will consequently tend against a steering deflection and make the vehicle directionally stable. Moreover, by the inclination of the link, the whole second frame together with the rider will get an inclination in inwards direction towards the centre of the curve, which reduces the tilting tendency caused by the centrifugal force.*”

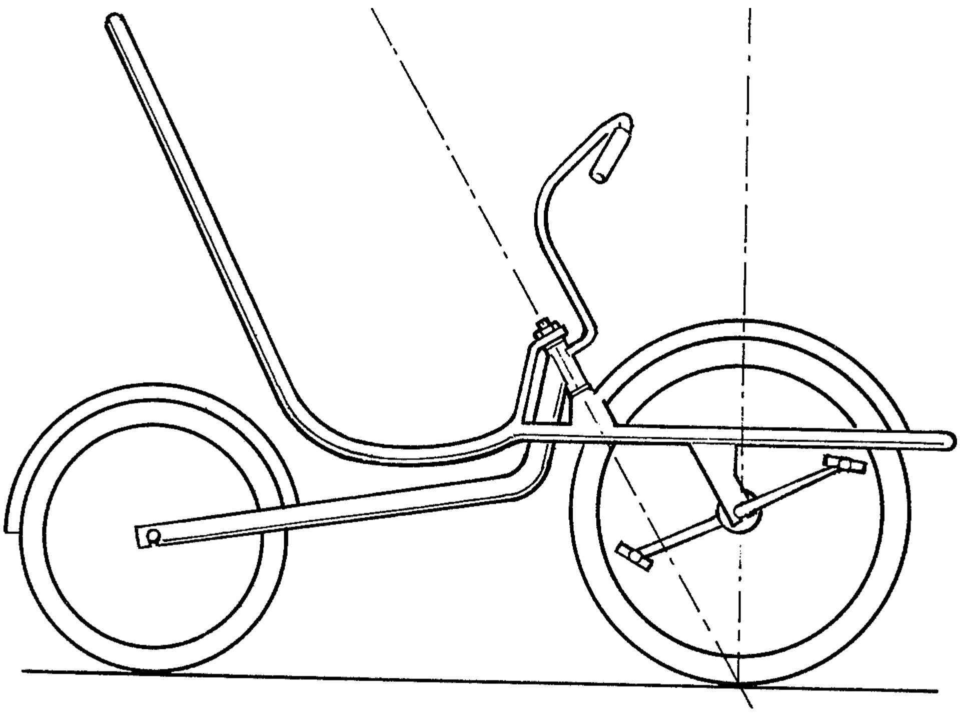

Figure A.28: Häggkvist’s 1976 bicycle with the rider on the front frame. [115]

A.26 1976 Laiterman 'Semi-Recumbent Bicycle'

Lee Howard Laiterman built this prototype bicycle (figure A.29) around 1976 (reported about it in 1977) in order to test his theories of stability on steering with the rear wheel. It was a bicycle he made "to find out if such a design could be made stable, and if not, to minimize its instability" [117]. To make experimentation more easy the bicycle was made adjustable in several ways.

The main piece of the bicycle is a 1020 seamless steel pipe with a 50.8 mm (2.0") outer diameter and a 1.651 mm (0.065") wall thickness. The headset tube was constructed of a 73.0 mm (2.125") outer diameter, 76.2 mm (3.0") long pipe welded perpendicularly at the end of the main pipe. The rear wheel fork was a straightened and shortened conventional fork placed with bearings in the headset. At the end of the rear wheel fork triangular blades were welded with multiple slits at different distances from the steer axis to provide an adjustable trail from 25 to 203 mm. Aluminum slotted brackets were used to attach the remaining components, i.e. rider seat, handlebars, front wheel, and bottom bracket, on to the keyed main pipe. This way all those components could be shifted over the pipe and geometric parameters could be adjusted. All in all, the following parameters could be adjusted: The wheelbase and trail length (and sign by turning the wheel 180°), and the height and longitudinal position of the seat, the handlebar and bottom bracket. Note that the steer axis angle could not be adjusted. A steer linkage reversal pulley was implemented by using 1.6 mm (0.0625") stainless-steel cable, the wheels had a 508 mm (20") diameter, and it totally weighted about 20.4 kg (45 lbs).

After trial and error, Laiterman settled on his ideal configuration of the RWSB. This configuration had a seat height of 610 mm, seat angle of 70°, and a bottom bracket height of 432 mm. Moreover, his minimum of 25 mm negative trail (steer axis intersects ground behind rear wheel) and a wheelbase of 889 mm were considered the best. He also decided to include a steer input/output ratio of 2.5:1, because rear-wheel steering produces supposedly a much sharper turn for a given steer angle as compared to an FWSB. Eventhough, Laiterman's thesis advisor, David Gordon Wilson, still called the RWSB almost impossible to ride on a personal note to Cornelius [8], Laiterman himself said the ridability of the bicycle was rather good at the time of an MIT press event for the RWSB in 1976 [117]:

> "*It's true that my recumbent was difficult to ride, but in point of fact I could ride it and had become reasonably proficient by the time of the press demonstration. I lived in Boston, and on that day I rode it to campus in Cambridge and then back home after the*

(a) (b)

Figure A.29: Lee Laiterman with his prototype semi-recumbent bicycle seen from the right-front (a) [4], and from the right-rear (b) [116].

demonstration; a distance of about one and a half miles each way.

During the demonstration I rode around the circular lawn in front of the Earth Sciences building. After a couple of laps around, I decided to end with a dramatic flourish. By braking hard with the front wheel and steering sharply it was easy to cause the rear end to pivot around the front wheel, resulting in a 180 degree skidding turn to stop. At least that was the plan, but as I initiated the maneuver I found myself being thrown off and had to 'drop' the bike to keep from being catapulted. I suppose David Wilson interpreted that as meaning I couldn't ride the thing."

Somewhat more concretely dynamically, Laiterman's bicycle showed counter-steering [4]:

"*As the bicycle began a right turn for example, the front end of the frame would first dip to the left before aiming to the right*"

However, it was not pleasant to ride since riding it requires a lot of control [4]:

"*This requires a great deal of concentration which detracts from riding pleasure.*"

Laiterman also made a design of a bicycle that was never built (figure A.30). This RWSB was less adjustable and should weigh about 11.3 kg (25 lbs) due to the use of aluminum-alloy components. Due to the obtaining of the best results with small trails, trail was completely absent in this final design.

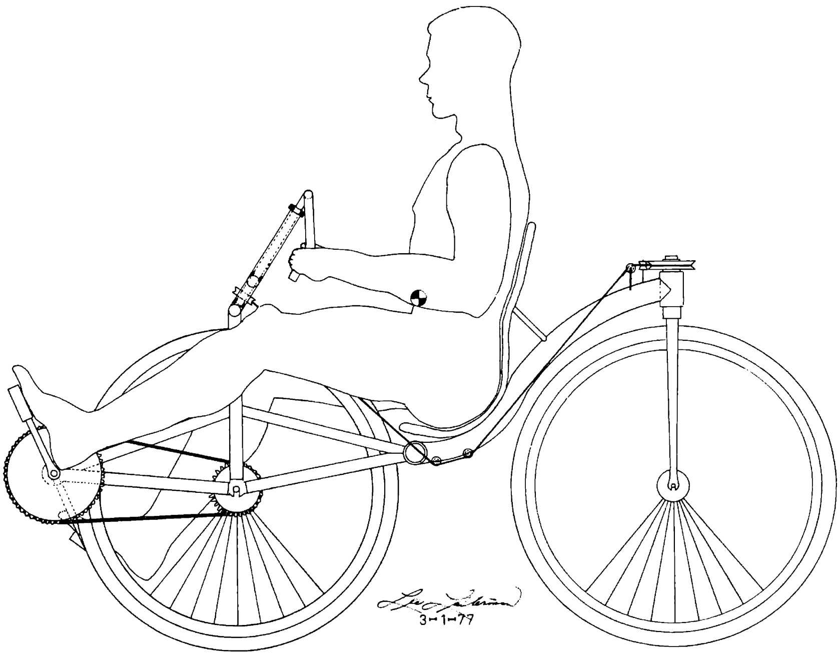

Figure A.30: Final semi-recumbent bicycle design of Laiterman which has never been built. Note that it has a vertical steer axis and zero rear wheel trail. [4]

A.27 1979 Schwarz (NHTSA) 'Rear Steered, front wheel drive test buck'

Robert Schwarz made this motorcycle in 1979 as a safer motorcycle for the National Highway Traffic Safety Administration (NHTSA) [5]. He did not list measurements, but it is basically a reversed conventional motorcycle which is elongated to be able lower the position of the rider with engine between the legs and in effect lower the position of the center of mass (figure A.31). Furthermore, the steer axis points down-rearwards and the steer-axis/ground intersection is in front of the rear wheel considering the forward driving direction. Reports state that despite poor stability prospects, NHTSA (headed by Joan Claybrook), insisted on continuing to build the 'backwards bike' and tons of dollars were invested [28]. Many saw this as a waste of public money [28] [30] when it appeared that, as expected, the motorcycle was very unstable and they were only able to let the machine ride on two wheels for a maximum of only 2.5 s [5]:

> "*The outriggers were essential; in fact, the only way to keep the machine upright for any measurable period of time was to start out down on one outrigger, apply a steer input to generate enough yaw velocity to pick up the outrigger and then attempt to catch it as the machine approached vertical.*"

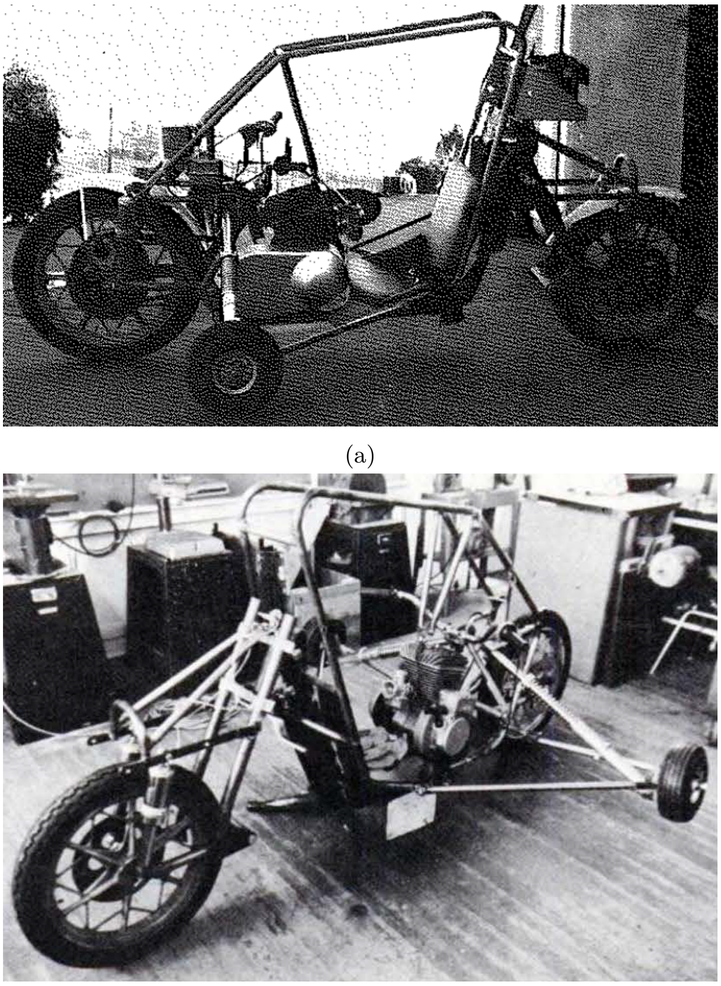

(a)

(b)

Figure A.31: Schwarz (NHTSA) 1979 safety bicycle from (a) left side [5] and (b) the right-rear [28].

A.28 1982 Van Wijnen ‘ChaCha Bike’

Ophthalmic surgeon Wim van Wijnen from Zuilinchem made the Charming Chair (ChaCha) Bike (figure A.32) in 1982 [118]. The rider sits on the rear frame while the front wheel on the front frame is driven. The steering axis is aligned with the back of the seat and intersects the ground close to the front wheel contact point. This bicycle forms the inspiration for all Flevobikes since it is a pretty ridable bicycle [119]:

> “*Cha-Cha II is a very compact bicycle with big (27-inch or there-abouts) wheels. The rider sits in a semi-reclining position. It has front-wheel drive.*
>
> *The unique setup has a frame of two parts. The seat, which has shock absorbers, is kept together with cables. (Looking at the photo, it appears the Cha-Cha may have a horizontal pivot in the middle. Cables at wheel-center level hold the front and back together. The cables are attached to springs at the rear. As the bike flexes in the middle as it is ridden, the cables and springs provide a springing action.)*
>
> *The bike offers a tremendous visibility (presumably because of the very high seating position). The bike is unique and comfortable, ‘but it’s a question of personal taste.’*
>
> *The design is effective, although some riders question this because of the light construction of the seat. When climbing hills, the seat flexes to the extent that the rider (presumably one of the authors, not Van Wijnen) is afraid of braking. There’s a lot of pressure on the seat.*
>
> *How does it ride and steer? After 10 minutes, an inexperienced rider could ride it pretty well. Maneuvers can result in some unexpected problems and situations, but overall, the bicycle is very stable and roadworthy.*
>
> *After riding 25-30 kilometers, the rider could ride it with folded arms. (I’m finding this is ‘common’ with FWD recumbents where the bottom bracket is attached to the forks. What happens is that the rider learns to steer with his legs – I assume only when riding in a straight line – while pedaling.)*”

(a) (b)

Figure A.32: The 1982 ChaCha Bike of Wim van Wijnen from (a) the right [118] and (b) from the left with splash-boards (as ChaCha II?) [119].

A.29 1985 Maebe ‘Bicycle with steerable wheels’

Richard M. Maebe received a patent for his two wheel steered bicycle design in 1985 [120]. Figure A.33a shows that both wheels can rotate independently about a vertical axis with respect to a rather stiff main frame. One wheel is connected to the handlebar and the other wheel with a direct pedal drive and optional brake is connected to the saddle. Steering of the front wheel can thus be done by turning the handlebar while steering the rear wheel can be done by means of the saddle or the pedals.

Technically, it cannot be regarded as bicycle in the most technical definition since it has two vertical steer axes with zero trails for either wheel. Note that trail might be a confusing concept here because one wheel has a zero trail with one steer axis and that same wheel has a wheelbase-length trail with the other steer axis. The Whipple model cannot be used to model such a bicycle, because it has two steer axes. Therefore, the concept of trail might also prove to be important to a different degree.

Maebe considers his design an improvement of past designs with synchronous but oppositely turning front and rear assemblies. Moreover, in the unsynchronous category his design is supposedly better than the design of Belden [113] (section A.24), because of the lack of trail of the wheels and that during steering the rear wheel the feet are no longer obstructed by the main frame and can be kept easier on the pedal crank. Once the rider is accustomed to it and has obtained the skill of independently steering the front and rear assembly, the bicycle of Maebe is supposed to be a challenging alternative to riding conventional bicycles or trick bicycles of the same type due to the vertical steer axes and zero trail:

> “*Since the wheel assemblies rotate around perpendicular axes, it is easy to steer the bicycle, as it is not necessary to counteract forces which are prevalent in prior art bicycles having wheel assemblies which rotate around axes which are not substantially perpendicular to the riding plane. The constant riding position and ease in which the wheel assemblies are independently rotatable provide a bicycle which is more stable than bicycles disclosed in the past.*”

Different commercial versions of this concept are produced throughout the years. The Hoppley Circus Bike (figure A.33b) is an example that is very similar to the patent. In the 1980’s German manufacturer Brückl commercialized a bicycle similar to Maebe’s bicycle called the Super Trick Cycle (STC) (figure A.33c) [121]. This bicycle has a small front wheel trail with respect to the front steer axis due to a slight angle (in direction of conventional bicycle) of said axis.

(a) (b) (c)

Figure A.33: The bicycle with steerable wheels as seen in (a) a drawing from Maebe’s patent [120], (b) the Hoppley Circus Bike [122], and (c) the Brückl Super Trick Cycle (STC) [121].

A.30 1986 Vrielink 'Flevobike'

The Flevobike (named after the 'Flevo Polder' in the Netherlands in which the Flevobike birthplace Dronten lies) is a front wheel driven bicycle with center steering designed by Johan Vrielink in 1986 [118]. The bicycle evolved from the ChaCha-Bike (section A.28) which has a nice short chain, is compact, and absorbs shocks [123]. The Flevo is build with square tubing and had originally only rear wheel suspension and later on also the front wheel got suspension. Front and rear wheel are interchangeable and the bicycle can be easily taken apart. It's trail is often of the same sign as a conventional bicycle, because the steer axis is angled such that the steer axis intersects the ground in front of the front wheel. However, riding it is not as easy as on a conventional bicycle and does take some doing [123]:

> "*Learning to ride it is not a matter of course. It takes effort to become accustomed to it.*"

Although it takes some learning to ride it, it is a nice example of an unconventional bicycle design that became popular enough to evolve into a serial produced bicycle (figure A.34) [118]:

> "*...he met Wim van Wijnen, an ophthalmic surgeon who had many new ideas, and who had built the ChaCha bike (short for: Charming Chair Bike): This bike was pretty remarkable, with its center steering and front wheel traction. In 1986, Johan designed his own version of this bike. He used smaller wheels in order to make suspension possible. The front frame had to be altered. The new frame went over the front wheel. He also made the bike separable.*
>
> *Some more improvements were made (f.i. the motorbike springs were replaced by rubber blocks). In spring 1988 the serial production started, and in april 1989 the Flevobike company officially started. ...The company that had started in the cellar of the Vrielinks' home, expanded gradually. Three times, an each time bigger building was added to the Flevobike factory. In 1998, The company has grown to 13 employees.*
>
> *In the meantime, the bike has been improved technically in small steps. F.i. sometimes the steering axle broke. It was replaced by a somewhat thicker one. For many years, the bike could be purchased in all colors, as long as it was white or black.*
>
> *...In 1991, the FlevoRacer followed. It had two 26" or 28" wheels, no front spring and a more recumbent seat. The racer has a somewhat smaller frontal area, and is slightly faster than the bike.*
>
> *From this time, Flevobike company regarded the bike, trike and racer more or less finished. Many other HPVs were designed: Easy Rider, Forens, Amigo, Greenmachine, Rapido, Basic,*

Figure A.34: A Flevobike from the 1990's. [118]

Fifty-fifty, Alleweder, C-alleweder (Carbon Alleweder). But there were some improvements and variations. Most of them were made by technical students, cooperating with the Flevobike company. In 1990, an extremely lightweight show model was produced, and won a first prize in an aluminium construction contest. It was unsprung, and the seat was too narrow to be comfortable. But it looked amazingly beautiful!

. . . the rights of the bike, trike and racer came to 'Ligfietsshop Tempelman' (Tempelman recumbent bike shop). Harm Tempelman had since the beginning produced the seats and luggage boots of the Flevobikes, and later, he was the one to produce the C-alleweder in license for Flevobike. He and his son Gerrit had started their shop in one of the buildings of the former Flevobike. They do all service, also for the bikes that have been bought from Flevobike in the past. Moreover, they have a post order service for self-builders and people who want to replace parts of their Flevos."

A.31 198- Cornelius 'Rear-Steering Recumbent Bicycles'

Cornelius built seven RWSBs over 10 years from 1978 on and concluded that rear steering might hold the possibility of solving the recumbent packaging problem [8], but it is the least feasible solution [33]. As the packaging problem he considers that for a proper weight distribution the pedals should occupy the same volume as the front wheel, i.e. the bracket must be placed too close near or inside the wheel rim. The several RWSBs of Cornelius are described here to see the evolution his bicycle went through. The first bicycles are all made of plywood, aluminum, and pop-rivets while the last one is more sound. Moreover, all versions include a steer reversal to make a clockwise handlebar rotation result in a clockwise bicycle turn.

Plywood Flyer (figure A.35)

The 1978 Plywood Flyer had 508 mm wheels, a seat height of 152 mm, and used a 'four-bar-linkage wheel-positioning mechanism' with a vertical steer axis and 76 mm of negative trail. It was unrideable for all practical purposes.

MK I (figure A.36)

Cornelius teamed up with Jerry S. Onufer in 1981 to create the MK I which almost the same as Laiterman's [4] RWSB to test how hard it really was to ride this RWSB. With respect to Laiterman's bicycle, the MKI had an added adjustable steer axis angle and adjustable steering control. This means that along with the same measures as Laiterman's RWSB, the MK I also shares the ability of an adjustable wheel position in the fork. These features allowed for experimenting with different trails and steer axis angles. The MK I used 508 mm wheels, a seat height of 508 mm with almost vertical seat back, a bottom-bracket height of 406 mm. The wheel base could be varied between 1020 and 1270 mm and the steer axis angle could be varied from -30° to +30°. The wheel position in the fork, i.e. distance from wheel center perpendicular to the fork longest main part, could be varied from 0 to 100 mm. The fork could also be turned 180° about the vertical axis to allow for both negative and positive rear wheel trail (negative for steer axis/ground intersection behind rear wheel contact and positive when in front of rear wheel contact). Finally, the steer control input/output ratio was 1:1 and a steer reversal that makes a clockwise handlebar rotation result in a clockwise turn was included. For the MK I it was concluded that the positive trail configurations were easier to control than the negative trail configurations. Steer axis angle had little influence on the controllability. It was impossible to ride this bicycle below a certain 'critical balance speed', but for all positive and small negative trails it could be ridden without aid after an assisted start. Inspired by the Laubach Velocipede (where he read about in [91]) Cornelius increased the rear wheel trail first to +305 mm and eventually to +610 mm giving the bicycle a wheel base of 1600 mm. With this last configuration, an unassisted start was possible and stabilizing the bicycle was easy, although the handling felt strange and handlebar forces were large. This finding led to the creation of more large positive trail RWSB versions, but making the rear wheel trail larger and larger might be interpreted as shifting the bicycle more and more to front wheel steering.

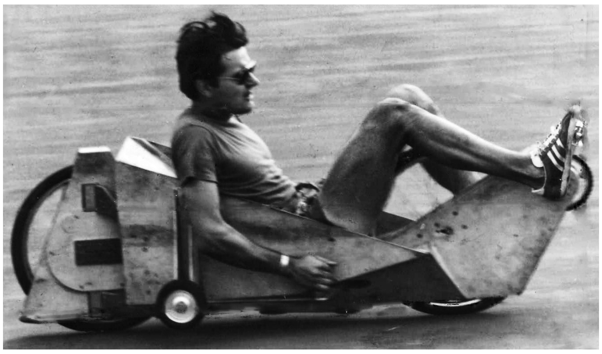

Figure A.35: Cornelius' 1978 'Plywood Flyer', first RWSB built. [33]

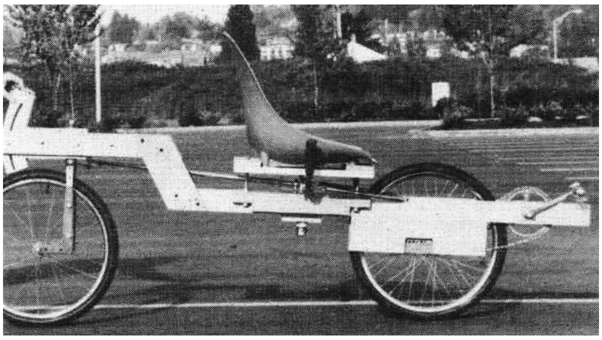

Figure A.36: Cornelius' 1981 MK I adjustable RWSB. [8]

MK II (no figure)

The wheel base of this bicycle was 1070 mm and an alternative system was implemented to steer. A four-bar linkage was used to pivot the wheel for steering. The idea was that the trail would be large for small steer angles, e.g. during starting, and small for large steer angles, e.g. in tight turns due to the displacement of the instantaneous rotation center, to reduce lateral offset associated with large trail. In steer-neutral position the rear wheel trail was about +914 mm and for a 30° the trail would be reduced to 102 mm. However, it did not work as good as the simple single pivot solution as seen on a conventional bicycle.

MK III (no figure)

For the MK III Cornelius returned to a single-pivot steer mechanism with a steer pivot beneath the seat. Three different rear wheel trails were tested: +762, +965 and +1170 mm. Also, different steer control input/output ratios were tested: from 1.5:1 to 3:1. The steer control linkage was such that the input-link length increased with handlebar angle which results in a variable-ratio control linkage. The best handling was obtained with +762 mm trail and 2:1 input/output ratio. This bicycle with vertical steer axis delivered acceptable performance for riding in a straight line, but was unsatisfactory for tight turns at low speed. Increasing the trail further had diminishing return and was impractical for packaging perspective. Note that stronger bearings are used in the headset to accommodate for larger forces from a larger arm of the contact point force.

MK IV (figure A.37)

The MK IV had a fixed rear wheel trail of +762 mm and a fixed input/output steer control ratio of 2:1. The seat height was 610 mm with upright seat back, the bottom bracket height was 406 mm and the steer axis angle was adjustable from -21° to +21°. The best steer performance was obtained by adjusting the steer axis angle such that the potential energy was maximal in steer-neutral position. This means that the steer axis angle was increased in positive direction, i.e. steer axis pointed diagonally upwards to the rear. To do so, the headset top bearing was moved backwards and the bottom bearing was moved forward. The maximum cornering performance was obtained with the maximal positive steer axis angle of 21°, but this worked against the stability in straight motion which required a smaller axis angle. Cornelius explains this by noticing that a positive steer axis configuration causes a potential energy peak when the wheels are centered: an energy peak is an unstable equilibrium and the bicycle thus tends to steer to either side to leave the instability. To compromise, a final angle of +14° was chosen as final solution and this resulted in the best low-speed stability of all versions yet.

MK V (no figure)

The MK V was designed with the goal of lowering the aerodynamic drag. The effect of a more recumbent posture and larger wheels was investigated. 700 x 25C wheels, a seat height of 483 mm, a seat back angle of 45° and a bottom-bracket height of 610 were used for the design. The steer axis made a 75° from the horizontal pointing upwards to the rear. Furthermore, the fork offset (perpendicular distance

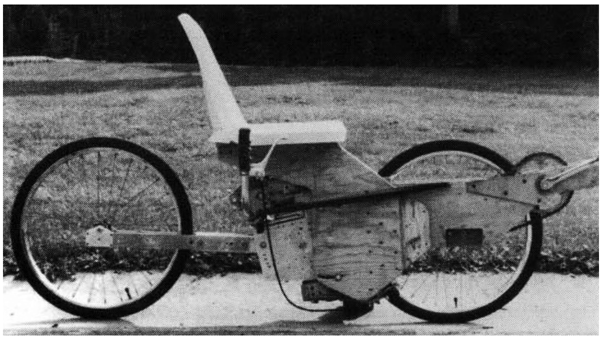

Figure A.37: Cornelius' MK IV. [32] (published as correction on misprint in original article)

of wheel axle to steer axis) could be 457 or 610 mm, depending on the position of the handlebars, before or behind the steer pivot. The 610 mm fork offset setting turned out to be the most stable and the bicycle could still be started unassisted. However, the speed at which the bicycle became stable was higher and the low speed stability was decreased. An increase of the steer control input from 2:1 to 3:1 reduced the large amplitude weaves occurring during riding with one hand at high speeds. The final version of the MK V had the same velodrome cruise speed as a conventional upright bicycle and was even faster than a front wheel steered recumbent of type Avatar 2000.

MK VI (figure A.38)

Chronologically, this version was built after the 'final' version of Cornelius' RWSBs; the VelAero. But this bicycle is introduced first, because it is more experimental than the VelAero. It is hypothesized that an infinite trail would come as close to the lean-steer relation of a conventional self stable bicycle as possible. Therefore, this bicycle is a modification of the MK V that includes a 'near-parallelogram four-bar linkage' to 'steer' the rear wheel by displacing it almost purely lateral. The linkage had an instantaneous rotation center at 7600 mm in front of the rear wheel and the rear wheel translated 100 mm with a 25° steering input. Steering corrections were hard to make and in effect it was only tested in straight line, but it was easier to start and was stable from a lower speed as compared to the upcoming VelAero. Cornelius reasoned that for an actual implementation the mechanism should be adapted to have two phases such that the rear wheel moves only lateral for small steer inputs and it rotates for larger inputs. Then, non straight line movements at higher speed would be easier while keeping the easy starting.

VelAero (figure A.39)

The ultimate RWSB design of Cornelius is named the VelAero from 1988 which is largely made of chrome-molybdenum. Note that the absolute trail of the front wheel is smaller than the absolute trail of the rear wheel and that is thus questionable whether this is truly an RWSB. However, just as with all Cornelius' RWSBs the seat is mounted on the front frame. The total mass is 15 kg, the wheelbase is 1020 mm, the seat height is 470 mm, the bottom bracket height is 597 mm, the steering axis angle

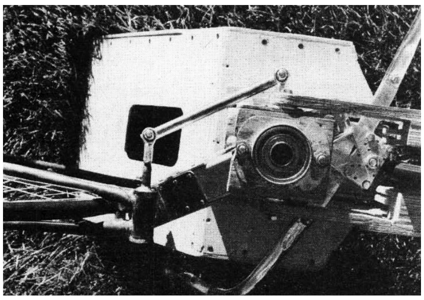

Figure A.38: Cornelius' MK VI bottom view. [8]

is 15°, the fork offset (perpendicular distance from steer axis to wheel axle) is 508 mm, and a 45/55 front/rear weight distribution. A hydraulic steering damper is added to ride with one hand while keeping direction. The handlebar to headset steering linkage is made variable: The input/output ratio is 3:1 in the neutral position, but this ratio reduces progressively during increased steer so that 47.4° handlebar angle results in 30° steer frame rotation.

Over 800 km with trips of maximal 80 km are ridden on the VelAero. The dynamical behavior was such that the stability of the bicycle increased significantly during acceleration, even for sprints to speeds up to 13 m/s. This made starting easy, although a lot of weaving was necessary to balance the bicycle at constant velocities below 2-3 m/s. For hill climbing (max climb angle 5%) the weaving was present until 4 m/s. For the Avatar 2000 recumbent bicycle, the 'critical balance speed' is less than 0.5 m/s on flat roads and 2 m/s on steep hills. Deceleration of the VelAero might have destabilized the bicycle, were it not that braking was almost exclusively done by using the rear wheel. Probably this causes a couple that opposes the steer out of fall couple (assumed inherently for positive trails bicycles), thereby maintaining stability.

All in all, the VelAero could be balanced at medium and higher speeds, but heavy weaving was necessary to ride the bicycle at low speeds [33]. The final RWSB showed somewhat too large critical balance speeds, but it was a predictably controlled recumbent in a racing situation [8]:

> "*I feel the stability of the VelAero is close to the maximum for the long-trail approach to an RSRB* (Rear-Steering Recumbent Bicycle)*, given the low rider posture. Unfortunately, the level of stability is not adequate for a general-purpose recumbent. The important lesson relating to the beneficial effects of long trail is that the rear-steering stability problem requires solutions that will differ drastically from conventional front-steering geometries.*"

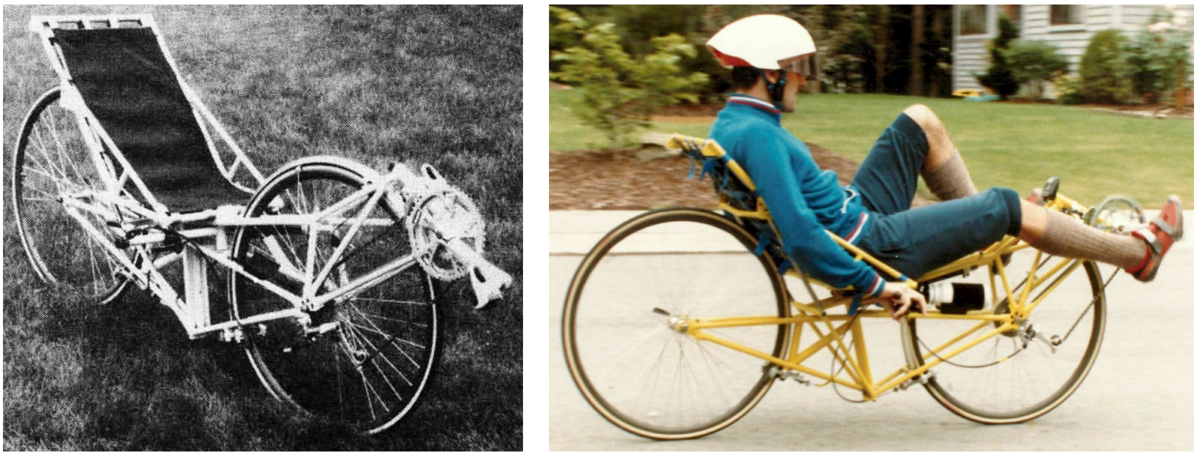

(a) (b)

Figure A.39: VelAero; Cornelius' 1988 final 'RWSB' (a) front right view [8] and (b) Cornelius riding it [33].

A.32 198- Klein 'Rear Steered Bikes'

From the 1980's on, Klein uses RWSBs to motivate students for dynamics and control by letting them experience it in a direct manner [40] [14]. The importance of integrated process and control design, the effects of poles and zeros in the right-half plane, the fundamental limitations caused by bad system dynamics, and the role of sensors and actuators can all be discussed with the help of Klein's RWSBs: [40]:

> "*As a consequence of experimenting with modified bicycles, a connection emerges between the hardware prototypes and the theoretical aspects and methodology of dynamic systems and controls. As an example, several rear-steered bicycles were built and tested.*"

Klein has two main RWSB examples for hands-on experience with the counter-intuitive properties of an RWSB. Both those RWSBs are unstable on itself (no self-stability), but one is 'unridable' while the other one can be ridden.

Rear Steered Bike I

The first RWSB, shown in figure A.40, was used by University of Illinois undergraduate students in the 1980's to conduct additional bicycle experiments [124], while Klein uses it as demonstration model. It can easily be made from a conventional bicycle. Basically, the saddle and handlebars have switched positions, where the saddle is still on the larger frame, but this frame is now the front frame. The handlebars, which turn around a different angled axis compared to a conventional bicycle, are connected to the head tube by means of a crossed linkage via chains and wires makes sure that a clockwise handlebar turn still results in a rightward (clockwise) bicycle turn [40]:

> "*The first rear-steered bicycle incorporates a seat mounted over the steering head, and then an extra steering head is welded into the frame in the former position of the seat post, and a conventional bicycle chain connects, via sprockets, the handlebars to the steered wheel in the rear. Thus, the bike is reversed completely; handlebars in the front turn the rear wheel and the pedals drive the front wheel.*"

Because this bicycle is more or less a conventional bicycle ridden reversedly, it has all positive real part eigenvalues. This becomes clear when one realizes that an eigenvalue plot is point symmetric about the complex axis; when a system has all negative real parts of eigenvalues in forward values, then these eigenvalues are positive in the opposite direction. This bicycle is thus unstable by itself and, in fact, due

Figure A.40: Original RWSB of Klein. Basically, a reversedly ridden conventional bicycle and therefore unstable. [14] [36]

to the large positive eigenvalues it was thought that such a bicycle would be unridable (uncontrollable) by humans. Experience did indeed show that this hypothesis might be truth [40]:

> "*It is an annual challenge with students to ride this bicycle, but nobody has mastered this particular rear-steered bicycle.*"

Since they were so convinced that it could not be ridden, Klein put an award (US$1,000/US$5,000 depending on the source, it might have increased throughout the years) on it for the first person that could ride it under specified conditions. But even when they did not let excusively students try it, or when they allowed long practice time and some constructional changes, everyone failed to ride it [124]:

> "*There is a standing offer, under certain stipulated conditions, of a prize of US$5,000 to the first person who can successfully ride this bike. Please don't spend the prize money in advance, as better people than you have already tried, about 500 in all, and all attempts to date have failed. Rear-Steered Bike I has never been ridden, although hundreds of average and even skilled riders have tried. The best attempt made so far occurred in the 1980's when the bicycle was placed on loan for about one month to the then president of the University of Illinois Unicycle Riding Club. With practice the rider, a skilled unicyclist, was able to eventually remain upright on the bike, but in doing so the rider had to do two things:*
>
> 1. *Configure the chain connecting the handlebars and the rear fork in a conventional circular loop, as opposed to being in a 'figure 8' or crossed which is the usual connection configuration.*
> 2. *The rider ended up riding haphazardly in an open and flat parking lot as opposed to being able to follow a prescribed path.*
>
> *Being able to follow a prescribed path is one of the requirements in order to qualify for the US$5,000 prize. In addition there are additional requirements, all quite reasonable but nonetheless bike riding challenge requirements must be adhered to. The contribution of John Becker, former University of Illinois graduate student in Mechanical Engineering, is acknowledged as it was through John's effort that this particular bike was built. As photos show, this UIUC bike has been through its share of trials and tribulations. Hundreds upon hundreds of overly optimistic riders have tried for the prize reward - but to no avail! Our money is very safe. We've hauled and crated this popular bike to seemingly countless shows and exhibitions across the nation. We never fail to attract attention as well as suckers who think that it's easy to ride. In short we have tons of fun just laughing as this bike draws would-be riders like a pile of hundred dollar bills flying about in the wind draws all who want to scoop up what then can grab.*"

However, a video shows someone carefully, slowly, and with many steering motions riding this bicycle [125]. It is not clear whether the 'specified conditions' are met, but presumably this video shows Brianno Coller who won the price and proudly mentions it in a small biography [126]:

> "*Recently Dr. Coller successfully completed the 'Rear-Steer Bike Challenge.' He became the first human to ride Richard Klein's Rear-Steer Bike I. Built in 1986, no one had ever been able to ride the bike. The bicycle had been studied by several prominent scholars and had been deemed unridable. In October of 2009, Dr. Coller proved them wrong and gave the $5,000 prize money to a worthy cause.*"

Rear Steered Bike II

Klein's second RWSB is shown in figure A.41 and is rather different from a conventional bicycle. This bicycle is designed by undergraduates of Klein [124]:

> "*This particular research bicycle was the result of a succession of three semester long projects by students in mechanical engineering. The essence is that this bike is rideable, as it has been ridden by approximately fifty different persons at various times. We confess that it is not a bike for the timid. Rear Steered Bike II differs from Rear Steered Bike I in a number of ways. The rider's center of mass is higher, the rider's center of mass is more forward, the wheel base is shorter, the rear steered fork is naive as it is vertical and has zero*

trail, and lastly, the steering action of the rider is reduced due to the use of different sized sprockets on the connecting steering chain assembly, that is, the chain and cable apparatus that connects the handlebars to the rear-steered fork."

It convinced him that RWSBs (or bicycles in general) are a great tool in making students enthusiastic [40]:

> "*The power of analysis and synthesis techniques is made vividly clear to the students as related to the rear-steered bicycle. Specifically, analysis of the equations of motion, based on an idealized rigid mass inverted pendulum and an appropriate kinematic ground track model, suggests several design changes, including shifting of the center of mass forward and upward, and use of a shorter wheelbase. This design modification yields conditions suitable for stable closed-loop control assuming a first-order controller. Students also have investigated the use of pole-placement techniques in order to stabilize the inherently unstable rear-steered bicycles. The discussion of pole-placement techniques then triggers a need for the discussion of observability and controllability of state equation models. The class really starts to believe in the power of systems-theoretic techniques when class members report that they experimentally modified a rear-steered bicycle, as suggested by analysis of the equations, and that the bicycle is ridable, although challenging to ride.*"

The closed-loop controlled system can be made better ridable (robust control) by increasing the ratio between the right-half-plane zero (numerator in transfer function) and the right-half-plane pole (denominator in transfer function); the separation between them can be increased by making the zero larger and the pole smaller. First off, the zero can be made larger by increasing the forward velocity while the pole value is not influenced by forward velocity such that the ratio between unstable pole and zero is increased for larger velocities, thereby making control easier. Thus, these RWSBs become better ridable with increasing velocity.

Moreover, the zero value is inversely proportional to the horizontal distance of the center of mass to the front wheel contact point. So to increase the value of the zero, the center of mass needs to be horizontally close to the front wheel contact point. The pole value, however, is inversely dependent on the center of mass height value. A small pole thus requires a high center of mass. To implement these dynamics, the rider, whose position is the main contributor to the center of mass position of the whole bicycle rider assembly, is placed close to the front wheel on a high saddle.

Figure A.41: Rear Steered Bike II; the second RWSB of Klein. Due to a high rider center of gravity and the small distance between the vertical projection of the rider center of mass and the front contact point, this bicycle is rather ridable compared to the earlier version. [14] [36]

Furthermore, compared to a conventional bicycle, this RWSB has smaller wheels and a higher crank position to accommodate for the higher rider position. The linkages between the handlebars and headset are once again crossed. Moreover, while the steer axis is almost vertical, the rear wheel has a negative trail due to a small bend in the rear wheel fork. Indeed, this bicycle is ridable [124]:

> "*Travis Williams, University of Illinois scholarship athlete, tried our RSB II and was successful even on his first try. Within about ten minutes of riding experience, Travis was quite proficient - as well as being a great sport. Persons riding this bike comment that it is easier to ride in somewhat circular arcs, as when the bike is in a circular arc, the rider can apply controlled pedaling power or even brake some, as desired, to influence what we'll call the lateral centrifugal force reactions. In essence, just as when you are riding any conventional bike and leaning into a turn, by applying pedaling power and increasing speed, the bike will tend towards the upright as the speed is increased. The converse also happens when speed is reduced. As a point of technical clarification, the notion of centrifugal force is illusionary. Centrifugal forces do not exist in nature, but only appear to exist (and contrary to Newton's Laws) for example when the human is in a moving coordinate system. To be correct, the rider in a turning maneuver experiences centripetal forces, typically lateral forces that act at the tire's point of contact with the ground.*"

A.33 1988 Berger 'QED'

Warren A. Berger experimented with bicycle steering in 1988 [127] and came up with his bicycle 'QED' (quod erat demonstrandum, which was to be demonstrated). He tried to imitate the layout of a high front wheel driven 'lean-to-steer' tricycle by using a two-wheeled design in order to have the magic of riding on a single track vehicle. He interpreted this tricycle as a rear wheel steerer and in accordance his derivative bicycle would also be rear wheel steered.

Not discouraged by messages of impossible or hard to balance rear wheel steered bikes, he went on with a trial and error based design process. The bicycle frame of the QED I was made of chrome-moly and was adjustable in several ways. It turned out that the steering axis could not be too horizontal nor should it be too steep and he settled on a rear and upward pointing steering axis making a 70° angle with the horizontal to have the best turn into fall behavior. Moreover, the steer axis intersects the ground between the two wheel contacts and to reduce steering effort, the wheelbase should be as short as possible. Eventually he used a 900 mm wheelbase on the 13.9 kg weighing bicycle which further includes a 550 mm high seat and a 62/38 front-to-rear weight distribution shown in figure A.42a. Notable is that a steering ratio was implemented in order to make steering possible, the final ratio being 1.6:1 for 30° turning right or left. With this configuration he was able to climb 20% steep hills without wheel slip and is rather happy with the result:

> "*This seems the best compromise so far. The steering is light enough, even with 17 pounds (7.6 kg) of stuff in the rear panniers. And I can usually still turn around in our road without putting my foot down.*"

Installing a smaller rear wheel of 500 mm further forward on the bicycle made the wheelbase 800 mm long while the rear wheel trail became 100 mm shorter, but this did not make the bicycle less stable. This bicycle configuration is shown in figure A.42b, however, due to larger rolling resistance this smaller rear wheel was unfavorable nevertheless. Berger already had plans for the QED II which would be made of aluminum and thus would be lighter (11 kg). The bottom bracket would be higher (375 mm) for more clearance and the seat would be lowered to 450 mm for easier steering. To improve braking and to prevent 'front-wheel plowing (understeer)', while keeping enough traction and the ability to climb steep hills, the weight distribution should be altered to about 53/47 (front/rear). This could be done by using smaller wheels of 500 mm which makes pushing the bottom bracket and seat backwards by 87 mm possible.

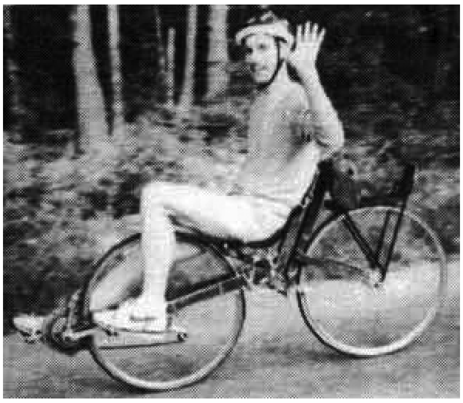

(a)

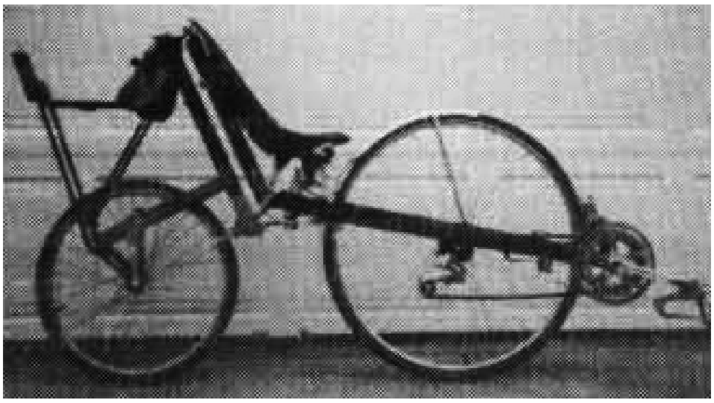

(b)

Figure A.42: Berger's QED I with (a) his favorite configuration and (b) a shorter wheelbase and smaller rear wheel configuration. [127]

A.34 1988 Sudheimer 'Niedriges Zweirad'

In 1988 Arnold Sudheimer patented a bicycle with low rider position, the 'Niedriges Zweirad' (low bicycle) [128]. Most bicycles with low rider seat need a long wheel base, long chain, and heavy construction to position the rider in between the two wheels. This bicycle however, places the pedals ahead of the front wheel such that the rider can be seated in a semi-recumbent position close behind the front wheel on a bucket seat (see figure A.43a). The handlebar is placed between the front wheel and the seat and is connected by a cross-linkage to the head tube at the rear. This way a clockwise handlebar movement results in a clockwise turn (see figure A.43b). By adjusting the Pitman arm of the crossed linkage, one can adjust the steering transmission ratio from handlebar to rear wheel fork [translation by P.H. de Jong]:

> "*Um Abmessungen, Eigengewicht, Luftwiderstand und Aufwand der Kraftübertragung bei Zweirädern mit niedriger Sitz-position gering zu halten und zugleich mit hoher Wendigkeit des Fahrzeuges größtmögliche Sicherheit und Bequemlichkeit für der Fahrenden zu erreichen, wird folgende Konstruktion hier angewendet:*
>
> *An einem entsprechenden Stahlrahmen mit geringem Radstand werden ein gefederter Schalensitz mittig zwischen beiden Rädern und der Pedalantrieb vor dem anzutreibenden Vorderrad angeordnet. Die Pedale sind mit Fersenstützen versehen. Das Hinterrad wird mittelbar über ein Gestänge mit variabler Übersetzung gelenkt.*"

> "*In order to minimize the dimensions, weight, air drag, and propulsion effort of two-wheelers with a low seating position, and at the same time, with the greatest possible maneuverability of the vehicle, achieve the greatest possible safety and comfort for the riders, the following construction is used here:*
>
> *On an appropriate steel frame with a small wheelbase, a sprung bucket seat is arranged centrally between both wheels and the pedal drive is arranged in front of the front wheel to be driven. The pedals are equipped with heel necks. The rear wheel is steered indirectly via a rod with variable transmission.*"

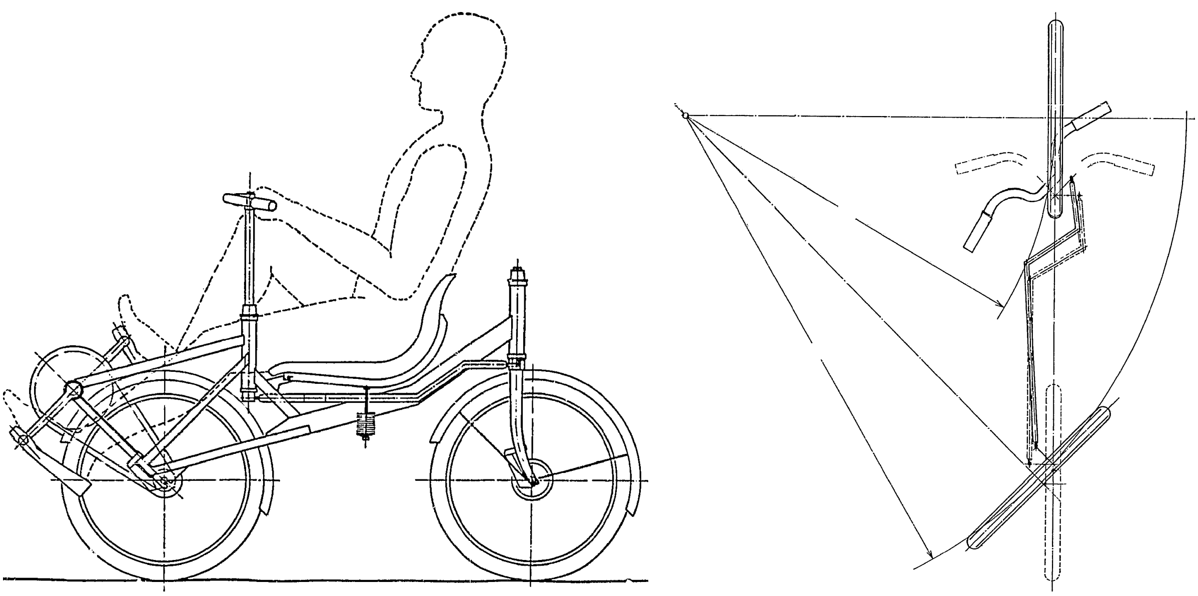

(a) (b)

Figure A.43: Sudheimer 1988 low bicycle seen (a) from the left, and (b) from above in a (counterclockwise) lefward turn. [128]

A.35 1989 Trzaska 'Fahrrad'

Martin Trzaska patented his 'Fahrrad' (bicycle) in 1989 [129] (figure A.44). With his design Trzaska attempts to make the bicycle better ridable, more stable, and safer in turns and under bad weather and road conditions. With one small wheel the center of mass of the frame can be lower, while the larger wheel still allows for a normal drive wheel diameter. This is claimed to be beneficial for the ride stability and decreases the severity of falling over. Furthermore, the front wheel drive is apparently better for stability, while rear wheel steering aids in parking into small spaces [translation by P.H. de Jong]:

> "*Ein weiterer Vorteil ergibt sich aus der Anbringung des gelenkten Rades am in Fahrtrichtung hinteren Ende des Fahrrades. Auch hier wird der Vorteil, den beispielsweise gewöhnliche Kraftfahrzeuge beim rückwärtigen Einparken in Parklücken beim Lenken haben, ausgenutzt, wobei allgemein bekannt ist, daß dabei eine gute Lenkbarkeit erreicht wird, d.h. Kraftfahrzeuge können beim Rückwärtsfahren selbst in Kleinstparklücken einparken. ...*"

> "*A further advantage results from the attachment of the steered wheel to the, in travel direction, rear end of the bicycle. In this case too, the advantage which for example normal motor vehicles have with steering in the case of reverse parallel parking in parking spaces, is exploited. It is generally known that in that case good steerability is achieved, i.e. motor vehicles can park themselves in the smallest possible parking space when moving in reverse. ...*"

The bicycle has a frontally upwards pointing steer axis that intersects the ground close to the rear wheel contact. To steer, the handlebar can for example be connected to the head tube by means of a chain, a belt, a wire rope, or a Bowden cable, and so on.

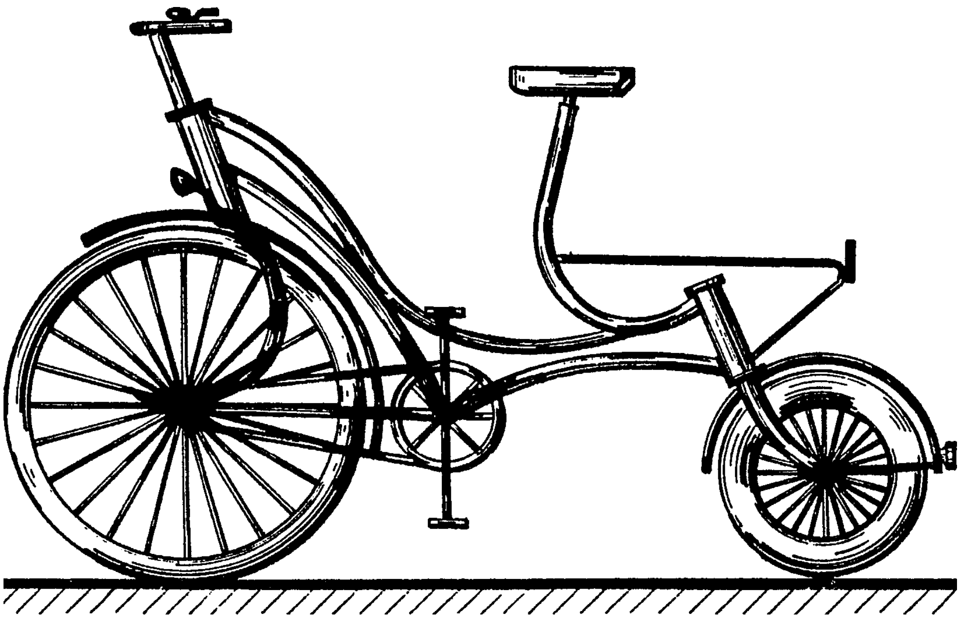

Figure A.44: Trzaska's 1989 'Fahrrad'. [129]

A.36 1990 Brown 'Rear Steering Recumbent Design'

Charles Brown was fascinated by Cornelius' work on rear wheel steering and came up with an own design idea in 1990 [130]. As can be seen in figure A.45 the rider sits on the front frame and drives the front wheel while steering is done with help of some kind of steering reversal. However, the steer axis intersects the ground in front of the front wheel and is thus alike a conventional bicycle making it technically front wheel steered [130]:

> "*After reading Craig Cornelius's fascinating account of his experiments with rear-steering recumbents (HP 8/2/90), I wondered if the following design would work. Although technically a front-steering bicycle, it would seem to meet Craig's goals, without the steering problems. Like Craig's bikes, the handlebars would turn the rear portion of the frame in the opposite direction the handlebars were turned.*"

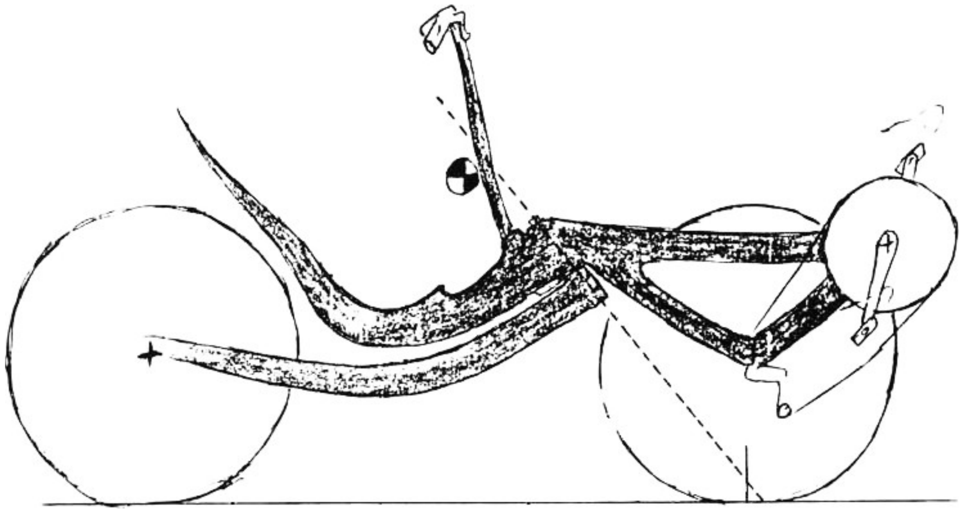

Figure A.45: Rear-steering recumbent design of Brown. The steering axis (dashed line) angle should be no less than 47° from the horizontal and the center of gravity (black and white quadrants circle) should be at or slightly behind the steering axis. [130]

A.37 199- De Weert 'ABT'

Fred de Weert built an RWSB around 1991 which he called 'AchterwielBestuurde Tweewieler' (Dutch translation of rear wheel steered bicycle) or short 'ABT' [85]. He reported about this bicycle in the dutch magazine 'HPV-nieuws' (volume 7, number 2, July 1991). The front wheel driven bicycle has a negative steering axis angle and a rather large negative rear wheel trail (figure A.46). The steering mechanism had a reversal mechanism, such that a handlebar turn to the right resulted in a steer angle to the right. This bicycle was ridable to a certain degree as reported by Erik Wannee who borrowed the bicycle [85]:

> "*It appears to be possible to ride such a thing, but it is very unstable. Steering requires much brute force, and while making a turn, it wants to steer stronger than you want it to do. So strong counter-steering is necessary.*"

Around 1995 Jurriaan Bol modificated the ABT in several ways (figure A.47) and reported about it in 'HPV-nieuws' (volume 11, number 3, May 1995). The motivations for building an RWSB are nicely described by Jurriaan Bol and in fact this probably describes why in general many enthusiasts take up the challenge of building an RWSB [85]:

> "*Many years ago I set out to design my own recumbent bicycle. Like so many others, when I started thinking and sketching I soon found that front wheel steering, that seems so natural in a upright-bike, generates a lot of problems in a recumbent. Holland is a great recumbent country so I was able to consult several experienced recumbent designers. They all told me 'we have tried it, but it just does not work, forget it!' When I asked them what they had tried the standard response was 'everything'. When I asked them why it would not work the answer was 'it's just not stable'. I know now that they where right, but at the time I just was annoyed, nobody seemed to know WHY it did not work. For after all, understanding why something does not work is the key to a solution. So the main motivation for my RearWheelSteeringBikes work was to try to prove them wrong, finding out 'why not?' would be the second best outcome.*"

Despite several attempts in improving the ridability of the RWSB by modifying it, Bol was not successful; His results with modifications always proved disappointing. He developed a theory where he distinguishes the riding of a bicycle in two phases: A rather static starting phase, and a dynamic riding phase. according to Bol, for one RWSB configuration, stability could never be reached in both these phases; An RWSB can be build that can be easily started, but not ridden safely when going faster, or

Figure A.46: The 'ABT' of Fred de Weert has a negative steer axis angle and negative rear wheel trail. [85]

Figure A.47: One version of the modified ABT by Jurriaan Bol. Here the headset is behind the rear wheel, the steer axis angle and rear wheel trail are both positive. [85]

an RWSB can be made that cannot be started from standstill, but is easily ridden at higher speeds. Basically, he acknowledges the existence of a critical speed above which some bicycles are stable, but he was not able to obtain this stable behavior with an RWSB [85]:

> "*Now, of course there are stories of RearWheelSteeringBikess actually being ridden. They are probably true. Actually, I drove one around the house block myself (the block was 500 m with lots of curves and bumps). But I only succeeded once or twice in doing the entire block without stopping. The point is, driving a RearWheelSteeringBike is like driving a one wheeler. Yes, it is possible, but no, it is no substitute for a real bike. You just cannot use it to travel from A to B.*"

Finally, a theory of Bol on the increasing of the turning radius during leaning and the difference for an RWSB as compared to an FWSB is noteworthy [85]:

> "*Also some behaviours in geometry that are felt in the dynamic stage are different. When it leans over in a corner a ForeWheelSteeringBike shifts the contact area between road and frontwheel forward. This increases the radius of the turn. (wider turn) Thus requiring the driver to steer more to maintain the intended radius. This is a process that no cyclist is aware of. What it comes down to is that a turning instruction is dampened. A ForeWheel-SteeringBikes does exactly the opposite this means that when you steer into a corner the minute you lean over the bike dives into the corner. If you are not trained to correct you simply fall. It takes all your attention to just make it through a corner.*"

A.38 199- Wannee 'ABT-2'

Erik Wannee saw potential in rear wheel steering for two wheelers, because it was implemented with succes on four wheeled vehicles. For example, the first four wheeled vehicle that broke through the sound barrier on land, the Thrust Super Sonic Car, uses rear wheel steering. As a two-wheeled rear wheel steering example Erik Wannee noticed the RWSB of De Weert (section A.37) and philosophized about advantages and dynamics of an RWSB on his website [85]:

Simple lightweight drivetrain Short chain to the front wheel.

Simple equal assemblies Possible simple implementing equal sized rear and front assembly without long chain trouble.

Unhindered steering Steering wheel (rear wheel) may be placed behind the shoulders where every desired steer movement can be performed.

Low air resistance Low placed driver seat is possible due to absence of chain to rear wheel.

Narrow fast fairing Legs can move close to the front wheel.

Exciting Excitement of exploring the unknown.

Although an RWSB might have some advantages, the behavior in steering of an RWSB is different than that of an FWSB. Wannee describes the (big) differences between the two bicycle types as he sees them, but seemingly seems to miss the point that one has to steer into the fall to recover from the fall. However, he acknowledges the difficulty in bicycle dynamics and that one straightforward physical explanation is hard to provide. He concludes that it is difficult to predict how all different steering behavior determining factors will work together in practice. With his theory in mind, he thought about improving the ABT of De Weert:

> "*The biggest disadvantage of the ABT lies in the fact that the long trail pulls the center of gravity so strongly to the wrong direction, while making a steering movement. In order to avoid that effect, the steering head could better be placed behind the center of the rear wheel. But then you create a negative trail, making the rear wheel unstable. So the question is: Is it possible to move the center of gravity of the bike to the right side, without creating a negative trail? That won't be possible with a single turning axis. But I considered that such could be possible with a complex movement. With that in mind, I designed a completely different prototype. I called it ABT-2* (figure A.48)"

Figure A.48: The ABT-2 of Erik Wannee. [85]

Wannee's ideas resulted in the creation of 'ABT-2' ('AchterwielBestuurde Tweewieler 2' Dutch translation of rear wheel steered bicycle 2). It is not that apparent what the trail and the steer axis angle of the ABT-2 are, but the working principle is described by Wannee. Sadly, the complex steering mechanism had not the desired effect and Wannee was not able to built a practical RWSB:

> "*This prototype had no steering head tube, but the front fork was attached to a ball-and-socket joint (left in top of the picture), while the movements of the fork were determined by two bars with screw-threads (bottom of the picture), connecting frame to both ends of the rear axle. The attachment-points of the bars could easily be displaced (because of all those Mecano-like holes). By replacing the bars with longer or shorter ones, their length could also be easily changed. The steering mechanism works through two separate short handle-bars on both sides of the seat (comparable to the system of the Jouta-tricycles) and a bar on both sides, connected to both sides of the top of the fork. This system makes possible a typical lemniscate ('8'-shaped) movement that cannot be made with a normal head tube.*
>
> *I would have thought that it should be a Columbus' egg, but after four months of intense trying and changing all parameters of the bike, I couldn't ride a single meter on it! Unfortunately, the movements of all parts are so complex that it is impossible to understand why this bike was unsuccessful. I couldn't solve a couple of fundamental problems with my 'solution'. Disappointing but instructive.*
>
> *Of all these things it may be apparent that until now, it has not been succesful to build a well-usable RWSB. Also from the theoretical view-point, there are some reasons why this principle will inevitably keep having big disadvantages: If you'd ride a RWSB and would have to avoid a suddenly opened car door, you can only steer with the rear wheel in the direction of that car. It would be very difficult to avoid a collision. If you would for any reason ride just along the pavement, it would be difficult to get away from it. Moreover, a bicycle is principally a vehicle that is permanently losing its balance. So it must be corrected continuously by steering. When losing your balance on a frontwheel-steered bicycle, you can turn the handlebars in a way that the front wheel moves directly under the centre of gravity of the bike. On a RWSB, it's just going the wrong way: As you want to pull the rear wheel under the centre of gravity, the bike turns the other way, thus increasing the dis-balance.*"

A.39 199- Reimers 'Kalle'

During the 1990's Hans-Ulrich Reimers ((von) Waldow) built several prototypes of a bicycle where the rider sits on the front frame and because of this rider position claims to have 'Hecklenkung' which is German for rear steering. It is a compact vehicle with small wheels and he called this type of bicycle the 'Kalle' [132]. This bicycle was patented in 1992 and does require the front wheel as the driven wheel, and the head tube placed slightly ahead of the seat around the middle of the bicycle [131].

In 1992 he had a ridable version, witnessing a movie on his site [132] in which he maneuvers the bicycle seemingly without any effort. Later, in 1995, he built version 3E (figure A.50) and even 3F (figure A.51). Reimers does not state much about the exact stability except for that it functions 'quite convincing' and that some theoretical calculations of a (unknown) university show that the bicycle is ridable. However, others also noted that the bicycle appears quite ridable [85] (although some are not convinced, see section A.66):

> "*...I found a photo on a german HPV home page of an RWSB, named 'Kalle', on which the driver seems to ride quite relaxed on a cycle-track. I could find this bike on two photographs in the (no more existing) magazine Bike Culture Quarterly (resp. no. 11, page 52 and no. 18, page 49), from which I took the following pictures:* A.50b A.51b. *Supplementary information from this magazine and readers of my page taught me that this bike is made by Hans-Ulrich Reimers from Reinickendorf (near Berlin, Germany). He builds them on custom order. It seems to be well rideable. The manufacturer claims speeds up to 40 km/h. The design resembles to a FlevoBike, but with the seat attached to the front part. Just like the Flevo, both wheels are sprung. Moreover, I remark that the rider is in a pretty vertical position, there is a positive steering head angle, and the steering head is far to the front. In contrast to the Flevo, I expect this bike will not be rideable without using your hands.*"

It has supposedly some advantages with respect to conventional bicycles [131]. Conventional bicycles have either a very straight sitting position or a leaned forward sitting position (for racing bicycles), giving either problems for an aerodynamic and weather resistant fairing or for head collision prevention respectively. Moreover, a conventional saddle has a small contact patch such that the pressure on a rider's buttock is considerable and might cause uncomfortable pain. Waldow's invention solves these problems by incorporating a comfortable and deep sit position which allows for better fore-aft-stability, aerodynamics and fairing, easy (dis-)mounting the bicycle by means of the handlebar, and the bicycle can be equal or smaller than conventional bicycles, making transportation easier.

Whether this bicycle is actually rear wheel steered is doubtable, because the front frame can be seen as the leading frame that determines the riding direction, since the front frame is said to be directioned with respect to the rear fork by means of a steering mechanism [131] [translation by P.H. de Jong]:

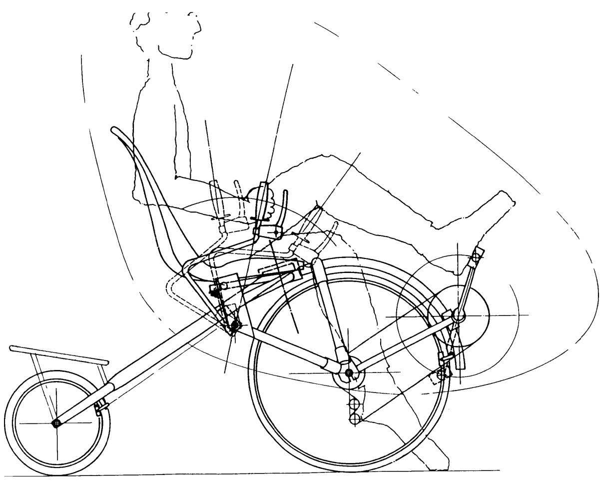

Figure A.49: 1992 Patent drawing of the Kalle with possible fairing. [131]

(a) (b)

Figure A.50: The Kalle-3E from 1995 with Hans-Ulrich Reimers (a) from the right side [132] and (b) from the right rear [85].

> "*... daß sich vorne ein Rahmen befindet, der sich durch ein Gelenk gegenüber dem nach hinten gerichteten Schaft der Hinterradgabel lenken läßt.*"

> "*... that a frame is located at the front, which can be steered by a steer joint opposite to the rearwardly aimed shaft of the rear wheel fork.*"

This becomes especially clear when looking at the wheel trails of the bicycle, i.e. the distances from the wheel contact points to the steer axis ground intersection [85]:

> "*... another special property of this bike: The steering head line points towards the ground in front of the front wheel. With some fantasy, you could say that both wheels have a positive trail. By the way, you can wonder if this bike can be really called a RWSB. You can also consider it as a FWSB on which the rider is actually sitting on the handlebars.*"

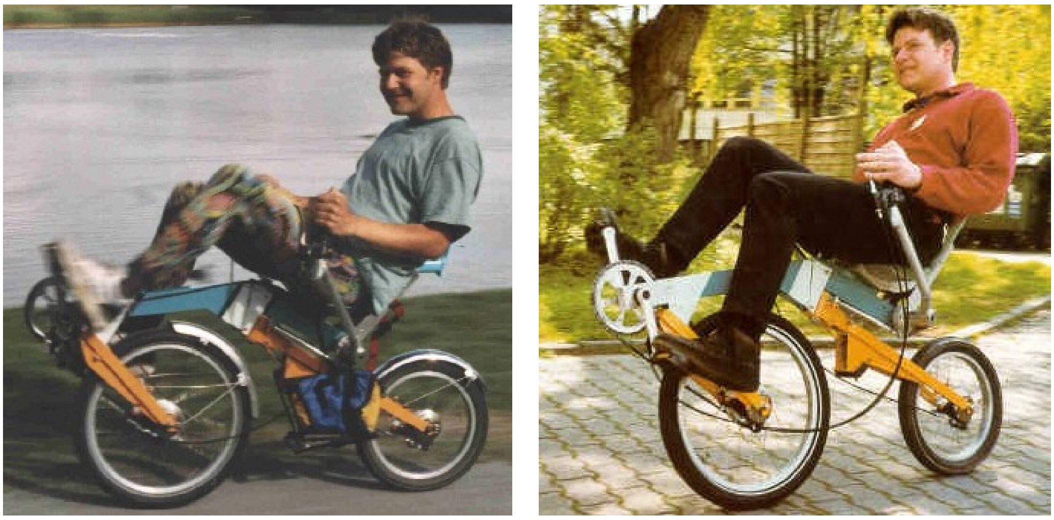

(a) (b)

Figure A.51: The Kalle-3F (a) [132] and (b) [85] from the left side.

A.40 1993 Schmidt 'Airbike'

The Airbike concept is designed by Uwe Schmidt and his brother in 1993 [133]. Staiger took on production of the bicycle and their version weighs about 17 kg, has 26" wheels and a suspension by means of a rubber block [134]. The bicycle can be folded at the central hinge such that several heights, and lengths as the wheel base and the trail, as well as the steer axis angle can all be altered. Once mastered, riding it is reported as quite comfortable [134]:

> "*Riding the centre steering principle has the whole drive train fixed to the front half of the frame which turns on a hinge just below the front end of the seat. So for steering, the legs of the rider have to move sideways which is quite an new experience for the beginner. Yes, there is an under seat handlebar, too, but you should not be surprised to find your legs much stronger than your arms. Thus, the airbike is in fact steered by the legs, the handlebars mainly being the support for brake handles and gear levers. Not quite what the average cyclist is used to.*
>
> *Very few cases have been reported of people who stepped on an airbike and were able to ride off without problems. However, any average mortal person can also learn how to ride the bike, it's just a matter of determination and patience, to different degrees. The latter usually is counted in days or weeks. After having gained full control over the machine (we are talking months now), the ride on an airbike is said to have a kind of metaphysical quality which more than rewards the candidate for all the pain and suffering he has gone through on his way towards perfection.*
>
> *...A sense of gliding over the street tarmac similar to flying is often reported.*"

Figure A.52: Airbike from around 1995 made by Staiger. The steering axis is aligned with the diagonal part of the front frame. [134]

A.41 1993 Hofman & Bakker 'Swing Chinkara'

The Swing Chinkara is a bicycle from 1993 created by Rob Hofman and Marnix Bakker in Delft, the Netherlands [118]. Swing Cycle in the Netherlands produced the Chinkara which can be seen as an evolution of the Flevobike [135]. The rider sits on the rear frame and the steer axis intersects the ground near the driven front wheel contact point. Dave Ductor described his experience with this bike in Recumbent and Tandem Rider Magazine [135]:

> "*...I used the bike to run errands, to go out to eat, and to visit friends. Several hundred miles later, it has become a little easier to ride, but it still requires a fair amount of effort to keep upright.*
>
> *Should a bicycle require such an extensive training period? Almost all of us learned to ride as kids, and most people can jump on a recumbent and ride without too much trouble. I have read that the Flevobike front drive concept can be easily mastered, but in the case of the Chinkara it seems that it will be a while longer before I can ride it without hands. I have since seen it done though, and was very impressed!! I suspect that for most people, learning to ride a bike like the Chinkara is somewhat improbable. For some, perhaps impossible. But it can be done! And I am left wondering how long it will take?*
>
> *Is the front wheel drive system the holy grail of recumbent design? There have been several front wheel drive recumbent designs that were based on a more conventional geometry, with a headtube and a steerable front fork. And while the front wheel drive concept is interesting from a technical perspective and may have some merit in practice, I am not sure that the Chinkara represents a step forward for recumbent design. Calling it a creative breakthrough may be more appropriate, as it does demonstrate what is possible in steering geometry. But I think that the Chinkara, and by association the Flevobike front drive concept, probably isn't a very good choice of bike for novice riders, barring any significant design refinements that may have taken place. Flevobike fans are an enthusiastic bunch though, and there is a fan site. At the same time I suspect that even veteran recumbent riders can still look forward to an intense learning experience with such a design. And for most of us, isn't that part of the fun?*"

Figure A.53: A sideview of the 1993 Swing Chinkara. [135]

A.42 1993 Riggenmann 'Liegefahrrad kettenlos frontantrieb'

Konrad Riggenmann patented in 1993 his 'Liegefahrrad kettenlos mit frontantrieb' (chainless recumbent bicycle with front drive) [136]. He saw advantages in the reduced air drag of a recumbent bicycle, were it not that popular recumbent bicycle designs have long, pollution-sensitive and high-friction low hanging chains running from the bracket at the feet to the driven rear wheel. Moreover, the relative long wheel base makes larger steer movement for balancing necessary, as well as that it requires a heavier frame coming at the cost of lower ridability.

Therefore, Riggenmann introduces a bicycle with direct-drive on the front wheel, just as in classic penny-farthing bicycles, with the difference that Riggenmann's bicycle has two equal-sized standard 26"-28" wheels. The rear wheel is steered with the handlebar located underneath the seat and connected with the rear wheel with a cross-linkage that makes sure that a clockwise handlebar turn results in a clockwise bicycle turn. Riggenmann's design stands or falls with the introduction of his mechanism in the bracket that supplies free-running and a transmission ratio, or else the bicycle will have the disadvantages of the penny-farthing without its benefit of high speed cycling. He does not expect the rear steering to be a problem in terms of stability, but rather sees a special advantage in it [translation by P.H. de Jong]:

> "*Die Steuerung über das 'nachlaufende' Hinterrad neigt (etwa auf stark gekiesten Wegen oder im Schnee) weniger zum 'Ausbrechen' als eine Vorderradlenkung.*"

> "*The steering of the trailing rear wheel reduces, e.g. on heavy gravel paths or in the snow, the tendency of the bicycle to break out.*"

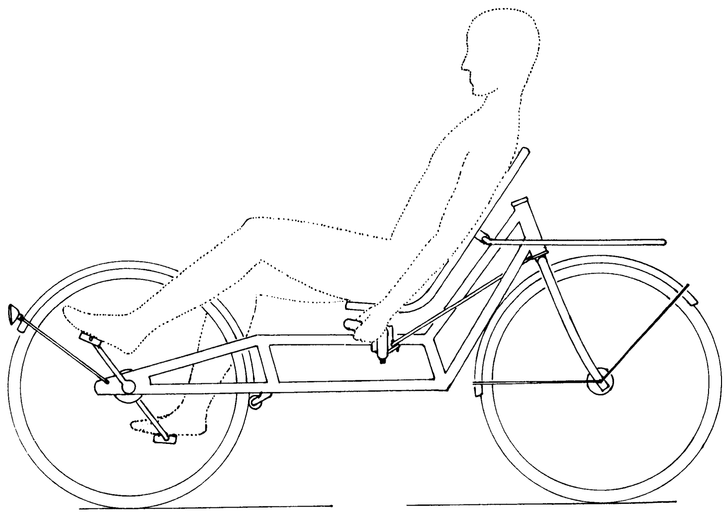

(a)

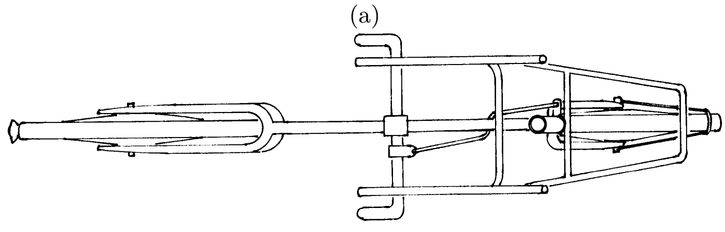

(b)

Figure A.54: The 1993 'kettenlose Liegefahrrad' (chainless recumbent bicycle) of Konrad Riggenmann seen from (a) the left, and (b) from above. [136]

A.43 1994 Langen 'Two-Wheeled Vehicle'

In 1994 Christianus P. Langen got a patent for a 'two-wheeled vehicle', or bicycle, he invented for Langenberg B.V. in Cuijk, The Netherlands [137]. According to Langen, conventional bicycles are of rather large dimensions such that transporting them in the trunk of a car is difficult. Folding bicycles that should solve this problem are generally unpleasant to ride due to the small wheels or folding them involves a lot of work. Langen's invention obviates these drawbacks of folding bicycles. Therefore, he implements a 'reversal of wheel function' where the driven wheel is underneath the handlebar and the steerable wheel underneath the seat, making a small wheel base bicycle with considerable large wheels possible.

The steerable rear wheel has a zero steer axis angle and no trail. The foldable hinged handlebar is connected to the rear wheel sub-frame with a coupling mechanism in such a way that a clockwise handlebar turn results in a clockwise bicycle turn. Furthermore, the direct drive of the front wheel requires a transmission ratio to be ridden comfortably, which is provided by a specially designed pedaling mechanism with crank arms complemented with 'contoured gear', making the pedals rotate with a different rate as the crank axle. Langen does not state anything about the ridability of the bicycle.

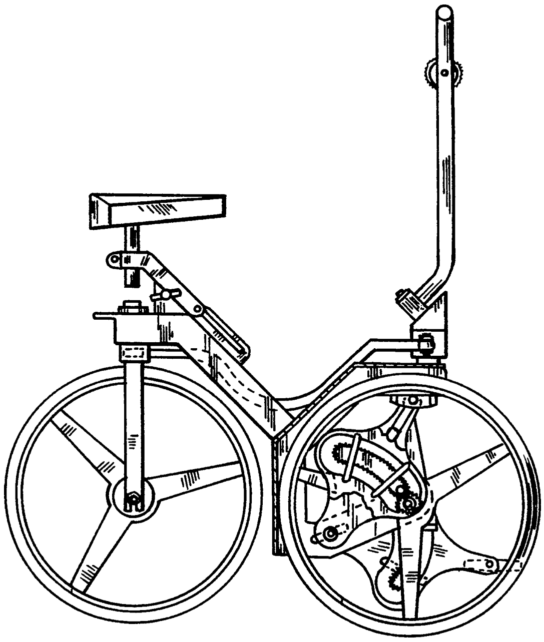

(a)

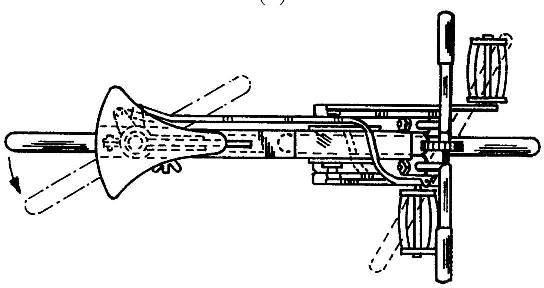

(b)

Figure A.55: Langen 'Two Wheeled Vehicle', seen from (a) the right side, and from (b) above; forward riding is to the right in the drawings. [137]

A.44 1995 Knoop 'Slingerding'

Sacha Knoop (building recumbent bicycles from 1985 [138]) built an RWSB around 1995 with front wheel drive, and called it 'Slingerding'. As it appears in figure A.56 the bicycle has a vertical steer axis which intersects the ground approximately in the middle between the front and rear wheel contact point. It was possible to ride the bicycle, but it occasionally shows dangereous unexpected behavior [85] (Summary of 'Van Slingerding tot Tweetwee, nogmaals achterwielbesturing', no. 3, pp. 12, May 1995, in Dutch):

> "*Sacha Knoop describes an RWSB, called 'Slingerding' (swinging thing). This vehicle has an even longer trail than Fred de Weert's ABT. You can't almost talk about rear wheel steering; it is more like centre steering. The 'head' tube is placed just under the seat. But the principal difference between this bike and an (also centre-steered) FlevoBike is, that in the latter one, the seat is attached to the rear part. It turned out to be possible to ride on it, but while riding at higher speeds, suddenly very hazardous things can happen: You can literally be launched off. And with this bike, too, you continuously have to countersteer very strongly. (That's why there are such long handlebars.) Very fatiguing and unpractical.*"

(a) (b)

Figure A.56: Knoop's 'Slingerding' (a) without rider, and (b) while being ridden. ('Photos taken from HPV-CD-ROM 1997' [85])

A.45 199- Gustavson 'Idea of rear wheel steering'

In the 1990's Åke Gustavson made had an 'idea of rear wheel steering' for bicycles originating from his interest for human powered machines and especially bicycles [139]. He argues that such a bicycle can be low and compact with a short chain, because one can drive the front wheel. Due to this properties an RWSB should also be easy to be made faired (covered, e.g for air drag reduction or bad weather protection). For his prototype (figure A.57a) he basically used a fore-aft flipped conventional bicycle configuration and he applied some shifting in wheel and rider position. The result looks somewhat as Zaidman's bicycle. It turned out that he was not able to ride this bicycle at all. To be able to learn the bicycle, he placed some helping wheels on it (figure A.57b), and he made some progress in the ability to ride it [139]:

> "*To tell the truth: I have not been able to ride it at all!*"

He theorized also that bringing the steer axis/ground intersection more to the front and flipping the steer axis angle such that it resembles a more conventional bicycle configuration could benefit the ridability. The rider is then still placed on the front frame, which would still leave it an RWSB or make it a 'hybrid'. However, before building a bicycle with this adjusted steering axis he concluded, backed-up by Erik Wannee, that it would also be very hard to ride, and in effect he never built it.

(a)

(b)

Figure A.57: Gustavson's prototype of his 'idea of rear wheel steering' on a bicycle (a) seen from the left and (b) from the right front. Forward riding direction is to the direction of the pedals with the steering mechanism coming straight from a conventional bicycle, but placed reversely. Gustavson included help wheels in order to help learning to ride the bicycle. [139]

A.46 1995 Suijker 'Wave'

The 'Wave' (see figure A.58) is a bicycle from around 1995 by Erik Suijker who made it as final examination project at the Academy for Industrial Design in Eindhoven, The Netherlands [140] [118]. The steer hinge of the bicycle is probably located at around the front of the seat with a steer axis angle direction as on a conventional bicycle. The frame looks like that of the Chinkara (see section A.41) and is also made of stainless steel tube. The wheels are standard 26" and the bicycle weighs 17.5 kg. A gas strut (much alike those in office chairs) is used for continuous height adjustment and does also act as shock absorber. This height adjustment makes it possible to change the bicycle from a racer (low position) to a slower urban bicycle (high position). Moreover, the bicycle is foldable to make transport easier.

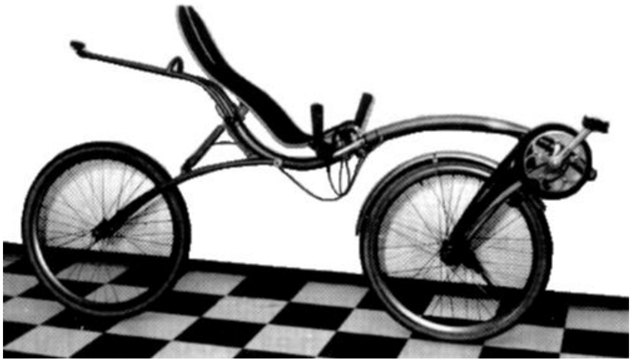

(a)

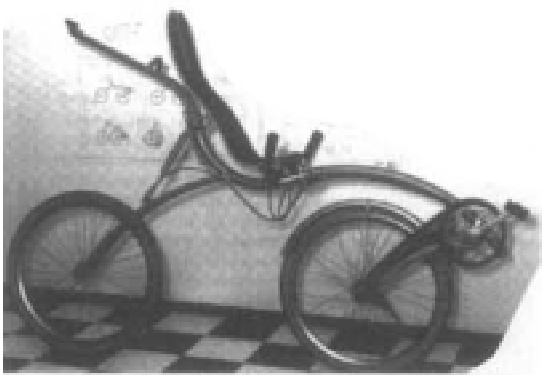

(b)

Figure A.58: The 1995 'Wave' of Erik Suijker seen from the right in (a) a low position [118], and (b) a high position [140]

A.47 1996 Summers 'Vehicle'

Thomas W. Summers received a patent in 1996 for his ideas on incorporating rear wheel steering on single track vehicles [141]. He assumed rear wheel steering beneficial for making high speed 'tight' turns. His rear wheels steered concepts, both a motorcycle (figure A.59a) and a bicycle (figure A.59b), have a steer axis pointing downward to the front and intersecting the ground at the midpoint between the two wheels. By doing this, Summers claims that both wheels follow the same track during a turn, giving the vehicle better turning qualities [141]:

> "*...the invention provides at least a single track vehicle which can be driven through turns at higher speeds but with the same safety factor as conventional single track vehicles, or at the same speeds but with increased safety. Power is applied to a traction surface substantially in the turn direction without skidding or scuffing as the front and rear tires track the same path.*"

A crossed linkage is used between the handlebar and the rear wheel assembly in order to make a clockwise handlebar rotation result in a clockwise bicycle turn. To improve steering of single-track vehicles, Summers also presents improvements of this handlebar mechanism in order to prove bicycle handling. One of these is the elliptical chain wheels used in the steering linkage in order to make the steering ratio variable for different steer angles.

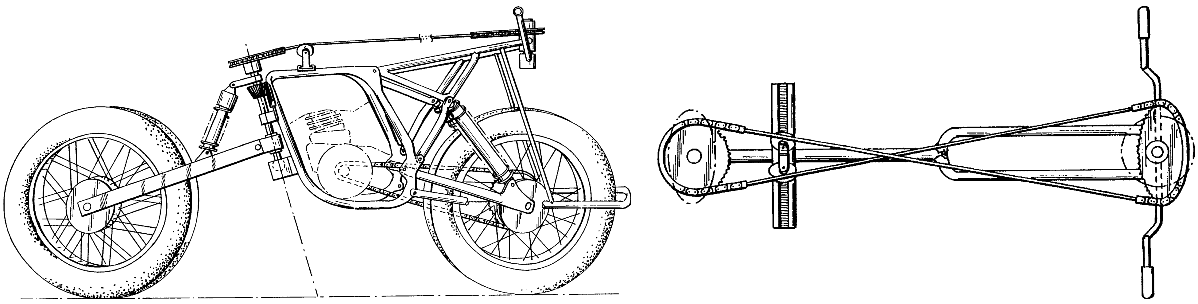

(a) (b)

Figure A.59: Summers' motorcycle (a) seen from the right side and (b) a top view of the crossed steering linkage with some some motorcycle parts left out for clarity. [141]

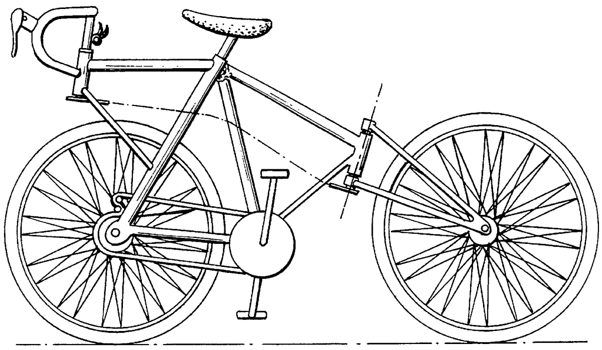

Figure A.60: Summers bicycle with rear wheel steering seen from the left. [141]

A.48 200- De Rooij 'RWSB'

In 2001 a notion is given on the rear wheel steered bicycle of Kees de Rooij [85]. This bicycle (figure A.61) has a back- and downward pointing steer axis intersecting the ground slightly in front of the rear wheel. In contrary to many other examples, this bicycle has no steering reversal, such that here a clockwise handlebar turn results in a counter-clockwise bicycle turn. However, the bicycle is still ridable [85]:

> "*On CycleVision 2001, I saw this RWSB with it's rider: Kees de Rooij. This bike has about the same design as Fred de Weert's ABT. Only this bike has no steering reversal mechanism, so that it steers towards the opposite direction. The riding behavior is comparable. As long as the excursions of the handlebars remain moderate, everything goes well. But sometimes a strong steering movement is necessary. Kees had ridden several hundreds of kilometres on it.*"

Figure A.61: De Rooij's rear wheel steered bicycle. [85]

A.49 200- Zaidman 'RWSB'

It was noticed in 2001 that Mati Zaidman performed some experiments with rear wheel steered bicycles in Israel [85]. The steer hinge is created by using the complete head tube and front fork of a conventional bicycle and placing this reversed at the back of a newly built bicycle (see figure A.62). Therefore, the steer axis of his prototype is angled such that it points downwards to the back and it intersects the ground at a similar distance from the steered wheel contact as on a conventional bicycle, but now behind it in stead of ahead of it. However, until the moment of report is was never been successfully ridden [85].

Figure A.62: First prototype RWSB of Mati Zaidman, seen from the right side. [85]

A.50 2002 Grimm 'SNAIX'

German architect/designer Friedrich Björn Grimm invented the SNAIX fitness bicycle in 1996 [142] and received a patent for it in 1998 [143] [144]. The latest version of the bicycle is from 2002. It can be imagined as a conventional bicycle with the steer axis shifted such that it now has a vertical steer axis which is located close to midway between the rear and front wheel contact points (figures A.63 and A.64). Just as for a conventional bicycle, the rider sits on the rear frame with the driven rear wheel, and the handlebar is attached to the front frame. The SNAIX bicycle evoluted from a hobby project into a very healthy way of transporation due to the movements it forces on the rider's body, but at the same time it is not safe for road use [142]:

> "*In the beginning the SNAIX neuro bike was a result of plain interest in geometry and bikes. But soon after it turned out that its most important effects are the neuronal (coordination) and muscular training caused by the special geometry.*
>
> *As far as we know now, it is the only training gear that combines prevention, therapy and medically correct training with lots of sport and fun indoors and outdoors. Meanwhile there is lots of proof that the holistic SNAIX training pattern, that evolved from learning with the bike, is a simple but effective answer for the growing number of health problems like back pain, overweight and motor–neuronal disorders.*
>
> *. . . There is a pivot right in the middle between the two wheel axles which causes the frame to bend left or right in curves. This special movement pattern is the 'mechanical core' of all SNAIX training gear.*
>
> *Because of its special geometry the SNAIX neuro bike can only be steered with body, saddle and rear wheel. It has a low rolling resistance, high adhesion in curves and it is foldable. It was constructed to to be a effective medical training machine that should not be used in traffic for safety reasons.*"

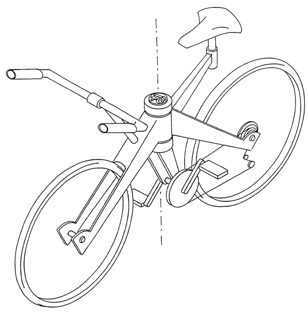

Figure A.63: Patent drawing showing Grimm's 'SNAIX' bicycle from the front left. [143] [144]

(a) (b)

Figure A.64: Grimm's 'SNAIX' bicycle (a) Prototype 1 from around 1997 seen from the left, and (b) Serial model 2 from 2002 seen from the right. [142]

A.51 2003 Efflandt 'Rear wheel steering bicycle'

Darrold Efflandt received a patent for his 'chain driven front wheel drive and rear wheel steering bicycle' in 2003 [145]. He invented his bicycle to provide 'superior maneuverability, handling, and stability' as compared to conventional front wheel steered and rear wheel driven bicycles. These conventional bicycles have the front wheel sharing both the main steering and the main braking functionality, which tends to make a bicycle perceptible to uncontrollable skidding under heavy braking. Moreover, rear wheel drive in stead of front wheel drive makes it harder to ride over obstacles directly ahead of the front tire, e.g. a curb, without using a 'hop'. However, Efflandt reasons that, although conventional bicycles can thus be improved by implementing rear wheel steering and front wheel drive, it is beneficial to keep the conventional familiarities of a bicycle, i.e. 'seating position, pedaling angle, overall geometry etc.'. This familiarity of a bicycle makes it 'here to stay', because people are used to it and interchangeable off-the-shelf bicycle components are readily and generally cheaply available for such conventional bicycles.

Therefore, Efflandt proposes a design as in figure A.65, which is basically a reversely ridden conventional bicycle with only minor changes in the construction. The driven wheel is now the front wheel, but still a chain transmission is used. The steer axis passes through the rear wheel in an exactly mirrored way as it passes through the front wheel of a conventional bicycle; it points downwards to the rear and intersects the ground behind the rear wheel contact point. The handlebar is connected to the rear wheel by steering wires that are crossed underneath the saddle, such that a clockwise steering motion results in a clockwise bicycle turn as displayed in figure A.65b.

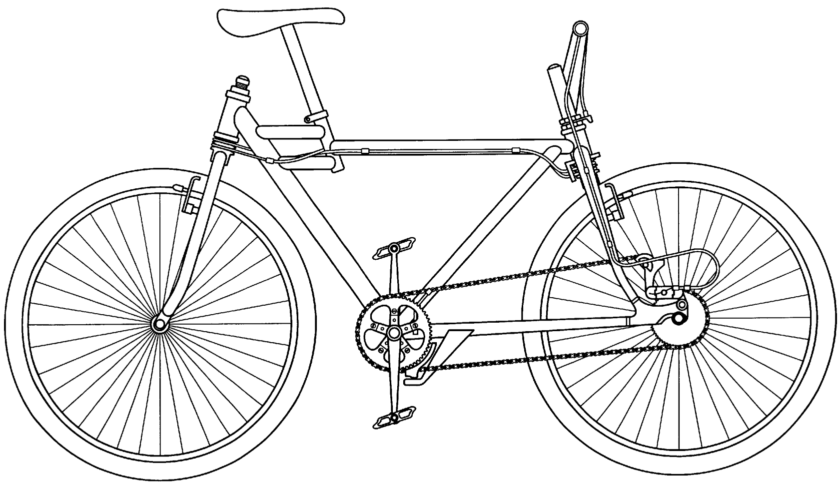

(a)

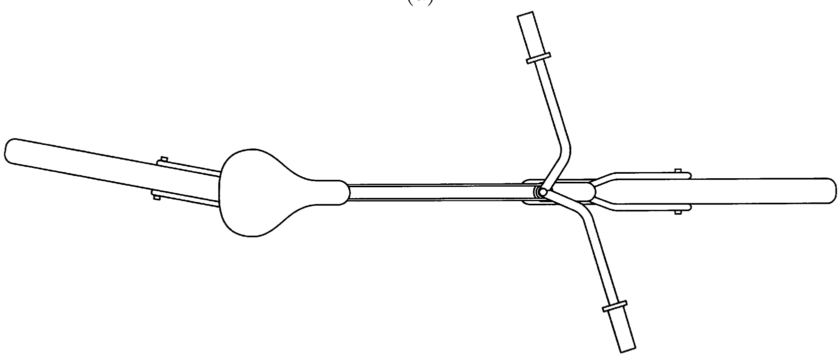

(b)

Figure A.65: Efflandt rear wheel steering bicycle from 2003 (a) from the right, and (b) from above with nonzero steer angle. [145]

A.52 2003 Mages 'Python'

Jürgen Mages built the first Python in 2003. It looks like the Flevobike (section A.30), Airbike (section A.40), and Chinkara (section A.41), but differs in that the steer axis intersects the ground in between the two wheels instead of in front of the front wheel (front wheel trail of 0.3 m, see figure A.66). It has a wheelbase of 1.29 m and a steer axis angle of 65∘. Reportedly, the Python's ridability is reasonable [146]:

> "*Some people asked me if the python is steerable at all because of its negative trail. In general, bikes with NT are not stable, especially at high velocities or when applying the front brake. But the steering geometry of the python is different, because the construction behaves like a "hanging pendulum". This means that the drivers weight forces the front part into a centered position, thus stabilizing the system.*
>
> *. . . When riding a bike, it is good to have steering feedback and a force that pulls the steered wheel back into a centered position. In normal bikes this centering force is realized by the Caster Effect caused by the pivot angle and the positive trail. This effect is zero when the bike is stopped and it is increasing with the speed. When trying to build a very low center-steered recumbent one has to face the fact that, with the steering pivot being beneath the seat, one has to implement a very shallow pivot angle to achieve positive trail. This shallow angle (around 30 deg) has big disadvantages: First the steered front wheel wants to tip into the curve by its own weight (Wheel Flop). A strong steering damper is needed to bring the wheel back to the center. Second the bike is very hard to maneuver because of its huge turning circle. So what to do? Allowing a negative trail and thus obtaining bigger pivot angles resolves the mentioned problems. But what about the centering force? The caster effect is gone but another force comes into play now: By turning the wheel, the pivot rises and as the rider sits above the pivot he is also lifted. As the lowest pivot position is the centered wheel, it is pulled back automatically (by gravity) after each steering action. This Seat Rising Effect is present at any speed and also when the bike is stopped.*
>
> *. . . Meanwhile* (June 2003) *I spent more than 2500 km on the python and I really love this bike. I use it daily for commuting, recreation and even in urban traffic. And still have many plans with it . . .*"

Figure A.66: The Python 1 from 2003. [146]

A.53 2004 Flatmo 'Badass'

Artist Duane Flatmo showed in 2004 a bicycle with rear wheel steering [147] [148] [149] [150]. His RWSB has a small rear wheel and a large front wheel (figure A.67). The steer axis intersects with the ground inbetween the two wheel contact points and the center of mass is positioned horizontally close to the front wheel contact point. Moreover, the center of mass is placed rather high. This all comes close to a self-stable RWSB configuration as found and described by Kooijman *et al.* [15], Broxterman *et al.* [17], Van Dijk *et al.* [18]. The handlebar is connected with wires to the rear wheel in such a manner that a clockwise handlebar turn results in a rightward turn, as can be seen in some videos [149] [150] [147].

The videos show that the bicycle is pretty well ridable [147] [148] [149] [150] and makes one wonder if this is a close to ideal configuration for rear wheel steering [85]:

> "*On the 2004 DaVinci art festival the Kinetic Sculpture artist Duane Flatmo was tooling around on this RWSB quite well. Steering is done via steel cables. Actually the position on this bike is so vertical that it doesn't take much to go forward over the front wheel, so it can be basically seen as an RWS unicycle. This brings me to the thesis that rear wheel steering is easier if the riding position is more upright, and/or more towards the front wheel.*"

And the bicycle leaves people in awe, and making them wonder how it exactly works [151]:

> "*How is this possible? Well, the short answer is that Duane didn't know it was impossible when he built the bike. Like when the Coyote didn't fall off the cliff until he looked down. Bikes work this way. But I suspect the answer is 'tuck'. I learned from an old pennyfarthing maker that one of the secrets that makes an ordinary ride is 'tuck', the proximity of the rear wheel to the front. I suspect that he's brought the rear wheel in close enough that one can compensate for the bike's squirrelliness by simply turning into the direction of the fall.*"

(a)

(b)

Figure A.67: Duane Flatmo on his (decorated) RWSB (a) from the right [85] (Erik Wannee received this picture from Paul Hanrahan), and (b) from the left with Flatmo actually riding it by making tight counterclockwise turns [147]. Steering is done by means of small handlebars.

A.54 2004 Dechenne 'Moan'

Belgian Laurent Dechenne made a bicycle in 2004 based on the Python of Jürgen Mages (see section A.52) with the inclusion of a four bar linkage idea of Michael Rienstra [152]. Dechenne claims that the four bar linkage allows for rear steering ('direction arrière') while leaving a positive front wheel trail with a conventional angle. The aligning of all parts took a while and the bicycle turned out rather heavy, because Dechenne wanted to make sure that the bicycle would be stiff and would not break. An early version of the 'Moan' (figure A.68a) left room for improvement:

> "*Just back from an empty parking lot... verdict 7 meters for a half turn... about the same as for a python... still acceptable as I do know I can improve this. The limit for the moment is not caused by the 4 bars itself, but by the handlebar which bangs onto the 4bars linkage, as they come towards each other with the inversion. I took my three wheels, 28", 26" and 20"... well no noticeable difference... For the rest, apart from this fucking* (sic) *right pull, (I have to pull on left... I'm not dyslexic...) it rides straight pleasant... Now I'm fully motivated, going to re-cut again the frame to solve this 'right pull', take advantage of the re-cut to lower down the 4bars and keep it flat... I will have maybe to look into the trail angle, I think for the moment it's nearly positive... going to study closely a lighter steering linkage... The Moan re-cut and re-welded with the 4 bars lying well flat.*
>
> *I've tested, by putting on the 20" wheel, an increase of positive trail...and the steering, with this set up, remains light up to bigger steering angles. With the '4bars linkage', the virtual pivot moves, causing a smaller positive trail as the steering angle increases... up to a point where it gets negative. As the trail gets negative the steering gets heavy. With the set up '4bars' lying flat, and 700 wheel, the trail is positive by 3 cms only...*"

With the 'Moan z' Dechenne was able to solve some of the issues:

> "*as a result, I've redrawn this set up... by tilting the pivots, I tilt the trail angle too, and I get back a positive trail with the 700 wheels, similar to the one I had with the 20" wheel. All parts are cut out, works in progress... It's a pity: this sketch looks like to one of the very first I did for the '4bars', that I put aside trying to do simpler.*
>
> *Here is the set up which solves the stability matter* (figure A.68c)*, allowing enough trail, as it looks now. I've ridden once again on the empty parking lot. You've got to get used in the beginning to the odd relationship between the handlebar's angle, the angle formed by the wheels, and to a feeling of balance somewhat different, but it is quite doable; it's just a 'the first 3 minutes to get moving' matter. The good side of the empty parking lot is you can, at the start, focus on the balance only, as a result it gets in much quicker. For now all the little subsidiaries matters are pending... the first one: the handlebar is too low and touches the ground on a turn a bit quick or sharp. I'll have to find out bits and pieces to put on pulleys and cables instead of gears.*"

(a) (b) (c)

Figure A.68: The 'Moan' of Dechenne (a) as an early version with (b) the four bar steer mechanism with the transmission system ('système de transmition de la direction'. (c) The 'Moan z' which solved stability issues of the early versions. [152]

A.55 2005 Ungar and Goczey 'Magic wheel' ('Gauswheel')

Hungarian Soma Gabor Ungar and Andras Goczey invented a gadget-like 'Foot-propelled hobby and/or sport device without handlebar' around 2005 [153], also known as 'Magic wheel', or 'Gauswheel' (although Gauswheels are sometimes also reversed ridden Magic wheels, i.e. smaller wheel ahead) [154] [155] [156] [157] [158]. It is a vehicle that is more of a handlebarless scooter than a conventional bicycle with saddle, handlebar, and drivetrain (see figure A.69). The rider has to stand on it and propel it by pushing off on the floor with one foot while steering is done by upper body motions. However, it does fit the technical bicycle definition of two wheel/frame assemblies that can rotate with respect to each other about a rotational steer hinge.

The vehicle has a vertical steer axis slightly ahead of the small rear wheel such that the steer axis intersects the ground also slightly ahead of the rear wheel making it a caster wheel. Probably, this vehicle requires some training time, but videos show that it is possible to ride it with success [154] [155] [156].

(a) (b) (c)

Figure A.69: Ungar's and Goczey's 'foot-propelled hobby device' (a) as right side view patent drawing [153], and (b) a commercial 'Magic wheel' from the front right [157], and (c) being ridden [158].

A.56 2005 Killian ‘Sideways bike’

Michael Killian made a symmetric bicycle with two steer axes and called it the ‘Sideways bike’, or ‘Snowboard bike’ [159]. He received several patents for his single-track vehicles with sidewards rider, with a bicycle patent in 2005 [160] [161] [162] [163]. The bicycle has two independent steer axis and has a saddle in the middle (see figures A.70 and A.71). The first version of Killian’s bicycle, the ‘Terrible two bicycle’ has a saddle such that the rider is facing in longitudinal direction of the bicycle, and this bicycle was already quite satisfactory [159]:

> “*Introducing a new bicycle invention by myself, Michael Killian. This bicycle is ridden forward and is balanced by using human Left to Right balance. This bicycle uses independant (non linked) Front and Rear steering. The ride is very wavy sort of like skiing with a capacity to drift to the right or left. The front and rear steering makes the bike much more maneuverable than a single steer bike. Your hands are by your side and you don’t exert a lot of pull on the steering. Its sort of like riding a horse where you cannot lean on the reins but all body movements come out of your seat and saddle. The saddle is necessarily a unicycle saddle (You would slip forward off a regular bike saddle).*”

A later version called the ‘Snowboard bike’ has the rider facing to the side such that this is a true ‘Sideways bike’, which can even function as snowboard trainer[159]:

> “*This Snowboard Bicycle or Snowboard Stance Bicycle can be used as a Snowboard Trainer. The rider’s body is positioned in Regular Stance. Riding this bicycle exercises the balance detection and correction mechanisms that a Snowboard Rider would use.The more you isolate and exercise this particular balance; the better you will snowboard.*”

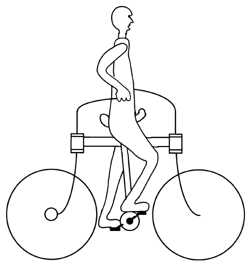

Figure A.70: Patent drawing of the bicycle of Michael Killian.

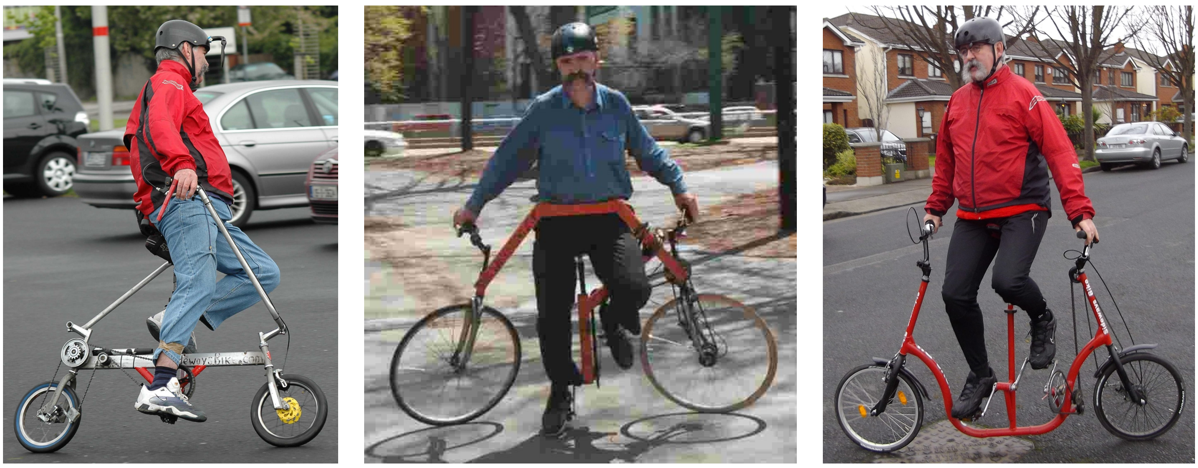

(a) (b) (c)

Figure A.71: Michael Killian on his ‘Sideways bike’ in different versions: (a) The terrible two bike, (b) the original sideways bike, and (c) the snowboard bike in 2011. [159]

A.57 2006 Gaea 'Rotative frames bicycle'

In 2006 Albert J. Gaea received a patent for his 'Bicycle having front and rear rotative wheel frames with actuatable means for engaging and disengaging the rear wheel frame rotation' [164]. Gaea uses a conventional bicycle head tube with front fork and attaches this to a horizontal 'swinger' (see figure A.72). On the rear end of this swinger a second head tube is introduced that holds a rear assembly with saddle, wheel and drive train. It is thus not a bicycle in the technical sense that it has only two wheel/frame assemblies connected by a steer hinge, but this vehicle has three frames with two steer axis.

When the foldaway bar on the 'swinger' is put into the rear frame, the rear frame rotation with respect to the 'swinger' is locked and it becomes a true bicycle with only one steer hinge. When unlocked, the rear assembly provides a second axis to steer about where the saddle turns along with the rear assembly to exercise control. The front steer axis is placed in such a way that it gives an angle and trail similar to that of a conventional bicycle, and the rear steer axis is vertical intersecting the ground ahead of the rear wheel.

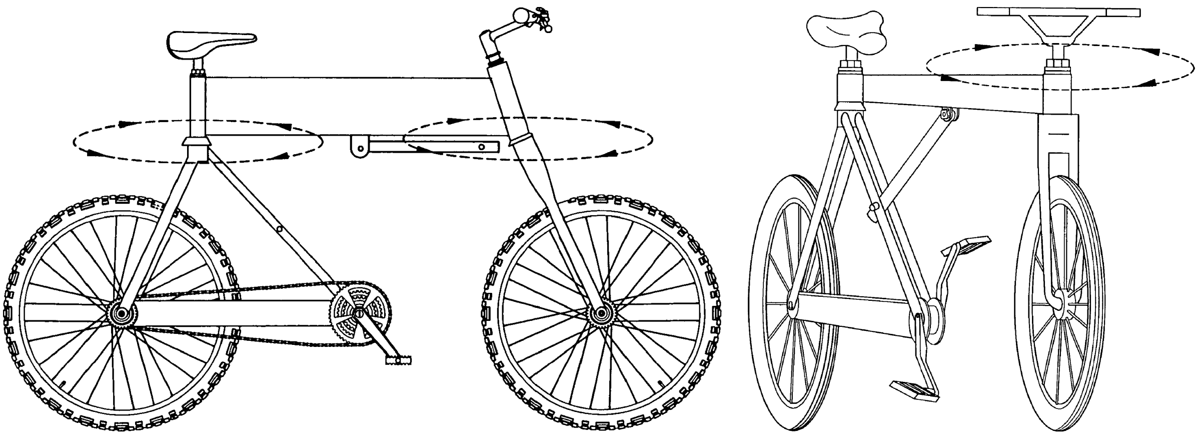

(a) (b)

Figure A.72: Gaea 2006 'rotative frames bicycle' (a) seen from the side with unlocked rear assembly, and (b) seen from the front right with locked rear assembly. [164]

A.58 2007 Zurlinden 'Legato GT'

Graduate Mathew Zurlinden from Detroit designed his recumbent bicycle 'Legato GT' in 2007 [165] [166]. The bicycle has two 20" hubless wheels and is driven by a continuously variable transmission at the front wheel (see figure A.73). The steer axis is located close to the rear wheel and is angled such that it points down to the rear and intersects the ground slightly ahead of the rear wheel. It is uncertain whether this bicycle is actually built and how it rides.

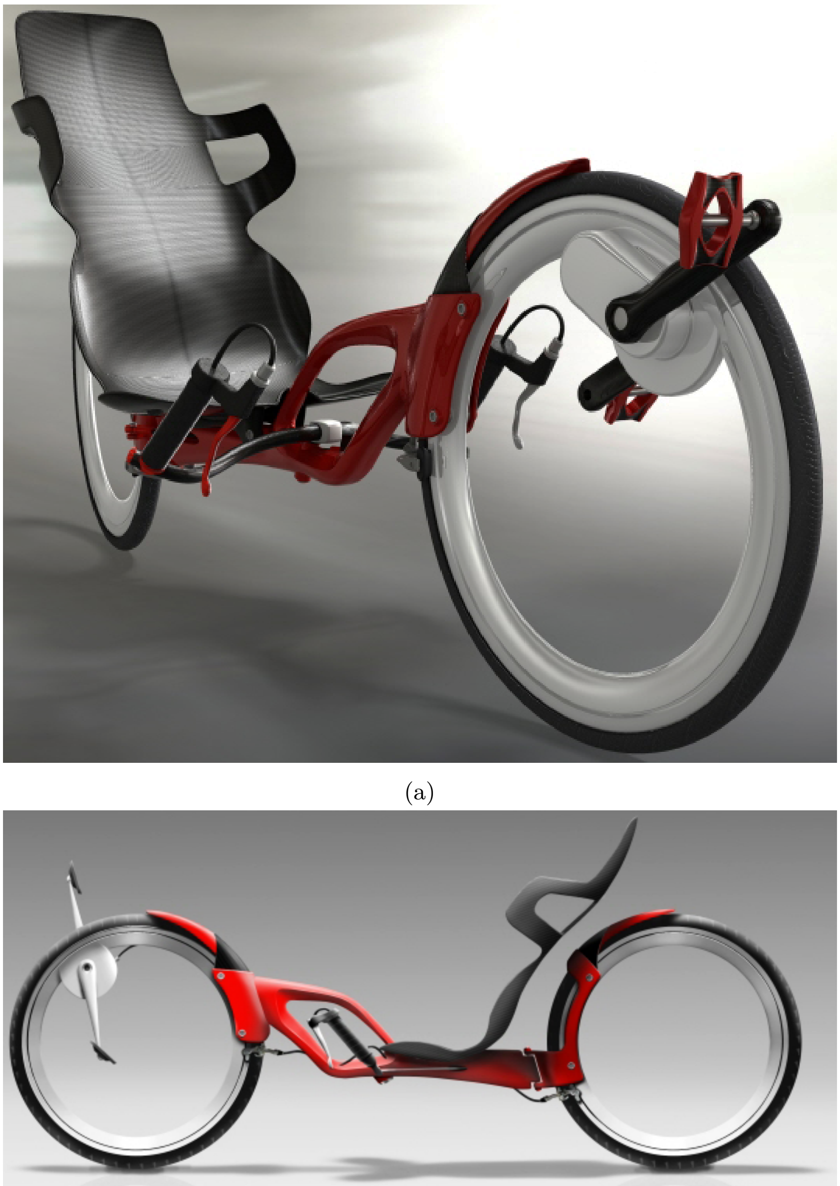

(a)

(b)

Figure A.73: Zurlinden's 'Legato GT' (a) seen from the front right, and (b) from the left side. [165]

A.59 2008 Renner 'Front Wheel Drive RWS Recumbent'

Dennis Paul Renner created at least two versions of his 'Front wheel drive rear wheel steering recumbent' bicycle design from somewhere before 2004 to 2008 [167] [168] [169] [110]. The RWSBs were created to prove that it could be done, but riding is not per definition better than riding a front wheel steering recumbent. However, in his philosophy a recumbent bicycle with rear wheel steering and front wheel drive can have benefits at the price of only small disadvantages [167]:

> "*Many of you might wonder why build a recumbent with front wheel drive. Why not stick with rear wheel drive? Well front wheel drive provides many advantages. First is that it requires much less chain than a normal recumbent. Second is it reduces weight by needing less chain and chain guides. Third in slippery situations like sand or an oily road the front wheel pulls the bike through the mess which is easier than the rear wheel trying to push the bike and rider through slick situations. The same holds true in cars.*
>
> *So if front wheel drive is so good why do most bikes have rear wheel drive? Well there are more and more recumbents entering the market all the time with front wheel drive. The difference between my design and others is that my design steers with the rear wheel. Most other front wheel drive recumbents still steer with the front wheel. Others like the Flevo and Python articulate just behind the front wheel. Still others like the Cruz Bike steer with a head tube in a normal fashion. The problem with these designs are that they have a lot of pedal steer that has to be compensated for by man handling the handle bars at high pedal power to stop excessive wiggle. This uses a lot of energy and strain the arms. The rear wheel steering removes pedal steer. This improves peddle energy efficiency. This makes for a smoother more efficient riding machine.*
>
> *So what is the down side of a front wheel drive rear wheel steering recumbent? I suppose it is the learning to ride such a bike. It still feels like a bicycle but has a slower rhythm. At least that is the best way I can describe its handling. It is a very relaxed ride. Still learning to ride one is a new adventure. It is my opinion that this design has very good potential to make a more efficient recumbent. In a lowracer design this configuration could push the efficiency envelope farther forward. I am currently working such a design.*"

1st RWS recumbent

Renner's first RWS recumbent bicycle is made of rather thick pipes and is given a red paint job. While the head tube is placed closer to the rear wheel than to the front wheel, the absolute trail of the rear wheel is only slightly smaller due to the positive tilt angle (steer axis points diagonally downwards to the front of the bicycle) (figure A.74). Most weight is on the front wheel, because that is the driven wheel and more traction can be created that way. The steering mechanism linkages are placed such that a clockwise-like handlebar movement results in a clockwise bicycle turn.

(a) (b)

Figure A.74: Renner's first front wheel drive RWS recumbent (a) without [110] and (b) with rider [168].

2nd RWS recumbent

The difference between the versions seems to be merely cosmetic with the most notable difference the more horizontal rider posture with respect to the first version. This second 10.5 to 11.5 kg bike has 700c wheels with vectran spokes for lightness and comfort [170]. Furthermore, the frame is chromoly nickel silver brazed and the seat frame and handle bars are 6061T6 Aluminum with a component set that is full Ultegra.

The bicycle is pretty ridable, as can be seen in some videos [171] [170]. Dennis states that riding it is rather stable and easy [personal communication Renner]:

> "*I would say that it is not self stable like a conventional bike. There is no riding it hands off. Same as most of my recumbents. . . . The wheel base is 45 inches, 114.3 cm. The head tube angle is 71 degrees. Seat height is 23 inches, 58.42 cm. I tried to keep the steering in line with the torso of the rider. Even though it is called a rear wheel steering, most of the steering is done by leaning the front wheel in the direction you want to go. The handling seems very slow compared to a normal bike but it is surprisingly stable and able to dodge the smallest object just like a normal bike. When learning to ride one you need to just relax and not fight the slow rhythmic feel that the long trail creates.*"

Although his relative succes, he does not see his design to become a large commercial succes [171]:

> "*. . . there is no suspension but the ride is very forgiving cause of the light weight tubing. . . . I don't have to plan turns, its just like riding a bike. It is still very responsive. . . . It is easy but it does take a learning curve. No one can just jump on it and ride away. I think this is why it will never hit main stream.*"

Both designs can give raise to the question if Renner has a rear or front wheel steered bicycle [172]:

> "*I have to say that I'm still unclear whether to call the design a true FWDRWS, or whether I should think of it as a centre-steer, with the hinge right at the back end of the centre section, but – crucial condition – with the rider carried on the front part of the bike, just in front of the steering hinge, though with his back leaning backwards over it. I notice that the hinge is only just behind your hip-line.*"

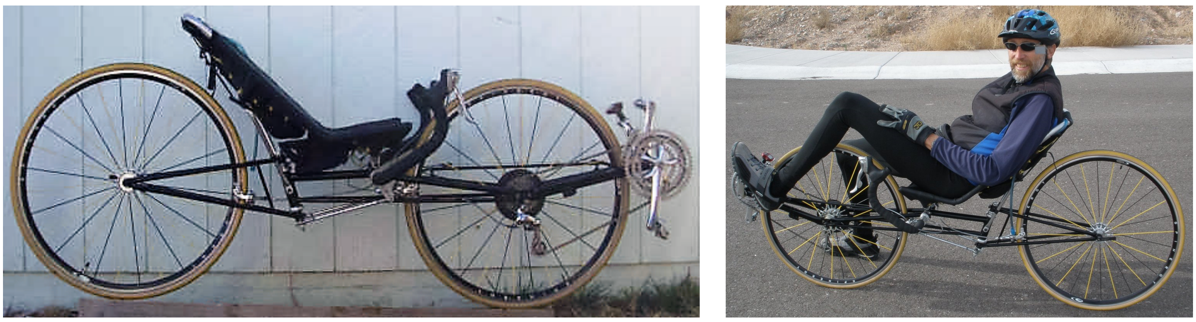

(a) (b)

Figure A.75: Second front wheel drive RWS recumbent of Dennis Renner (a) without [110] and (b) with rider [168].

A.60 2008 Delcambre 'Rear Wheel steering bike'

Mark Delcambre posted a photo of a 'Rear wheel steering bike' in 2008 [173]. The bicycle has a standard frame of a conventional bicycle as front frame which is elongated at its rear side to hold the steered rear fork in a new extra head tube (see figure A.76). This rear fork is connected to the handlebar, which has its own head tube, by a bar that is installed such that a clockwise handlebar turn results in a clockwise bicycle turn. At the location of the head tube of the original donor bicycle, the saddle is placed. Nothing is known about the ridability of this bicycle.

Figure A.76: Delcambre's 'Rear wheel steering bike' from the left side. [173]

A.61 2008 Petit 'ZNB'

From 2008 to at least 2010 Frenchman Nicolas Petit (NP) experimented with a bicycle lay out he called 'le ZNB'. He wanted to create a bicycle with direct front wheel drive by placing the seat on the same front frame as the pedals, a 'monobloque' [174]. The steer pivot was incorporated by means of two pivots lying far from each other. He noted that an ordinary bicycle ridden backwards is not stable. He tested this by more or less recreating an experiment by Jones [3] by pushing backwards an ordinary bicycle with different trail and steer axis angle and letting it loose.

The first version of his bicycle (figure A.77a) had a ball bearing just in front of the seat and a four bar mechanism underneath and besides the seat. The steer axis then goes through the rotational pivot and an instantaneous point at the intersection of two of the four bars. However, it was not stable and in effect hard to ride. To improve the ridability, the second version (figure A.77b) dropped the four bar mechanism and used two rotational pivots to span the steer axis; one at the front of the seat and one behind the rider's head. It was better ridable, but still demanded a large effort of the arms and the stability felt unnatural.

(a)

(b)

(c)

Figure A.77: Early versions of Petit's bicycle; (a) the first, (b) second and (c) third. [174]

Another change in the design of the bicycle in 2008 as depicted in figure A.77c made the bicycle pretty easy to ride. It again uses a four bar mechanism behind the seat with an instantaneous turn center somewhere in front of the seat making the steer axis intersect the ground about 250 mm ahead of the front wheel contact with an angle of about 55°. Due to the four bar mechanism behind the seat, the steer axis is positioned such that it goes from the upper high hinge to a point in front of the front wheel. The front wheel trail is thus actually positive which is not directly clear from the pictures. The problem with this version was the rather abominable ergonomic without brakes and bad placed handlebar. In less than 5 minutes a small speed was developed and with larger velocity, the stability seemed to increase. To increase stability during braking, the seat might need to be lowered. Petit himself concluded that this is a front wheel steered bicycle, because the rear wheel has a trajectory inside the front wheel trajectory; RWSB has a larger turn radius for the rear wheel with respect to the front wheel.

A later version of August 2009 was pretty well ridable with a wheelbase of about 1030 mm, a seat height of 250 mm and a seat back angle of 35° [175]. Two videos show that riding it is indeed possible [176] [177], but reportedly it is still not optimal. The development went on after this version and the bicycle became better and better [178].

Figure A.78: 2009 version of Petit's ZNB. [176]

A.62 2008 Figaro 'croquis de géométries'

Figaro (forum alias) presented two 'croquis de géométries' (French for 'geometry sketches') in 2008 for a bicycle with a peculiarly placed headset [179]. The headset is placed (partly) underneath the rear wheel with the steer axis angled downward to the front and intersecting the ground ahead of the rear wheel (see figure A.79). Only difference between the two sketches is the bending of the rear fork which is downwards for one and upwards for the other design.

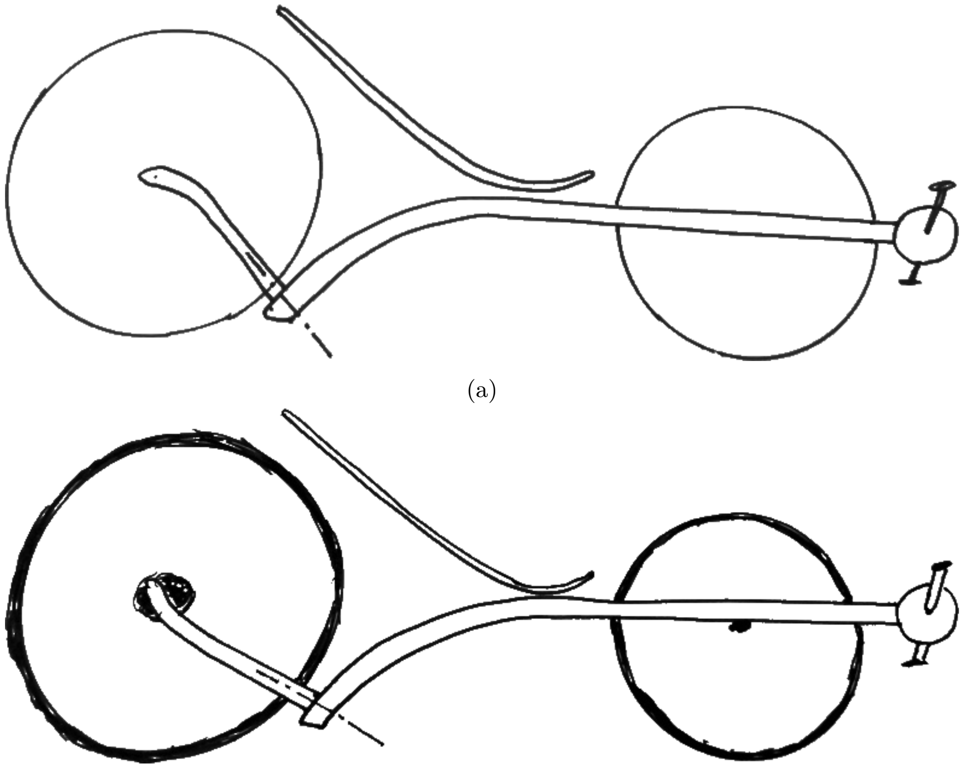

(a)

(b)

Figure A.79: Figaro's ideas on rear wheel steering with (a) rear fork bending downwards, and (b) rear fork bending upwards. [179]

A.63 2009 Ryan 'YikeBike'

Grant Ryan from New Zealand designed the 'YikeBike' [180] (which looks like an old bicycle design [181]), released it on 2 September 2009, and received a patent in 2010 [182]. This vehicle is a motorized compact and foldable bicycle that, due to the larger front wheel, looks something like a classic penny-farthing bicycle (actually this bicycle is sometimes categorized as mini-farthing, see figure A.80). It has a steer axis that is positioned in a similar way to conventional bicycles as can be seen in figure A.80a. Although it cannot be clearly seen from the pictures, videos show that the handlebar is attached to the front assembly, and the saddle is attached to the rear frame. Several videos do also show that the vehicle is rather ridable.

(a) (b) (c)

Figure A.80: Ryan's 2009 'YikeBike' (a) as patent drawing [182], (b) the Model C, and (c) being ridden. [180]

A.64 2009 Graham and McGowan 'Spin Scooter'

Brad Graham and Kathy McGowan (known as KoolKat and Radical Brad on the AZ Builders Forum) from Ontario, Canada made a peculiar scooter around 2009 [183]. The scooter has a 'normal' front part with steer axis, but at the rear a wheel is attached with an extra steer axis, making this a single-track vehicle with both wheel steering (see figure A.81). Here, the rear wheel is much alike a shopping cart small caster wheel with vertical steer axis and a trail. Both steer joints can rotate independent of each other, since they are unconnected, which gives extra opportunities for riding this vehicle in comparison with a conventional scooter.

(a) (b)

Figure A.81: Graham's and McGowan's 'Spin scooter' (a) from the rear left, and (b) being ridden. [183]

A.65 2009 NIU 'Rear steered bicycle'

Students mechanical engineering at the Northern Illinois University (NIU) built this RWSB for a senior design project in fall 2009 [184]. From the videos it can be seen that the steer axis is nearly vertical and that it intersects the ground in front of the rear wheel (see figure A.82). Steering is done by handlebars that are connected with cross linked wires to the rear fork. A clockwise handlebar turn results in a rightwards turn. Moreover, it is told that the saddle and the handlebars are adjustable in both the horizontal and vertical direction [185]. Also, the videos show that riding this bicycle seems rather effortless.

(a)

(b)

Figure A.82: Snapshots of the NIU 'Rear steered bicycle' (a) as overview [184], and (b) a close-up [185].

A.66 200- Moriguchi 'Kalle clone'

A video of Japanese Nobuo Moriguchi riding his 'Kalle clone' recumbent bicycle clone (see section A.39) was published in 2009 [186]. As would be expected from a clone, this bicycle has the same main features as the original Kalle with the steer axis intersecting the ground at around the front wheel contact point (see figure A.83). Although the video shows Moriguchi riding the bicycle rather smoothly, he found it impractical to ride, saying [186]:

> "*I am not sure about the original Kalle made by Mr. Hans-Ulrich Reimers, however, my Kalle clone is not good at turning small corners and I found it is not a proper bike for use in city traffic.*"

(a) (b)

Figure A.83: Moriguchi's 'Kalle clone' (a) fromt he right, and (b) from behind. [186]

A.67 2010 Cal Poly 'Rear wheel steering'

Students of the California Polytechnic State University, San Luis Obispo (Cal Poly) built several 'rear wheel steering' bicycles as a senior project for their Mechanical Engineering undergraduate degrees during 2009 and 2010. This RWSB is strongly based on the design of Dennis Renner. Three versions were created and the final version eventually participated in a mechanical design competition, but the builders of the bicycle are not those who ride it in competition.

Prototype I

The first version (figure A.84) of their prototype did not have propulsion and in effect was used downhill only. Steering is done by using sticks and a video shows that the bicycle could be ridden with one hand for small periods of time [187]. The steer axis can be seen to point diagonally upwards to the rear.

Prototype II

For the second version, propulsion was included by means of pedals and a chain, and the steer axis could be rotated to test which angle is best. After testing, they settled with a steer axis pointing diagonally upwards in forward direction, witnessing the angle for the final version. The dynamical behavior of this bicycle are extensively recorded in numerous videos: [188] [189] [190] [191] [192] [193] [194] [195] [196] [197] [198] [199]. It appears that this bicycle is fairly easy ridden and some videos show that speeds of 33 mph (53.1 km/h) are reached. According to one of the builders experimenting with this prototype gave gave interesting findings, but was not very easy [192]:

> "*Many of the features are adjustable, including the head tube angle (the angle of the hinge), the wheelbase by multiple dropouts for the front and rear wheels, the control sensitivity by the lever-arm linkages, and the seat position.*
>
> *After testing many different angles and wheel configurations, the riders found a forward-leaning head tube angle more desirable at high speeds. That's their preference, not mine. I was/am too short to reach the pedals. The final bike had a forward-leaning head tube angle and it worked for the racers. If you don't like that configuration you can build your own bike.*
>
> *There are a lot of factors in play. Because some features are adjustable, each time we changed something, we had to get used to riding all over again. This configuration sacrifices stability for agility: hence the really tight turns you see in this video. The prototype is also much heavier than the Renner bike, and heavier than our final bike.*"

Figure A.84: Snapshot of the prototype I of Cal Poly students seen from the left [187].

(a) (b)

Figure A.85: Prototype II of Cal Poly students with adjustable steer axis angle (a) during turning [199], and (b) riding straight ahead [192].

Artemis (Final version)

The final version, the Artemis, competed in the 2010 West region Human Powered Vehicle Challenges (HPVC) of The American Society of Mechanical Engineers (ASME). It participated in the speed class and finished 12$^{\text{th}}$ out of 14 contestants in the overall ranking [200]. The bicycle is made of tig welded 4130 steel and uses bike tubing, carbon and a heat-moldable-foam seat. The total mass adds up to 14.5 kg. At some point during the development, protecting wheels were included to help the steering mechanism from being damaged, but hey limited the turning. Also for this bicycle several runs were filmed: [201] [202] [203] [204] [205] [206] [207] [208] [200]. As the videos show, this bicycle is pretty good ridable and one of the builders (Kevin Moynihan) described that the design process made interesting things clear [207]:

> "*We built a proof-of-concept frankenstein's monster to see if it would work, then a prototype to find out what angle's, wheel positions, and seat positions worked, then built this race bike. We haven't high speed tested the race bike as much - but the prototype has been up to 35 or so and it seems to behave intuitively - mistakes made at that speed are entirely correctable, as we came to learn from some harrowing experiences.*
>
> *Push the left steering arm forward, rear wheel turns out behind you to your right which would be a turn to the right. Much more intuitive than the other way around - we tried. The arms pivot separately along the same axis - each of those tubes has a machined surface for cane creek IS bearings and are also internally relieved to save some weight. We were able to ride it one-handed pretty easily. No-hands was hard.*
>
> *We did take an advanced dynamics class on single-track vehicle design and control theory. It was pretty clear in the class that there are mathematical models for normal bikes, but none are really complete. For example, we had a model for the 'control spring' - the force/deflection of rider input required to initiate turns, but the model wasn't stable on it's own. I'm not saying the math is too hard (actually, yes I am: for a side-project) but I don't think there is a complete model FOR normal bikes or AGAINST rear wheel bikes.*
>
> *However (and a big one), we suppose that the main centering effect of our vehicle came from mass in the seat. The weight of the rider would tend to 'pull' the bike towards straight. When you turn, I imagine the rider would find himself lifting up away from the ground, similar to how a door with a canted hinge will center to a low spot when released. . . . The weight centers the rear wheel - not as self-stabilizing as the normal bikes tendency to lean away from a steer and then steer into the lean to self correct, but it does the job. The centering effect was not something dependent on speed. That's the golden ticket - make the stability increase with speed. It's a combo of a centering moment while upright, and a correcting, natural steer towards the direction of lean that keeps normal bikes from dumping you. It is less stable than an upright, sure. But as you can see from the videos we posted*

Figure A.86: Final version of Cal Poly students, the Artemis. [209]

and others out there, they aren't unstable. I think a better understanding of either uprights or a rear-wheel steer bike could lend information to make these more stable."

The final results was quite satisfying, as one of the riders of the racing team states[207]:

> "*I was one of the riders on the team that they built this bike for and can attest that it is entirely rideable. Instantly comfortable? No. Coming from a background of years of trials competition and mtb racing I have some rather good handling skills and this bike took me an hour to be able to ride.*
>
> *My biggest problem in learning to ride this vehicle was that it wasn't naturally correcting in the same way a bike was. If you tried to steer through weight transfer and let it sort of roll into corners, it would just fall over. However, once you got used to the feeling of how it steered and behaved, it was exceptionally responsive to input and could really carve corners. Think pedaling while leaned over into a turn tight enough to fit in two parking spaces.*
>
> *I'd say that this is a HUGE step forward in rear-steer bikes and that with further development could very well become a viable alternative to front-steer bikes.*"

(a) (b)

Figure A.87: The Artemis with fairing for the race (a) without front cap, and (b) with. [208]

A.68 2010 Raynor 'Independent rear wheel steering bicycle'

Maurice Raynor received in 2010 a patent for his 'Bicycle having independent rear wheel steering' [210]. The front part of the bicycle is rather conventional with a front steer axis, bu at the rear an extra vertical steer axis is included right through the center of the rear wheel (see figure A.88). A conventional handlebar is used to steer the front wheel, while the rear wheel is steered by a longitudinally sliding control lever on the horizontal member of the main frame connected by a flexible cable to the rear steer joint. The rear wheel is not attached to the frame by a fork, but by a single rod on the right side of the wheel. This way the wheel can be turned around its vertical axle. A Cardan shaft in the steer rotation joint of the rear wheel makes it possible that the rear wheel can be driven when it is steered. He calls this bicycle a 'special effects vehicle', because tricks can be performed with it, e.g. with both the rear and front wheel steered 90° with respect to the middle frame, the bicycle could be ridden laterally [210]:

> "*The rear wheel steered vehicle provides new avenues in special effects vehicles. Illustratively, with the rear wheel turned to a right angle to the frame, pedaling can result in the rear wheel describing circles around the front wheel. The rear wheel may be turned to a lesser degree, and with the front wheel being steered, the entire vehicle may travel at an acute angle to the longitudinal direction of the frame. If the front and rear wheels are steered either simultaneously or one at a time while the vehicle is under propulsion, many additional effects may be enjoyed which would not be available from for example a traditional bicycle or even an articulated bicycle.*"

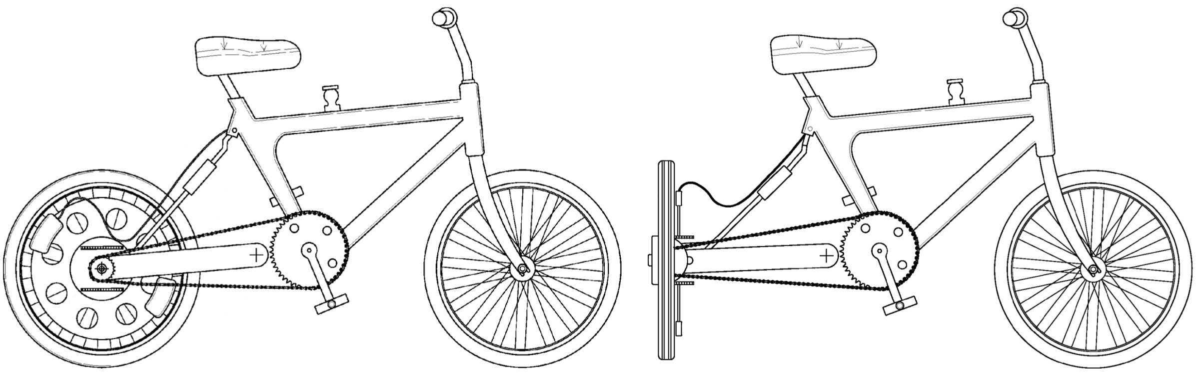

(a) (b)

Figure A.88: Raynor's 2010 'Bicycle having independent rear wheel steering' right side view patent drawings, (a) with the rear wheel in a conventional straight ahead position, and (b) with the rear wheel in an alternative steer position; 90° turned. [210]

A.69 2010 Yneges 'Intense'

Roman Yneges designed his 'foldable multi-purpose mountain bike', the 'Intense' (figure A.89), in 2010 [211]. This two wheel steered bicycle was never built, but is supposed to have nice riding and transportation features [211]:

> "*A foldable bike with two wheel steering and a method of locomotion which drives both the front and rear wheels by the operator's pedal up/down movement. ... Weight load selector controls the amount of tension placed on the suspension spring.*
>
> *Folding configuration*
>
> *The mountain bike can be folded for easy carry. Weighing 22lbs, the bike is ideal for long hikes deep into rough country. The handle bars can be removed and folded. They can then be clipped to the spine of the outer shell body. The pedals are foldable and the entire pedal casing is then rotated to stowed position.*"

(a)

(b)

Figure A.89: Yneges concept model created in Maya and enhanced in Photoshop. (a) The bicycle seen from behind and (b) the rear wheel turned at 45 degrees counter to the direction of travel with a locked front wheel. [211]

A.70 2010 Ziganime 'Dirfesse'

The 'Ziganime' is a French group of artists founded in 2004 by Didier Gomard, aka BRICOLO, consisting of artists of the 'Ecole de Cirque du Nord Isère' (Circus school of Nord Isère) and 'l'association sportive Pour Ailes' (the athletic association For Ailes), who made the 'Dirfesse' in 2010 [212]. It appears that BRICOLO is the designer and/or builder and he built, among others, the rear wheel steered 'Dirfesse' (see figure A.90). As act they built and ride weird bicycles and therefore they also required an RWSB. The 'Dirfesse' is a reversed small bicycle with the steer axis adjusted to be vertical. This makes it possible to put the saddle on the steer wheel frame such that one can steer by move the saddle with ones hips. To have some support, a handlebar is placed and locked in the old saddle pin tube.

(a) (b)

Figure A.90: Ziganime's or BRICOLO's 2010 'Dirfesse' seen from the left in (a) a straight ahead course, and (b) a counterclockwise turn. [212]

A.71 2010 Go *et al.* 'X-Bike'

Woogyeong go, Dong-ha Kim en Kyeongpyo Cho from Korea designed their folding bicycle, the 'X-Bike', at the Cheongju University for the Seoul Cycle Design Competition 2010 [213] [214] [215]. The bicycle looks like a classic design (see section A.13) and has a direct planetary gears drive on the front wheel, while the rear wheel is steered (figure A.91). The front frame contains the driven front wheel and the saddle, and the rear frame has the rear wheel and the handlebar attached to it. The head tube is placed perpendicular to the front frame and collinear to the rear frame, making a compact design. This way, the steer axis is aligned with the rear frame that points down to the rear and the steer axis intersects the ground behind the rear wheel contact point. Advantages should be the absence of the chain and the easy folding mechanism, but whether it is easily ridable does not become clear.

Figure A.91: Go *et al.* 2010 X-Bike seen from the front left. [213]

A.72 2010 Meeks 'Quantum Leap'

Eddie Alexander Meeks (EAM studios) presented his motorcycle, the 'Quantum Leap', in 2010 [216] [217]. Its is a custom designed motorycle that incorporates front wheel drive with rear wheel steering (see figure A.92). It was never built with the idea of being dynamically stable, but rather to make a technically working (although, does it work when it is dynamically unstable?) alternative to conventional motorcycles [216]:

> "*Meeks is the only person to hitch a leg over Quantum Leap and experience the dynamics of his front wheel driven creation. This was done under the controlled conditions of a parking lot at low speeds.*
>
> *'The bike's so expensive, it's a concept that's going to be shown and to ride it and to take a chance of chipping or scratching it, it's not worth it. All we wanted to do was make sure it worked, which we did.'*
>
> *Meeks said the steering felt 'kind of weird' explaining that when you do something for the first time totally different from what you've done your entire life, it naturally is going to feel odd at first. Learning to steer it definitely takes a learning curve. The bike was built as a show piece and will ultimately end up in a private collection after it makes the bike show rounds. It is titled in North Carolina, though, has undergone state inspection and has been granted a serial number and frame sticker.*"

(a)

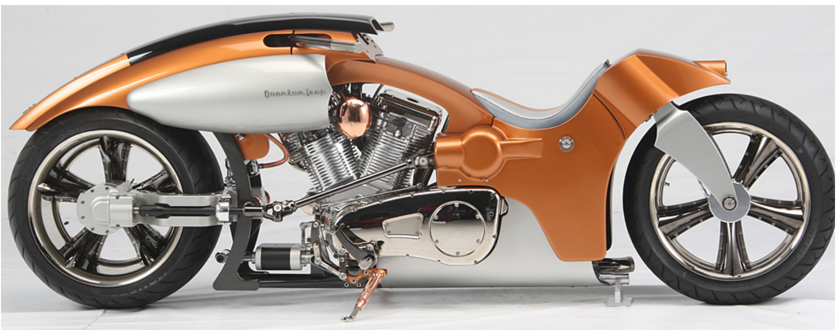

(b)

Figure A.92: Meeks' Quantum Leap (a) from the front left, and (b) from the left. [216]

A.73 2011 Bechtel 'Bicymple'

Product and graphic designer Josh Bechtel created the 'Bicymple' in late 2011 and teamed up with 'co-conspirator and operations manager' Gabe Starbuck to commercialize the bicycle [218]. The bicycle is longitudinally nearly symmetrical with two steer axes (see figure A.93). The front fork can be turned by turning the attached handlebar, and the rear fork can be turned by turning the attached saddle or by feet movement on the pedals. If desired, the rear steer axis can be locked, to make the bicycle more conventional. Frame and forks are made of CroMo Steel, and the driving mechanism has an integrated freewheel mechanism with single speed transmission. Some dimensions are a wheel base of 31" (0.79 m), head angle of 74°, wheels of 29" (700c) with 29×1.75" tires, a top tube length of 23" (0.58 m), and a height of 35" (0.89 m). The bicycle is designed to be simple, but is yet well ridable [218]:

> "*Is it possible to evolve from the established bicycle design while adhering to the basic principles of simplicity, functionality, style, and excitement? This is the question that gave birth to the bicymple. By removing the chain, the number of moving parts and overall complexity is significantly reduced. A direct-drive, freewheeling hub joins the crank arm axis with the rear-wheel axis, shortening the wheelbase and minimizing the design. More than just a stylish concept bike, the bicymple is comfortable, easy to ride, and brilliantly simple to maintain. The lightweight design and short wheelbase make for a nimble ride. The optional rear-steer mode is reminiscent of custom 'swing bikes' and allows tighter turns and 'crab-riding'. The ultra-compact design makes it effortless to get in and out of tight spaces and easily squeezes into stairwells, hallways, fire escapes, nooks, and crannies. bicymple. Designed by Josh Bechtel: a bicycle, simplified.*"

(a) (b)

Figure A.93: Bechtel's 2011 'Bicymple' (a) from the right in a straight ahead position, and (b) from the rear right in a counterclockwise two wheel-steered position. [218]

A.74 2011 Zhang 'Front wheel driving rear wheel steering type bicycle'

In 2011 Wei Zhang received a patent for his 'Front-wheel-driving and rear-wheel-steering type bicycle' [219]. This foldable bicycle is a variation on a simple and compact design that comes along more often (see section A.13 and A.71). The bicycle has two straight frames with a front frame holding the driven wheel and a locked saddle, while the rear frame holds the rear wheel and handlebar (see figure A.94). The head tube is positioned such that the steer axis is aligned with the rear frame and intersects the ground behind the rear wheel contact point.

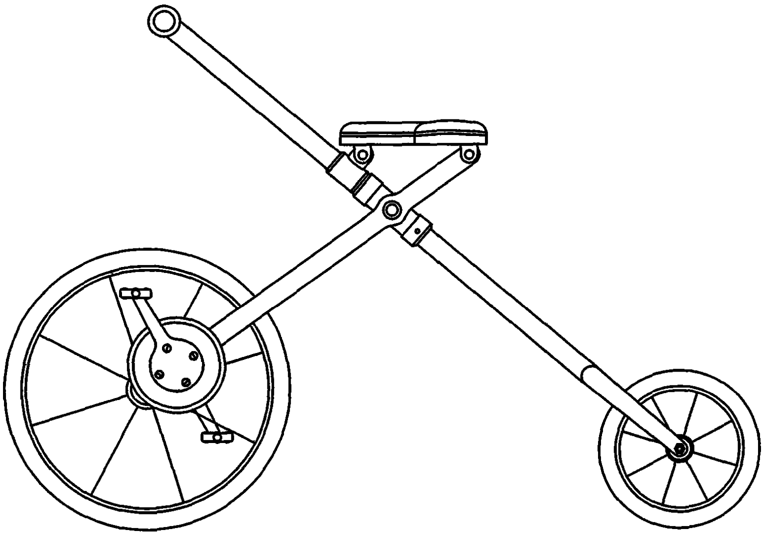

(a)

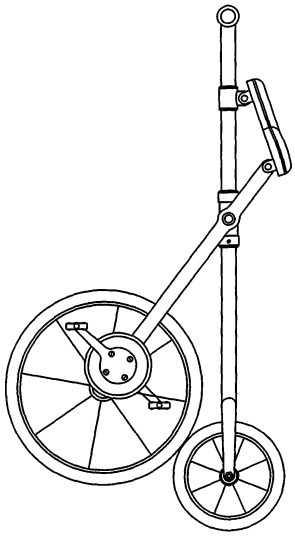

(b)

Figure A.94: Zhang's 2011 foldable 'Front wheel driving rear wheel steering type bicycle' (a) unfolded and seen from the left, and (b) folded. [219]

A.75 2011 Morrow 'Contraption'

Mark Morrow built his bike, which he refers to as 'Contraption', around 2011 when he felt like doing something different from his first bicycle[220]. The front wheel drive bicycle configuration is similar to that of the Badass of Flatmo (see section A.53), but although Morrow's bicycle has a vertical steer axis, it differs from the Badass in that it has no rear wheel trail (see figure A.95). The bicycle is constructed from simple spare parts that were available [220]:

> "*Almost a year or so after building my first regular bike, I felt like making something a little bit different. One day an idea popped into my head for making a rear-wheel steering bicycle. - The frame is from scrap pipe that was laying around. - The wheels, tires, gears, cranks, headset, and chain were parted from an old (free) dumpster bike. - The 'steering shaft' is made from a piece of exhaust pipe tubing, welded to the bottom of a headset stem. - The fork in the rear (and small tire) are from a thriftstore childrens bicycle. It was cut in half at the stem, where I added in square tubing for the steering cable to connect to. - I used plastic pulleys, attached to the frame for the steering cable to run thru. - The seat frame was made from steel tubing, and the seat itself was cut from 3/8" plywood. I was originally going to cover the wood with cushioning and fabric. But I never got around to it.*"

A video shows that the bicycle can be ridden, and that a counterclockwise handlebar motion results in a leftwards turn [221]. However, Morrow reported some issues he encountered:

> "*If there is ever a day I decide to build another one of these contraptions, their are a couple of things I would do differently. - The steering is way too sensitive. I need to enlarge the 'steering shaft' in the front. And use a larger diameter wheel. - The handle bars come in too close to the chest. - In this current version, I eliminated the use of all the gears so that it is a single speed. This was mainly do to laziness. In the future I would keep it multi-speed. - The pedals are almost too far down, anybody shorter has trouble riding. If it could somehow be more universal, or an adjustable seat. - When I first had the idea in mind I pictured being able to make very sharp turns, almost being able to stay in one place but in circles. Unfortunately, it did not work out this way. There was probably something that could have be changed for this to be possible.*"

Figure A.95: Morrow's 2011 'Contraption' seen from the left. [220]

A.76 2012 Despins 'Front-wheel driven, rear-wheel steered vehicle'

American Colin Despins received a patent for his 'Front-wheel driven, rear-wheel steered vehicle' in 2011 [222]. With his design, Despins attempts to improve the maneuverability, handling, and stability as compared to conventional two-wheeled vehicles. Using rear wheel-steering decouples the steering function from the main breaking function by bringing these respectively to the rear and front wheel, which increases stability, he reasons. Furthermore, making the front wheel the driven wheel, makes it easier to climb a curb or a similar stationery object. Therefore, his invention is a single-track vehicle with rear wheel steering and front wheel drive. He chose to put the rider in a recumbent position with a possible power source located below and ahead of the bicycle geometrical midpoint (see figure A.96). He also provides 'kits' to transform a conventional bicycle into a version of his rear wheel steered vehicle vision (see figure A.97).

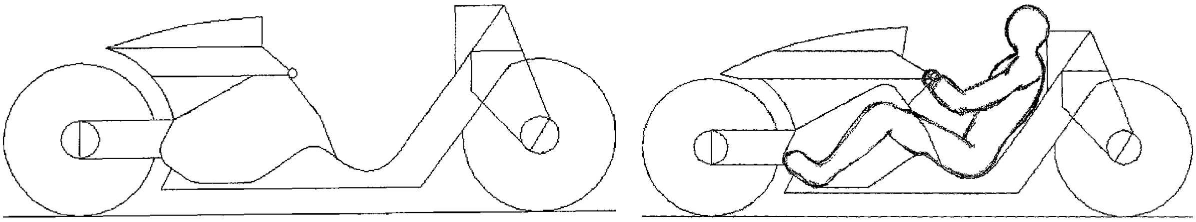

(a) (b)

Figure A.96: Despins' vehicle patent drawing seen from the left (a) without rider, and (b) with. [222]

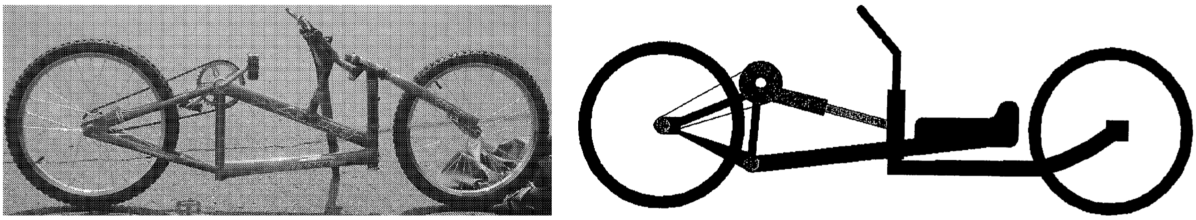

(a) (b)

Figure A.97: Despins' human-powered bicycle design seen from the left (a) as built realization, and (b) a schematic drawing. [222]

A.77 2012 Priority Designs ‘Cannondale CERV’

Priority Designs (PD) designed the ‘CERV’ for Cannondale in 2012 [223]. Broadly speaking, this concept bicycle is rather conventional, but has a negative front wheel trail; the steer axis intersects the ground behind the front wheel contact point (see figure A.98 and A.99). Being a concept bicycle, this vehicle has some interesting but maybe impractical features. For example, in stead of forks, single bars are used, and the steering mechanism works with some transmission in stead of directly [223]:

> “*The CERV features a dynamically adjustable headset that moves both fore-and-aft and up-and-down. The genius lies in achieving the above without altering the seat-to-crank height. This system puts the rider in an optimal position based on the terrain. The headset translates forward and down for a clean, low-drag position when descending. When climbing, it moves up and back, creating a more upright position for maximum leverage on the crank. Doing all this with a traditional fork in place wasn’t going to cut it, so a single-sided swing arm was proposed. Designing a forkless front-end has its own challenges, integrating it into a multi-axis adjustable system is another degree of difficulty altogether.*
>
> *Priority Designs took the original concept sketch and got to work exploring mechanical solutions to the challenges presented. In addition to working through the mechanisms in SolidWorks, mock-ups were built and key components were tested. Ultimately, a proof-of-concept bike was fabricated to validate the engineering principles and define the working envelope. Cannondale reviewed the mechanical solutions and dimensional realities revealed by the test mule. A revised concept illustration was created and the team at Priority Designs was given the green light to turn the vision into a reality.*”

Figure A.98: Priority Design’s prototype of the Cannondale CERV seen from the right. [223]

(a) (b)

Figure A.99: The final CERV design seen from the left (a) from the outside, and (b) a depiction of the internal parts. [223]

A.78 2012 Mauletti 'Bicis'

Italian Enrico Mauletti [224], aka recumbent, presented some 'Bicis' (Italian for bikes) around 2012 [225]. He was interested in a 'rear wheel steering (RWS), front wheel driven (FWD), direct traction (TD)' two wheeled vehicle. The direct traction means here that the pedals are on the same frame as the driven front wheel and thus that the chain does not buckles during steering. A two wheeled vehicle had his preference because three wheeled RWS vehicles are inherently (more) stable. Other than for great technical pleasure, Mauletti attributes two advantages to such a design for recumbent bicycles in order to make them competitive for conventional bicycles. First, pedaling can be more efficient because the rider is on the same frame as the drive train. Secondly, the chain can be just as long as on a traditional bicycle, causing even less energy losses.

RWS ispirate alle bici tradionali

In his search Mauletti presents a bicycle which is probably not his own. He believes this concept (figure A.100 and figure A.101) is a logical first step in making an RWSB, because it is more or less simply a reversed normal recumbent, hence, his 'RWS ispirate alle bici tradionali' (RWS inpired by traditional bicycles). Sadly, he concludes that this bicycle, or any bicycle such as this one, for that matter, do not function. He proposes that a better approach is a more mid-steered recumbent bicycle which havee proven to be better ridable. Interestingly, Mauletti notices that rear wheel steering has the strange behavior that initially the rear moves away from a turn. Only later on does the bicycle move in the wanted direction. This causes a strange (and maybe non correctable) experience for the rider.

(a) (b)

Figure A.100: A concept, referred to by Mauletti, being somewhat 'ethereal' (a) seen from the right rear, and (b) from the right front. [225]

(a) (b)

Figure A.101: The bicycle as realized from the earlier concept as referred to by Mauletti (a) with extra handlebar, and (b) without. [225]

RWS recumbent 01

Mauletti's own concept uses several links which support and connect the steered rear wheel to the frame (see figure A.102). He wrote about it and shows the movement in a video [226] (free translation by P. H. de Jong):

> "*It has two links working in parallel: A more 'horizontal' which serves to give the steering direction and to laterally move the wheel so as to position the center of gravity of the bicycle and rider inside of the curve (almost to cause it to fall inside). A more 'vertical' link that serves to create the first with a kind of rear similar to that of a traditional bicycle, completing the load-bearing structure of the rear wheel and which, thanks to its measures, tends to maintain the rear wheel in a virtually vertical position. The two links are imagined as a set of 'rods' in which all the ends are equipped with ball joints; This structure is not stable on its own, but you have to imagine that it will become in the moment that the cyclist will have challenged the (not yet designed) handlebar.*
>
> *The length of the link is absolutely 'a muzzo', just to see how he does, obviously playing on the geometry of the 'bi-link' (©) you will get everything you can imagine in terms of the RWS behavior. The wheelbase of 700C wheels, the seat position (angle of 30°) and the chock, are 'reasonable'. The frame seems easy to imagine. The 'dual-link', being formed by a lattice structure made of rods and struts, may be somewhat lighter. It remains to be seen how to practically implement the ball joints at the wheel axis where three links converge , but maybe you can remove a bit of the ends of at least one of the three links (to be studied later). The handlebar (to be imagined) could also be based on some simple link commanded by a traditional handlebar or, better, by a pair of side levers. In short, an LSS - Lateral Seat Steering (©).*"

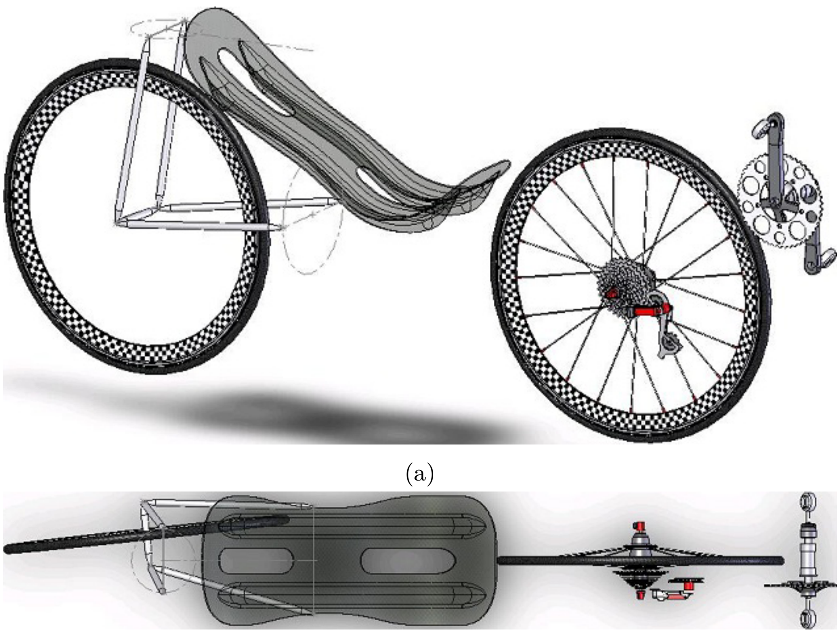

(a)

(b)

Figure A.102: Mauletti's concept (as of yet without frame) (a) in isometric view, and (b) from a top view. [225]

A.79 2012 De Lorenzi 'Cosa che potrebbe funzionare'

Italian Luciano De Lorenzi made a simple 'Cosa che potrebbe funzionare' (Italian for 'Thing that might work') in 2012 to make a rear wheel steered bicycle steer into a fall by redistributing the mass [227]. His idea has the steer axis close to the rear wheel and incorporates a center of mass of the rear frame that is placed behind the rear wheel (see figure A.103). At least in a static situation does a lean of the bicycle then result in a steer angle that steers the bicycle in the direction of the fall [227] (free translation by P. H. de Jong):

> "*One thing that would work would have a very small trail and a mass behind. The balancing mass for the length of its arm (up steering axis) should be larger than that of the bike for the trail measure. In this way the wheel is pulled and when leaning on one side you steer that way. It would probably work but who would like to carry around unnecessary weight.*"

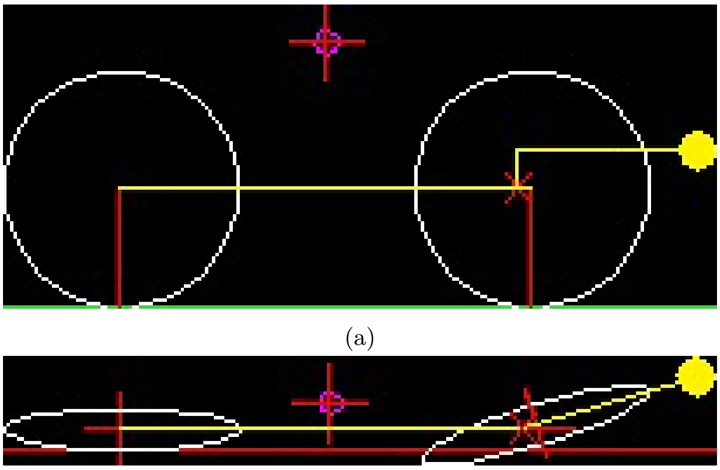

(a)

(b)

Figure A.103: De Lorenzi's concept (a) from the left side, and (b) from a top view. [227]

A.80 2012 Song 'Bicycle using front wheel to drive, rear wheel to steer'

Song Zheng Liang issued a patent in 2012 that shows a 'Bicycle using front wheel to drive, rear wheel to steer' [228] (figure A.104). The bicycle has a positive rear wheel trail (steer axis intersects ground ahead of rear wheel) and a vertical steer axis (see figure A.104). The rider is positioned far backward at a position behind the rear wheel contact point. It seems from the patent description that a string and pulley system is used that connects the handlebars to the rear frame. These strings are mounted such that a clockwise handlebar movement results in a rightward steer. However, this system is not depicted in figure A.104. Song claims that the bicycle is safer, requires less material, is easier in maintenance and is comfortable to ride.

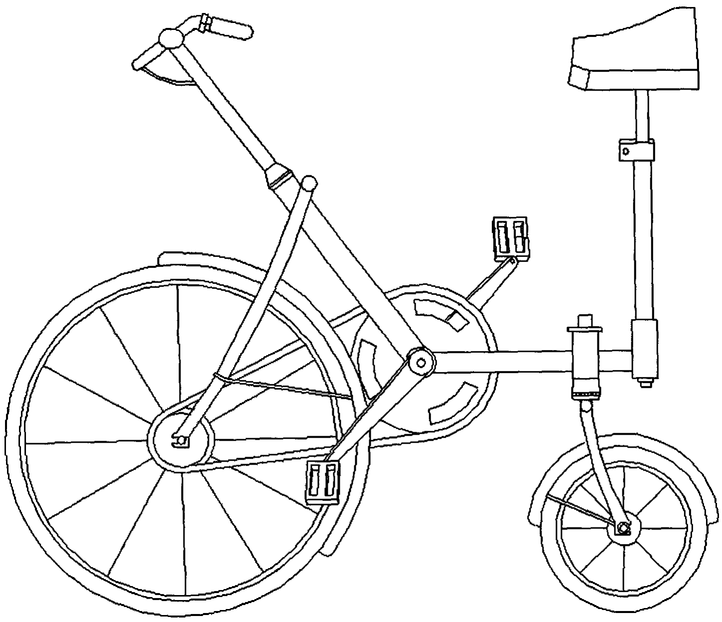

Figure A.104: Song's 'Bicycle using front wheel to drive rear wheel to steer'. [228]

A.81 2012 Carling bicycles

Darling Cris Carling of Chicago Rat Patrol Bike Club made two weird bicycle around 2012 [229]. It appears that this bicycle club makes strange bicycles just for fun where an RWSB is not ill-suited.

Unridable front pedal rear steer

This is a front pedaled rear steered bicycle with a simple lay-out of only two tubes made from recycled material (see figure A.105). The headset crosses the front fork bar leaving a very small trail for the rear wheel. However, this 'mutant' bicycle turned out to be unridable [229]:

> "*Cris' front pedaling-rear steering bike. It is as difficult to ride as it looks, in fact no one has made more than 2 crank rotations at a time on it. Some improvements are planned to make it slightly more rideable.*"

Bike you steer with your rear

In an attempt to make a less difficult front pedaling rear steering bike Carling made this backwards bike. It is basically a BMX with the handlebar and saddle interchanged. The handlebar are fixed to the (now) front frame while the saddle is fixed to the rear fork. Thus, the saddle turns with the steered rear wheel and steering is done by moving the saddle. Reportedly, it is relatively better ridable than Carling's previous RWSB [229]:

> "*It is less difficult, it can make about 4 crank rotations.*"

Figure A.105: Carling's first unridable front pedal rear steer bicycle seen from the left. (Photo by Alexis Ellers [229])

(a) (b)

Figure A.106: The second rear steer bicycle of Carling (a) without rider from the left, and (b) being ridden. Note that the saddle turns with the rear fork while the handlebar is fixed to the front frame. (Photos by Alexis Ellers [229])

A.82 2012 Saleh 'RWS recumbent bicycle'

Mohsen Saleh made his 'RWS recumbent bicycle' in 2012 [230] [231] [232]. He aimed to get rid of long chains on recumbent bicycles, to get rid of interference of the legs with a steering front wheel, and to make the recumbent bicycle better suited for frequent starts and stops. Therefore, he uses a direct front driven rear wheel steered bicycle with a four bar steer linkage (see figure A.107). Saleh claims that this four bar linkage makes the trail negative (steer axis intersects ground behind rear wheel) in neutral steer position, but with nonzero steer angles, the trail is positive, causing stabilizing lean/steer and caster effects. However, despite his claims he was not able to ride the bicycle [230]:

> "*Known Issues with current design: Long wheelbase which results in larger turning radius; Weight distribution: almost 60% rear to 40% front wheel, I would probably have to change this configuration for next design; Using cable to steer the rear wheel seems that is not so practical, I used cable as it enables us to integrate bicycle seat and steering handle bars. Connecting the handle bars stem to seat is an advantage as by adjusting the position of seat, the handle bars would also be in the right place without any further adjustments; The steering center of gravity is located in a position which doesn't contribute to lean steering and actually it produces a reverse torque that resists against lean steer. The whole design is not yet ridable as a result of aforementioned issues.*
>
> *Known Issues with current prototype: Despite my efforts to build a high quality prototype, This model is still too wobbly . . . I could have done a better job . . .*
>
> *I started this project and my aim was not only to have a ridable bicycle... i wanted a totally stable bicycle that every recumbent rider could ride it. unfortunately in first attemmpt, riding the first prototype made it clear that even if i could manage to ride this bike with some modification, yet the chances to ride it as easy as a Normal FWS bike is so low. that's why the project was left as it is. I Don't assume that riding Denis Renner's FWDRWS is as easy as you see him in his video... the Kalle bicycle was also discontinued probably because it was not as safe and ridable as a normal FWS bike. I am not disappointed though. I know that with this configuration i may solve the problem however it requires enough time to recalculate and reconstruct this design and at the moment i don't have any. i would work on this again.*"

Figure A.107: Saleh's 'RWS recumbent bicycle' seen from the right side. [231]

A.83 2011 Kooijman *et al.* 'Stable with rear wheel steering'

In 2011 Kooijman *et al.* found probably the first theoretical self-stable RWSB configuration [16]. By chance they discovered this self-stable configuration when trying to model a monocycle with non-rotating mass [from personal conversation with A. Schwab]. Such a monocycle model requires a massless frame attached to the nonrotating mass with frictionless contact point somewhere on the ground in order to prevent the mass from rotating (without this frame the mass would be free to rotate in the wheel and the model would be under-defined). Under the assumption that such a frictionless contact can also be modeled by a small massless caster wheel, an attempt was done to model the monocycle in JBike6, but surprisingly, the results where not identical. In hindsight it is obvious that a frictionless point on the ground is not identical to a small massless castor wheel. Indeed, the stick can not generate lateral forces, the caster wheel can. A frictionless contactpoint cannot be modeled with the Whipple model, nor with JBike6, for that matter. However, by this serendipity they discovered a selfstable RWSB.

Their found parameter values of the reported configuration are given in table A.2 and in figure A.108 a graphical representation along with eigenvalues are presented. Following the findings of Kooijman *et al.* [16] concerning rear wheel steering, several student groups from Delft University of Technology built RWSBs.

Table A.2: The non-zero Kooijman *et al.* self-stable theoretical RWSB parameters ($\lambda_s = 0°$).

Parameter	**Symbol**	**Value**
Wheel base	w	1 m
Front wheel trail	c	−0.9 m
Rear wheel R radius	r_R	0.1 m
Rear wheel R mass	m_R	1 kg
Rear wheel R mass moment of inertia	I_{Ryy}	0.005 kgm^2 $(= 2I_{Rxx})$
Front frame H center of mass	(x_H, z_H)	(1.1, −0.15) m
Front frame H mass	m_H	10 kg
Front wheel F radius	r_F	0.35 m
Front wheel F mass	m_F	5 kg
Front wheel F mass moment of inertia	I_{Fyy}	0.6125 kgm^2 $(= 2I_{Fxx})$

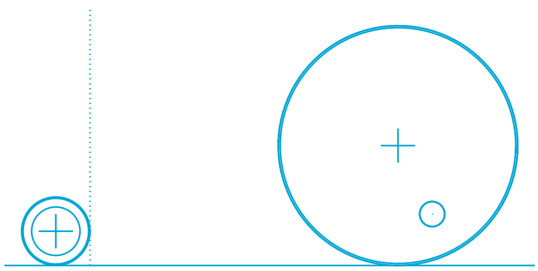

(a)

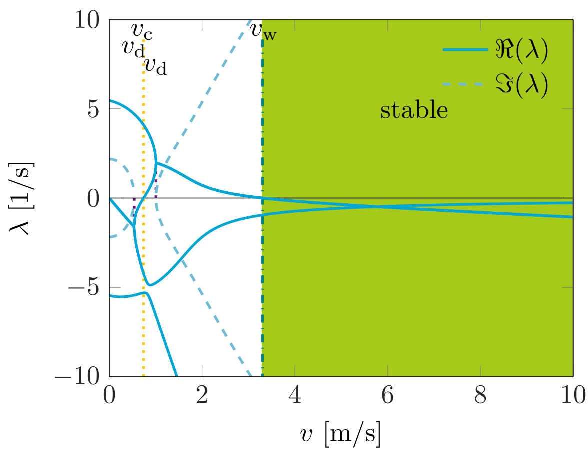

(b)

Figure A.108: The Kooijman 'Stable with rear wheel steering' (a) configuration, and (b) eigenvalue plot. $v_{capsize} = 0.738$, $v_{doubleroot} = 0.538$, 1.005, and $v_{weave} = 3.3011$ m/s (Recreated with JBike6 from [16])

A.84 2012 Broxterman *et al.* 'Zelfstabiele achterwiel gestuurde fiets'

This bicycle, 'Zelfstabiele achterwiel gestuurde fiets' (Dutch for 'self-stable rear wheel steered bicycle') was built in the autumn of 2011 by a group of students, Broxterman *et al.* [17], including the author of this study. The front wheel is a large 28" standard bicycle wheel and has steel rings in it to increase it's mass moment of inertia. In contrary, the rear wheel is a small 6" wheel chair wheel (see figure A.109). Moreover, the rear frame is a light small frame, while the front frame is larger and has extra (adjustable) mass added in front of the front wheel axle. At the rear axle, extra weights are added to prevent the bicycle from tipping over to the front. The two frames are hinged by a headset taken completely from an old bicycle. The two assemblies can be subdivided in the 4.611 kg front frame, the two added shaft masses at the front weighing together 3.085 kg, the 0.718 kg rear frame, and two weights at the rear axle weighing together 1.784 kg. Thus, to be self-stable, a rather inconvenient mass distribution is applied as can be seen in table A.3 and figure A.113. The RWSB's noticed and measured test behavior suggests that one could indeed obtain self-stable behavior with rear wheel steering.

The bicycle has some features that make it suitable for experimenting. First off, the front frame is made higher than essentially needed, which is in order to make it simpler to operate; It is now easier to push the bicycle without bending over too much. This had as extra advantage that a measuring unit could easily be placed on top of the frame. Moreover, the bicycle now more resembles a ridable bicycle; a seat can be placed on the upper frame tube. Another feature is the adjustability of the front weights. These weights are made of steel shafts and are placed in tubes at either side of the front wheel. These holder tubes are mounted at the front wheel axle such that they can be slightly adjusted vertically. The weight shafts, on their part, can slide in those tubes and therewith the place of the center of mass of the bicycle can be altered. It is even possible to retract the shafts up to a point where they stick out of the back of the holding tubes (opposing the forward position as depicted in figure A.109). That way, the center of mass of the bicycle can be shifted from in front of the front wheel axle to a location behind the front wheel axle. Some set-screws in the tube walls hold the shafts in place. The weights at the rear axle are only to prevent tipping over to the front and are nonadjustable in location. These weights barely influence the dynamics of the whole bicycle.

The lean rate of the front frame was measured with a gyrometer and the forward speed was measured with a standard bicycle speed measurement method with magnets and a magnet switch. Measurements indicated that the the lean angular rate of the bicycle damped out at forward speeds at around 5 m/s and that the RWSB is thus self-stable. This speed can be reached by pushing the bicycle while running and is also a reasonable speed for normal bicycle riding. This let to the conclusion that an RWSB can indeed be self-stable and that it is likely possible to make a ridable RWSB. Adding weight above the front axle is possible while still keeping the bicycle self-stable. This notion resulted in the ridable RWSB concept drawing (never built) shown in figure A.111. The concept attempts to put the most mass around the spokeless front wheel (imaginary) axle. To drive the bicycle a chainless mechanism is placed at the front wheel.

Figure A.109: The riderless TU Delft bicycle seen from the left side. Note the two weights at the front sticking out rather far to bring the center of mass of the bicycle near the front wheel axle. [17]

Table A.3: The Broxterman *et al.* self-stable no-rider RWSB parameters.

Parameter	Symbol	Value
Wheel base	w	0.9910 m
Front wheel trail	c	-0.7902 m
Steer axis tilt	λ_{s}	-0.0175 rad
Gravity	g	9.81 N/kg
Rear wheel R radius	r_{R}	0.0760 m
Rear wheel R mass	m_{R}	0.2710 kg
Rear wheel R MMOI	$(I_{\mathrm{R}xx}, I_{\mathrm{R}yy})$	(0.000954, 0.000477) kgm^2
Rear frame B COM	$(x_{\mathrm{B}}, z_{\mathrm{B}})$	(0.0385, -0.0859) m
Rear frame B mass	m_{B}	2.502 kg
Rear frame B MMOI	$\begin{bmatrix} I_{\mathrm{B}xx} & 0 & I_{\mathrm{B}xz} \\ 0 & I_{\mathrm{B}yy} & 0 \\ I_{\mathrm{B}xz} & 0 & I_{\mathrm{B}zz} \end{bmatrix}$	$\begin{bmatrix} 0.0254 & 0 & 0.0041 \\ 0 & 0.0176 & 0 \\ 0.0041 & 0 & 0.0349 \end{bmatrix}$ kgm^2
Front frame H COM	$(x_{\mathrm{H}}, z_{\mathrm{H}})$	(1.0585, -0.2569) m
Front frame H mass	m_{H}	7.696 kg
Front frame H MMOI	$\begin{bmatrix} I_{\mathrm{H}xx} & 0 & I_{\mathrm{H}xz} \\ 0 & I_{\mathrm{H}yy} & 0 \\ I_{\mathrm{H}xz} & 0 & I_{\mathrm{H}zz} \end{bmatrix}$	$\begin{bmatrix} 0.4052 & 0 & -0.2779 \\ 0 & 1.4625 & 0 \\ -0.2779 & 0 & 1.0763 \end{bmatrix}$ kgm^2
Front wheel F radius	r_{F}	0.3575 m
Front wheel F mass	m_{F}	5.020 kg
Front wheel F MMOI	$(I_{\mathrm{F}xx}, I_{\mathrm{F}yy})$	(0.2245, 0.4490) kgm^2

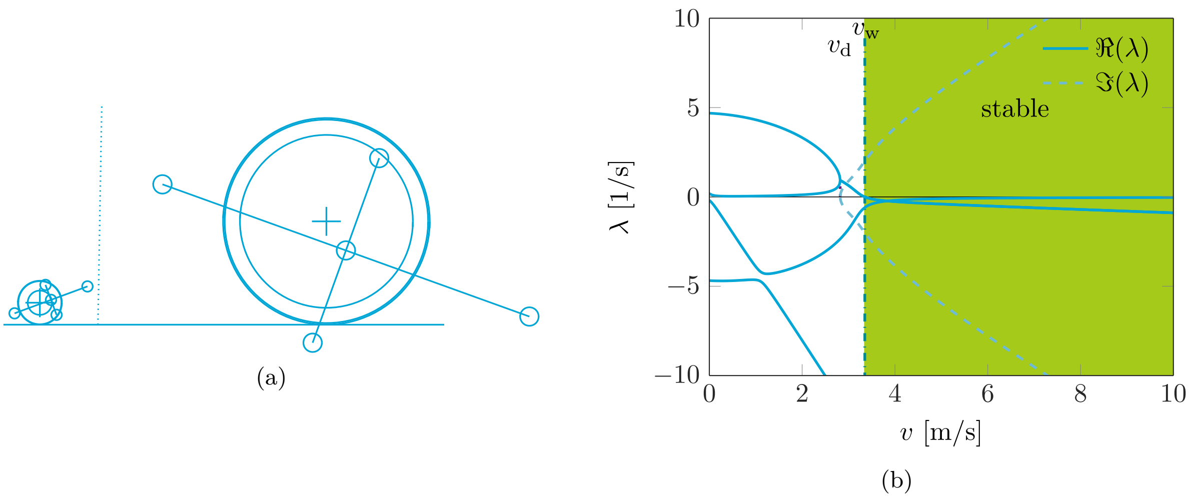

Figure A.110: Broxterman *et al.* RWSB (a) configuration, and (b) eigenvalue plot. $v_{\mathrm{doubleroot}} = 2.8195$ and $v_{\mathrm{weave}} = 3.3498$ m/s (Recreated with JBike6 from [17])

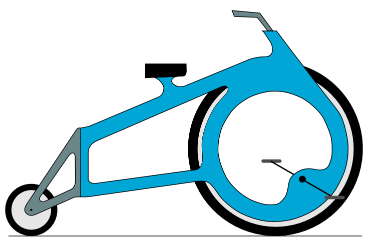

Figure A.111: An impression of how the riderless bicycle could be developed into a ridable version. The placing of the bottom bracket in the spokeless wheel brings the center of mass of the front frame more to the front. [17]

A.85 2012 Van Dijk *et al.* 'Zelfstabiele achterwiel gestuurde fiets'

In 2012 Van Dijk *et al.* built a bicycle that is supposedly self-stable with a no-hands rider on it, the 'Zelfstabiele achterwiel gestuurde fiets' (Dutch for self-stable rear wheel steered bicycle') [18]. An algorithm they made to find the best RWSB, e.g. most self-stable or self-stable at lowest speed, found a configuration resembling the bicycle of Broxterman *et al.* (section A.84). However, their bicycle includes a rider and all other parts that are needed to ride a bicycle (see figure A.112). The algorithm used simplified frames and other parts so that they could not directly built the bicycle from the outcome. A CAD design was made in SolidWorks that used the algorithm output as lead. The parameters and eigenvalues of the final design are given in table A.4 and figure A.113 and the bicycle of A.112 is based on these parameters. According to calculated, but not measured, values the bicycle with rigid no-hands rider is self-stable from 3.2 to 6.1 m/s.

They discarded the idea of direct drive of the front wheel, because the rider position was not ideal enough for that. Instead they used a conventional chain transmission with a hub brake. As steering mechanism normal handlebars with are placed with a headset below the saddle and are connected by steel wires to a bar/plate attached to the rear fork at the headset. The wires are crossed such that a clockwise turn of the handlebars results in a clockwise bicycle turn. Moreover ,the points of attachment of the wires on the handlebars and fork can be adjusted to realize different steer ratios. The front frame consists of the wheel suspension and bottom bracket part of a conventional bicycle frame with additional square pipes. The headset of the donor frame is removed and used at a different location to supply the steering of the RWSB. Salient detail is that the headset makes the same but reversed angle with the vertical on this RWSB as it did on the donor bicycle. The saddle and the back rest are mounted to the upper horizontal bar in such a way that the fore-aft position and the back lean angle can be altered to position the rider differently. Moreover, the wheels are standard 12" and 28" wheels.

The built and measured bicycle without rider differs a little bit from the initial design parameters from table A.4. In total it weighs 32.6 kg with a front frame of 11.2 kg, a rear frame (including separate rear axle weights of 4.5 kg in total) of 13.0 kg, a front wheel of 7.5 kg, and a rear wheel of 0.9 kg. Note that the parameters in table A.4 show that the rear weights are modeled into the rear wheel parameter. This way the weights are located at the rear wheel axles and by not altering the rear wheel mass moments of inertia, the dynamics should not be affected very much. Despite these rear axle weights, the high layout of the RWSB with the center of mass close to the front axle reduced the braking ability

Figure A.112: Ridable RWSB of Van Dijk *et al.*, an evolution of the Broxterman *et al.* riderless RWSB. [18]

(maximum of 1.5 m/s^2 deceleration) of the bicycle due to danger of tipping forward.

Some of the group members were able to ride the bicycle with less than 10 minutes of practice time, and thus qualitatively the ridability seemed good. The main problem was the unstable behavior at low speeds which made it hard and somewhat scary to start cycling. Self-stability was tested by measuring two angular rates with gyrometers: The front frame lean angle and an angular rate related to the steer rate (probably the rear frame yaw rate). The forward speed was measured by using a standard bicycle speed meter with magnets in the wheel. They performed tests by bringing the bicycle in a curve and then releasing the hands from the handlebars. Then self-stability should bring the bicycle back to a straight forward motion. The measurement showed diminishing sinusoidal angular rates at the two locations on the bicycle.

Table A.4: The built Van Dijk *et al.* self-stable ridable RWSB parameters.

Parameter	**Symbol**	**Value**
Wheel base	w	1.05 m
Front wheel trail	c	-0.82 m
Steer axis tilt	λ_s	-0.4712 rad
Gravity	g	9.81 N/kg
Rear wheel R radius	r_R	0.15 m
Rear wheel R mass	m_R	10 kg
Rear wheel R MMOI	(I_{Rxx}, I_{Ryy})	(0.03, 0.02) kgm^2
Rear frame B COM	(x_B, z_B)	(0.31, -0.49) m
Rear frame B mass	m_B	2.09 kg
Rear frame B MMOI	$\begin{bmatrix} I_{Bxx} & 0 & I_{Bxz} \\ 0 & I_{Byy} & 0 \\ I_{Bxz} & 0 & I_{Bzz} \end{bmatrix}$	$\begin{bmatrix} 0.1382 & 0 & 0.0798 \\ 0 & 0.1800 & 0 \\ 0.0798 & 0 & 0.1218 \end{bmatrix}$ kgm^2
Front frame H COM	(x_H, z_H)	(1.0298, -0.8362) m
Front frame H mass	m_H	83.77 kg
Front frame H MMOI	$\begin{bmatrix} I_{Hxx} & 0 & I_{Hxz} \\ 0 & I_{Hyy} & 0 \\ I_{Hxz} & 0 & I_{Hzz} \end{bmatrix}$	$\begin{bmatrix} 10.5062 & 0 & -3.4651 \\ 0 & 14.0722 & 0 \\ -3.4651 & 0 & 4.6060 \end{bmatrix}$ kgm^2
Front wheel F radius	r_F	0.3750 m
Front wheel F mass	m_F	5 kg
Front wheel F MMOI	(I_{Fxx}, I_{Fyy})	(0.35, 0.7) kgm^2

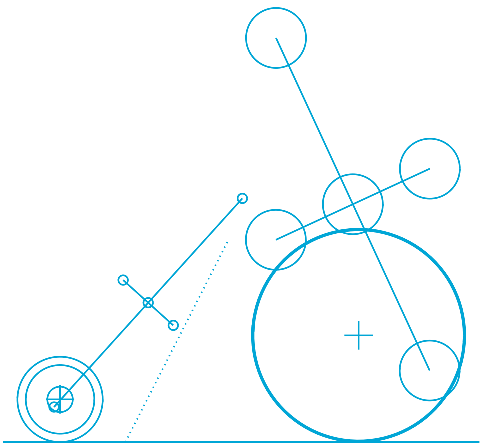

(a)

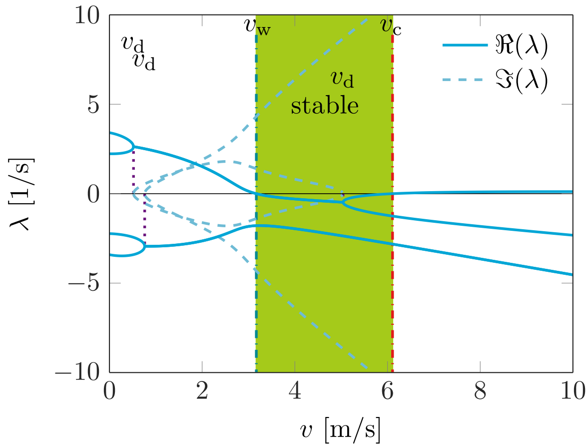

(b)

Figure A.113: Van Dijk *et al.* RWSB (a) configuration , and (b) eigenvalue plot. $v_{\text{doubleroot}}$ = 0.5195, 0.7605, 5.040, $v_{\text{weave}} = 3.169$, and $v_{\text{capsize}} = 6.1082$ m/s (Recreated with JBike6 from [18])

Concept RWS recumbent

The optimization algorithm of Van Dijk *et al.* produced another promising bicycle configuration based on a different to-be-optimized starting configuration [18]. This configuration can be seen in table A.5 and figure A.114, but it was never elaborated further. The bicycle resembles a recumbent bicycle with an almost horizontal rider positioned low between the wheels. With the center of mass further behind the front wheel and lower as compared to the built and tested bicycle of Van Dijk *et al.*, the chance of pitching over frontally is reduced. They disregarded this design, because it is only stable in a too small and high speed region for their purposes, but it does still show self-stability and might serve as an inspiration for a more practical ridable RWSB in the future.

Table A.5: Concept Van Dijk *et al.* self-stable ridable RWSB parameters.

Parameter	**Symbol**	**Value**
Wheel base	w	0.75 m
Front wheel trail	c	-0.40 m
Steer axis tilt	λ_s	0.6441 rad
Gravity	g	9.81 N/kg
Rear wheel R radius	r_R	0.1504 m
Rear wheel R mass	m_R	0.6123 kg
Rear wheel R MMOI	(I_{Rxx}, I_{Ryy})	(0.0064, 0.0125) kgm^2
Rear frame B COM	(x_B, z_B)	(0.2197, -0.1329) m
Rear frame B mass	m_B	1.1233 kg
Rear frame B MMOI	$\begin{bmatrix} I_{Bxx} & 0 & I_{Bxz} \\ 0 & I_{Byy} & 0 \\ I_{Bxz} & 0 & I_{Bzz} \end{bmatrix}$	$\begin{bmatrix} 0.00030725 & 0 & -0.0014 \\ 0 & 0.0183 & 0 \\ -0.0014 & 0 & 0.0182 \end{bmatrix}$ kgm^2
Front frame H COM	(x_H, z_H)	(0.5749, -0.3803) m
Front frame H mass	m_H	85.845 kg
Front frame H MMOI	$\begin{bmatrix} I_{Hxx} & 0 & I_{Hxz} \\ 0 & I_{Hyy} & 0 \\ I_{Hxz} & 0 & I_{Hzz} \end{bmatrix}$	$\begin{bmatrix} 3.4701 & 0 & -2.6208 \\ 0 & 13.4416 & 0 \\ -2.6208 & 0 & 10.9717 \end{bmatrix}$ kgm^2
Front wheel F radius	r_F	0.2315 m
Front wheel F mass	m_F	9.9974 kg
Front wheel F MMOI	(I_{Fxx}, I_{Fyy})	(0.2629, 0.5227) kgm^2

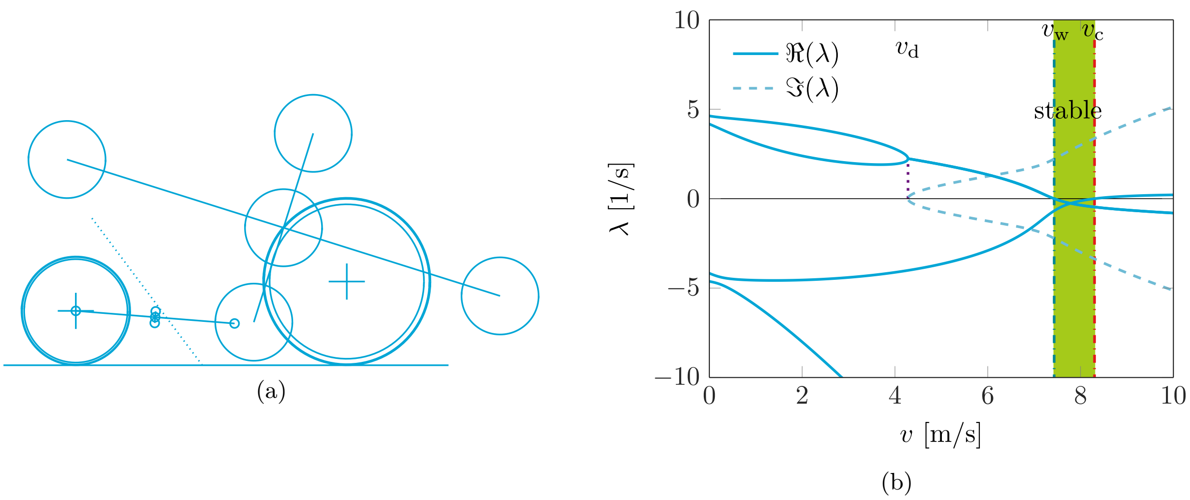

Figure A.114: Van Dijk *et al.* concept RWSB (a) configuration, and (b) eigenvalue plot. $v_{\text{doubleroot}} = 4.2815$, $v_{\text{weave}} = 7.4308$, and $v_{\text{capsize}} = 8.3005$ m/s (Recreated with JBike6 from [18])

A.86 2013 Harrop 'Rear Steering Bicycle attempt'

With his 'Rear Steering Bicycle attempt' Ross J. Harrop tried to improve the design of Stroud (section A.13) in 2013 [233]. He saw some deficienies in Stroud's design, and with several adjustments he improved the design (figure A.115a) and made a more drastical redesign (figure A.115b) [233]:

> "*A bit of history Edward Mansfield STROUD of USA in 1890 came up with this fully adjustable velocipede which could be pedalled via chain or directly by the front wheel. The rear wheel was self centering and steered through the central shaft. The handle bar was pressed down on the side in-which the rider wanted to go. The problems I foresee are that the steering force required would be rather high even acknowledge that most of the overall weight is on the front wheel. The other draw back is that the handlebar movement is opposite to that of a normal bicycle.*
>
> *To overcome these deficiencies I have devised a mechanism to reverse and variable increase the mechanical advantage of the steering system.*
>
> *Below is my attempt at improving on Strouds' bicycle. With greater steering leverage and a more gradual rear wheel turning movement, a higher cornering speed should be navigated more easily. The proposed bike shown left has normal handlebars and seat placing the rider near the centre, however a 45 degree turn will produce the same degree of rear wheel lean 45 degrees, a bit excessive I think, so a redesign is required.*
>
> *A Rethink*
>
> *Like everything comes a compromises, the handlebar positioning becomes more relaxed, and a better braced frame has resulted. The seat position stayed the same and head angle changed from 45 to 22.5 degrees, with a slight increase of frame movement sidewards caused by increased trail from 85mm to 180mm. The reduced wheel lean may make steering more manageable? The front wheel points into a corner 1/5 of the angle of the rear wheel which points in the opposite direction.The centre of gravity will need to be maintained within the wheel alignment so the rider will need to lean themself into corners.*
>
> *And would be to have the weight over the front wheel like a penny farthing or unicycle. The riders centre of gravity would be less effected by the sideward movement of the frame when the rear wheel is turned but more tip able in the forward direction.*"

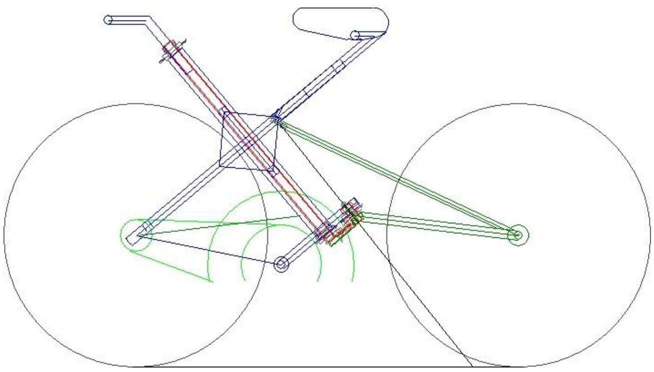

(a)

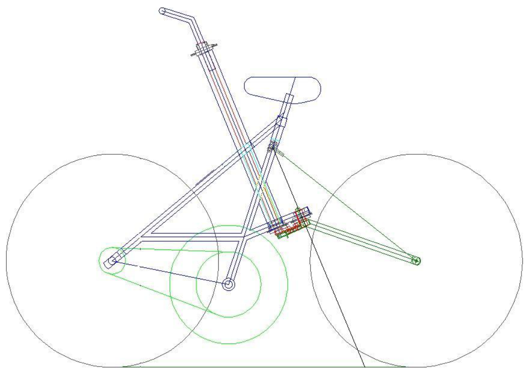

(b)

Figure A.115: Harrop's two improvements on Stroud's bicycle, (a) incorporating his steering mechanism, and (b) a rethink of the total bicycle. [233]

A.87 2014 Schwab and Kooijman ‘RWSVeloX’

This RWSB configuration was presented in 2014 by Schwab and Kooijman after a research on implementing rear wheel steering into the world speed record breaking VeloX bicycle [19]. The design space was limited due to the fact that they used the VeloX 1 and its recumbent rider position and limited spaced fairing as given properties. Therefore, only the steer axis angle, the trail, and the center of mass position of the steer assembly could be altered. Subsequently, the best (least unstable) configuration they could find by trial and error is the one given in table A.6 and shown in figure A.116. The bicycle is never stable in the forward speed range, but the positive real eigenvalue does grow only minimally with increasing speed, such that this recumbent race bicycle might be ridden by a human controller. However, being too unstable, this configuration was not worked out any further. For future work, it would be better to use a less strict design space, e.g. allow for a different fairing or rider position.

Table A.6: Concept RWSVeloX parameters.

Parameter	**Symbol**	**Value**
Wheel base	w	1.4 m
Front wheel trail	c	-1.2 m
Steer axis tilt	λ_s	-1.0472 rad
Gravity	g	9.81 N/kg
Rear wheel R radius	r_R	0.2860 m
Rear wheel R mass	m_R	1 kg
Rear wheel R MMOI	$(I_{\mathrm{R}xx}, I_{\mathrm{R}yy})$	(0.0350, 0.0700) kgm^2
Rear frame B COM	$(x_\mathrm{B}, z_\mathrm{B})$	(0.2, -0.2) m
Rear frame B mass	m_B	2 kg
Rear frame B MMOI	$\begin{bmatrix} I_{\mathrm{B}xx} & 0 & I_{\mathrm{B}xz} \\ 0 & I_{\mathrm{B}yy} & 0 \\ I_{\mathrm{B}xz} & 0 & I_{\mathrm{B}zz} \end{bmatrix}$	$\begin{bmatrix} 0.0162 & 0 & -0.0065 \\ 0 & 0.0250 & 0 \\ -0.0065 & 0 & 0.0088 \end{bmatrix}$ kgm^2
Front frame H COM	$(x_\mathrm{H}, z_\mathrm{H})$	(0.7182, -0.3591) m
Front frame H mass	m_H	110 kg
Front frame H MMOI	$\begin{bmatrix} I_{\mathrm{H}xx} & 0 & I_{\mathrm{H}xz} \\ 0 & I_{\mathrm{H}yy} & 0 \\ I_{\mathrm{H}xz} & 0 & I_{\mathrm{H}zz} \end{bmatrix}$	$\begin{bmatrix} 1.3409 & 0 & 0.0818 \\ 0 & 20.0045 & 0 \\ 0.0818 & 0 & 18.6636 \end{bmatrix}$ kgm^2
Front wheel F radius	r_F	0.3340 m
Front wheel F mass	m_F	1 kg
Front wheel F MMOI	$(I_{\mathrm{F}xx}, I_{\mathrm{F}yy})$	(0.0450, 0.0900) kgm^2

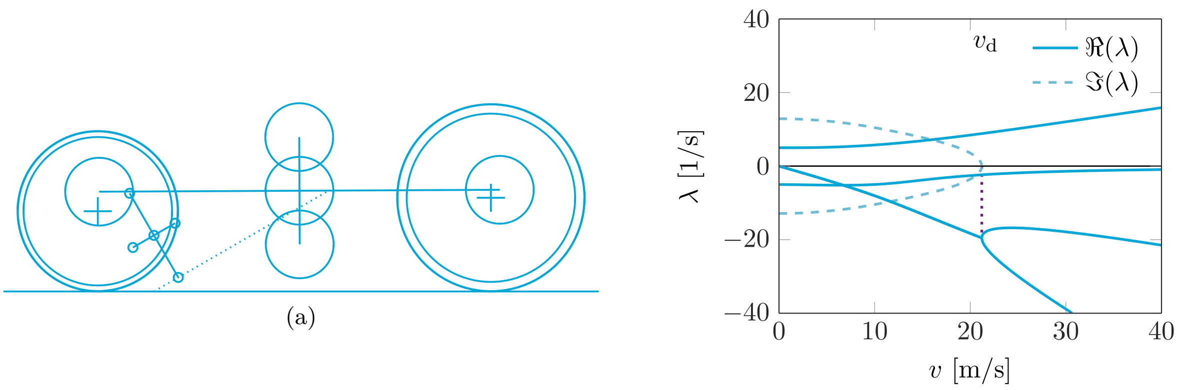

(a) (b)

Figure A.116: Schwab and Kooijman ‘RWSVeloX’ (a) configuration, and (b) eigenvalue plot. Unstable for all forward velocities; $v_\mathrm{doubleroot} = 5.8747$ m/s. (Recreated with JBike6 from [19])

A.88 2014 Mars 'DirectDrive Recumbent with RWS'

Rik Mars developed a recumbent bicycle idea around 2014 that incorporated direct drive of the front wheel combined with rear wheel steering, the 'DirectDrive Recumbent with rear wheel steering' [110]. He was inspired by some earlier rear wheel steered recumbents like the one of Dennis Renner (section A.59) and a study on a direct drive recumbent of Jeremy Garnet [234]. He implements rear wheel steering by placing the steer axis such that it points downward to the front and intersects the ground close to the midpoint in between the wheel contacts (figure A.117). Furthermore, by implementing a directly driven front wheel, he saw his concept as a better alternative to those designs [110]:

> "*Better would be a DirectDrive Recumbent with rear wheel steering: DDRRWS, of which I present a model. It has 28" (622 mm) rims. A gearing in the wheel hub still needs to be developed to ride this bike at higher speeds.*"

(a) (b)

Figure A.117: Model of Mars' direct drive recumbent with rear wheel steering (a) seen from the right, and (b) from the rear right. [110]

A.89 2014 hf61 'Rigging rear wheel steering bike'

In 2014 forum user hf61 tried to model the recumbent bicycle of Dennis Renner (section A.59) in the 'Blender' software, as a 'Rigging rear wheel steering bike' [235]. He wanted to find which pivot angle is the best for that recumbent bicycle design. Therefore, he incorporated different steer axis angles as the one used by Renner (figure A.118), making the trail also very different in magnitude from Renner's trail.

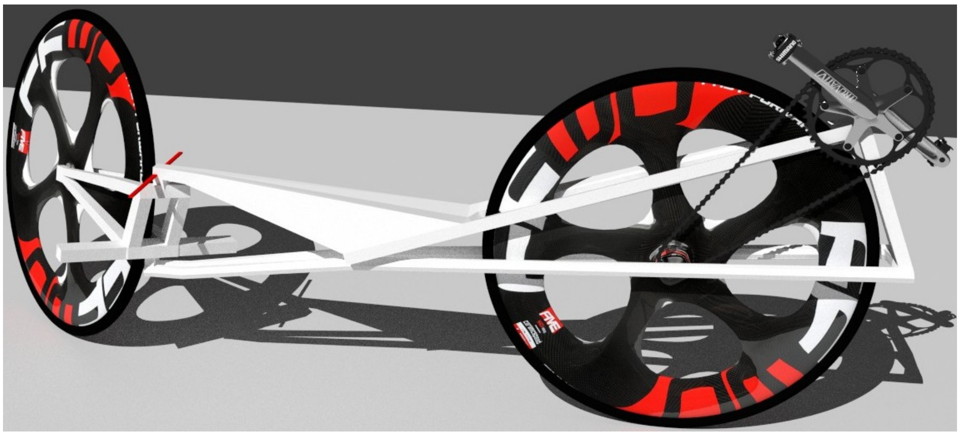

Figure A.118: hf61's Blender model of Renner's bicycle seen from the front right. [235]

A.90 2015 Pinkerton Cycles 'Back 2 front bike'

Pinkerton Cycles made at least two versions of a 'Back 2 front bike' between 2013 [236] and 2015 [237]. The bicycle is simply a reversed conventional BMX bicycle with an altered steer mechanism to make a clockwise handlebar turn results in a clockwise bicycle turn (see figure A.119). A video shows the difficulties in riding it [236], which is endorsed by their own words [237]:

> "*Steer the front wheel which is at the back....A real mind bender.....*"

(a) (b)

Figure A.119: Pinkerton Cycles' 'Back 2 front bike' (a) early 2013 version from the left side [236], and (b) the later 2015 version from the right side [237].

A.91 2015 Baid 'Flexion bike'

Shreyans Baid experimented with rear wheel steering around 2014/2015 by building his 'Flexion' bicycle [238] [239]. This bicycle is a reversed recumbent with the steer axis intersecting the ground slightly behind the rear wheel (figure A.120). Steering is done by pulling and pushing two levers, but videos show that the bicycle is not ridden in a stable fashion [238] [239]; The bicycle often rests on the training wheels and bystanders often push the bicycle or intervene the rider to avoid collisions with other objects. Baid made the RWSB to have the advantages of a recumbent bicycle, while maintaining a short drivetrain [239]:

> "*Flexion is a rear steering recumbent bicycle. Unlike normal cycles where the user's back gets absolutely no support, recumbent cycles give you total back support. It is tested that this position while driving, gives the rider better momentum and driving ability. Well, the existing recumbent bikes are all front steering with long connected chains till the rear. So to avoid that and let's say, to move away from the conventional design, I, under the guidance of Mr. Sudipto Sengupta started this project. Its just the first stage, a lot of development can be done to make it better. But it was fun working on this project got to learn a lot of things and looking forward to quickly start the second improved version of it.*"

(a) (b)

Figure A.120: Baid's 2015 'Flexion' (a) first version with rear-side view with a look on the steer mechanism [238], and (b) a later version (main difference with the earlier version seems to be a higher bracket) from a side view [239].

A.92 2015 Zakaria Toro-X

Norul Ridzuan Zakaria designed and posted a bicycle design in 2015 called 'Toro-X' [240]. He designed several bicycles with the same steering principal: The handlebar is attached to the rear assembly which steers by turning about its own axis, and the rider sits on the front assembly which also contains the driven front wheel (see figure A.121). This configuration makes that the two frames are crossed. Moreover, in his designs this makes that the steer axis points downward to the rear and the steer axis intersects the ground behind the rear wheel. The several bicycle designs of Zakaria had all their own specific purpose and were adjusted to meet specific requirements [240]:

> "*Each Toro-X bicycle has its chain ring connected via the chain to the front wheel, while its handle is connected to the rear wheel. . . . Toro-X Uno is the lightest Toro-X bicycle with the simplest frame design and built with the least construction materials. If Toro-X Uno is to be constructed based on a conventional design, it will require 40% more construction materials. . . . Toro-X Duro is equipped with a twin shock-absorber under the saddle for comfort. Toro-X Duro-S* (Stylo) *is the stylish version of Toro-X Duro. . . . Toro-X Veloce is designed to be cycled fast. Toro-X Veloce-S is the stylish version of Toro-X Veloce. . . . Front wheel drive & rear wheel steering configuration as in Toro-X is suitable for chopper bicycle design. Toro-X Chopper resembles chopper bicycle by having high handle bar and lower saddle. Toro-X Chopper-S is the stylish version of Toro-X Chopper. . . . Toro-X Citta is designed to be cycled in the city. Toro-X Citta-S is the stylish version of Toro-X Citta.*"

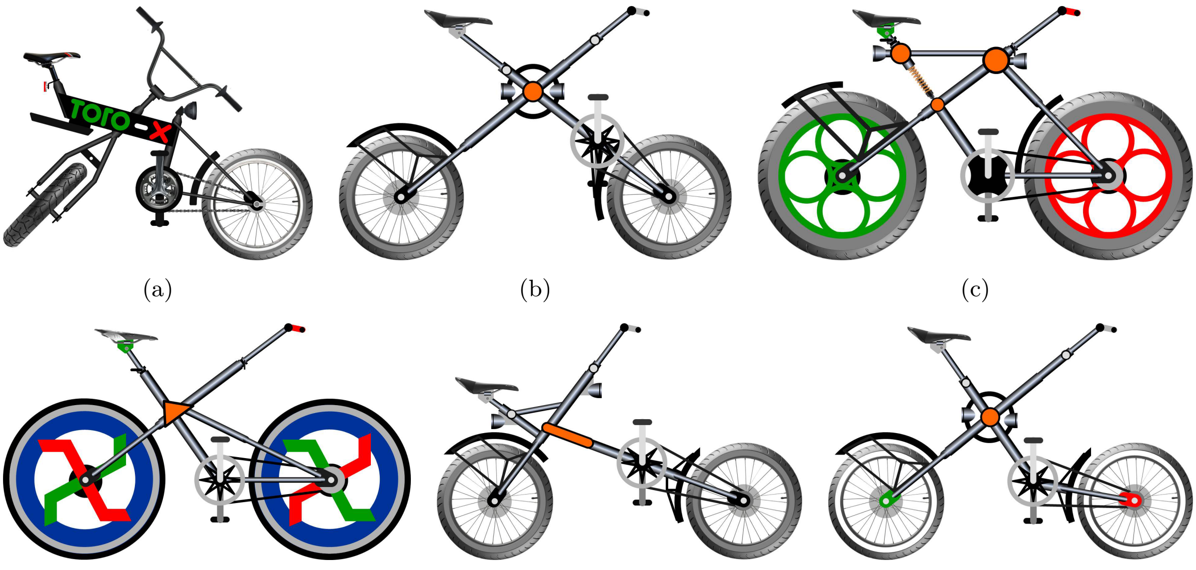

(a) (b) (c)

(d) (e) (f)

Figure A.121: Different versions of Zakaria's 'Toro-X' seen from the right side: (a) Prototype 1, (b) Uno, (c) Duro, (d) Veloce, (e) Chopper, and (f) Citta. [240]

A.93 2015 Aßmann 'Heck-Knicklenker'

In 20015 Bernd Aßmann, aka Nemberch, presented his bicycle design the 'Heck-Knicklenker' (German for 'rear bend steerer') [241] [242]. The bicycle has front wheel drive with a steer axis intersecting the ground close to the midpoint in between the wheel contacts (see figure A.122) The bicycle is adjustable by changing the angle between the two frames, such that mass heights, wheelbase, steer axis angle, and trail can be varied, although not independently (see figure A.123). To enable this adjustments, the steer joint is a universal joint. Furthermore, the steering mechanism is such that when the left and ride steer rod are moved in a 'clockwise' direction, then the bicycle also turns in a clockwise direction. Although his bicycle was ridable, it was not perfect [241] [translation by P.H. de Jong]:

> "*Das Teil ist fahrbar aber nicht gutwillig.*"
>
> "*The part is ridable, but not willingly.*"

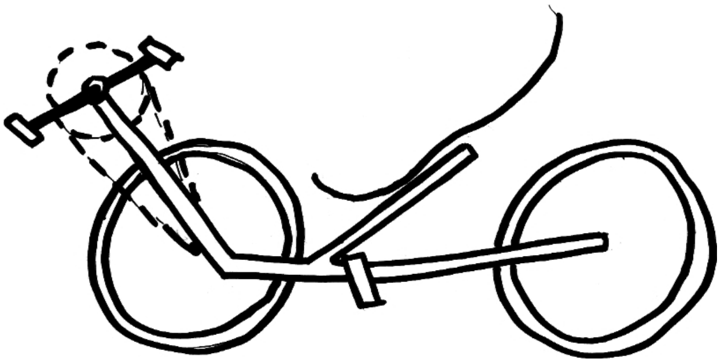

Figure A.122: left side view drawing of Aßmann's 'Heck-Knicklenker' idea. [241]

(a) (b)

Figure A.123: Aßmann's 'Heck-knicklenker' seen from the left (a) in a low adjusted position, and (b) in a higher position. [242]

A.94 2016 Haloche *et al.* ‘Trocadero’

Three Frenchmen Alban Haloche, Alexis Honoré, and Johan Le Bon built a fixie bicycle for fun in 2016 [243]. It is a singlespeed bicycle named ‘Trocadero’(-fixie) and it has besides the normal steering pivot an extra more horizontal pivot (see figure A.124). This hinge is placed in the down tube close to the head tube and its turning axis is aligned with the down tube. The second steer axis thus intersects the ground close to the rear wheel contact point. Hence, the rear wheel trail with respect to this second steer axis is smaller than the front wheel trail with respect to that same axis. As figure A.124b shows, without steering about the conventional axis, the bicycle behavior seems rear wheel steered. The rider is now able to steer by moving the hips and as witnessed by a video [244] it is quite ridable and small turns and slaloms are no problem. Apparently, it takes only ten minutes to learn to ride the Trocadero. Moreover, one can make it a conventional bicycle by locking the down tube hinge by plugging in a pin.

(a) (b)

Figure A.124: The ‘Trocadero’ of Haloche *et al.* (a) with an extra hinge in the down tube of the frame [243], (b) allowing this bicycle to do some weird, but smooth and ‘rear-wheel-steer-like’ moves [244].

A.95 ---- Lund University 'Un-Ridable Bike'

This 'Un-ridable bike' is created by the Lund University in Sweden [36] and is similar to the first bicycle of Klein [14]. Just as Klein's, it is a converted conventional bicycle, but the saddle and handlebars location is slightly different (see figure A.125). The rider sits a little closer to the front wheel and the handlebars are angled such that they turn around a same angled axis as on a conventional bicycle. Because it is a reversed conventional bicycle, the steer axis is such that it points downward to the rear and intersects the ground behind the rear wheel in forward riding direction. Also, the linkages between the handlebars and headset are crossed; a clockwise turn of the handlebars results in a clockwise turn of the bicycle.

Figure A.125: Lund University's 'Un-ridable bike' seen from the right side. [36]

A.96 ---- Smith 'To be determined'

Roy Smith mentioned this reaar wheel steered bicycle of which the stability has 'yet to be determined' [245]. Just as others have done this is simply a reversed and slightly altered conventional bicycle (figure A.126. This gives the bicycle a steer axis that intersects the ground behind the rear wheel and a driven front wheel. A rod connects the handlebar to the rear frame (fork) in a fashion such that a clockwise handlebar turn results in a clockwise bicycle turn.

Figure A.126: Smith's mentioned 'To be determined' bicycle seen from the left side. [245]

A.97 ---- ‘Milwaukee bicycle’

At the International Bicycle and Motorcycle Dynamics Conference at the Kern Center at Milwaukee School of Engineering (MSOE), among a weird bicycles display with bicycles from all over Milwaukee, also a rear wheel steered bicycle could be tested [246]. This bicycle was a reversed conventional bicycle with the handlebar at the original saddle location and the saddle at the original handlebar location, and the steer axis intersects the ground behind the rear wheel (figure A.127). In stead of what is often done for RWSBs, this bicycle has no steer reversal; a clockwise handlebar turn results in a counterclockwise bicycle turn. This bicycle was quite badly ridable, but some persons were able to ride it for about half a minute after a few hours of practice [personal conversation with A. L. Schwab, George Dialynas, and Oliver Lee].

(a) (b)

Figure A.127: Milwaukee conference bicycle (a) from the front right, and (b) from the right [Photos by G. Dialynas and A.L. Schwab]

A.98 ---- UCSB ‘Rideable Bike’

The University of California, Santa Barbara (UCSB) has designed a bicycle with rear wheel steering with the idea that it should be ridable under certain conditions [14]. Dave Bothman supervised the construction of the bicycle which can be seen as a conventional bicycle ridden backwards, having a negative rear wheel trail and a smaller-than-conventional rear wheel (figure A.128). The connection between handlebars and headset is crossed to make steering more intuitive; a clockwise handlebar motion results in clockwise bicycle turn. Pictures show a rather deflated rear wheel tire, it is not sure if this is done to benefit the ridability. The bicycle is ridable, but starting it requires as special procedure which involves ‘skill and dare’ since high acceleration is needed [14]:

> “*The rear-steered UCSB bicycle . . . is designed to be ridable under certain conditions. One way is to start by leaning forward (making a* (horizontal distance center of mass to front wheel contact) *small) and standing up on the pedals (making h* (center of mass height) *large) and then pedaling rapidly to quickly reach a high speed. This skill takes fortitude, but several students and one faculty member, Roy Smith, have mastered the technique.*”

(a) (b)

Figure A.128: The UCSB ‘rideable’ rear-steered bicycle ridden by Dave Bothman (a) from a front right view [14] [36], and (b) a left side view [245].

A.99 ---- 'Rear Steer Allegedly rideable'

This 'allegedly rideable' bicycle presented by Critical Mass in Vancouver has a simple implementation of rear wheel steering with seemingly unknown builder or owner, [247]. Built at latest in 2005 it is not sure when exactly this bicycle was created, but Jon-Richard Little, aka Johnny Payphone, reported in 2010 about it [151]. The bar connecting the driven front wheel to the saddle is crossed by the headset setting up a nonzero steer axis angle (figure A.129). In effect, the fork attached to the handlebar is such that the rear wheel trail is nearly zero with the steer axis intersecting the ground close to the rear wheel contact point. Apparently, this front wheel driven bicycle can be ridden [151]:

> "*Here's another bike that is technically rear-steered and allegedly somewhat rideable.*"

Figure A.129: The 'allegedly rideable' rear steer bicycle seen from the left side. [247]

A.100 ---- Reversely ridden bicycles

Some people are trained in riding a bicycle backwards while positioned on it in an ordinary fashion. A conventional bicycle only needs to be altered such that pedaling it backwards drives the bicycle in stead making the pedals run free; a fixed-gear bicycle would thus require no alteration at all. Curan Wright did it in 2008 while trying to raise money for the good cause (figure A.130a) [248] [249]. He used an almost unchanged bicycle (BMX) and is able to ride it pretty fast backwards witnessing a video [250]. He rode at least 53-hundred miles on the highway and across the U.S.A.. Romanian Orban-Barra Gabor also does it and he officially set a distance world record in 2014 (set to 27.58 m by him) (figure A.130b) [251]. However, he balances and steers it differently in that he adjusts for straight-track leaving by 'bunnyhopping' it back in the desired straightly rearward direction [252]. This way he probably does not have to master the different dynamics of the now rear wheel steered bicycle, and moreover the Whipple bicycle model does no longer apply since the constant contact assumption is violated.

The lack of evidence showing people performing this act, and Gabor's desired alternative way of balancing makes one think that it is rather difficult to perform this backwards bicycle riding. This is in line with the stability theory that states that a bicycle that is stable in one riding direction (as many conventional bicycles are) is unstable in the reversed direction. The eigenvalue plot is point symmetric about the eigenvalue axis and thus when an eigenvalue is negative for positive forward velocity, it is positive for negative forward velocity. Reversing the parameters of the benchmark bicycle and analyzing the eigenvalues, shows that indeed a backwards ridden conventional bicycle is unstable, because it has never all negative real eigenvalues for one velocity (see section 4.2). The eigenvalue corresponding with the caster mode is large and increasingly positive. Where this mode is of least importance in normal ridden conventional bicycles, it is here a large concern.

(a) (b)

Figure A.130: These men ride the bicycle with the driven wheel ahead and steered wheel behind. (a) Curan Wright on his roadtrip across the U.S.A., he rides the bicycle by pedaling it backwards while sitting on it normally except for a turned head to see where he is going [248]. (b) Orban-Barra Gabor during his backwards cycling distance world record attempt pedaling the bicycle in the direction of his back and looking at the pavement for orientation [252]. Gabor cleverly avoids the mastering of the odd dynamics by 'bunnyhopping' it into balance.

A.101 ---- Reversed rider cycling

Another way of looking at rear wheel steering is rotating the rider 180° and ride the bicycle with ones back facing in the ride direction. By sitting reversedly on the handlebar, the steered front wheel of the unaltered conventional bicycle is then placed at the rear of the rider. The mass distribution of the bicycle is thus altered by making the handlebar assembly a lot heavier and the rear assembly lighter. 'Hands-off' riding may be a lot more difficult because the connection between the two assemblies, i.e. the handlebar/fork assembly and the frame with saddle and drive-train assembly, is now done by the legs. Numerous examples of people performing this 'act' just for fun or as art performance. For example, German Christian Adam (né Patzig) (figure A.131a) who plays violin while doing it around 1990 [253], or 2013 world record breaking (337.60 km in 24 h) Australian Andrew Hellinga (figure A.131b) [254] [255] [256] [257].

Some people even make customized bicycles that incorporate a reversed rider position [6]. Around 1980 M. W. Raymond experimented with it to make an enclosed streamlined recumbent 'backward' bicycle (figure A.131c). The idea was that then advantages such as a simpler driving transmission and forward placed center of mass could be obtained and still have a rather conventional (and stable) steer placement which makes that the pedaling motion of the rider does not affect the steering of the front wheel. Raymond was able to balance the bicycle at 0.25 m/s and could even maneuver in circles and figure-eights at low speed. However, the low center of mass made balancing harder, and more importantly, since the rider sits reversed on it he requires a mirror to look ahead of the bicycle which was too repellent for convenient ordinary use no matter what kind of mirror he tried.

(a) (b) (c)

Figure A.131: Three examples of people riding a bicycle in a reversed position while the bicycle still moves with its steered wheel ahead. (a) Christian Adam playing violin while cycling in a reversed position in Kurt Felix' Swiss television show 'Supertreffer' around 1990 [253] and (b) Andrew Hellinga doing the same without making music but setting a world record distance [254]. (c) Raymond tests his recumbent bicycle with reversed rider position and mirror [6].

List of Figures

List of Tables

List of Symbols

Symbols

Latin

Symbol	Units	Description
$\mathbf{A}$	–	state space matrix
A	–	front assembly
A	$\mathrm{kg^2m^4}$	Routh coefficient
$\mathcal{A}$	–	general coefficient
$\mathbf{B}$	–	state space matrix
B	–	rear frame
B	$\mathrm{kg^2m^4/s}$	Routh coefficient
$\mathcal{B}$	–	general coefficient
b	m	rear wheel trail
$\mathbf{C}$	–	state space matrix
$\mathbf{C}_\mathrm{f}$	$\mathrm{kgm^2/s}$	feedback control ‘damping’ matrix
$\mathbf{C}_1$	kgm	velocity ‘damping’ matrix (to be multiplied by v)
C_f	$\mathrm{kgm^2/s}$	feedback control ‘damping’
C_1	kgm	velocity ‘damping’
C	$\mathrm{kg^2m^4/s^2}$	Routh coefficient
$\mathcal{C}$	–	general coefficient
c	–	capsize
c	m	front wheel trail
$\mathbf{D}$	–	state space matrix
D	$\mathrm{kg^2m^4/s^3}$	Routh coefficient
$\mathcal{D}$	–	difference measure of model and measurements
d	–	double root
d	m	horizontal distance wheel axle to front frame COM
E	$\mathrm{kg^2m^4/s^4}$	Routh coefficient
$\mathcal{E}$	Nm	pendulum stiffness
e	–	mathematical constant (Euler’s number)
F	–	front wheel
F	N	force
$\mathbf{f}$	Nm	generalized forces vector
f	–	feedback
f	Nm	generalized force
g	–	gait
g	N/kg	gravitational acceleration
H	–	front frame
h	–	headtube
$\mathbf{I}$	–	identity matrix
I	–	applied impulse
I	$\mathrm{kgm^2}$	mass moment of inertia
$\mathcal{I}$	$\mathrm{kgm^2}$	mass moment of inertia about pendulum axis

Symbol	Units	Description
i	–	image frame
i	–	imaginary unit
J	–	JBike6
J	–	quadratic cost function
j	–	counter
$\mathbf{K}$	–	feedback control gains matrix
$\mathbf{K}_\mathrm{f}$	kgm^2/s^2	feedback stiffness matrix
$\mathbf{K}_0$	kgm	gravity stiffness matrix (to be multiplied by g)
$\mathbf{K}_2$	kg	velocity stiffness matrix (to be multiplied by v^2)
K_f	kgm^2/s^2	feedback control stiffness
K_0	kgm	gravity stiffness
K_2	kg	velocity stiffness
$\mathcal{K}$	–	constant
$\mathcal{L}$	m	length
$\mathbf{M}$	kgm^2	mass matrix
M	–	middle point of support line (also base-point)
M	kgm^2	inertial mass
$\mathcal{M}$	kg	mass
m	kg	mass
$\mathbf{N}$	–	reference gains matrix
$\mathcal{N}$	–	number
N	–	reference gain
n	–	nominal
n	–	number
O	–	origin
$\mathcal{O}$	m	fork offset
P	–	rear wheel contact point
P	Nm/s	power
$\mathbf{p}$	–	coordinate system
p	–	pulse
p	–	part counter (= R, B, H, F, A)
$\mathbf{Q}$	–	state cost weights
Q	–	front wheel contact point
$\mathbf{q}$	rad	generalized coordinates vector
q	rad	generalized coordinate
$\mathbf{R}$	–	input cost weights
R	–	rear wheel
R	m	turn radius
$\mathcal{R}$	m	radius
$\mathbf{r}$	–	state space reference vector
r	–	reference
r	m	wheel radius
S	kgm	gyrostatic coefficient
$\mathcal{S}$	m	displacement
s	–	steer (axis)
s	1/s	Laplace frequency parameter
$\mathbf{T}$	–	transformation matrix
T	–	total assembly
T	Nm	torque
$\mathcal{T}$	s	oscillation/time period
t	–	tick
t	s	time
U	–	Unicycle
$\mathcal{U}$	V	voltage
$\mathbf{u}$	–	state space input vector

Symbol	Units	Description
u	m	perpendicular distance to steer axis
$\mathcal{V}$	–	line slope
v	m/s	forward velocity
W	–	wheel
$\mathcal{W}$	m	line vertical axis intercept
w	–	weave
w	m	wheel base
X	$\mathrm{kg^6 m^{12}/s^6}$	Routh determinant
$\mathcal{X}$	m	pendulum coordinates axis
$\mathbf{x}$	–	state space state vector
x	m	axis, coordinate, direction
$\mathbf{y}$	–	state space output vector
y	m	axis, coordinate, direction
$\mathcal{Z}$	m	pendulum coordinates axis
z	m	axis, coordinate, direction
$\mathbf{0}$	–	zero matrix
Ø	m	diameter

Greek

Symbol	Units	Description
α	rad (°)	angle nominal bicycle to principal coordinates
β	rad	angle nominal bicycle to pendulum coordinates
γ	rad	headtube angle in pendulum frame
Δ_{s}	–	steer-side coefficient
δ	rad	steer angle
ζ	–	damping ratio
θ	rad	pitch angle (about bicycle y-axis)
ι	–	mass moment of inertia coefficient/factor
λ	1/s	eigenvalue
λ_{h}	°	headtube angle
λ_{s}	rad	steer axis angle
μ	–	ratio
π	–	mathematical constant (Archimedes' constant)
ϕ	rad	lean/roll angle (about bicycle x-axis)
φ	rad	phase
ψ	rad	heading/yaw angle (about bicycle z-axis)
ω	1/s	(oscillation) frequency

Functions, brackets and diacritics (letter modifiers)

Diacritic	Description
$\arg(\square)$	argument function
$\cos$	cosine
$\sin$	sine
$\tan$	tangent
$\arctan$	arctangent
$\det(\square)$	determinant
$\mathrm{diag}(\square)$	diagonal elements matrix
$\mathrm{rank}(\square)$	matrix rank
$\mathrm{sgn}(\square)$	signum function
$\Im(\square)$	imaginary part of complex number
$\Re(\square)$	real part of complex number

Diacritic	Description
$\lvert\square\rvert$	modulus (absolute value)
$\lVert\square\rVert$	Euclidean norm (2-norm)
$\dot{\square}$	first time derivative
$\ddot{\square}$	second time derivative
$\int$	integral
$\overset{\frown}{\square}$	arc
$\hat{\square}$	eigenvector
$\overline{\square\square}$	line length
$\bar{\square}$	mean, average
$\square^*$	projection, alternative, calibrated
$\square^\mathsf{T}$	transpose

Acronyms

Acronym	Description
AC	Alternating Current
A/D	Analog to Digital
BPM	Beats Per Minute
CAD	Computer-Aided Design
COM	Center of Mass
DC	Direct Current
DUT	Delft University of Technology
EOM	Equations of Motion
FWS(B)	Front Wheel Steered (Bicycle)
GND	Ground
GUI	Graphical User Interface
HPV	Human Powered Vehicle
IMU	Inertial Measurement Unit
I/O	Input to Output
LQR	Linear-Quadratic Regulator
LSB	Least Significant Bit
MMOI	Mass Moment of Inertia
MSE	Mean Squared Error
NHTSA	National Highway Traffic Safety Administration
NIU	Northern Illinois University
NRMSE	Normalized Root Mean Square Error
ODE	Ordinary Differential Equation
PD	Proportional Derivative
RSRB	Rear Steered Recumbent Bicycle
RWS(B)	Rear Wheel Steered (Bicycle)
2D	Two-Dimensional
3D	Three-Dimensional

References

[1] W. J. M. Rankine, "On the dynamical principles of the motion of velocipedes," *The Engineer*, vol. 28 and 29(1870), pp. 28:79,129,153,175 and 29:2, 1869.

[2] A. Sharp, *Bicycles and Tricycles: An Elementary Treatise on Their Design and Construction, with Examples and Tables.* Longmans, Green, and Company, 1896.

[3] D. E. H. Jones, "The stability of the bicycle," *Physics Today*, vol. 23, no. 4, pp. 34–40, 1970. (reprinted in September 2006).

[4] L. H. Laiterman, "Theory and applications of rear-wheel steering in the design of man-powered land vehicles," bachelor's thesis, Massachusetts Institute of Technology, May 1977.

[5] R. Schwarz, "Accident avoidance characteristics of unconventional motorcycle configurations," sae technical paper 790258, Society of Automotive Engineers, 1979. doi:10.4271/790258.

[6] F. R. Whitt and D. G. Wilson, *Bicycling Science.* MIT Press, 2nd ed., 1982.

[7] R. L. Price, "Human-powered vehicle steering and suspension design," *Human Power - The technical journal of the IHPVA*, vol. 7, no. 3, pp. 18–22, 1989.

[8] C. J. Cornelius, "Rear-steering recumbent bicycles," *Human Power - The technical journal of the IHPVA*, vol. 8, no. 2, pp. 6–7,17–20, 1990.

[9] J. C. Whitehead, "Rear-wheel-steering basics," *Human Power - The technical journal of the IHPVA*, vol. 8, no. 4, pp. 9–12, 1990.

[10] T. Hikichi and Y. Tezuka, "Study on improving the motorcycle high speed stability using a rear wheel self-steering system," 1995. SAE Technical Papar 950198.

[11] S. Suryanarayanan, M. Tomizuka, and M. Weaver, "System dynamics and control of bicycles at high speeds," in *Proceedings of the American Control Conference, Anchorage, AK May 8-10, 2002*, vol. 2, pp. 845–850 vol.2, 2002.

[12] D. Karnopp, *Vehicle Stability.* Mechanical Engineering, CRC Press, 2004.

[13] D. G. Wilson and J. Papadopoulos, *Bicycling Science.* MIT Press, 3rd ed., 2004.

[14] K. Åström, R. E. Klein, and A. Lennartsson, "Bicycle dynamics and control: adapted bicycles for education and research," *Control Systems, IEEE*, vol. 25, pp. 26–47, Aug 2005.

[15] J. D. G. Kooijman, J. P. Meijaard, J. M. Papadopoulos, A. Ruina, and A. L. Schwab, "A bicycle can be self-stable without gyroscopic or caster effects," *Science*, vol. 332, no. 6027, pp. 339–342, 2011.

[16] J. D. G. Kooijman, J. P. Meijaard, J. M. Papadopoulos, A. Ruina, and A. L. Schwab, "A bicycle can be self-stable without gyroscopic or caster effects - supporting online text material," Apr. 14 2011. `http://www.sciencemag.org/content/332/6027/339/suppl/DC1`, `http://bicycle.tudelft.nl/stablebicycle/`, `http://ruina.tam.cornell.edu/research/topics/bicycle_mechanics/stablebicycle/`.

[17] S. Broxterman, P. de Jong, M. Korevaar, and W. Kuijsters, “Het ontwerpen van een zelfstabiele achterwiel gestuurde fiets,” bachelor’s thesis, Delft University of Technology, January 2012. in Dutch.

[18] T. van Dijk, T. Huiskens, M. Knol, and M. de Vette, “Rijden op een achterwiel gestuurde fiets,” bachelor’s thesis, Delft University of Technology, June 2012. in Dutch.

[19] A. Schwab and J. Kooijman, “Balance and control of a rear-wheel steered speed-record recumbent bicycle,” *Procedia Engineering; ISEA 2014: 10th Conference of the International Sports Engineering Association*, vol. 72, pp. 459–464, 2014.

[20] Wikipedia, “Bicycle — wikipedia, the free encyclopedia,” 2016. `https://en.wikipedia.org/wiki/Bicycle`, [Online; accessed 28-January-2016].

[21] G. Gimini, “Behance - gianluca gimini - velocipedia,” Mar. 27 2016. `https://www.behance.net/gallery/35437979/Velocipedia`, [Online; accessed 15-December-2016].

[22] J. P. Meijaard, J. M. Papadopoulos, A. Ruina, and A. L. Schwab, “Linearized dynamics equations for the balance and steer of a bicycle: a benchmark and review,” *Proceedings of the Royal Society of London A: Mathematical, Physical and Engineering Sciences*, vol. 463, no. 2084, pp. 1955–1982, 2007.

[23] J. Meijaard, J. M. Papadopoulos, A. Ruina, and A. Schwab, “Historical review of thoughts on bicycle self-stability,” 2011. `http://hdl.handle.net/1813/22497`.

[24] A. L. Schwab, “History of bicycle steer and dynamics equations,” Sept. 10 2009. `http://bicycle.tudelft.nl/schwab/Bicycle/BicycleHistoryReview/index.htm`, [Online; accessed 1-June-2015].

[25] D. Limebeer and R. Sharp, “Bicycles, motorcycles, and models,” *Control Systems, IEEE*, vol. 26, pp. 34–61, Oct 2006.

[26] J. Meijaard, J. M. Papadopoulos, A. Ruina, and A. Schwab, “Linearized dynamics equations for the balance and steer of a bicycle: a benchmark and review – supplementary appendices,” June 2007. Electronic Supplementary Material, `http://bicycle.tudelft.nl/benchmarkbicycle/`, `http://bicycle.tudelft.nl/benchmarkbicycle/meijaard2007linearizedESM.pdf`, [Online; accessed 1-June-2015].

[27] R. Sharp, “The stability and control of motorcycles,” *Journal of Mechanical Engineering Science*, vol. 13, no. 5, pp. 316–329, 1971.

[28] D. Despain, “175,000... the challenge and the alternative,” *American Motorcyclist - The monthly journal of the American Motorcyclist Association*, vol. 33, p. 4, April 1979.

[29] AM, “Proxmire says nhtsa fleeced the public,” *American Motorcyclist - The monthly journal of the American Motorcyclist Association*, vol. 33, p. 22, June 1979.

[30] W. Proxmire, *The fleecing of America.* Houghton Mifflin Company, 1980.

[31] F. R. Whitt and D. G. Wilson, *Bicycling Science: Ergonomics and Mechanics.* MIT Press, 1st ed., 1974.

[32] HP, “Letter to the editor - correction,” *Human Power - The technical journal of the IHPVA*, vol. 8, no. 1, p. 3, 1990.

[33] Hephaestus (Craig Cornelius), “The left-handed cyclist - recumbents and convergent evolution,” March 2012. `http://lefthandedcyclist.blogspot.nl/2012/03/recumbents-and-convergent-evolution.html`, [Online; accessed 16-April-2015].

[34] M. Tomizuka, *Control and Modeling of Complex Systems: Cybernetics in the 21st Century Festschrift in Honor of Hidenori Kimura on the Occasion of his 60th Birthday*, ch. Computer Control of Vehicles: Overcoming Limitations of Human Drivers, pp. 283–301. Boston, MA: Birkhäuser Boston, 2003.

[35] D. Karnopp, *Vehicle dynamics, stability, and control.* CRC Press, Taylor and Francis Group, 2nd ed., 2013.

[36] K. J. Åström, “Bicycle dynamics and control,” 2006. lecture notes, `http://www.control.lth.se/media/Staff/KarlJohanAstrom/Lectures/BikeTalkKTH2006.pdf`, [Online; accessed 4-May-2015].

[37] J. M. Papadopoulos, “Bicycle steering dynamics and self-stability: a summary report on work in progress,” technical report, Cornell University, Ithaca, NY, 1987. Preliminary draft, 15 December 1987, `http://ruina.tam.cornell.edu/research/topics/bicycle_mechanics/papers.php`, `http://ruina.tam.cornell.edu/research/topics/bicycle_mechanics/bicycle_steering.pdf`, [Online; accessed 20-February-2015].

[38] K. Åström, “Limitations on control system performance,” *European Journal of Control*, vol. 6, no. 1, pp. 2 – 20, 2000.

[39] R. E. Klein, “Novel systems and dynamics teaching techniques using bicycles,” in *American Control Conference, 1988*, pp. 1157–1160, June 1988.

[40] R. E. Klein, “Using bicycles to teach system dynamics,” *Control Systems Magazine, IEEE*, vol. 9, pp. 4–9, April 1989.

[41] K. Aström and R. Murray, *Feedback Systems: An Introduction for Scientists and Engineers*. Princeton University Press, 2010.

[42] M. J. Coleman and J. M. Papadopoulos, “Intrinsic stability of a classical monocycle and a generalized monocycle.” Unpublished manuscript, 30 October 2010.

[43] P. Gewirtz, “On “I Know It When I See It”,” *Yale Law Yournal, Faculty Scholarship Series*, vol. 105, pp. 1023—-1047, 1996. Paper 1706. `http://digitalcommons.law.yale.edu/fss_papers/1706`.

[44] J. Kooijman, *Bicycle Rider Control: Observations, Modeling & Experiments.* Dissertation, Delft University of Technology, Sept. 18 2012. uuid:3Ada8e3e64-0f3e-4932-adf7-dd80d9008040.

[45] Schwab, Papadopoulos, Ruina, and Dressel, “JBike6 - A Benchmark for Bicycle Motion (linearized ODEs),” Feb. 8 2015. `http://ruina.tam.cornell.edu/research/topics/bicycle_mechanics/JBike6_web_folder/`.

[46] A. L. Schwab and J. P. Meijaard, “A review on bicycle dynamics and rider control,” *Vehicle System Dynamics*, vol. 51, no. 7, pp. 1059–1090, 2013.

[47] Schwab, Papadopoulos, Ruina, and Dressel, “Jbike6 help,” Feb. 8 2015. `http://ruina.tam.cornell.edu/research/topics/bicycle_mechanics/JBike6_web_folder/JBhelp.htm`, [Online; accessed 8-February-2016].

[48] Destin - SmarterEveryDay, “The backwards brain bicycle - smarter every day 133 - youtube,” Apr. 24 2015. `https://www.youtube.com/watch?v=MFzDaBzBlL0&nohtml5=False`, [Online; accessed 6-April-2016].

[49] Gaël COSTE, “Reverse steering bike demo3 master biker - youtube,” Apr. 29 2012. `https://www.youtube.com/watch?v=-rUdaeOVGC8`, [Online; accessed 6-April-2016].

[50] Gael - Tim, “Reverse steering bike - instructables,” Apr. 29 2012. `http://www.instructables.com/id/Reverse-steering-bike/`, [Online; accessed 6-April-2016].

[51] M. Olley, “Road manners of the modern car,” *Proceedings of the Institution of Automobile Engineers*, vol. 41, no. 1, pp. 147–182, 1946.

[52] L. Strandberg, “Danger, rear wheel steering,” *Journal of Occupational Accidents*, vol. 5, no. 1, pp. 39 – 58, 1983.

[53] M. J. Coleman, *A stability study of a three-dimensional passive-dynamic model of human gait.* Dissertation, Cornell University, February 1998.

[54] A. K. Kundu, *Aircraft Design.* Cambridge Aerospace Series, Cambridge University Press, 2010.

[55] D. Witt, "Riding a boat like a bicycle," *Human Power - The technical journal of the IHPVA*, vol. 13, no. 1, pp. 3–6, 1997. issue no. 44.

[56] P. L. Jakab, *Visions of a flying machine: the Wright brothers and the process of invention.* Smithsonian history of aviation series, Smithsonian Institution Press, 1990.

[57] SAE International, 2008. SAE J670 (R) Vehicle Dynamics Terminology.

[58] A. L. Schwab and J. P. Meijaard, "How to draw euler angles and utilize euler parameters," in *ASME 2006 International Design Engineering Technical Conference & Computers and Information in Engineering Conference, Philadelphia, Pennsylvania, USA, September 10–13, 2006*, pp. 1–7, 2006. `http://bicycle.tudelft.nl/schwab/Publications/SchwabMeijaard2006.pdf`.

[59] J. Kooijman, A. Schwab, and J. Meijaard, "Experimental validation of a model of an uncontrolled bicycle," *Multibody System Dynamics*, vol. 19, no. 1-2, pp. 115–132, 2008.

[60] J. K. Moore, M. Hubbard, A. L. Schwab, and J. D. G. Kooijman, "Accurate measurement of bicycle parameters," in *Proceedings, Bicycle and Motorcycle Dynamics 2010 Symposium on the Dynamics and Control of Single Track Vehicles, 20—22 October 2010, Delft, The Netherlands*, 2010. `http://bicycle.tudelft.nl/schwab/Publications/moore2010accurate.pdf`.

[61] J. K. Moore, M. Hubbard, J. D. G. Kooijman, and A. L. Schwab, "A method for estimating physical properties of a combined bicycle and rider," in *Proceedings of the ASME 2009 International Design Engineering Technical Conferences & Computers and Information in Engineering Conference, IDETC/CIE 2009, August 30 – September 2, 2009, San Diego, California, USA*, 2009. `http://bicycle.tudelft.nl/schwab/Publications/MooreHubbardKooijmanSchwab2009.pdf`.

[62] Dassault Systèmes, "Solidworks help - mass properties dialog box," 2016. `http://help.solidworks.com/2017/english/SolidWorks/sldworks/hidd_massproperty_text_dlg.htm`, [Online; accessed 18-October-2016].

[63] A. L. Schwab, J. D. G. Kooijman, and J. P. Meijaard, "Some recent developments in bicycle dynamics and control," in *Fourth European Conference on Structural Control (4ECSC), St.Petersburg, Russia, September 8—12, 2008*, pp. 695–702, 2008. `http://bicycle.tudelft.nl/schwab/Publications/SchwabKooijmanMeijaard2008.pdf`.

[64] W. Laubach, "Improvement in velocipedes," Jan. 26 1869. US Patent 86,235.

[65] E. J. Routh, "Stability of a dynamical system with two independent motions," *Proceedings of the London Mathematical Society*, vol. 1, no. 1, pp. 97–99, 1873.

[66] N. Apppelman, "Dynamics and control of a steer-by-wire bicycle," master's thesis, Delft University of Technology, Nov. 27 2012.

[67] T. Öberg, A. Karsznia, and K. Öberg, "Basic gait parameters: reference data for normal subjects, 10-79 years of age," *Journal of rehabilitation research and development*, vol. 30, no. 2, p. 210—223, 1993.

[68] Shimmer Research - Realtime Technologies Ltd, "SDLog for Shimmer3 Firmware User Manual Rev 0.13b," 2016. `http://www.shimmersensing.com/images/uploads/docs/SDLog_for_Shimmer3_Firmware_User_Manual_rev0.13b.pdf`.

[69] Shimmer Research - Realtime Technologies Ltd, "IMU User Guide Revision 1.4," 2016. `http://www.shimmersensing.com/images/uploads/docs/IMU_User_Guide_rev1.4.pdf`.

[70] Shimmer Research - Realtime Technologies Ltd, "Shimmer PROTO3 Series User Guide Revision 1.4," 2016. `http://www.shimmersensing.com/images/uploads/docs/Shimmer_PROTO3_Series_User_Guide_Rev1.4.pdf`.

[71] Shimmer, "Shimmer - Discovery in Motion," 2016. http://www.shimmersensing.com/, [Online; accessed 22-October-2016].

[72] O. Dong, C. Graham, A. Grewal, C. Parrucci, and A. Ruina, "The bricycle: a bicycle in zero gravity can be balanced or steered but not both," *Vehicle System Dynamics*, vol. 52, no. 12, pp. 1681–1694, 2014.

[73] A. L. Schwab, *Dynamics of Flexible Multibody Systems; Small Vibrations Superimposed on a General Rigid Body Motion.* PhD thesis, Delft University of Technology, 2002.

[74] D. Greenwood, *Principles of Dynamics.* Prentice Hall PTR, 2nd ed., 1988.

[75] J. I. Neĭmark and N. A. Fufaev, *Dynamics of Nonholonomic Systems.* Translations of mathematical monographs, American Mathematical Society, 2004.

[76] P. Paris and L. Zhang, "A disk rolling on a horizontal surface without slip," *Mathematical and Computer Modelling*, vol. 36, no. 7, pp. 855 – 860, 2002.

[77] "Rear wheel steered bicycle (rwsb)." http://www.bicycle.tudelft.nl/rwsb/.

[78] Pryor Dodge, "Bicyclearts - the pryor dodge collection," 2008. http://www.bicyclearts.com/bicycles.php, [Online; accessed 19-April-2015].

[79] Grace's Guide, "Grace's guide - british industrial history - reynolds and mays," 2009. http://www.gracesguide.co.uk/Reynolds_and_Mays#cite_note-1, [Online; accessed 19-April-2015].

[80] B. Trepanier, "B(yikes!) | eccentric mobility - phantom velocipede, 1865.," Oct. 10 2006. http://www.artcenter.edu/williamson/recent/byikes/byikesimages/3.html, [Online; accessed 20-February-2016].

[81] Reynolds and Mays, "The "phantom," the velocipede of the period: Reynolds & mays's patent," Apr. 21 1869. British patent 1,216; French patent 85,885.

[82] H. W. Bartleet, *Bartleet's Bicycle Book.* Burrow and Company, 1931. Reprinted in 1983 by Pinkerton.

[83] T. Hadland and H.-E. Lessing, *Bicycle Design – An Illustrated History.* MIT Press, 2014.

[84] Munn & Co., "Improved style of two-wheeled velocipedes," in *Scientific American*, vol. 20, p. 264, Munn & Company, 1869.

[85] E. Wannee, "Rear wheel steered bike (rwsb) page," May 7 2005. http://wannee.nl/hpv/abt/e-index.htm, http://wannee.nl/hpv/abt/e-abt-deel2.htm, http://wannee.nl/hpv/abt/bol.htm, [Online; accessed 6-June-2015].

[86] J. Granger, "Bicycling, 1869," June 28 2012. http://granger.pixels.com/featured/1-bicycling-1869-granger.html, http://images.fineartamerica.com/images-medium-large/1-bicycling-1869-granger.jpg [Online; accessed 14-April-2016].

[87] A. Combs, "Improved velocipede," Aug. 24 1869. US Patent 93,967.

[88] J. I. Stassen, "Velocipedes," Apr. 8 1869. The Great Seal Patent Office, British Patent 1065.

[89] Stassen & Co. Engineers, "The patent velocipede "eagle"." flyer of unknown origin.

[90] National Museum of American History, "America on the move - laubach velocipede." http://amhistory.si.edu/onthemove/collection/object_270.html, [Online; accessed 17-April-2015].

[91] S. H. Oliver and D. H. Berkebile, *Wheels and Wheeling: The Smithsonian Cycle Collection.* Smithsonian studies in history and technology, Smithsonian Institution Press, 1974.

[92] Canada Science & Technology Museum, "Pinterest - 1869 boneshaker velocipede," 2013. https://www.pinterest.com/pin/178173728978527114/, [Online; accessed 19-April-2015].

[93] M. G. Crane, "Bicycle," May 30 1882. US Patent 258,559.

[94] E. McCall, "Mccall bicycle," June 26 1883. US Patent 280,054.

[95] De Lancy Kennedy, "Bicycle," Nov. 6 1883. US Patent 287,943.

[96] C. Leddell, "Leddell bicycle," Oct. 14 1884. US Patent 306,498.

[97] C. Leddell, "Leddell bicycle," June 16 1885. US Patent 319,983.

[98] S. D. Reynolds, "Bicycle," June 4 1889. US Patent 404,562.

[99] E. M. Stroud, "Velocipede," Apr. 28 1891. US Patent 451,080.

[100] Štěrba, "sterba-bike.cz - national technical museum - prague, czech republic," 2012. `http://www.sterba-bike.cz/item/national-technical-museum-prague-czech-republic/category/czech-republic/group/velo-museums?lang=EN`, [Online; accessed 16-August-2015].

[101] H. W. Libbey, "Bicycle," Dec. 5 1893. US Patent 509,919.

[102] Štěrba, "sterba-bike.cz - fenner 1894," 2012. `http://www.sterba-bike.cz/album/800`, `http://www.sterba-bike.cz/fotka/23565/category/katalogy-f-gal`, `http://www.sterba-bike.cz/media/foto/23/imgcbf22249b40d99441c4c77bbc0143f44.jpg` [Online; accessed 7-February-2016].

[103] Grace's Guide, "Grace's guide - british industrial history - fenner rear-steerer, front-driver cycle co," 2012. `http://www.gracesguide.co.uk/Fenner_Rear-steerer,_Front-driver_Cycle_Co`, `http://www.gracesguide.co.uk/File:Im189311Eng-Fenner.jpg`, `http://www.gracesguide.co.uk/images/9/91/Im189311Eng-Fenner.jpg` [Online; accessed 7-February-2016].

[104] Anonymous, "Fahrräder.," *Polytechnisches Journal*, vol. 296, pp. 101–110, 1895.

[105] A. P. Stephens, "Steering mechanism for cycles," July 18 1899. US Patent 629,179.

[106] J. Anderson, "Military bicycle.," Sept. 26 1899. US Patent 633,745.

[107] J. Anderson, "Bicycle.," Sept. 26 1899. US Patent 633,746.

[108] J. Anderson, "Military bicycle.," Sept. 26 1899. US Patent 633,748.

[109] Various, *Punch, or the London Charivari.*, vol. 147. The Project Gutenberg EBook, July 8 1914. `http://www.gutenberg.org/ebooks/29217`, `http://www.gutenberg.org/files/29217/29217-h/29217-h.htm`, [Online; accessed 13-April-2016].

[110] Openbike-Contributors, "Openbike – RearWheelSteeringConcepts," Oct. 21 2014. `http://en.openbike.org/wiki/RearWheelSteeringConcepts`, [Online; accessed 6-March-2016].

[111] M. Beneke, T. Noakes, G. Beneke, and M. Reynolds, *The Lore of Cycling*. Oxford University Press Cape Town, 1989.

[112] G. H. Mieher, "Bicycle," Dec. 5 1939. US Patent 2,182,345.

[113] R. A. Belden, "Bicycle with pivotable rear wheel," Apr. 2 1974. US Patent 3,801,130.

[114] The Strong, "Swing bike - online collections - museumofplay.org." `http://www.museumofplay.org/online-collections/5/21/113.2286`, [Online; accessed 11-September-2015].

[115] B. Häggkvist, "Bicycle and tricycle of low wind resistance and of low center of gravity," Sept. 21 1976. US Patent 3,981,516.

[116] AP Wirephoto, "New type bicycle," *Eau Claire Leader-Telegram*, p. 7A, Oct. 16 1976. October 16.

[117] P. Bruneau, "Ryan owners club - the beginning," 2004. `http://ryanownersclub.com/history/beginning.htm`, [Online; accessed 20-May-2015].

[118] E. Wannee and M. Anderseck, "The official flevobike fanclub site." http://flevofan.ligfiets.net/?doc=home&lang=en, http://flevofan.ligfiets.net/?doc=ch1&lang=en, http://flevofan.ligfiets.net/?doc=ch4-01&lang=en, http://flevofan.ligfiets.net/?doc=ch4-13&lang=en, [Online; accessed 3-April-2016].

[119] B. Zwikker and B. Moens, "Cha-cha bike," *Human Power - The technical journal of the IHPVA*, vol. 9, no. 2, pp. 16–17, 1991.

[120] R. M. Maebe, "Bicycle with steerable wheels," Mar. 26 1985. US Patent 4,506,902.

[121] Bike Shaped Objects, "Weird bruckl swing bike on ebay," June 23 2013. http://www.bikeshapedobjects.com/2013/06/23/weird-bruckl-swing-bike-on-ebay/, [Online; accessed 27-March-2015].

[122] Unicycle.com, "Hoppley 20" circus bike - blue." http://www.unicycle.com/unicycles/ultimate-wheel/hoppley-circus-bike.html, [Online; accessed 21-April-2015].

[123] T. ten Brinke, "Johan vrielink and the flevo bike," *Human Power - The technical journal of the IHPVA*, vol. 9, no. 2, pp. 15–16, 1991.

[124] Rainbow Trainers, "Lose the training wheels - front fork," Oct. 27 2005. http://www.losethetrainingwheels.org/default.aspx?Lev=2&ID=35, [Online; accessed 9-February-2016 per http://web.archive.org].

[125] Jared Herbig, "Rear steer bike," Dec. 6 2012. https://www.youtube.com/watch?v=_qHP6oJlXnk, [Online; accessed 11-September-2015].

[126] AAAS, "Bigraphical sketch - brianno coller," Oct. 15 2012. http://media.eurekalert.org/aaasnewsroom/2010/FIL_000000001099/biosketch.pdf, [Online; accessed 28-October-2015].

[127] W. A. Berger, "Off the beaten trail: Experiments in bicycle stability," *Human Power - The technical journal of the IHPVA*, vol. 10, no. 1, pp. 16–18, 1992.

[128] A. Sudheimer, "Niedriges Zweirad," Apr. 28 1988. DE Patent 8,622,822.

[129] M. Trzaska, "Fahrrad," Mar. 2 1989. DE Patent App. DE19,873,727,771.

[130] C. Brown, "Rear-steering recumbents," *Human Power - The technical journal of the IHPVA*, vol. 8, no. 1, p. 3, 1990.

[131] H.-U. Waldow, "Front wheel drive bicycle - is steered by levers either side of seat, acting on rear wheel fork," Mar. 5 1992. DE Patent App. DE19,904,027,643.

[132] H.-U. Reimers, "Die "kalle"-serie," May 5 2013. http://www.hecklenker.de/index.htm, http://www.hecklenker.de/prototypen.htm [Online; accessed 31-July-2015].

[133] Wikipedia, "Airbike — wikipedia, die freie enzyklopädie," 2014. https://de.wikipedia.org/w/index.php?title=Airbike&oldid=136298244, [Online; accessed 25-August-2015].

[134] J. Mages, "airbike.de," Sept.16 2001. http://www.airbike.de/index2.htm, [Online; accessed 25-August-2015].

[135] D. Ductor, "pedersenbicycles.com - the chinkara," Aug. 10 2012. Reprinted from Recumbent and Tandem Rider Magazine, http://www.pedersenbicycles.com/chinkara.htm, [Online; accessed 25-August-2015].

[136] K. Riggenmann, "Liegefahrrad, kettenlos mit frontantrieb," Feb. 18 1993. DE Patent App. DE19,914,127,174.

[137] C. P. Langen, "Two-wheeled vehicle," Oct. 4 1994. US Patent 5,351,979.

[138] S. Knoop, "Sacha knoop - over mij." in Dutch, http://en.ligfiets.net/user/13831/sachaknoop.html, [Online; accessed 31-March-2016].

[139] Å. Gustavson, "My bike page - the idea of rear wheel steering - the project of a faired bike - how to ride impossible bikes," Apr. 24 2003. http://users.abo.fi/agustavs/hpv/index.html, http://users.abo.fi/agustavs/hpv/rbike.html, http://users.abo.fi/agustavs/hpv/fbike.html, http://users.abo.fi/agustavs/hpv/lbike.html [Online; accessed 29-July-2015].

[140] M. A. Ruitenbeek, "Low, high, foldable and gorgeous: The wave," *Human Power - The technical journal of the IHPVA*, vol. 13, no. 1, pp. 14–15, 1997.

[141] T. Summers, "Vehicle," Jan. 23 1996. US Patent 5,485,893, WO patent 1995001276.

[142] SNAIX training, "About us - snaix.com," 2008. http://www.snaix.com/snaix/index.html, http://www.snaix.com/snaix/company/company_en.php?lang=en, http://www.snaix.com/snaix/trainingsprinzip/knicklenker_en.php?lang=en [Online; accessed 17-January-2017].

[143] F. B. Grimm (Dipl,-Ing), "Einspuriges zweirad," Jan. 15 1998. DE Patent App. DE1,997,110,950,A1.

[144] F. B. Grimm (Dipl,-Ing), "Einspuriges zweirad," July 15 1998. DE Patent App. DE1,997,110,950,C2.

[145] D. Efflandt, "Chain driven front wheel drive and rear wheel steering bicycle," July 8 2003. US Patent 6,588,786.

[146] J. Mages, "python-lowracer.de," Nov.28 2011. http://www.python-lowracer.de/index.html, http://www.python-lowracer.de/pics/gallery/index.html, http://www.python-lowracer.de/geometry.html, [Online; accessed 25-August-2015].

[147] swingbikechick, "Duane flatmo's badass! - youtube," Oct. 6 2007. https://www.youtube.com/watch?v=oIuETJ17Xhw, [Online; accessed 14-August-2015].

[148] swingbikechick, "The badass and the swing bike - youtube," Oct. 6 2007. https://www.youtube.com/watch?v=F41PK22JaU8, [Online; accessed 14-August-2015].

[149] D. Flatmo, "bad ass - youtube," Nov. 16 2011. https://www.youtube.com/watch?v=oStBEuVWfuw, [Online; accessed 14-August-2015].

[150] D. Flatmo, "Duane flatmo on the tonight show - youtube," Apr. 28 2015. https://www.youtube.com/watch?v=zwNPH7Qwv1s, [Online; accessed 14-August-2015].

[151] J.-R. Little (Johnny Payphone), "Duane flatmo's "badass", the bike that shouldn't be. - chicagofreakbike.org," Mar. 2010. http://non.primate.net/chicagofreakbike/2010/03/duane-flatmos-badass-bike-that-shouldnt.php, [Online; accessed 12-April-2016].

[152] L. Dechenne, "Les "progres" et les étapes de mes bricolage vélo - vélo couché artisanal," 2004. in French, http://les-velos-de-laurent.skynetblogs.be/archive/2004/09/index.html, http://les-velos-de-laurent.skynetblogs.be/archive/2004/10/index.html, http://les-velos-de-laurent.skynetblogs.be/archive/2004/week45/index.html, [Online; accessed 22-April-2016].

[153] S. G. Ungar and A. Goczey, "Foot-propelled hobby and/or sport device without handlebar," June 11 2013. US Patent 8,459,667.

[154] macigwheel, "Magic wheel - youtube," Nov. 10 2006. https://www.youtube.com/watch?v=v96i8ldtdbE, [Online; accessed 15-March-2016].

[155] designsonline, "The magicwheel the latest craze to hit the streets - youtube," Sept. 26 2007. https://www.youtube.com/watch?v=Yab_UA0ERZY, [Online; accessed 15-March-2016].

[156] magicwheelbrasil, "Magic wheel - xtreme sports - youtube," July 2 2009. https://www.youtube.com/watch?v=ZNAaI_zlI_c, [Online; accessed 15-March-2016].

[157] 650Steve Restoration Overload ltd., "Products - shanghai steve," Jan. 12 2014. http://www.shanghaisteve.com/products/products.htm, http://www.shanghaisteve.com/products/MagicWheel1.gif, [Online; accessed 15-March-2016].

[158] Jumper-online, "Magic wheel - jumper-online." http://jumper-online.ru/site/magic-wheel/, http://jumper-online.ru/images/magic-wheel-2.jpg [Online; accessed 15-March-2016].

[159] M. Killian, "Sidewaysbike – Not Your Father's Bicycle !," July 15 2007. http://www.sidewaysbike.com/, [Online; accessed 29-March-2016].

[160] M. Killian, "Two wheel steering scooter with latitudinal aligned wheels," Sept. 25 2003. US Patent App. 10/102,161.

[161] M. Killian, "Two wheel steering bicycle with operator positioned facing sideways whose support frame passes under operator supporting operator unicycle like saddle," Feb. 10 2005. US Patent App. 10/635,151.

[162] M. Killian, "Two wheel steering bicycle with each wheel having its own steering control operated by rider's left and right hand respectively and rider positioned facing the direction of motion," Apr. 11 2006. US Patent 7,025,366.

[163] M. Killian, "Two wheel steering bicycle with each wheel having its own steering control operated by rider's left and right hand respectively and rider positioned facing an angle greater than zero and less than ninty degrees with respect to the direction of motion," Jan. 18 2011. US Patent 7,871,095.

[164] A. J. Gaea, "Bicycle having front and rear rotative wheel frames with actuatable means for engaging and disengaging the rear wheel frame rotation," Oct. 17 2006. US Patent 7,121,567.

[165] M. Zurlinden, "Coroflot - recumbent bicycle," Dec. 3 2007. http://www.coroflot.com/mzurlinden/Recumbent-Bicycle, [Online; accessed 4-March-2016].

[166] S. Khan, "Trends updates - boy, cycling with comfort sounds inviting," Jan. 7 2009. http://trendsupdates.com/boy-cycling-with-comfort-sounds-inviting/, [Online; accessed 4-March-2016].

[167] D. Renner, "Recumbents, art, and poems - front wheel drive rear wheel steer recumbent," Dec. 27 2008. http://recumbentsartandpoems.blogspot.nl/2008/12/many-of-you-might-wonder-why-build.html, [Online; accessed 15-October-2016].

[168] D. Renner, "Recumbent bicycles," Dec. 4 2008. https://plus.google.com/photos/114755469029244806605/albums/5187329097320926865?banner=pwa, [Online; accessed 15-October-2016].

[169] D. Renner, "FWDRWS Recumbent," Aug. 2 2010. https://get.google.com/albumarchive/114755469029244806605/album/AF1QipO21KrPmE-b6AQxgJZC6aaL3hBVR1N8HETpNWIE?source=pwa, [Online; accessed 15-October-2016].

[170] D. Renner, "Rear wheel steering recumbent - youtube," December 2009. https://www.youtube.com/watch?v=9ijzld_X0eg, [Online; accessed 5-December-2014].

[171] D. Renner, "Recumbent fwdrws - youtube," December 2008. https://www.youtube.com/watch?v=KMA7CTfbpwo&list=UUV8pe9d2w2H-mmuKAC-KkBw, [Online; accessed 5-December-2014].

[172] R. Gwilym, "Recumbents, art, and poems - rear wheel steering - comments," Dec. 23 2009. http://recumbentsartandpoems.blogspot.nl/2009/12/rear-wheel-steering.html#comments, [Online; accessed 15-October-2016].

[173] M. Delcambre, "Rear wheel steering bike – flickr.com," Aug. 14 2008. https://www.flickr.com/photos/mdelcambre/2764892330/, http://c3.staticflickr.com/4/3087/2764892330_a8ffb86dcf_b.jpg, [Online; accessed 13-May-2016].

[174] N. Petit (NP), "Direction arrière - page 3 - velorizontal.bbfr.net," 2008. in French, http://velorizontal.bbfr.net/t204p50-direction-arriere, http://i45.servimg.com/u/f45/12/75/46/00/vel0110.jpg, http://i45.servimg.com/u/f45/12/75/46/00/pa070010.jpg, http://i45.servimg.com/u/f45/12/75/46/00/pa170010.jpg, http://i75.servimg.com/u/f75/12/75/46/00/pb110010.jpg, http://i75.servimg.com/u/f75/12/75/46/00/pb110011.jpg [Online; accessed 14-April-2016].

[175] N. Petit (NP), "Tad : Le znb - page 1-4 - velorizontal.bbfr.net," 2009. in French, http://velorizontal.bbfr.net/t7559-tad-le-znb, http://velorizontal.bbfr.net/t7559p25-tad-le-znb, http://velorizontal.bbfr.net/t7559p50-tad-le-znb, http://velorizontal.bbfr.net/t7559p75-tad-le-znb, [Online; accessed 14-April-2016].

[176] niafron26, "znb video 1 - youtube," Aug. 20 2009. https://www.youtube.com/watch?v=SGlNhdxesbc, [Online; accessed 14-April-2016].

[177] niafron26, "znb video2 - youtube," Aug. 20 2009. https://www.youtube.com/watch?v=9GOYHBqU1a8, [Online; accessed 14-April-2016].

[178] N. Petit (NP), "vélo couché à traction avant et direction arrière - page 1 - velorizontal.bbfr.net," 2011. in French, http://velorizontal.bbfr.net/t14765-velo-couche-a-traction-avant-et-direction-arriere, [Online; accessed 19-April-2016].

[179] Figaro, "Direction arrière - page 5 - velorizontal.bbfr.net," 2008. in French, http://velorizontal.bbfr.net/t204p100-direction-arriere, http://i73.servimg.com/u/f73/11/93/93/67/direct10.jpg, http://i73.servimg.com/u/f73/11/93/93/67/direct11.jpg, [Online; accessed 19-April-2016].

[180] YikeBike, "YikeBike – fully electric folding bike.," 2015. http://www.yikebike.com/, http://www.yikebike.com/wp-content/uploads/2015/11/banner-Nov1.jpg, [Online; accessed 10-May-2016].

[181] J. Hehr, "Bicycle.," Mar. 5 1901. US Patent 669,201.

[182] G. Ryan, P. Higgins, and C. Smith, "Cycle," Jan. 21 2010. WO Patent App. PCT/IB2009/006,267.

[183] B. Graham and K. McGowan, "The Spin Scooter - AtomicZombie," Dec. 18 2009. http://www.atomiczombie.com/Tutorial%20-%20The%20Spin%20Scooter%20-%20Page%201.aspx, http://www.atomiczombie.com/Tutorial%20-%20The%20Spin%20Scooter%20-%20Page%202.aspx, http://www.atomiczombie.com/Tutorial%20-%20The%20Spin%20Scooter%20-%20Page%203.aspx, http://www.atomiczombie.com/Tutorial%20-%20The%20Spin%20Scooter%20-%20Page%204.aspx, http://www.atomiczombie.com/Tutorial%20-%20The%20Spin%20Scooter%20-%20Page%205.aspx, [Online; accessed 15-March-2016], or http://www.atomiczombie.com/ct-spinscooter.html [Online; accessed 15-March-2016 per http://web.archive.org].

[184] NIUEngineerful, "Adjustable rear steered bicycle - youtube," Nov. 30 2009. https://www.youtube.com/watch?v=OngYfiiC0Bo, [Online; accessed 11-September-2015].

[185] NIUEngineerful, "Niu adjustable rear steered bicycle - youtube," Nov. 30 2009. https://www.youtube.com/watch?v=mQLatUDFwwg, [Online; accessed 11-September-2015].

[186] T. Levand, "kalle.wmv - youtube," Dec. 29 2009. https://www.youtube.com/watch?v=SVwmGiH-HPg, [Online; accessed 31-July-2015].

[187] ausnessa, "2 week prototype - youtube," Mar. 11 2009. https://www.youtube.com/watch?v=gBR-rPoZlsg, [Online; accessed 11-September-2015].

[188] ausnessa, "Recumbent down turri i - youtube," Oct. 6 2009. https://www.youtube.com/watch?v=3Is8QpWXNpg, [Online; accessed 11-September-2015].

[189] ausnessa, "Recumbent down turri ii - youtube," Oct. 6 2009. https://www.youtube.com/watch?v=tLjmFtfRTr4, [Online; accessed 11-September-2015].

[190] K. Moynihan, "Reat triangle pov rear wheel steering prototype - youtube," Jan. 19 2010. https://www.youtube.com/watch?v=xvNIKzNWCiE, [Online; accessed 11-September-2015].

[191] K. Moynihan, "Rear wheel steering prototype - cal poly mech eng senior project - youtube," Jan. 19 2010. https://www.youtube.com/watch?v=nugn2DbL-uw, [Online; accessed 11-September-2015].

[192] FatalNoogie, "Rear-wheel-steering recumbent bike prototype testing - youtube," Aug. 26 2009. https://www.youtube.com/watch?v=VbqnSTa-gQY, [Online; accessed 11-September-2015].

[193] FatalNoogie, "Sept 21 testing 1 - youtube," Sept. 23 2009. https://www.youtube.com/watch?v=64h8XdEugq8, [Online; accessed 12-September-2015].

[194] FatalNoogie, "Sept 21 testing 2 - youtube," Sept. 23 2009. https://www.youtube.com/watch?v=HH-cOw3HybY, [Online; accessed 12-September-2015].

[195] FatalNoogie, "Sept 21 testing 3 - youtube," Sept. 23 2009. https://www.youtube.com/watch?v=_so1vLPiFkU, [Online; accessed 12-September-2015].

[196] FatalNoogie, "Sept 21 testing 4 - youtube," Sept. 23 2009. https://www.youtube.com/watch?v=D9JnbzwEh44, [Online; accessed 12-September-2015].

[197] FatalNoogie, "Sept 21 testing 5 - youtube," Sept. 23 2009. https://www.youtube.com/watch?v=18NOdSbfM50, [Online; accessed 12-September-2015].

[198] FatalNoogie, "Sept 21 testing 6 - youtube," Sept. 23 2009. https://www.youtube.com/watch?v=wa9wq2ljPGs, [Online; accessed 12-September-2015].

[199] FatalNoogie, "Prototype riding jan 14 part 1 - youtube," Jan. 19 2010. https://www.youtube.com/watch?v=s-SYVuSqTNY, [Online; accessed 12-September-2015].

[200] ASME, "Human powered vehicle challenge (hpvc) results 2010 west - competitions - events - asme." https://www.asme.org/events/competitions/human-powered-vehicle-challenge-(hpvc)/hpvc-results, [Online; accessed 12-September-2015].

[201] K. Moynihan, "Rob circling rear wheel steering race bike - cal poly mech. eng. senior project - youtube," Jan. 30 2010. https://www.youtube.com/watch?v=yfzRNhJIOIk, [Online; accessed 11-September-2015].

[202] K. Moynihan, "Rob head-cam rear wheel recumbent race bike through slalom and into death turn washout - youtube," Feb. 1 2010. https://www.youtube.com/watch?v=8QhqJo48MEc, [Online; accessed 11-September-2015].

[203] K. Moynihan, "Austin testing out, f and mid, r steering through slalom on rear wheel steering recumbent race bike - youtube," Feb. 1 2010. https://www.youtube.com/watch?v=GicxrGWzulQ, [Online; accessed 11-September-2015].

[204] K. Moynihan, "Austin testing fast on out, f, and out, r, slalom on rear steering recumbent race bike. - youtube," Feb. 1 2010. https://www.youtube.com/watch?v=v3lnRmSWKPE, [Online; accessed 11-September-2015].

[205] FatalNoogie, "Final rws bike test run a1 - youtube," Jan. 27 2010. https://www.youtube.com/watch?v=GBntbE-WN8o, [Online; accessed 12-September-2015].

[206] FatalNoogie, "Final rws bike test run a2 - youtube," Jan. 27 2010. https://www.youtube.com/watch?v=_AaWkNJNATc, [Online; accessed 12-September-2015].

[207] kjmoynih, "Novel rear wheel steering recumbent - mtbr.com," Feb. 28 2010. http://forums.mtbr.com/frame-building/novel-rear-wheel-steering-recumbent-596685.html, [Online; accessed 11-September-2015].

[208] Cal Poly Human Powered Vehicle, "Artemis - past vehicles - cal poly human powered vehicle," Sept. 11 2013. http://hpv.calpoly.edu/PastVehicles/Artemis/index.html, [Online; accessed 12-September-2015].

[209] Berniche, "Direction arrière - page 12 - velorizontal.bbfr.net," Apr. 2 2012. in French, http://velorizontal.bbfr.net/t204p275-direction-arriere, http://img15.hostingpics.net/pics/64315723B.jpg, [Online; accessed 13-April-2016].

[210] M. Raynor, "Bicycle having independent rear wheel steering," Feb. 4 2010. US Patent App. 12/184,985.

[211] R. Yneges, "Multi Use Mountain Bike – Bicycle Design Projects," Apr. 15 2010. http://www.coroflot.com/yneges/Bicycle-Design-Projects, [Online; accessed 16-May-2016].

[212] Ziganime, "Voici les nouveautés 2010 - nouveautés - ziganime.com," Mar. 28 2010. in French, http://www.ziganime.com/, http://www.ziganime.com/new2010.htm, http://www.ziganime.com/2010new/dirfesse1.jpg, http://www.ziganime.com/2010new/dirfesse2.jpg [Online; accessed 13-April-2016].

[213] Woogyeong Go, "x bike by woogyeong go from korea - seoul cycle design competition 2010 - designboom," Sept. 17 2010. http://www.designboom.com/project/x-bike/, [Online; accessed 12-April-2016].

[214] iF World Design Guide, "X bike / Minivelo." http://ifworlddesignguide.com/entry/66163-x-bike, [Online; accessed 12-April-2016].

[215] 2020, "Xbike - verkeersnet," June 13 2011. in Dutch, http://www.verkeersnet.nl/5388/xbike/, [Online; accessed 12-April-2016].

[216] B. Harley, "Motousa - custom builder eddie meeks quantum leap," Nov. 30 2010. http://www.motorcycle-usa.com/2010/11/article/custom-builder-eddie-meeks-quantum-leap/, http://www.motorcycle-usa.com/photo-gallery/custom-builder-eddie-meeks-quantum-leap/, [Online; accessed 5-March-2016].

[217] E. A. Meeks, "Eddie Alexander Meeks Artist - The Custom Bikes," Nov. 25 2010. http://www.eamstudios.net/, [Online; accessed 5-March-2016].

[218] J. Bechtel, "bicymple. – a bicycle, simplified.," 2016. http://www.bicymple.com/, [Online; accessed 10-May-2016].

[219] W. Zhang, "Front wheel driving and rear wheel steering type bicycle," Sept. 21 2011. CN Patent 201,980,369.

[220] M. Morrow, "About the rear-steerer bike - markism.net," Oct. 2 2011. http://markism.net/Bike_RS.html, [Online; accessed 4-September-2015].

[221] sockozz, "Rear steerer bike - markism.net - youtube," Sept. 11 2013. https://www.youtube.com/watch?v=qsm3uLnxzh0, [Online; accessed 4-September-2015].

[222] C. Despins, "Front-wheel driven, rear-wheel steered vehicle," May 31 2011. US Patent 7,950,682.

[223] Priority designs (PD), "Cannondale CERV Bike," Oct. 22 2013. http://www.prioritydesigns.com/work/#bicycle-design-engineering-and-development-consulting, [Online; accessed 10-May-2016].

[224] E. Mauletti, "Enrico Mauletti's web pages," Oct.30 2009. in Italian, http://digilander.libero.it/maulettilandia/index.htm, [Online; accessed 20-April-2016].

[225] E. Mauletti (recumbent), "Velocipede a ruota posteriore sterzante - rws - page 1-6 - bicireclinateitalia.forumfree.it," 2012. in Italian, http://bicireclinateitalia.forumfree.it/?t=60244966, http://bicireclinateitalia.forumfree.it/?t=60244966&st=15, http://bicireclinateitalia.forumfree.it/?t=60244966&st=30, http://bicireclinateitalia.forumfree.it/?t=60244966&st=45, http://bicireclinateitalia.forumfree.it/?t=60244966&st=60, http://bicireclinateitalia.forumfree.it/?t=60244966&st=75, [Online; accessed 20-April-2016].

[226] Canale di maulettilandia1, "CIMG5726.AVI - YouTube," Mar. 4 2012. https://www.youtube.com/watch?v=m-FInHtAMwE, [Online; accessed 16-May-2016].

[227] L. De Lorenzi, "Velocipede a ruota posteriore sterzante - rws - page 4 - bicireclinateitalia.forumfree.it," Feb. 24 2012. in Italian, http://bicireclinateitalia.forumfree.it/?t=60244966&st=45, [Online; accessed 16-May-2016].

[228] Song Zheng Liang, "Bicycle using front wheel to drive rear wheel to steer," Nov. 14 2012. CN Patent 202,529,083.

[229] Rat Patrol Bike Club, "Rat Bikes - Other Experiments," Apr. 9, 16 2012. http://rat-patrol.org/MiscBikes/index.html, http://rat-patrol.org/MiscBikes/content/20120406_000_large.html, http://rat-patrol.org/MiscBikes/content/oe1_large.html, http://rat-patrol.tumblr.com/archive, http://rat-patrol.tumblr.com/post/20779423016/cris-front-pedaling-rear-steering-bike-it-is-as, http://36.media.tumblr.com/tumblr_m27vpn87Ha1rtuicqo1_1280.jpg, http://rat-patrol.tumblr.com/post/21244587703/in-an-attempt-to-make-a-less-difficult-front, http://41.media.tumblr.com/tumblr_m2logvbZ101rtuicqo4_1280.jpg, http://41.media.tumblr.com/tumblr_m2logvbZ101rtuicqo3_1280.jpg, [Online; accessed 13-April-2016].

[230] M. Saleh, "Rws recumbent bicycle - mohsen-saleh.com," Jan. 23 2012. http://www.mohsen-saleh.com/2012/01/rws-recumbent.html, [Online; accessed 16-January-2017].

[231] M. Saleh, "Rws recumbent - google+," Jan. 13 2012. https://plus.google.com/photos/+MohsenSaleh/albums/5700836541269847121, [Online; accessed 16-January-2017].

[232] Design Temptation, "Recumbent bike- rear wheel steering," Jan. 23 2012. https://www.youtube.com/watch?v=BFOLgY_eE_I, [Online; accessed 16-January-2017].

[233] R. J. Harrop, "Rear Steering Bicycle attempt.," Apr. 27 2013. http://members.westnet.com.au/rjharrop/rear%20steering/stroud.htm, [Online; accessed 13-May-2016].

[234] J. M. Garnet, "Ergonomics of direct-drive recumbent bicycles," *Human Power eJournal*, vol. 5, 2008. http://www.hupi.org/HPeJ/0017/GarnetDirectDriveRecumbents.pdf.

[235] hf61, "Rigging rear wheel steering bike - blenderartists," June 2014. http://blenderartists.org/forum/showthread.php?354248-Rigging-rear-wheel-steering-bike, [Online; accessed 22-May-2016].

[236] gladwell61, "rear steer bicycle.pinkerton cycles.," Oct. 4 2013. https://www.youtube.com/watch?v=JnFmcAgFgBE, [Online; accessed 11-September-2015].

[237] pinkertoncycles, "Our very own design back 2 front bike..steer the front wheel which is at the back....a real mind bender.....," Apr. 28 2015. https://instagram.com/pinkertoncycles/, https://instagram.com/p/2BnEbNsiLb/, [Online; accessed 11-September-2015].

[238] S. Baid, "Vid 20140919 143024 - youtube," Oct. 20 2014. https://www.youtube.com/watch?v=C0la0a8s35g, [Online; accessed 5-September-2015].

[239] S. Baid, "Flexion bike - youtube," Feb. 24 2015. https://www.youtube.com/watch?v=_IUdPxMi2Rs, [Online; accessed 5-September-2015].

[240] N. R. Zakaria, "Toro-x front wheel drive rear wheel," June 2015. http://langkasa-norul.blogspot.nl/2015/06/toro-x-front-wheel-drive-rear-wheel.html?view=timeslide, [Online; no longer available].

[241] B. Aßmann (Nemberch), "Heck-knicklenker – velomobil," 2015. in German, http://www.velomobilforum.de/forum/index.php?threads/heck-knicklenker.42381/, http://www.velomobilforum.de/forum/index.php?threads/heck-knicklenker.42381/page-2 [Online; accessed 1-June-2016].

[242] Bernd Aßmann, "Heck-Knick-Lenker - YouTube," Aug. 4 2015. https://www.youtube.com/watch?v=MBHMMFT-II8, [Online; accessed 1-June-2016].

[243] J. L. B. Alban Haloche, Alexis Honoré, "Trocadero - fixie," 2016. in French, http://www.trocadero-fixie.fr/, https://www.facebook.com/Trocaderofixie, https://www.instagram.com/trocaderofixie/ , https://twitter.com/trocaderofixie, [Online; accessed 25-May-2016].

[244] Trocadero Fixie, "Trocadero-fixie," Apr. 28 2016. https://www.youtube.com/watch?v=Bk-PfmvCLuE, [Online; accessed 25-May-2016].

[245] R. Smith, "Control systems 2 lecture 5: Rhp poles and zero limitations & how to design and ride a bike," 2016. lecture notes, http://control.ee.ethz.ch/~ifa_cs2/CS2_lecture05.small.pdf, [Online; accessed 30-March-2016].

[246] FOX6News, "Something new on 2 (or more) wheels: Msoe hosts intl. bicycle & motorcycle dynamics conference," Sept. 22 2016. http://fox6now.com/2016/09/22/something-new-on-2-or-more-wheels-msoe-hosts-intl-bicycle-dynamics-conf/, [Online; accessed 4-October-2016].

[247] Critical Mass Vancouver, "Random home made bike shots," Apr. 4 2005. http://www.bikesexual.org/cm/misc-foto.htm, http://www.bikesexual.org/cm/pic/foto/misc/211_1173.jpg [Online; accessed 13-April-2016].

[248] C. Wright, "Wonderful counsellor, the mighty god, the everlasting father, the prince of peace - bikingbackwards," Oct. 10 2010. http://bikingbackwards.us/, [Online; accessed 14-March-2016 per http://web.archive.org].

[249] Associated Press, "Backwards Biker Treks Across Country - YouTube," Apr. 17 2008. https://www.youtube.com/watch?v=YWcFj4ZruPk, [Online; accessed 18-March-2016].

[250] Associated Press - KAKE, "Dvs backward biker," April 2008. Associated press story number 774584, http://www.aparchive.com/metadata/DVS-Backward-Biker/d1b5a00bdf4a34ff7a081269df308569?query=774584&current=1&orderBy=Relevance&hits=1&referrer=search&search=%2fsearch%2ffilter%3fquery%3d774584%26from%3d1%26orderBy%3dRelevance%26allFilters%3dKAKE%253ASource%26ptype%3dIncludedProducts%26_%3d1431695894952&allFilters=KAKE%3aSource&productType=IncludedProducts&page=1&b=308569, [Online; accessed 15-May-2015].

[251] Guinness World Records, "Longest distance riding backwards (free wheel) - guinnessworldrecords.com," May 3 2014. http://www.guinnessworldrecords.com/world-records/longest-distance-riding-backwards-(free-wheel), [Online; accessed 9-March-2016].

[252] O. Gabi, "Orban barra gabor 2x guinness world records 2014," May 31 2014. https://www.youtube.com/watch?v=yzzoDtzD2gQ, [Online; accessed 9-March-2016].

[253] C. Adam (né Patzig), "bicycle-world-records," Aug. 8 2008. http://www.bicycle-world-records.com/Guinness/Worldrecord.html, http://www.bicycle-world-records.com/Guinness/worldrecordsNav.html, http://www.bicycle-world-records.com/worldrecords/Guinnessbook.html [Online; accessed 9-March-2016].

[254] Ms. Purple, “Cyclist rides bicycle backwards for 24 hours, covers 337 kilometers - odditycentral,” Oct. 11 2013. http://www.odditycentral.com/news/cyclist-rides-bicycle-backwards-for-24-hours-covers-337-kilometers.html, [Online; accessed 9-March-2016].

[255] EWAustraliaChannel, “24 hour Backwards Cycling challenge,” Sept. 23 2013. https://www.youtube.com/watch?v=pl5MvRtI89g, [Online; accessed 9-March-2016].

[256] Guinness World Records, “Longest distance cycling backwards - guinnessworldrecords.com,” Oct. 8 2013. http://www.guinnessworldrecords.com/world-records/longest-distance-cycling-backwards, [Online; accessed 9-March-2016].

[257] Guinness World Records, “Longest distance cycling backwards in 24 hours - guinnessworldrecords.com,” Oct. 8 2013. http://www.guinnessworldrecords.com/world-records/longest-distance-cycling-backwards-in-24-hours, [Online; accessed 9-March-2016].

TU Delft